

# **Identification and characterization of EFR-interacting proteins**

A thesis submitted to the University of East Anglia for the degree of Doctor of  
Philosophy

**Milena Roux**

The Sainsbury Laboratory  
John Innes Centre  
Norwich UK

October 2010

This copy of the thesis has been supplied on condition that anyone who consults it is understood to recognize that its copyright rests with the author and that no quotation from the thesis, nor any information derived there from, may be published without the author's prior, written consent ©

## ABSTRACT

Plants rely on their innate immune system to defend themselves from myriad potential pathogens. Fundamental to this immunity is the detection of conserved microbial markers called pathogen-associated molecular patterns (PAMPs) by host pattern recognition receptors (PRRs), some of which are trans-membrane leucine-rich repeat receptor-like kinases (RLKs). EF-Tu receptor (EFR) is the PRR for the bacterial PAMP elongation factor Tu (EF-Tu). Signaling following receptor activation results in the activation of PAMP-triggered immunity (PTI). Despite the importance of PTI only few of the molecular mechanisms underlying PTI signaling have been discovered to date. In this thesis, I have used immunoprecipitation followed by mass spectrometry to identify EFR-interacting proteins (EIPs) in *Nicotiana benthamiana* and Arabidopsis expressing functional GFP-tagged EFR. Among the putative EIPs identified in this study are several chaperones responsible for EFR receptor maturation, as well as RLKs from different subfamilies – named receptor kinases associated with EFR (RAEs). Notably, members of the somatic embryogenesis receptor like kinase (SERK) family of RLKs, including SERK1, SERK3/BAK1 and SERK4/BKK1, were identified as RAEs. I further conducted a comprehensive study of the role of SERKs in Arabidopsis PTI signaling and disease resistance in collaboration with Benjamin Schwessinger in the laboratory. Firstly, I found that upon transient over-expression, EFR and FLS2 are capable of interacting in a ligand-inducible manner with all SERKs except SERK5. Interestingly, FLS2 showed with a clear preference for BAK1, while EFR equally interacted with SERK1 to 4. Next, I showed that BAK1 is capable of trans-phosphorylating EFR *in vitro*. Finally, I took advantage of the newly discovered *bak1-5* allele, which does not lead to constitutive cell death when combined with *bkk1* null mutations to study the function of BAK1 and BKK1 in immunity. We found that *bak1-5 bkk1-1* mutant plants are severely compromised in all FLS2- and EFR-dependent signaling responses, as well as resistance to hemi-biotrophic bacteria and obligate biotrophic oomycetes.

I also initiated the study of RAE5 and RAE6, and preliminary results indicate that RAE5 may be an important positive regulator of PAMP-induced reactive oxygen species (ROS) burst.

All together, these results unveil an unexpected regulation of the EFR-dependent pathway by a suite of RKs.

## Table of Contents

<b>ABSTRACT .....</b>	<b>II</b>
<b>LIST OF TABLES .....</b>	<b>VII</b>
<b>PART II .....</b>	<b>VII</b>
<b>LIST OF FIGURES .....</b>	<b>VIII</b>
<b>PART I .....</b>	<b>VIII</b>
<b>LIST OF PUBLICATIONS .....</b>	<b>XI</b>
<b>ABBREVIATIONS .....</b>	<b>XII</b>
<b>PART I .....</b>	<b>1</b>
<b>1 Literature Review .....</b>	<b>1</b>
1.1 Plant-microbe interactions: general overview .....	1
1.1.1 Preformed defenses .....	1
1.1.2 Overview of innate immunity .....	3
1.2 Defense level 1: PAMP-triggered immunity (PTI) .....	5
1.2.1 Bacterial PAMP perception .....	5
1.3 ER-QC of immune-related proteins .....	18
1.4 Signaling downstream from pathogen perception .....	21
1.4.1 Receptor Kinase Complexes .....	22
1.4.2 Receptor endocytosis .....	27
1.4.3 Ion fluxes .....	31
1.4.4 ROS burst .....	34
1.4.5 MAPK signaling .....	35
1.4.6 Changes in gene expression .....	36
1.4.7 Epigenetic regulation of defense responses .....	38
1.4.8 Callose deposition .....	41
1.4.9 The hypersensitive response .....	42
1.4.10 Lesion mimicry, PCD and guards .....	43
1.4.11 Too much fat will kill you .....	45
1.4.12 Mysterious kinases, cell death and lipids .....	46

1.4.13 Negative regulation of defense signaling .....	49
1.4.14 Plant Hormones.....	51
1.5 Effector-triggered susceptibility (ETS).....	59
1.5.1 Virulence effectors .....	59
1.5.2 RIN4: bullseye .....	63
1.6 Effector-triggered Immunity (ETI), Level 2 Defense .....	65
1.6.1 Resistance genes .....	65
1.7 Comparison of ETI and PTI signaling modes.....	79
<b>PART II .....</b>	<b>81</b>
<b>2 Materials and Methods.....</b>	<b>81</b>
2.1 Plant material and growth conditions.....	81
2.1.1 <i>Arabidopsis thaliana</i> .....	81
2.1.2 <i>Nicotiana transient expression</i> .....	83
2.2 PAMP assays .....	84
2.2.1 pamps .....	84
2.2.2 Seedling growth inhibition.....	84
2.2.3 ROS burst assay .....	84
2.2.4 MAP kinase assay .....	85
2.2.5 PAMP-induced defense gene induction .....	85
2.2.6 PAMP-induced ethylene production .....	86
2.2.7 Crude elicitor extract preparation.....	86
2.3 Pathogen assays .....	87
2.3.1 Bacterial spray-inoculation of <i>Arabidopsis</i> .....	87
2.4.2. <i>H. Arabidopsis</i> inoculation and scoring on <i>Arabidopsis</i> .....	87
2.3.2 Pathogens used in this study .....	88
2.4 Molecular biology.....	88
2.4.1 DNA methods .....	88
2.4.2 RNA methods.....	96
2.4.3 Protein methods .....	97
2.5 Cellular biological methods .....	104
2.5.1 Confocal laser scanning microscopy.....	104
2.6 Antibiotics used in this study .....	104
2.7 Media used in this study .....	104
2.8 Primers used in this study .....	105
<b>PART III .....</b>	<b>108</b>
<b>3 Original Thesis Proposal .....</b>	<b>108</b>

## **PART IV: THESIS RESULTS.....118**

<b>1 IDENTIFICATION OF EFR-INTERACTING PROTEINS (eips) IN NICOTIANA BENTHAMIANA .....</b>	<b>118</b>
1.1 Preface .....	118
1.2 Results .....	118
1.2.1 Development of specific anti-EFR antibodies.....	118
1.2.2 Development of tagged <i>EFR</i> constructs for transient expression.....	121
1.2.3 Production of transgenic <i>Arabidopsis</i> plants stably expressing functional atefr .....	123
1.2.4 Immunoprecipitation of transiently expressed tagged EFR from <i>N. Benthamiana</i> .....	126
1.2.5 The EFR protein may undergo fragmentation.....	137
1.2.6 Pleiotropic drug resistance (PDR) ABC transporters .....	139
1.3 Discussion.....	149
1.3.1 Large scale EFR immunoprecipitation.....	149
1.3.2 The role of pleiotropic drug resistance (PDR) transporter role in PTI remains elusive .....	150
<b>2 IDENTIFICATION OF EFR-INTERACTING PROTEINS (EIPS) IN ARABIDOPSIS.....153</b>	
2.1 Preface .....	153
2.2 Results .....	153
2.2.1 EFR-egfp is enriched in immunoprecipitates .....	153
2.2.2 EFR <i>N</i> -glycosylation and quality control.....	158
2.2.3 EFR Phosphorylation .....	160
2.2.4 Putative EFR-interacting proteins .....	163
2.3 Discussion.....	169
2.3.1 EFR Immunoprecipitation in <i>Arabidopsis</i> .....	169
2.3.2 ER-QC components as putative eips .....	169
2.3.3 <i>N</i> -glycosylation .....	172
2.3.4 EFR phosphorylation .....	172
2.3.5 PEN3 does not have a clear role in PTI .....	175
<b>3 SERKS: REGULATORY CO-RECEPTORS FOR MULTIPLE RECEPTOR KINASES..177</b>	
3.1 Preface .....	177
3.2 Results .....	178
3.2.1 Identification of serks in the EFR complex .....	178
3.2.2 EFR interacts with BAK1 in <i>Arabidopsis</i> .....	180
3.2.3 Interactions between ligand-binding receptors and regulatory receptor kinases do not require active kinase .....	182
3.2.4 EFR, FLS2 and BAK1 undergo trans-phosphorylation <i>in vitro</i> .....	184
3.2.5 EFR, FLS2 and BRI1 have differential specificity for serks in <i>N. Benthamiana</i> .....	186
3.2.6 BAK1 and BKK1 are required for EFR-, FLS2- and PEP1/2-dependent responses .....	188
3.2.7 BAK1 and BKK1 are required for disease resistance .....	196

3.3 Discussion.....	201
3.3.1 The regulatory LRR-RLK BAK1 interacts <i>in planta</i> with several ligand-binding LRR-rks, including EFR .....	201
3.3.2 EFR, FLS2 and BRI1 form complex(es) with multiple serks .....	202
3.3.3 The regulatory LRR-rks BAK1 and BKK1 are important regulators of FLS2-, EFR- and PEP1/2-dependent signaling.....	203
3.3.4 BAK1 and BKK1 are required for immunity to hemi-biotrophic and obligate biotrophic pathogens .....	204
3.3.5 Possible molecular functions of BAK1 and BKK1.....	206
<b>4 RAE5: AN EFR-INTERACTING LRR-RLK FUNCTIONING AS A REGULATOR OF PTI AND ETI .....</b>	<b>209</b>
4.1 Preface .....	209
4.2 Results .....	212
4.2.1 RAE5 was identified in EFR ips .....	212
4.2.2 RAE5 interacts with rlks in <i>N. Benthamiana</i> .....	212
4.2.3 Anti-RAE5 antibody development.....	215
4.2.4 RAE5 interactions in Arabidopsis.....	218
4.2.5 RAE5 is present at the plasma membrane.....	220
4.2.6 RAE5 is required for optimal PAMP-triggered ROS responses .....	221
4.3 Discussion.....	222
4.3.1 RAE5: PRR regulator?.....	222
4.3.2 RAE5 and its potential link with OXI1, lipid signaling and cell death control .....	225
4.3.3 RAE5 complex dynamics and potential ETI-PTI bridge .....	228
<b>5 Parting shots - raes of insight.....</b>	<b>231</b>
5.1 Preface .....	231
5.2 Preliminary results .....	233
5.3 Discussion.....	237
<b>6 General Conclusions and Outlooks .....</b>	<b>239</b>
<b>APPENDIX.....</b>	<b>247</b>
<b>ACKNOWLEDGEMENTS .....</b>	<b>278</b>
<b>REFERENCES .....</b>	<b>279</b>

## List of Tables

### Part II

Table 2-1 List of <i>Arabidopsis thaliana</i> and <i>N. plumbaginifolia</i> lines used in this study .....	81
Table 2-2 Summary of pathogens used in this study .....	88
Table 2-3 Standard thermal program .....	89
Table 2-4 High-fidelity PCR thermal program .....	90
Table 2-5 Targeted mutagenesis PCR thermal program .....	90
Table 2-6 Summary of plasmids used in this study .....	95
Table 2-7: Generation of polyclonal antibodies .....	99
Table 2-8 Primers used in this study .....	105

### Part IV

Table 1-1 Proteins identified by MS analysis of EFR immunoprecipitates .....	133
Table 1-2 <i>NbSERK</i> tryptic peptides identified by MS analysis of EFR immunoprecipitates .....	134
Table 2-1 Potential EFR-interacting proteins .....	156
Table 2-2 Glycosylated EFR peptides identified by MS analysis of EFR IPs .....	159
Table 2-3 EFR phosphopeptides identified by MS analysis of EFR IPs .....	161
Table 2-4 PEN3 peptides identified by MS analysis of EFR IPs .....	164
Table 3-1 Identification of SERK tryptic peptides by MS analysis of elf18-treated EFR immuno-precipitates .....	179
Table 4-1: RAE5 peptides identified by MS analysis of EFR IPs .....	212
Table 5-1 RAE peptides identified by MS analysis of EFR immunoprecipitates .....	234

### Appendix Tables

Table A1.1 EFR peptides identified in comparison extraction .....	247
Table A1.3 NbSERK MS data .....	250
Table A2.1 Attached .xls spreadsheet .....	
Table A2.2 AHA peptides identified by MS analysis of EFR IPs .....	258
Table A4.1 RAE5 co-expressed genes predicted by Expression Angler .....	262
Table A5.1 RAE6 co-expressed genes predicted by Expression Angler .....	272
Table A5.2 RAE7 co-expressed genes predicted by Expression Angler .....	274
Table A5.3 RAE8 co-expressed genes predicted by Expression Angler .....	276

## List of Figures

### Part I

Figure 1: Basolateral epithelial flagellin detection. ....	6
Figure 2: Pathway for N-glycosylation for nascent polypeptides in plants.....	19
Figure 3 EFR requires a SDF2-ERdj3B-BiP complex for maturation .....	20
Figure 4: SERK receptor complexes.....	25
Figure 5: Promotion of signaling through endocytosis. ....	28
Figure 6: Overview of FLS2-induced PTI signaling .....	42
Figure 7: Negative regulation of defense signaling .....	51
Figure 8: <i>Pseudomonas</i> effectors subvert innate immunity .....	62
Figure 9: Model for NB–LRR protein activation.....	69
Figure 10: Signaling network interactions governed by PTI and ETI.....	80

### Part IV

Figure 1.1 Anti-EFR antibodies cannot detect endogenous <i>Arabidopsis</i> EFR ....	120
Figure 1.2 Transiently expressed EFR is functional and detectable in the cell periphery in <i>N. benthamiana</i> .....	122
Figure 1.3 Transgenic <i>Arabidopsis</i> over-expressing EFR complements <i>efr-1</i> for <i>elf18</i> responses. ....	124
Figure 1.4 Transgenic lines expressing EFR under the control of the native promoter complement <i>efr-1</i> .....	125
Figure 1.5: Immunoprecipitation of transiently expressed EFR-HA <sub>3</sub> or GUS-HA <sub>3</sub> from total protein or microsomal preparations .....	128
Figure 1.6 Immunoprecipitation of <i>N. benthamiana</i> transiently expressed EFR .	131
Figure 1.7 Alignment of SERK proteins of <i>Arabidopsis</i> , <i>Nicotiana</i> and <i>Solanum</i> spp.....	135
Figure 1.8 EFR protein coverage obtained by mass spectrometry analysis of EFR IP in <i>N. benthamiana</i> . ....	139
Figure 1.9 Pleiotropic drug resistance (PDR) ABC Transporter Family. ....	140
Figure 1.10 <i>N. plumbaginifolia</i> <i>NpPDR1</i> -silenced lines have sensitized ROS responses. ....	143
Figure 1.11 Schematic representation of PDR12 gene organization and protein domains. ....	144

Figure 1.12 <i>pdr12</i> mutants are compromised in PAMP-induced gene expression .....	146
Figure 1.13 <i>pdr12-1</i> mutants are slightly more susceptible to weakly virulent <i>Pseudomonas</i> .....	148
Figure 2.1 Immunoprecipitation of EFR in transgenic Arabidopsis.....	155
Figure 2.2 Conservation of N-glycosylation sites in selected LRR-RKs .....	159
Figure 2.3 Multiple alignment of EFR, Xa21, FLS2, BRI1, BAK1 cytoplasmic domains .....	162
Figure 2.4 PEN3 interacts with FLS2 but not with EFR under conditions tested.....	165
Figure 2.5 <i>pen3</i> mutants do not have severely compromised PTI responses....	167
Figure 3.1 EFR and BAK1 interact in a ligand-specific manner. ....	181
Figure 3.2 Role of kinase activity for receptor heteromerization and signaling. ..	183
Figure 3.3: BAK1 transphosphorylates EFR <i>in vitro</i> .....	185
Figure 3.4 EFR, FLS2 and BRI1 have different specificity for the SERK proteins in <i>N. benthamiana</i> . ....	187
Figure 3.5 PAMP-induced ROS burst and seedling growth inhibition of single serk mutants. ....	188
Figure 3.6 SERK1 and SERK2 are not required for flg22 and elf18 responses in Arabidopsis. ....	189
Figure 3.7 BAK1 and BKK1 are required for flg22 and elf18 responses in Arabidopsis .....	192
Figure 3.8 BAK1 and BKK1 are required for flg22 and elf18 responses in Arabidopsis .....	195
Figure 3.9 BAK1 and BKK1 are required for AtPep1 responses. ....	196
Figure 3.10 BAK1 and BKK1 are required for resistance to adapted and non-adapted bacteria. ....	198
Figure 3.11 BAK1 and BKK1 are required for resistance to the obligate biotrophic oomycete pathogen <i>Hyaloperonospora arabidopsis</i> .....	200
Figure 4.1. Phylogenetic tree of members of LRR-RK subfamily XII.....	209
Figure 4.2 Primary structure of RAE5 protein .....	210

Figure 4.3. RAE5 is capable of interaction with EFR, FLS2, BRI1, BAK1 and OXI1 in <i>N. benthamiana</i> .....	214
Figure 4.4. Anti-RAE5 antibodies can detect RAE5 in total protein extracts .....	217
Figure 4.5. RAE5 complex formation in Arabidopsis.....	219
Figure 4.6. Transiently over-expressed RAE5 is localized in the plasma membrane.....	221
Figure 4.7. RAE5 is a positive regulator of ROS burst.....	222
Figure 5.1 RLK/Pelle subfamilies enriched in up- and down-regulated genes under abiotic and biotic stress conditions .....	233
Figure 5.2 <i>rae6</i> single mutants respond with wild-type-like ROS burst and seedling growth inhibition.....	236

## Appendix Figures

Figure A2.1 Putative N-glycosylation sites in EFR .....	251
Figure A2.2 Multiple sequence alignment of PDR family members .....	252
Figure A2.3 Workflow for identification of PTMs .....	255
Figure A2.4 EFR phosphopeptides spectra and fragmentation tables .....	256
Figure A2.5 Multiple sequence alignment of various receptor-like kinases .....	261
Figure A4.1 Multiple alignment of members of Family XII of LRR-RKs.....	265
Figure A4.2 Kinase domain phylogeny of selected LRR-RLK genes in four plant species .....	266
Figure A4.3 Pairwise alignment for comparison of proteins encoded by alternative <i>RAE5</i> transcripts .....	267
Figure A4.4 Formation and attenuation of phosphatidic acid (PA) .....	268
Figure A4.5 Phylogenetic tree of Pt1-related Arabidopsis protein kinases.....	268
Figure A4.6 Pathway for sphingolipid metabolism .....	269
Figure A5.1 Phylogenetic tree of RAE6 family VIII-2 members.....	270
Figure A5.2 Multiple alignment of RAE6 family VII-2 members .....	271
Figure A5.3 Phylogenetic tree of RAE7 family members .....	273
Figure A5.4 Phylogenetic tree of CRK family members .....	275

## List of publications arising from the work in this thesis:

Roux, M\*, Schwessinger, B.\* , Albrecht, C., Chinchilla, D., Jones, A., Holton, N., Malinovsky, F.G. , Tör, M, de Vries, S. and Zipfel, C. (2010) The Arabidopsis leucine-rich repeat receptor kinases BAK1/SERK3 and BKK1/SERK4 cooperate to regulate innate immunity. *In preparation.*

\*co-first authors

Schwessinger, B., Roux, M., Sklenar, J, Kadota, Y., Jones, A. and Zipfel, C. (2010) Phosphorylation-dependent differential regulation of plant growth, cell death and innate immunity by the regulatory receptor-like kinase BAK1. Submitted to PloS Genetics.

## Abbreviations

ABA	Abscisic acid
ACA	Arabidopsis $\text{Ca}^{2+}$ -ATPase
ACC	1-aminocyclopropane-1-carboxylic acid
ACD11	Accelerated cell death 11
ACR4	Arabidopsis Crinkly 4
ACRE	Avr9/Cf-9 rapidly elicited
ACS	ACC synthase
Adi3	AvrPto-dependent Pto-interacting kinase 3
AGC	cAMP-dependent protein kinase A, cGMP-dependent protein kinase G and phospholipids-dependent protein kinase C
AGO	Argonaute
AHA	Arabidopsis $\text{H}^+$ -ATPase
APAF	Apoptotic protease-activating factor
ASC	Apoptosis-associated speck-like protein
ASK	Apoptosis signal-regulating kinase 1
ATX	Arabidopsis homolog of trithorax 1
Avr	Avirulence protein/gene
BAK1	BRI1-associated kinase 1
BAP1	BON1-associated protein 1
bHLH	Basic-helix-loop-helix
BIK1	Botrytis-induced kinase 1
BiP	Luminal binding protein
BIR1	BAK1-interacting RLK
BL	Brassinolide
BKK1	BAK1-like 1
BON	BONZAI
BR	Brassinosteroid
BRI1	Brassinosteroid insensitive 1
CARD	Caspase activation and recruitment domain
CBB	Coomassie brilliant blue
CBRLK	Calmodulin binding S-locus receptor kinase

CC	Coiled-coil
CDC5 (MAC1)	Cell division cell cycle 5 (transcription factor)
CDC48	Cell division cycle protein 48 (ATPase)
CDPK	Calcium-dependent protein kinases
CED4	Cell death abnormality
CERK1	Chitin elicitor receptor kinase 1
CEBiP	Chitin elicitor binding protein 1
CHORD	Cysteine- and histidine-rich domain
CID	Collision-induced dissociation
CK	Cytokinins
CMPG1	Cys, Met, Pro and Gly or ACRE74
CNGC	Cyclic nucleotide-gated channels
CNL	CC-NB-LRR
CNX	Calnexin
COR	Coronatine
CPR	Constitutive expressor of PR genes
CRK	Cysteine-rich RLK
CRT1	Compromised recognition of TCV (Hsp90)
CRT3	Calreticulin 3
CS	Crystallin and small heat shock protein-like
CSP	Cold shock protein
CTR1	Constitutive triple response 1
cv.	Cultivar
DAD	Defender against cell death
DAG	Diacylglycerol
DDE1	Delayed dehiscence 1
DET3	De-etiolated 3
Dex	Dexamethasone
DGL1	Defective glycosylation1
DGK	DAG kinase
DND	Defense no death
dpi	Days post-infiltration/inoculation
DRM	Detergent resistant membranes

DUF	Domain of unknown function
EBF1	EIN3-binding F-box protein 1
ECD	Electron capture dissociation
EDS	Enhanced disease susceptibility
EFR	EF-Tu receptor
EGF	Epidermal growth factor
EIL	EIN3-like
EIN	ET-insensitive
EIP	EFR-interacting protein
EIX	Ethylene-inducing xylanase
EF-Tu	Elongation factor Tu
ERAD	ER-associated degradation
ERF	Ethylene response factor 1
ERQC	ER quality control
ERS	ET sensor
ESI	Electrospray ionization
ET	Ethylene
ETD	Electron transfer dissociation
ETI	Effector-triggered immunity
ETP	EIN2-targeting protein
ETR	ET response 1
ETS	Effector-triggered suppression
EV	Empty
FB1	Fumonisin B1
FBR	Fumonisin B1 resistant
FER	FERONIA
FLS2	Flagellin-sensing
FT-ICR	Fourier transform ion cyclotron resonance
GA	Gibberellins
GCS	Glucosidase
GlcNAc	N-acetylglucosamine
GPI	Glycosylphosphatidylinositol
Grp78	Glucose-regulated protein 78

GSL	Glucan synthase-like
HERK1	HERCULES
Hlm	HR-like lesion mimic
Hop/Sti	Hsp70/Hsp90 Organizing Protein/Stress-inducible protein
Hpa	Hyaloperonospora arabidopsis (formerly <i>P. parasitica</i> )
HR	Hypersensitive Response
Hrc	Hypersensitive response and conserved
Hrl	hypersensitive response-like lesions
Hrp	Hypersensitive response and pathogenicity
Hsp	Heat shock protein
HUB1	Histone monoubiquitination 1
HypSys	Hydroxyproline-rich glycopeptides
ICE	IL-1-converting enzyme
ICS1	Isochorismate synthase 1
IL	Interleukin
Ile	Isoleucine
Ins(4,5)P <sub>3</sub>	Inositol-1,4,5,-triphosphate
IP	Immunoprecipitate
IPAF	ICE-protease-activation factor
IPCS	Inositolphosphorylceramide synthase
IPS	1L-myo-inositol-1-phosphate synthase 1
I κβ	Inhibitor of NF- κβ
IRAK4	IL-1-associated receptor kinase 4
JA	Jasmonic acid
JAR1	Jasmonate-Resistant 1
JAZ	Jasmonate ZIM domain
JM	Juxtamembrane
LAZ	LAZARUS
LCB1	Long-chain base 1
LPS	Lipopolysaccharides
LRR	Leucine-rich repeat
LSD	Lesion simulating disease resistance response
IsiRNA	Long siRNAs

MAC	MOS4-associated complex
MAMP	Microbe-associated molecular pattern
MAPK	Mitogen-activated protein kinase
miRNA	MicroRNA
MED	Mediator
MKP	MAPK phosphatase
MKS1	MAP kinase substrate 1
MOS	Modifier of snc1
MS	Mass spectrometry
MS/MS	Tandem MS
MyD88	Myeloid differentiation primary response protein 88
NAIP5	NLR apoptosis-inhibitory protein 5
natsiRNA	Natural antisense transcript small interfering RNA
NBS	Nucleotide-binding site
NDR1	Nonrace-specific disease resistance 1
Nep	Necrosis- and ethylene-inducing protein
NF-κβ	Nuclear factor κβ
NFR	Nod factor receptor
NINJA	Novel Interactor of JAZ
NLP	Nep-like protein
NLRs	NOD-like receptors
NLRC4	NLR family, CARD-domain containing 4
NLRP3	NLR family, pyrin domain containing 3; also called Nalp3/cryopyrin
NLS	Nuclear localization sequence
NO	Nitric oxide
NOD	Nucleotide binding and oligomerization domain
NPP1	Necrosis-inducing Phytophthora protein 1
NPR1	Nonexpressor of PR genes
NRIP	N-receptor interacting protein 1
OG	Oligogalacturonides
OST	Oligosaccharide transferase
OXI	Oxidative signal-inducible

PA	Phosphatidic acid
PAD4	Phytoalexin deficient 4
PAMP	Pathogen-associated molecular pattern
PBS1	AvrPphB susceptible
PCD	Programmed cell death
PCNA	Proliferating cells nuclear antigen A
PDF	Plant defensin
PDI	Protein disulphide isomerase
PtdIns(4,5)P <sub>2</sub>	Phosphatidylinositol-4,5-biphosphate
PDK	3'-phosphoinositide-dependent kinase
PDR	Pleiotropic drug resistance
Pep13	13 aa oligopeptide elicitor
PEPR	AtPep receptor
PG	Endopolygalacturonase
PGIP	Polygalacturonase-inhibiting protein
PGN	Peptidoglycan
PIR	Protein interaction reporter
PLC or D	Phospholipase C or D
PMR4	Powdery mildew resistant 4
Pph	<i>Pseudomonas syringae</i> pv. <i>phaseolicola</i>
PR	Pathogenesis-related
PRL1	Pleiotropic regulatory locus 1
PRR	Pattern-recognition receptor
Pta	<i>Pseudomonas syringae</i> pv. <i>tabaci</i>
PTI	PAMP-triggered immunity
Pti1	Pto-interacting 1
Pto	<i>Pseudomonas syringae</i> pv. <i>tomato</i>
Pto	Resistance to Pto
PUB	Plant U-box
pv.	Pathovar
PVDF	Polyvinylidifluoride
PVX	Potato virus X
R	Resistance protein/gene

RACK1	Receptor for Activated C-Kinase 1
RAE	RK associated with EFR
RAR1	Required for Mla12 resistance
RBP-DR1	RNA-binding protein defense-related 1
Rboh	Respiratory burst oxidase homolog
RdDM	RNA-directed DNA methylation
RIN	RPM1-interacting protein
RIPK	RPM1-induced kinase
RLCK	Receptor-like cytoplasmic kinase
RLK	Receptor like kinase
RNP-1	RNA-binding motif 1
ROS	Reactive oxygen species
RPM1	Resistance to <i>P. maculicola</i> protein 1
RPP	Resistance to <i>P. parasitica</i>
RPS	Resistance to <i>P. syringae</i>
RPW	Resistance to powdery mildew
RRS	Resistance to <i>R. solanacearum</i>
RTE	Reversion-to-ethylene sensitivity 1
RTK	Receptor tyrosine kinase
SA	Salicylic acid
SAR	Systemic acquired resistance
SCD1	Stomatal cytokinesis defective 1
SCF	Skp1–Cul1–F box/ Skp1p-Cdc53p-F box
SDF2	Stromal-derived factor 2
SDG	SET domain group 8
SERK	Somatic embryogenesis related kinase
SET	SuVar-3-9-E(2)-trithorax
SID2	SA induction deficient 2
SGI	Seedling growth inhibition
SGT1	Suppressor of the G 2 allele of skp1
siRNA	Small interfering RNA
SNC	Suppressor of npr1-1, constitutive 2
SPT	Serine palmitoyltransferase

SSI	Suppressor of SA insensitivity of npr1-5
SST3	Staurosporin and temperature-sensitive 3
STAND	Signal <u>trans</u> duction <u>A</u> TPas with <u>n</u> umerous <u>d</u> omains
SuVar	Suppressor of variegation 3-9
TAL	Transcription activator-like
TAP	Tandem affinity purification
THE1	THESEUS 1
TIR	Toll/Interleukin receptor
TIR1	Transport inhibitor response 1
TLR	Toll-like receptor
TM	Transmembrane
TMV	Tobacco mosaic virus
TNL	TIR-NB-LRR
TPL	TOPLESS
TPR	TOPLESS-related
TRAF	Tumor necrosis factor Receptor-Associated Factor
TRV	Tobacco rattle virus
TTSS	Type three secretion system
UGGT	UDP-glucose:glycoprotein transferase
VSP	Vegetative storage protein
WB	Western blotting
WIN	HopW1-1-interacting 2
WRKY	WRKY DNA binding protein

# Part I

## 1 Literature Review

### 1.1 *Plant-microbe interactions: general overview*

The following is not a comprehensive review of plant-pathogens interactions, as we have learned so much over the last 100 years that I would need several volumes to sketch out the entire field. I have just outlined major important concepts and tried to highlight areas that I think are of particular interest or relevance to the thesis topic.

The interaction between plants and the myriad pathogens that constantly attempt to attack them is a battle over the centuries, and evolution has armed each with an array of tools, both defensive and offensive. Plants are mostly resistant to incursion however, and this is due to their fine-tuned, multilayered innate immune system. I will discuss some of the strategies used by each side of this battle for dominance, and try to put into perspective the progress that has been made in the field until now.

Innate immunity is due to non-host resistance provided by pre-invasive defenses such as those afforded by plant cell itself, as well as induced defenses, and the activation of immunity through the recognition of non-self (Bent and Mackey, 2007; Nürnberg and Lipka, 2005).

#### 1.1.1 Preformed defenses

##### 1.1.1.1 Mechanical defenses

Plant tissues are reinforced with structural barriers to prevent pathogen attachment or penetration. Firstly, the cell wall, composed of cellulose polymers, cross-linking glycans and pectins, provides some protection against bacterial and fungal pathogens (Huckelhoven, 2007). Lignin in the cell wall is a polymer of

phenolic compounds, and provides rigidity to cells, forming a primary component in wood. In addition, cutin, suberin and waxes create fatty deposits in cell walls (Schreiber, 2010), preventing pathogens from contacting the epidermis (Reina-Pinto and Yephremov, 2009). This primary layer is supplemented by the action of inducible defense responses. Reactive oxygen species released in response to pathogen perception catalyze cross-linking of cell wall polymers (Passardi *et al.*, 2004), signaling to neighbouring cells to put up defenses.

### 1.1.1.2 Chemical defenses

Secondary metabolites or phytoanticipins, including terpenoids, phenolics and alkaloids, function in the constitutive defense of many plant species. For example, the monoterpenoid pyrethrin produced by *Chrysanthemum* acts as an insect neurotoxin (Hitmi *et al.*, 2000), while the diterpenoid gossypol produced in cotton has antibacterial and antifungal properties (Olson *et al.*, 2008) and triterpenoid cardiac glycosides are toxic to herbivores (Dobler, 2001).

A wide range of phenolic compounds produced in plants have roles in defense, including tannins, lignins, flavonoids and phytoalexins. Phytoalexins, such as camalexin produced in *Arabidopsis*, are antifungal and antibiotic (Glazebrook and Ausubel, 1994; Glazebrook *et al.*, 1997; Zhou *et al.*, 1999).

Another important class of compounds is the nitrogenous alkaloids, produced in vascular plants. For example, capsaicin, responsible for the spicy taste of chilli peppers (Molina-Torres *et al.*, 1999) and cyanogenic glycosides, which break down to form hydrogen cyanide, are toxic to aerobic organisms (Zagrobelny *et al.*, 2004).

Brassicaceae produce sulfur-containing glucosinolates, the mustard oil glucosinolates being responsible for the characteristic taste of brassica vegetables. Myrosinases hydrolyse the beta-thioglucoside bond of glucosinolates to produce aglycones (Burmeister *et al.*, 1997), which break down to form isothiocyanates with chemical properties deterring insect feeding. In *Arabidopsis*, the myrosinase PEN2 (penetration 2) hydrolyzes indole glucosinolates into indol-3-methylamine and raphanusamic acid, which may be toxic to fungal pathogens (Bednarek *et al.*, 2009) and have not been identified in insect interactions. Furthermore, the 4-

methoxy-indol-3-ylmethylgluconsinolate is required for callose deposition in response to inoculation with pathogens (Clay *et al.*, 2009).

### **1.1.1.3 Protein and peptide defenses**

Pathogenesis-related (PR) proteins comprise several classes of proteins and peptides induced by microbe, insect or herbivore attack (reviewed in (van Loon *et al.*, 2006). Defensins (PR-12 family), first identified in barley and wheat, are small cysteine-rich proteins with broad antimicrobial activity, especially against fungal infection (Stotz *et al.*, 2009). The defensin *PDF1.2a* gene is induced by pathogens and JA/ET application, and is used as a marker for defense against necrotrophic fungal pathogens (Penninckx *et al.*, 1998).

Thionins (PR-13 family) are also cysteine-rich peptides, with broad antifungal and antibacterial activities (Epple *et al.*, 1995). Protease inhibitors (PR-6 family), commonly induced by herbivore attack, inhibit digestive enzymes such as chymotrypsin (Sels *et al.*, 2008).

Interestingly, PR-1 protein accumulation is used as a marker for defense activation and is associated with systemic acquired resistance (SAR), although its biological function has not been characterized (van Loon *et al.*, 2006). Other enzymes may also directly target pathogens, for example by degradation of fungal or oomycete cell walls by chitinases or glucanases, respectively which have both been shown to possess antimicrobial properties (van Loon *et al.*, 2006).

### **1.1.2 Overview of innate immunity**

**Pathogen-associated molecular patterns (PAMPs)** are conserved molecules, typical of a whole class of microorganisms and essential to microbial survival, making them less likely to evolve away from recognition (Janeway and Medzhitov, 2002). PAMPs may be present on the surface of the microbe (such as flagellin), be released through enzyme activity (such as chitinases) or may be released from dying cells (as proposed for EF-Tu) (Zipfel and Felix, 2005). These molecules are usually absent from host organisms and can be found across

kingdoms, from bacteria to fungi and oomycetes (Medzhitov, 2007). PAMPs are sometimes referred to as microbe-associated molecular patterns (MAMPs), as they are also found in non-pathogenic microorganisms (Medzhitov, 2007). Hence, invading microorganisms betray their presence to potential hosts by the presence of PAMPs that are detected by **pattern recognition receptors (PRRs)**, notable for their specificity and sensitivity of detection (Janeway, 1989). This recognition sets in motion a series of downstream cellular events that induce **PAMP-triggered immunity (PTI)** (Chisholm *et al.*, 2006). Only a few PRRs have been identified in plants so far, most of which are members of the large family of receptor-like kinases, numbering around 600 in *Arabidopsis* and 1000 in rice (Shiu *et al.*, 2004). To subvert PTI, pathogens have developed effectors that compromise PTI by suppressing defense responses or evading detection. In this way, pathogens bring about **effector-triggered susceptibility (ETS)**. In the early days of study of PAMPs, the importance of this layer of defense was overlooked in favour of that afforded by resistance (R) proteins. Initially termed gene-for-gene resistance (Flor, 1971), this branch of innate immunity relies on the recognition between would-be pathogen effector molecules (avirulence/Avr) and host resistance (R) proteins, which results in either further colonization or ultimately resistance of the plant. If the plant host recognizes the effector, it sounds the alarm and defenses go up to prevent any further spread of the pathogen, usually using the **hypersensitive response (HR)** cell death to sequester the infection. This type of response has recently been termed **effector-triggered immunity (ETI)**. In the current view of plant-pathogen interactions, the molecular events culminating in susceptibility or resistance are no longer viewed as solid permanent features of plant or microbe, but rather as a dynamic interaction between these opponents, pushed on by selective pressure and evolving to dominate. This manifests as a continuous cycle of evolution between plants and pathogens as they try to outsmart each other at each turn, and was succinctly defined in the zig-zag model of Jones and Dangl (Jones and Dangl, 2006).

## **1.2 Defense level 1: PAMP-triggered immunity (PTI)**

PAMPs, historically referred to as general elicitors, a term coined by Noel Keen in 1972 (Keen *et al.*, 1972), have fascinated plant scientists for decades. Early work studied the induction of soybean defense responses by an elicitor from *Phytophthora megasperma* var. *sojae* (Keen *et al.*, 1972), which was later identified as  $\beta$ -glucan (Ayers *et al.*, 1976), which is released from oomycete cell walls by the activity of glucanases (Yoshikawa *et al.*, 1981). Since then, many PAMPs have been identified and the search continues.

### **1.2.1 Bacterial PAMP perception**

#### **1.2.1.1 Flagellin detection in mammals**

The discovery of the immunogenicity of flagellin occurred during the study of *Salmonella* infection of gut epithelium. The observation was made that while only a few epithelial cells had been colonized, all displayed activation of the pro-inflammatory transcription factor nuclear factor (NF)- $\kappa$ B (Gewirtz *et al.*, 2001). Subsequently, the presence of a soluble mediator was proven when the media of the infected cells could be used to induce interleukin (IL)-8 secretion in uninfected cells (Gewirtz *et al.*, 2001). Flagellin, the primary structural component of bacterial flagella, was thereafter purified and has been shown to be a potent immune inducer even in the picomolar range (McSorley *et al.*, 2002).

The flagellin receptor Toll-like receptor 5 (TLR5) (Hayashi *et al.*, 2001) is expressed on the basolateral surface of polarized epithelia (Figure 1), specifically positioned to recognize invasive pathogens that have managed to breach the epithelium (Vijay-Kumar *et al.*, 2008).

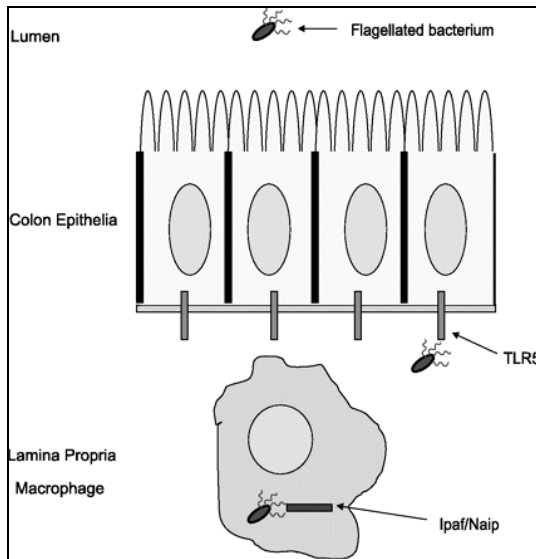


**Figure 1: Basolateral epithelial flagellin detection from Neish, 2007.**

Epithelial cells use basolateral Toll-like receptor (TLR) TLR5 to detect extracellular flagellate pathogens that have breached the apical epithelial barrier. These cells respond with proinflammatory transcriptional responses. Macrophages utilize intracellular IL-1 $\beta$ -converting enzyme protease-activating factor (Ipaf)/neuronal apoptosis inhibitory protein (Naip)5 to detect intracytoplasmic flagellin and respond with IL-1 release and/or apoptosis.

The region of flagellin recognized by TLR5 is a highly conserved region, which is exposed in free monomers but buried within the assembled flagellar structure (Smith *et al.*, 2003). Given the conservation of flagellin, TLR5 enables the recognition of a wide variety of flagellated bacteria.

Following flagellin binding to TLR5, receptor dimerization occurs (Hayashi *et al.*, 2001), followed by recruitment of the adaptor MyD88 (Medzhitov *et al.*, 1998). Interleukin-1 (IL-1) receptor-associated kinase (IRAK) (Moors *et al.*, 2001) is activated, and associates with TRAF6 and this leads to activation of MAP kinases (p38 and ERK) and inhibitor of NF- $\kappa$ B (Ik $\beta$ ) kinases, which results in activation of transcription factors nuclear factor  $\kappa$ B (NF- $\kappa$ B) (Tallant *et al.*, 2004); Berin *et al.*, 2002; Khan *et al.*, 2004). This in turn drives the expression of several proinflammatory genes including the neutrophil chemoattractant IL-8 (Yu *et al.*, 2003). Downstream signaling results in the transcriptional activation of a panel of at least 500 defense-related genes that protect the cells against various challenges (Zeng *et al.*, 2003). Flagellin can also be detected intracellularly by members of the nucleotide-binding oligomerization domain-leucine-rich repeats (NOD-LRR; NLR) family of receptors, specifically NLRC4 (NLR family, CARD-domain containing 4) and NLRP3 (NLR family, pyrin domain containing 3; also called Nalp3/cryopyrin)

(Miao *et al.*, 2006; Warren *et al.*, 2008). NLRC4, also called IPAF for ICE-protease-activation factor (where ICE stand for IL-1-converting enzyme), possesses a nucleotide binding oligomerization domain (NOD), and a PAMP-recognition domain (LRR). NLRC4 also heterologomerizes with NLR apoptosis-inhibitory protein 5 (NAIP5), and this protein is required for inflammasome activation (Lightfield *et al.*, 2008). The inflammasome contains NLRC4, the adaptor protein apoptosis-associated speck-like protein (ASC), which contains a caspase activation and recruitment domain (CARD) domain, and the cysteine protease caspase 1 (Agostini *et al.*, 2004).

These authors provide evidence for the recognition of the carboxy-terminal end of *Legionella pneumophila* flagellin by NLRC4 (Lightfield *et al.*, 2008), while a conflicting report suggests the N-terminal amino acids of *Pseudomonas aeruginosa* flagellin are critical (Franchi *et al.*, 2007), though neither report could distinguish whether the mutations compromised translocation of flagellin into the cytosol. This conflict should be resolved when further studies reveal the nature of PRR-PAMP binding for cytosolic flagellin.

Flagellin may be secreted via the type III or IV secretion system, leading to its recognition in the cytoplasm (Franchi *et al.*, 2006; Miao *et al.*, 2006). NLRC4 can interact with pro-caspase-1 through CARD-CARD domain interactions, however the adaptor ASC also has a role to play, though this remains unclear. Thereafter, caspase-1 processes pro-inflammatory cytokines including IL-1 $\beta$  and IL-18 as part of the pyroptotic response to infection (Chang and Yang, 2000). Importantly, non-flagellated *Shigella* can also activate the NLRC4 inflammasome to result in caspase-1 activity (Martinton *et al.*, 2002).

### 1.2.1.2 Plant flagellin perception

Flagellin extracted from *P. syringae* pv. *tabaci* was originally shown to induce medium alkalinization of tomato cells (Felix *et al.*, 1999). A meticulous study using synthetic flg peptides based on *P. aeruginosa* flagellin showed that a conserved peptide from the N-terminus, with a minimum of 15 amino acids (flg15) (in tomato) and up to 22 amino acids (flg22) (in Arabidopsis) was required to elicit defense responses.

Importantly, although the receptor architectures of the plant flagellin receptor and TLR5 are similar, they are not orthologous proteins, and thus the portions of flagellin which are immunogenic in mammals differ from the plant-active epitope. Interestingly, flagellins of the plant-associated bacteria *Agrobacterium tumefaciens* and *Rhizobium meliloti* showed little conservation in the flg15 domain and were completely inactive, even at high concentrations (Felix *et al.*, 1999). Moreover, flg22, but not flg15, elicited defense responses in *Arabidopsis*, while tomato cells responded to either peptide (Bauer *et al.*, 2001). Further truncations of the peptide from the C-terminus created competitive antagonist peptides (Felix *et al.*, 1999; Bauer *et al.*, 2001), likely competing for binding sites at the receptor, FLS2 (flagellin sensing 2), which was subsequently identified (Gómez-Gómez *et al.*, 2001; Chinchilla *et al.*, 2006).

Rice was reported to be insensitive to flg22 (Felix *et al.*, 1999). However, recent results showed that flg22 is recognized by rice, but that this response is weaker than with full-length flagellin (Takai *et al.*, 2008). In addition, flagellins derived from non-adapted bacteria but having identical protein sequences differentially induce strong defense responses in non-host plants, illustrating that other domains and/or post-translational modifications of flagellin are also recognized (Taguchi *et al.*, 2003, 2006, 2009; Takeuchi *et al.*, 2003, 2007). Finally, analysis of *Xanthomonas campestris* pv. *campestris* flagellin sequences has revealed some polymorphisms within strains, however the flg22 region was the only part of the molecule able to elicit responses (Sun *et al.*, 2006).

In exceptional cases, some virulent phytopathogenic bacteria are able to mask recognition of a PAMP (e.g. flagellin) by mutating residues within the recognized epitope (Felix *et al.*, 1999; Pfund *et al.*, 2004; Sun *et al.*, 2006). This reflects a virulence strategy evolved by successful pathogens complementary to effector secretion.

FLS2 is a LRR-receptor-like kinase (RLK), with 28 extracellular LRRs, a transmembrane domain and an intracellular Ser/Thr kinase domain (Chinchilla *et al.*, 2006). A systematic alanine-scanning mutagenesis approach narrowed down the flg22-binding region to solvent-exposed LRRs 9-15 (Dunning *et al.*, 2007), although the exact binding site was not identified.

FLS2 orthologs have been identified in tomato (Robatzek *et al.*, 2007), *N. benthamiana* (Hann and Rathjen, 2007), rice (Takai *et al.*, 2008) and Brassica spp. (Dunning *et al.*, 2007). Furthermore, functional conservation of FLS2 has been demonstrated by expression of the rice *FLS2* gene, *OsFLS2*, in an *A. thaliana* *fls2* mutant (Takai *et al.*, 2008), suggesting that the associated signaling pathways are also functionally conserved.

FLS2 is important for resistance to bacterial pathogens, as *fls2* mutants show enhanced growth of *Pto* DC3000 and flg22 pre-treatment limits growth of subsequently inoculated bacteria (Zipfel *et al.*, 2004). However, Arabidopsis accessions Dra-0 and Po-0 have non-functional FLS2 and yet are not generally immuno-compromised (Dunning *et al.*, 2007). Nonetheless, lack of flagellin recognition allows more growth of the non-adapted bacteria *Pseudomonas syringae* pv. *phaseolicola* and *P. syringae* pv. *tabaci* (Li *et al.*, 2005; de Torres *et al.*, 2006). To avoid detection, it is logical for pathogens to suppress the expression of flagella once they have entered the apoplast. Indeed, the virulence regulator HrpL suppresses flagellar expression in *Erwinia amylovora* (Cesbron *et al.*, 2006) and *P. syringae* pv. *phaseolicola* 1448a (Ortiz-Martín *et al.*, 2010), while in *Pto* DC3000 HrpR is responsible for this function (Lan *et al.*, 2006). These data point to the importance of flagellin perception in innate immunity.

### **1.2.1.3 Elongation factor Tu (EF-Tu)**

Elongation factor Tu (EF-Tu) was identified as a PAMP when crude *fliC* *E. coli* GI826 extracts lacking flagellin were applied to cell cultures and seen to induce extracellular alkalinization (Kunze *et al.*, 2004). Biochemical purification resulted in the identification of EF-Tu, and the elicitor-active portion of the protein was revealed by a process of proteolytic cleavage. Synthetic peptides of EF-Tu fragments were tested for activity, and this revealed an N-terminal 18 amino acid peptide (elf18) derived from a predicted exposed surface of the protein as the minimum epitope to induce strong responses in Arabidopsis cell cultures (Kunze *et al.*, 2004).

EF-Tu is an abundant bacterial protein, and it is conceivable that some of this should be released during colonization of host plants betraying the presence of the

bacteria. Evidence of EF-Tu has been found in the secretome of *Xanthomonas campestris*, *Pseudomonas fluorescens* and *Erwinia chrysanthemi* (Zipfel et al., 2006). Furthermore, EF-Tu plays a role in the adhesion of bacteria to mammalian host cells and is an activator of pro-inflammatory responses (Granato et al., 2004). Interestingly, *E. coli* EF-Tu is modified by acetylation of the N-terminal Serine residue, and this modification enhances elicitor activity of synthetic elf peptides. Analysis of elf18 peptides of *Erwinia amylovora* and *E. chrysanthemi* revealed identical peptides to *E. coli*, while *Agrobacterium tumefaciens* and *Sinorhizobium meliloti* elf18 peptides differ slightly, but maintain activity. In contrast, elf18 derived from phytopathogenic strains of *Pseudomonas syringae* pv. *tomato* DC3000 and *Xanthomonas campestris* pv. *campestris* had significantly reduced activity (Lacombe et al., 2010). A truncated peptide elf12 behaved as a weak competitive antagonist of elf18 activity (Kunze et al., 2004).

The receptor for elf18, EFR (EF-Tu receptor) is a LRR-RLK belonging to the same subfamily (XII) as FLS2, with 21 LRRs in the extracellular domain, an N-terminal signal peptide and an intracellular Ser/Thr kinase domain (Zipfel et al., 2006). EF-Tu perception is unique to Brassicaceae; however, poplar and rice encode receptors with similar architecture, presumably for the perception of as yet unidentified PAMPs (Boller and Felix, 2009). In the case of rice, the closest EFR homolog is Xa21 (discussed below). Interestingly, transiently expressed EFR is fully functional in Solanaceous plants, suggesting that downstream components are conserved between families (Lacombe et al., 2010; Zipfel et al., 2006). EFR plays an important role in disease resistance and elf26 pretreatment reduces bacterial growth in plants subsequently inoculated with *Pto* DC3000 (Zipfel et al., 2006). *efr-1* null mutants are also susceptible to the less virulent *Pto* DC3000 COR<sup>-</sup> and  $\Delta$ AvrPto $\Delta$ AvrPtoB strains (Nekrasov et al., 2009), which lack the phytotoxin coronatine or the effectors AvrPto and AvrPtoB, respectively. EFR confers resistance to *A. tumefaciens*, as *efr-1* plants are more amenable to transient expression (Zipfel et al., 2006), and EFR-over-expressing *N. benthamiana* plants are conversely more recalcitrant to transient expression. Furthermore, transgenic EFR-expressing *N. benthamiana* plants display enhanced resistance to the adapted virulent bacteria *P. syringae* pv. *syringae* B728a, as well as *P. syringae* pv. *tabaci* 11528 (Zipfel et al., 2004). This has also been extended

to tomato plants, where EFR over-expression provides resistance to important pathogens of solanaceous plants, such as *Ralstonia solanacearum* GMI1000 and *Xanthomonas perforans* T4-4B (Lacombe *et al.*, 2010).

#### **1.2.1.4 Xa21: from R to PRR**

Xa21, identified as a resistance gene in the wild rice cultivar *Oryza longistaminata*, confers resistance to *Xanthomonas oryzae* pv. *oryzae* (Xoo) (Khush *et al.*, 1990; Song *et al.*, 1995). Xa21 is a LRR-RLK with 23 extracellular LRRs and has similar receptor architecture to EFR. Recently, it has been shown that in fact Xa21 is a PRR, as it recognizes and binds the small sulfated type-I secreted peptide ax21 (Lee *et al.*, 2009). Peptide sulfation is critical to its recognition by Xa21 and although ax21 is present in all sequenced *Xanthomonas* sp., the unmodified peptides do not elicit Xa21-mediated defense responses (da Silva *et al.*, 2004).

#### **1.2.1.5 Other bacterial PAMPs**

Lipopolysaccharides (LPS) are the principal component of the outer membrane of Gram-negative bacteria and act as PAMPs in dicots and monocots (Newman *et al.*, 2007). LPS is composed of a variable long-chain polysaccharide region, O-antigen, and a more conserved lipid A moiety. The lipid A part of LPS is as effective as intact LPS in inducing a defense response in *Arabidopsis* (Zeidler *et al.*, 2004) and this activity depends in its phosphorylation and acylation (Silipo *et al.*, 2010). In addition, synthetic oligorhamnans, which are common components of the otherwise highly variable O-chain in LPS, can trigger defense responses in *Arabidopsis* (Bedini *et al.*, 2005).

In addition to activating defenses, LPS and other exopolysaccharides can suppress defense responses, by chelating calcium ions for example (Newman *et al.*, 2007; Tellstrom *et al.*, 2007; Aslam *et al.*, 2008).

Peptidoglycan (PGN) is a component of the bacterial cell wall composed of  $\beta$ -1,4-linked N-acetylglucosamine (GlcNac) and N-acetyl muramic acid cross-linked by peptides. Species specificity is encoded in the peptide portion of PGN and either this or the conserved glycan structure can act as PAMPs for recognition by vertebrates, insects and *Arabidopsis* (Guan and Mariuzza, 2007; Charroux *et al.*, 2010; Gust *et al.*, 2007; Erbs *et al.*, 2008). Although PGN and chitin are structurally related, the as-yet unidentified receptor is distinct from the chitin receptor, as cells saturated with PGN were still able to respond to chitin (Gust *et al.*, 2007).

Cyclic lipopeptides derived from multiple strains of *Bacillus subtilis* have also been demonstrated to stimulate defense responses in tobacco (Jourdan *et al.*, 2009). The RNA-binding motif (RNP-1) of bacterial cold shock proteins (CSP) acts as a PAMP in *Solanaceae* by recognition of its 22-amino acid core, CSP22 (Felix and Boller, 2003). Other proteinaceous PAMPs perceived by plants include the superoxide dismutase SodM (Watt *et al.*, 2006) and harpins (Engelhardt *et al.*, 2009). Recent work showed that bacterial non-methylated CpG DNA was also recognized as a PAMP in *Arabidopsis* (Yakushiji *et al.*, 2009). Recently, the type III secretion system (TTSS) was shown to elicit strong ROS burst in *N. benthamiana* when delivered from the pHIR11 cosmid by *Pfo*, compared to *Pfo* without pHIR11 (Oh *et al.*, 2010a). pHIR11 carries the conserved cluster of *hrp/hrc* genes cloned from *P. syringae* pv. *syringae* 61, but HrpK and HrpZ are largely responsible for the ROS-inducing property of the TTSS (Oh *et al.*, 2010a). HrpK, a translocase responsible for the delivery of other effectors (Petnicki-Ocwieja *et al.*, 2005) could be the actively inducing PTI, or may cause delivery of another unknown elicitor. The functionally redundant translocase HrpZ (Kvitko *et al.*, 2007), also contributes to this elicitation. HrpZ is capable of lipid binding and pore formation, and also induces HR in tobacco (Haapalainen *et al.*, 2010) and MAP kinase activation in parsley (Engelhardt *et al.*, 2009) when applied exogenously. Interestingly, *hrpA*, a pilus protein encoded by the HrpZ operon, is subject to diversifying selection (Guttman *et al.*, 2006), supporting the hypothesis that the TTSS is detected by the innate immune system.

### 1.2.1.6 Recognition of Fungal PAMPs

#### 1.2.1.6.1 Chitin perception

Chitin is a polymer of N-acetyl-D-glucosamine, which comprises the fungal cell wall and is not found in plants. This component of fungal cell wall is required for pathogenicity and defects in its synthesis reduce fungal virulence (Wan *et al.*, 2008). Plants have cleverly evolved a means of enzymatically degrading fungal cell walls and can recognize the breakdown products, such as chitin fragments (chitooligosaccharides) as PAMPs.

In rice, the lysin motif (LysM) domain-containing protein CEBiP (chitin elicitor binding protein) was found to directly bind chitin (Kaku *et al.*, 2006). Interestingly, in legumes LysM-domain containing RLKs Nod factor receptors NFR1 and NFR5 are responsible for chitooligosaccharide (Nod factor) recognition resulting in symbiosis (Radutoiu *et al.*, 2003). This suggests that perception systems for symbiosis have been adapted to the detection of dangerous microorganisms.

Importantly, CEBiP is a glycosylphosphatidylinositol (GPI)-anchored protein (Shibuya *et al.*, unpublished results) without an intracellular domain, therefore it must collaborate with other protein/s to transduce this signal into the cell and bring about PTI signaling. In *Arabidopsis*, homologs of CEBiP exist in a family of 3 LYM proteins, but it is not known if these proteins are able to bind chitin. However, the LysM-RK CERK1/LysM-RLK1 was found to be required for chitin perception and also contributes to resistance to fungal pathogens (Wan *et al.*, 2008; Miya *et al.*, 2007). Evidence for chitin binding by AtCERK1 is partial. Recent work using *in vitro* binding assays in yeast showed binding of AtCERK1 to chitin (Iizasa *et al.*, 2010). Moreover, the ectodomain of AtCERK1 was also shown to bind chitin with low affinity while the kinase domain was modified by phosphorylation in response to chitin elicitation (Petutschnig *et al.*, 2010). Rice cultivar Kinmaze possesses a homologous protein OsCERK1 (Chen *et al.*, 2010b) responsible for chitin perception and defense against fungal pathogens (Kishimoto *et al.*, 2010). Recently, cross-linking and blue native PAGE analysis has shown that OsCERK1 and CEBiP form hetero-oligomers in response to chitin elicitation, though CEBiP already exists as homo-oligomers in the membrane (Shimizu *et al.*, 2010).

Interestingly, *Arabidopsis* *cerk1* mutant are also more susceptible to spray-inoculated bacterial pathogens (Gimenez-Ibanez *et al.*, 2009a; Gimenez-Ibanez *et al.*, 2009b), thus CERK1 may also recognize some bacterial oligosaccharide PAMP or endogenous cell wall breakdown product released during bacterial infection, implying dual specificity for this important receptor. Recent work has revealed a LysM receptor-like protein (RLP) as the putative PGN receptor, required for disease resistance to *Pto* DC3000 (Andrea Gust and Thorsten Nürnberg, personal communication). It is conceivable that AtCERK1 may oligomerize with different PAMP receptors for altered specificity, thus engaging with CEBiP homologs for chitin perception, or with PGN receptor for PGN perception.

#### **1.2.1.6.2 Ethylene-inducing xylanase (EIX) and LeEIX1/2**

Ethylene-inducing xylanase (EIX), a protein of 22 kDa derived from the fungus *Trichoderma viride* (Fuchs *et al.*, 1989), induces ethylene production, PR protein expression, electrolyte leakage and HR in tobacco and tomato (Bailey *et al.*, 1990; Bailey *et al.*, 1992; Ron *et al.*, 2000; Elbaz *et al.*, 2002; Bargmann *et al.*, 2006). Importantly, the xylanase activity of EIX is not required for it to act as an elicitor of defense responses (Furman-Matarasso *et al.*, 1999).

In tomato, two EIX receptors LeEIX1 and LeEIX2 were cloned and identified as LRR-RLPs. Interestingly, in usually EIX-nonresponsive tobacco, transient over-expression of LeEIX1/2 allows EIX binding, but only LeEIX2 can transmit the signal that induces HR (Ron and Avni, 2004).

#### **1.2.1.7 Oomycete PAMPs**

##### **1.2.1.7.1 Pep-13**

A conserved peptide fragment (Pep-13) of an abundant cell wall glycoprotein (GP42) derived from the phytopathogenic oomycete *Phytophthora sojae* was found to elicit defense gene expression and synthesis of antimicrobial phytoalexins

in parsley (Nürnberger *et al.*, 1994; Hahlbrock *et al.*, 1995), and was later identified as a PAMP (Brunner *et al.*, 2002). Furthermore, it was shown that GP42 is a *P. sojae* cell wall-associated  $\text{Ca}^{2+}$ -dependent transglutaminase (TGase), the first such enzyme reported from an oomycete species. Pep-13 mutagenesis showed that the same amino acid residues that were important for plant defense-eliciting activity in parsley (Nürnberger *et al.*, 1994) and potato were also essential for TGase activity (Brunner *et al.*, 2002). Despite the identification of a high-affinity binding site for Pep13 in parsley cells, the receptor could not be purified and remains elusive (Nennstiel *et al.*, 1998; Nürnberger *et al.*, 1995).

#### **1.2.1.7.2 Nep-like proteins (NLPs): toxin or PAMP?**

A 24-kD necrosis- and ethylene-inducing protein (Nep1) was first purified from culture filtrates of *Fusarium oxysporum*, and was intriguing in its ability to trigger plant cell death (Bailey, 1995). The Nep1 sequence is unrelated to any known protein or functional domain (Nelson, 1998; Pemberton and Salmond, 2004), but several Nep1-like proteins (NLPs) have since been discovered in a variety of organisms including fungi, oomycetes and bacteria. A novel necrosis-inducing *Phytophthora* protein 1 (NPP1) domain is present in all NLPs (Fellbrich *et al.*, 2002), and features a conserved heptapeptide motif (Gijzen and Nürnberger, 2006).

NPP1 is an NLP derived from *P. parasitica*, which induces necrosis in dicotyledonous plants, including parsley, tobacco and *Arabidopsis* (Fellbrich *et al.*, 2002), which is distinct from immunity-induced programmed cell death (PCD) (Qutob *et al.*, 2006). NPP1 application also results in calcium influx, ROS production, ethylene biosynthesis, MAP kinase activation, callose deposition and phytoalexin production (Fellbrich *et al.*, 2002). Although NLPs cause a range of responses typical of PAMP-induced signaling, no receptors have yet been identified, and difficulty in classifying these molecules as toxins or PAMPs persisted for many years.

Recently, the crystal structure of the NLP from the oomycete *Pythium aphanidermatum* was obtained, and interestingly, the protein fold was structurally similar to marine cytolytic pore-forming toxins (actinoporins) derived from *Actinia*

*equina* (equinatoxin II) and *Stichodactyla helianthus* (sticholysin) (Ottmann *et al.*, 2009). Furthermore, three-dimensional modeling of the structure of NLPs from *P. parasitica* and the phytopathogenic bacterium, *Pectobacterium carotovorum* displayed high conservation. Indeed, virulence of *nlp*<sup>-</sup> *P. carotovorum* was rescued by expression of the 2 oomycete NLPs, suggesting that these NLPs are orthologous proteins (Ottmann *et al.*, 2009). Mutagenesis analysis revealed that the same structural properties were required for plasma membrane permeabilization and cytolysis in plant cells, as well as to restore bacterial virulence (Ottmann *et al.*, 2009).

### 1.2.1.8 Potential PRRs of unknown PAMPs

In *Arabidopsis*, the membrane-localized AtRLP30 was shown to be required for resistance to the non-adapted bacterial pathogen *P. syringae* pv. *phaseolicola* 1448A (Wang *et al.*, 2008a), though no function as a R protein has been demonstrated, and this protein could be a PRR. More recently, RLP51/SNC2 was identified in a screen for mutants with constitutive defense in the absence of *nonexpressor of PR genes* (*NPR1*) (Zhang *et al.*, 2010c). The semi-dominant mutant *snc2-1D* (suppressor of *npr1-1*, constitutive 2) had dwarf morphology similar to *snc1*, partially suppressed by elevated temperatures (Zhang *et al.*, 2010c). The mutation in *snc2-1D* is present within the conserved GxxxG motif (Fritz-Laylin *et al.*, 2005) in the TM domain. *snc2-1D npr1-1* plants display increased SA accumulation compared to *npr1-1*, as well as enhanced resistance to *Pto* DC3000 and *Hpa* Noco 2, while *snc2* loss-of-function lines were more susceptible to *Pto* DC3000 (Zhang *et al.*, 2010c). It is possible that SNC2 detects an unknown PAMP or guards some component of innate immunity.

A similar screen also identified *snc4-1D*, another semi-dominant mutant with a phenotype similar to *snc1* (Bi *et al.*, 2010). The mutation, resulting in increased resistance and constitutive *PR-1* expression, was identified within the kinase domain of an atypical receptor kinase with extracellular glycerophosphoryl diester phosphodiesterase domains (Bi *et al.*, 2010). The *snc4-1D* phenotype is suppressed by loss of the positive regulator of defense *MAP kinase substrate 1*

(MKS1) (Bi *et al.*, 2010). At this point the function of SNC4 is unknown, but could be as a PAMP receptor or regulator of other PRRs.

### 1.2.1.9 Host-derived Danger Signals, DAMPs

In addition to the recognition of non-self molecules, plants and animals also respond to markers of “danger” or cellular damage (danger/damage-associated molecular pattern, DAMP) (Matzinger, 2002), resulting in a similar set of responses to PAMP perception. The action of fungal hydrolases on plant cell wall pectin releases the DAMP oligo- $\alpha$ -galacturonides (OGs) (Ferrari *et al.*, 2007). OGs were originally found as inducers of proteinase inhibitors in tomato leaves, and act when present at high concentrations, without moving systemically within plant tissues (Bishop *et al.*, 1981). OGs induce responses similar to flg22 in *Arabidopsis*, including ROS burst, MAPK activation and defense gene expression (Denoux *et al.*, 2008; Galletti *et al.*, 2008), while enhancing resistance to fungal pathogen *Botrytis cinerea* (Ferrari *et al.*, 2007).

In the 1970s, the discovery that leaf damage systemically induces proteinase inhibitors, which inhibit insect digestive enzymes (Green and Ryan, 1972), forged the idea that mobile signals generated at injury sites create systemic protection against herbivores and insects. Endogenous signals, released by plant cells in response to wounding and pathogen attack, include the peptides systemin (Ryan and Pearce, 2003), AtPep1 (Huffaker *et al.*, 2006) and hydroxyproline-rich glycopeptides (Pearce and Ryan, 2003). Systemin and AtPep1 are produced from precursor polypeptides while systemin is stored in the cytoplasm (Narváez-Vásquez and Ryan, 2004). Systemin provided the first example of a systemic wound signal in plants and reaches the apoplast where its binding to a tissue-specific receptor, likely a BRI1-related protein, leads to expression of polyphenol oxidase and protease inhibitors (Berger *et al.*, 1996; Holton *et al.*, 2007; Malinowski *et al.*, 2009).

The AtPep1 precursor PROPEP1 is induced in response to wounding, jasmonates, ethylene and PAMPs (Huffaker *et al.*, 2006), and processed AtPep1 is transported to the apoplast where it is detected by the LRR-RKs PEPR1 and PEPR2 (Yamaguchi *et al.*, 2006, 2010; Krol *et al.*, 2010; Postel *et al.*, 2010).

*AtPep1*-induced responses mirror PTI and include ROS burst, membrane depolarization, and ethylene production (Yamaguchi *et al.*, 2010). As such, *AtPep1* and its paralogs are hypothesized to act as amplifiers of PTI signaling (Huffaker and Ryan, 2007; Krol *et al.*, 2010; Yamaguchi *et al.*, 2010), though the contribution of *AtPep1* perception to disease resistance remains to be tested in the *pepr1 pepr2* mutant.

Hydroxyproline-rich glycopeptides, members of a systemin subfamily called HypSys peptides, are derived from post-translationally modified precursors in tobacco and tomato cell walls (Narváez-Vásquez *et al.*, 2005). In tobacco, HypSys peptides induce trypsin inhibitor activity in response to wounding (Pearce *et al.*, 1993), while tomato homologs induce protease inhibitor synthesis (Pearce and Ryan, 2003) and petunia HypSys peptides activate *defensin 1* expression (Pearce *et al.*, 2007). Endogenous wound-responsive peptides activate the jasmonic acid (JA) signaling pathway and JA is part of the mobile signal for proteinase inhibitor expression in tomato (Schilmiller and Howe, 2005).

### **1.3 ER-QC of immune-related proteins**

During the production of transmembrane glycoproteins, nascent secretory proteins travel through the ER where they encounter chaperones, which aid their folding and ultimately their delivery to the plasma membrane where they function. The correct folding of proteins during this maturation process is monitored by a mechanism called ER quality control (ER-QC) (Ellgaard and Helenius, 2003). If proteins are terminally misfolded or aberrant they are delivered to ER-associated degradation (ERAD) machinery (McCracken and Brodsky, 1996; Vembar and Brodsky, 2008) in the cytosol, or the vacuole (Pimpl *et al.*, 2006). This ER-QC pathway can follow different routes and is largely conserved from mammals to yeast (Brodsky and McCracken, 1999).

A major route for ER-QC depends on N-glycosylation of nascent proteins. This co-translational modification of newly synthesized polypeptides is catalyzed by the oligosaccharide transferase (OST) complex (Figure 2), comprised of subunits including DAD1/2 (defender against cell death); STT3a and 3b (staurosporine and temperature sensitive) and DGL1 (defective glycosylation1) (Koiwa *et al.*, 2003;

Lerouxel *et al.*, 2005). In this process, a glycosyl moiety GlcNaAc<sub>2</sub>Man<sub>9</sub>Glc<sub>3</sub> (GlcNAc: N-acetylglucosamine; Man: mannose; Glc: glucose) is conjugated to the Asn (N) of the consensus sequon Asn-X-Ser/Thr (X is any amino acid except Pro) (Helenius and Aebi, 2001). The outermost Glc residues are trimmed by the action of glucosidases I and II (GCSI/II), while the antagonistically acting UDP:glucose:glycoprotein glucosyltransferase (UGGT) specifically recognizes aberrantly folded proteins and adds one glucose. These mono-glucosylated glycan-conjugated proteins are then recognized by the ER lectin-like chaperones calreticulin (CRT) and calnexin (CNX) that act to assist in proper folding. If following glucose removal by glucosidase the protein is properly folded, it will exit the ER; however if it contains hydrophobic patches, it will be recognized by UGGT, which will add another glucose, again targeting the monoglucosylated non-native polypeptide to the CRT/CNX cycle. This continues until the correct conformation is obtained and the protein will be exported to the Golgi to finally arrive at its correct PM destination (Pattison and Amtmann, 2009). Finally, protein disulphide isomerase (PDI) and oxidoreductases are responsible for the formation of disulphide bonds between thiol groups of nascent polypeptides (Figure 2).

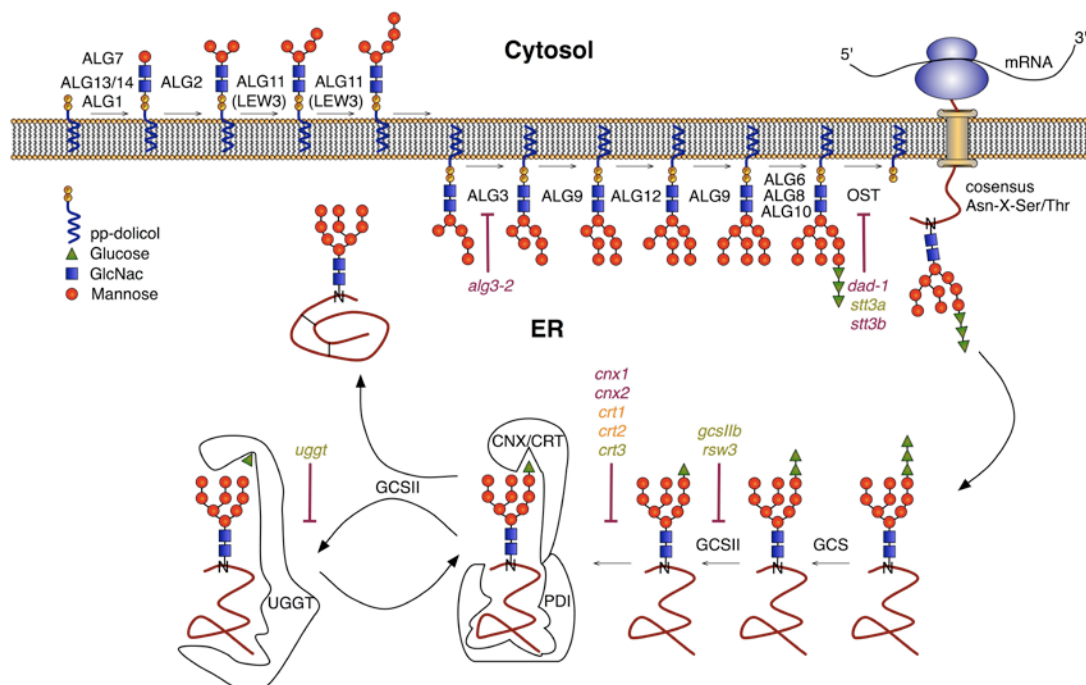


**Figure 2: Pathway for N-glycosylation for nascent polypeptides in plants. Figure made by Frederikke Gro Malinowsky.**

Another pathway specifically required for EFR occurs in parallel or in cooperation with the CRT3 pathway. Here, misfolded proteins are retained by the Hsp70 luminal binding protein (BiP). The Hsp40 Erdj3b recruits BiP and activates BiP ATPase activity, transferring the client to BiP and releasing Erdj3b (Jin *et al.*, 2008, 2009b). In Arabidopsis, the unique protein stromal derived factor 2 (SDF2) interacts with Erdj3b and is essential for the correct folding of EFR (Nekrasov *et al.*, 2009; Figure 3).

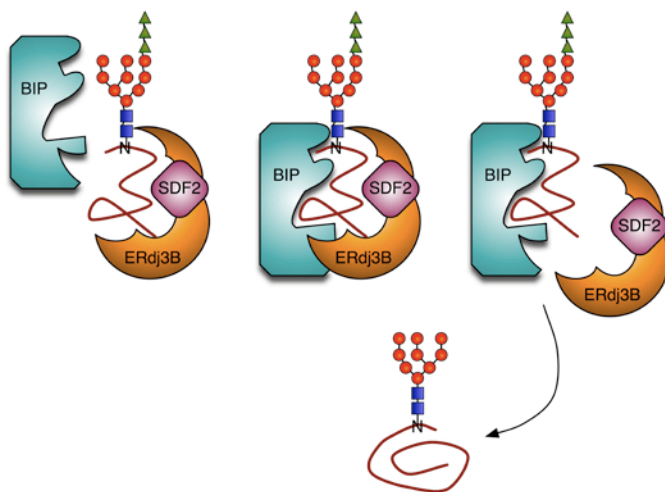


**Figure 3: EFR requires a SDF2-ERdj3B-BiP complex for maturation.**

The chaperones SDF2 and ERdj3B recruit incorrectly unfolded EFR to a complex including BiP. Following receptor maturation, EFR is released from the ER. BiP: luminal binding protein; SDF2: stromal-derived factor 2 (Figure made by Frederikke Gro Malinowsky).

In yeast and mammalian cells, CDC48 (p97) contributes to retrotranslocation of ERAD substrates prior to proteasomal degradation (Braun *et al.*, 2002; Jarosch *et al.*, 2002; Schrader *et al.*, 2009). The Arabidopsis homolog AtCDC48 complements yeast *cdc48* (Rancour *et al.*, 2002) and is required for the degradation of aberrant MLO protein (Müller *et al.*, 2005), suggesting that the plant homolog plays a similar role in ERAD, though this protein also functions in cytokinesis and cell expansion (Rancour *et al.*, 2004; Rancour *et al.*, 2002).

Recently, genetic screens in Arabidopsis have revealed that elements of the ER-QC pathway are specifically required for production of functional EFR. These include UGGT, CRT3, STT3a and GCSIIb (Saijo *et al.*, 2009; Li *et al.*, 2009a; Häweker *et al.*, 2010; Lu *et al.*, 2009; Christensen *et al.*, 2010). Importantly, these chaperones act specifically for EFR folding and none of these pathways are

essential to the function of the related FLS2 receptor (Nekrasov *et al.*, 2009; Saijo *et al.*, 2009). This suggests an additional requirement of this more recently evolved receptor for folding assistance.

The requirement of ER-QC for innate immunity seems to be conserved in the closest rice homolog of EFR, the PRR Xa21. The rice homolog of BiP, OsBiP3, was identified as an interactor of Xa21 (Park *et al.*, 2010a), while a rice *OsSDF2*-silenced line is more susceptible to *Xanthomonas* (Park *et al.*, 2010b). Similarly, the chitin receptor in rice OsCERK1 interacts with Hsp90 and its co-chaperone Hop/Sti1 in the ER (Chen *et al.*, 2010a) and these chaperones are required for receptor maturation and innate immunity. Furthermore, in *N. benthamiana*, CRT3 and BIP5/GRP78-5 (glucose-regulated protein 78) are among the ER-resident chaperones that are up-regulated during N-mediated defense and *CRT3*-silenced plants are compromised in N-mediated TMV (tobacco mosaic virus) resistance (Caplan *et al.*, 2009).

Interestingly, misfolded BRI1 mutant proteins (*bri1-9*; *bri1-5*) are retained in the ER in a UGGT- and CRT3-dependent manner (Jin *et al.*, 2007; Hong *et al.*, 2008; Jin *et al.*, 2009a). *bri1-9* and *bri1-5* mutants, which are structurally compromised but signaling competent, interact with calnexin and BiP (Jin *et al.*, 2007; Hong *et al.*, 2008). BiP-mediated ER retention has more impact than the CNX/CRT cycle in retaining *bri1-5* in the ER (Hong *et al.*, 2008), while *bri1-9* ER-retention is compromised by mutations in *UGGT* (Jin *et al.*, 2007) and *CRT3* (Jin *et al.*, 2009a).

#### **1.4 Signaling downstream from pathogen perception**

PAMPs bind to their cognate receptors and activate a signaling cascade to alert the plant that pathogens are attempting to infect, and prompt the initiation of defense responses. Immediately following PAMP perception, within seconds the receptor engages with a regulatory co-receptor. This probably results in trans-phosphorylation and activation of the receptor to enhance its activity and amplify signaling (Zipfel, 2009). This is followed by other temporally controlled responses, including ion fluxes across the plasma membrane, changes in cytosolic calcium concentration, oxidative burst, MAP kinase activation, changes in gene

expression, callose deposition and seedling growth inhibition (Nicaise *et al.*, 2009). Similar responses occur in response to R-mediated effector/Avr recognition, including oxidative burst, hormonal changes and transcriptional reprogramming. The striking HR following Avr recognition (Morel and Dangl, 1997) is what distinguishes ETI in most cases.

### 1.4.1 Receptor Kinase Complexes

#### 1.4.1.1 Mammalian RTKs as a model for complex formation

Receptor proteins from diverse systems are known to engage in interactions, to form homo- or heteromers in order to co-ordinate signaling responses, often through reciprocal phosphorylation events (Schlessinger, 2002). Mammalian growth factor receptors, one class of receptor tyrosine kinases (RTKs), are composed of a glycosylated ligand-binding extracellular domain, a single transmembrane region and a cytoplasmic domain with catalytic tyrosine kinase activity (Schlessinger, 1988). RTKs can be envisaged as membrane-associated allosteric enzymes, where ligand binding and enzyme activity are separated by their topology in the plasma membrane (Ullrich and Schlessinger, 1990). Thus receptor activation by ligand binding must somehow be translated across this divide into altered function of the intracellular domain.

Receptor oligomerization, which occurs universally among growth factor receptors, is such a mechanism for ligand-induced activation (Schlessinger, 1988; Williams, 1989). Ligand binding stabilizes interactions between receptor molecules, leading to trans-phosphorylation, and this combines to create positive feedback, with enhanced ligand binding and kinase activity (Ullrich and Schlessinger, 1990). For example, insulin receptor activation loop auto-phosphorylation increases its catalytic efficiency up to 200-fold (Cobb *et al.*, 1989). Inactive receptor kinases are auto-inhibited by intramolecular interactions specific to each type of receptor, and the release of this inhibition is achieved when kinase domain phosphorylation releases the active site into a conformation suitable for phosphotransfer. Interestingly, auto-phosphorylation occurs in *trans* and in particular sequence, each subsequent phosphorylation event further destabilizing the auto-inhibitory

interactions (Lemmon and Schlessinger, 2010). Auto-phosphorylation occurs in addition to exogenous substrate phosphorylation, the phosphorylated receptor then becoming the site for assembly of complexes of signaling proteins.

Many examples of the importance of receptor protein-protein interactions exist in nature and illustrate the importance of this mechanism of receptor activation.

#### 1.4.1.2 SERK receptor complexes

Plant receptor kinases (RKs) share a similar domain organization to growth factor receptors, although the intracellular domain is Ser/Thr kinase and is more closely related to *Drosophila* Pelle kinases and human IRAKs (Shiu and Bleecker, 2001). However, plant RKs, such as brassinosteroid insensitive 1 (BRI1) and BRI1-associated kinase 1 (BAK1), do auto-phosphorylate tyrosine residues despite their characterization as Ser/Thr kinases (Oh *et al.*, 2009; Oh *et al.*, 2010b). Nowhere near as much mechanistic detail is yet available for plant receptor kinases, which number over 600 in *Arabidopsis* (Shiu and Bleecker, 2001), however it is clear that receptor complex formation is also key to plant RK signaling.

BAK1/SERK3 (somatic embryogenesis related kinase 3) is a LRR-RLK with 5 extracellular LRRs and an active intracellular Ser/Thr kinase domain. This versatile protein was originally identified as an interactor of the LRR-RLK brassinosteroid (BR) receptor BRI1 (Li *et al.*, 2002; Nam and Li, 2002; Wang *et al.*, 2005b). *In planta*, BRI1 has been identified as homodimers (Wang *et al.*, 2005a), however ligand binding enhances BRI1-BAK1 heteromerization and provokes reciprocal receptor trans-phosphorylation, which ultimately increases the kinase activity of BRI1 and enhances downstream signaling (Wang *et al.*, 2008d). This receptor pair provides a good example of plant receptor complex formation following the model put forward for animal RTKs at least to some extent. BRI1 kinase activity is negatively regulated by its C-terminus, which is a site of phosphorylation (Wang *et al.*, 2005a). Extensive work has been done to characterize the nature of receptor phosphorylation in BRI1 and BAK1, and several parallels have been found between these receptors and epidermal growth factor (EGF) receptor. BRI1 homodimers can mediate basal level of brassinosteroid signaling without co-

receptors, but the amplitude of signaling is enhanced with their co-operation. BRI1 can bind ligand and carry out auto-phosphorylation of the activation loop. BAK1 binds to the receptor to receive phosphorylation of its activation loop residues. The activated BAK1 then trans-phosphorylates BRI1 on juxtamembrane and C-terminal residues to enhance its activity (Wang *et al.*, 2008d).

BAK1 belongs to a sub-class of the subfamily II of LRR-RLKs, referred to as the SERK family based on sequence homology with the carrot LRR-RLK SERK protein (Hecht *et al.*, 2001). The SERK family contains 5 closely related members in Arabidopsis, many of which are engaged in several receptor complexes. The Arabidopsis SERK proteins are involved in diverse signaling pathways (Figure 4) and are often functionally redundant (Albrecht *et al.*, 2008). In BR signaling, BAK1, SERK1 and BAK1-like (BKK1/SERK4) all interact with BRI1 to positively regulate BR responses (Karlova *et al.*, 2006; He *et al.*, 2007; Albrecht *et al.*, 2008; Jeong, 2010). SERK1 and SERK2 have redundant roles in male sporogenesis (Albrecht *et al.*, 2005; Colcombet *et al.*, 2005; Albrecht *et al.*, 2008), and SERK1 was recently showed to be involved in organ separation in flowers (Lewis *et al.*, 2010). Importantly, BKK1 and BAK1 are both required to control cell death and senescence (He *et al.*, 2007; Kemmerling *et al.*, 2007; Jeong *et al.*, 2010). It is therefore possible that SERKs can combine in different oligomeric complexes specific to distinct cellular pathways.

Unpredictably, BAK1 was recently found to form a ligand-inducible complex with FLS2 (Chinchilla *et al.*, 2007; Heese *et al.*, 2007). This association occurs within seconds of flg22 binding, and leads to rapid phosphorylation of FLS2 and BAK1 (Schulze *et al.*, 2010). BAK1 loss-of-function and knockout lines have reduced responsiveness to flg22, elf18, LPS, PGN, HrpZ, CSP22, the oomycete PAMP INF1, and the DAMP AtPep1 (Chinchilla *et al.*, 2007; Heese *et al.*, 2007; Shan *et al.*, 2008; Krol *et al.*, 2010), hinting that BAK1 forms ligand-dependent complexes with their corresponding PRRs. The receptors for endogenous peptide AtPep1, PEPR1 and PEPR2, also interact with BAK1 in a yeast-two hybrid (Postel *et al.*, 2010). Treatment of cell cultures with elf26 leads to rapid phosphorylation of BAK1 and of a co-immunoprecipitated protein that migrates at the same size as the glycosylated form of EFR (Schulze *et al.*, 2010). Importantly, the effect of BAK1 loss-of-function on elf18 responses is less striking than for flg22 responses

(Chinchilla *et al.*, 2007; Shan *et al.*, 2008). This indicates that EFR may preferentially interact with other RRs than BAK1, and that additional complex components are required for signaling downstream of FLS2 and EFR.

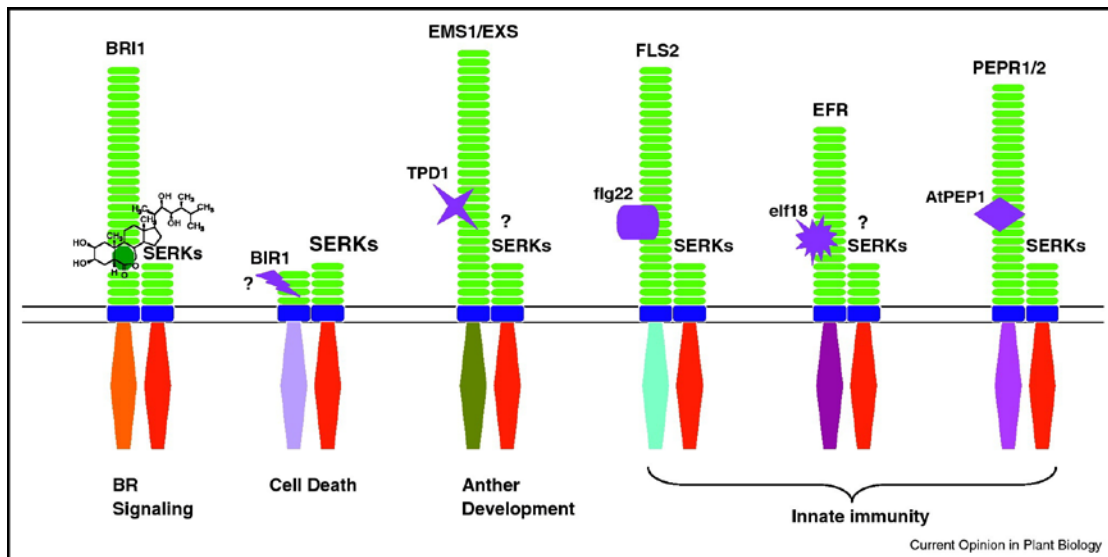


**Figure 4: SERK receptor complexes from Li, 2010.**

BAK1 interacts with BRI1 for brassinosteroid signaling; in an unknown pathway with the LRR-RK BIR1. SERK1 and SERK2 may control the same pathway as EMS1/EXS1 although an interaction has not been shown yet. BAK1 interacts with FLS2 in response to flg22 detection for innate immunity, as well as the PEP receptors PEPR1/2. An interaction has not been shown for BAK1 and EFR.

#### 1.4.1.3 FLS2-associated proteins

In addition to its interaction with BAK1, other proteins have been identified as FLS2-associated. Recently, stomatal cytokinesis defective 1 (SCD1) was recently identified as an *in vivo* interaction partner for FLS2 by mass spectrometry analysis (Korasick *et al.*, 2010). *scd1* mutants display SA-dependent enhanced resistance to infection with syringe-infiltrated *Pto* DC3000, correlated with hyper-accumulation of *PR1* transcripts and hydrogen peroxide. However, the same mutants are less sensitive to PAMP application, manifested as reduced seedling growth inhibition and ROS production in response to flg22 or elf18 (Korasick *et al.*, 2010). The authors did not investigate FLS2 endocytosis in this mutant, although SCD1 is co-expressed with coatomers, dynamins and adaptins (ATTED-II, <http://atted.jp>) suggesting a potential role in trafficking of FLS2.

#### 1.4.1.4 The rice defensome

Several proteins important for rice innate immunity have been identified, and are proposed to exist as a large complex called the defensome (Chen *et al.*, 2010b). Firstly, rice Rac GTPase OsRac1 was found to be a key regulator of PTI signaling (Wong *et al.*, 2004; Lieberherr *et al.*, 2005). Required for *Mla12* resistance (RAR1), required for the function of several R genes, is required for OsRac1-mediated rice disease resistance (Thao *et al.*, 2007). OsRac1 forms a complex with RAR1, Hsp90 and Hsp70 in rice (Thao *et al.*, 2007). Furthermore, OsRac1 interacts with Receptor for Activated C-Kinase 1 (RACK1A), which in turn is associated with the N-terminus of NADPH oxidase (OsRbohB), RAR1 and SGT1 (Nakashima *et al.*, 2008). An analysis of detergent resistant membrane (DRM)-associated proteins revealed several proteins important for rice innate immunity including OsRac1, Xa21, CEBiP, Hsp70, Rboh and Pt1 (Fujiwara *et al.*, 2009). OsRac1 was found to be enriched in DRMs following chitin elicitation, along with OsRACK1 (Fujiwara *et al.*, 2009). Recently it was shown that chitin receptors CEBiP and OsCERK1 exist in hetero-oligomeric complexes stabilized by ligand binding (Shimizu *et al.*, 2010). Finally, the defensome comprises OsCERK1 and OsRac1 linked by Hop/Sti to the chaperone complex including Hsp90, RAR1 and SGT1 (Chen *et al.*, 2010b).

#### 1.4.1.5 Receptor-like cytoplasmic kinase complexes

Botrytis-induced kinase 1 (BIK1) is a receptor-like cytoplasmic kinase (RLCK) that acts as a positive regulator of PAMP-induced signaling (Lu *et al.*, 2010), but was originally identified for resistance to fungal pathogens (Veronese *et al.*, 2006). *Bik1* mutants display reduced seedling growth inhibition and compromised PAMP-induced bacterial disease resistance (Lu *et al.*, 2010), as well as elevated salicylic acid levels (Veronese *et al.*, 2006). BIK1 is phosphorylated in response to flg22 and elf18 and responsible for phosphorylation of BAK1 and FLS2 (Lu *et al.*, 2010; Zhang *et al.*, 2010a). However, these results are contentious, as no FLS2 kinase activity can be detected *in vitro*, and it is thus impossible to classify BIK1 as a

substrate for FLS2 (Zhang *et al.*, 2010a). Arabidopsis protoplasts were used to demonstrate association between BIK1 and FLS2 as well as BAK1 in co-immunoprecipitation assays (Lu *et al.*, 2010), but subsequent examinations failed to identify BIK1-BAK1 interactions (Zhang *et al.*, 2010a), suggesting that these were artefacts of over-expression.

Further work has identified molecular connections between PTI and ETI based on BIK1 and related proteins. BIK1 belongs to a family of RLCKs, which includes PBS1 and PBS1-like protein (PBLs). *Bik1 pb1* mutants are more compromised than single mutants in PTI responses, suggesting that these kinases co-operate in PTI (Zhang *et al.*, 2010a). In un-stimulated plants, BIK1 interacts with FLS2, EFR and CERK1 and is rapidly phosphorylated upon flg22 application. Following flg22 elicitation, when BIK1 dissociates from FLS2, presumably to allow it to carry out some other function required for PTI (Zhang *et al.*, 2010a).

The *P. syringae* effector AvrPphB, a cysteine protease, cleaves PBS1 to activate ETI controlled by the cytoplasmic immune receptor RPS5 (Ade *et al.*, 2007). AvrPphB can also inhibit PTI by cleaving PBS1-like (PBL) kinases, including BIK1, PBL1, and PBL2 (Zhang *et al.*, 2010a). Interestingly, the *bik1* mutant phenotype, with dwarfing and elevated salicylic acid levels is reminiscent of the resistance protein-triggered HR. BIK1 and PBLs are likely to be guarded by RPS5, which detects AvrPph-induced cleavage.

#### **1.4.2 Receptor endocytosis**

Endocytosis is one of the most highly conserved cellular processes for regulation of plasma membrane receptor-mediated signaling eukaryotes, considering that many signaling receptors undergo rapid endocytosis after ligand-induced activation (von Zastrow and Sorkin, 2007). Individual receptors differ, and can selectively enter distinct clathrin-dependent and clathrin-independent pathways by various mechanisms. One aim of endocytosis is to reduce the number of receptors present on the cell surface and bring about attenuation of ligand-responsive cellular signaling. Alternatively, endocytosis provides additional membrane surface area for signaling (Figure 5a). As there are hundreds of receptor kinases encoded in the Arabidopsis genome, it is conceivable that the

plasma membrane could have limited space, while endocytic vesicles provide an additional platform for signaling. A further advantage could be that the diffusion of endosomal compartments containing signaling molecules allows important components of a signaling cascade to make contact rapidly, regardless of the size of the cell (Figure 5b) (Geldner and Robatzek, 2008).

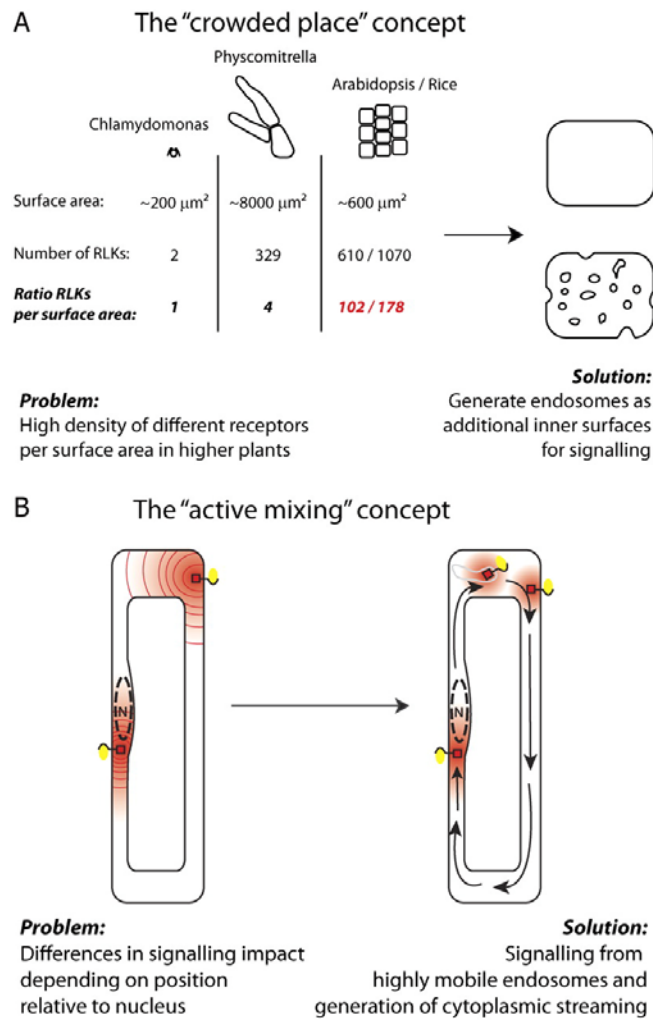


**Figure 5: Promotion of signaling through endocytosis from Geldner and Robatzek, 2008.**  
A. Endocytic compartments increase available surface area for the many encoded RRs. B. Mobile signaling provided by endosomes facilitates rapid signaling in a plant cell with large vacuole.

BRI1-GFP has been detected at the plasma membrane and within intracellular mobile vesicles of root meristem cells (Russinova *et al.*, 2004; Geldner *et al.*, 2007). BRI1-GFP co-localizes with the endocytic marker FM4-64 and this was sensitive to the inhibitor of endosomal trafficking, Brefeldin A (Geldner *et al.*, 2007). Interestingly, BRI1 endosomal localization enhances its signaling output, providing a good example of the efficacy of signaling from endosomes (Geldner *et al.*, 2007). The RLK Arabidopsis Crinkly4 (ACR4) controls ovule cell organization

(Gifford *et al.*, 2003), as well as differentiation in the epidermis (Watanabe *et al.*, 2004) and root tip meristem (De Smet *et al.*, 2008; Stahl *et al.*, 2009). ACR4 undergoes endocytosis, and this is linked to its rapid turnover, which requires the extracellular crinkly repeat domain (Gifford *et al.*, 2005). The LRR-RLP LeEIX2, the tomato receptor for the fungal PAMP EIX, features a conserved endocytosis motif Yxxø on the cytoplasmic tail, which is required for its function (Ron and Avni, 2004). EIX-triggered LeEIX2 internalization has recently been shown, with LeEIX2 co-localizing with FYVE endosomes (Bar and Avni, 2009). To further regulate EIX endocytosis, EH-domain containing 2 (EHD2), which interacts with LeEIX2 cytoplasmic domain, inhibits LeEIX2 endocytosis, and in so doing, inhibits EIX-induced HR (Bar and Avni, 2009). Recent work revealed EIX-induced heteromerization of LeEIX1 and LeEIX2, where LeEIX1 acts as a negative regulator of LeEIX2 internalization and signaling in a BAK1-dependent manner (Bar *et al.*, 2010).

When expressed in the natural *fls2* mutant accession Ws-0, FLS2-GFP restores flg22 responsiveness, and can be seen accumulating at the cell periphery in mesophyll and epidermal cells, including guard cells (Robatzek *et al.*, 2006). FLS2-GFP can be seen in roots, leaves, stems and flower petals (Robatzek *et al.*, 2006). Upon flg22 application, the protein begins to accumulate in vesicles, and ultimately disappeared, likely through proteasomal degradation (Robatzek *et al.*, 2006). The signal returned to the PM in a cycloheximide-sensitive manner, suggesting that *de novo* receptor synthesis was responsible for the signal recovery (Robatzek *et al.*, 2006). This appears to be a form of ligand-induced receptor endocytosis. Vesicle formation was inhibited in the presence of chemical inhibitors of tubulin and actin polymerization, suggesting that cytoplasmic streaming is involved in this process. Furthermore, application of the inhibitor of formation of pre-vacuolar compartments, Wortmannin, inhibited FLS2-GFP endocytosis, as did the kinase inhibitor K252a (Robatzek *et al.*, 2006). Endocytosis is reduced in the absence of the FLS2 regulatory receptor BAK1 (Chinchilla *et al.*, 2007).

These observations are in line with what has been observed with the mammalian RTK EGF receptor (EGFR). EGFR is subject to ligand-induced endocytosis followed by degradation. EGFR also continues to signal from endosomes, as certain components of the signaling cascade, such as the MAPK scaffold protein, are localized to endosomal compartments (Teis *et al.*, 2002).

Subsequent studies of FLS2 also observed FLS2-YFP fluorescence in the cell periphery, but in protoplasts endocytosis could not be induced by flg22 application (Ali *et al.*, 2007a). The study further scrutinized FLS2 mobility in plasma membranes by FRAP (fluorescence recovery after photobleaching) analysis. It is hypothesized that mobile receptors are free to diffuse within the membrane environment, while those sequestered in complexes within membrane microdomains may be more limited in mobility. In this way, a laser is used to bleach the fluorescence of the recombinant protein within a narrow region of the membrane, and the recovery of fluorescence in this region is a measure of the diffusion co-efficient of the protein. FRAP analysis showed that FLS2-YFP is mobile in the PM, and this was quantitatively reduced following flg22 treatment. The same study did not detect FLS2 homodimerization occurring, when assessed by BiFC or FRET analysis (Ali *et al.*, 2007a).

#### **1.4.2.1 Signaling from lipid microdomains**

Lipid rafts are comprised of membranes organized through interactions between sterols and sphingolipids, and are thought to spatially control signaling through dynamic association of partners. Proteomic studies of lipid raft-associated proteins are achieved through the isolation of DRMs, as the tight association of lipids in microdomains reduces their detergent solubility (Borner *et al.*, 2005; Kierszniowska *et al.*, 2009). The lipid raft hypothesis remains controversial, though DRMs have been studied by several groups (Mongrand *et al.*, 2004; Borner *et al.*, 2005; Morel *et al.*, 2006; Fujiwara *et al.*, 2009; Kierszniowska *et al.*, 2009). Proteomic studies of DRMs provide knowledge of protein associations, which could be due to direct interactions, and thus can provide insight into function.

PTI signaling could be facilitated by close association of proteins involved in the cascade, for example by association with DRMs. A recent study used quantitative proteomics to investigate flg22-induced changes in *Arabidopsis* DRM-associated proteins (Keinath *et al.*, 2010). 64 proteins were enriched in DRMs upon PAMP elicitation, including FLS2, though unexpectedly not BAK1 (Keinath *et al.*, 2010). DRM-associated differentially identified proteins include LRR-RLKs FERONIA (FER), HERCULES (HERK1), remorins, H<sup>+</sup>-ATPases (AHA1, AHA2, AHA3,

AHA4),  $\text{Ca}^{2+}$ -ATPases (ACA8 and ACA10) and vacuolar ATPase subunit C DET3 (de-etiolated 3) (Keinath *et al.*, 2010). AHA1, AHA2 and FER were previously found to be phosphorylated in response to flg22 treatment (Benschop *et al.*, 2007; Nühse *et al.*, 2007). An independent study of DRMs to identify core sterol-associated proteins (Kierszniowska *et al.*, 2009) also identified FLS2 in DRMs, but not strictly sterol-associated, likely due to its role in dynamic signaling.

Mutants of FERONIA, DET3 and AHA1 were compromised for flg22-induced stomatal closure and concordantly had enhanced susceptibility to *Pto* DC3000  $\Delta$ AvrPto $\Delta$ AvrPtoB (Keinath *et al.*, 2010). Interestingly, FER is involved in signaling for pollen tube reception (Escobar-Restrepo *et al.*, 2007), as well as cell elongation, where it functions with related RLKs HERCULES1 (HERK1) and THESEUS1 (THE1) (Guo *et al.*, 2009). Given the promiscuous nature of this protein in several signaling pathways, FER could be a signaling adaptor, however a specific FLS2-FER interaction has yet to be proven.

A similar quantitative study was carried out to identify proteins differentially DRM-associated in response to the elicitor cryptogein in tobacco BY-2 cells (Stanislas *et al.*, 2009). In this study a 14-3-3 protein required for ROS burst was identified, as well as several dynamin-related proteins that play a role in trafficking (Stanislas *et al.*, 2009).

Proteomic analysis of DRM-associated proteins revealed several proteins important for rice innate immunity including OsRac1, Xa21, CEBiP, Hsp70, Rboh and Pt1 (Fujiwara *et al.*, 2009) (see §1.4.1.4).

### 1.4.3 Ion fluxes

One of the earliest measurable responses to PAMP perception is ion ( $\text{H}^+$ ;  $\text{Ca}^{2+}$ ) fluxes across the plasma membrane, resulting in extracellular alkalinization (Felix *et al.*, 1999; Bauer *et al.*, 2001; Kunze *et al.*, 2004; Garcia-Brugger *et al.*, 2006; Jeworutzki *et al.*, 2010). Electrophysiological analysis has shown that flg22 and elf18 rapidly induce the same transient ion fluxes and membrane depolarization in *Arabidopsis* mesophyll cells and root hairs (Jeworutzki *et al.*, 2010). This response depends on increases of cytosolic calcium and overlaps with

the production of reactive oxygen species, but precedes transcriptional activation of *PR* genes (Jeworutzki *et al.*, 2010).

Although the receptors have not been identified, this influx of calcium from the apoplast could be responsible for the activation of AtRbohD and calcium-dependent protein kinases. However, *rbohD/F* mutants exhibit wild-type changes in membrane potential, suggesting that activation of NADPH oxidases occurs in parallel with or downstream of ion fluxes (Jeworutzki *et al.*, 2010).

#### 1.4.3.1 Calcium signaling

Calcium has many important functions as a second messenger in plant signaling, with roles described in growth and development, as well as response to stress (Dodd *et al.*, 2010; Kudla *et al.*, 2010). Calcium homeostasis is maintained by the opposing actions of calcium influx and efflux systems (Sanders *et al.*, 2002). Elicitation with PAMPs including flg22 rapidly induces calcium signatures in the cytoplasm and nucleus (Lecourieux *et al.*, 2005; Gust *et al.*, 2007). Furthermore, calcium influx is essential for responses to PGN (Erbs *et al.*, 2008) and cryptogein (Lecourieux *et al.*, 2005) as well as the HR (Grant *et al.*, 2000; Urquhart *et al.*, 2007).

Calcium channels such as cyclic nucleotide-gated channels (CNGC) and glutamate receptor GLR channels conduct  $\text{Ca}^{2+}$  into plant cells and are potential candidates for the pathogen/PAMP/elicitor (or ETI)-activated  $\text{Ca}^{2+}$  influx pathway (Ma and Berkowitz, 2007). Ali *et al.* (2007) showed that the *Arabidopsis* 'defense no death 1' mutation (*dnd1*), located in AtCNGC2 (Clough *et al.*, 2000), is associated with a loss in a plasma membrane inward  $\text{Ca}^{2+}$  current (Ali *et al.*, 2007b). The authors link the CNGC2-dependent  $\text{Ca}^{2+}$  current to NO production in guard cell protoplasts responding to LPS, perhaps via  $\text{Ca}^{2+}/\text{CaM}$  complexes (Ali *et al.*, 2007b; Ma *et al.*, 2008). Later the same group further extended this model to show that cytosolic  $\text{Ca}^{2+}$  influx and NO production occurring in response to PAMPs or pathogen inoculation also depends on cyclic AMP (cAMP) (Ma *et al.*, 2009). However, *dnd1* exhibited a normal depolarization response towards flg22, suggesting that CNGC2 is not directly responsible for FLS2-mediated signaling (Jeworutzki *et al.*, 2010).

Elevation of cytoplasmic calcium is mediated by an increase in  $\text{Ca}^{2+}$  influx rather than a decrease in  $\text{Ca}^{2+}$  efflux from the cytosol (Takabatake *et al.*, 2007). However, until recently there was no direct link between calcium ATPases and calcium-mediated defense responses. Recent work has shown that silencing of *N. benthamiana* type BII  $\text{Ca}^{2+}$ -ATPase *NbCA1* results in accelerated Cf9- and N-mediated cell death, as well as cell death in response to the nonhost bacterium *Pto* DC3000 and PAMP cryptogein (Zhu *et al.*, 2010a). Furthermore, changes in amplitude and duration of calcium spikes in *NbCA1*-silenced plants translates into altered calcium signatures in the nucleus and cytoplasm. Finally, the authors place the action of *NbCA1* upstream of *NbRbohB* and *NbCaM* in the signaling cascade leading to HR (Zhu *et al.*, 2010a). Furthermore, work in *Arabidopsis* has shown that the vacuolar auto-inhibited  $\text{Ca}^{2+}$ -ATPases (ACA) ACA4 and ACA11 act as suppressors of SA-dependent PCD, providing a link between HR and calcium efflux (Boursiac *et al.*, 2010).

Changes in  $[\text{Ca}^{2+}]_{\text{cyt}}$  (calcium signatures) are translated /decoded into cellular events by calcium binding proteins such as calmodulin, calcium-dependent protein kinases and calcineurin B-like proteins, the targets of which are as yet largely unknown (Luan *et al.*, 2009; Ma *et al.*, 2008). Recently, a CaM-binding protein CBP60g has been identified with a role in linking  $\text{Ca}^{2+}$  to SA signaling (Wang *et al.*, 2009). CaM binds CBP60g only in the presence of  $\text{Ca}^{2+}$ , and CaM binding is required for CBP60g to promote SA signaling. Interestingly, respiratory burst oxidase homolog (Rboh) proteins contain EF hands and a tobacco Rboh can be directly activated by calcium (Keller *et al.*, 1998; Sagi and Fluhr, 2001).

Calcium-dependent protein kinases (CDPKs) are calcium sensors that play an indispensable role in transcriptional reprogramming in plant innate immune signaling (Boudsocq *et al.*, 2010). Using a functional genomic screen and genome-wide gene expression profiling, it was found that four CDPKs, CDPK4, CDPK5, CDPK6 and CDPK11 and MAPK cascades act differentially in the control of genes involved in the synthesis of defense peptides and metabolites, cell wall modifications and redox signaling (Boudsocq *et al.*, 2010). CDPKs appear to be the convergence point of signaling triggered by most PAMPs as multiple *cpk* mutants have reduced ROS burst and gene induction in response to flg22, as well

as increased susceptibility (Boudsocq *et al.*, 2010). In tobacco cell cultures expressing the RLP Cf9 (resistance to *C. fulvum* 9), NtCDPK was activated by Avr9 elicitation (Romeis *et al.*, 1999; Romeis *et al.*, 2000). Furthermore, *NtCDPK2* silencing results in compromised Avr9-induced HR in *N. benthamiana*, suggesting a role for CDPKs in immunity (Romeis *et al.*, 2001).

Notably, the importance of calcium in PTI is illustrated by the fact that bacterial extracellular polysaccharides target calcium as a means of inhibiting innate immune responses (Aslam *et al.*, 2008).

#### 1.4.4 ROS burst

Another early PAMP-induced response is the production of reactive oxygen species (ROS) - highly toxic intermediates of reduced oxygen, such as superoxide ( $O_2^-$ ) and hydrogen peroxide ( $H_2O_2$ ). ROS produced during pathogen challenge is largely derived from the activity of membrane-localized NADPH oxidases (respiratory burst oxidase homologs, Rboh) (Torres *et al.*, 2002), with AtRbohD being the most important for PAMP-triggered oxidative burst (Meszaros *et al.*, 2006; Nühse *et al.*, 2007; Zhang *et al.*, 2007). Cell wall type III peroxidases (Prx) are also responsible for ROS production, through a mechanism resembling that of Rbohs, the dismutation of superoxide into peroxide (Almagro *et al.*, 2009). Furthermore, expression of French bean peroxidase (FBP)-specific antisense constructs rendered *Arabidopsis* plants more susceptible to fungal and bacterial pathogens (Bindschedler *et al.*, 2006).

R-mediated ROS production is biphasic: an initial low amplitude phase, likely triggered by PAMPs, is followed by a more intense, persistent phase, also reliant on the activity of RbohD (Torres *et al.*, 2006).

The relative position of oxidative burst in the sequence of signaling events during PTI and ETI remains to be clarified. In *Arabidopsis* at least, RbohD-dependent ROS production seems to be downstream or independent of MAP kinase activation (Zhang *et al.*, 2007). In potato (*Solanum tuberosum*), calcium-dependent protein kinases StCDPK4 and StCDPK5 were recently shown to mediate oxidative burst by directly phosphorylating NADPH oxidase RbohB (respiratory burst

oxidase homologue) (Kobayashi *et al.*, 2007), while in *Arabidopsis* AtRbohD is phosphorylated in response to flg22 (Benschop *et al.*, 2007; Nühse *et al.*, 2007).

It is important to note that ROS production associated with the HR in response to Avr recognition by corresponding R proteins is not required for resistance. This is exemplified by *AtrohodD/F* double mutants, which do not produce ROS but show more cell death than Col-0 in weakly resistant interactions (Torres *et al.*, 2002).

ROS, in concert with SA, has been implicated in the establishment of SAR (Durrant and Dong, 2004). AtRbohD-produced ROS were recently shown to mediate a rapid, systemic, cell-to-cell signal in response to diverse stimuli, including pathogens and wounding. This implies a role for ROS in mediating general long distance communications (Miller *et al.*, 2009).

#### 1.4.5 MAPK signaling

Changes in phosphorylation, including activation of MAP kinases and AtRbohD occurs within 5-10 minutes of PAMP application (Boller and Felix, 2009). MAPK signaling relies on sequential phosphorylation events between three elements, MAPKK-kinases (MEKK), MAPK kinases (MKK) and MAPKs (MPK). In *Arabidopsis*, a complete MAP kinase cascade comprising MEKK1-MKK4/5-MPK3/6 was initially proposed to be involved in PTI downstream of FLS2 (Asai *et al.*, 2002). More recent work showed that MEKK1 does not regulate flg22-activated MPK3/6, but rather activates MPK4, a negative regulator of defense (Ichimura *et al.*, 2006; Nakagami *et al.*, 2006; Suarez-Rodriguez *et al.*, 2007; Gao *et al.*, 2008). At the MAPKK level, flg22-induced activation of MPK3/4/6 is dependent on MKK1, while MPK3 and MPK6 are also activated by MKK4 (Meszaros *et al.*, 2006). Furthermore, MKK1 and MKK2 seem to act redundantly to control MPK4 (Gao *et al.*, 2008; Qiu *et al.*, 2008). Thus FLS2 activates two simultaneous MAPK cascades, one consists of an unknown MEKK-MKK4/5-MPK3/6 and acts positively on PTI, while the other, consisting of MEKK1-MKK1/2-MPK4, acts negatively on PTI. MPK3 and MPK6 are also activated by *P. syringae* infection, but this is much more sustained than PTI-induced MAPK activation (Underwood *et al.*, 2007).

Although PAMPs trigger the simultaneous activation of positive (MPK3/6) and negative (MPK4) regulators of defense gene expression, these antagonistic pathways are regulated by the same protein phosphatase 2C (PP2C), AP2C1 (Schweighofer *et al.*, 2007). It may seem counterintuitive, but in practice this may provide a sensitive mechanism for the control of defense responses by maintaining a careful balance of positive and negative regulators during signaling. MAPK phosphatase 2 (MKP2) interacts with MPK3 and MPK6 to regulate ROS and pathogen-induced signaling responses (Lumbreras *et al.*, 2010). *Mkp2* mutants are more resistant to necrotrophic bacterial pathogen *R. solanacearum*, suggesting that this pathway is negatively regulated by MKP2 activity (Lumbreras *et al.*, 2010).

HopW1-1-interacting 2 (WIN2) is a PP2C required for resistance to *Pto*, which interacts with HopW1 (Lee *et al.*, 2008), though the target is as yet unidentified. Another phosphatase, PP2C induced by AvrRpm1 (PIA1), was identified in a proteomic screen as differentially expressed during RPM1-AvrRpm1 interactions (Widjaja *et al.*, 2009), and was subsequently shown to be required for signaling in response to AvrRpm1 but not AvrB (Widjaja *et al.*, 2010). The target of PIA1 also remains elusive, but RIN4 phosphorylation does not appear to be affected in the *pia1* mutant (Widjaja *et al.*, 2010). The expression level of RPM1-induced kinase (RIPK) (de Torres *et al.*, 2003) was also unaffected in the *pia1* mutant, although the post-translational modification of this protein by PIA1 was not further investigated (Widjaja *et al.*, 2010).

#### 1.4.6 Changes in gene expression

Major transcriptional changes occur in response to elicitation by flg22 (Navarro *et al.*, 2004; Zipfel *et al.*, 2004), with many of the genes similarly regulated by elf18 (Zipfel *et al.*, 2006). There is partial overlap of differential gene expression in response to chitin and PGN (Gust *et al.*, 2007). Interestingly, many RLKs are upregulated in response to PAMP treatment, including EFR, FLS2, BAK1 and BKK1 (Zipfel *et al.*, 2006; Postel *et al.*, 2010).

Approximately 80% of flg22-induced genes are also upregulated by cycloheximide application (Navarro *et al.*, 2004). This suggests that genes involved in PTI may be

negatively regulated by repressors, which themselves are subject to rapid proteolysis (Navarro *et al.*, 2004). Thus, the release of negative regulation is necessary for PTI signaling.

Interestingly, downstream responses following elf18 and flg22 perception overlap, with high correlation in the transcriptome changes occurring 30 - 60 minutes after treatment (Zipfel *et al.*, 2006). A large number of genes (441) are also similarly up-regulated by flg22, elf26 and chitoctaose (Wan *et al.*, 2008). There was also an overlap between the genes induced by flg22 and PGN (Gust *et al.*, 2007). This evidence indicates that PTI signaling in response to diverse PAMPs share the same downstream machinery. The same machinery appears to be used by ETI, as gene expression changes in response to flg22 and effector proteins were also similar (Navarro *et al.*, 2004). Thus it appears that the purportedly later-evolving ETI simply appropriated the extant signaling cascades and adjusted their intensity.

Important gene expression changes are controlled downstream of MAP kinase activation by WRKY-type transcription factors, key regulators of plant defenses (Eulgem and Somssich, 2007; Pandey and Somssich, 2009). WRKY22 and WRKY29 act as positive regulators downstream of the MPK3/6 cascade (Asai *et al.*, 2002) while MPK4 directly regulates gene expression by interaction with WRKY25 and WRKY33 and the MPK4-interacting protein MKS1 (Andreasson *et al.*, 2005; Zheng *et al.*, 2006; Zheng *et al.*, 2007; Qiu *et al.*, 2008). Interestingly, MPK4 exists constitutively in nuclear complex with MKS1 and WRKY33. Pathogen challenge leads to MPK4 activation and MKS1 phosphorylation, which ultimately results in the release of MKS1 and WRKY33 and the activation of gene expression (Qiu *et al.*, 2008). Thus, WRKY factors both positively and negatively regulate PAMP-triggered transcriptional changes. Recently, it was found that WRKY11 and 17 and WRKY18/40/60 function as negative regulators of basal resistance in bacterial and fungal interactions (Xu *et al.*, 2006b; Journot-Catalino *et al.*, 2006; Shen *et al.*, 2007; Pandey *et al.*, 2010).

The antagonistic functions of MAPKs and WRKYS in the regulation of PTI allude to the importance of negative feedback inhibition in controlling the severity of the defense response. Negative feedback inhibition (mediated by WRKY18/40/60 for example) of the basal defenses may occur to prevent accumulation of harmful secondary metabolites or uncontrolled cell death. In one example it was shown

that components of ETI (resistance proteins) then relieve this negative regulation of PTI to allow the more potent responses of ETI to occur (Shen *et al.*, 2007).

#### **1.4.7 Epigenetic regulation of defense responses**

Epigenetic effects are those mechanisms that alter chromatin structure to bring about activation or repression of gene expression. Covalent modification of the histone-tail amino acids creates a code for gene activity, and is varied ranging from phosphorylation, ubiquitination to methylation and acetylation. These epigenetic tags on nucleosomes are sites of recognition for activating or repressing complexes that determine whether genes are on or off (Noma *et al.*, 2001; Sims *et al.*, 2006).

The Su(Var)3-9-E(2)-trithorax (SET) domain, conferring methyltransferase activity, is found in components of Polycomb/trithorax group complexes, which regulate development and homeotic genes. Members of the trithorax family methylate lysine 4 of histone H3 (H3K4), creating a mark associated with the 'on' state of genes. The *Arabidopsis* homolog of trithorax 1 (ATX1) is an interesting SET-domain-containing protein, which has been shown to cause H3K4 methylation, but causes antagonistic effects on gene expression (Saleh *et al.*, 2008). The action of ATX1 is not genome-wide H3K4 methylation, but 1600 genes are transcriptionally affected in *Arabidopsis atx1* mutants (Alvarez-Venegas *et al.*, 2006). The likely explanation for such a phenomenon is that a transcription factor is the primary target of ATX1, and its histone modification results in altered activity and downstream changes in secondary target genes. WRKY70 is a transcription factor with an important role in balancing outputs from the antagonistic hormone signaling pathways, by upregulating SA-related genes and downregulating JA-signaling (Li *et al.*, 2004; Li *et al.*, 2006). WRKY70 is induced by pathogen inoculation (Li *et al.*, 2004; Li *et al.*, 2006) and 24 hours after *Pto* DC3000 infiltration, WRKY70 gene expression peaks (Alvarez-Venegas *et al.*, 2007). At peak expression, increased WRKY70 H3K4 di- and trimethylation can be detected, in parallel with decreased H3K27 methylation. In *atx1*, WRKY70 trimethylation is lost, making ATX1 responsible for activation of WRKY70 (Alvarez-Venegas *et al.*, 2007). ATX1 likely has additional transcription factors as primary targets, and as

such is a master regulator of thousands of genes (Alvarez-Venegas *et al.*, 2006; Alvarez-Venegas *et al.*, 2007).

WRKY38 and WRKY62, acting together as negative regulators of defense, are induced early in pathogen responses, likely to prevent over-reaction of plant defenses (Kim *et al.*, 2008b). WRKY38 and 62 also interact with histone deacetylase 19 (HDA19), which is a positive regulator of defense and inhibits the activity of these WRKYs (Kim *et al.*, 2008b).

Recently, the RING E3 ligase histone monoubiquitination 1 (HUB1) was reported to have a role in resistance to necrotrophic fungal pathogens. *hub1* mutants, which have thinner cell walls but enhanced callose around infection sites, are more susceptible to *B. cinerea* and *A. brassicola*, but not to *P. syringae* DC3000 or *Pto* DC3000 *AvrRpm1* (Dhawan *et al.*, 2009). Furthermore, HUB1 interacts with MED21, a subunit of the Arabidopsis Mediator, a conserved complex regulator of RNA polymerase II. MED21 knockdown lines show enhanced susceptibility to the same pathogens. However, HUB1-mediated histone H2B modification is independent of histone H3 and DNA methylation. Thus, histone H2B monoubiquitination is another important chromatin modification with regulatory roles in plant defense against necrotrophic fungi most likely through modulation of gene expression (Dhawan *et al.*, 2009). Another example of this regulation pertaining to defense signaling is provided by the histone methyltransferase SET domain group 8 (SDG8). SDG8 is responsible for the regulation of genes involved in JA and ET signaling, and thus resistance to necrotrophic fungal pathogens (Berr *et al.*). Importantly, *sdg8-1* mutants are impaired in JA-induced alterations of H3K36 methylation of defense marker genes (e.g. *PDF1.2*; *MYC2*) and MKK3 and MKK5. This suggests a role for SDG8 in allowing histone methylation to operate as a record of permissive transcription for a subset of defense genes, expediting transcriptional induction (Berr *et al.*, 2010). Histone modification has recently been directly implicated in the regulation of resistance genes. SDG8 is also required for the expression of the RPS4-like *R* gene *LAZ5*, which requires H3K36 trimethylation for transcriptional activation (Palma *et al.*, 2010).

Furthermore, the ATP-dependent-chromatin remodeling factor gene *SPLAYED* (*SYD*) is required for basal and inducible *PDF1.2a* and *VSP2* expression in plant defense against necrotrophic fungal pathogens (Walley *et al.*, 2008).

Intriguingly, the *Shigella* effector OspF dephosphorylates nuclear MAP kinases to prevent them from phosphorylating H3 (Arbibe *et al.*, 2007). This prevents the activation of NF- $\kappa$ B-responsive defense genes, and is a clever trick by the pathogen for manipulating epigenetic regulation to its own benefit. Importantly, the *Pseudomonas* effector HopAI1 belongs to the same family of phosphatases, with a similar role in MAPK deactivation (Li *et al.*, 2007); (Zhang *et al.*, 2007). However, modification of histones by nuclear MAP kinases has not been shown in plants. If this is possible, MPK4 would be a good candidate as it is already known for nuclear localization with WRKY33.

Thus mechanisms of histone modification and chromatin remodeling contribute to the intricate control of defense responses. This epigenetic control system is a clever mechanism for rapid, wide-ranging and flexible alterations in gene expression, such as those required during plant-pathogen interactions and is likely to continue to be an interesting area of exploration in the future.

#### 1.4.7.1 RNA silencing

Flg22 treatment leads to the rapid down-regulation of several primary auxin-response genes (Navarro *et al.*, 2004; Zipfel *et al.*, 2004; Navarro *et al.*, 2006). This initial observation was later linked to the flg22-induced accumulation of the conserved microRNA *miRNA393* that targets the auxin receptor transport inhibitor response 1 (TIR1) and its close paralogs (Navarro *et al.*, 2006). Constitutive over-expression of *miRNA393* drastically restricts *Pto* DC3000 growth. Therefore, anti-bacterial immunity involves a rapid down-regulation of auxin responses mediated by RNA silencing. Consistently, *Pto* DC3000 effectors target the silencing machinery to achieve full virulence, with AvrPto interfering with the processing of *miRNA393*, while AvrPtoB leads to degradation of *miRNA393* precursors (Navarro *et al.*, 2008). In addition to *miRNA393*, 2 other miRNAs namely *miRNA167* and *miRNA160*, which target auxin response factors/receptors to negatively regulate auxin signaling, are also induced after infection with *Pto* DC3000 TTSS<sup>+</sup> (Fahlgren *et al.*, 2007).

*Pto* DC3000 carrying AvrRpt2 specifically induces the production of a natural antisense transcript (nat) small interfering RNA (siRNA) nat-siRNAATGB2 in a

pathway that depends on the resistance protein RPS2 and its signaling component nonrace-specific disease resistance 1 (NDR1) in Arabidopsis (Katiyar-Agarwal *et al.*, 2006). Later, another class of endogenous siRNA - long siRNAs (lsiRNAs) - was shown to be induced by pathogen infection (Katiyar-Agarwal *et al.*, 2007). In this case, AtlsiRNA-1 was also induced in response to AvrRpt2, and this requires Argonaute 7 (AGO7) (Katiyar-Agarwal *et al.*, 2007). miRNA-deficient Arabidopsis mutants support growth of *Pto DC3000 TTSS*<sup>-</sup> and non-adapted bacterium *P. syringae* pv. *phaseolicola* (Navarro *et al.*, 2008), and Arabidopsis plants lacking AGO4, which is involved in RNA-directed DNA methylation (RdDM), are more susceptible to *Pto DC3000* and to the non-adapted strain *P. syringae* pv. *tabaci* (Agorio and Vera, 2007). Most recently, AGO1 was shown to be a positive regulator of PTI responses, including defense gene expression and callose deposition, as well as resistance to *Pto DC3000* (Li *et al.*, 2010b). Furthermore, miR160a, miR398b and miR773 were AGO1-bound miRNAs differentially regulated by flg22 elicitation (Li *et al.*, 2010b). Over-expression of miR160a enhanced flg22-induced callose deposition while miR398b and miR773 caused the opposite effect, as well as enhanced disease susceptibility to *Pto DC3000* and *Pto DC3000 hrcC*<sup>-</sup> (Li *et al.*, 2010b). Overall, gene silencing appears as an inherent component of anti-bacterial immunity.

#### 1.4.8 Callose deposition

One of the later responses is the accumulation of callose between the cell wall and the plasma membrane (Bestwick *et al.*, 1997; Gómez-Gómez *et al.*, 1999). The Arabidopsis callose synthase glucan synthase-like 5 (GSL5) / powdery mildew resistant 4 (PMR4) is responsible for the synthesis of this  $\beta$ -1,3-glucan polymer in response to PAMPs and fungal pathogens (Jacobs *et al.*, 2003; Nishimura *et al.*, 2003; Kim *et al.*, 2005c). *Pmr4* mutant plants are more susceptible to the type-III secretion system (TTSS<sup>-</sup>) mutant strain *Pto DC3000 hrcC*<sup>-</sup> (Kim *et al.*, 2005c), while the double-mutant *pmr4 pad4* allows some growth of the non-adapted bacterium *Pseudomonas syringae* pv. *phaseolicola* in comparison to the respective single mutants (Ham *et al.*, 2007). This suggests a role for PMR4-dependent callose deposition in anti-bacterial immunity.

Although the order of events is not yet obvious, callose deposition may be downstream of ROS production, as *AtrbohD* mutants produce fewer callose deposits following flg22 elicitation (Zhang et al., 2007). However this remains controversial, as *AtrbohD* mutants have conversely also been reported to have wild-type-like callose deposition (Keinath et al., 2010). Recently, it was shown that callose deposition depends on PAMP-induced glucosinolates (Clay et al., 2009), components that are linked to anti-microbial immunity (Mishina and Zeier, 2007a; Bednarek et al., 2009).

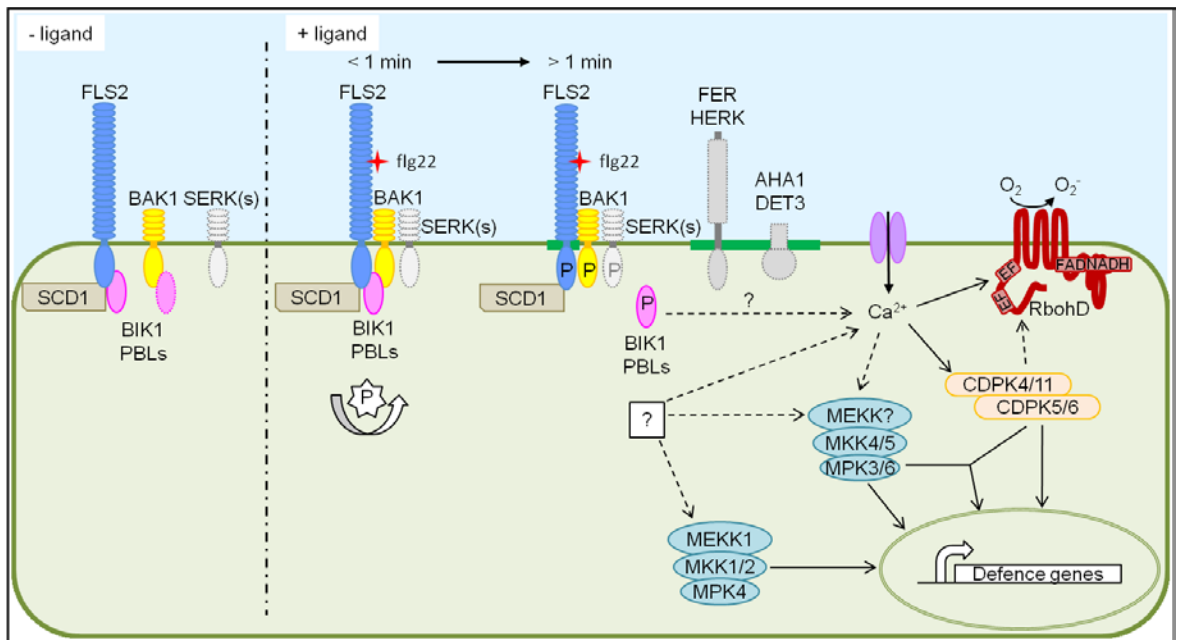


**Figure 6: Overview of FLS2-induced PTI signaling from Segonzac et al., 2010.**

FLS2 interacts constitutively with the DENN-domain protein SCD1 and the RLCKs BIK1 and PBLs. BIK1 might also be associated with BAK1 in the resting state. Upon flg22 binding, a complex forms between FLS2, BAK1 and BIK1 almost instantaneously. Other SERKs, such as BKK1 might also be part of the FLS2 complex. The RLKs FER and HERK as well as the proton pumps AHA1 and DET3 are present in flg22-induced DRMs where FLS2 resides. Following flg22 binding, multiple phosphorylation events occur rapidly. Upon phosphorylation, BIK1 is released from the complex. Flg22 perception leads to the activation of at least two MAPK cascades, both involved in the induction of defence gene expression. Flg22 binding also triggers a Ca<sup>2+</sup> burst that might activate Ca<sup>2+</sup>-dependent protein kinases (CDPKs) and the NADPH-oxidase AtRbohD required for the ROS burst. Arabidopsis CDPK4, 5, 6 1 and 11 act synergistically and independently of the MAPKs to induce defence gene expression.

#### 1.4.9 The hypersensitive response

R protein-mediated defense is often associated with a form of controlled or programmed cell death (PCD) at the site of pathogen infection, called the HR

(Morel and Dangl, 1997). This response is thought to limit the spread of the infecting pathogen and prevent disease progression. The HR is associated with several physiological changes, including transient opening of ion channels, in particular  $\text{Ca}^{2+}$  and  $\text{K}^+$  channels, and/or the production of reactive oxygen species (ROS) (Ma and Berkowitz, 2007; Mur *et al.*, 2008). The study of lesion mimic mutants has identified several regulators of cell death (see § 1.4.10). Recent work has shown that AvrRps4-induced HR depends on components of autophagy, while HR responding to AvrRpt2 does not (Hofius *et al.*, 2009), suggesting some mechanistic specificity encoded by R proteins.

Importantly, although the classical view is that ETI induces HR while PTI does not, the situation refuses to be so simplified as PAMPs can also induce cell death responses. *P. aeruginosa*-derived flg22 does not cause cell death in *Arabidopsis*, while full-length *P. syringae* pv. *tabaci* 6605 flagellin as well as recombinant N-terminal flagellin polypeptides do induce HR dependent on FLS2 (Naito *et al.*, 2007). Flagellin protein derived from *P. syringae* pv. *tabaci* induces cell death in non-host soybean, while *E. coli*-derived flagellin similarly causes HR in tobacco (Taguchi *et al.*, 2003). These cell death responses were both dependent on the glycosylation of flagellin protein (Taguchi *et al.*, 2003). Full-length flagellin derived from *Acidovorax avenae* (*Pseudomonas avenae*) strain N1141, but not the *A. avenae*-flg22 induces HR in rice cell cultures (Che *et al.*, 2000). Furthermore, LPS also induced PCD in rice, but not *Arabidopsis*, cells (Desaki *et al.*, 2006).

#### 1.4.10 Lesion mimicry, PCD and guards

Several *Arabidopsis* lesion mimic mutants have been isolated over the years, displaying enhanced disease resistance and HR-like lesion formation, either independent or dependent on SA and NPR1. Examples include *accelerated cell death 11* (*acd11*), *lesion simulating disease resistance response* (*lsd*), *constitutive expressor of PR genes* (*cpr*), *suppressor of SA insensitivity of npr1-5* (*ssi*), *hypersensitive response-like lesions* (*hrl1*) and *HR-like lesion mimic* (*hlm1*) (Jirage *et al.*, 2001; Brodersen *et al.*, 2002; Bowling *et al.*, 1994; Dietrich *et al.*, 1997; Shirano *et al.*, 2002; Balague *et al.*, 2003). Most of these mutants display defective growth and constitutive defense responses in the absence pathogen inoculation.

*lsd1* however, displays runaway cell death upon inoculation with HR-inducing bacteria (Jabs *et al.*, 1996). Several lesion mimic mutants, including *snc1-1*, *bir1*, *bon1-1* and *cpr1* are temperature-dependent and their dwarf phenotypes can be rescued by incubation at elevated temperatures (Bowling *et al.*, 1994; Hua *et al.*, 2001; Zhang *et al.*, 2003; Yang and Hua, 2004; Yang *et al.*, 2006b; Gao *et al.*, 2009).

BONZAI1 (BON1) belongs to a family of *Arabidopsis* copines, which are calcium-responsive phospholipid-binding proteins (Yang *et al.*, 2006b). BON1 and its interactor, BON1-associated protein 1 (BAP1), may function in vesicle fusion to plasma membranes, a temperature-dependent process (Hua *et al.*, 2001). BON1 functions as a negative regulator of defense through its suppression of SNC1 (Yang and Hua, 2004; Lee and McNellis, 2009) and other *R* genes (Li *et al.*, 2009b).

The recently identified BAK1-interacting receptor kinase BIR1 is also linked to cell death, as *bir1* mutants are temperature-sensitive, dwarf and show elevated disease resistance (Gao *et al.*, 2009). In addition, *mpk4* and *mekk1* mutants display dwarfism, associated with elevated SA levels, and a constitutive necrosis phenotype (Suarez-Rodriguez *et al.*, 2007; Petersen *et al.*, 2000; Ichimura *et al.*, 2006). Proteins whose absence confers lesion mimic phenotypes, such as BIR1, MEKK1 and MPK4, may not be involved in PCD *per se*, but may be guardes of unidentified R proteins that activate HR when their elimination is detected. At least for ACD11 this could be the case (see § 1.6.1.1 for guard hypothesis). An *acd11* suppressor screen (Malinovsky *et al.*, 2010) resulted in the identification of the *R* gene *LAZARUS 5* (*LAZ5*) (Palma *et al.*, 2010), which may be guarding ACD11, though an interaction between these has yet to be shown. The same screen also revealed a putative new PCD regulator - LAZ1, a DUF300 protein related to a mammalian tumour suppressor (Malinovsky *et al.*, 2010).

Investigating plant homologs of known mammalian cell death regulators has revealed insights into PCD regulation. In mammals, proliferating cells nuclear antigen A (PCNA) is involved in regulation of cell proliferation through its role as a DNA polymerase processivity factor (Maga and Hubscher, 2003). *Arabidopsis* SET domain-containing proteins able to bind PCNA have recently been isolated – ATXR5 and ATXR6 (Raynaud *et al.*, 2006) and found to be involved in histone methylation and heterochromatin formation (Jacob *et al.*, 2009). These proteins

also induce cell death when over-expressed, suggesting a role in PCD control (Raynaud *et al.*, 2006). Interestingly, subsequent work has identified an interaction between ATXR5 and ATXR6 and 1L-myo-inositol-1-phosphate synthase 1 (AtIPS1) (Meng *et al.*, 2009). *Atips1* mutants also show spontaneous cell death, providing a promising link between inositol metabolism and cell death control (Meng *et al.*, 2009).

#### 1.4.11 Too much fat will kill you

Over the last 10 years, the role of lipids in plant defense responses has come to light. Firstly, oxylipins such as JA produced by the lipoxygenase pathway (Reinbothe *et al.*, 2009), are important signaling molecules for plant defense. In addition, the unsaturated fatty acid pathway plays a role in membrane remodeling (Upchurch, 2008) while the very long chain fatty acid pathway is responsible for cuticle and sphingolipid biosynthesis (Samuels *et al.*, 2008). Ceramides are lipid molecules comprised of a long-chain base and amide-linked acyl chain. These are precursors to the more complex sphingolipids, which feature sugar or phosphate residues attached to the ceramide group (Dunn *et al.*, 2004).

Sphingolipid biochemistry ([Appendix Figure A4.6](#)) plays an important role in the control of cell death in animals and plants. The sphinganine analog myctotoxin fumonisin B1 (FB1) induces cell death in plant and animals and is a competitive inhibitor of ceramide biosynthesis (Gilchrist, 1997). Ceramides have been shown to induce calcium-dependent cell death in *Arabidopsis* (Townley *et al.*, 2005). The lesion mimic mutants *acd5*, a putative ceramide kinase (Liang *et al.*, 2003) and *acd11*, a sphingosine transfer protein (Brodersen *et al.*, 2002), are both involved in lipid metabolism. The FB1-resistant mutant *fbr11-1* (*fumonisin B1 resistant 11-1*) was identified in a screen for mutants that do not produce ROS in response to FB1 treatment (Shi *et al.*, 2007). The mutation responsible for *fbr11-1* phenotype was found within the long-chain base 1 (LCB1) subunit of serine palmitoyltransferase (SPT), an enzyme upstream of ceramide synthase in the ceramide (N-acetylsphingosine) biosynthetic pathway (Shi *et al.*, 2007). The penultimate products of this pathway, sphingosine and dihydrosphingosine, have antagonistic roles in the induction of cell death (Shi *et al.*, 2007). Thus, free sphingolipid bases

are likely involved in PCD induction in *Arabidopsis*, possibly via the regulation of ROS in response to pathogen detection. Work in *N. benthamiana* showed that the LCB2 subunit of SPT can induce HR, and this function depends on the cofactor binding-site of the enzyme (Takahashi *et al.*, 2009). Furthermore, resistance to the nonadapted bacterium *Pseudomonas cichorii* could be pharmacologically compromised by an SPT inhibitor, or silencing of the SPT subunits (Takahashi *et al.*, 2009). The importance of sphingolipid synthesis for nonhost resistance is supported by these data. This hypothesis is supported by sphingolipidomic profiling using mass spectrometry analysis of *Arabidopsis*-*Pseudomonas* interactions, which revealed the rapid elevation of free sphingobase t18:0 (phytosphinganine) during HR-inducing infections with *Pto* DC3000 (Peer *et al.*, 2010).

In a screen for enhanced RPW8 [powdery mildew resistance gene]-mediated HR-like cell death (*erh*), the plant homolog of inositolphosphorylceramide synthase (IPCS) was identified and named ERH1 (Wang *et al.*, 2008c). ERH1 is induced by pathogen infection and acts as a negative regulator of RPW8-dependent HR (Wang *et al.*, 2008c). IPCS converts ceramide to inositolphosphorylceramide, and when ERH1 is absent the accumulation of ceramide results in cell death (Wang *et al.*, 2008c).

#### 1.4.12 Mysterious kinases, cell death and lipids

Oxidative signal-inducible 1 (OXI1/AGC2-1) is a member of subfamily VIIb of the AGC (named for cAMP-dependent protein kinase **A**, cGMP-dependent protein kinase **G** and phospholipids-dependent protein kinase **C**) family of Ser/Thr protein kinases. In mammals and yeast, AGC kinases are important for signal integration related to growth, cell proliferation and apoptosis (Pearce *et al.*, 2010). OXI1 falls into a plant-specific AGC subclade featuring DFD instead of DFG in subdomain VII of the kinase domain, which is also marked by a 50-80 amino acid insertion in the activation loop (T-loop insertion). Kinases in subfamily VIIb are related to mammalian protein kinase A with a signature C-terminal hydrophobic FxxF motif for 3'-phosphoinositide-dependent kinase 1 (PDK1)-interaction (Bögre *et al.*, 2003). Originally OXI1 was singled out for its inducibility in response to ROS

sources such as  $H_2O_2$  and cellulase. Subsequently, it was shown that OXI1 is required for disease resistance to biotrophs such as *Pto* DC3000 and virulent *Hpa* strains, but not necrotrophs (Rentel *et al.*, 2004; Petersen *et al.*, 2009). Confoundingly, OXI1 over-expressing lines are also more susceptible to these pathogens, leading to the suggestion that any perturbation in OXI1 disturbs disease resistance signaling pathways (Petersen *et al.*, 2009). The role of OXI1 in *Arabidopsis* defense remains elusive as the preceding work has given incomplete answers. Peroxide and cellulase were shown to induce phosphorylation of OXI1, MPK3 and MPK6, and *oxi1* mutants displayed reduced MAPK activation, putting OXI1 upstream of MAPK activation and downstream of ROS (Rentel *et al.*, 2004). Later, a yeast-two hybrid screen provided OXI1-interacting proteins as *Arabidopsis* relatives of tomato *Pti1*. Tomato SIPti1 was previously identified in a Y2H screen as an interactor of *Pto* (Zhou *et al.*, 1995). *Pti1* is phosphorylated by *Pto* and was placed downstream of *Pto*, as *Pto* is not a substrate for SIPti1 kinase activity. SIPti1 is thought to regulate cell death during the defense response as tobacco transiently expressing SIPti1 has an enhanced HR in response to inoculation with *P. syringae* pv. *tabaci* carrying *AvrPto* (Zhou *et al.*, 1995).

Although only *Arabidopsis* SIPti1 homologs designated PTI1-1, PTI1-2 and PTI1-3 were reported as OXI1 interactors (Anthony *et al.*, 2006), there are 10 *Arabidopsis* homologs, several with higher overall sequence similarity to SIPti1. PTI1-1 and PTI1-2 are phosphorylated by OXI1, and appear to lack the ability to use OXI1 as a substrate, although they possess kinase activity *in vitro* (Anthony *et al.*, 2006). This phosphorylation is reduced when a conserved threonine, T238 in SIPti1, is mutated to alanine, suggesting that this could be an OXI1 target phosphosite. Kinase activity of PTI1-2 was enhanced by treatment with flg22, xylanase and phosphatidic acid (PA) (Anthony *et al.*, 2006). In this work however, no loss-of-function lines were explored for the role of PTI1 in disease resistance, making it impossible to determine whether PTI1 phosphorylation by OXI1 leads to changes in cell death and disease susceptibility. Interestingly, PTI1-1 is predicted to be co-expressed with the LCB2 subunit of serine palmitoyltransferase, an enzyme upstream of ceramide synthase (Shi *et al.*, 2007). Mutations in this pathway, such as *acd11*, which is mutated in sphingosine transfer protein, lead to constitutive cell death (Brodersen *et al.*, 2002). Furthermore, the penultimate products of this

pathway sphingosine and dihydrosphingosine have antagonistic roles in the induction of cell death (Shi *et al.*, 2007).

In rice, OsPti1 was identified as an interactor of OsOXI1 in Y2H (Matsui *et al.*, 2010). OsOXI1 gene expression and protein phosphorylation are induced by peroxide and chitin, suggesting a role in PTI and ETI. Moreover, OsPti1 is phosphorylated by OsOxi1, mirroring the situation in Arabidopsis. In rice, OsPti1 also negatively regulates cell death but this does not depend on OsOXI1 phosphorylation (Matsui *et al.*, 2010).

What's more, PDK1 is an upstream activator of Arabidopsis OXI1, and specifically phosphorylates OXI1 at a conserved site in its activation domain (T-loop). PDK1 activity is itself enhanced by binding PA and phosphatidylinositol-4,5-bisphosphate (PI(4,5)P<sub>2</sub>) (Anthony *et al.*, 2004). These clues all link lipid metabolism to cell death responses, and PTI1 could be this connection. A tomato OXI1 homolog AvrPto-dependent Pto-interacting kinase 3 (Adi3) interacts with Pto when AvrPto is present and is similarly subject to activation in response to PDK1 in tomato (Devarenne *et al.*, 2006). Silencing of *Adi3* leads to spontaneous lesions and enhanced disease resistance, in a pathway that requires MKKK $\alpha$  (Devarenne *et al.*, 2006). The authors propose a model wherein PDK1 and Adi3 interact at the plasma membrane. Upon phosphorylation by PDK1, Adi3 translocates to the nucleus and negatively regulates cell death through an unknown mechanism. Upon inoculation with pathogen, Adi3 exits the nucleus and is phosphorylated by Pto, releasing cell death suppression and leading to HR (Ek-Ramos *et al.*, 2010). Most recently, in mammals an association was uncovered between PDK1 and the apoptotic regulator, apoptosis signal-regulating kinase 1 (ASK1) (Seong *et al.*, 2010), a MKKK that activates p38 and JNK/SAPK MAPK cascades and mediates cell survival in mammals. PDK1 negatively regulates ASK1 activity by phosphorylating a 14-3-3-binding site on the kinase, while ASK1 reciprocally phosphorylates PDK1 to inhibit its activity (Seong *et al.*, 2010). ASK1-mediated signaling is activated by ROS produced in response to LPS binding to TLR4 and is required for innate immunity in mammals (Matsuzawa *et al.*, 2005). This links PAMP perception, ROS and PDK1 function with apoptosis control, and it would be interesting to explore similar relationships in plants.

Here we have much evidence for OXI1 and its substrates in the control of cell death as it relates to disease resistance, but many questions remain. The subcellular location of OXI1 and its PTI substrates has not been tested in rice or Arabidopsis. Loss-of-function for rice and Arabidopsis Pti homologs have to be assessed for the influence of Pti on disease resistance, as well as PTI signaling.

#### **1.4.13 Negative regulation of defense signaling**

During normal growth and development, defense responses are repressed by a set of negative regulators, in order to conserve plant resources. Several negative regulators of defense have been identified as mutants with constitutive defense responses (see below). Negative regulation of defense responses could be achieved with diverse mechanisms, including protein degradation and transcriptional control, mentioned here.

Polyubiquitination serves to target proteins for proteasomal degradation, or can regulate protein function depending where the ubiquitin molecules are ligated. Thus the action of E3 ligases is used to control the activity of several plant and animal defense signaling pathways (Bhoj and Chen, 2009; Craig *et al.*, 2009; Trujillo and Shirasu, 2010) (Figure 7). In mammals TLR-mediated responses are inhibited by the action of the Pellino family of E3 ligases that polyubiquitinate IRAK in TLR signaling pathways to control activation of NF- $\kappa$ B and MAPK cascades (Moynagh, 2009). Ubiquitination also presents a means of controlling other receptor activities. For example, EGF receptor is ubiquitinated prior to its endocytosis (Marmor and Yarden, 2010). This could be the case for PRRs, which share homology to EGFR and may be subject to endocytosis, like FLS2 (Robatzek *et al.*, 2006). Several regulators of Xa21-mediated signaling have been identified, including a RING finger ubiquitin ligase XB3 (Wang *et al.*, 2006c), a WRKY transcription factor (OsWRKY62 or XB10) (Peng *et al.*, 2008), and a protein phosphatase 2C (XB15) (Park *et al.*, 2008), XB24, a unique ATPase (Chen *et al.*, 2010c), all of which have negative regulatory effect on Xa21 activity.

Recently, the EDS1 and NDR1-dependent *cpr30* mutant was identified, characterized by elevated defense gene expression, and constitutive disease

resistance to virulent and avirulent pathogens. This aided the identification of CPR30 as a negative regulator of defense, both basal and *R*-gene mediated. CPR30 is an F-box protein that was shown to interact with SKP1/ASK proteins, and is thought to form an SCF E3 ligase complex responsible for degradation of positive regulators of defense (Gou *et al.*, 2009).

Pathogen-induced E3 ligases plant U-box (PUB) AtPUB22, AtPUB23 and AtPUB24 are negative regulators of PTI (Trujillo *et al.*, 2008), while tomato E3 ligase Avr9/Cf-9 rapidly elicited 74 (ACRE74) is induced in response to flg22 elicitation (Navarro *et al.*, 2004). In tobacco, the ACRE74 orthologous U box CMPG1 also mediates Cf9-triggered HR and disease resistance (Gonzalez-Lamothe *et al.*, 2006). ACRE276 is an Avr9-induced U box required for Cf9- and Cf4-mediated HR in tobacco, as well as tomato Cf9-mediated HR and fungal disease resistance (Yang *et al.*, 2006a). The Arabidopsis ACRE276 homolog PUB17 is required for RPM1 and RPS4-mediated resistance to *Pto* DC3000 (Yang *et al.*, 2006a). Thus E3 ligases can play contradictory roles in innate immunity.

Transcriptional control is an important means of control for negative regulation of defense responses. WRKY48 is a negative regulator of *PR* gene expression and basal resistance to *Pto* DC3000 (Xing *et al.*, 2008). The MYB30 transcription factor, whose expression is specifically induced by avirulent bacteria (Daniel *et al.*, 1999), acts as a positive regulator of defense in the control of pathogen-induced cell death (Vailleau *et al.*, 2002). Potential MYB30 target genes identified by microarray analysis include those involved in very long chain fatty acid biosynthesis, implicating this pathway in cell death control (Raffaele *et al.*, 2008). Recent work has found that phospholipase A2- $\alpha$ , responsible for hydrolysis of membrane glycerophospholipids to free fatty acids, interacts with MYB30 to negatively regulate its activity (Froidure *et al.*, 2010). This provides an interesting link between negative regulation of defense responses and fatty acid metabolism, which is also discussed in the following paragraph.

The calmodulin binding S-locus receptor kinase CBRLK1 is reported to be a negative regulator of defense, as *cbrlk1* mutants display enhanced pathogen-induced *PR1* gene expression as well as resistance to *Pto* DC3000 (Kim *et al.*, 2009a).

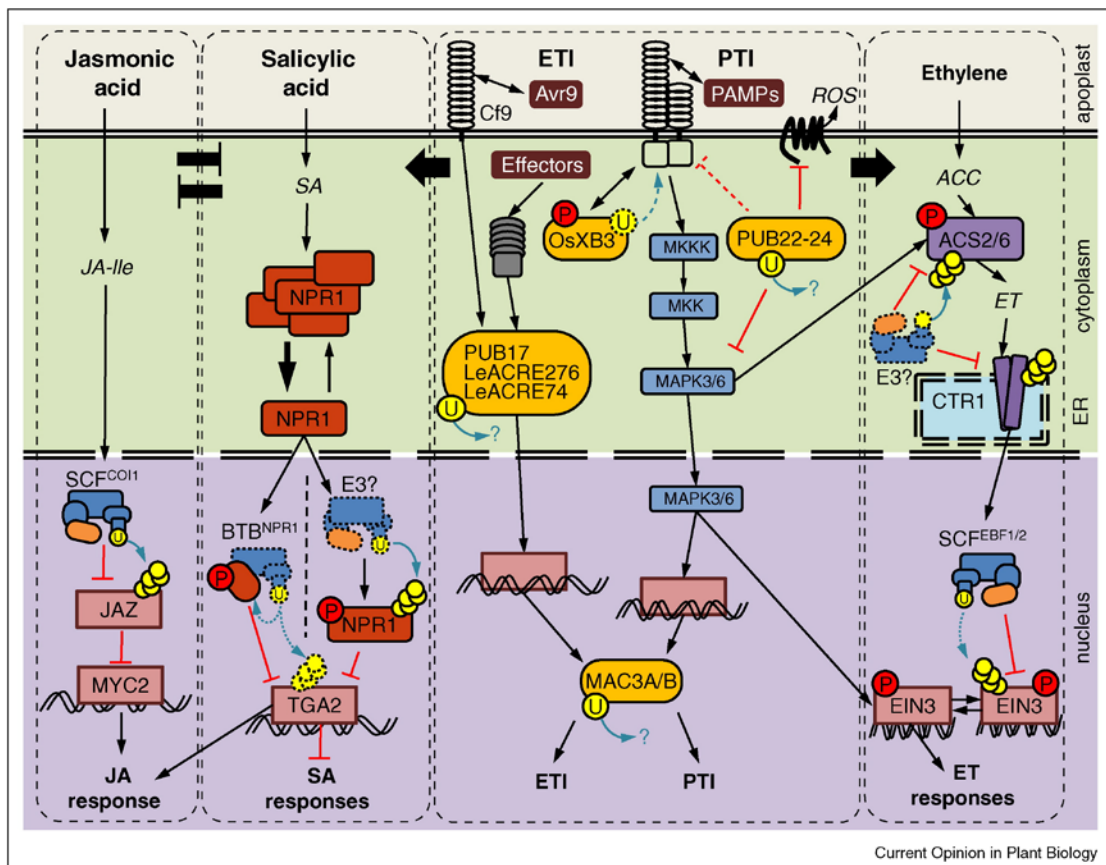


**Figure 7: Negative regulation of defense signaling from Trujillo and Shirasu, 2010.**

Arrows and bar-headed lines indicate functional interactions, and double-headed arrows indicate a physical interaction. Dotted forms and arrows denote inferred interactions and components for which data are not available. Light blue arrows indicate ubiquitination, a question mark (?) indicates an unknown target, yellow dots indicate ubiquitin (U), and red dots indicate phosphorylation (P).

### 1.4.14 Plant Hormones

#### 1.4.14.1 Take 2 aspirin and call me in the morning: the wonders of Salicylic acid

Over thirty years ago, White noticed that exogenous salicylic acid (SA) application induced *pathogenesis-related* (PR) gene expression and partial resistance to TMV in tobacco (White, 1979), and scientists have spent years unravelling SA-related signaling mechanisms.

The function of SA in plant defense was initially studied using transgenic tobacco and Arabidopsis plants expressing the bacterial *NahG* gene encoding a salicylate hydroxylase. These plants are hyper-susceptible to virulent pathogens and

impaired in SAR and ETI (Delaney *et al.*, 1995; Raordan and Delaney, 2002). SA is also required for HR, but is unable to induce HR alone (Ward *et al.*, 1991). Systemic acquired resistance (SAR) is a broad-spectrum induced resistance triggered by local infection with pathogens, resulting in HR (Ryals *et al.*, 1996). SAR is accompanied by increased endogenous SA (Metraux *et al.*, 1990) in parallel with upregulation of defense genes (Ward *et al.*, 1991) including those encoding pathogenesis-related (PR) proteins (van Loon *et al.*, 2006).

Signal transduction in the SA pathway requires NPR1 (nonexpressor of *PR* genes), a master regulator identified in a screen for SAR-impaired mutants (Cao *et al.*, 1994; Delaney *et al.*, 1995; Shah *et al.*, 1997). Indeed, *npr1* plants accumulate SA in response to pathogen infection but are compromised in *PR* gene induction and SAR. Under low-SA conditions, NPR1 exists in an oligomeric form in the cytoplasm (Mou *et al.*, 2003), and this is facilitated by S-nitrosylation (Tada *et al.*, 2008). In response to increased SA, NPR1 dissociates into monomers, which translocate to the nucleus (Kinkema *et al.*, 2000) to engage in interactions with TGA-type TFs (Figure 7) (Fan and Dong, 2002; Choi *et al.*, 2010; Johnson *et al.*, 2003; Despres *et al.*, 2003). TGA2, 5 and 6 are requisite for SA-induced *PR1* expression (Zhang *et al.*, 2003a), while WRKY70 is also induced by SA and is NPR1-dependent (Li *et al.*, 2004). Thus, NPR1 functions as a transcriptional co-activator. Recent work has revealed a proteasome-dependent mechanism of NPR1 regulation, which constantly removes NPR1 from the nucleus to prevent inappropriate SAR activation. SAR inducers cause dual phosphorylation of NPR1 at a phosphodegron motif followed by recruitment to Cullin3-based ubiquitin ligase (Spoel *et al.*, 2009). Subsequent degradation of phospho-NPR1 is essential for SAR activation and downstream gene induction (Spoel *et al.*, 2009).

SA is known to act antagonistically to JA, suppressing this signaling pathway in plants to favor resistance to microbial pathogens over JA-dependent necrotroph and herbivore resistance (Felton and Korth, 2000; Leon-Reyes *et al.*, 2010; Koornneef and Pieterse, 2008).

Interestingly, this antagonism resembles the effect of the nonsteroidal anti-inflammatory drug acetylsalicylic acid (aspirin), a SA-derivative, on prostaglandin formation in animal cells. Prostaglandins are structurally similar to jasmonates and

are involved in inflammation (Thoma *et al.*, 2004). Indeed, SA suppresses expression of JA-responsive genes such as *PDF1.2* and *vegetative storage protein (VSP)*, and this is NPR1-dependent, although it does not require NPR1 nuclear localization, suggesting a cytoplasmic role for NPR1 in JA-related antagonism (Spoel *et al.*, 2007).

In contrast, SAR against *Pto* DC3000 also requires systemic induction of JA biosynthetic and JA-responsive genes (Truman *et al.*, 2007), nicely illustrating that SA and JA pathways are also capable of acting synergistically.

Importantly, SA a role to play in PTI, as *SA induction deficient 2 (sid2)* mutants, compromised in the SA-biosynthetic enzyme isochorismate synthase 1 (ICS1) (Wildermuth *et al.*, 2001), display reduced flg22-induced disease resistance (Tsuda *et al.*, 2008). This requirement of SA for PTI is corroborated by another study, where it was shown that *sid2* mutants produce less flg22-induced H<sub>2</sub>O<sub>2</sub> and callose deposition (Zhang *et al.*, 2010a).

#### **1.4.14.2 Jasmonates**

Jasmonates are oxylipin phytohormones that share significant structural and functional properties with the animal hormones prostaglandins. Jasmonates are involved in responses to diverse stresses including insects, pathogens, ozone, UV light, wounding, and other abiotic stresses (Wasternack and Kombrink, 2009).

Jasmonic acid (JA) biosynthesis initiates with  $\alpha$ -linolenic acid oxygenation in the chloroplast and terminates with synthesis of (+)-7-iso-JA in the peroxisome. This molecule epimerizes to a more stable *trans* configuration, generally known as JA (Wasternack, 2007; Creelman and Mullet, 1997). JA can be enzymatically converted into several conjugates, for example, ethyl-jasmonate, or MeJA, cis-jasmone and JA-amino acid conjugates. Interestingly, JA requires conjugation with amino acids to achieve biological activity, and this is carried out by the JA-amido synthetase Jasmonate-Resistant 1 (JAR1) (Katsir *et al.*, 2008; Staswick, 2008; Staswick and Tiryaki, 2004; Thines *et al.*, 2007).

(-)-JA-L-isoleucine was initially thought to be the molecularly active form of the hormone, and this molecule is structurally and functionally mimicked by the *Pseudomonas syringae* phytotoxin coronatine (COR) (Katsir *et al.*, 2008; Staswick,

2008). Recent work on bioactive jasmonates has shown that COI1 (coronatine-insensitive 1) is the JA-L-Ile receptor and (+)-7-iso-JA-Ile is the natural ligand of COI1-JAZ (jasmonate ZIM domain) complexes, while the previously proposed (-)-JA-L-Ile is inactive (Fonseca *et al.*, 2009). Indeed, previous contamination by active enantiomer of (-)-Ja-Ile preparations masked the identity of the true active components.

COI1, an F-box, determines the target specificity as part of the SCF<sup>COI1</sup> (SKIP-CULLIN-F box) E3 ligase complex responsible for JA-induced JAZ protein degradation (Figure 7) (Thines *et al.*, 2007; Chini *et al.*, 2007; Devoto *et al.*, 2002; Xu *et al.*, 2002) and has only recently been confirmed as the jasmonate receptor (Yan *et al.*, 2009).

JA signaling is repressed by dimeric JAZ proteins (Chini *et al.*, 2009b; Chung and Howe, 2009); once they are degraded they liberate the basic-helix-loop-helix (bHLH) type transcription factor MYC2 (and possibly other TFs), which directs JA-dependent transcriptional activation (Chini *et al.*, 2007; Chini *et al.*, 2009a). It has recently been found that in Arabidopsis in the presence of the hormone, JAZ3 interacts with COI1 via the C-terminal Jas motif (Katsir *et al.*, 2008; Thines *et al.*, 2007; Chico *et al.*, 2008; Melotto *et al.*, 2008; Chini *et al.*, 2009b).

Ultimately, jasmonate signaling brings about significant changes in gene expression which signals a transition from growth to defense (Pauwels *et al.*, 2008; Zhang and Turner, 2008). Recent work, using a tandem affinity purification (TAP) approach to isolate JAZ-interacting proteins, has revealed the molecular mechanisms by which JAZ proteins repress gene expression (Pauwels *et al.*, 2010). It was shown that the Arabidopsis JAZ proteins engage the Groucho/Tup1-type co-repressor TOPLESS (TPL) TPL8 and TPL-related proteins (TPRs) via an adaptor protein, Novel Interactor of JAZ (NINJA). NINJA functions as a transcriptional repressor whose activity is mediated by a functional TPL-binding EAR repression motif. Consequently, NINJA and TPL proteins function as negative regulators of jasmonate responses. TPL proteins may behave as general co-repressors that affect multiple signaling pathways through the interaction with specific adaptor proteins.

#### **1.4.14.2.1 Coronatine**

The first JA-insensitive mutant *coi1* was identified by the ability of the phytotoxin coronatine (COR) to mimic MeJA-induced root-growth inhibition (Feys *et al.*, 1994). Intriguingly, COR functions as an agonist of the JA receptor, and indeed is 1000-fold more efficient than JA-Ile in promoting COI1-JAZ3 interactions *in vitro* (Katsir *et al.*, 2008). It is not yet clear whether the toxic properties of COR result solely from an overstimulation of the JA signaling pathway, due to its high receptor-binding efficiency, or whether COR has additional properties that alter normal cellular processes. *Arabidopsis* and *tomato* *coi1* mutants are far less susceptible to infection by COR-producing strains of *P. syringae* (Feys *et al.*, 1994) and *Pto* DC3000 *COR*<sup>-</sup> strains are severely compromised in virulence (Brooks *et al.*, 2004). However, *Pto* DC3000 *COR*<sup>-</sup> is able to grow to a level approximating wild-type *Pto* DC3000 in *sid2* and *fls2* mutants, illustrating a role for COR in suppressing SA-mediated defenses (Brooks *et al.*, 2004; Block *et al.*, 2005; Melotto *et al.*, 2006; Zeng *et al.*, 2010). COR also represses abscisic acid (ABA)-mediated stomatal closure to facilitate pathogen entry (Melotto *et al.*, 2006). Thus, COR is an important virulence factor for *Pto*, which illustrates the clever targeting of eukaryotic hormone receptors by pathogen virulence factors providing an efficient mechanism to manipulate genome-wide transcriptional programs and other processes to effectively suppress host cell defenses.

#### **1.4.14.3 Ethylene**

Ethylene (ET) is a hormone involved in several essential processes in plants including fruit ripening, germination, senescence and defense (Lin *et al.*, 2009). *Arabidopsis* encodes 5 ET receptors, related to bacterial two-component histidine kinase sensors: ET response 1 (ETR1), ETR2, ET sensor 1 (ERS1), ERS2 and ET-insensitive 4 (EIN4) (Lin *et al.*, 2009). These receptors bind to ET via their ER-localized N-terminus (Wang *et al.*, 2006a). ET receptor signaling is thought to occur through an inverse agonist model, where in the absence of ET signaling is constitutive, and in its presence, the receptors are deactivated (Figure

7) (Hua and Meyerowitz, 1998; Lin *et al.*, 2009). An *etr1-2* suppressor screen led to the identification of *rte1*, *reversion-to-ethylene sensitivity 1* (Dong *et al.*, 2008). RTE1, a transmembrane protein and positive regulator of ETR1 (Dong *et al.*, 2008), functions by direct interaction with ETR1 (Dong *et al.*, 2010).

Constitutive triple response 1 (CTR1) is a putative Raf-like MAPKKK, which interacts with ETR1 and ERS1 (Clark *et al.*, 1998; Huang *et al.*, 2003), to act as a negative regulator of ET signaling (Kieber *et al.*, 1993), though its true molecular activity remains unknown. Downstream signaling components include the transcription factors EIN3 and EIN3-like (EILs) that are responsible for activation of downstream signaling cascades through activation of ethylene response factor 1 (ERF1), EIN3-binding F-box protein 1 (EBF1) and other targets (Chao *et al.*, 1997; Solano *et al.*, 1998; Potuschak *et al.*, 2003; Guo and Ecker, 2003). EIN2 is a pivotal player in ET signaling where it acts downstream of CTR1, and loss of *EIN2* results in ethylene insensitivity (Alonso *et al.*, 1999). EIN2 is rapidly turned over in the cell, but ET stabilizes ET protein levels (Qiao *et al.*, 2009). Two F-box proteins identified as EIN2-interactors, EIN2-targeting proteins (ETPs) ETP1 and ETP2 (Qiao *et al.*, 2009), are required for EIN2 degradation (Qiao *et al.*, 2009). Furthermore, it was recently shown that ER-localized EIN2 specifically interacts with ETR2 (Bisson *et al.*, 2009). Post-transcriptional stability of EIN3 has emerged as pivotal in ET signaling regulation (Solano *et al.*, 1998). EIN3 accumulates in the nucleus in an ET-dependent manner, and is constantly degraded via the 26S proteasome in the absence of ET. EBF1 and EBF2 target EIN3 for degradation by serving as substrate recognition subunits for the E3 ubiquitin ligases (Gagne *et al.*, 2004; Guo and Ecker, 2003; Potuschak *et al.*, 2003).

Interestingly, divergent MAPK cascades were found to regulate EIN3 levels and modulate ET signaling (Yoo *et al.*, 2008). However, this was later contested with evidence that EIN2, not MKK9, is required for nuclear EIN3 stability (An *et al.*, 2010).

Most recently, it was shown that the steady-state *FLS2* expression is directly controlled by ethylene-induced EIN3 and EIN3-like transcription factors (Boutrot *et al.*, 2010). This suggests the operation of a positive feedback loop for PAMP signaling, presumably facilitating a more robust response.

#### 1.4.14.4 PAMP and pathogen-responsive hormone signaling

Flg22 treatment results in the production of SA (Mishina and Zeier, 2007b; Tsuda *et al.*, 2008), which is required for both local and systemic-acquired resistances (Durrant and Dong, 2004) and defense against biotrophic and hemibiotrophic pathogens (Glazebrook, 2005). Treatment of potato with the oomycete elicitor Pep13 results in production of SA and JA (Halim *et al.*, 2004). Moreover, bacterial PAMPs induce ET production (Felix *et al.*, 1999), which follows an intricate path of feedback regulation. MPK6 phosphorylates and stabilizes the ET biosynthetic enzyme isoforms 1-aminocyclopropane-1-carboxylic acid (ACC) synthase (ACS) ACS2 and ACS6, resulting in increased ethylene biosynthesis (Liu and Zhang, 2004). In a further layer of complexity, it was shown that MPK6 interacts with the ethylene response factor ERF104 and brings about its phosphorylation (Bethke *et al.*, 2009). In the presence of ET, ERF104 is released from MPK6, presumably allowing MPK6 to activate ET biosynthesis.

To determine the contribution of different hormone signaling pathways to PTI and ETI, Tsuda *et al* used combinations of mutants compromised in key signaling pathways: *dde1* (*Delayed dehiscence 1*; JA), *ein2* (ET), *pad4* (*Phytoalexin deficient 4*; SA and others) and *sid2* (SA) (Tsuda *et al.*, 2009). AvrRpt2-induced ETI and flg22-induced PTI remained intact in any of the single mutants, but were completely compromised in the quadruple mutant. PAMP-induced signaling and disease resistance relies on synergistic signaling of SA and ET/JA pathways, while Avr-induced signaling exploits a combination of pathways that is compensatory (Tsuda *et al.*, 2009).

The requirement of SA for ETI signaling depends on the *R* gene involved. Arabidopsis downy mildew resistance genes *Resistance to Peronospora parasitica* (*RPP*) *RPP4* depends on SA for signaling (van der Biezen *et al.*, 2002), while *RPP7* and *RPP8* do not have this requirement (Takahashi *et al.*, 2002); (McDowell *et al.*, 2000).

Flg22 upregulates the expression of the Arabidopsis microRNA *miRNA393*, which reduces auxin receptor levels by targeting TIR1-like proteins (Navarro *et al.*,

2006), and SA antagonises auxin signaling by stabilizing auxin-response repressors (Wang *et al.*, 2007). Indeed, AvrRpt2-overexpressing plants display altered morphology associated with elevated auxin levels (Chen *et al.*, 2007). Taken together, these results suggest that PTI and auxin signaling pathways are antagonistic. Consistently, the phytopathogenic bacteria *Xanthomonas campestris* pv. *campestris* and *Pto* DC3000 increase plant auxin levels (O'Donnell *et al.*, 2003), potentially by upregulating the expression of auxin biosynthetic genes (Schmelz *et al.*, 2003).

ABA is required for stomatal closure in response to the perception of *Pto* DC3000 and this response is inhibited by the phytotoxin coronatine (Melotto *et al.*, 2006). SA and ABA act antagonistically, with exogenous ABA application resulting in inhibition of SAR (Yasuda *et al.*, 2008). A recently identified RNA-binding protein defense-related 1 (AtRBP-DR1) was found to activate SID2-dependent SA signaling, and thus regulate immunity to hemi-biotrophic *Pto* DC3000 (Qi *et al.*, 2010). Congruently, *Pseudomonas* effectors such as AvrPtoB induce ABA synthesis in an effort to undermine SA signaling and thus promote bacterial virulence (de Torres-Zabala *et al.*, 2007). Investigation of the antagonistic relationship between SA and ABA revealed that SA is required for the full induction of PAMP-responsive genes, while ABA suppresses their expression (de Torres Zabala *et al.*, 2009).

Thus, careful modulation of these different hormone signaling pathways during plant-pathogen interactions is designed to respond appropriately to prevent infection, while balancing plant resources towards growth and development.

#### **1.4.14.5 Phytopathogens: it's a lifestyle choice**

Phytopathogens are classified depending on their lifestyle during plant colonization. Biotrophic pathogens depend on living plant tissue for survival, while necrotrophs encourage plant cell death and thrive on the dead tissue. Examples of obligate biotrophs include bacteria *Xanthomonas oryzae*, oomycete downy mildew *Hyaloperonospora arabidopsis*, powdery mildew *Erysiphe pisi*. While *Erwinia carotovora* and *Botrytis cinerea* offer good examples of necrotrophic pathogens

(van Kan, 2006). Many pathogens also bridge the two categories, living a hemibiotrophic lifestyle, where in early infection pathogens suppress cell death and later transition to a destructive necrotrophic phase. Hemibiotrophs include bacterium *Pseudomonas syringae*, fungi *Colletotrichum graminicola* and *Cladosporum fulvum*, and oomycete *Phytophthora infestans* (Collmer *et al.*, 2009) (Hammond-Kosack and Parker, 2003).

The different modes of infection used by these classes of pathogens results in differential deployment of plant defenses required for their defeat. The observation was made that *coi1* mutants, defective in jasmonic acid (JA) perception, are more susceptible to the necrotrophs *Botrytis cinerea* and *Alternaria brassicicola* but not to the biotrophic *Hyaloperonospora arabidopsis* (*Hpa*). Conversely, salicylic acid (SA)-non-responsive mutant *npr1* and salicylate hydroxylase transgenic *NahG* show opposite resistance phenotypes, with increased resistance to *B. cinerea* and *A. brassicicola*, and increased susceptibility to *Hpa* (Thomma *et al.*, 1998; Münch *et al.*, 2008). This led to the paradigm that in most cases, biotrophic pathogens are thwarted by SA-mediated defenses and the hypersensitive response (HR), while necrotrophs are susceptible to JA and ethylene (ET)-mediated defenses (Glazebrook, 2005).

Of course this is a simplified view to allow us to generally understand plant-pathogen interactions, and there are many exceptions to the rule. One example is the surprising increased resistance of *jin1* (MYC2 mutant) to *Botrytis cinerea*, in contrast to the purported function of JA signaling in resistance to necrotrophic pathogens (Nickstadt *et al.*, 2004).

## **1.5 Effector-triggered susceptibility (ETS)**

### **1.5.1 Virulence effectors**

To infect plants, pathogens need to circumvent PTI responses. An effective strategy employed by various pathogenic microorganisms makes use of effector proteins to suppress defense responses, either by preventing PAMP perception or inhibiting PAMP-induced signaling (Figure 8).

Bacterial effectors are mostly secreted into plant cells by the type-three secretion system (TTSS). This function has been shown to be important for pathogen virulence. Indeed, plant pathogenic bacteria lacking a functional TTSS induce a primary defense response and are non-pathogenic (Collmer *et al.*, 2000; Grant *et al.*, 2006). Fungal effectors may be secreted into the apoplast or delivered into the host cytoplasm by an as yet unknown mechanism(s), while oomycete effectors delivered into the host cytoplasm harbour a conserved RxLR domain that may gain entry to host cells by exploiting the plant endocytic pathway (Rehmany *et al.*, 2005; Birch *et al.*, 2009; Dou *et al.*, 2008).

The majority of plant effector targets that have been identified are for bacterial effectors, however the studies of *P. infestans* effectors have begun to provide insight into the virulence mechanisms employed by oomycetes. The *P. infestans* effector Avr3a interacts with and stabilizes the E3 ligase CMPG1 to prevent INF1-induced cell death (Bos *et al.*, 2010). Furthermore, the cysteine protease C14 is inhibited by apoplastic *P. infestans* effectors EPIC1 and EPIC2B in *N. benthamiana*, and C14 is required for resistance to *P. infestans* (Kaschani *et al.*, 2010).

*Pto* DC3000 has been a useful model for the study of bacterial effectors, this pathogen encodes over 30 effectors (<http://www.pseudomonas-syringae.org/>; {Hann, #1365}; Abramovitch *et al.*, 2006; Zhou and Chai, 2008).

Among them, AvrPto is a small triple helix protein, potentially acting as a kinase inhibitor (Xing *et al.*, 2007). In resistant tomato plants, the cytoplasmic protein kinase Pto recognizes AvrPto and AvrPtoB in plants carrying the NBS (nucleotide-binding site)-LRR gene *Prf*, leading to ETI responses (Mucyn *et al.*, 2006). In susceptible tomato and Arabidopsis plants AvrPto is a virulence factor and inhibits PTI upstream of MAPK activation (Scofield *et al.*, 1996; He *et al.*, 2006; Hann and Rathjen, 2007). AvrPto is a kinase inhibitor (Xing *et al.*, 2007), however its activity is not required for resistance mediated by Pto and Prf. In order to elucidate the target of AvrPto, other plant kinases were considered. Interestingly, Pto, FLS2 and EFR kinase domains share a high degree of homology (Shan *et al.*, 2008). AvrPto has been shown to interact *in vivo* with FLS2 and EFR (Xiang *et al.*, 2008; Xiang *et al.*, 2010). AvrPto was shown to inhibit FLS2, EFR and BIK1 auto-phosphorylation *in vitro* (Xiang *et al.*, 2010; Zhang *et al.*, 2010a), however it is possible that the amount of AvrPto delivered into plant cells under natural

conditions would be unable to suppress kinase activity. In addition, AvrPto was thought to target BAK1 thereby preventing the formation of PRR/BAK1 complexes (Shan *et al.*, 2008). However, further work confirmed that FLS2 and not BAK1 is the molecular target of AvrPto (Xiang *et al.*, 2010).

Strikingly, ETI triggered by Pto and Prf in resistant tomato plants results from the inhibition of the AvrPtoB E3 ligase activity by Pto (Ntoukakis *et al.*, 2009). AvrPtoB activity leads to degradation of FLS2 and CERK1, using a very direct tactic for preventing PTI activation (Göhre *et al.*, 2008; Gimenez-Ibanez *et al.*, 2009b).

Many *P. syringae* effectors, including AvrPto, AvrRpt2, AvrRpm1, HopAO1 and HopAI1 target PTI responses (Janjusevic *et al.*, 2006; Kim *et al.*, 2005b; Underwood *et al.*, 2007; Xiang *et al.*, 2008), making the study of effector function a means of unraveling PTI signaling. The diversity of effector manipulation of plant metabolism is impressive. AvrRpt2 alters auxin physiology in the host, and the resulting elevation in auxin levels suppresses plant defenses and promotes disease (Chen *et al.*, 2007). HopAI1, a *P. syringae* TTSS effector, acts as a phosphothreonine lyase, which inactivates mitogen-activated protein (MAP) kinases (Li *et al.*, 2007). Indeed, HopAI1 interacts with AtMPK3 and AtMPK6, and its overexpression in Arabidopsis suppresses their activation by flg22 (Zhang *et al.*, 2007). In contrast, HopAO1 uses its intrinsic phosphatase activity to somehow suppress PTI downstream or independently of MAPKs (Underwood *et al.*, 2007), though its target has not been identified. Intriguingly, the glycine-rich binding protein 7 (GRP7), which plays a role in stomatal closure in response to abiotic stress (Kim *et al.*, 2008a), has been identified as a positive regulator of PTI against bacteria and is a target of the ADP ribosyltransferase activity of effector HopU1 (Fu *et al.*, 2007). HopM1 harnesses the host proteasome to bring about degradation of AtMIN7, a protein involved in innate immunity (Nomura *et al.*, 2006).

A family of *Xanthomonas* transcription activator-like (TAL) effectors directly binds to plant genes, mimicking transcription factors to modulate host metabolism to suit the pathogen (Boch and Bonas, 2010). TAL effectors are composed of a central characteristic repeat domain, nuclear localization signals and a transcriptional activation domain (Bogdanove *et al.*, 2010). The number and sequence of repeats determines the specificity of TAL effectors (Herbers *et al.*, 1992; Yang *et al.*, 2005). *X. campestris* pv. *vesicatoria* AvrBs3 (17.5 repeats) binds directly to a

specific promoter sequence (*UPA* box) in the pepper *UPA20* (*upregulated by AvrBs3*) gene to activate its transcription and enhance hypertrophy, which is beneficial to bacterial colonization (Kay *et al.*, 2007; Romer *et al.*, 2009). Interestingly, AvrBs3 comprises nearly identical 34 amino acid repeats, with the exception of the 12th and 13th hypervariable repeats, which are used to classify effectors into types (Boch and Bonas, 2010). Since the *UPA* box of 18 - 19 bp almost corresponds to the number of AvrBs3 repeats, the hypothesis developed that certain repeat types correspond to specific base pairs in the target DNA (Moscou and Bogdanove, 2009; Bogdanove *et al.*, 2010). In this way the authors identified target specificity in a 2 amino acid motif per repeat (e.g. HD = C; NG = T; NS = A/C/G/T; NN = A/G; IG = T) and thus are able to predict TAL effector targets (Moscou and Bogdanove, 2009; Bogdanove *et al.*, 2010).

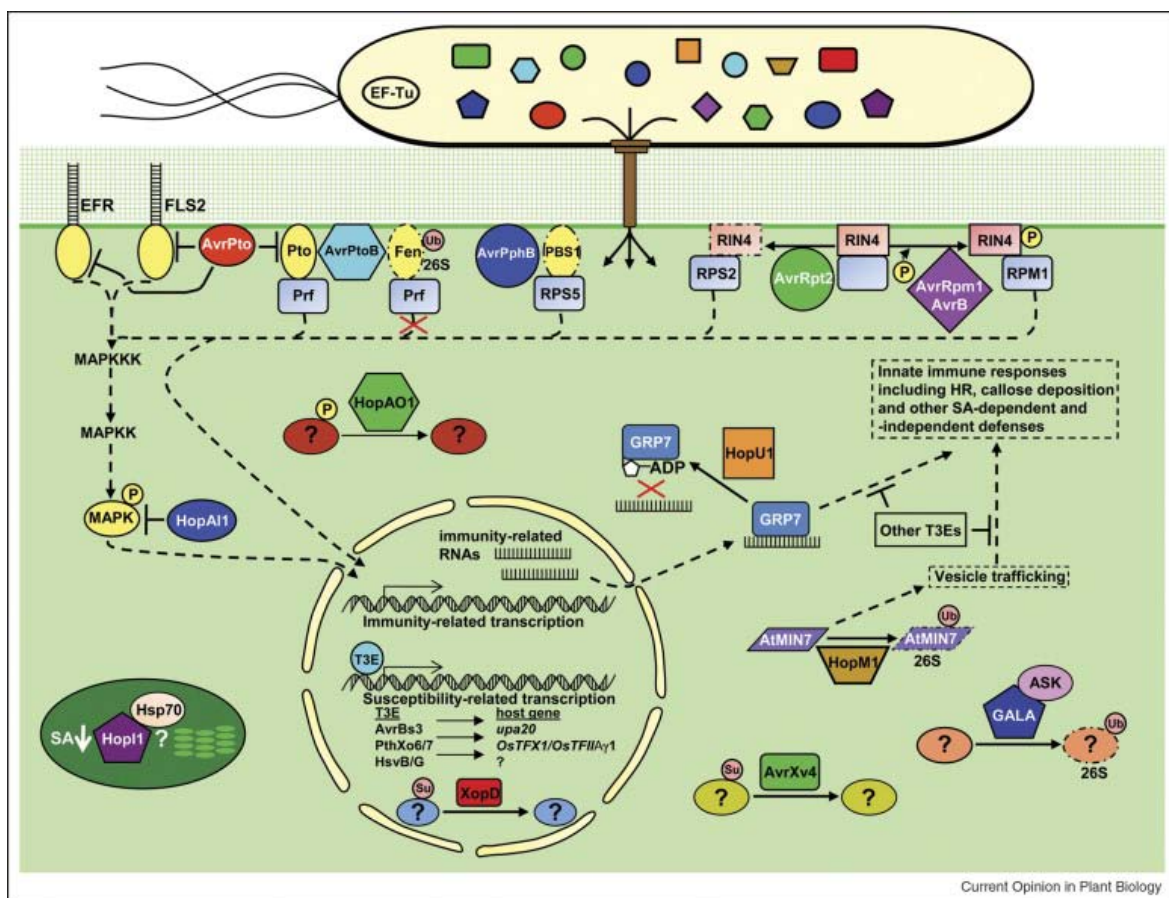


Figure 8: *Pseudomonas* effectors subvert innate immunity from Block *et al.*, 2008.

### 1.5.2 RIN4: bullseye

RIN4 was initially identified as an AvrB-interacting protein in a Y2H screen, and was also found to interact with RPM1, hence it was called RPM1-interacting 4 (RIN4) (Mackey *et al.*, 2002). RPS2 interacts with RIN4 at the plasma membrane (Belkhadir *et al.*, 2004), and degradation of RIN4 by cysteine protease effector AvrRpt2 (Axtell *et al.*, 2003) results in RPS2 activation, and subsequent HR (Mackey *et al.*, 2003). RIN4 is also targeted for phosphorylation by AvrRpm1 and AvrB, and this modification is detected by RPM1, which triggers defense responses (Mackey *et al.*, 2002). Importantly, AvrRpt2, AvrRpm1 and AvrB retain virulence functions in the absence of their cognate resistance proteins and RIN4 (Belkhadir *et al.*, 2004), opening up the possibility that these effectors are targeting other host proteins, which are protected by RIN4 that acts as a decoy (see Decoy Model § 1.6.1.1). Alternatively, some as yet uncharacterized manipulation of RIN4 by these effectors may promote pathogen virulence.

The key regulators of stomatal opening, the H<sup>+</sup>- ATPases AHA1 and AHA2, were recently found to be enriched in detergent-resistant membranes (DRMs) upon flg22 elicitation, along with other immunity-related proteins including FLS2 (Keinath *et al.*, 2010). Although RIN4 was not identified in DRMs, RIN4 is known to interact with AHA1/2 and in this way plays a role in the control of stomatal opening (Liu *et al.*, 2009). The failure of *Pto* DC3000 to activate re-opening of stomata in *rin4* plants supports this role (Liu *et al.*, 2009).

It seems counterintuitive that an effector should instigate destruction of RIN4, described as a negative regulator of basal defense responses (Kim *et al.*, 2005c). However, while RIN4 degradation negatively affects PTI responses, it simultaneously prevents ETI activation in response to RIN4 modification detected by RPM1. In 1996 Ritter and Dangl noticed that AvrRpt2 inhibits RPM1-mediated responses (Ritter and Dangl, 1996), this is achieved through the destruction of RIN4 and is suppressed when *RIN4* is overexpressed (Mackey *et al.*, 2003). RPM1-induced ETI responses are more intense than those initiated by RPS2; RPS2-induced HR occurs at 15 hours as opposed to 5 hours for RPM1 (Ritter and Dangl, 1996; Katagiri and Tsuda, 2010; Kim *et al.*, 2005c) - this could offer an advantageous compromise for the pathogen. Furthermore, RIN4 is required for

RPM1 protein stability (Mackey *et al.*, 2002), and decreased RIN4 levels are associated with reduced RPM1-induced signaling. Thus, by eliminating RIN4 the pathogen also sidesteps RPM1 activation, although RPS2 is then activated. To complicate matters even more, AvrRpm1 can induce defense responses dependent on *RPS2*, in plants lacking *RPM1* (Kim *et al.*, 2009b). However, it is important to bear in mind that *Pto* DC3000 does not naturally contain AvrRpt2, AvrRpm1 and AvrB, making the competitive interaction between these effectors during infection of *Arabidopsis* unlikely.

RIN4 is an enigmatic protein – it has no domains of known function and aside from a role in stomatal aperture control and as a negative regulator of PTI (Kim *et al.*, 2005c), its mechanism of action remains elusive. This mystery has attracted the attention of several groups over the last years, revealing that RIN4 succumbs to not only the effects of AvrRpt2, AvrRpm1 and AvrB, but also HopF2, AvrPto, AvrPtoB, HopAM1 and HopPtoQ (Wilton *et al.*, 2010; Luo *et al.*, 2009). The fact that RIN4 is ‘persecuted’ by sequence divergent effectors hints at the idea that effectors have convergently evolved to target this important protein.

Recently, it was shown that AvrPto can also cause degradation of tomato RIN4 homologs *in planta* in a Prf- and Pto-dependent manner (Luo *et al.*, 2009). This degradation occurs via the proteasome and is not required for HR in *N. benthamiana* and tomato (Luo *et al.*, 2009). Tomato homolog S/RIN4 interacts with both AvrPto and AvrPtoB, and loss of S/RIN4 is associated with increased resistance to *Pto* T1 expressing AvrPto (Luo *et al.*, 2009). Furthermore, the interaction between Pto and AvrPto is required for RIN4 breakdown, as is the AvrRpt2-targeted cleavage site. Interestingly, AvrPto itself is not required, as auto-active Pto can initiate RIN4 proteolysis. This suggests that RIN4 degradation is occurring as a consequence of Pto activation and relies on an endogenous plant proteolytic pathway independent of HR (Luo *et al.*, 2009).

HopF2 is a *Pto* DC3000 effector previously studied for its potent suppression of PTI responses (Li *et al.*, 2005). In recent work, HopF2 was shown to interact with RIN4 and specifically suppress AvrRpt2-mediated HR upon overexpression, but not when delivered from TTSS (Wilton *et al.*, 2010). RIN4 was proposed to be a virulence target for HopF2, as HopF2 ETI suppression and enhanced bacterial growth occurred only in the presence of RIN4 (Wilton *et al.*, 2010). Importantly, TTSS-delivered HopF2 PTI suppression is maintained in the absence of RIN4,

pointing to the existence of other HopF2 targets (Wilton *et al.*, 2010). Subsequently, HopF2 was found to ADP-ribosylate RIN4, as well as MKK4 and MKK5, thus inhibiting PAMP-induced MAP kinase activation (Wang *et al.*, 2010b). HopF2 could also interact with other MKKs including MKK1, the upstream activator of MPK4. Work by the same group revealed RIN4-MPK4 interactions as well as a role for MPK4 in the AvrB-induced phosphorylation of RIN4 *in vitro* (Cui *et al.*, 2010), further implicating MAP kinases upstream of RIN4-mediated signaling pathways.

## **1.6 *Effector-triggered Immunity (ETI), Level 2 Defense***

During the evolution of pathogens, certain phytopathogenic organisms have developed the ability to overwhelm PTI through evasion or suppression of the plant defense system using acquired virulence factors. The susceptible plants became hosts to those specific microbes. Consequently, certain cultivars of originally susceptible plants evolved *R* genes for the specific recognition of a pathogen strain, which confers resistance to this particular strain/race of pathogen. This type of resistance is referred to as effector-triggered immunity (ETI).

### **1.6.1 Resistance genes**

*R* genes encode receptors designed to perceive microbial virulence proteins, called effectors (avirulence, Avr). Over 40 *R* genes have been cloned over the last twenty years, most of them sharing the same structural organization: a nucleotide-binding site (NB) combined with a C-terminal LRR domain. Interestingly, similar domains are found in mammalian NOD-like receptors (NLRs) that are PRRs (Ausubel, 2005).

The NB domain forms part of a larger domain, the NB-ARC, shared between R proteins and human APAF1 (apoptotic protease-activating factor 1) and the *C. elegans* homolog CED4 (cell death abnormality). The NB and ARC domains in combination form a functional nucleotide-binding pocket (Tamelink *et al.*, 2002). Proteins in possession of the NB-ARC domain belong to the STAND (signal

transduction ATPases with numerous domains) family of ATPases (Lukasik and Takken, 2009). The N-termini of NB-LRRs proteins are variable: either a Toll interleukin1 receptor homology (TIR) domain [TIR-NB-LRR or TNL] (e.g. RPS4; N) or a coiled-coil (CC) domain [CC-NB-LRR or CNL] (e.g. RPM1; RPS2; RPS5; Rx; Mla) is usually present (Meyers *et al.*, 2003). This N-terminal variable region binds to specific host proteins, either effector targets or downstream regulatory components (discussed below). The C-terminal LRR domain, which ostensibly forms a solenoid shape, also has a proposed role in protein-protein interactions (Lukasik and Takken, 2009).

In plants and mammals, stress signaling follows a similar pattern. First, stressors are detected in/directly by a sensor protein (NLR or R protein); this is followed by sensor oligomerization facilitating recruitment of downstream signaling proteins and initiation cellular repair/defense responses. The archetypal example of this scheme is the formation of the NLRP3 inflammasome in response to PAMPs or DAMPs in mammals. In contrast to mammalian transmembrane TLRs and NLRs, plant NB-LRR receptors recognize pathogen-encoded effector proteins and are often cytoplasmic. NB-LRR proteins are activated by the delivery of virulence factors (effectors) into the cell (Jones and Dangl, 2006).

Studies of NB-LRR proteins have been dominated by the following questions: (1) how do R proteins work? (2) how have they evolved for recognition of Avr products?

### **1.6.1.1 How R proteins work: Avr against guards, decoys and evolution**

The LRR domain, which is under diversifying selection, (McDowell and Simon, 2006) appears to be the site of NB-LRR recognition specificity. At the outset, it appeared as if this would mediate direct interactions between NB-LRR and Avr, but this type of receptor-ligand relationship has seldom been detected. A direct mode of R-Avr recognition was shown for the *Magnaporthe grisea* Avr-Pita effector and cognate rice CNL Pi-ta (Jia *et al.*, 2000). Similarly, flax multigenic loci (K, L, M, N, P) encode allelic variants, which interact with effectors from the flax rust fungus

(Ellis *et al.*, 2007). A direct interaction was also detected *in planta* between the *Hpa* effector ATR1 and the LRR domain of the cognate R protein RPP1 (Krasileva *et al.*, 2010). However, these examples appear to be the exception rather than the rule leading to the development of the **guard hypothesis** (Dangl and Jones, 2001). Here, the NB-LRR detects changes in a distinct host protein, the **guardee**, which is the victim of Avr action. The model suggests that **guardees** should be virulence targets, and this has been shown in some cases.

RIN4 is a classic case of the guard hypothesis. RIN4 is constitutively bound to the CNL receptors RPM1 (resistance to *P. maculicola* protein resistance to *P. maculicola* protein 1) and RPS2 (resistance to *P. syringae* 2). RIN4 preserves RPS2 in an inactive state until its cleavage (Day *et al.*, 2005) by AvrRpt2, a cysteine protease (Axtell *et al.*, 2003; Mackey *et al.*, 2003; Kim *et al.*, 2005a). Likewise, AvrRpm1 and AvrB bring about phosphorylation of RIN4, resulting in RPM1 activation (Mackey *et al.*, 2002). RIN4 modification functions as an activator of RPS2 or RPM1, to trigger plant defense.

In the case of the *Nicotiana glutinosa* receptor N, the host target is not constitutively bound to the receptor, but rather in the presence of p50, the TMV avirulence effector (Caplan *et al.*, 2008). The indirect interaction between N and p50 is mediated by N-receptor interacting protein 1 (NRIP1). Normally localized to chloroplasts, NRIP1 can be found in the cytoplasm and nucleus in response to p50 (Caplan *et al.*, 2008). NRIP1-p50 probably associates with N, leading to defense activation.

A further refinement of the guard model has recently been proposed. In the **decoy model**, van der Hoorn and Kamoun suppose that a given effector has a host target which is distinct from the cognate R proteins, but they put forward that the **guardee** is in an precarious situation, subject to two opposing natural selection forces in individual plants, driving maintenance or loss of functional R genes. The two opposing selective pressures acting on the effector-interaction surface of the **guardee** provokes the evolution of a host protein, the “decoy,” that specializes in perception of the effector by the R protein but itself has no specific function in disease or resistance. Simply put, the decoy does not constitute a true virulence target, but it should resemble one. As a consequence, the decoy imitates effector

targets to block the pathogen into a recognition event (van der Hoorn and Kamoun, 2008).

The decoy model is illustrated by the tomato Ser/Thr kinase Pto, which acts as a decoy for the molecular targets (EFR, FLS2, CERK1, BAK1) of effectors AvrPto and AvrPtoB. Pto mediates the association of Prf, a CC-NB-LRR and AvrPto (Mucyn *et al.*, 2006). AvrPto is a kinase inhibitor, but inhibition of Pto kinase does not initiate defense (Xing *et al.*, 2007), rather the AvrPto-Pto association triggers defense (Scofield *et al.*, 1996); (Tang *et al.*, 1996). Usually Pto and Prf interact and stabilize each other (Mucyn *et al.*, 2006) in an inactive complex; the disruption of this complex by AvrPto abolishes the inhibitory action of Pto, allowing Prf to activate defense. Pto also inhibits the AvrPtoB E3 ligase activity to induce ETI in resistant tomato plants (Ntoukakis *et al.*, 2009). The Pto kinase domain is similar to that of EFR, FLS2 and BAK1, and Pto competes with FLS2 for interaction with AvrPto (Xiang *et al.*, 2008), luring the effector away from its virulence targets. Thus, Pto prevents the targeting of PTI and also induces activation of the immune receptor, which feeds into defense signaling.

The CNL RPS5 detects the proteolysis of the RLCK decoy PBS1 (AvrPphB susceptible 1) by the *Pseudomonas* effector AvrPphB, activating HR (Shao *et al.*, 2003); (Swiderski and Innes, 2001). PBS1 interacts with RPS5 CC domain prior to its cleavage by AvrPphB, and the loss of PBS1 interaction results in ATP-mediated activation of RPS5 (Ade *et al.*, 2007). However, AvrPphB can also cleave related RLCKs involved in PTI, namely BIK1 and PBS1-like (Zhang *et al.*, 2010a). Thus PBS1 may behave as a decoy for these virulence targets to promote RPS5 activation.

### **1.6.1.2 How R proteins work: Intramolecular switch**

The mechanism of immune receptor activation is of great importance to plants, as resistance responses such as HR come at a high cost, and should not be erroneously activated, yet they must be swiftly switched on in response to attack. This occurs via intramolecular rearrangements, thought to open the NB domain, and allowing cleavage and cycling of the bound nucleotide (Ting *et al.*, 2006). The CNL Rx, which provides resistance to potato virus X (PVX), has been used as a

model to understand intramolecular activation of immune receptors (Lukasik and Takken, 2009).

The NB-ARC domain can be considered as a molecular switch for R activation: the state where ADP is bound is “off”, while the “on”-state features bound ATP. The CC and LRR domains bind the NB-ARC, creating a recognition platform for Avr binding, in this case for PVX coat protein (CP). The negative regulatory LRR domain stabilizes this closed conformation. Following perception of Avr, the surface between the LRR N-terminus and the ARC2 subdomain shifts to release the auto-inhibition. This is followed by nucleotide exchange and subsequent conformational changes, making the NB domain available to interact with downstream signaling components. Hydrolysis of ATP would switch the receptor “off” (see Figure 9). In Rx, a well-conserved motif of the CC domain (EDVID) mediates intramolecular interactions, while the N-terminus offers possibilities for interaction with diverse proteins. For example, Rx requires RanGAP2 for its function, and this interaction is mediated by the sequences bordering the EDVID and the N-terminus (Rairdan *et al.*, 2008).

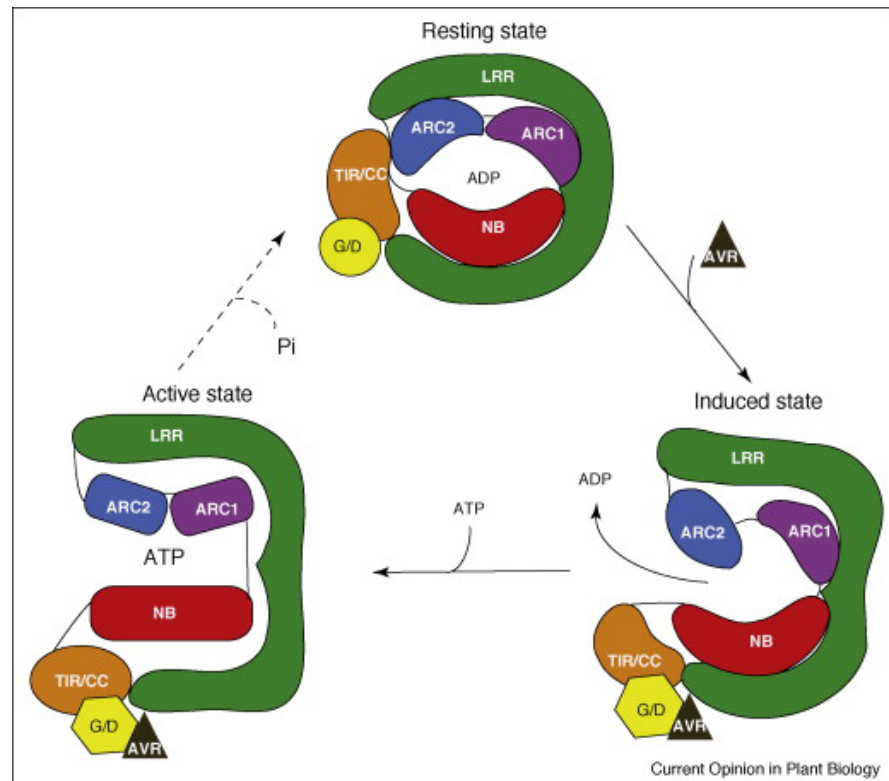


**Figure 9: Model for NB-LRR protein activation from Lukasik and Takken, 2009.**

In the absence of a pathogen an NB-LRR protein resides in its resting (ADP) state, in which the LRR stabilizes the closed conformation. The recognition platform for the AVR protein (brown triangle) is provided by the C-terminal part of the LRR together with CC/TIR domain (CC) and the latter could be bound to an

interactor (referred to as guardee or decoy – G/D). Perception of the AVR (direct or via the G/D) changes the interaction surface between the N-terminal part of the LRR and the ARC2 subdomain, thereby releasing the autoinhibition conferred by the LRR. Subsequent nucleotide exchange triggers a second conformational change, altering the interactions of the NB-ARC domain with CC and LRR domains (induced state). In the activated state the NB subdomain is accessible to interact with downstream signalling partners. Hydrolysis of ATP could return the protein to its resting state.

A synthesis of the decoy model and the model for R activation with a focus on evolution is described by the bait-and-switch model (Collier and Moffett, 2009). Here, the interaction between the bait (decoy) and the R protein precedes R protein activation using the mechanism described above. The bait draws in the Avr protein, which will activate the R protein (“on” switch) through the release/degradation of the bait. In this way, the interaction between the R and the bait via the less evolutionarily constrained LRR can be used to fish for diverse Avrs, expanding R recognition specificity. At the same time, conservation of the nucleotide-binding pocket allows activation of the R protein funneled into a conserved set of downstream signaling responses.

The idea that nucleotide binding pocket modification brings about NB-LRR activation is well established, however this has not been confirmed for TNLs and CNLs. These 2 groups of NB-LRRs have differential signaling requirements (Aarts *et al.*, 1998), and as such it would not be surprising if their activation mechanisms also differ. For example, no CC domain can function autonomously, but the RPS4 and RPP1A TIR domains are sufficient to induce defense responses (Swiderski *et al.*, 2009).

### **1.6.1.3 Resistance genes pair up for action**

Several examples have been found where disease resistance to a pathogen isolate or response to an Avr gene product sometimes requires pairs of NB-LRRs (Eitas and Dangl, 2010). It is known that multiple effectors can be detected by a single R protein, indeed the sequence unrelated *P. syringae* effectors AvrB and AvrRpm1 activate disease resistance mediated by the CNL1 RPM1 (Bisgrove *et al.*, 1994; Grant *et al.*, 1995). These effectors are N-myristoylated and localized at the plasma membrane, where they interact with RIN4, resulting in RIN4 phosphorylation, which is detected by RPM1 and leads to its activation. AvrB and AvrRpm1 have multiple targets in *rpm1* (Belkhadir *et al.*, 2004), indicating that

multiple R genes have evolved to detect molecular changes in effector targets. However, it had been difficult to take apart the ability of each effector to induce disease resistance.

In the absence of *RPM1*, expression of AvrB leads to chlorosis in a RIN4-independent manner (Belkhadir *et al.*, 2004), which could represent the virulence function of AvrB *in planta*. To identify AvrB-specific host targets required for chlorosis, Eitas and colleagues screened mutagenized population of *RPM1* mutant accession Mt-0/Dex::AvrB plants for this inducible phenotype (Eitas *et al.*, 2008). Thus, the TNL TAO1 was identified as required for chlorosis as well as *PR-1* gene induction in response to AvrB (Eitas *et al.*, 2008). In Col-0, *TAO1* is required for resistance to *Pto* DC3000 but not *Pto* DC3000/AvrRpm1. Importantly, the protein level of *RPM1* is unaffected in *tao1* alleles with compromised disease resistance, thus *TAO1* is not simply required for *RPM1*, but rather these R proteins act in concert to provide robust resistance to *Pto* DC3000 expressing AvrB. This finally disconnects AvrB and AvrRpm1 effector recognition in *Arabidopsis*, and provides an illustration of enhanced flexibility and disease resistance amplitude gained through cooperation of immune receptors.

*RPS2* is a CNL R protein required for resistance to *Pto* carrying AvrRpt2 (Kunkel *et al.*, 1993). In *rpm1* plants, AvrRpm1 induces necrosis, chlorosis and PR-1 accumulation (Kim *et al.*, 2009b). However, in *rpm1 rps2* *Arabidopsis* plants conditionally expressing AvrRpm1, these responses, and disease resistance was reduced (Kim *et al.*, 2009b). Similarly, plants lacking *RPS2* display AvrRpt2-induced chlorosis, necrosis and PR-1 expression. However in *rpm1 rps2* plants expressing Dex:AvrRpt2, symptoms were reduced (Kim *et al.*, 2009b). Overall, *RPS2*-mediated responses to AvrRpm1 contribute to defense responses against *Pto*, despite being weaker than those triggered by AvrRpt2 (Kim *et al.*, 2009b). As discussed previously, *RPM1* and *RPS2* guard RIN4. Thus, perturbations of RIN4 may mediate the weak activation of *RPM1* by AvrRpt2 and of *RPS2* by AvrRpm1.

The tandem TNLs *RRS1* and *RPS4* together confer resistance to strains of *Ralstonia solanacearum*, as well as *Pto* carrying AvrRps4 and the fungal pathogen *Colletotrichum higginsianum* (Deslandes *et al.*, 2003; Narusaka *et al.*, 2009; Birker *et al.*, 2009). This provides an interesting case of two related R proteins co-

operating to overcome infection by three different pathogens.

#### 1.6.1.4 Sneaky resistance: SNC1

SNC1 is a TNL type resistance protein, which was identified in a screen for *npr1* suppressors, as a dominant mutant *snc1-1*, for *suppressor of npr1-1, constitutive 1* (Li *et al.*, 2001). *Snc1-1* as well as *snc1 npr1* constitutively expresses *PR* genes and accumulate SA, leading to resistance to *P. syringae* pv. *maculicola* ES4326 and *Hpa* Noco2. Resistance triggered by SNC1 follows SA-dependent and independent pathways, and is dependent on PAD4 (Zhang *et al.*, 2003b). Importantly, *snc1* does not display spontaneous lesions (Zhang *et al.*, 2003b), suggesting that R-mediated resistance can be dissected from cell death, and SNC1 activation in *snc1* follows a unique mechanism. The mutation in SNC1 responsible for the constitutively active *snc1* phenotype is located between the NB-ARC and LRR (Zhang *et al.*, 2003b). Interestingly, SNC1 is clustered with *RPP4* and *RPP5*, with which it shares amino acid similarity. The *R* genes in the RPP5 cluster are co-regulated through gene-silencing machinery (Yi and Richards, 2008). Due to the fitness costs associated with maintenance of *R* gene loci in plants (Tian *et al.*, 2003), *R* regulation is very important and occurs via several mechanisms. *R* genes in the RPP5 locus are also transcriptionally regulated by an SA-dependent positive feedback loop, and over-expressed SNC1 can cause co-suppression of these *R* genes (Yi and Richards, 2007). Furthermore, steady state expression of is elevated in mutants of RNA silencing machinery, including *dcl4-4* and *ago1-36* (Yi and Richards, 2007).

A suppressor screen in *snc1* and *snc1 npr1* backgrounds identified several *modifier of snc1 (mos)* mutants (Zhang and Li, 2005). MOS1, which corresponds to DDM1 (decrease in dna methylation1), regulates SNC1 expression through its role in chromatin remodeling and DNA methylation (Li *et al.*, 2010a). *Mos1* reduces SNC1 expression and causes aberrant DNA methylation upstream of SNC1 (Li *et al.*, 2010a). The inability of MOS1 to regulate expression of transgenic SNC1 proves that MOS1 functions at chromatin level (Li *et al.*, 2010a).

MOS3 is a putative nucleoporin 96 (Zhang and Li, 2005) and MOS6 is an importin  $\alpha$ 3-homolog, while MOS7 is related to nucleoporin Nup88 from *Drosophila* and

mammals, which limits nuclear export of activated NF- $\kappa$ B TFs (Cheng *et al.*, 2009). In *mos7* plants, nuclear accumulation of SNC1, EDS1 and NPR1 is reduced (Cheng *et al.*, 2009). The importance of these nuclear proteins in regulation of innate immunity highlights the role of nucleo-cytoplasmic trafficking in resistance signaling. MOS2, a nuclear protein with RNA-binding motifs also suggests that RNA processing plays a role in innate immunity (Zhang *et al.*, 2005). MOS5, a component of ubiquitin pathway implicates ubiquitination in plant defense (Goritschnig *et al.*, 2007).

Subsequently, a complex was identified comprising several immune regulators: MOS4; the MYB transcription factor cell division cell cycle 5 (AtCDC5/MAC1) and pleiotropic regulatory locus 1 (PRL1/MAC2), all of which are required for resistance signaling (Palma *et al.*, 2007). MOS4 and PRL1 interact with AtCDC5, suggesting that these proteins belong to a large immune complex, MOS4-associated complex (MAC) (Palma *et al.*, 2007). In humans and yeast, the homologs of these proteins belong to the Nineteen Complex (NTC), a complex associated with the spliceosome assembly (Ajuh *et al.*, 2001), and the plant MAC may have similar associations. Further work to characterize the nature of the MAC in *Arabidopsis* led to the identification of 24 MAC components by proteomic analysis (Monaghan *et al.*, 2009). Among those identified were homologous proteins resembling the human and yeast E3 ligase Prp19, named MAC3A and MAC3B, and found to possess E3 ligase activity (Figure 7) (Monaghan *et al.*, 2009). These functionally redundant proteins are required for basal and R-gene-mediated resistance (Monaghan *et al.*, 2009). It is possible that the MAC targets defense repressors for degradation, MOS4 acting as a scaffolding protein for AtCDC5/MAC1 coordinating transcriptional changes, perhaps in close association with the spliceosome, in parallel with protein degradation by MAC3A/MAC3B.

### **1.6.1.5 Receptor like proteins**

In addition to the CNL or TNL R proteins described, several others have been identified. In tomato, an array of Cf LRR-RLPs provide resistance to the biotrophic fungus *Cladosporium fulvum*, through the recognition of their cognate Avr genes (Fritz-Laylin *et al.*, 2005).

The best-studied example is Cf9, which confers resistance to *C. fulvum* carrying Avr9 - a small cysteine-rich peptide (Jones *et al.*, 1994), and recognition results in HR in Cf9 tobacco and Cf9 tomato (Hammond-Kosack and Jones, 1997). Interestingly, Cf9 encodes a short cytoplasmic tail but lacks an intracellular signaling domain, suggesting that it interacts with an adaptor to facilitate signal transduction. This adaptor has not been identified, however the Cf9-Avr9 interaction has been used to elucidate several aspects of resistance gene-mediated signaling. Interestingly, resistance to the fungal pathogen *Venturia inaequalis* is conferred by the apple *Vf* locus, which has homology to tomato Cf (Vinatzer *et al.*, 2001). The *Ve1* gene encodes a tomato RLP that provide resistance to *Verticillium* wilt (Kawchuk *et al.*, 2001; Fradin *et al.*, 2009).

### 1.6.1.6 Chaperones associated with R-mediated signaling

RAR1 (required for *Mla12* resistance), which facilitates *R* gene function in plants (Freialdenhoven *et al.*, 1994), contains 2 CHORDs (Cysteine and histidine-rich domains), which often occur in pairs. Animal CHORD-containing proteins such as Chp1 and melusin (Brancaccio *et al.*, 2003), have an supplementary CS (crystallin and small heat shock protein-like) domain, with structural similarity to heat shock proteins (Garcia-Ranea *et al.*, 2002). RAR1 and melusin can interact with another CS domain-containing protein SGT1 (suppressor of G2 allele of *skp1*) (Azevedo *et al.*, 2002), originally known from yeast (Kitagawa *et al.*, 1999). RAR1 and SGT1 are fundamental for the function of NLRs in plants (Shirasu and Schulze-Lefert, 2003), while mammalian SGT1 plays a similar part in the activation of animal NLRs (da Silva Correia *et al.*, 2007; Mayor *et al.*, 2007). Importantly, not all R proteins require RAR1, although members of both CNL and TNL classes are RAR1-dependent, and include barley *Mla1* and *Mla6*; *Arabidopsis* RPP4, RPP5, RPM1, RPS2, RPS4 and RPS5; soybean *Rpg1b* and potato *Rx* (Musket *et al.*, 2002; Tornero *et al.*, 2002; Bieri *et al.*, 2004; Fu *et al.*, 2008).

Historically, conflicting results have prevented the confirmation of a role for mammalian CHORD proteins in NLR function (da Silva Correia *et al.*, 2007; Hahn, 2005). SGT1 function is reliant on its interaction with Hsp90 (heat shock protein 90), the molecular chaperone (Botér *et al.*, 2007; Liu *et al.*, 2004; Mayor *et al.*,

2007; Zhang *et al.*, 2008; Shirasu, 2009). CHORD proteins can bind Hsp90 and SGT1, creating stable Hsp90-Sgt1-CHORD complexes (Botér *et al.*, 2007; Shirasu and Schulze-Lefert, 2003). In these complexes, the CS domain possesses distinct binding sites for Hsp90 (Catlett and Kaplan, 2006; Lee *et al.*, 2004) and RAR1 (Botér *et al.*, 2007). In contrast, the SGT1-specific (SGS) domain of SGT1 facilitates its interaction with LRR domain of NLRs such as potato Rx, tobacco N and human Nod1 (Bieri *et al.*, 2004; da Silva Correia *et al.*, 2007; Leister *et al.*, 2005).

SGT1 and the CHORD proteins are not dependent on Hsp90 as client proteins, but rather function as co-chaperones. SGT1 also functions downstream of NLR function as part of the SCF E3 ubiquitin ligase complex (Catlett and Kaplan, 2006; Kadota *et al.*, 2008), targeting proteins for proteasomal degradation (Azevedo *et al.*, 2002). SGT1 links HSP90 chaperone to the SCF complex to bring about ubiquitination of client proteins (Zhang *et al.*, 2010b), possibly to degrade negative regulators of defense responses (Zhang *et al.*, 2010b; Botér *et al.*, 2007).

Recently, the crystal structure of a complex comprising the N domain of Hsp90, SGT1 CS domain and RAR1 CHORD domain was determined (Zhang *et al.*, 2010b). Mutagenesis of the interaction surfaces compromises NLR-mediated resistance to viruses, providing evidence of a biological role for the interactions. Analysis of the complex suggests that CHORD domain proteins structurally influence the chaperone to regulate ATPase-coupled conformational cycles, though the role in NLR activation is not known.

CRT1 (compromised recognition of TCV) is a member of the same GHKL (Gyrase, Hsp90, histidine kinase, MutL) ATPase/kinase superfamily as Hsp90 (Kang *et al.*, 2008). CRT1, localized to endosomes (Kang *et al.*, 2010), has been shown to interact with the ARC domains of diverse CNLs and TNLs (including Rx, RPS2, SNC1, RPP8 and RPM1) in their inactive states (Kang *et al.*, 2010). Furthermore, CRT1 has been shown to interact weakly with Hsp90 (Kang *et al.*, 2010), possibly functioning as a co-chaperone or scaffolding protein. Finally, the resistance protein N relies on several chaperones including NbCRT2 and NbCRT3 and protein disulphide isomerases NbERp57 and NbP5 for its function in TMV resistance (Caplan *et al.*, 2009).

### 1.6.1.7 Functions of NB-LRR proteins

The question of how resistance proteins activate immune responses following effector recognition has been plaguing researchers since the discovery of this phenomenon. Recent discoveries related to the nuclear localization of R proteins have started to shed some light on their mechanisms of action.

Allelic barley Mla CNL type receptors have been localized in the cytoplasm and nucleus of epidermal cells (Shen *et al.*, 2007), with the amount of Mla10 increasing in the nucleus during the defense response to *Blumeria graminis*. Similarly, the tobacco TNL type receptor N in *N. benthamiana* is nuclear and cytoplasmic localized (Burch-Smith *et al.*, 2007). Nuclear N is not required for recognition of p50. Interestingly, neither of these proteins possesses a nuclear localization sequence (NLS). In contrast, the Arabidopsis TNL type RPS4 protein recognizing *P. syringae* strains expressing AvrRps4 (Gassmann *et al.*, 1999) contains a NLS, which is required for nuclear import and disease resistance (Wirthmueller *et al.*, 2007).

Taken together, these findings suggest that nuclear localization of certain R proteins may be the key to their function. This localization seems fitting, considering the extensive transcriptional reprogramming that occurs upon pathogen attack, affecting 3-12% of the 24 000 Arabidopsis genes tested in response to fungal or bacterial infection (Thilmony *et al.*, 2006; de Torres *et al.*, 2003; van Wees *et al.*, 2003; AbuQamar *et al.*, 2006; Hu *et al.*, 2008; Wang *et al.*, 2008b; Chandran *et al.*, 2009; Tischner *et al.*, 2010). A physical interaction between Mla10 receptor and 2 WRKY transcription factors (TFs) in barley (Shen *et al.*, 2007) suggests a role for TFs as downstream targets for immune receptors. In this example, the function of the interaction seems to be in de-repression of PTI, as Arabidopsis mutants of the corresponding WRKYs display enhanced basal resistance (Shen *et al.*, 2007).

Recently, Topless-related 1 (TPR1) or MOS10 was shown to be a positive regulator of SNC1-mediated immunity (Zhu *et al.*, 2010c). TPR1 is a transcriptional co-repressor that associates with histone deacetylase 19 *in vivo* (Zhu *et al.*, 2010c). TPR1 targets include negative regulators of immunity DND1 and DND2,

suggesting that inhibition of negative regulators is the mechanism by which R-mediated immunity is achieved (Zhu *et al.*, 2010c).

An early indication of R protein function in the nucleus came with the characterization of the *Arabidopsis* receptor RRS1-R (Deslandes *et al.*, 2003). This immune receptor has an unusual domain organization, possessing a C-terminal WRKY domain attached to the usual TNL module. RRS1-R recognizes the *Ralstonia solanacearum* effector PopP2, which co-localizes with RRS1-R in the nucleus and stabilizes RRS1-R (Deslandes *et al.*, 2003). An RRS1-R mutant without DNA-binding activity displays chronic defense gene expression and occasional cell death in the absence of pathogens (Noutoshi *et al.*, 2005). This suggests a role for the immune receptor in binding DNA and suppressing defense gene expression, a function that is inhibited in the presence of the effector PopP2.

### 1.6.1.8 ETI signaling pathways

Analysis of *Arabidopsis* mutants with enhanced disease susceptibility has allowed the delineation of several of plant defense pathways. The membrane-localized protein nonrace-specific disease resistance 1 (NDR1) is required for the function of many CNL R proteins, while many TNL R proteins require the lipase-like proteins enhanced disease susceptibility 1 (EDS1) and phytoalexin deficient 4 (PAD4) (Aarts *et al.*, 1998; Feys *et al.*, 2001), describing at least two separate pathways for ETI signaling. In contrast, the *RPP7* and *RPP8* *H. parasitica* R genes function independently of *EDS* and *NDR1* (McDowell *et al.*, 2000). Interestingly, NDR1 interacts with the C-terminus of RIN4, likely after its cleavage by AvrRpt2, to modulate RPS2 activation (Day *et al.*, 2006).

SA is involved in *avr-R*-mediated defenses and it is required for establishment of SAR and for basal resistance to some virulent pathogens (Cao *et al.*, 1994; Nawrath and Metraux, 1999). There are two classes of enhanced disease susceptibility (*eds*) mutants: those impaired in SA accumulation such as *eds5/sid1* and *eds16/sid2*, (Nawrath and Metraux, 1999; Rogers and Ausubel 1997; Volko *et al.* 1998), and those that are unresponsive to exogenously applied SA such as *npr1/him1* (Cao *et al.*, 1994; Delaney *et al.*, 1995; Shah *et al.*, 1997). *Ndr1* plants

display a partial reduction in SA accumulation following infection (Shapiro and Zhang, 2001), while *EDS16/SID2* encodes isochorismate synthase, a central protein in SA biosynthesis, the loss of which essentially eliminates SA production (Wildermuth *et al.*, 2001). *NPR1* acts downstream of SA to mediate activation of defense genes (Cao *et al.*, 1994; Delaney *et al.*, 1995; Pieterse and Van Loon, 2004) and also affects SA levels, which are often elevated in *npr1* plants (Ryals *et al.*, 1997; Shah *et al.*, 1997). However, SA-dependent defense responses independent of *NPR1* do occur (Glazebrook *et al.*, 1996; Bowling *et al.*, 1997; Rate *et al.* 1999).

Several RPM1-interacting proteins were identified in a Y2H screen, including RPM1-interacting (RIN) RIN1, RIN2, RIN3 and RIN13. RIN1 is the *Arabidopsis* homolog of TIP49a (TBP-interacting protein 49a), a helicase domain-containing protein that interacts with TATA-binding protein (TBP) and is important for nuclear events in mammals and *Drosophila* (Kanemaki *et al.*, 1997; Kanemaki *et al.*, 1999). The link between TIP49 and transcriptional control could be through its modification of chromatin structure, though this has not been shown (Holt *et al.*, 2002). RIN1 is required for meristem development in addition to its role in negative regulation of disease resistance (Holt *et al.*, 2002). TIP49a also interacts with other resistance proteins in addition to RPM1, including RPP5 (resistance to *Peronospora parasitica* 5) (Holt *et al.*, 2002).

RIN2 and RIN3 are both membrane-localized E3 ubiquitin ligases, which have a role in positive regulation of RPM1 and RPS2-responsive HR, but no effect on pathogen growth (Kawasaki *et al.*, 2005). In contrast, RIN13 enhances RPM1-mediated bacterial resistance in the absence of HR when ectopically expressed, and thus has a positive regulatory role for RPM1 function (Al-Daoude *et al.*, 2005). RIN4 was also identified in a Y2H screen, for AvrB interactors, and subsequently also found to interact with RPM1 and AvrRpm1 (Mackey *et al.*, 2002) (see §1.5.2).

## 1.7 Comparison of ETI and PTI signaling modes

PTI and ETI are associated with many of the same molecular responses (Tao *et al.*, 2003; Navarro *et al.*, 2004; Abramovitch *et al.*, 2006; Zipfel *et al.*, 2006), suggesting overlapping signaling cascades. Some researchers consider ETI as an accelerated and amplified PTI response, as PTI typically does not result in cell death, suggesting that this might be to avoid over-reaction to PAMPs, signals that can be considered as less specific than effector targets. A more sophisticated perspective considers that ETI and PTI exploit the same set of signaling components, split into sectors controlled by JA, ET, SA and PAD4, but employ different tactics. PTI uses distinct signaling sectors synergistically, while ETI uses the sectors in a compensatory manner, allowing a more robust form of immune signaling to occur (Figure 10). In this view, signaling is not a linear path but rather a network, which can be manipulated by different input signals to cause responses that differ in intensity and timing (Katagiri and Tsuda, 2010). Also, antagonistic signaling pathways, such as those controlled by SA and JA/ET, are not necessarily engaged simultaneously, but rather serve as back-ups for each other, to create a signaling network that is robust in the face of many threats from effector manipulation and environmental changes (Katagiri and Tsuda, 2010). This is based on the fact that the quadruple mutant *dde2/ein2/pad4/sid2* (compromised in all sectors) is compromised for almost all responses to the PAMP flg22, as well as the effector AvrRpt2 (Tsuda *et al.*, 2009). However, in the same study, AvrRpm1-responsive ETI was not dependent on all 4 signaling sectors (Tsuda *et al.*, 2009). The authors propose that the difference between AvrRpt2- and AvrRpm1-dependent responses can be characterized not by their use of signaling machinery, but rather in their rapidity, with AvrRpm1 responses being faster (Tao *et al.*, 2003; Ritter and Dangl, 1995; Tsuda *et al.*, 2009). The same group made similar observations upon expression profiling of *Arabidopsis* - *P. syringae* incompatible and compatible interactions, specifically AvB vs AvrRpt2-responsive genes (Tao *et al.*, 2003). AvrRpm1 could be considered a more powerful effector than AvrRpt2 (Kim *et al.*, 2005c) while RPM1 offers inflated fitness costs compared to RPS2 (Tian *et al.*, 2003).

Whatever the case, these hypotheses underscore that there is certainly a connection between PTI and ETI, and we are approaching an understanding of this link with each new discovery. Future work will aim to identify components linking PTI and ETI, perhaps through differential proteomic analysis of *Arabidopsis-Pseudomonas* interactions. However, we should approach oversimplified views of defense signaling with caution, as there is a danger of overlooking crucial aspects in an attempt to fit data into a model of our design, rather than that of nature.

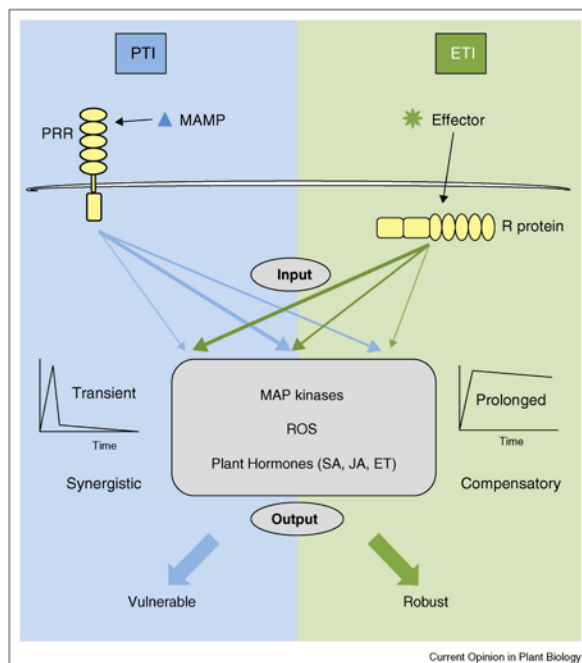


**Figure 10: Signaling network interactions governed by PTI and ETI from Tsuda and Katagiri, 2010.** A common signaling machinery is used differently in PTI and ETI. A MAMP is recognized by a PRR and triggers downstream responses for PTI. An effector is recognized by an R protein to trigger downstream responses for ETI. Although signaling machinery employed in PTI and ETI is extensively shared, it is utilized differently in PTI and ETI. The shared network is likely to have multiple input points, and we speculate that differences in levels and/ or timing of multiple inputs, which are symbolized by different weights of the arrows in the figure, result in different ways of using the shared network. The different ways of using the network are manifested by: induced responses are transient in PTI and prolonged in ETI; synergistic relationships among the signaling sectors are evident in PTI; compensatory relationships among the sectors dominate in ETI. These differences might explain vulnerability of PTI to perturbations caused by pathogens and robustness of ETI against both pathogenic and genetic perturbations.

## Part II

## 2 Materials and Methods

### 2.1 Plant material and growth conditions

#### 2.1.1 *Arabidopsis thaliana*

##### 2.1.1.1 Growth conditions

*Arabidopsis thaliana* ecotype Columbia-0 (Col-0) was the background for all mutants and transgenic lines used in this study (Table 2.1). The *Arabidopsis* plants used in this study were grown as 4 plants per pot (9 x 9 cm) at 20–21 °C with a 10 h photoperiod and 65 % humidity, or on plates containing Murashige-Skoog (MS) salts medium (Duchefa), 1% sucrose, and 1% agar with a 16 h photoperiod. The third backcross of *bak1-5* with Col-0 was used for all experiments.

**Table 2-1 List of *Arabidopsis thaliana* and *N. plumbaginifolia* lines used in this study**

Allele/line	Polymorphism	Description	Reference
Col-0	-	Columbia 0, wild-type reference line	
<i>fls2</i>	<i>fls2-17;G1064R</i>	knock-out mutant of the PRR FLS2	(Zipfel <i>et al.</i> , 2004)
<i>efr-1</i>	Salk_044334	knock-out mutant of the PRR EFR	(Zipfel <i>et al.</i> , 2006)
<i>efr-1 fls2</i>	-	double knock-out mutant of FLS2 and EFR	(Nekrasov <i>et al.</i> , 2009)
<i>efr-1/pEFR::EFR-eGFP-HA</i>	-		(Nekrasov <i>et al.</i> , 2009)
<i>bak1-4</i>	Salk_116202	knock-out mutant of BAK1	(Chinchilla <i>et al.</i> , 2007)
<i>bak1-5</i>	C408Y point mutation	EMS-induced missense substitution mutant in BAK1, three times back-crossed to Col-0	(Schwessinger <i>et al.</i> , submitted)
<i>bkk1-1</i>	Salk_057955	knock-out mutant of BKK1	(He <i>et al.</i> , 2007)
<i>bak1-4 bkk1-1</i>	-	double mutant generated by crossing <i>bak1-4</i> with <i>bkk1-1</i>	(He <i>et al.</i> , 2007)
<i>bak1-5 bkk1-1</i>	-	double mutant generated by crossing <i>bak1-5</i> with <i>bkk1-1</i>	(Schwessinger <i>et al.</i> , submitted)
<i>serk1-1*</i>	Salk_044330	Insertion in At1g71830; truncated protein lacking last 130 aa	(Albrecht <i>et al.</i> , 2005)
<i>serk1-3*</i>	GK_448E10	Insertion in At1g71830	(Albrecht <i>et al.</i> , 2008)
<i>serk2-2*</i>	SAIL_119_G03	Insertion in At1g34210	(Albrecht <i>et al.</i> , 2005)
<i>bak1-3/serk3-1*</i>	Salk_034523	Insertion in At4g33430	(Russinova <i>et al.</i> , 2004)
<i>bkk1-1 or serk4-1*</i>	Salk_057955	Insertion in At2g13790	(He <i>et al.</i> , 2007; Kemmerling <i>et al.</i> , 2007)
<i>serk4-2</i>	Salk_089460	Insertion in At2g13790	Gift from Birgit Kemmerling

**Table 2.1 List of *Arabidopsis thaliana* and *N. plumbaginifolia* lines used in this study  
continued**

Allele/line	Polymorphism	Description	Reference
serk5-1	Salk_147275	Insertion in At2g13800	(Albrecht <i>et al.</i> , 2008)
bak1-3 serk4-2	-	Weak alleles	Unpublished
serk1-3 bak1-4*	-		
serk2-2 bak1-4*	-		
<i>N. plumbaginifolia</i> NpPDR1-S1	N/A	Stable line silenced for NpPDR1	Marc Boutry (Stukkens <i>et al.</i> , 2005) (Bultreys <i>et al.</i> , 2009)
pdr12-1	Salk_013945	Insertion in At1g5520	Youngsook Lee (Lee <i>et al.</i> , 2005)
pdr12-2	Salk_005635	Insertion in At1g5520	Youngsook Lee (Lee <i>et al.</i> , 2005)
pdr10-1	Salk_118823	Insertion in At3g30842	Unpublished
pen3-1 /PEN3p::PEN3- GFP	N/A		Gift from Somerville Shauna
<i>pdr12-1 pdr10-1</i>	N/A	Double mutant generated from crossing <i>pdr12-1</i> and <i>pdr10-1</i>	Unpublished
<i>pen3-1</i>	N/A	point mutation causing G354D amino acid change in At1g59870	Gift from Somerville Shauna (Stein <i>et al.</i> , 2006)
<i>pdr8-1</i>	Salk_000578	Insertion in At1g59870	Masayoshi Maeshima Nagoya Uni, Japan (Kobae <i>et al.</i> , 2006)
<i>pdr8-2</i>	Salk_142256	Insertion in At1g59870	Masayoshi Maeshima Nagoya Uni, Japan (Kobae <i>et al.</i> , 2006)
<i>rae5-1</i>	Salk_061769	Insertion in At4g08850	Unpublished, Freddy
<i>rae6-1</i>	Salk_040386	Insertion in At3g14840	Unpublished
<i>xii1-1</i>	GK_031G02	Insertion in At1g35710	Unpublished, Freddy

\*Gift from Sacco de Vries, Wageningen University, The Netherlands

### 2.1.1.2 Stable transformation of *A. thaliana*

The transgenic *Arabidopsis* plants were generated using floral dip method (Clough and Bent, 1998). Briefly, flowering *Arabidopsis* plants were dipped into a suspension culture of *Agrobacterium tumefaciens* AGL1 or GV3101 carrying the indicated plasmid (this was carried out by Matthew Smoker and Jodie Pike). Plants carrying a T-DNA insertion event were selected either on MS media containing the appropriate selection or as soil grown seedlings by the spray application of PPT (phosphinothricine, Duchefa) (this part was carried out by me when on agar plates).

### **2.1.1.3 Generation of *Arabidopsis* F<sub>1</sub> and F<sub>2</sub> progeny**

*(This was used to generate double mutants e.g. pdr12-1 pdr10)*

Fine tweezers were used to emasculate individual flowers. To prevent self-pollination, only flowers that had a well-developed stigma but immature stamen were used for crossing. Fresh pollen from three to four independent donor stamens was dabbed onto each single stigma. Mature siliques containing F<sub>1</sub> seed were harvested and allowed to dry. Approximately five F<sub>1</sub> seeds per cross were grown as described above and allowed to self-pollinate. Produced F<sub>2</sub> seeds were collected and stored.

### **2.1.1.4 *Arabidopsis* seed sterilization**

For *in vitro* growth of *Arabidopsis*, seeds were sterilized. Approximately 50 - 100 *Arabidopsis* seeds were placed into 1.5 ml tubes in plastic racks. 100 ml of 12 % sodium hypochlorite solution (chlorine bleach) was poured into a beaker and put together with the seed into a desiccator. 10 ml of 37 % HCl was directly added into the bleach. The lid of the desiccator was left closed for 4 – 8 h. After the sterilization period, the desiccator was slightly opened under a fume hood for 5 min to let out the gas.

## **2.1.2 *Nicotiana* transient expression**

### **2.1.2.1 Growth conditions**

*N. benthamiana* and *N. plumbaginifolia* plants were grown in controlled environment chambers at an average temperature of 24°C (range 18 – 26°C), with 45-65% relative humidity under long day conditions (16h light).

### **2.1.2.2 Transient expression**

*(Transient expression was used in Chapter 1-5 to test functionality of recombinant proteins or for protein productin for co-immunoprecipitation.)*

*Agrobacterium tumefaciens* GV3101 overnight cultures grown at 28 °C in low-salt LB were harvested by centrifugation at 3500 rpm and resuspended in 10 mM

MgCl<sub>2</sub> to a final OD<sub>600</sub> of 0.3. The cultures were incubated at room temperature for 1 H and then hand-infiltrated on leaves of three to four week old *N. benthamiana* or *N. plumbaginifolia* leaves using a 1 mL needleless syringe. All samples were taken 2 days post infiltration.

## **2.2 PAMP assays**

### **2.2.1 PAMPs**

The following elicitors were used in this study: crab shell chitin (c9752, Sigma, UK), flg22 peptide (CKANSFREDRNEDREV) (Peprton, South Korea), elf18 peptide (ac-SKEKFERTKPHNVGTIG) (Peprton, South Korea), CSP22 (AVGTVKWFNAEKGFGFITPDGG) (Peprton, South Korea) and AtPep1 peptide (ATKWKAKQRGKEKVSSGRPGQHN) (Peprton, South Korea).

### **2.2.2 Seedling growth inhibition**

*(This was done in Chapter 1 for characterization of transgenic lines; also for mutant phenotyping in Chapter 1-3.)*

Freshly harvested seeds were surface-sterilized, sown on MS media, stratified for 2 days at 4°C in the dark and put in the light. Five-day-old seedlings were transferred into liquid MS with or without the indicated amount of peptide and incubated for eight further days. Dry weight of six replicates per treatment was measured using a precision scale (Sartorius) and graphically plotted relative to the untreated control.

### **2.2.3 ROS burst assay**

*(This was done in Chapter 1 for characterization of transgenic lines; also for mutant phenotyping in Chapter 1-3.)*

Eight leaf discs (4 mm diameter) of four 3-4 week-old plants were sampled using a cork borer and floated overnight on sterile water in a white 96-well plate (Bioone). The following day the water was replaced with 100µl/well of solution of 17 mg/ml (w/v) luminol (Sigma) and 10 mg/ml horseradish peroxidase (Sigma) containing 100 nM elf18, flg22, AtPep1 or 100 µg/ml chitin. Luminescence was captured

either using a Varioskan Flash (Thermo Scientific) multiplate reader or Photek camera (East Sussex, UK). The amount of relative light units might differ depending on the light capturing apparatus used.

For ROS assays on whole seedlings, seedlings were grown on GM agar plates before being transferred to GM liquid medium in white 96-well plates. After 8 days or when the seedling was almost the size of the well, the ROS assay was conducted as for leaf discs, except 150  $\mu$ l of solution was added per well.

#### **2.2.4 MAP kinase assay**

*(This method was used to characterize serk mutants in Chapter 3.)*

14-day-old *Arabidopsis* seedlings were grown for five days on MS plates and then transferred to liquid MS. Triplicates of two seedlings each were treated with water, 100 nM elf18 or 100 nM flg22 for 0, 5 and 15 min before being pooled for harvest. Seedlings were ground to fine powder in liquid nitrogen and solubilised in buffer Iacus buffer [50 mM Tris-HCl pH 7.5; 100 mM NaCl; 15 mM EGTA; 10 mM MgCl<sub>2</sub>; 1 mM NaF; 1 mM Na<sub>2</sub>MoO<sub>4</sub>.2H<sub>2</sub>O; 0.5 mM NaVO<sub>3</sub>; 30 mM  $\beta$ -glycerophosphate; 0.1% IGEPAL CA 630; 100 nM calyculin A (CST); 0.5mM PMSF; 1 % protease inhibitor cocktail (Sigma, P9599)]. The extracts were centrifuged at 16,000xg, the supernatant cleared by filtering through Miracloth and  $\frac{1}{4}$  vol of 4xLDS loading buffer (Invitrogen) was added. Samples were heated at 70°C for 20 minutes before loading 40  $\mu$ g of total protein on SDS-PAGE gels for separation at 100V. Gels were blotted onto PVDF membrane (BioRad). Immunoblots were blocked in 5% (w/v) BSA (Sigma) in TBS-Tween (0.1%) for 1-2 H. The activated MAP kinases were detected using anti-p42/44 MAPK primary antibodies (1:1000, Cell Signaling Technology) overnight, followed by anti-rabbit-HRP conjugated secondary antibodies (Sigma).

#### **2.2.5 PAMP-induced defense gene induction**

*(This method was used to characterize pdr and serk mutants in Chapter 1 and 3.)*

14-day-old *Arabidopsis* seedlings grown for five days on MS plates and then transferred to liquid MS were used for all gene induction studies. RNA was extracted using RNeasy Plant Mini kit (Qiagen) followed by DNase-treatment with

Turbo DNA-free (Ambion). RNA was quantified with a Nanodrop spectrophotometer (Thermo scientific). cDNA was synthesized from 2.5 µg total RNA using SuperScript III reverse transcriptase (Invitrogen). SybrGreen master mix (Sigma) was used for qPCR reactions.

For defense gene induction analysis a triplicate of two seedlings each was treated either with water, 100 nM elf18 or 100 nM flg22 for 0, 30, 60 and 180 min and pooled before harvesting. Gene expression of *At2g17740* (*DC1-domain containing protein*), *At5g57220* (*CYP81F2*) and *At1g51890* (*LRR-RLK*) was monitored by qPCR analysis. The expression of each marker gene was normalized to the internal reference gene *At4g05320* (*UBQ10*) and plotted relative to the Col-0 steady-state expression level.

## **2.2.6 PAMP-induced ethylene production**

*(This method was used to characterize serk mutants in Chapter 3.)*

Plants were grown for 6 weeks before sampling 2 mm leaf strips from 4 plants per genotype. Ethylene assays were performed as described by Felix *et al* (1999) using 1µM flg22, elf18 or AtPep1.

## **2.2.7 Crude elicitor extract preparation**

*(These extracts were used in characterization of serk mutants in Chapter 3.)*

*P. syringae* pv. *tabaci* 6605 was grown O/N at 28°C in Kings B medium supplemented with appropriate antibiotics. Cells were pelleted at 4,000 x g for 15 min, washed with 1 volume sterile water and re-suspended in 1/10 volume sterile water. The extract was boiled for 10 min at 95°C, spun down and supernatant applied at a final concentration of 0.1 (v/v).

*Hyaloperonospora arabidopsis* (*Hpa*) crude elicitor was prepared as follows: The aerial parts of 3-4 week old *Ws-0 eds1-1* infected (*Hpa* Emoy2, 7dpi) or non-infected plants were harvested and frozen in liquid nitrogen. 20 ml of cold sterile water was added and mixed vigorously by vortexing. The suspension was cleared of plant debris by filtering through Miracloth and enriched for heavier particles by centrifugation at 300 rpm for 15 mins. The supernatant was decanted and the pellet resuspended in 3ml of sterile water and heated at 95°C for 10 mins. These suspensions were used at a concentration of 1:100.

## 2.3 Pathogen assays

### 2.3.1 Bacterial spray-inoculation of *Arabidopsis*

(This method was used to characterize *pdr* and *serk* mutants in Chapter 1, 2 and 3.)

The strains of *Pseudomonas syringae* pv. *tomato* DC3000 (*Pto* DC3000), *Pto* DC3000 *COR*<sup>-</sup> (coronatine mutant) or *Pto* DC3000  $\Delta$ *AvrPto*/ $\Delta$ *AvrPto* (lacking effectors *AvrPto* and *AvrPtoB*) and *P. syringae* pv. *tabaci* 6605 (*Pta*) were grown overnight in Kings B medium supplemented with appropriate antibiotics. Cells were harvested by centrifugation and pellets resuspended in sterile water to appropriate OD<sub>600</sub> (0.2 for *Pto* DC3000  $\Delta$ *AvrPto*/ $\Delta$ *AvrPto* and *Pto* DC3000 *COR*<sup>-</sup>; 0.02 for *Pto* DC3000). Immediately prior to spraying, Silwett L-77 was added to bacteria to 0.04 % (v/v).

Bacteria were sprayed onto leaf surfaces until run-off and plants maintained at high humidity for 3 days. For syringe inoculation of *P. syringae* pv. *tabaci* (*Pta*) 6605, bacteria were similarly grown and harvested. Cell pellets were resuspended in sterile water to O.D. <sub>600</sub> 0.002 and infiltrated using a needleless syringe into 2 leaves each of 4 plants per genotype.

Samples were taken using a cork-borer (2 mm) to cut leaf discs from 2 leaves per plant and 4 plants per genotype. Leaf discs were ground in water, diluted and plated on TSA with appropriate selection. Plates were incubated at 28°C and colonies counted 2 days later.

### 2.4.2. *H. arabidopsis* inoculation and scoring on *Arabidopsis*

(This method was used to characterize *serk* mutants in Chapter 3; this was done by Nick Holton, Laboratory of Mahmut Tör, University of Warwick.)

*Hpa* infections were performed as described by Tör *et al.*, 2002. Spores were harvested from infected Ws-eds1 seedlings 7 days post-inoculation, suspended in cold water at a density of  $5 \times 10^4$  spores/mL and spray-inoculated onto 7-day-old seedlings to the point of run-off. Inoculated seedlings were incubated at high humidity at 18°C for 7 days then sporulation was assessed. The growth of the *Hpa* strains Cala2 and Emoy2 was assessed by counting the number of

sporangiophores per cotyledon. The reproduction of the *Hpa* strain Emco5 infection was determined by vortexing sporulating seedlings in water and by quantifying spores using a haemocytometer.

### 2.3.2 Pathogens used in this study

**Table 2-2 Summary of pathogens used in this study**

Pathogen	Reference
<b><i>Pseudomonas</i> strains</b>	
<i>Pta</i> 6605	(Shimizu <i>et al.</i> , 2003)
<i>Pto</i> DC3000	(Whalen <i>et al.</i> , 1991)
<i>Pto</i> DC3000 $\Delta$ AvrPto/ $\Delta$ AvrPto	(Lin and Martin, 2005)
<i>Pto</i> DC3000 COR <sup>+</sup>	(Melotto <i>et al.</i> , 2006)
<b><i>Hyaloperonospora arabidopsis</i> isolates</b>	
Cala2	(Holub <i>et al.</i> , 1994; McDowell <i>et al.</i> , 2000)
Emco5	(Holub <i>et al.</i> , 1994; McDowell <i>et al.</i> , 2000)
Emoy2	(Holub <i>et al.</i> , 1994; McDowell <i>et al.</i> , 2000)

## 2.4 Molecular biology

### 2.4.1 DNA methods

#### 2.4.1.1 Isolation of genomic DNA from *Arabidopsis*

*This method was used for genotyping mutants.*

This DNA extraction method yields relatively poor quality DNA sufficient for standard PCR. Aliquots were stored at -20° C. Small leaf samples of an area of about 25 mm<sup>2</sup> were taken with a pair of tweezers and 400 µl of DNA extraction buffer (0.2 M Tris-HCl pH 7.5; 0.25 M NaCl; 0.025M EDTA; 0.5 % (w/v) SDS) were added. The tissue in the tube was crushed either using an electric grinder with blue pestles or by adding a small steel or glass ball to Costar plates and using a Retch grinder. The solution was centrifuged at 3000 rpm for 10 minutes (plates) or 13 000 rpm (eppies) for 5 minutes and 300 µl supernatant was transferred to a fresh tube. One volume of isopropanol was added to precipitate DNA and centrifuged for 15 minutes. The supernatant was discarded carefully. The pellet was washed with 80 % ethanol and dried. Finally the pellet was dissolved in 100 µl

sterilized water and 1  $\mu$ l of the DNA solution was used for a 20  $\mu$ l PCR reaction mixture.

### 2.4.1.2 PCR methods

All PCR reactions were carried out in using a PTC-225 Peltier thermal cycler (MJ Research).

#### 2.4.1.2.1 Standard PCR

This method was used when sequence accuracy was not required. Briefly; the PCR reaction mix contained 2  $\mu$ l 10 x reaction buffer, 0.6  $\mu$ l of each 10 mM primer, 0.4  $\mu$ l 2 mM dNTP mix, 0.1  $\mu$ l Taq polymerase (NEB), 13.6  $\mu$ l dH<sub>2</sub>O and 1  $\mu$ l of the DNA template solution. A typical Standard PCR thermal program is shown below.

**Table 2-3 Standard thermal program**

Stage	Temperature (°C)	Time period	Cycles
Initial denaturation	94	3 min	1 x
Denaturation	94	15 sec	
Annealing	50-60	15 sec	25 – 40 x
Extension	72	1 min per kb	
Final extension	72	10 min	1 x

#### 2.4.1.2.2 Colony PCR

The previously described PCR conditions were used with slight adjustments. A small pipette tip of colonies showing antibiotic resistance were added to each reaction and the volume was adjusted adding 1 $\mu$ l of dH<sub>2</sub>O. Additionally, the samples were heated for 10min at 94°C before the first cycle. Each colony was streaked out onto a fresh LB plate containing the appropriate antibiotic selection

#### 2.4.1.2.3 High-fidelity PCR

*This method was used for cloning e.g. PDR12*

This method was used when sequence accuracy was required. Briefly; the reaction mix contained 2  $\mu$ l 2 mM dNTP mix, 1  $\mu$ l of each 2 mM primer, 4  $\mu$ l 5 x

hifidelity buffer, 0.6  $\mu$ l DMSO, 1  $\mu$ l of the template cDNA and, 11.2  $\mu$ l dH<sub>2</sub>O and 0.2  $\mu$ l Phusion polymerase (Finzyme). The mix was kept on ice and put in the thermocycler when it reached 98°C. A typical hi-fidelity PCR thermal program is shown below.

**Table 2-4 High-fidelity PCR thermal program**

Stage	Temperature (°C)	Time period	Cycles
Initial denaturation	98	1 min	1 x
Denaturation	98	10 sec	
Anealing	55-62	15 sec	20 – 30 x
Extension	72	20 sec per kb	
Final extension	72	5 min	1 x

#### **2.4.1.2.4 Targeted mutagenesis PCR**

*This method was used to create the kinase-dead mutants of EFR, FLS2, BAK1 and BRI1 kinase domains.*

This method was used to introduce a desired mutation with a DNA sequence. Briefly; the reaction mix contained 4  $\mu$ l 2 mM dNTP mix, 2.5  $\mu$ l of each 2 mM primer, 10  $\mu$ l 5 x GC-rich buffer, 1.5  $\mu$ l DMSO, 1  $\mu$ l of the template plasmid (25  $\mu$ g/ $\mu$ l) and, 28.25  $\mu$ l dH<sub>2</sub>O and 0.75  $\mu$ l Phusion polymerase (Finzyme). The mix was kept on ice and put in the thermocycler when it reached 98°C. A typical high-fidelity PCR thermal profile is shown below. A typical targeted mutagenesis PCR thermal program, is shown below.

**Table 2-5 Targeted mutagenesis PCR thermal program**

Stage	Temperature (°C)	Time period	Cycles
Initial denaturation	98	1 min	1 x
Denaturation	98	10 sec	
Anealing	55	15 sec	12 x
Extension	72	20 sec per kb	
Final extension	72	5 min	1 x

The PCR reactions were equilibrated to room temperature and 1  $\mu$ l DpnI was added to each. Reactions were incubated O/N at 37°C and 5  $\mu$ l used to transform *E. coli* DH5 $\alpha$ .

#### **2.4.1.2.5 DNA sequence verification**

Dideoxy DNA sequencing reactions were carried out in a final volume of 10 µl containing 80-100 ng template DNA, 0.5 µl of 3.2 µM primer, 1.5 µl 5x buffer and 1µl ABI Big Dye Terminator Ready Reaction Mix (Perkin Elmer, Massachusetts, USA). The PCR cycle conditions were: initial denaturation step at 96°C for 1 min, denaturation at 96°C for 10 sec, annealing at 50°C for 5 sec and elongation at 60°C for 4 min (25 cycles total). Sequencing was carried out on a 377 or 3700 ABI PRISM™ Dye-Deoxy Terminator Cycle Sequencer (Perkin Elmer, Massachusetts, USA) in the Genome centre (John Innes Centre). Sequences were analysed using the software package Vector NTI version 11 (Invitrogen).

#### **2.4.1.2.6 Agarose gel electrophoresis**

DNA fragments were separated by electrophoresis in horizontal agarose gels. The gels were prepared in 1 x TAE (40 mM Tris, 20 mM NAOAc, 1 mM EDTA, pH 7.9) including 1 µg/ml ethidium bromide (Sigma) for visualization purposes. The concentration of agarose varied between 0.8 - 2 % (w/v) depending on the sizes of the DNA fragments to be separated but 1 % (w/v) gels were normally used for analytical purposes. DNA samples were prepared by adding 0.1 vol of 10 x loading buffer (50% (w/v) glycerol, 50 mM EDTA, 10 x TAE, 0.25 % (w/v) 64 bromophenol blue, 0.25% (w/v) xylene cyanol) and were loaded into the wells of the gel submerged in 1 x TAE. Gels were run at 10 - 100 V until the desired separation was achieved. Analytical gels were photographed on a short wavelength UV transilluminator (GelDoc 1000, BioRad).

#### **2.4.1.2.7 DNA purification from agarose gel pieces**

DNA was visualised on a long wavelength UV transilluminator (TM40, UVP) and the desired fragment was excised using a razor blade. Fragments were purified using QIAquick spin columns (Qiagen) following the manufacturer's instructions.

#### **2.4.1.2.8 *bak1-5* marker design**

*This method was used to verify *bak1-5* mutants from crosses.*

For *bak1-5* homozygous mutant identification a dCAPS marker was designed using dCAPS Finder 2.0 (Neff *et al.*, 2002). The genomic region around the *bak1-5* mutation was PCR amplified using Taq polymerase (Qiagen). The corresponding product was cut with RsaI (NEB) and *bak1-5* derived PCR products contained an additional RsaI site in addition to the internal restriction control site.

#### **2.4.1.3 Cloning**

The desired DNA sequences were amplified by high-fidelity PCR ([2.4.1.2.3](#)) using the appropriate template and primers. All sequences were verified in the primary plasmid ([2.4.1.3.1-3](#)) by DNA sequencing analysis ([2.4.1.2.5](#)). Secondary plasmids ([2.5.1.3.4-5](#)) were verified by restriction analysis (2.4.1.3.10).

##### **2.4.1.3.1 Blunt end cloning**

*This method was used for subcloning kinase domains.*

The blunt end DNA fragment was ligated into the pCR-Blunt-II-TOPO (Invitrogen) primary vector combining 0.5 µl vector solution, 0.5 µl 6 x buffer salt solution, 0.5-2 µl of DNA fragment solution and making it up to 3 µl using sterile dH<sub>2</sub>O. The reaction was left for 30 min at RT. The whole reaction volume was used to transform *E. coli* DH5α.

##### **2.4.1.3.2 Gateway entry vector cloning**

The DNA fragment containing a CACC at the 5'-end was ligated into the pENTR-D-TOPO (Invitrogen) entry/primary vector combining 0.5 µl vector solution, 0.5 µl 6 x buffer salt solution, 0.5 - 2 µl of DNA fragment solution and making it up to 3 µl using sterile dH<sub>2</sub>O. The reaction was left for 30 min at RT. The whole reaction volume was used to transform *E. coli* DH5α.

#### **2.4.1.3.3 IN-Fusion cloning**

*This method was used for subcloning kinase domains.*

The DNA fragments were amplified with primers carrying the following extension: 5'-AAGTTCTGTTCAGGGCCCG- for the forward primer and 5'-ATGGTCTAGAAAGCTTTA- for the reverse primer. The destination vectors pOPINM and pOPINF were linearised previously using KpnI (NEB) and HindIII (NEB). 50 ng of purified insert and 100 ng of linearised destination vector were mixed in a total volume of 10 µl sterile dH<sub>2</sub>O. The reaction mix was added to a well of dry-down In-Fusion (Clontech) reaction powder and mixed by pipetting up and down. The reaction was incubated at 42°C for 30 min and terminated by adding 40 µl TE immediately afterwards. Up to 30 µl of the reaction volume was used to transform *E. coli* DH5α.

#### **2.4.1.3.4 Classical “cut and paste” cloning**

The DNA fragments of interest (inserts) were released from the primary vector (2.4.1.3.1) using appropriated restriction enzymes. The secondary vector was also pre-digest with appropriate restriction enzymes creating compatible ends. For DNA ligation 2 µl purified insert, 6 µl purified linearised vector, 1 µl ligase buffer and 1 µl of T4 DNA ligase were combined in one reaction tube, mixed and incubated at 16°C O/N. The whole reaction volume was used to transform *E. coli* DH5α.

#### **2.4.1.3.5 Gateway LR reaction**

LR Gateway reaction was used to introduce the insertion of the entry vector into a destination vector that was either from the pGWB or pEarleygate series (Nakagawa *et al.*, 2007; Earley *et al.*, 2006). The reaction mix contained 50 - 150ng of the entry vector (2.4.1.3.2), 200 - 250ng of the destination vector, TE buffer pH 8.0 up to a final volume of 4 µl, and 1 µl of the LR Clonase II mix (Invitrogen). The reaction was vortexed shortly and incubated for 4-6 H at RT. The reaction was stopped adding 1µl of Proteinase K (Invitrogen) and incubating samples for 15min at 37°C. Normally, 2 µl of the reaction volume was used to transform *E. coli* DH5α.

#### **2.4.1.3.6 Vector map generation**

Vector maps of primary and secondary plasmids were generated using VNTI version 11 (Invitrogen). In silico digests were performed to identify appropriated endonucleases for restriction analysis (2.4.1.3.10).

#### **2.4.1.3.7 Transformation of bacteria by heat-shock**

For transformation an aliquot of DH5α (made by Karen Morehouse) cells were mixed with indicated amount of ligation or plasmid solution and left on ice for 10-30min. The cells were heat shocked at 42°C for 1-2 min and immediately chilled on ice for another 5min. The cells were re-suspended in 750 µl of liquid LB and incubated while shaking at 300 rpm at 37°C for 1-2 H. The solution was plated on LB-agar plates containing the appropriate antibiotic selection.

#### **2.4.1.3.8 Transformation of bacteria by electroporation**

Prior to electroporation, electro-competent bacterial cells were thawed on ice for 5 - 10 min. The desired amount of desalted plasmid up to 5 µl was added to 20 µl of electrocompetent cells. Cells were transformed in an electroporation cuvette with a width of 1 mm in a Bio-Rad electroporator (Bio-Rad, Hercules, CA, USA). The settings were 1800 V with a capacity of 25 µF, over 200 Ω resistance. Cells were recovered from the cuvette by adding 1 ml of liquid LB medium and transferring the suspension to a sterile Eppendorf tube. The bacteria were incubated while shaking at 300 rpm for 1-2 H in the case of *E. coli* at 37°C and for *A. tumefaciens* at 28 °C. The bacterial solution was plated on LB-agar plates containing the appropriate antibiotic selection.

#### **2.4.1.3.9 Plasmid miniprep**

Single colonies corresponding to positive colony PCR results were incubated O/N in 5 ml LB containing the appropriate antibiotics and spun down for 10 min at

4,000 rpm. Plasmids were extracted from the bacterial cell pellet using QIAprep spin miniprep kits (Qiagen) following the manufacturers protocol.

#### **2.4.1.3.10 Restriction analysis**

The restriction reaction mix contained 200-400 ng of the plasmid, 1  $\mu$ l of 10 x reaction buffer, 0.5  $\mu$ l of each of the cutting enzymes (NEB), and was incubated for 1.5 H at 37°C. The product was analyzed by agarose gel electrophoresis.

#### **2.4.1.3.11 Plasmids used in this study**

**Table 2-6 Summary of plasmids used in this study**

Name	Insert	Backbone	Reference
<b>Plant expression vectors</b>			
35S::GUS-HA <sub>3</sub>	GUS	pBIN19	
35S::EFR-YFP-HA <sub>3</sub>	EFR	pEarleyGate101	Gift from V. Nicaise
35S::EFR-CFP-HA <sub>3</sub>	EFR	pEarleyGate102	Gift from V. Nicaise
35S::EFR-GFP-His	EFR	pEarleyGate103	Gift from V. Nicaise
35S::EFR-HA <sub>3</sub>	EFR	pGWB14	
pEFR::EFR-eGFP	EFR	pEpigreenB5	(Nekrasov <i>et al.</i> , 2009)
pEFR::EFR-eGFP-HA <sub>3</sub>	EFR	pEpigreenB5	(Nekrasov <i>et al.</i> , 2009)
35S::PIP2-GFP	PIP2 (aquaporin)		Gift from S. Schornack
pBAK1::BAK1:HA <sub>3</sub>	genomic region of BAK1 including 1.5 kb upstream sequence	pEpiGreenB5(HA)	B. Schwessinger
pBAK1::BAK1:GFP	genomic region of BAK1 including 1.5 kb upstream sequence	pEpiGreenB5(GFP)	B. Schwessinger
pBAK1::BAK1:Myc			(Chinchilla <i>et al.</i> , 2007)
pFLS2::FLS2:Myc			(Robatzek <i>et al.</i> , 2006)
35S::SERK1-HA <sub>3</sub>	SERK1	pGWB14	with B. Schwessinger
35S::SERK2-HA <sub>3</sub>	SERK2	pGWB14	with B. Schwessinger
35S::SERK4-HA <sub>3</sub>	SERK4	pGWB14	with B. Schwessinger
35S::SERK5-HA <sub>3</sub>	SERK5	pGWB14	with B. Schwessinger
35S::BRI1-GFP-His	BRI1	pEarleyGate103	with B. Schwessinger
35S::FLS2-GFP-His	FLS2	pEarleyGate103	with B. Schwessinger
p35S::BRI1:HA <sub>3</sub>			gift of Freddy Boutrot Sainsbury Laboratory UK
pCERK1::CERK1:HA <sub>3</sub>			(Gimenez-Ibanez <i>et al.</i> , 2009a)

**Table 2.6 continued**

Name	Insert	Backbone	Reference
<b>Plant expression vectors</b>			
35S:RAE5-GFP-His	RAE5.1 cDNA	pEarleyGate103	Gift from V. Nicaise
35S::RAE5-HA <sub>3</sub>	RAE5.1 cDNA	pGWB14	Cloned from above entry clone
35S::RAE5_D905N-GFP-His	Kinase mutant RAE5	pEarleyGate103	Cloned from above entry clone
35S::OXI1-eYFP-cMyc	OXI1 cDNA		Gift from Marc Knight
35S::OXI1-HA <sub>3</sub>	OXI1 cDNA	pGWB14	Cloned from above vector
35S::PEN3-GFP	PEN3		Gift from Shauna Somerville
<b><i>E.coli</i> expression vector</b>			
pGST:BAK1	BAK1 CD (256-615aa)	pGEX-4T1	primary vector (Karlova <i>et al.</i> , 2009); B. Schwessinger
pGST:BAK1m	derivate of pGST:BAK1 expressing BAK1 (D418N) CD	pGEX-4T1	
pMBP:EFR	EFR CD (682-1031aa)	pOPINF	with B. Schwessinger
pMBP:EFRm	derivate of pMBP:EFR expressing EFRm (D849N) CD	pOPINF	with B. Schwessinger
pMBP:FLS2	FLS2 CD (840-1173aa)	pOPINF	with B. Schwessinger
pMBP:FLS2m	derivative of pMBP:FLS2 expressing FLS2m (D977N) CD	pOPINF	with B. Schwessinger
<b><i>E. coli</i> expression vector</b>			
pMBP:BRI1	BRI1 CD (814-1196aa)	pOPINF	with B. Schwessinger
pMBP:BRI1m	derivate of pMBP:BRI1 expressing BRI1m (D977N) CD	pOPINF	with B. Schwessinger
pHis <sub>6</sub> :FLS2	see above	pOPINM	with B. Schwessinger
p His <sub>6</sub> :FLS2m	see above	pOPINM	with B. Schwessinger
p His <sub>6</sub> :BRI1	see above	pOPINM	with B. Schwessinger
p His <sub>6</sub> :BRI1m	see above	pOPINM	with B. Schwessinger

## 2.4.2 RNA methods

### 2.4.2.1 Isolation of total RNA from *Arabidopsis*

RNA was extracted using RNeasy Plant Mini kit (Qiagen) following the manufacturer's protocol. RNA quality was evaluated by agarose gel electrophoreses.

### **2.4.2.2 Reverse transcription PCR**

*This method was used to characterize pdr12 mutants and verify knock-out lines for pdr and serk mutants.*

This method was used to generate single stranded cDNA from total RNA. All reactions mixes were always kept on ice if not indicated otherwise. Briefly; the reaction mix contained 2.5 µg total RNA, 2 µl 2 mM oligo(dT)<sub>15</sub> , 4 µl 2 mM dNTP and was made up with sterile dH<sub>2</sub>O to a final volume of 13 µl. The reaction mix was heated for 5 min at 65°C and put on ice immediately for 1-5 min. The contents of the tube were collected by brief centrifugation. 7 µl of the second reaction mix were added containing 4 µl First-Strand buffer, 1 µl 0.1 M DTT, 1 µl RNase OUT (Invitrogen) and 1 µl SuperScript III RT polymerase (Invitrogen). The reactions were vortexed briefly, spun down and incubated at 50°C for 50 min. The reactions were terminated by heating at 70°C for 15 min and kept at -20°C for storage.

### **2.4.3 Protein methods**

#### **2.4.3.1 Immunoblotting and general protein methods**

*These methods were used for small and large-scale immunoprecipitations and for verifying protein expression of transgenic lines.*

##### **2.4.3.1.1 SDS-polyacrylamide gel electrophoresis**

The reagents and SDS-polyacrylamide gel preparation methods were followed according to Laemmli, 1970. Gels were run in Mini PROTEAN III gel tanks (Bio-Rad) filled with Tris-glycine electrophoresis buffer (25 mM Tris, 250 mM glycine (electrophoresis grade, pH 8.3, 0.1% SDS). The gel electrophoresis was performed in a continuous buffer system at 2.1 - 3.4 mA cm/gel. All gels included a molecular size marker 10-250 K Bio-Rad Precision Plus Marker (Bio-Rad) or NEB broad range marker (NEB). Electrophoresis was continued until the loading dye band migrated to the bottom of the gel.

#### **2.4.3.1.2 *Electroblotting***

Two Whatman papers and sponges per gel were equilibrated for 5 min in pre-chilled transfer buffer (25mM Tris, 192mM glycine, 20% (v/v) methanol, pH 8.3). The PVDF membrane (BioRad) was activated for 1 min in methanol. The sandwich and device were assembled according the manufacturer's protocol (BIO-RAD). The membrane was facing the anode and the gel the cathode. The transfer took place at 4°C overnight at 30 V or for 2 H at 95 V.

#### **2.4.3.1.3 *Coomassie staining***

The proteins in the gel or on the membrane were visualized by Coomassie staining. The gel was transferred to a tray containing Coomassie stain solution (0.5% (w/v) Coomassie brilliant blue R-250, 50% (v/v) methanol, and 7.5% (v/v) glacial acetic acid), agitated at RT for 30 min, and de-stained three times under agitation for 30min with de-stain (20% (v/v) methanol, 5% (v/v) acetic acid).

#### **2.4.3.1.4 *Immunodetection***

The PVDF transfer membrane containing immobilised, denatured proteins was blocked for one hour at room temperature with 0.1% TBST buffer (0.5M NaCl, 200mM Tris-HCl, 0.05% (v/v) Tween-20, 0.2% (v/v) Triton X-100, pH 7.5) containing 5% dried skimmed milk powder (w/v) with gentle agitation on a platform shaker. After removal of the blocking solution, the membrane was washed for 2 min with TBS buffer.

The membrane was then incubated with the primary antibodies directed against the target protein with 0.1% TBST buffer containing 5% dried skimmed milk powder (w/v) for 1 H at RT or O/N at 4°C. The membrane was washed three times for 15 min each with 0.1% TBST buffer. The membrane was than incubated for 1 H at RT with 0.1% TBST buffer containing 5% dried skimmed milk powder (w/v) and secondary antibodies directed against the anti-immunoglobulin of the primary antibody covalently coupled to horseradish peroxidase (HRP).

The membrane was washed three times for 15 min each with 0.1% TBST buffer. Detection of the peroxidase signal of the secondary antibody-HRP conjugate was performed with ECL (Amersham Biosciences), or SuperSignal West Femto (Pierce) chemiluminescent detection reagent for Western blotting. The membrane was exposed onto AGFA Blue CP-BU film (AGFA) or ECL Hyperfilm (Amersham Biosciences). Film exposure ranged from 10 sec to 20 min. The film was aligned to the membrane and the protein standards were marked on the film to confirm the relative molecular weight of the signal.

Primary antibodies were diluted in 0.1% TBST buffer containing 5% dried skimmed milk powder (w/v) solution to the following concentration: anti-GFP (AMS Biotechnology) 1: 5000; anti-BAK1 1:500; anti-HA-HRP (Santa Cruz) 1: 2000; anti-FLS2 1:1000; anti-BRI1 1:1000; anti-RAE5 1:500; anti-PDR8 1:1000 (Kobae *et al.*, 2006).

Secondary antibodies were diluted in 0.1% TBST buffer containing 5% dried skimmed milk powder (w/v) solution to the following concentration: anti-rabbit-HRP (Sigma) 1:5000 or anti-rabbit-HRP (Ebioscience) 1:5000.

#### 2.4.3.1.5 Antibodies

**Table 2-7: Generation of polyclonal antibodies**

Antibody	Peptide sequence	Peptide location	Reference
Anti-BAK1	DSTSQIENEYPSGPR	C-terminus	(Schulze <i>et al.</i> , 2010)
Anti-EFR	EPO71644:CSEEVPRDRMRTDEAV EPO71645:KNNASDGNPSDSTTLGM	JM kinase	This work
Anti-RAE5	EPO92743:TKQIEEHTDSESGG EPO92742:NETTDSSISNPSTKQ	JM kinase	This work
Anti-FLS2	KANSFREDRNEDREV	C-terminus	(Chinchilla <i>et al.</i> , 2007).

Polyclonal antibodies were generated by immunizing rabbits with synthetic peptides. Antibodies (final bleed) were affinity purified against the peptide (Eurogentec).

#### 2.4.3.1.5.a Anti-EFR antibody purification

*This was done by me in order to try enrich anti-EFR antibodies, Chapter 1*

In order to enrich for EFR-specific antibodies, further affinity purification of the antisera obtained from rabbits immunized with both peptides was undertaken. The peptide EPO71644 (isoelectric point 4.21) was dissolved in 50 mM HEPES pH 7. Peptide sufficient for preparation of 0.5 x column bed volume (100 µl per 200 µl matrix) at a concentration of 0.4 mg peptide/ 100 µl resin was dissolved. Sufficient Affi-gel 15 matrix (Bio-Rad) (suitable for ligands with *pI* < 6.5) was prepared for 2 small plastic columns with internal diameter 0.8 cm. (Bed volume (b.v.) =  $\pi(0.8/2)^2 \times 0.5\text{cm} = \pm 250 \mu\text{l}$ ) and rinsed three times with water.

The peptide was incubated with the Affi-Gel 15 in a 1.5 ml eppendorf for 4 hours at 4°C to create an affinity matrix to enrich for peptide-specific antibodies. 0.1 ml Ethanolamine-HCl pH 8 1M was added/ml Affi-Gel and incubated for 1 hour. The gel was transferred to the mini columns and washed 3 times with water and then with 50 mM HEPES pH 7 until the eluate  $\text{OD}_{280} = 0$ . The column was washed with 100 mM glycine pH 2.5, then with 50 mM HEPES pH 7. The large bleed was diluted 1:10 with 10 mM Tris pH 7.5 and centrifuged.

The column was washed with 10 b.v. 10 mM Tris pH 7.5, 2 b.v. 100 mM glycine pH 2.5; 10 b.v. 10 mM Tris pH 8.8 until the column pH = 8.8 (pH paper). The column was then washed with 10 b.v.s triethylamine pH 11.5, then 10 mM Tris pH 7.5 until the column pH = 7.5. 5ml of the diluted serum was applied to the affinity column and the flow-through re-applied 3 times. The column was washed with 20 b.v. of 10 mM Tris pH 7.5, then 20 b.v. of 10 mM Tris pH 7.5/500 mM NaCl.

The acidic fraction of antibodies was eluted with 10 b.v. 100 mM glycine pH 2.5 and basic antibody fraction was eluted with 10 b.v. 100 mM triethylamine pH 11.5, each directly eluted into an eppendorf containing 1 b.v. 1M Tris pH 7.5. The fractions were then combined and dialyzed against PBS overnight using a Slide-a-Lyzer mini-dialysis kit (Pierce). The purified antibodies were preserved by the addition of sodium azide to 0.02 % (w/v), aliquoted and stored at -80°C.

#### **2.4.3.1.6 SDS-PAGE, colloidal Coomassie staining and gel excision**

*This method was used for large-scale IPs described in Chapter 1 and 2.*

For protein separation prior to mass spectrometry, pre-cast NuPage Novex 4 – 12 % gradient 1.5 mm Bis-Tris gels were used (Invitrogen). Immunoprecipitates were loaded across 2 or 3 wells, with one empty well separating different samples. Gels were run at 200 V in 1 x MOPS buffer (Invitrogen). Following electrophoresis, gels were stained as follows: Two solutions were freshly combined: Solution A 10 % (w/v)  $(\text{NH}_4)_2\text{SO}_4$  in, acidified with 1.25 % (v/v) concentrated 85 % phosphoric acid and Solution B: 5 % (w/v) CBB G in water. To prepare the stain, 4 parts solution A was combined with 1 part methanol and solution B and 1.6 % (v/v) solution B and well mixed before adding to the gel. The gel was incubated overnight at room temperature. Destaining was done by the addition of fresh distilled water until the background had destained.

Bands of interest were excised using a fresh razor blade for each band. Bands were cut into cubes on a clean glass slide and cubes destained with 50 % (v/v) ethanol before preparation for mass spectrometry analysis (at this stage samples were handed over to the mass spectrometry team).

#### **2.4.3.1.7 HPLC and Mass Spectrometry**

*This method was used for large-scale IPs described in Chapter 1 and 2.*

Protein samples were prepared for the mass spectrometry analysis as described previously (Ntoukakis *et al.*, 2009). LC-MS/MS analysis was performed using a LTQ-Orbitrap mass spectrometer (Thermo Scientific) and a nanoflow-HPLC system (nanoAcuity, Waters Corp.) as described previously (Ntoukakis *et al.*, 2009). The entire TAIR9 database was searched (TAIR9 33596 sequences; 13487687 residues) ([www.arabidopsis.org](http://www.arabidopsis.org)) using Mascot (with the inclusion of sequences of common contaminants such as keratins and trypsin).

Parameters were set for  $\pm 5$  ppm peptide mass tolerance and allowing for methionine oxidation and two missed tryptic cleavages. Carbiodomethylation of cysteine residues was specified as a fixed modification and oxidized methionine and phosphorylation of serine, threonine or tyrosine residues were allowed as variable modifications. Scaffold (v2\_06\_01, Proteome Software Inc., Portland, OR) was used to validate MS/MS based peptide and protein identifications. Peptide

identifications were accepted if they could be established at greater than 95.0% probability as specified by the Peptide Prophet algorithm. Protein identifications were accepted if they could be established at greater than 95.0% probability and contained at least 2 identified peptides.

### **2.4.3.2 *In vitro* protein analysis**

#### **2.4.3.2.1 Recombinant protein purification**

*This method was used to generate proteins for kinase domains for in vitro testing of kinase activity.*

Recombinant fusion proteins were produced in *E. coli* BL21 (Novagen), extracted using BugBuster reagent (Novagen) containing 1 µl/ml Benzoase (Novagen), 1 KU/ml Lysozyme (Novagen) and 150 µl/ml protease inhibitor cocktail set II (Novagen) and the soluble fraction was used to enrich for fusion proteins. GST-tagged fusion proteins were enriched using Glutathione Sepharose Fast Flow (GE Healthcare) according to the manufactures protocol. MBP-tagged fusion proteins were enriched using Amylose Resin (NEB) according to manufactures protocol. His-tag fusion proteins were enriched using His-Bind Resin (Novagen) according to the manufactures protocol. After elusion fusion proteins were adjusted to the same concentration in 10% glycerol solution and stored at -20°C until usage.

#### **2.4.3.2.2 Radioactive *in vitro* kinase assays**

*This method was used to generate proteins for kinase domains for in vitro testing of kinase activity.*

The fusion proteins were incubated in 30 µl kinase buffer (50 mM Tris, pH 7.5, 10 mM MgCl<sub>2</sub>, 10 mM MnCl<sub>2</sub>, 1 mM DTT) in the presence of 1 µM unlabeled ATP and 183 kB of [<sup>32</sup>P]-γ-ATP for 30 min at 30°C with shaking at 900rpm. The reactions were stopped by adding 2 x LDS loading buffer (Invitrogen). The phosphorylation status of fusion proteins was analyzed by autoradiography after separation of one-fourth of the *in vitro* kinase assay by SDS-PAGE followed by western blotting, if not indicated otherwise. Incorporated [<sup>32</sup>P]-groups were visualised exposing the membrane onto ECL Hyperfilm (Amersham Biosciences). In auto-phosphorylation assays 1 µg fusion protein for MBP- and GST-tagged proteins and 5 µg for His-

tagged proteins was incubated with 1 µg of MBP (Fluka). In transphosphorylation assays 1µg of each fusion protein was used.

#### **2.4.3.3 *In vivo* protein analysis**

##### **2.4.3.3.1 Protein extraction and immunoprecipitation in *N. benthamiana***

*This method was used for testing protein expression, for co-IP experiments or for large-scale protein expression and IP.*

Leaves were harvested 2 dpi. Leaves were ground to fine powder in liquid nitrogen and 5 ml extraction buffer [50 mM Tris-HCl pH 7.5; 150 mM NaCl; 10 % glycerol; 10 mM DTT; 10 mM EDTA; 1 mM NaF; 1 mM Na<sub>2</sub>MoO<sub>4</sub>.2H<sub>2</sub>O; 1% (w/v) PVPP; 1% (v/v) P9599 protease inhibitor cocktail (Sigma); 1% (v/v) IGEPAL CA-630 (Sigma)] added. Samples were cleared by centrifugation at 16.000xg for 15 min at 4°C and adjusted to 2 mg/ml total protein concentration. Immunoprecipitation were performed on 1.5 ml total protein by adding 20 µl GFPTrap-A beads (Chromotek) (Rothbauer *et al.*, 2006; Rothbauer *et al.*, 2008), 20 µl anti-HA sepharose beads (Roche), or 20 µl true-blot anti-rabbit Ig beads (Ebioscience) in combination with 15 µl antibody and incubation at 4°C for 3-4 H. Beads were washed 4 times with TBS containing 0.5% (v/v) IGEPAL CA-630, immunoprecipitates eluted with 30 µl 2xLDS (Invitrogen) and heating at 70°C for 10 min.

##### **2.4.3.3.2 Protein extraction and immunoprecipitation in *A. thaliana***

*This method was used for testing protein expression in transgenic lines or for antibody specificity, for co-IP experiments or for large-scale protein expression and IP.*

Frozen tissue was ground to fine powder in liquid nitrogen and extraction buffer [50 mM Tris-HCl pH 7.5; 150 mM NaCl; 10 % glycerol; 5 mM DTT; 2mM EDTA; 1 mM NaF; 1 mM Na<sub>2</sub>MoO<sub>4</sub>.2H<sub>2</sub>O; 1 mM PMSF (Sigma); 5 mM Na<sub>3</sub>VO<sub>4</sub>, 1 % (v/v) P9599 protease inhibitor cocktail (Sigma); 1 % (v/v) IGEPAL CA-630 (Sigma)] added. Samples were cleared by centrifugation at 16.000xg for 15 min at 4°C and adjusted to 2mg/ml total protein concentration. Immunoprecipitations were performed on 1.5 ml total protein by adding 20 µl GFPTrap-A beads (Chromotek), 20 µl anti-HA sepharose beads (Roche), or 20 µl true-blot anti-rabbit Ig beads

(Ebioscience) in combination with 15 µl antibody and incubation at 4°C for 3-4 H if not indicated otherwise. Beads were washed 4 times with TBS containing 0.5% (v/v) IGEPAL CA-630, immunoprecipitates eluted with 50 µl 2xLDS (Invitrogen) and heated at 70°C for 10 min.

## **2.5 Cellular biological methods**

### **2.5.1 Confocal laser scanning microscopy**

*Nicotiana benthamiana* leaf tissue transiently over-expressing the indicated proteins, or transgenic *Arabidopsis* plants were analysed by CLSM employing the Leica SP5 Confocal Microscope (Leica Microsystems, Wetzlar, Germany). After excitation at 488 nm, eYFP emission and remaining autofluorescence were detected using the PI (>660 nm) filter set. All samples were imaged with the 40x objectives. Pictures were taken giving an average of four scans.

Plasmolysis was achieved by the addition of 1 M NaCl to leaf slices for 20 minutes prior to microscopy.

## **2.6 Antibiotics used in this study**

Final concentrations of 50 µg/mL, 25 µg/mL, 100 µg/mL, 100 µg/mL and 50 µg/mL were used for kanamycin, gentamycin, carbenicillin, rifampicin and spectinomycin for bacterial cultures, respectively. For the selection of *Arabidopsis* transgenic lines, 50 µg/mL, 40 µg/mL or 10 µg/mL of kanamycin, hygromycin, or phosphinothricin respectively, were used. All antibiotic solutions were filter-sterilized using 22 µm syringe filter.

## **2.7 Media used in this study**

All recipes are for the scale of 1 liter.

### **LB**

10 g tryptone, 5 g yeast extract, 10 g NaCl, pH 7.0. For solid Medium, 10g agar was included.

## King's B

20 g Peptone, 1.5g Heptahydrated Magnesium Sulfate, 1.5g Potassium Hydrogen Phosphate, 10mL glycerol. pH7.0. For solid medium, 10 g agar was included.

## MS

4.3 g MS salts, 0.59 g MES, 0.1 g myo-inositol, 1 ml of 1000x MS vitamin stock, 10 g sucrose pH was adjusted to 5.7 with KOH . For solid medium, 8 g phyto-agar was included.

## GM

4.3 g MS salts, 0.59 g MES, 0.1 g myo-inositol. 1 ml 1000x GM vitamins, pH 5.7. For solid medium 8 g phytoagar was included.

## 2.8 Primers used in this study

Table 2-8 Primers used in this study

Primer name	5' to 3' sequence
BAK1_4_F_GT	CATGACATCATCATCATTGC
BAK1_4_R_GT	ATTTGCAGTTGCCAACAC
BKK1-1_F_GT	TGGCTCAGAAGAAAACCACAG
BKK1-1_R_GT	CTGCTCCACTTCTGTTCCAC
BAK1_dCAPS_F_GT	AAGAGGGCTTGCATGATGTCAGT
BAK1_dCAPS_R_GT	GAGGCAGCAAGATCAAAAG
EFR_KD_F	AAGTTCTGTTCAAGGCCGGCCAGTGATGGTAACCCATC
EFR_KD_R	ATGGTCTAGAAAGCTTACATAGTATGCATGTCGTATTAACATC
FLS2_KD_F	AAGTTCTGTTCAAGGCCGGAAATTACATCAGAGTCCTCATTAACCG
FLS2_KD_R	ATGGTCTAGAAAGCTTAAACTCTCGATCCTCGTTACGATC
BRI1_KD_F	AAGTTCTGTTCAAGGCCGGTAGAGAGATGAGGAAGAGACG
BRI1_KD_R	ATGGTCTAGAAAGCTTATAATTTCCTTCAGGAACCTCTTTTATAC
BAK1_(D416N)_F	CCCAAAGATTATTATCGAAATGTGAAAGCTGCAAATATTGTTG
BAK1_(D416N)_R	CAACAAATATTGCAGCTTCACATTGATGAATAATCTTGGG
EFR_(D848N)_F	GACCCTGTAGCTCACTGTAATATTAAGCCAAGCAACA
EFR_(D848N)_R	TGTTGCTGGCTTAATATTACAGTGAGCTACAGGGTC
FLS2_(D997N)_F	GGTTTCCCATCGTCATTGTAATCTGAAGCCAGCTAATATACTC
FLS2_(D997N)_R	GAGTATATTAGCTGGCTTCAGATTACAATGAACGATGGGAAAAC
BRI1_(D1009N)_F	GTCCGCATATCATCCACAGAAACATGAAATCCAGTAATGTGTTG
BRI1_(D1009N)_R	CAACACATTACTGGATTCATGTTCTGTGGATGATGCGGAC

---

**Table 2.8 continued**

<b>Primer name</b>	<b>5' to 3' sequence</b>
AtPDR12_RT_Fw	GAAGCGGCTTAGGAGTCGATTCGC
AtPDR12_RT_Rv	CGTCCACTCGAATCCTATCATAGCG
AtPDR12cDNA_Fw	GAATCGATATGGAGGGAACTAGTTTCACCA
AtPDR12cDNA_Rv	GAGGATCCTCGTTTGGAAATTGAAACT
AtPDR12pENTRFw	CACCATGGAGGGAACTAGTTTCAC
AtPDR12pENTRRv	TCGTTTGGAAATTGAAACTCTTG
serk1-1_Fw	CGTGACAACAGCAGTCCGTGGCACCATCGG
serk1-1_Rv	CCCTTTAATCGAACCATAGCAC
serk1-3_Fw	AGCAATTGGTTGCAGAAAAGT
serk1-3_Fw	AGAGATATTCTGGAGCGATGTGACCGATGG
serk2-2_Fw	CTCTGGTATGGGAAGATGGTAATGTGGTCTGAG
serk2-2_Rv	CGGCTAGTAACTGGGCCGCATAGATCC
bak1-3_Fw	GCAC TGAAAACAGTTAGC
bak1-3_Rv	GATGCAGGAAGGGGAGTCAA CTTGGTG
serk4bkk1-1_Fw	CTGAAGAAGACCCAGAGG
serk4bkk1-1_Rv	ACGCTCAAGTGGAGTAATGA
serk5_Fw	CTGAAGAAGACCCAGAGG)
serk5_Rv	GCTTAATGGAAGTGGAGAGA
pdr8-1Fw	TGAAGATATCTTCTCATCTGGTTC
pdr8-1Rv	CCATAACGAGTACCAACACCTTG
pdr8-2Fw	TTGATTGGTACAGTCTTCTGGC
pdr8-2Rv	TTGAGAGTTCTGATGCAGAAGG
serk4-2_Fw	ACTTTTTTGTGGCTGGTTG
serk4-2_Rv	ATCTCCCTGAAATACTTACACAAGACC
bak1-4gtR	CGG CCA CTA AAG TAC CAT CAG CTA A
bak1-4gtF	CCT CTC ACC GGA GAT ATT CCT G
rae6-1_F	CTCAAAAGGAATTGGAATGTTG
rae6-1_R	CTTCAGATAAGCTGAGGCAGC
qFRK1_F	ATCTTCGCTTGGAGCTTCTC
qFRK1_R	TGCAGCGCAAGGACTAGAG
qAt1g51890_F	CCAGTTGTTCTGTAATACTCAGG
qAt1g51890_R	CTAGCCGACTTGGGCTATC
qAt2g17740_F	TGCTCCATCTCTCTTGTGC
qAt2g17740_R	ATGCGTTGCTGAAGAAGAGG
qAt5g57220_F	AATGGAGAGAGCAACACAATG
qAt5g57220_R	ATACTGAGCATGAGCCCTTG
qUBQ10_F	AGATCCAGGACAAGGAGGTATT
qUBQ10_R	CGCAGGACCAAGTGAAGAGTAG
LB3SAIL	TAGCATCTGAATTCTATAACCAATCTCGATACAC
LBb1.3	ATTTGCCGATTTCACCGTAATATTAGTAGTGGAAATA
RAE5_D905N_fw	CCGGCGATTGTTCACCGTAATATTAGTAGTGGAAATA
RAE5_D905N_rv	TATTCCCACCTACTAATATTACGGTGAACAATCGCCGG
EFR_S683E_fw	TGAAGAGGAAAAAGAAAAACAATGCCGAAGATGGTAACCCATC
	TGATTCTACTAC

---

---

**Table 2.8 continued**

<b>Primer name</b>	<b>5' to 3' sequence</b>
EFR_S683E_rv	GTAGTAGAACATGGATGGTTACCATCTTCGGCATTGTTTTCTT TTTCCTCTTC
EFR_S683A_fw	GAAGAGGAAAAAGAAAAACAATGCCGCAGATGGTAACCCATCT GATTCTACTA
EFR_S683A_rv	TAGTAGAACATGGATGGTTACCATCTGCAGCATTGTTTTCTT TTCCTCTTC
OXI1_Fw	CACCATGCTAGAGGGAGATGAGAACAGA
OXI1_nostopRv	AAATACCAAAAAATTGTTATCACTTCTAA
RAE 6_RT1_Fw	GTATAGCAATTGGGAAGACGATACTTCG
RAE 6_RT1_Rv	ACCACCTCTCCGATCTGTTGCA
RAE 6_RT2_Fw	CTGGAAAGGACTAGAGAAACTGGTT
RAE 6_RT2_Rv	CACAGTTATATGAAGGCCGTAGAA
RAE 6_RT3_Fw	ATTCAGATTTGGGCTTGCTAAGC
RAE 6_RT3_Rv	TAGTTGTCGTGTTGTTATCTCCTC
Serk4_RT1_fw	AATTCACTCTCAGAGTCGCTGGAA
Serk4_RT1_rv	TGAGCCGATTGTTGAGATATCCAG
Serk4_RT2_fw	GTACGCGGTACAATTGGCCATATAG
Serk4_RT2_rv	CCTTTGCCATTCTCCCATCTCTC
RAE5_kinase_fw_pO PIN	AAGTTCTGTTCAAGGGCCGTTCATCTGTTCCGTAAACGAACA
RAE5_kinase_rv_pO PIN	ATGGTCTAGAAAGCTTAAGAAAAGGCAGTGGAGATAGAGAGC
EFR_T709A_Fw	GAAGAGCTTCATAGTCAGCAAGTCGCTTCTCTCAA
EFR_T709A_Rv	TTGAAGAGAACGCACTTGCTGCACTATGAAGCTCTTC
EFR_T709E_Fw	GTTATGAAGAGCTTCATAGTCAGAAAGTCGCTCTCTCAACC AATT
EFR_T709E_Rv	AATTGGTTGAAGAGAACGCACTTCTGCACATATGAAGCTCTCA TAAC
EFR_T709E_Fw2	GAAGAGCTTCATAGTCAGAAAGTCGCTTCTCTCAA
EFR_T709E_Rv2	TTGAAGAGAACGCACTTCTGCACATATGAAGCTCTTC
RAE5.1+.2 F1	GGTGTGCTGCTCACTCGGG
RAE5.1+.2 R1	TCGAGTTGAGAACCGTCCCCA
RAE5.1 F2	CTATGTTGCTCCAGAACTAG
RAE5.1 R2	GTTCCGGTAGCCGGTGGTCG
RAE5.2 F3	CTATGTTGCTCCAGgtacg
RAE5.2 R3	ACCCGACCCGACCATAACCG

---

## Part III

### 3 Original Thesis Proposal

*I wrote this proposal (with input from my supervisor) in advance of the start of my 3-year PhD project, in October 2007. Obviously during the course of the project, the methodology and objectives were adjusted according to the progress of the project. However, I have included it as it was written to illustrate the comparison of the original proposal with the ultimate outcomes of this PhD project.*

#### 1. Significance of Research

In order to gain insight into PTI signaling, we need to unravel how PAMPs are perceived and how this perception is linked to intracellular responses. To this aim, we propose to search for proteins that interact with the EF-Tu receptor EFR. The identification of EFR interacting proteins (EIPs) could lead to the discovery of positive and negative regulators of PTI signaling. Indeed, EIPs could be targets for pathogen effectors so their identification could also contribute to the understanding of ETI. Furthermore, as EFR is a transmembrane leucine-rich repeat receptor kinase, it can also shed light on mechanisms controlling transmembrane receptor activation and function.

Preliminary phenotypic analysis by the Zipfel lab of *Arabidopsis* mutants insensitive to *elf18* (*elfin* mutants) suggest that the signaling cascades induced by the two unrelated PAMPs EF-Tu and flagellin are more divergent than originally supposed. Indeed, out of ~100 non-*efr* *elfin* mutants, only one mutant is compromised in responses triggered by both PAMPs. This project should provide further insight into this unexpected observation. This will connect with other projects in the lab that focus on identifying genes mutated in the *elfin* mutants. The results of the projects will further our understanding of PAMP signaling.

Ultimately, the understanding of innate immunity in plants could contribute to the development of strategies for immunizing plants against infection and new environmentally friendly approaches to crop protection.

## 2. Main objectives

The main focus of this project is to identify proteins that associate with the leucine-rich repeat (LRR) receptor kinase EFR (EFR-interacting proteins, EIPs). This will be done *in vivo* to elucidate the dynamic interactions and signaling involved in plant defense following bacterial PAMP perception.

Putative EIPs will be identified using quantitative immunoprecipitation combined with knock-down (QUICK). Briefly, co-immunoprecipitation (co-IP) will be done with antibodies recognizing EFR itself, or tagged versions of EFR. In order to have a quantitative idea of the proteins involved in the EFR complex, *Arabidopsis* seedlings will be subjected to metabolic labelling using <sup>15</sup>N. The labelled plants will be treated with elf18, while the unlabelled plants will be left untreated. Elicited and control extracts will be combined and proteins will be extracted. The reciprocal labelling experiment will also be done as an additional control to account for any changes due to labelling. Proteins will be fractionated to enrich for membrane proteins and the total, soluble and membrane fractions will be incubated with matrix-bound anti-EFR antibodies or antibodies against the tags. Immunoprecipitated proteins will be separated by SDS-PAGE and the bands of interest will be excised and subjected to analysis by liquid chromatography tandem mass spectrometry (LC-MS/MS).

Proteins identified by this method will be reconfirmed individually using co-IPs and fluorescence resonance energy transfer analyses. In addition, co-localization of proteins will be assessed by fluorescence microscopy. Finally, the dynamics of the interactions will be tested by determining the effect of elf18 elicitation on complex formation. The specificity of interactions between EFR and EIPs will also be addressed by testing interaction between EIPs and other LRR receptor kinases (e.g. FLS2, BRI1, ERECTA).

Once EIPs have been confirmed, their role in innate immunity will be investigated. This will be done by isolating homozygous knockout mutants and generating over-expressing lines for *EIP* genes of interest. First, the role of EIPs in EF-Tu responses will be characterized. After PAMP treatment, several responses can be measured including reactive oxygen species (ROS) and activation of mitogen-activated protein kinases (MAPKs), altered gene expression and the inhibition of

seedling growth. These studies will be further extended to assess EIP general function in innate immunity. Responses to other PAMPs, such as flg22, lipopolysaccharides (LPS), chitin and oligogalacturonides (OGA) will be similarly tested in the mutant lines. Disease susceptibility to bacterial, fungal and oomycete pathogens will also be analyzed in these lines. Further biochemical and molecular characterization of individual EIPs will be carried out, depending on the identity of the EIPs.

#### **4. Research Design and Methodology**

##### **Objective 1: Identify EFR-interacting proteins (EIPs) *in vivo***

###### **1. Development of experimental tools**

Before this project can begin, specific antibodies are necessary for the co-immunoprecipitation (co-IP) of EFR to be carried out. Anti-EFR antibodies against specific peptides have been ordered and will be tested for specificity in the first stage of the project using wild-type *Arabidopsis* and *efr* null mutant. Concurrently, tagged versions of EFR will be generated in the event that no appropriate anti-EFR antibody is found, and for use in other stages of the project (discussed below). Fluorescent (GFP, CFP, YFP) and immunological (Myc; FLAG; HA) tags will be used. C-terminal tagging will be employed to prevent disruption of the signal peptide at the N-terminus of the EFR protein. Tagged versions of EFR will be expressed preferably under the native EFR promoter. However if expression levels are unacceptable for the biochemical experiments, constructs under the control of the strong constitutive 35S promoter will be used. To rapidly test for functionality, these tagged EFR proteins will be expressed transiently using *Agrobacterium tumefaciens* in *Nicotiana benthamiana* leaves. *N. benthamiana* plants have no perception system for EF-Tu, but gain the ability to respond to EF-Tu when transiently transformed with EFR (Zipfel *et al.*, 2006). In parallel, we will generate stable transgenic lines of *A. thaliana* expressing the tagged EFR constructs in an *efr* null background to avoid possible interference with endogenous untagged EFR proteins.

The functionality of the tagged EFR versions will be assessed by testing cellular responses in transgenic plants after elf18 elicitation, such as the production of reactive species (ROS) using a luminol-based assay.

## **2. Identifying EIPs**

Co-IP using anti-EFR antibodies or antibodies reacting with the tags mentioned above will be used to pull-down EFR and EIPs *in vivo*. This approach has been widely used to detect protein-protein interactions (Phizicky and Fields, 1995), and as it reflects the *in vivo* situation, provides more convincing results than *in vitro* methods or in yeast.

### **2.1. Qualitative study**

A preliminary investigation will be done in order to optimize conditions of protein solubilization, IP and test antibodies. Initially, total protein extracts will be used directly for co-IP experiments. Total protein has successfully been used for interaction studies involving SERK1 to identify multiple interaction partners (Karlova *et al.*, 2006). In other studies, the microsomal fraction has been used to identify RLK interactors (Heese *et al.*, 2007). LRR-RLKs may reside in lipid raft microdomains at the plasma membrane, which have proven recalcitrant to Triton X-100 solubilization (Shahollari *et al.*, 2004). A report has identified a highly efficient method combining two-phase partitioning (Larrson *et al.*, 1994) and methanol (Mitra *et al.*, 2007) for the solubilisation of membrane proteins, especially LRR-RLKs. Using this method to enrich for membrane proteins prior to mass spectrometry will increase the sequence coverage of highly hydrophobic membrane proteins, which may include EIPs. Initially total protein will be used for IP, if this approach is not effective, microsomal fractions will be used.

In this experiment, *Arabidopsis thaliana* Col-0 and *efr* plants will be cultivated in shaking liquid MS medium for 7 days prior to elf18 treatment. Protein extracts from elicited and control plants will be immunoprecipitated with anti-EFR (or anti-TAG) antibodies. Extracts will be analyzed by anti-EFR or anti-TAG western blotting to confirm the presence of EFR in the immunoprecipitate. Extracts will also be separated by SDS-PAGE and the gels Coomassie stained. Bands of interest will be excised and subjected to liquid chromatography-tandem mass spectrometry (LC-MS/MS) to identify proteins.

## **2.2. Quantitative study**

Quantitative immunoprecipitation combined with knock-down (QUICK) (Selbach and Mann, 2006) - a method of co-IP employing stable isotope labelling - will be used to quantitatively assess EIP-EFR interactions and to reduce the rate of false-positives. As opposed to using a knock-down line, the negative control used in this study will be *efr* null-mutant plants. Methods incorporating isotopic labels into proteins using chemical derivatization, such as isotope coded affinity tag (ICAT), do not account for differences in sample handling prior to labelling. An alternative is the use of metabolic labelling by feeding organisms with heavy isotopes during growth – stable isotope labelling with amino acids in cell culture (SILAC). In this approach, control and experimental samples are combined before homogenization and extraction, providing an internal control for all subsequent steps. SILAC has proved difficult and inefficient in plant studies (Engelsberger *et al.*, 2006), but an alternative method of metabolic labelling using  $^{15}\text{N}$  has been successfully implemented for plants.  $^{15}\text{N}$  labelling has recently been used in comparative membrane proteomic studies of *Arabidopsis* cell suspension cultures (Lanquar *et al.*, 2007) and whole plants (Nelson *et al.*, 2007).

In the present study, *Arabidopsis* plants will be cultivated in shaking liquid culture using light ( $^{14}\text{N}$ ) or heavy ( $^{15}\text{N}$ ) medium. These experiments will be done in duplicate to compare (1) *elf18* treatment in wild type and *efr* plants (control) or (2) using wild type plants with *elf18* treatment or addition of medium alone.

For interaction studies, *elf18* (treatment) will be added to heavy ( $^{15}\text{N}$ ) Col-0 and light *efr* plants. The converse will also be carried out for comparison [inverse metabolic labelling – the isotopic pattern should be reversed in the reciprocal experiment]. Plant extracts from heavy and light plants will be combined and membranes isolated (Wang *et al.*, 2005). EFR will be immunoprecipitated from membrane and cytoplasmic fractions with anti-EFR or anti-TAG antibodies. Proteins will be analyzed by western blotting to detect the presence of EFR and confirm successful immunoprecipitation of EFR. Extracts will also be separated by SDS-PAGE and the gels Coomassie stained. Bands of interest will be excised and subjected to liquid chromatography-tandem mass spectrometry (LC-MS/MS) to identify proteins. The utility of metabolic labelling as a control for eliminating false positives will be evident at this stage. EFR and EIPs should be more abundant in

the heavy than the light form while contaminating proteins should be present equally as heavy and light.

### **3. Confirmation of EIPs**

Once the identity of an EIP is known, the EIP-EFR interactions need to be confirmed *in vivo* using biochemical and cell biology approaches.

#### **3.1. By biochemical means**

The first step to confirm IP results will be to generate specific anti-EIP antibodies and transgenic plants expressing tagged versions of the EIPs. Then, reciprocal co-IP between EFR and the EIPs using anti-EIP or anti-TAG antibodies can be conducted before and after *elf18* treatment.

#### **3.2. By microscopic means**

Real-time monitoring and localization of protein interactions within living cells requires instant read-out. This can be achieved by attaching a spectroscopic probe to the proteins of interest in the cell and measuring fluorescence resonance energy transfer (FRET). FRET involves the excitation of an acceptor fluorophore (yellow fluorescent protein, YFP) by a donor fluorophore (cyan fluorescent protein, CFP), which only occurs when they are less than 52 Å apart (Tsien, 1998). FRET can be detected in living cells as a change in emission intensity of the donor and acceptor, and as a change in the fluorescent life-time (Yan and Marriot, 2003). FRET can occur between different variants of green fluorescent protein (GFP) (Miyawaki and Tsien, 2000) and can be monitored in living cells using fluorescence microscopy techniques (Kenworthy, 2001). Fluorescence lifetime imaging microscopy (FLIM) coupled with fusions of cyan and yellow fluorescent proteins to BAK1 and BRI1 was used to show heterodimerization of BRI1 and BAK1 in protoplast endosomes (Russinova *et al.*, 2004). This served to confirm the validity of the co-IP as an assay of their association *in planta*. This method will be used to confirm the EFR-EIP interactions detected in the initial co-IP experiments. For this purpose, YFP and CFP derivatives of EFR and the EIPs will be generated. Although some analyses can be performed using transient expression in protoplasts, double-transgenic plants will also be generated. In addition, fluorescence microscopy will be used to determine where complex components are localized. Proteins which function as part of the EFR receptor

complex are likely to be found in or at the periphery of the membrane. The co-localization of EFR and EIPs will thus confirm co-IP results.

In order to analyze the dynamic nature of EIP-EFR interactions, a time study of protein interactions will be done using the co-IP and microscopic techniques described above. *Arabidopsis* seedlings will be elicited for 2, 5, 10, 30 and 60 minutes with *elf18* and the progress of complex formation will be followed.

#### **4. Specificity of the interaction**

The proteins BAK1 and KAPP interact with several RLKs (Chinchilla *et al.*, 2007; Ding *et al.*, 2007; Heese *et al.*, 2007; He *et al.*, 2007). This suggests that RLK signaling pathways partially share certain signaling components. Thus, the specificity of the interaction between EIPs and EFR will be determined by comparing the ability of EIPs to interact with other RLKs. Co-IP of EIPs with RLKs, such as FLS2 (Chinchilla *et al.*, 2006; Robatzek *et al.*, 2006), BRI1 (Nam and Li, 2001; Russinova *et al.*, 2004; Wang *et al.*, 2005), CLV1 (Trottochaud *et al.*, 1999; De Young *et al.*, 2006) and ERECTA (Shpak *et al.*, 2003) will be carried out using available tagged lines and/or antibodies.

#### **5. The role of EIPs in innate immunity**

##### **5.1. EF-Tu related responses**

Once putative EIPs are confirmed interactors of EFR, their role in defense signaling will need to be addressed. To this aim, potential insertional mutants will be ordered from available stock centres and homozygous null *eip* mutants will be isolated. In addition, EIP over-expressing lines will be generated.

The possibility exists that any given EIP may exist as part of a multigene family, resulting in functional redundancy. This would preclude the identification of EIP function in single mutants. If necessary, multiple mutants could be obtained or artificial miRNA constructs could be designed to target several members of the corresponding multigene family.

We will test whether the absence or over-abundance of an EIP has any consequences for EFR signaling. *Elf18*-induced responses will be measured in *eip* null mutants, EIP over-expressing lines and compared to Col-0 responses. These *elf18*-induced responses include induction of an oxidative burst, expression of early marker genes, MAP kinase activation, callose deposition and seedling

growth inhibition. All these responses will be measured over a range of elf18 concentrations.

### **5.2. Responses to other PAMPs**

The involvement of EIPs in signaling related to other PAMPs can also be assessed using the approaches described in 5.1. These experiments will provide an indication of whether any EIPs are involved in other PAMP signaling pathways and should also expose cross-talk between PAMP signaling pathways. PAMPs that will be used to induce mutant plants include flg22, LPS, chitin and oligogalacturonides (OGAs).

### **5.3. EIPs in disease susceptibility**

The *Arabidopsis fls2* mutant is more susceptible than wild-type Col-0 to infection by the virulent pathogen *Pseudomonas syringae* pv. *tomato* DC3000 (*Pto* DC3000), and pre-treatment of wild-type but not the *fls2* mutant plants with flg22 enhances resistance to *Pto* DC3000 (Zipfel *et al.*, 2004). *Fls2* plants are also more susceptible to *P. syringae* pv. *phaseolicola* (de Torres *et al.*, 2006) and *P. syringae* pv. *tabaci* lacking flagellin are more virulent on wild-type plants (Li *et al.*, 2005).

*Efr* plants are also more amenable to transformation by *Agrobacterium tumefaciens*, revealing that plant transformation is normally restricted by plant defenses (Zipfel *et al.*, 2006). In addition, *efr* plants are more susceptible to colonization by the weakly virulent mutant strains *Pto* DC3000  $\Delta$ avr*Pto* $\Delta$ avr*PtoB* and *Pto* DC3000 *COR* $^-$  (rotation project). Thus, PAMP perception contributes to PAMP-triggered immunity (PTI) against bacterial growth.

Disease susceptibility of *EIP* lines to adapted and non-adapted *Pseudomonas* strains will be assessed by bacterial growth curve experiments. Strains that will be used include *Pto* DC3000, *Pto* DC3000 *COR* $^-$ , *Pto* DC3000  $\Delta$ avr*Pto* $\Delta$ avr*PtoB*, *Pto* DC3000 *hrcC* $^-$ , *P. syringae* pv. *tabaci* and *P. syringae* pv. *phaseolicola*.

PAMP-triggered responses are targeted by pathogen effectors (de Torres *et al.*, 2006; Hauck *et al.*, 2003; He *et al.*, 2006; Janjusevic *et al.*, 2006) and thus PAMP signaling components may also be important components of effector-triggered immunity (ETI). The role of EIPs in ETI will be established by bacterial growth curve experiments in *EIP* lines using strains of *Pseudomonas syringae* pv. *tomato* DC3000 carrying the Avr genes *AvrRpm1*, *AvrRpt2* and *AvrRps4*.

We will also assess the susceptibility of *EIP* lines to the fungi and oomycetes *Alternaria brassicicola*, *Botrytis cinerea* and *Hyaloperonospora parasitica* (Noco2

andEmco5). In addition, susceptibility to adapted and non-adapted powdery mildews will be done in collaboration with the group of Volker Lipka in the Sainsbury Laboratory.

## **6. Further characterization of EIPs**

A more detailed analysis of EIPs will become clearer upon identification of specific EIPs, but potential molecular and biochemical relationships between EIPs and EFR can already be considered.

### **6.1. Are EIPs substrates for EFR?**

Some of the identified EIPs might be direct substrates of the EFR kinase. If an EIP is a RLK it is possible that there may be a trans-phosphorylation event whereby each kinase is activated through phosphorylation by its interaction partner. The importance of phosphorylation in receptor activation can be investigated in this case. In this case, we will test *in vitro* and *in vivo* if EFR phosphorylates the EIPs. The specificity can then be tested using EFR with a mutated kinase domain.

### **6.2. Are EIPs involved in endocytosis?**

FLS2 is internalized after flg22 treatment (Robatzek *et al.*, 2006). Receptor endocytosis may be important to attenuate PAMP-triggered signaling or to facilitate internal signaling cascades. It is unknown whether EFR is subject to endocytosis, though it contains a cytosolic adaptin binding motif (Yxxφ) (ELM Database <http://elm.eu.org/>) which is a signal for clathrin-mediated endocytosis in animals. The receptor internalization motif is recognized by adaptin, which binds to the receptor, targeting the complex to intracellular compartments for further processing (Pérez-Gómez and Moore, 2007). If EFR is in fact subject to endocytosis, we will test if there is a requirement for any EIPs in this process. This work will be done in collaboration with Silke Robatzek at the Max Planck Institute in Cologne (Germany).

### **Host Institution and Expertise:**

The Sainsbury lab has a worldwide reputation for conducting excellent research in the study of plant-pathogen interactions. As such, the lab has an abundance of expertise in this field. The Sainsbury lab has the latest in mass spectrometry technology and combined with the on-site expertise, is an ideal location for this

project. Alex Jones has the primary role in the Sainsbury lab for facilitating and supporting entry-level usage of mass spectrometry for the identification of proteins and their post-translational modifications. She is ideally suited to assist the development of methods and analysis of results in this project. In addition, the lab will soon obtain an Orbitrap LTQ mass spectrometer (Thermo Fischer) with increased mass accuracy for more precise protein identification.

The Sainsbury Lab recently purchased a state-of-the-art Leica confocal TCS SP5 microscope which will be useful for the co-localization experiments that have been planned.

## Part IV: Thesis Results

# 1 IDENTIFICATION OF EFR-INTERACTING PROTEINS (EIPs) IN *NICOTIANA BENTHAMIANA*

## 1.1 Preface

The molecular details of the signaling cascades following PAMP perception in plants remain elusive, despite years of effort towards their characterization. This may be partly due to redundancy in signaling components, which limits the utility of forward- and simple reverse-genetic approaches. An alternative approach is to identify protein interactors of key components of PAMP signaling, such as the PRR EFR. In order to uncover important regulators or substrates of EFR, I aimed at identifying specific EFR-interacting proteins *in planta*. At the onset of this project, no tools were available for immunodetection of endogenous EFR or EFR transient expression. To this end I had to produce tools, including anti-EFR antibodies, *EFR* constructs for transient and stable expression, and tagged *EFR* transgenic *Arabidopsis* lines. It was not possible to generate anti-EFR antibodies for immunoprecipitation. My goal was then to use transiently expressed EFR to probe for EIPs. To optimize the method, I had to compare extraction methods and IP protocols for EFR, which can be challenging for transmembrane proteins. Putative EIPs identified in this study include *NbBAK1/SERK3*, components of ER quality control (luminal binding protein; calnexin) and ABC transporter PDR1.

## 1.2 Results

### 1.2.1 Development of specific anti-EFR antibodies

In order to develop specific polyclonal anti-EFR antibodies, I had to identify peptides unique to EFR and of a suitable nature for immunization of rabbits. Two such appropriate sequences (EPO71644: CSEYPRDRMRTDEAV and EPO71645 KNNASDGNPSDSTTLM; [Figure 1.1A](#)) were identified in the kinase domain of EFR (see [Appendix Figure A4.1-3](#) for multiple sequence alignment of kinase domains of family XII LRR-RKs) and synthetic peptides of these sequences were used to immunize rabbits over a 3-month period (Eurogentec). The final

bleed was obtained and used to assess the specificity of the antibodies. In the first instance, both antisera were tested against protein extracts derived from *efr-1* null mutant and wild-type Col-0 plants but no signal was detected by western blotting, even when using femtomole-sensitive chemiluminescent substrates (data not shown). I reasoned that perhaps the specific antibodies were present at low concentrations. In order to enrich for EFR-specific antibodies, further affinity purification of the antisera obtained from rabbits immunized with both peptides was undertaken. I coupled the peptide EPO71644 to AffiGel 15 to create an affinity matrix to enrich for peptide-specific antibodies. I then applied diluted large bleed to the affinity column and eluted acidic and basic antibody fractions, which were subsequently pooled and dialyzed against PBS. Western blotting of *Arabidopsis* protein extracts derived from *efr-1* null mutant and Col-0 plants did not detect any specific bands, either in seedlings or adult plants, but a faint band could be detected in protein extracts derived from transgenic *N. benthamiana* stably expressing untagged EFR under the control of the native promoter ([Figure 1.1B and C](#)); Lacombe *et al.*, 2010). This suggested that the additional purification step may have enriched for EFR-specific antibodies, but endogenous EFR levels in *Arabidopsis* remain below the detection limit.

In a subsequent experiment, I compared the ability of anti-HA affinity matrix and the affinity-purified anti-EFR antibodies to immunoprecipitate transiently expressed EFR-YFP-HA<sub>3</sub> from *N. benthamiana* extracts ([Figure 1.1D](#)). As a negative control, I similarly immunoprecipitated transiently expressed GUS-HA<sub>3</sub>. Although EFR is predicted to be a protein of 113 kDa, the untagged protein is known to migrate to 150 kDa on SDS-PAGE, likely due to glycosylation of the LRR domain (Zipfel *et al.*, 2006; Chapter 2). With the addition of the C-terminal tags, the recombinant protein has a predicted molecular weight of approximately 175 kDa. Anti-HA immunoblotting of total protein extracts detected a weak band at the correct size for tagged EFR but this was not detectable with anti-EFR immunoblotting ([Figure 1.1D](#)). In the corresponding anti-HA IP, a band could be detected for EFR-YFP-HA<sub>3</sub> at the correct size, which was absent from the GUS-HA<sub>3</sub> sample, suggesting that this band is specific to EFR-YFP-HA<sub>3</sub>. Similarly, a band was also detected at this size by anti-HA immunoblotting of the same protein extract but which had been subjected to anti-EFR immunoprecipitation ([Figure 1.1D](#)). These results suggest that the anti-EFR antibodies are not sufficiently

sensitive to detect native levels of EFR in *Arabidopsis*, but can detect heterologously expressed EFR when it has been enriched by immunoprecipitation.

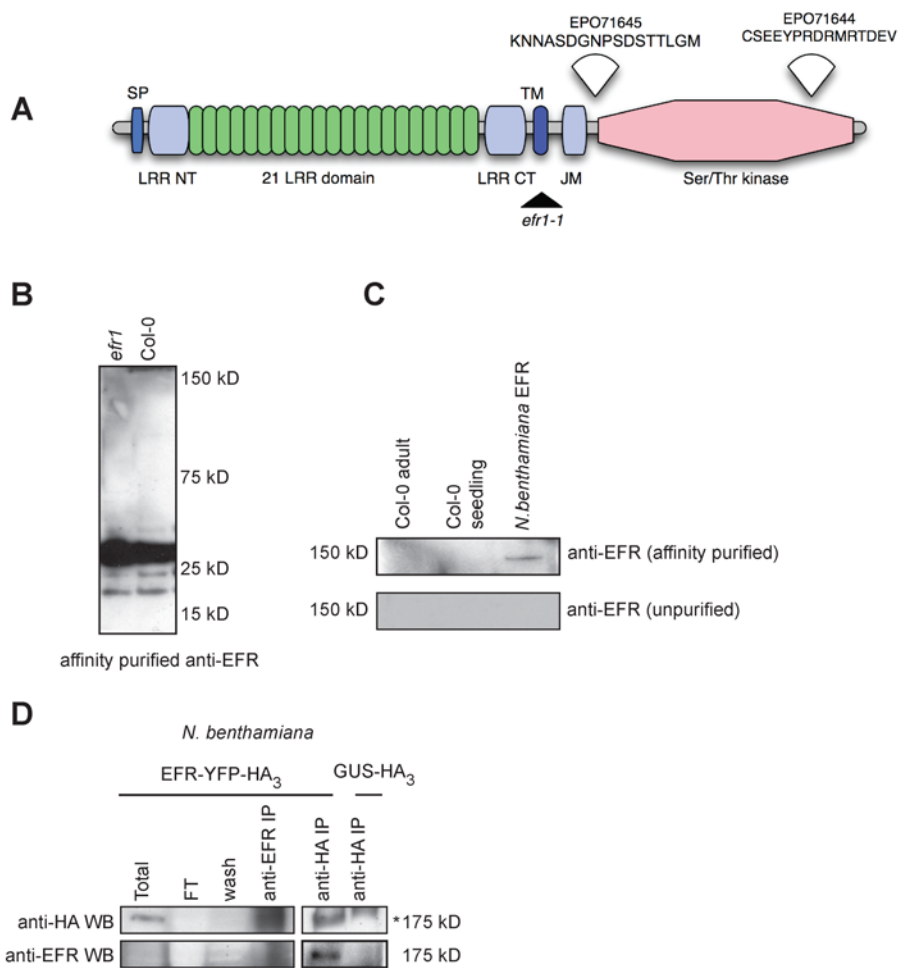


**Figure 1.1 Anti-EFR antibodies cannot detect endogenous *Arabidopsis* EFR**

A. Schematic representation of EFR protein. The LRR domain is represented in green ovals, followed by the transmembrane domain in blue and the kinase domain in pink. The location of peptides selected for immunization is indicated by wedges with the sequence above. SP = signal peptide; LRR = leucine-rich repeat; NT= N terminal; CT= C terminal; TM = transmembrane domain.

B. Immunoblot of *Arabidopsis* total protein extracts probed with affinity-purified primary anti-EFR antibody (1:1000).

C. Immunoblot of *Arabidopsis* and *N. benthamiana* expressing *EFR* total protein extracts probed with unpurified or affinity-purified primary anti-EFR antibody (1:500).

D. Immunoblot of total, flow-through (FT), wash and anti-EFR or anti-HA immunoprecipitate (IP) derived from *N. benthamiana* expressing either EFR-YFP-HA<sub>3</sub> or GUS-HA<sub>3</sub>. The anti-HA immunoblot is indicated in the top panel and the anti-EFR (affinity purified; 1:1000) is indicated in the bottom panel. The molecular weight is indicated as 175 kDa, asterisk indicates nonspecific band.

### 1.2.2 Development of tagged *EFR* constructs for transient expression

As I was unable to develop anti-*EFR* antibodies suitable for *EFR* immunoprecipitation, I tested affinity-tagged *EFR* constructs for transient expression in *N. benthamiana* and stable expression in transgenic *Arabidopsis*. The full-length *EFR* cDNA was cloned by Valerie Nicaise into the Gateway-compatible *pEarleyGate* binary expression vectors (Earley *et al.*, 2006). Three constructs were cloned, each with a constitutive 35S promoter and C-terminal tags as follows: *pEarley101-EFR-YFP-HA*<sub>3</sub>; *pEarley102-EFR-CFP-HA*<sub>3</sub>; *pEarley103-EFR-GFP-His*<sub>6</sub>. The fluorescent tags facilitate detection of *EFR* *in planta* by confocal microscopy, while the GFP, HA<sub>3</sub> and His<sub>6</sub> can be used for immunoprecipitation of *EFR*.

I tested the transient expression of the constructs in transient expression in the model plant *Nicotiana benthamiana* that allows *Agrobacterium*-mediated transient expression of defined tagged proteins (Goodin *et al.*, 2008). Leaf samples were harvested 2 days post-infiltration and total proteins extracted using a crude SDS-based extraction buffer. Proteins were separated by SDS-PAGE and detected by Western blotting using anti-His primary antibodies for detection of *EFR-GFP-His*<sub>6</sub> ([Figure 1.2A](#), left panel) and anti-HA-HRP HRP-conjugated primary antibodies for detection of *EFR-YFP-HA*<sub>3</sub> and *EFR-CFP-HA*<sub>3</sub> ([Figure 1.2A](#), right panel). In each case, a band was detected at the appropriate size (175 kDa), which was absent from proteins extracted from wild-type *N. benthamiana*. Thus, tagged *EFR* proteins can be successfully expressed and detected in *N. benthamiana*.

In order to establish the localization of *EFR* upon transient expression in *N. benthamiana*, I used the same system of agro-infiltration followed by confocal microscopy of leaf strips. *EFR-GFP-His* could be detected in the cell periphery 2 days post-infiltration ([Figure 1.2B](#)), suggesting a plasma membrane localization, as expected for a receptor-like kinase containing a predicted transmembrane domain (Zipfel *et al.*, 2006).

To test if the tagged *EFR* protein is functional, the production of ROS in response to elf18 was measured in leaf discs transiently expressing *EFR*, and compared to *N. benthamiana* stably expressing untagged At*EFR* under the native promoter. As shown in [Figure 1.2C](#), no ROS burst was produced in response to

elf18 when GUS-HA<sub>3</sub> was transiently expressed in *N. benthamiana*. However, as previously reported (Lacombe *et al.*, 2010), the stable transgenic EFR *N. benthamiana* produced a burst of ROS within 5 minutes of elf18 elicitation (Figure 1.2C, black line). A similar burst, of even greater amplitude was produced in leaf discs transiently over-expressing any of the tagged EFR constructs (Figure 1.2C, yellow, green and blue lines). The ROS bursts peaked at 10 minutes and decreased within 35 minutes but did not reach baseline levels.

These results suggest that tagged EFR is able to function in *N. benthamiana*, as measured by ROS production in response to elf18.

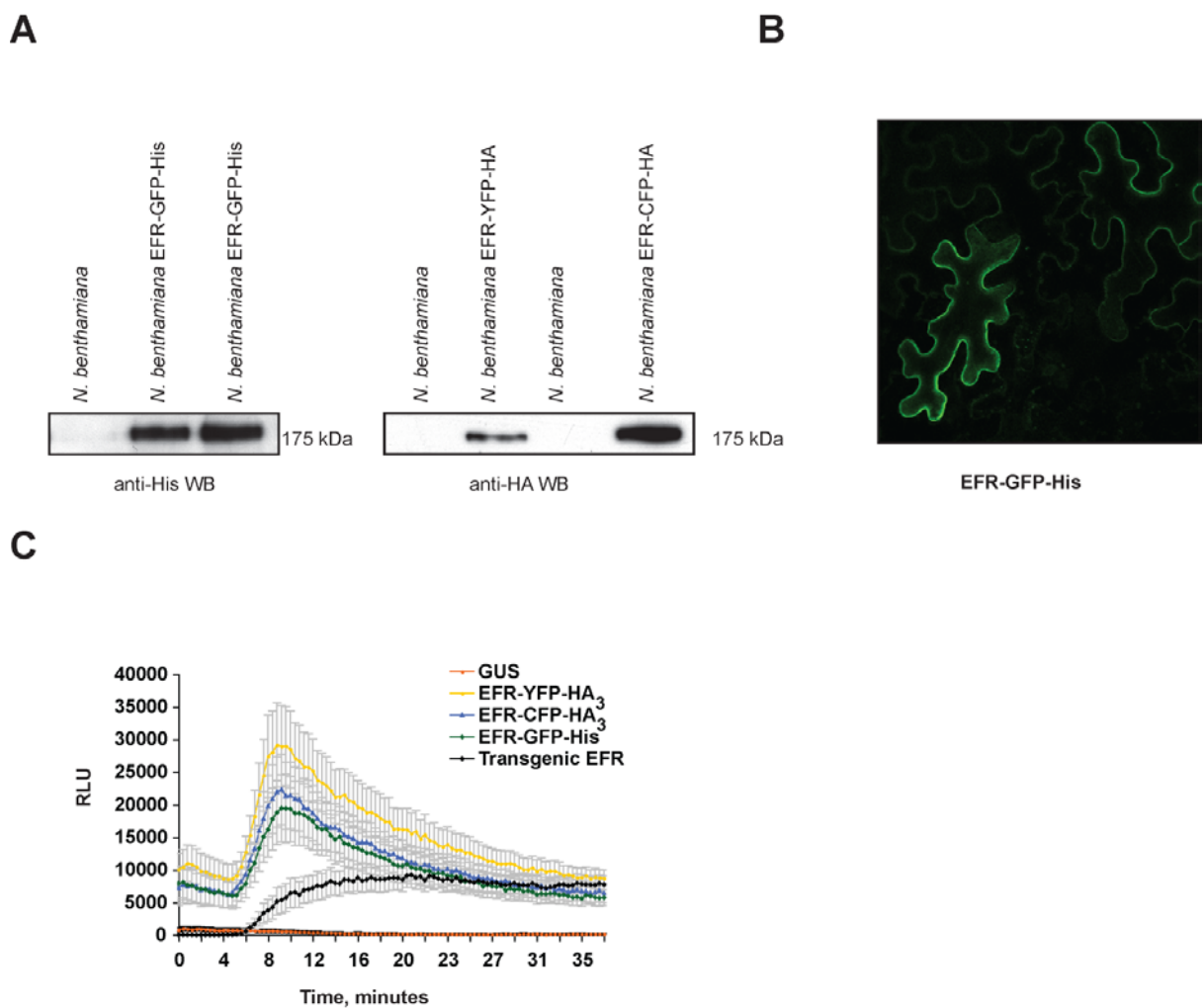


**Figure 1.2 Transiently expressed EFR is functional and detectable in the cell periphery in *N. benthamiana*.**

A. Western blotting of total protein extracts derived from wild-type *N. benthamiana* or *N. benthamiana* expressing EFR-GFP-His - left panel, anti-His (1:1000); EFR-YFP-HA<sub>3</sub> or EFR-CFP-HA<sub>3</sub> - right panel, anti-HA-HRP (1:2000).

B. Confocal image of EFR-GFP-His expressed in *N. benthamiana* under the control of the 35S promoter, 2 days post-agro-infiltration.

C. Production of ROS burst in response to addition of 100 nM elf18 in *N. benthamiana*, stably expressing AtEFR (black) or transiently expressing GUS (orange); EFR-YFP-HA<sub>3</sub> (yellow), EFR-CFP-HA<sub>3</sub> (blue) or EFR-GFP-His (green), 2 days post-agroinfiltration. RLU, relative light units. Results are average ± standard error (n=8).

### 1.2.3 Production of transgenic *Arabidopsis* plants stably expressing functional AtEFR

Upon confirming the functionality of tagged EFR in *N. benthamiana*, I initiated production of stable *Arabidopsis* transgenic lines expressing the same proteins (in collaboration with Valerie Nicaise). Null mutant *efr-1* and wild-type Col-0 *Arabidopsis* were transformed by floral dipping with EFR-YFP-HA<sub>3</sub>, EFR-CFP-HA<sub>3</sub> or EFR-GFP-His<sub>6</sub> under the control of the 35S promoter. Despite recovery of several primary transformants, only one suitable stable transgenic line was obtained in *efr-1* expressing 35S::EFR-YFP-HA<sub>3</sub> (line 5-1-3; [Figure 1.3A](#)). It is possible that few stable transgenic lines were obtained as the plant is attempting to limit PRR expression to prevent excessive immune signaling.

The tagged EFR protein could be detected by confocal microscopy and was localized to the cell periphery ([Figure 1.3B](#)), in agreement with the expected subcellular localization and the localization observed when expressed in *N. benthamiana*. The transgenic EFR line responded even more intensely to elf18 elicitation, and produced a sustained ROS burst of greater amplitude than wild-type Col-0 ([Figure 1.3C](#)). This shows that *efr-1* is complemented by functional, over-expressed tagged EFR protein. The transgenic line responded similarly to Col-0 in a seedling growth inhibition assay ([Figure 1.3D](#)). Inhibition of seedling growth is a late PAMP-induced response measurable in *Arabidopsis*, where even low concentrations of flg22 or elf18 inhibit the expansion of roots and shoots when included in growth medium (Gómez-Gómez *et al.*, 1999; Gómez-Gómez and Boller, 2000; Zipfel *et al.*, 2006). The fact that the tagged EFR is able to functionally complement *efr-1* in this assay illustrates that the full signaling pathway can be activated by the tagged protein.

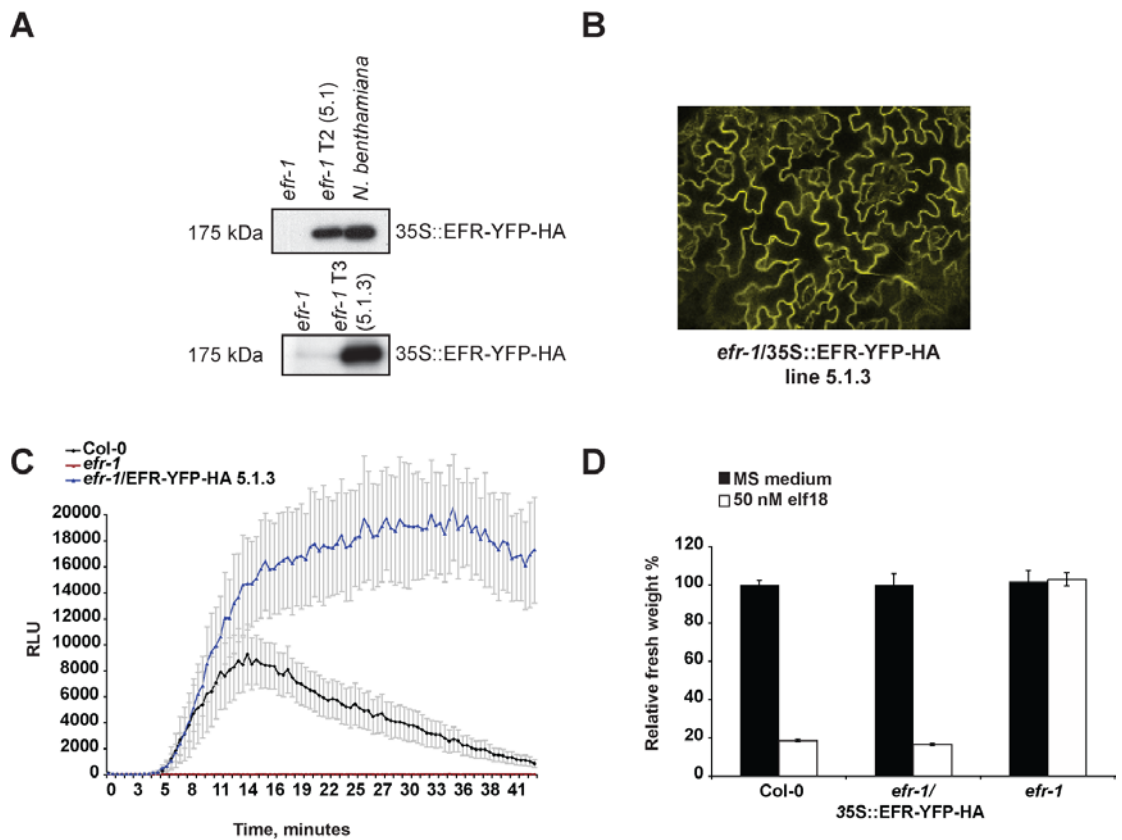


**Figure 1.3 Transgenic Arabidopsis over-expressing EFR complements *efr-1* for elf18 responses.**

A. Immunoblot detection (anti-HA, 1:2000) of crude protein extracts of T2 (line 5.1) and T3 (line 5.1.3) transgenic *efr-1* Arabidopsis seedlings expressing 35S::EFR-YFP-HA compared to *N. benthamiana* transiently expressing the same construct, 2 days post-agroinfiltration.

B. Confocal imaging of Arabidopsis epidermal leaf tissue expressing 35S::EFR-YFP-HA.

C. Production of ROS in response to 100 nM elf18 elicitation in Col-0, *efr-1* and *efr-1*/EFR-YFP-HA leaf discs. Results are average  $\pm$  standard error ( $n = 8$ ).

D. Seedling growth inhibition of Col-0, *efr-1* and *efr-1*/EFR-YFP-HA following incubation in MS medium or 50 nM elf18. Data are represented as relative fresh weight compared to untreated seedlings. Results are average  $\pm$  standard error ( $n = 10$ ).

In the next phase of the project, I went on to develop transgenic lines expressing tagged EFR under the control of its native promoter, in order to more closely approximate natural expression levels of EFR (in collaboration with Vladimir Nekrasov). Arabidopsis *efr-1* plants were transformed with EFR-eGFP or EFR-eGFP-HA in a binary vector (*epiGreenB5*) containing the native *EFR* promoter (Nekrasov *et al.*, 2009). The tagged EFR-eGFP protein expressed from T3 lines 1.33.12 and 1.33.17 was detectable by western blotting of crude total protein extracts (Figure 1.4A). Although the native promoter was used, it is likely that the levels of EFR in these lines exceed those in Col-0, as the transgenic lines showed heightened responsiveness to elf18. The ROS burst in response to elf18

was of greater amplitude and duration than that of wild-type Col-0 ([Figure 1.4B](#)), and the growth of EFR-eGFP seedlings was more inhibited by elf18, even at concentration of 1 nM elf18 ([Figure 1.4C](#)). Similar results were obtained for characterization of EFR-eGFP-HA lines (done by Vladimir Nekrasov; [Figure 1.4 E-F right panel](#)). Nonetheless, the expression levels and responsiveness were lower than seen for the over-expression lines ([Figure 1.3](#)).

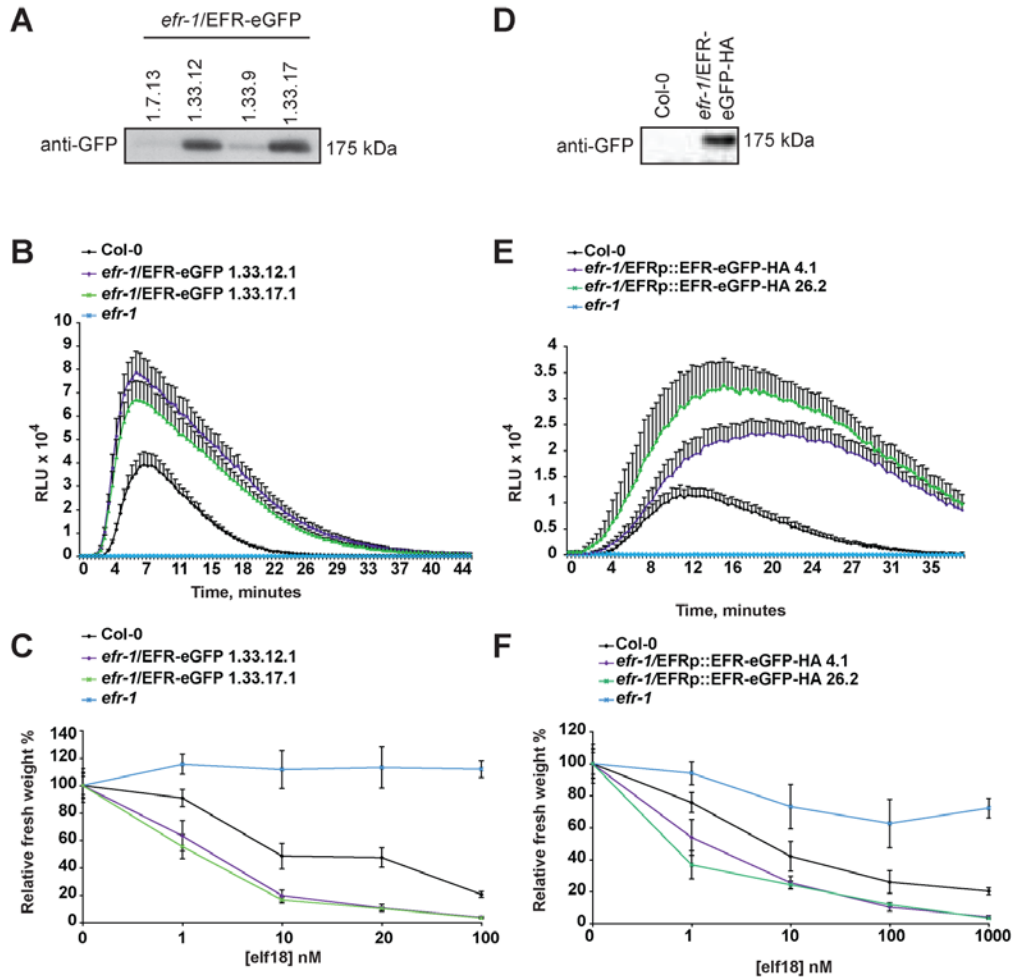


**Figure 1.4 Transgenic lines expressing EFR under the control of the native promoter complement *efr-1*.**

A and D. Immunoblot detection (anti-GFP, 1:5000) of crude protein extracts derived from independent T3 transgenic *efr-1* Arabidopsis lines expressing *EFRp::EFR-eGFP* (A) or *EFRp::EFR-eGFP-HA* (D).

B and E. Production of ROS in response to elf18 (100 nM) elicitation in Col-0, *efr-1* and *efr-1/EFR-eGFP* (B) or *efr-1/EFR-eGFP-HA* (E) leaf discs. Results are average  $\pm$  standard error ( $n = 8$ ).

C and F. Seedling growth inhibition of Col-0, *efr-1* and *efr-1/EFR-eGFP* (C) or *efr-1/EFR-eGFP-HA* (F) in response to increasing elf18 concentration. Data are represented as relative fresh weight compared to untreated seedlings. Results are average  $\pm$  standard error ( $n = 6$ ).

## 1.2.4 Immunoprecipitation of transiently expressed tagged EFR from *N. benthamiana*

### 1.2.4.1 Immunoprecipitation method development

While selecting homozygous EFR transgenic lines in Arabidopsis, I carried out EFR IPs in *N. benthamiana*. I made use of the agro-infiltration system for transient expression of EFR in *N. benthamiana* to produce large amounts of tissue for immunoprecipitation. In order to establish a working protocol, I compared extraction of total protein with the isolation of the microsomal fraction prior to immunoprecipitation of EFR. I agro-infiltrated either EFR-HA<sub>3</sub> or GUS-HA<sub>3</sub> under the control of the 35S promoter into 2-week-old *N. benthamiana* plants. Two days post-infiltration, I harvested 15 g of tissue for each protein extraction. I extracted total protein from tissue expressing EFR-HA<sub>3</sub> or GUS-HA<sub>3</sub> or wild-type *N. benthamiana*. Following tissue grinding, the sample was split to compare extraction methods. The total protein was extracted from tissue expressing EFR-HA<sub>3</sub> or GUS-HA<sub>3</sub> using a buffer containing the non-denaturing detergent IGEPAL CA-630 to extract EFR from the plasma membrane with minimal disruption of protein-protein interactions. Microsomal proteins were isolated from wild-type *N. benthamiana* or tissue expressing EFR-HA<sub>3</sub> by ultracentrifugation of total protein and solubilization of pelleted membrane proteins in a buffer containing the same detergent. Anti-HA affinity matrix was added to either microsomal or total protein to immunoprecipitate EFR-HA<sub>3</sub> or GUS-HA<sub>3</sub>.

A faint band around the correct size of 175 kDa could be detected for EFR-HA<sub>3</sub> in the total protein extracted in each case ([Figure 1.5A-B](#), indicated by arrow), which was absent from either GUS-HA<sub>3</sub> expressing or wild-type *N. benthamiana*. Interestingly, the same volume of the microsomal fraction was significantly enriched in EFR-HA<sub>3</sub>. Following immunoprecipitation, the amount of EFR-HA<sub>3</sub> was further increased, from both the total protein and microsomal fraction. The volume of immunoprecipitate loaded on the gel was half that of the total protein, demonstrating that the EFR-HA<sub>3</sub> protein was pulled out of the total or microsomal protein successfully ([Figure 1.5A-B](#)).

The remaining immunoprecipitate was loaded on a SDS-PAGE gel and stained with colloidal Coomassie brilliant blue. EFR-HA<sub>3</sub> can be seen as a

distinctly stained band on the gel at around 175 kDa, and the band is absent from the corresponding IP derived from wild-type *N. benthamiana* ([Figure 1.5C](#)) or GUS-HA<sub>3</sub>-expressing tissues ([Figure 1.5D](#)). GUS-HA<sub>3</sub> was also successfully immunoprecipitated from total protein, and is represented by a large band at around 60 kDa ([Figure 1.5D](#)). In order to determine the best extraction method to obtain high-quality EFR peptides, I used tandem mass spectrometry (MS/MS) analysis to analyze the IPs. I excised the EFR band from each of the gels, carried out an in-gel trypsin digestion and subjected extracted peptides for HPLC-MS/MS analysis. Mass spectrometry analysis revealed a coverage EFR of 4 % of the EFR sequence in the IP recovered from the microsomal fraction, compared to 30 % from the total protein ([Figure 1.5E-F](#); [Appendix Table A1.1](#)).

Given that a similar amount of EFR could be immunoprecipitated from total protein and microsomal fraction, but that the total protein IP seemed to provide a better coverage across the length of EFR, I decided to exclude the microsomal fractionation to avoid possible degradation due to the additional time taken to pellet the microsomes. For all future IPs, I used total protein extracted using a non-denaturing detergent to solubilize EFR from membranes.

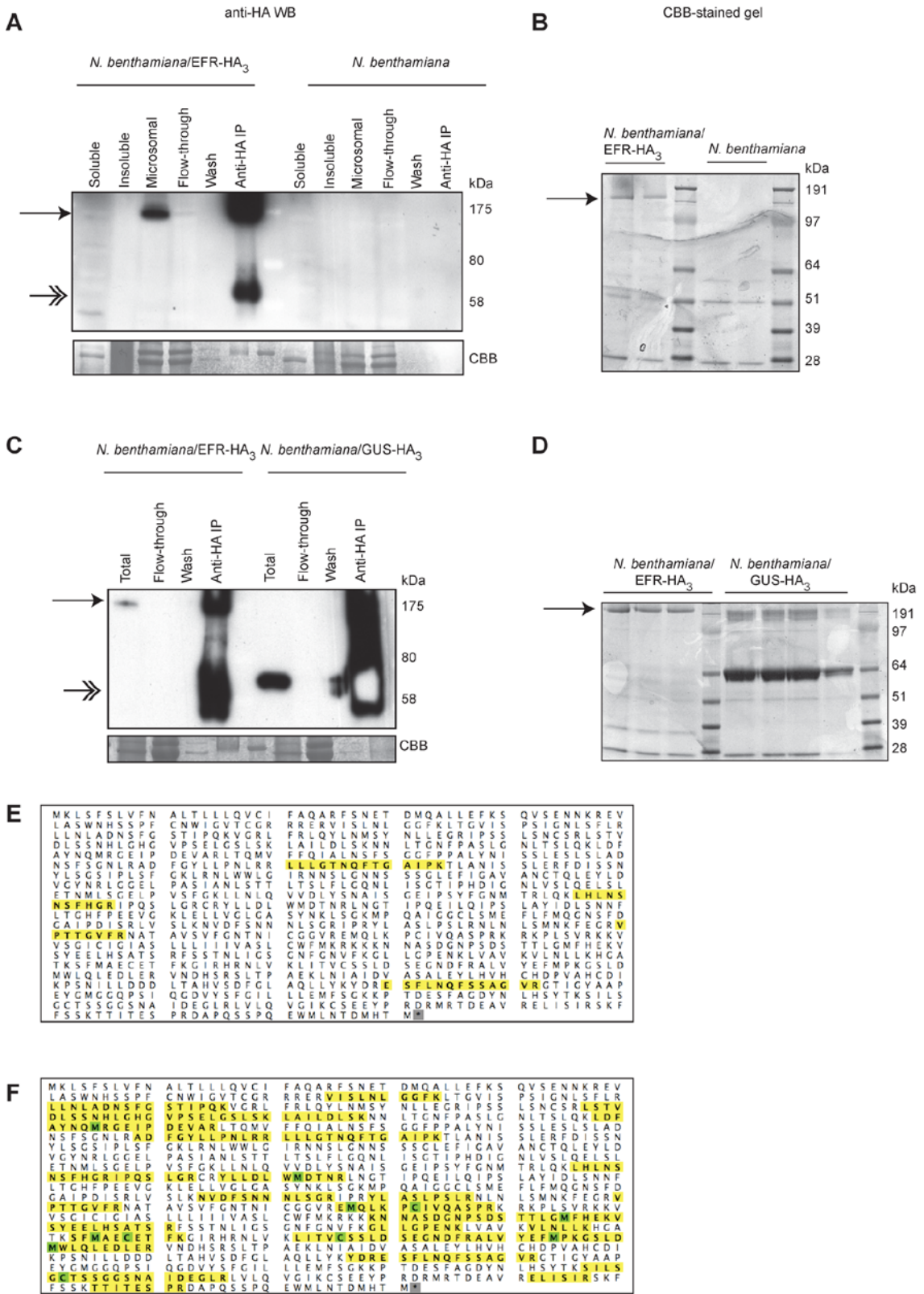


**Figure 1.5: Immunoprecipitation of transiently expressed EFR-HA<sub>3</sub> or GUS-HA<sub>3</sub> from total protein or microsomal preparations.** A. Western blot illustrating microsomal protein extraction followed by anti-HA immunoprecipitation from wild-type or EFR-HA<sub>3</sub> transiently expressing *N. benthamiana*; anti-HA immunoblot, film (top) and Coomassie-stained PVDF membrane (CBB, bottom). Single-head Arrows indicate EFR-HA<sub>3</sub>; double-headed arrows indicate cleavage product.

- B. Colloidal Coomassie-stained SDS-PAGE of anti-HA IP prepared from microsomal fraction proteins from wild-type or EFR-HA<sub>3</sub> transiently expressing *N. benthamiana*. Arrows indicate EFR-HA<sub>3</sub>.
- C. Western blot illustrating total protein extraction followed by anti-HA immunoprecipitation from *N. benthamiana* transiently expressing EFR-HA<sub>3</sub> or GUS-HA<sub>3</sub>; anti-HA immunoblot, film (top) and Coomassie-stained PVDF membrane (CBB, bottom). Arrows indicate EFR-HA<sub>3</sub>.
- D. Colloidal Coomassie-stained SDS-PAGE of anti-HA IP prepared from total proteins extracted from *N. benthamiana* transiently expressing EFR-HA<sub>3</sub> or GUS-HA<sub>3</sub>. Approximate molecular weight in kDa indicated on right. Arrows indicate EFR-HA<sub>3</sub>.
- E. Illustration of sequence coverage of EFR (4 %) as determined by mass spectrometry analysis of IPs generated from microsomal proteins. Peptides are indicated by yellow shading of the sequence, with oxidized residues green.
- F. Illustration of sequence coverage of EFR (30 %) as determined by mass spectrometry analysis of IPs generated from total proteins. Peptides are indicated by yellow shading of the sequence, with oxidized residues green.

#### 1.2.4.2 *N. benthamiana* EFR IP

Once the method had been established, I set out to carry out large-scale IPs of EFR-HA<sub>3</sub> that had been transiently expressed in *N. benthamiana* in order to identify EFR-interacting proteins (EIPs). In these experiments I made use of GUS-HA as a negative control for the IPs, to allow me to exclude proteins simply adhere to IP beads. In the initial biological replicate I prepared 15 g each of GUS-HA<sub>3</sub> and EFR-HA<sub>3</sub> infiltrated tissue, and I further vacuum infiltrated EFR-HA<sub>3</sub>-expressing tissue with 100 nM elf18 for 5 minutes prior to freezing. I extracted total proteins and enriched for GUS-HA<sub>3</sub> or EFR-HA<sub>3</sub> by anti-HA immunoprecipitation. I separated the total protein using SDS-PAGE and compared this to the flow-through (the protein remaining after the immunoprecipitation) to ascertain the efficiency of the immunoprecipitation using anti-HA beads. In this experiment it appeared that the IP had enriched for EFR-HA<sub>3</sub> and GUS-HA<sub>3</sub> although not all the transiently expressed GUS-HA<sub>3</sub> had been captured by the IP ([Figure 1.6A,C,E](#)). Some protein still remained in the flow-through, however this was not surprising given the high level of GUS expression obtained. For EFR, the total protein extract contained a weak band corresponding to EFR-HA<sub>3</sub>; this band was absent from the flow-through and highly enriched in the IP ([Figure 1.6A](#)). Thus EFR has been efficiently immunoprecipitated from the total protein in this experiment.

The remaining immunoprecipitate was separated on SDS-PAGE and stained with colloidal Coomassie brilliant blue to visualize the proteins present in the immunoprecipitate ([Figure 1.6B](#)). The band corresponding to EFR could be clearly seen around 175 kDa (indicated by arrow). I expected to observe more striking

differences in the band patterns obtained for EFR and GUS, to suggest the presence of potential EFR-interacting proteins. Despite the lack of obvious differences, each lane of the gel was sliced into 10 slices and subjected to mass spectrometry (MS) analysis.

Peptide sequences were searched against the SPtrEMBL database (<http://www.expasy.ch/sprot/>), and matches to closely related sequences assessed, as the *N. benthamiana* genome has not been sequenced. EFR was identified in the IP with a coverage of 25 % of the whole sequence ([Table 1.1](#)). The control GUS was covered up to 42 % across the whole protein; in each case the proteins were identified by 24 peptides. In this initial experiment 60 proteins were present in the EFR IP that were absent from the GUS negative control IP ([Appendix Table 1.2](#)).

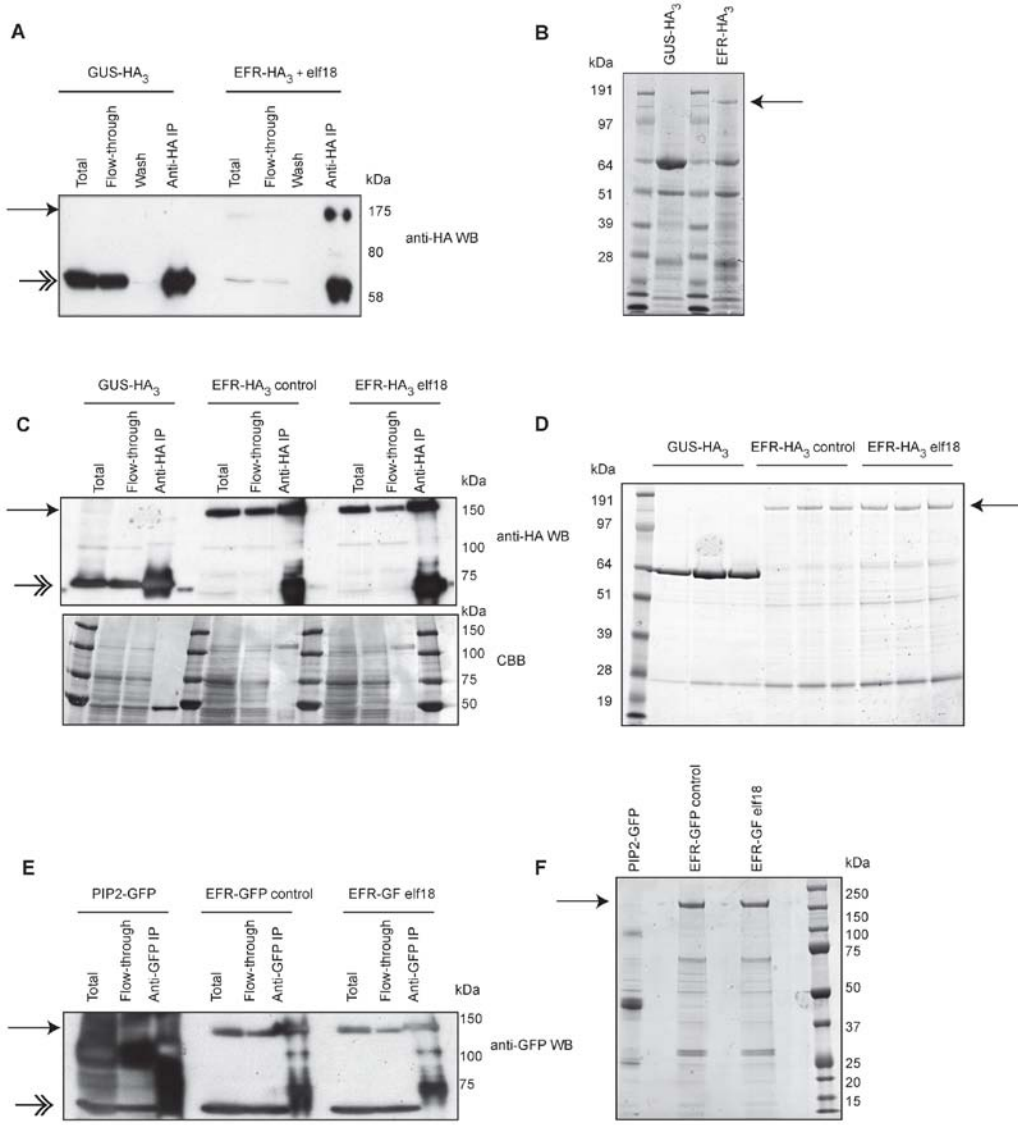


**Figure 1.6 Immunoprecipitation of *N. benthamiana* transiently expressed EFR.**

Arrows indicate EFR, double arrows indicate cleavage product.

A. Western blot illustrating first biological replicate of total protein extraction followed by anti-HA immunoprecipitation from *N. benthamiana* transiently expressing EFR-HA<sub>3</sub> or GUS-HA<sub>3</sub>; anti-HA immunoblot.

B. Colloidal Coomassie-stained SDS-PAGE of anti-HA IP prepared in (A).

C. Western blot illustrating second biological replicate of total protein extraction followed by anti-HA immunoprecipitation from *N. benthamiana* transiently expressing EFR-HA<sub>3</sub> (with/out elf18 treatment) or GUS-HA<sub>3</sub>; anti-HA immunoblot, film (top), CBB-stained PVDF (bottom).

D. Colloidal Coomassie-stained SDS-PAGE of anti-HA IP prepared in (C).

E. Western blot illustrating third biological replicate of total protein extraction followed by anti-GFP immunoprecipitation from *N. benthamiana* transiently expressing EFR-GFP-His (with/out elf18 treatment) or PIP2-GFP; anti-GFP (1:5000) immunoblot, film.

F. Colloidal Coomassie-stained SDS-PAGE of anti-GFP IP prepared in (C).

Approximate molecular weight in kDa as indicated.

In the subsequent biological replicate of this experiment, I also prepared an EFR-HA sample without elf18 treatment in order to identify any potential EFR-

interacting proteins that may associate or dissociate from EFR following PAMP treatment. In addition, in this replicate I increased the amount of anti-HA affinity matrix added to each IP in order to recover more protein for MS analysis. Despite this improvement to the protocol, I still did not capture all the tagged protein as a significant band could be seen in the flow-through ([Figure 1.6C](#)). However, a significant amount of EFR was enriched ([Figure 1.6D](#)) and analyzed by MS after excision from the gel. EFR sequence coverage in this replicate amounted to 15 % of the entire protein, represented by 27 unique peptides. GUS coverage reached 57 % and was represented by 35 peptide identifications. Indeed, only half of the volume of IP was loaded compared to total protein or flow-through, thus EFR was highly enriched by IP ([Figure 1.6C](#)).

In the third biological replicate I sought to compare which proteins could be pulled out by immunoprecipitating EFR-GFP-His with GFP affinity matrix compared to anti-HA affinity matrix. I reasoned that true interactors should be identified whatever the epitope tag used for the IP. For the negative control I expressed a well-characterized membrane protein aquaporin PIP2-GFP. In this IP, EFR-GFP-His or PIP2-GFP was enriched by the addition of GFPTrap beads, where llama anti-GFP antibodies are immobilized on agarose beads (Rothbauer *et al.*, 2006). Once again, not all of the epitope-tagged protein was pulled out by the affinity matrix ([Figure 1.6E](#)), although I used additional beads in this replicate. Both PIP2-GFP (60 kDa) and EFR-GFP-His were enriched by the IP, as 1/5<sup>th</sup> of the volume of IP was loaded for comparison to the total and flow-through ([Figure 1.6E](#)).

The highest coverage of EFR was obtained in the final replicate, with 38 % coverage of EFR by 38 peptides ([Table 1.1](#)). This improved detection of EFR could either be due to better enrichment of EFR by GFPTrap than by anti-HA affinity beads or to improving technical skill over the course of the experiments. PIP2 was identified with 25 % sequence coverage ([Table 1.1](#)). The overall coverage of EFR by sequence over the course of the 3 replicates is indicated in [Figure 1.8A](#) and Table 1.1, and it is clear that the transmembrane domain is under-represented.

**Table 1-1 Proteins identified by MS analysis of EFR immunoprecipitates**

Putative Proteins	Accession	Mr	GUS_1	GUS_2	PIP2	Elf18					
						-	-	+	+	+	+
EFR_At5g20480	Q8S9I3	113	0	8	0	27	35	24	23	38	
BAK1/SERK3	Q94F62	68	0	0	0	0	0	1	2	3	
Luminal-binding protein (BiP)/GRP 78	P49118	73	0	0	0	3	2	0	3	3	
ER luminal-binding protein	B7U9Z3	?	0	0	0	1	3	0	0	3	
F7G19.5 protein	O04022 +1	73	0	0	0	2	3	0	1	3	
Calnexin-like protein	Q4W5U7	61	0	0	0	2	1	0	2	2	
Luminal-binding protein 1/AtBiP1	Q9LKR3	74	0	0	0	1	1	0	0	2	
BIP1	Q03681	32	0	0	0	1	2	1	0	3	
NpPDR1	Q949G3	162	1	1	8	0	3	1	3	8	
Endochitinase A	P08252 +2	35	0	0	0	2	0	2	1	0	
CYP81B2v2	A1XEH7	58	0	0	0	3	0	2	1	0	
CYP71D20v2	A1XEM1 +1	57	0	0	0	3	0	0	1	1	
Glycyl-tRNA synthetase 1	O23627	82	0	0	0	0	0	2	0	2	
Ras-related protein YPT3	Q01111 +1	24	0	0	0	0	1	2	0	1	
Vacuolar H+-ATPase A1 subunit isoform	Q84XW6	69	0	0	0	0	0	2	1	0	
Type III chlorophyll a/b-binding protein	Q6RUN3	9	0	0	0	0	0	1	2	0	
Dynamin-related protein	Q8LF21	69	0	0	0	0	0	2	1	0	
L-galactono-1,4-lactone dehydrogenase-like	A1YRI9	66	0	0	0	2	0	0	1	0	
Serine hydroxymethyltransferase	O23254 +2	52	0	0	0	0	0	2	0	0	
ATP:citrate lyase	Q9AXR6 +1	66	0	0	0	1	0	2	0	0	
Uncharacterized protein At1g51980.2	A8MQE5 +2	49	0	0	0	0	0	3	0	0	
uncharacterized protein	Q38HV9	45	0	0	0	0	0	2	0	0	
60S ribosomal protein	O82204	16	0	0	0	0	0	2	0	0	
Probable cytochrome b5 isoform 2	O48845 +1	15	0	0	0	0	0	2	0	0	
Putative uncharacterized protein At1g53210	Q8L636 +2	63	0	0	0	0	0	2	0	0	
Exportin 1b	Q94IV0 +2	123	0	0	0	0	0	0	2	0	
Rubisco	Q32507	52	0	0	0	0	0	2	0	0	
Ascorbate peroxidase	Q8W4V7	32	0	0	0	0	0	2	0	0	
Oxygen-evolving enhancer protein 1-2, chloroplastic	Q9S841	35	0	0	0	0	0	2	0	0	
12S seed storage protein	P15456	51	0	0	0	0	0	0	3	0	
40S ribosomal protein S7	Q8LD03	22	0	0	0	0	0	3	0	0	
Putative acyl-CoA synthetase(At2g47240/T8I13.8)	O22898	75	0	0	0	0	0	2	0	0	
Patellin-1	Q56WK6	64	0	0	0	0	0	2	0	0	
5-epi-aristolochene synthase 34	Q84LF1	63	0	0	0	0	0	0	2	0	
At2g45060	Q94AZ5	30	0	0	0	0	0	2	0	0	
Transcription factor APFI	Q9C5S7 +1	30	0	0	0	0	0	2	0	0	
Putative uncharacterized protein	Q8LD22 +2	27	0	0	0	0	0	2	0	0	
Uncharacterized protein At5g27640.2	Q2V341 +3	85	0	0	0	0	0	2	0	0	
Putative beta-glucosidase	Q8H169 +3	60	0	0	0	0	0	2	0	0	
uncharacterized protein	Q8LG44 +1	37	0	0	0	0	0	2	0	0	
Chloroplast methionine sulfoxide reductase B2	A7U629 +2	22	0	0	0	0	2	0	0	0	
Beta-glucuronidase/GUS	Q93VY4	68	24	35	0	2	0	19	1	0	
PIP2	P43286	30	0	0	7	0	4	0	0	5	

Mr: molecular weight (kDa); <sup>§</sup> Uniprot accession number <sup>\*</sup>EFR\_0: untreated prior to tissue harvest; <sup>§</sup>EFR\_elf18: 5 minutes 100 nM elf18 elicitation prior to tissue harvest; <sup>#</sup>GUS: GUS-HA; <sup>†</sup>PIP: PIP2-GFP (aquaporin). Proteins identified in 1/3 reps dark gray.

The results obtained for putative interactors over 3 complete biological replicate experiments were compared and reproducible interactors were considered potentially interesting to pursue if they were supported by strong peptide evidence (90 % peptide identification probability and 2 peptides per protein) and experimental reproducibility. Overall, if considering only proteins with a 90 % protein identification probability represented by a minimum of 2 peptides, 375 proteins were identified in the immunoprecipitates. Of these, 39 were absent from the negative controls in each replicate and present in at least 1 of the 3 replicates (text is dark gray), and 16 of these were present in 2 of the 3 replicates ([Table 1.1](#)).

Peptides matching *NbBAK1* and other members of the SERK family were identified in the final two biological replicates, but only in the elf18-treated IPs ([Table 1.2](#)). As the *N. benthamiana* genome has not been sequenced, only partial sequence information is available for *N. benthamiana* SERK proteins. A search of EST databases (KEGG, Kyoto Encyclopedia of genes and genomes; <http://www.genome.jp/>) for SERK proteins revealed partial ESTs K13416 (NbSERK1) and K13418 (NbBAK1) with homology to with the C-terminus of *Arabidopsis* and *Solanum* SERKs (see [Figure 1.7](#)).

**Table 1-2 *NbSERK* tryptic peptides identified by MS analysis of EFR immunoprecipitates**

Peptide Sequence	AtSERK					Mascot Ion Score*	Bio. Rep.
	1	2	3	4	5		
LANDDDVMlldWVK	100 %	100 %	100 %	Pos. 7 V to I	Pos. 7 V to I	79.7	2
TQGGELQFQTEVEMISM AVR	Pos. 2 Q to P	Pos. 2 Q to P	100 %	Pos. 2 Q to K	Pos. 2 Q to K	48	2
mLEGDGLAER (m1: oxidation)	Pos. 10 R to K	Pos. 10 R to K	100 %	100 %	100 %	38.9	3
ELQVASDNFSNK	Pos. 8 N to G	Pos. 6 S to T; Pos. 8 N to S	100 %	Pos. 3Q to L; Pos. 6 S to T	ELLVATEKFSKR	47.8	3
GTIGHIAPEYLSTGK	100 %	100 %	100 %	100 %	100 %	45.8	3

\* SpTREMBL database used; min. 90 % probability peptide and protein. Oxidation: +15.99

BAK1/1-615	1 -----MERRLMIPCFCFWLILVLDLVLRVSGNAEGDALSALKNSLAD--P	NKVLQSWDATLVT	PTCTWFHVCNSD	NSVTRV	DL	75																																																			
BKK1/1-620	1 MTSSKMEQRSLL-CFLYLLLLNFNTRVAGNAEGDALTLQKNSLSSGDP	PANNVLQSWDATLVT	PTCTWFHVCN	CPENK	VTRV	DL																																																			
SERK1/1-625	1 MES---SYVVFILLSLILLPNHSWL	ASANLEGDALHTLRVTTVD	--PNNVLQSWDPTLV	NPC	CTWFHVCNN	ENS																																																			
SERK2/1-628	1 MGRKKFEEAFGFCVLISLILLFN- -MEHGSSR-GFIWIL	SLWLASSMEGDAHLSLRAN	LVNPCTWFHVCNN	ENS	NSVIR	VRL																																																			
SERK5/1-601	1 -----MEHGSSR-GFIWIL	LSLFDVFSRTGKTV	TDALIALRSS	SSGDHTNNI	QLQSWNATH	HTPC																																																			
A6N8J2_SOLPE/1-629	1 MVKVMEKDTVVVSLVVWLL	LVVHHKKLIYANMEGDAHL	SLRVN	LQD	--PNNVLQSWDPTLV	NPC																																																			
A3R790_SOLTU/1-629	1 MVKVMEKDAVVVSLVVWLL	LVVHHKKLIYANMEGDAHL	SLRVN	LQD	--PNNVLQSWDPTLV	NPC																																																			
A3R789_SOLTU/1-629	1 MVKVMEKDAVVVSLVVWLL	LVVHHKKLIYANMEGDAHL	SLRVN	LQD	--PNNVLQSWDPTLV	NPC																																																			
NbSERK_EST/1-72	1 -----	-----	-----	-----	-----	-----																																																			
NbBAK1/1-129	1 -----	-----	-----	-----	-----	-----																																																			
BAK1/1-615	66 GNA	LSGQLV	MQLGQ	LPN	LQY	LELYSNNITG	T	PEQ	LGNT	ELV	SLDLY	LNN	LSGP	I	P	STL	GRL	KKL	RFL	R	NNNS	L	SGE	I	PR	158																															
BKK1/1-620	83 GNA	LSGKL	VLP	ELG	QNL	QNLQY	LELYSNNITG	I	PEEL	GDVL	ELV	SLDLY	YANSI	SGP	I	P	SS	LGK	L	KL	R	F	R	NNNS	L	SGE	I	PR	165																												
SERK1/1-625	77 GNA	ELSGH	LVP	ELG	VKL	NKLQY	LELYSNNITG	I	PIP	SNL	GNT	LN	SF	GP	I	P	ES	LGK	L	KL	R	F	R	NNNS	L	SGE	I	PR	159																												
SERK2/1-628	80 GNA	DLSGQLV	PQL	QNLK	NKLQY	LELYSNNITG	I	TCV	PS	ELG	N	LTN	NL	SF	GP	I	P	DS	LGK	L	KL	R	F	R	NNNS	L	SGE	I	PR	162																											
SERK5/1-601	78 GNA	LSG	LVP	QPL	QNLQY	LELYSNNITG	I	PE	ELG	DL	MELV	N	FANN	SGP	I	P	SS	LGK	L	KL	R	F	R	NNNS	L	SGE	I	PR	160																												
A6N8J2_SOLPE/1-629	81 GNA	ALSGL	LVP	QPL	QNLQY	LELYSNNITG	I	SGV	IP	PSD	LN	TN	S	LDLY	LNN	FV	GP	I	PD	LGK	L	KL	R	F	R	NNNS	L	SGE	I	PR	163																										
A3R790_SOLTU/1-629	81 GNA	ALSGL	LVP	QPL	QNLQY	LELYSNNITG	I	SGL	IP	PSD	LN	TN	S	LDLY	LNN	FV	GP	I	PD	LGK	L	KL	R	F	R	NNNS	L	SGE	I	PR	163																										
A3R789_SOLTU/1-629	81 GNA	ALSGL	LVP	QPL	QNLQY	LELYSNNITG	I	SGL	IP	PSD	LN	TN	S	LDLY	LNN	FV	GP	I	PD	LGK	L	KL	R	F	R	NNNS	L	SGE	I	PR	163																										
NbSERK_EST/1-72	-----	-----	-----	-----	-----	-----	-----	-----	-----	-----	-----	-----	-----	-----	-----	-----	-----	-----	-----	-----	-----	-----	-----	-----	-----	-----	-----	-----	-----																												
NbBAK1/1-129	-----	-----	-----	-----	-----	-----	-----	-----	-----	-----	-----	-----	-----	-----	-----	-----	-----	-----	-----	-----	-----	-----	-----	-----	-----	-----	-----	-----	-----																												
BAK1/1-615	159 S	LT	ATV	L	QV	VLD	LSNNP	L	TG	DP	I	PV	NG	F	S	L	F	T	P	AS	PP	PP	I	P	ST	TP	P	SP	AG	S	NR	I	TG	A	AG	229																					
BKK1/1-620	166 T	L	LT	SQ	-	-	-	-	-	-	-	-	-	-	-	-	-	-	-	-	-	-	-	-	-	-	-	-	-	-	-	-	-																								
SERK1/1-625	160 S	L	LT	N	T	QV	L	D	LSNNR	L	S	G	S	V	D	N	G	S	F	T	S	P	T	P	P	S	G	G	Q	M	T	A	A	I	AG	234																					
SERK2/1-628	163 S	L	LT	N	M	T	QV	L	D	LSNNR	L	S	G	S	V	D	N	G	S	F	T	S	P	T	P	P	S	G	G	Q	M	T	A	A	I	AG	242																				
SERK5/1-601	161 S	L	LT	A	P	L	-	-	-	-	-	-	-	-	-	-	-	-	-	-	-	-	-	-	-	-	-	-	-	-	-	-	-	-																							
A6N8J2_SOLPE/1-629	164 S	L	LT	N	S	Q	V	L	D	LSNNR	L	S	G	S	V	D	N	G	S	F	T	S	P	T	P	P	S	G	G	Q	M	T	A	A	I	AG	246																				
A3R790_SOLTU/1-629	164 S	L	LT	N	S	Q	V	L	D	LSNNR	L	S	G	S	V	D	N	G	S	F	T	S	P	T	P	P	S	G	G	Q	M	T	A	A	I	AG	246																				
NbSERK_EST/1-72	-----	-----	-----	-----	-----	-----	-----	-----	-----	-----	-----	-----	-----	-----	-----	-----	-----	-----	-----	-----	-----	-----	-----	-----	-----	-----	-----	-----	-----	-----	-----	-----																									
NbBAK1/1-129	-----	-----	-----	-----	-----	-----	-----	-----	-----	-----	-----	-----	-----	-----	-----	-----	-----	-----	-----	-----	-----	-----	-----	-----	-----	-----	-----	-----	-----	-----	-----	-----																									
BAK1/1-615	230 G	VAA	GA	A	LL	F	A	V	P	A	I	A	L	A	W	R	R	K	K	P	Q	D	H	F	D	V	P	A	E	D	P	E	V	H	G	K	V	K	G	R	A	D	G	T	312												
BKK1/1-620	235 G	VAA	GA	A	LL	F	A	V	P	A	I	A	F	W	R	R	K	K	P	Q	D	H	F	D	V	P	A	E	D	P	E	V	H	G	K	V	K	G	R	A	D	G	T	317													
SERK1/1-625	243 G	VAA	GA	A	LL	F	A	V	P	A	I	A	F	W	R	R	K	K	P	Q	D	H	F	D	V	P	A	E	D	P	E	V	H	G	K	V	K	G	R	A	D	G	T	325													
SERK2/1-628	246 G	VAA	GA	A	LL	F	A	V	P	A	I	A	F	W	R	R	K	K	P	Q	D	H	F	D	V	P	A	E	D	P	E	V	H	G	K	V	K	G	R	A	D	G	T	328													
SERK5/1-601	221 G	VAA	GA	A	LL	F	A	V	P	A	I	A	F	W	R	R	K	K	P	Q	D	H	F	D	V	P	A	E	D	P	E	V	H	G	K	V	K	G	R	A	D	G	T	298													
A6N8J2_SOLPE/1-629	247 G	VAA	GA	A	LL	F	A	V	P	A	I	A	F	W	R	R	K	K	P	Q	D	H	F	D	V	P	A	E	D	P	E	V	H	G	K	V	K	G	R	A	D	G	T	329													
A3R790_SOLTU/1-629	247 G	VAA	GA	A	LL	F	A	V	P	A	I	A	F	W	R	R	K	K	P	Q	D	H	F	D	V	P	A	E	D	P	E	V	H	G	K	V	K	G	R	A	D	G	T	329													
A3R789_SOLTU/1-629	247 G	VAA	GA	A	LL	F	A	V	P	A	I	A	F	W	R	R	K	K	P	Q	D	H	F	D	V	P	A	E	D	P	E	V	H	G	K	V	K	G	R	A	D	G	T	329													
NbSERK_EST/1-72	-----	-----	-----	-----	-----	-----	-----	-----	-----	-----	-----	-----	-----	-----	-----	-----	-----	-----	-----	-----	-----	-----	-----	-----	-----	-----	-----	-----	-----	-----	-----	-----	-----	-----	-----	-----	-----	-----	-----	-----	-----	-----	-----	-----													
NbBAK1/1-129	-----	-----	-----	-----	-----	-----	-----	-----	-----	-----	-----	-----	-----	-----	-----	-----	-----	-----	-----	-----	-----	-----	-----	-----	-----	-----	-----	-----	-----	-----	-----	-----	-----	-----	-----	-----	-----	-----	-----	-----	-----	-----	-----	-----													
BAK1/1-615	313 L	V	A	V	K	R	L	K	E	E	R	T	Q	G	E	L	O	G	E	L	Q	T	O	G	E	L	Q	T	N	S	N	K	I	N	L	G	R	G	F	K	V	K	R	L	A	D	G	T	395								
BKK1/1-620	318 L	V	A	V	K	R	L	K	E	E	R	T	Q	G	E	L	O	G	E	L	Q	T	O	G	E	L	Q	T	N	S	N	K	I	N	L	G	R	G	F	K	V	K	R	L	A	D	G	T	400								
SERK1/1-625	326 L	V	A	V	K	R	L	K	E	E	R	T	Q	G	E	L	O	G	E	L	Q	T	O	G	E	L	Q	T	N	S	N	K	I	N	L	G	R	G	F	K	V	K	R	L	A	D	G	T	408								
SERK2/1-628	329 L	V	A	V	K	R	L	K	E	E	R	T	Q	G	E	L	O	G	E	L	Q	T	O	G	E	L	Q	T	N	S	N	K	I	N	L	G	R	G	F	K	V	K	R	L	A	D	G	T	408								
SERK5/1-601	299 L	V	A	V	K	R	L	N	E	E	R	T	Q	G	E	L	O	G	E	L	Q	T	O	G	E	L	Q	T	N	S	N	K	I	N	L	G	R	G	F	K	V	K	R	L	A	D	G	T	381								
A6N8J2_SOLPE/1-629	330 L	V	A	V	K	R	L	N	E	E	R	T	Q	G	E	L	O	G	E	L	Q	T	O	G	E	L	Q	T	N	S	N	K	I	N	L	G	R	G	F	K	V	K	R	L	A	D	G	T	412								
A3R790_SOLTU/1-629	330 L	V	A	V	K	R	L	N	E	E	R	T	Q	G	E	L	O	G	E	L	Q	T	O	G	E	L	Q	T	N	S	N	K	I	N	L	G	R	G	F	K	V	K	R	L	A	D	G	T	412								
A3R789_SOLTU/1-629	330 L	V	A	V	K	R	L	N	E	E	R	T	Q	G	E	L	O	G	E	L	Q	T	O	G	E	L	Q	T	N	S	N	K	I	N	L	G	R	G	F	K	V	K	R	L	A	D	G	T	412								
NbSERK_EST/1-72	-----	-----	-----	-----	-----	-----	-----	-----	-----	-----	-----	-----	-----	-----	-----	-----	-----	-----	-----	-----	-----	-----	-----	-----	-----	-----	-----	-----	-----	-----	-----	-----	-----	-----	-----	-----	-----	-----	-----	-----	-----	-----	-----	-----													
NbBAK1/1-129	-----	-----	-----	-----	-----	-----	-----	-----	-----	-----	-----	-----	-----	-----	-----	-----	-----	-----	-----	-----	-----	-----	-----	-----	-----	-----	-----	-----	-----	-----	-----	-----	-----	-----	-----	-----	-----	-----	-----	-----	-----	-----	-----	-----													
BAK1/1-615	479 G	S	AR	GL	A	L	H	D	H	C	D	P	K	I	H	R	D	V	K	A	N	I	L	D	E	E	F	A	V	G	D	F	L	A	K	L	M	D	Y	K	D	T	H	V	T	A	V	GT	I	A	E	Y	L	ST	KG	Y	478
BKK1/1-620	484 G	S	AR	GL	A	L	H	D	H	C	D	P	K	I	H	R	D	V	K	A	N	I	L	D	E	E	F	A	V	G	D	F	L	A	K	L	M	Y	N	D	S	H	V	T	A	V	GT	I	A	E	Y	L	ST	KG	Y	483	
SERK1/1-625	492 G	S	AR	GL	S	L	H	D	H	C	D	P	K	I	H</																																										

BAK1/SERK3 was found as an interactor of the flagellin receptor FLS2 and a positive regulator of signaling (Chinchilla *et al.*, 2007; Heese *et al.*, 2007). Although no interaction between EFR and BAK1 has previously been reported, *bak1* mutants are compromised in *elf18* signaling, though less so than in *flg22* signaling (Chinchilla *et al.*, 2007).

The SERK peptides identified in these experiments are identical in AtBAK1, and a kinase domain peptide (GTIGHIAPEYLSTGK) matches all SERKs in the alignment provided ([Figure 1.7](#)). The *N. benthamiana* ortholog of BAK1 was probably pulled down in the IP, perhaps along with other NbSERKs for which sequence information is not available. Interestingly, the peptide sequence MLEGDGLAER is identical in all BAK1 homologs in the alignment except the KEGG DB-predicted NbBAK1 sequence, where the 5<sup>th</sup> position D (Asp) is replaced by an E (Glu) in NbBAK1 ([Figure 1.7](#)). This could be due to an error on the sequencing or translation of the EST, or it could represent a novelty of the protein. This could suggest that another NbSERK, which carries this polymorphism is present in the IP. In conclusion, it is likely that transiently expressed EFR interacts with the *N. benthamiana* homolog of BAK1, and perhaps other NbSERKs, in an *elf18*-dependent manner.

Several additional proteins with possible roles in defense responses (discussed below) were identified as putative EFR interactors, but were not further investigated due to time limitations.

Other putative interactors that were reproducibly identified in EFR IPs comprised a group of ER chaperones including calnexin-like and luminal binding protein (BIP), involved in protein folding (Ellgaard and Helenius, 2003). Although these could be present due to the over-expression of EFR creating an unfolded protein response (UPR), these proteins may also play a more specific role in EFR maturation, as they are specifically required for EFR protein folding in *Arabidopsis* (Li *et al.*, 2009a; Nekrasov *et al.*, 2009; Saijo *et al.*, 2009). Furthermore, *Arabidopsis* calreticulin and luminal binding protein were identified in EFR immunoprecipitates in *Arabidopsis* ([Chapter 2](#)), suggesting that these could be present in EFR complex(es).

In addition, the cytochrome P450s CYP81B3v2 and/or CYP71D2v20 were identified in EFR IPs. Due to the high homology in protein sequence, none of the

identified peptides allowed me to distinguish whether one or both of these CYPs are present in the IP. Interestingly, both CYPs are linked to defense responses. Membrane-localized tobacco CYP71D2v20 or 5-epi-aristolochene-1,3-dihydroxylase (EAH), which has pathogen/elicitor-inducible hydroxylase activity, is involved in synthesis of the phytoalexin capsidiol (Ralston *et al.*, 2001). *NbEAH*-silenced *N. benthamiana* plants are more susceptible to *P. infestans* infection and the expression of *EAH* is regulated by ET, suggesting that capsidiol production forms part of the basal defense response in *N. benthamiana* (Shibata *et al.*, 2010). CYP81B2v2 was identified in proteomic analysis of proteins differentially regulated by TMV infection of tobacco containing resistance protein N (Caplan *et al.*, 2009). Another potentially interesting putative interacting protein is endochitinase A (*N. tabacum*), which is induced by fungal pathogens (Neale *et al.*, 1990).

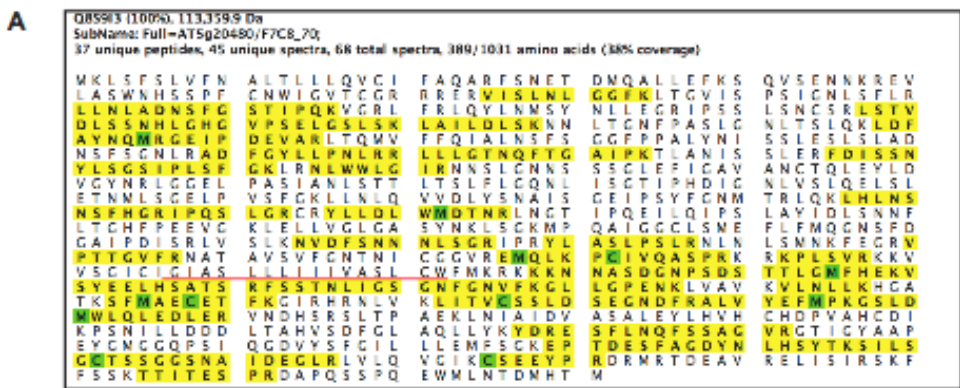
Ras-related protein YPT3 is a member of a large family of GTPases, and is named for its yeast homolog which functions in vesicle trafficking (Cheng *et al.*, 2002). These proteins appear to be functionally diverse in plants (Inaba *et al.*, 2002; Chow *et al.*, 2008). The pea homolog Pra2 reportedly interacts with DDWF1, a CYP450 involved in brassinosteroid synthesis (Kang *et al.*, 2001). Intriguingly, one of the tobacco homologs of DDWF1 is the pathogen-inducible CYP71D2v20 (Czernic *et al.*, 1996; Ralston *et al.*, 2001).

The remaining proteins, which were identified in the EFR- but not GUS- or PIP2- expressing tissues, were not detected in more than one biological replicate. Thus additional work would be required to determine whether they are truly interactors.

### 1.2.5 The EFR protein may undergo fragmentation

Notably, in each experiment I observed an additional band for EFR at a molecular weight of approx. 65 kDa ([Figure 1.6](#)). This was especially noticeable following IP, where the band was almost as intense as the full-length EFR band at 175 kDa ([Figure 1.6](#)). It is possible that EFR protein is unstable due to the presence of a potential degradation motif in the internal juxtamembrane region, which could be subject to cleavage. A consensus sequence P/GX<sub>5-7</sub>P/G, which corresponds to a proteolytic cleavage site in EGF receptors (Yuan *et al.*, 2003), is also present in the rice PRR Xa21 (Xu *et al.*, 2006a), which shows similarities to

EFR (Boller and Felix, 2009). Xa21 full-length protein is 140 kDa but a 100kDa product is detectable when visualizing the Myc-tagged protein by immunoblotting (Xu *et al.*, 2006a). This product corresponds to a potential cleavage product rendered by proteolytic activity that severs Xa21, possibly in the internal juxtamembrane region by cleavage at a degradation motif PSRTSMKG (Xu *et al.*, 2006a). A similar motif (PSDSTTLG) is revealed by alignment of the EFR amino acid sequence with that of Xa21, and this could be a site of instability of the EFR protein ([Figure 1.8B](#)). If the protein was cleaved at this site, a fragment of 65 kDa (including the YFP-HA tag) would be released, and this corresponds with the size of the band repeatedly detected by immunoblotting of EFR. However, I have not pursued this further and I have not conclusively identified the site of this potential cleavage. In addition, mass spectrometry data did not support this as no fragment peptides were recovered to suggest the cleavage occurring at this site. Indeed, the full-length peptide (K)NNASDGNPSDSTTLGmFHEK(V) has been identified with high Mascot scores on multiple occasions in all replicates of the IP-MS experiments, implying that this peptide is not cleaved at this potential degradation site (underlined) ([Figure 1.8C](#)). However, if the cleavage does occur in this peptide, it is possible that the cleavage products are too small to be detected by mass spectrometry.



biological membranes (Higgins, 2007). NpPDR1 was indirectly shown to transport the antifungal diterpene sclareol, suggesting a general role for NpPDR1 in the transport of antimicrobial compounds (Stukkens *et al.*, 2005). There is evidence suggesting a general role for PDRs in biotic stress responses in plants. *NpPDR1* expression is induced in response to infection by fungal and bacterial pathogens and *NpPDR1*-silenced plants are hyper-susceptible to necrotrophic fungal pathogens such as *Botrytis cinerea* but not to the hemibiotrophic bacterial pathogen *Pseudomonas syringae* pv. *tabaci* (*Pta*) (Stukkens *et al.*, 2005; Bultreys *et al.*, 2009).

In *Arabidopsis*, the closest homolog of NpPDR1 is AtPDR12 (69 % amino acid homology; Crouzet *et al.*, 2006 and [Figure 1.9](#)). AtPDR12 was shown to be involved in lead transport, as *pdr12* mutants are more sensitive to lead (Lee *et al.*, 2005). *AtPDR12* gene expression is highly induced by salicylic acid (SA) application and inoculation with fungal pathogens including *Alternaria brassicicola* (incompatible; Schenk *et al.*, 2003) and *Sclerotina sclerotiorum* (compatible; Dickman and Mitra, 1992), as well as *Pseudomonas syringae* pv. *tomato* (*Pto*) DC3000 (Campbell *et al.*, 2003). Contrastingly, *pdr12* mutants did not however display increased susceptibility to the bacterial pathogens *Pto* DC3000 or *Pta*, or the fungal pathogen *Fusarium oxysporum* (Campbell *et al.*, 2003). All these data point to an as yet undefined role for PDR12 in pathogen signaling, possibly as transporters of antimicrobial compounds.

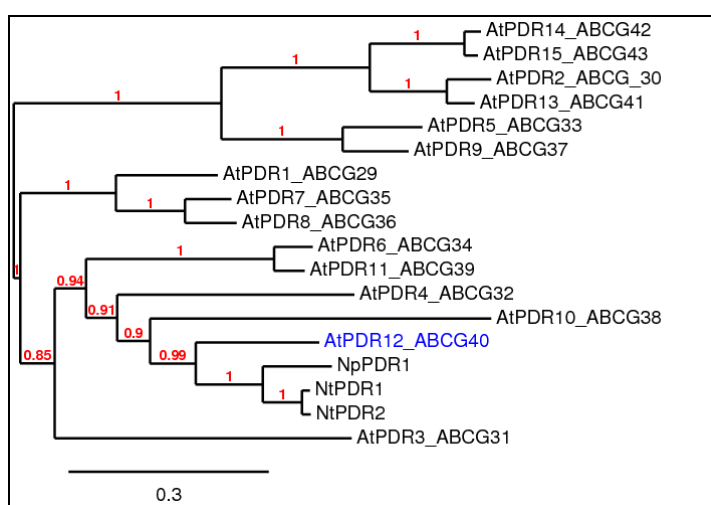


**Figure 1.9 Pleiotropic drug resistance (PDR) ABC Transporter Family.**  
Phylogenetic tree of *Nicotiana* and *Arabidopsis* PDR family members. At: *Arabidopsis thaliana*; Nt: *Nicotiana tabacum*; Np: *Nicotiana plumbaginifolia*. NtPDR1:Q76CU1; NtPDR2:Q76CU2; NpPDR1:Q949G3. AtPDR12 is indicated in blue. Full-length amino acid sequence used, MUSCLE for the alignment, PhyML for the phylogeny and TreeDyn for drawing the tree (at [www.phylogeny.fr](http://www.phylogeny.fr)). The branch support values are shown in red.

Considering the potentially important role of PDRs in plant defense, NpPDR1 made an interesting candidate interactor. In the third biological replicate, NpPDR1 was also identified in the negative control ([Table 1.1](#); for alignment of peptides see [Appendix Figure A2.2](#)), so it is possible that this protein only adheres non-specifically to agarose beads. Yet prior to carrying out this replicate, I already initiated work on this protein to determine whether it was a true interactor and/or had a clear PTI phenotype.

In order to confirm PDR as an EIP, I sought to directly test the interaction between EFR and the closest *Arabidopsis* NpPDR1-ortholog AtPDR12. PCR amplification of *PDR12* cDNA is difficult due to the low basal expression level of the gene. However, expression of PDR12 is induced by lead (Lee *et al.*, 2005) and indeed, in tissues previously treated with 0.5 mM Pb(NO<sub>3</sub>)<sub>2</sub> for 24 hours, *PDR12* could be sufficiently amplified (data not shown). In addition, due to the toxicity of PDR expressed in *E. coli* at 37°C (Marc Boutry, personal communication), all cloning procedures were carried out at 28°C. Despite cloning *PDR12* cDNA under the 35S promoter, I was never able to detect the protein by transient expression in *N. benthamiana* and thus could never carry out co-IP experiments to investigate possible interactions with EFR (data not shown).

Although I was unable to confirm any co-IP, I continued with characterization of *Arabidopsis* or *N. plumbaginifolia* PDR loss-of-function lines, in order to reveal any interesting phenotype. I obtained stable transgenic *N. plumbaginifolia* *PDR1*-silenced lines (*NpPDR1-S1*) (Stukkens *et al.*, 2005; Bultreys *et al.*, 2009) from the laboratory of Marc Boutry (Université Catholique de Louvain, Belgium) in order to determine whether they are compromised in PAMP-triggered responses. I tested the production of ROS in response to common PAMPs including flg22, CSP22 and chitin in wild-type *N. plumbaginifolia* and *NpPDR1-S1* lines. The *NpPDR1-S1* lines consistently had increased ROS production in response to CSP22 and chitin when compared to the wild-type *N. plumbaginifolia* ([Figure 1.10](#) A-B). Responses to flg22 were very weak and not reproducible (data not shown).

In order to determine whether elf18 responses were affected in the silenced lines, I transiently expressed 35S:EFR-YFP-HA<sub>3</sub> in 2-week-old wild-type *N.*

*plumbaginifolia* or *NpPDR1-S1* leaves. EFR-YFP-HA<sub>3</sub> was well expressed in *N. plumbaginifolia* as detected by Western blotting ([Figure 1.10D](#)). In contrast, no significant EFR expression was detectable in the silenced line over three replicate experiments ([Figure 1.10D](#)). This prevented any comparison of elf18-induced responses in these plants ([Figure 1.10C](#)), although the transient expression of EFR in *N. plumbaginifolia* conferred elf18-responsiveness similarly to *N. benthamiana*.

These lines are however hyper-susceptible to fungal pathogens and display spontaneous infection and chlorotic lesions when grown in the greenhouse in the absence of any pathogen inoculation (Stukkens *et al.*, 2005; data not shown). Therefore, the recalcitrance to transient expression could be due to constitutive activation of defense responses in the silenced plants. This could also explain the heightened sensitivity to other PAMPs in the ROS assay, and prevents any conclusions being drawn about the role of NpPDR1 in PTI signaling, at least using this method.

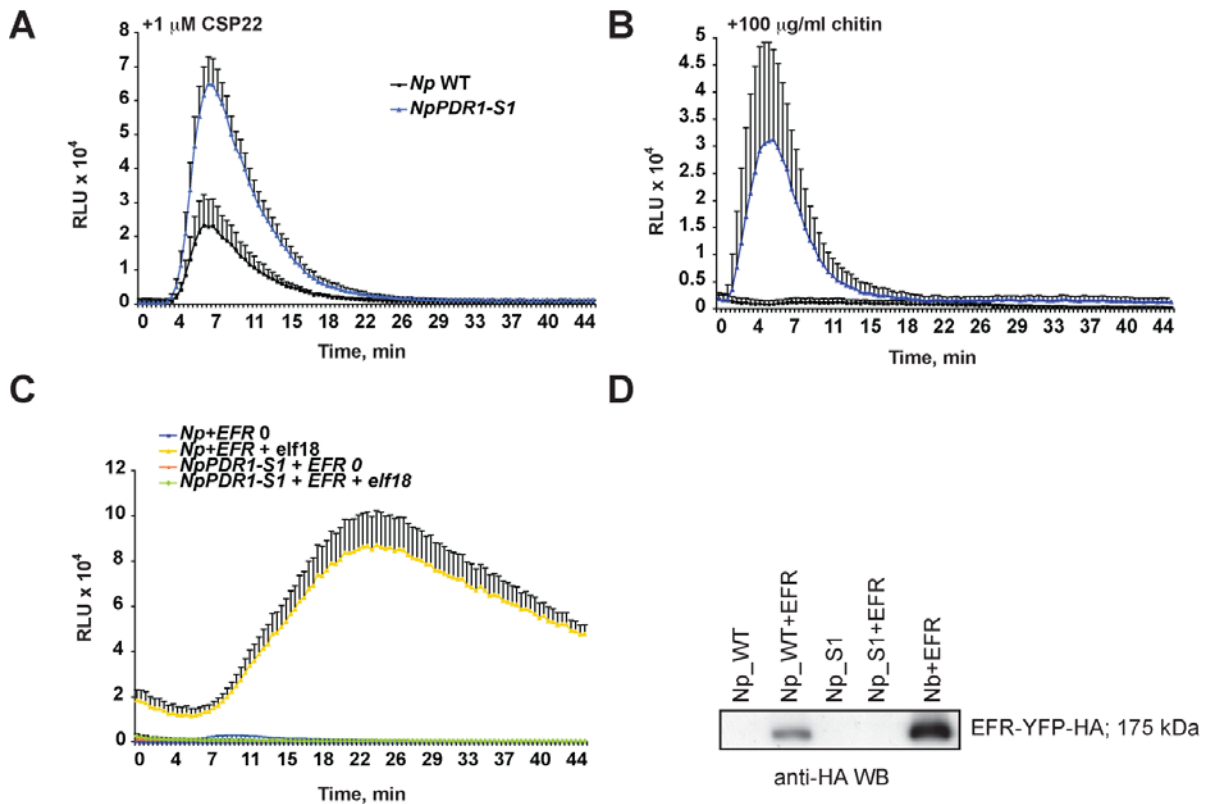


**Figure 1.10** *N. plumbaginifolia* *NpPDR1*-silenced lines have sensitized ROS responses.

A and B. Production of ROS in wild-type and *NpPDR1*-silenced *N. plumbaginifolia* plants responding to CSP22 (1 μM) (A) or chitin (100 μg/ml) (B) elicitation. Results are average ± standard error ( $n=8$ ).

C. Elf18-induced ROS production in wild-type (*Np*) and *NpPDR1*-silenced (*NpPDR1-S1*) *N. plumbaginifolia* plants transiently expressing EFR-YFP-HA (2 days post-agro-infiltration). Results are average ± standard error ( $n=8$ ).

D. Immunoblot analysis of transient expression of leaves in (C). Anti-HA western blotting of total protein extracts derived from wild-type (*Np*) and *NpPDR1*-silenced (*NpPDR1-S1*) *N. plumbaginifolia* and *N. benthamiana* (*Nb*) plants transiently expressing EFR-YFP-HA, 2 days post-agro-infiltration.

In order to determine if the *Arabidopsis* ortholog AtPDR12 (At1g15520) has a role to play in PAMP responses, I obtained 2 independent homozygous T-DNA insertion lines for AtPDR12, *pdr12-1* (Salk\_013945) and *pdr12-2* (Salk\_005635) (Figure 1.11A). Both insertions are close to the C-terminus of the gene and the position in *pdr12-2* corresponds to an insertion in one of the six transmembrane loops of the PDR12 protein, while *pdr12-1* has an insertion at the C-terminal tail of the protein (Figure 1.11B).

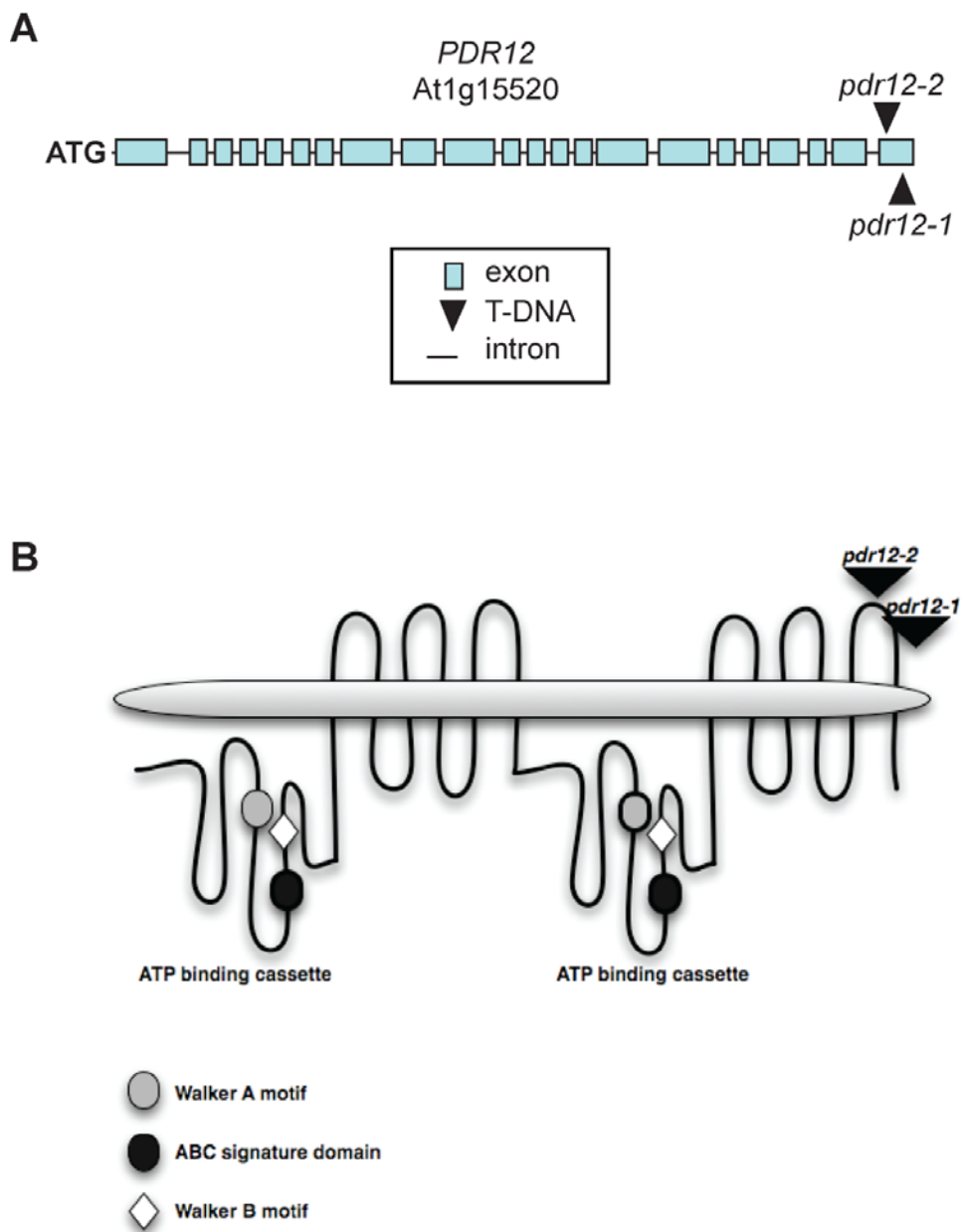


**Figure 1.11 Schematic representation of PDR12 gene organization and protein domains.**  
 A. *PDR12* gene (At1g15520) has 22 exons (blue boxes). T-DNA insertions in the final exon correspond to *pdr12-1* (Salk\_013945) and *pdr12-2* (Salk\_005635).  
 B. *PDR12* is an ABC (ATP-binding cassette) transporter with six transmembrane domains. The ATP binding cassette contains conserved motifs (Walker A and B; ABC signature). *pdr12-1* insertion corresponds to the C-terminus of the protein, *pdr12-2* insertion is within the transmembrane domain.

I went on to characterize the *pdr12* lines for PAMP responses and disease resistance. When elicited with *elf18*, *flg22* or chitin, Col-0 wild-type plants produce a burst of ROS within a few minutes of PAMP addition (Figure 1.12A), and this is maintained at wild-type levels in both of the *pdr12* lines tested (Figure 1.12A). Col-0, *pdr12-1* and *pdr12-2* all showed similar seedling growth inhibition over the

range of elf18 and flg22 concentrations tested ([Figure 1.12B](#)). In this experiment, an insertion line (Salk\_118823, *pdr10*) for the closest PDR12 paralog, PDR10 (At3g30842), was also included, but behaved as Col-0 in this assay ([Figure 1.12B](#)). I subsequently generated the double mutant *pdr12-1 pdr10* to resolve any potential functional redundancy among these closely related proteins, and repeated the growth inhibition assay. In this assay, the double mutant did not differ significantly from the single mutants or the wild-type Col-0, especially at high concentrations of elf18 or flg22, but at low concentrations displayed opposite phenotypes, with increased elf18 sensitivity compared to Col-0, and decreased flg22 sensitivity ([Figure 1.12C](#)).

*PDR12* gene expression is induced by inoculation with *A. brassicicola*, *S. sclerotiorum*, *F. oxysporum* and *P. syringae* (Campbell *et al.*, 2003). The publicly available microarray data (BAR, Arabidopsis eFP browser) indicate that *PDR12* gene expression is up-regulated in response to various biotic stresses including infection with *B. cinerea* and *P. infestans*, as well as treatment with the bacterial harpin (HrpZ) and *Phytophthora* elicitin NPP1. To further characterize its PAMP-induced gene expression, I carried out semi-quantitative RT-PCR analysis of *PDR12* gene expression in a time course experiment after elf18 and flg22 treatment ([Figure 1.12D](#)). I observed that Col-0 *PDR12* gene expression is slightly up-regulated within 1 hour of elf18 or flg22 elicitation, and this increases significantly by 3 hours, the expression remaining elevated even after 24 hours for elf18 ([Figure 1.12D](#), left). The cDNA of the constitutively expressed gene *RPL4* was used as loading control to indicate equal amounts of cDNA was used for each reaction. Interestingly, the *N. tabacum* PDR12-ortholog *NtPDR1* shows a similar pattern of gene expression, with transcript levels peaking after three hours of flagellin treatment (Sasabe *et al.*, 2002).

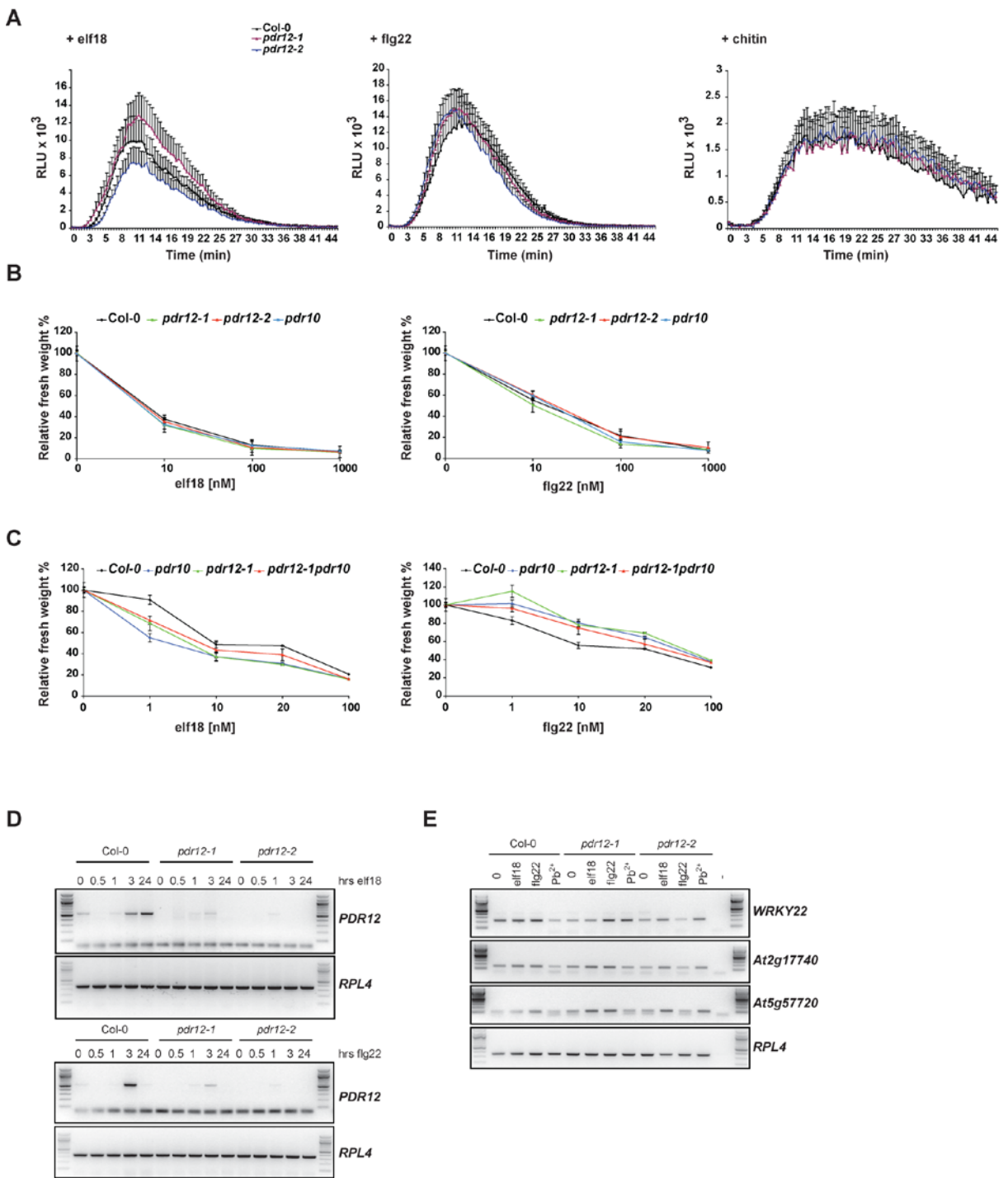


**Figure 1.12** *pdr12* mutants are compromised in PAMP-induced gene expression.

A. Production of ROS in Col-0, *pdr12-1* and *pdr12-2* in response to 100 nM elf18 (left), 100 nM flg22 (middle) and 100 µg/ml chitin (right) elicitation. RLU = relative light units. Results are average  $\pm$  standard error ( $n=8$ ).

B. Growth inhibition in response to increasing concentrations of elf18 (left) and flg22 (right) in Col-0, *pdr12-1*, *pdr12-2* and *pdr10* seedlings. Data are represented relative to the fresh weight of untreated seedlings. Results are average  $\pm$  standard error ( $n=6$ ).

C. Growth inhibition in response to increasing concentrations of elf18 (left) and flg22 (right) in Col-0, *pdr12-1*, *pdr12-1 pdr10* and *pdr10* seedlings. Data are represented relative to the fresh weight of untreated seedlings. Results are average  $\pm$  standard error ( $n=6$ ).

D. Semi-quantitative RT-PCR of *PDR12* (*At1g15520*) gene expression in response to time course treatment with 100 nM elf18 (top) or flg22 (bottom) for 0 – 24 hours (hrs) in Col-0, *pdr12-1* and

*pdr12-2* seedlings. Loading control is *RPL4* (*At3g09630*) gene expression (lower panel). Adjacent is 100 bp ladder for size reference.

E. Semi-quantitative RT-PCR of *WRKY22* (*At4g01250*), *At2g17740*, *At5g57720* gene expression in response to 60 minutes treatment with 100 nM *elf18*, 100 nM *flg22* or 0.1 mM *Pb(NO<sub>3</sub>)<sub>2</sub>* in Col-0, *pdr12-1* and *pdr12-2* seedlings. Loading control is *RPL4* (*At3g09630*) gene expression (lower panel). Adjacent is the 100 bp ladder for size reference.

Previous work indicated that no *PDR12* transcript was still present in either *pdr12-1* or *pdr12-2* (Lee *et al.*, 2005), however I sought to confirm the transcript levels in these lines. In *pdr12-1*, *PDR12* gene expression was weakly detectable, and was further reduced in *pdr12-2* ([Figure 1.12D](#)), suggesting that the expression in these lines is reduced but not eliminated.

Next I assessed the expression of the PAMP-induced marker genes (He *et al.*, 2006) *WRKY22*, *At2g17740* and *At5g57720* in response to 1 hour treatment with *elf18* and *flg22*, compared to water control or overnight *Pb(NO<sub>3</sub>)<sub>2</sub>* treatment which induces *PDR12* gene expression (Lee *et al.*, 2005). In each case I compared the *pdr12* mutants to Col-0. *WRKY22* expression was increased after treatment with *flg22* and *elf18*, but not *Pb(NO<sub>3</sub>)<sub>2</sub>*, as expected ([Figure 1.12E](#)). *WRKY22* *flg22*-induction was maintained in *pdr12-1*, with only a slight decrease in the *elf18*-induced sample, while *pdr12-2* showed markedly reduced *WRKY22* expression in response to *elf18* or *flg22* induction ([Figure 1.12E](#)). Expression of *At2g17740* and *At5g57720* was mildly induced within 1 hour of PAMP treatment in Col-0 and *pdr12-1*, but was reduced in *pdr12-2*, especially in response to *flg22* ([Figure 1.12E](#)).

In summary, these results indicate that PAMP-induced gene expression is impaired in *pdr12-2* lines, which also show the lowest level of *PDR12* expression ([Figure 1.12](#)). However, ROS burst and seedling growth inhibition of these mutants was not severely compromised.

To determine whether decreased PAMP-induced gene expression has an impact on disease resistance, I investigated the susceptibility of *pdr12* mutants to bacterial infection. Previous work has shown that *pdr12* mutants are not compromised in resistance to syringe-infiltrated *Pto* DC3000 (Campbell *et al.*, 2003). Thus, I opted for spray infection of *Pto* DC3000 to study pre-invasive defenses of the mutants. Col-0 plants supported the growth of *Pto* DC3000, which reached 6 - 7 log units of cfu/ml within 3 days of infection ([Figure 1.13A](#)). As shown previously, the *fls2* mutant and *efr-1 fls2* double mutant were both more susceptible than Col-0 (Zipfel *et al.*, 2004; Nekrasov *et al.*, 2009); ([Figure 1.13A](#)).

Bacterial growth was similar in Col-0 and both *pdr12-1* and *pdr12-2* (Figure 1.13A), indicating that their resistance to this virulent bacterial strain is intact. In order to reveal any subtle susceptibility phenotypes, I next infected the plants with a weakly virulent *Pto* strain lacking the phytotoxin coronatine (*Pto* DC3000 *COR*), which is important for bacterial colonization due to its role in re-opening stomata by mimicking isoleucine jasmonic acid (Ile-JA) (Melotto *et al.*, 2008; Melotto *et al.*, 2006). The *COR* strain is thus less virulent than the wild-type *Pto* DC3000, and reaches only 5 log units of cfu/ml growth when spray-inoculated on Col-0 plants (Figure 1.13B). However, this strain strikingly reveals the increased susceptibility in *fls2*, *efr-1* and *efr-1 fls2* mutants (Figure 1.13B; (Nekrasov *et al.*, 2009)). Interestingly, *pdr12-1* showed a reproducible slightly elevated bacterial growth while *pdr12-2* bacterial levels resembled the wild-type Col-0 (Figure 1.13B).

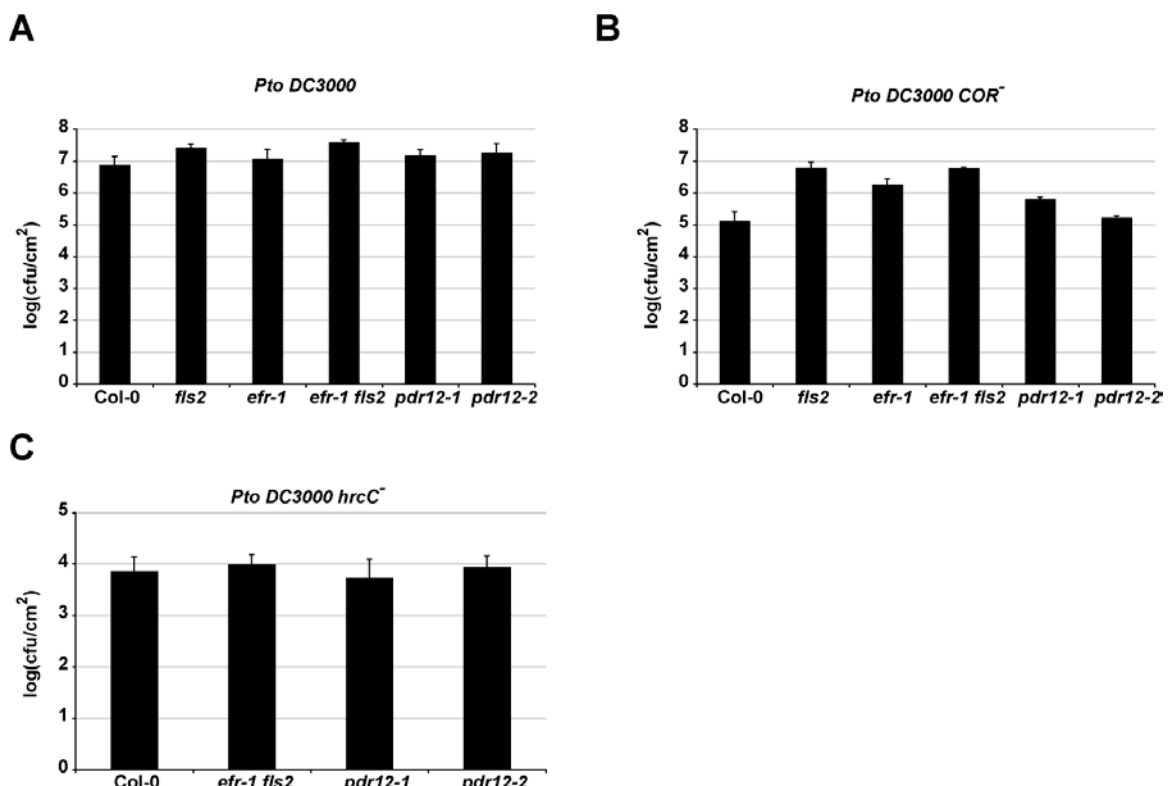


**Figure 1.13 *pdr12-1* mutants are slightly more susceptible to weakly virulent *Pseudomonas*.**  
A. Bacterial growth (cfu/cm<sup>2</sup>) in Col-0, *fls2*, *efr-1*, *efr-1 fls2*, *pdr12-1* and *pdr12-2* leaves spray-inoculated with 10<sup>7</sup> cfu/ml (O.D. 0.2) *P. syringae* pv. *tomato* DC3000 and sampled at 3 dpi. This experiment was repeated three times. Results are average ± standard error (n=4).  
B. Bacterial growth (cfu/cm<sup>2</sup>) in Col-0, *fls2*, *efr-1*, *efr-1 fls2*, *pdr12-1* and *pdr12-2* leaves spray-inoculated with 10<sup>7</sup> cfu/ml (O.D. 0.2) *P. syringae* pv. *tomato* DC3000 *COR*<sup>-</sup> and sampled at 3 dpi. This experiment was repeated three times. Results are average ± standard error (n=4).  
C. Bacterial growth (cfu/cm<sup>2</sup>) in Col-0, *fls2*, *efr-1*, *efr-1 fls2*, *pdr12-1* and *pdr12-2* leaves syringe-inoculated with 10<sup>5</sup> cfu/ml (O.D. 0.002) *P. syringae* pv. *tomato* DC3000 *hrcC*<sup>-</sup> and sampled at 3 dpi. This experiment was repeated twice. Results are average ± standard error (n=4).

Upon syringe inoculation of Col-0 with the non-virulent *Pto* DC3000 *hrcC* strain, which lacks a functional type-three secretion system (Roine *et al.*, 1997) and thus cannot inject effectors into plant hosts, there is a marked reduction in leaf colonization ([Figure 1.13C](#)). This level of growth is maintained in receptor mutant *efr-1 fls2*, as pre-invasive PAMP-induced defenses are not engaged when the bacteria are syringe infiltrated into the leaves ([Figure 1.13C](#)). *pdr12-1* and *pdr12-2* support a similar level of bacterial growth, with slightly reduced growth in *pdr12-1*. Although the mutants tested did not show strikingly compromised resistance to bacterial growth or PAMP responses, there was a mild reduction in PAMP-induced gene expression especially in *pdr12-2*, while *pdr12-1* was slightly more susceptible to *Pto* COR<sup>+</sup>.

## 1.3 Discussion

### 1.3.1 Large scale EFR immunoprecipitation

In this work, I initiated immunoprecipitation of EFR transiently expressed in *N. benthamiana* to identify possible cognate complex components, attempting to reveal components of the PAMP signaling cascade.

Initially I compared microsomal and total protein extraction prior to EFR immunoprecipitation, and decided to continue with total protein extraction, prioritizing a rapid extraction method with the aim of minimizing possible protein degradation. I carried out 3 biological replicates of the immunoprecipitation to identify reproducible interactors. I noticed that over the course of biological replication the identification of EFR peptides increased, showing an improvement of the technique as the method was optimized.

Using this strategy, I have detected peptides with high similarity to *AtBAK1* in EFR IPs, signifying that *Nicotiana benthamiana* SERK homolog(s), most likely at least *NbBAK1*, form(s) complex(es) with EFR in response to elf18 elicitation. No complete protein database exists for *N. benthamiana*, and the peptides obtained by mass spectrometry do not allow conclusive identification of the SERK family members interacting with EFR. This highlights one of the drawbacks of heterologous expression for conclusively identifying proteins with closely related

paralogs. However, this issue can probably be overcome by carrying out additional biological replicates, or transferring work to *Arabidopsis* (see Chapter 2 and 3). Previous work has shown that *NbBAK1* plays a prominent role in PAMP signaling, as silencing of *NbBAK1*, using a gene fragment cloned from *N. benthamiana*, compromises responses to flg22, INF1 and CSP22 (Heese *et al.*, 2007). The same is likely true for elf18 responses; this work is continued in [Chapter 3](#).

ER-QC components, including calreticulin (CRT), calnexin and luminal binding protein (BiP), are among the chaperones responsible for the correct folding of transmembrane proteins as they transit through the ER. For example, AtCRT3 is required for production of a functional EFR in *Arabidopsis* (Li *et al.*, 2009a; Saijo *et al.*, 2009). It is likely that EFR requires similar *N*-glycosylation and ER processing to be functional when transiently expressed. Thus it is appropriate to identify calnexin-like protein and luminal binding protein in EFR immunoprecipitates from *N. benthamiana*. These proteins have not been shown to interact directly with EFR in *Arabidopsis*, although several ER-QC-related proteins could later also be identified in EFR IPs in *Arabidopsis* ([Chapter 2](#)). Indeed it is likely that *N. benthamiana* homologs of these chaperones interact with EFR when heterologously expressed. Whether this interaction is specific or due to the accumulation of misfolded protein has not been addressed in this work, but the specific importance of these proteins for EFR in *Arabidopsis* suggests that this is not simply an artefact of transient over-expression.

### **1.3.2 The role of pleiotropic drug resistance (PDR) transporter role in PTI remains elusive**

Plant PDRs belong to a large family of ABC transporters that function as ATP-driven efflux pumps for a variety of substrates (Sánchez-Fernández *et al.*, 2001). *NpPDR1*, involved in the excretion of the antimicrobial sclareol to the leaf surface (Jasinski *et al.*, 2001), was identified as a putative EIP in the present study.

There is evidence supporting a general role for PDRs in biotic stress responses in plants. *NpPDR1* is constitutively expressed in leaf trichomes and roots, and its transcription is enhanced by jasmonic acid (JA) and sclareol but not salicylic acid (SA) (Stukkens *et al.*, 2005). *NpPDR1* expression in leaves is induced by infection with *B. cinerea* and bacteria *Pta* and *P. syringae* pv. *fluorescens* (*Pfo*), but not by

HR-inducing *P. syringae* pv. *syringae* (Stukkens *et al.*, 2005; Bultreys *et al.*, 2009). Interestingly, *NpPDR1*-silenced plants are not more susceptible to *Pta* infection, while they are hyper-susceptible to the necrotrophic fungal pathogens *B. cinerea* and *Fusarium oxysporum* as well as the necrotrophic oomycete *Phytophthora nicotianae* (Stukkens *et al.*, 2005; Bultreys *et al.*, 2009).

Based on amino acid similarity, *NpPDR1* clusters with PDR orthologs of *Arabidopsis* and *N. tabacum* (Crouzet *et al.*, 2006; [Figure 1.9](#)). The tobacco ortholog *NtPDR1* is similarly induced by JA, but interestingly also by flagellin elicitation (Sasabe *et al.*, 2002). In *Arabidopsis*, there are 15 PDRs, the closest ortholog of *NpPDR1* being *AtPDR12* (69 % homology). *AtPDR12* gene expression is highly induced (over 250-fold) by SA, and also by inoculation with fungal pathogens including *A. brassicicola* (incompatible) and *S. sclerotiorum* (compatible), as well as *Pto* DC3000 (Campbell *et al.*, 2003). However, this does not correlate with disease resistance. *pdr12* mutants do not display increased susceptibility to syringe inoculated bacterial pathogens *Pto* DC3000 or *Pto* 1065 or to the fungal pathogens *F. oxysporum* or *A. brassicicola* (Campbell *et al.*, 2003). Taken together, all these evidences suggest a role for PDRs in defense signaling. However, I was unable to confirm an interaction between *NpPDR1* or its ortholog *AtPDR12* and EFR. In addition, it was not possible to study the effect of *NpPDR1* on *elf18*-induced signaling, as *NpPDR1*-silenced plants were not amenable to transient expression. However, these plants displayed enhanced ROS burst responses to the other PAMPs tested. It cannot be excluded that these responses are related to the constitutive activation of defense in these hyper-susceptible plants. It is known that plant defense responses inhibit Agrobacterium transformation (Zipfel *et al.*, 2006), thus it is conceivable that the low expression of EFR in the *NpPDR1*-silenced leaves could be due to the activation of defenses in these plants.

*pdr12* mutants were not strikingly compromised in PAMP signaling or bacterial disease resistance, although defense gene expression was attenuated in these mutants. Further work is required to get closer to understanding the role of PDRs in PTI, as for instance, more in-depth characterization of the double mutant *pdr12-1 pdr10* or other true knock-out alleles that may now be available for study. Furthermore, it is important to determine whether PDR12 can transport antimicrobials, and how this is linked to activation of PAMP receptors. However

before embarking on such a study, it is worth considering that my subsequent work in *Arabidopsis* identified PDR8/PEN3 and not PDR12 in EFR immunoprecipitates, suggesting that PDR12 is actually not the *Arabidopsis* ortholog of interest in PAMP signaling ([Chapter 2](#)). This illustrates one of the drawbacks of using an unsequenced plant such as *N. benthamiana* for MS projects. In this way, proteins are identified based on partial sequence information and often only orthologous proteins are identified by MS. This leaves the choice of which *Arabidopsis* ortholog to pursue up to phylogenetic analysis, which is risky when proteins belong to large families, like PDRs.

Yet there was no conclusive evidence of a role for PDR8 in PTI either, and no association between PDR8/PEN3 and EFR could be detected by co-IP. Finally, the role of PDRs in biotic stress may be general and not specifically related to PAMP perception or signaling.

## 2 IDENTIFICATION OF EFR-INTERACTING PROTEINS (EIPs) IN ARABIDOPSIS

### 2.1 Preface

The *N. benthamiana* genome has not been sequenced and there is no complete database of all proteins for this organism. Thus, it is sometimes more informative to work in Arabidopsis. Following the establishment of the experimental protocol in *N. benthamiana* I adapted the method towards purification of the EFR complex from stable transgenic Arabidopsis *efr-1* plants expressing tagged EFR under the control of its own promoter to identify EIPs *in planta*. The objective was to purify large amounts of tagged EFR and its interactors by large-scale immunoprecipitation of EFR-eGFP-HA using GFP-binding protein beads. The immunoprecipitate was separated using gel electrophoresis and interactors identified using HPLC-MS analysis. This analysis was done to compare proteins interacting with EFR before and after the addition of elf18, in order to identify ligand-altered interactions. The experiment was repeated with 3 biological replicates. To compile a list of putative interactors, a set of conditions were applied to the list of proteins identified in the IP: the proteins selected as putative EIPs had to be absent from the negative control (*efr-1* knockout line) and have good quality peptides present in at least 2 biological replicates. The set of EIPs includes 2 especially interesting groups - several RJs, **Receptors Associated with EFR (RAE)** and proteins involved in receptor folding and glycosylation. In addition, other proteins with a potential role in PTI were identified, including H<sup>+</sup>-ATPases and a PDR family ABC transporter.

### 2.2 Results

#### 2.2.1 EFR-eGFP is enriched in immunoprecipitates

Total proteins were extracted from *efr-1* or *efr-1*/EFR-eGFP-HA tissue that had been treated with 100 nM elf18 or water for 5 minutes. Approximately 90 mg total protein was prepared and GFPTrap beads added to immunoprecipitate EFR. The IP was analysed by immunoblotting ([Figure 2.1](#) A, C, E) and the remainder separated by SDS-PAGE ([Figure 2.1](#) B, D, F). Each lane of the gel was sliced into

10 pieces and peptides extracted for HPLC-MS/MS analysis. The experiment was repeated with 3 independent biological replicates to ensure a better chance of identifying true reproducible interactors. In each replicate, there was clear enrichment of EFR-eGFP, though some protein remained in the flow-through, indicating incomplete immunoprecipitation, despite the use of large volumes of beads. Over the course of the replicates, the coverage of EFR reached 42 % ([Figure 2.1G](#)) and 52 unique peptides were identified ([Table 2.1](#) and [Appendix Table 2.1](#)).

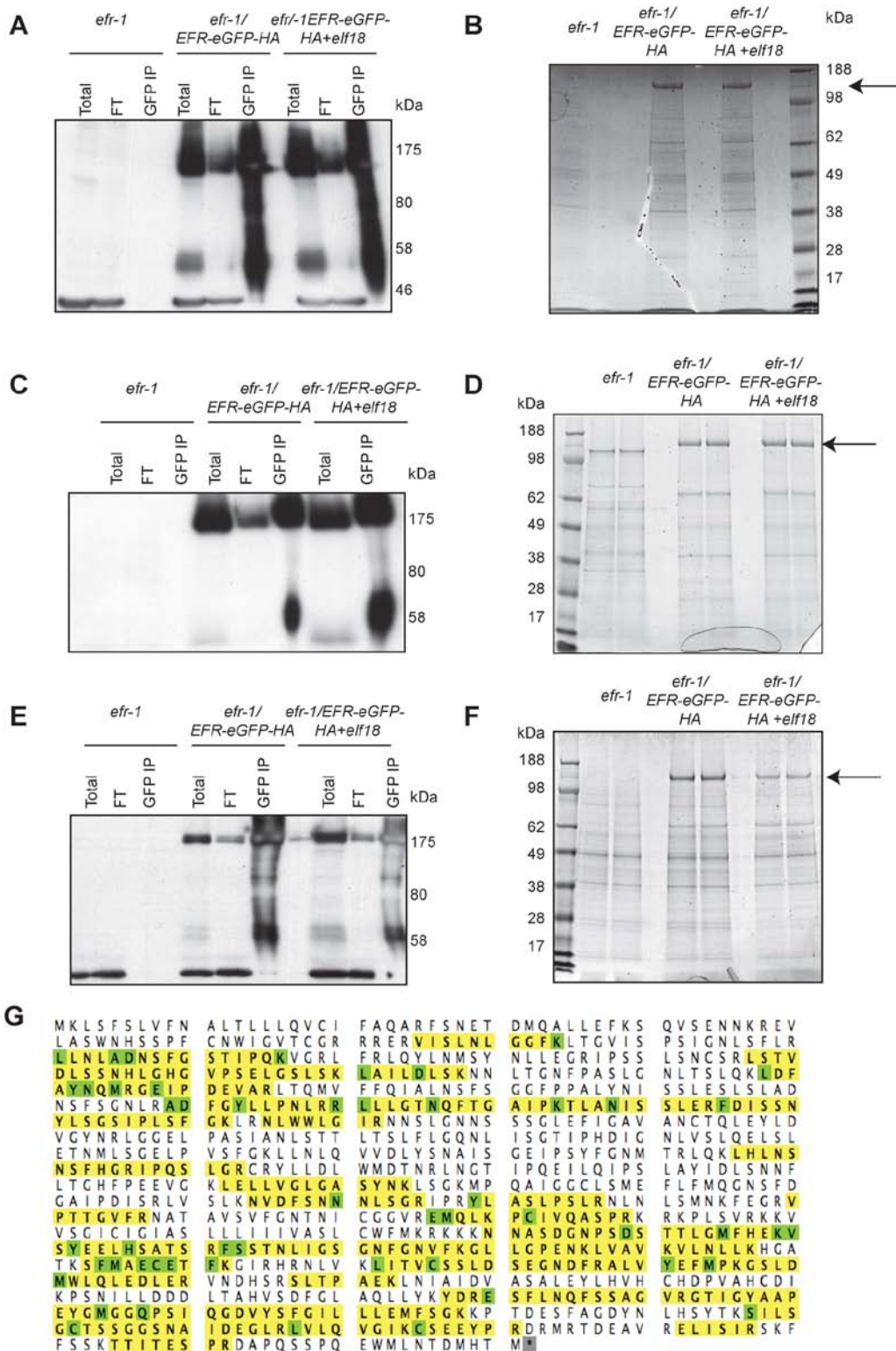


**Figure 2.1 Immunoprecipitation of EFR in transgenic *Arabidopsis*.**

A, C and E. Consecutive biological replicates of anti-GFP immunoprecipitation from *efr-1* or transgenic *efr-1* expressing EFR-eGFP-HA under the control of the native promoter; with or without 100 nM elf18 treatment; anti-GFP (1:5000) X-ray film. FT= flow-through.

B, D and F. Consecutive biological replicates of colloidal Coomassie-stained SDS-PAGE of anti-GFP IP prepared in A, C or E. Arrow indicates immunoprecipitated EFR-eGFP-HA. G. Illustration of coverage of EFR sequence by peptides identified in HPLC-MS/MS analysis of GFP IPs. Peptides are highlighted in yellow; green indicates post-translational modification e.g. methionine oxidation. Approximate molecular weight in kDa as indicated.

**Table 2-1 Potential EFR-interacting proteins**

Identified Protein *	Accession	no elf18			100 nM elf18			Location <sup>s</sup>
		Rep3	Rep2	Rep1	Rep3	Rep2	Rep1	
<b>Receptor-like kinases (RAEs)</b>								
BAK1 (BRI1-associated receptor kinase)	AT4G33430.1	0	0	2	9	2	7	PM
SERK4 (somatic embryogenesis receptor-like kinase 4)	AT2G13790.1	0	0	0	12	4	6	PM
SERK2 (somatic embryogenesis receptor-like kinase 2)	AT1G34210.1	0	0	0	4	2	2	PM
LRR-RK subfamily XII-7	AT4G08850.1/2	3	1	2	4	0	0	PM
LRR-RK subfamily VIII	AT3G14840.2	0	2	2	6	1	0	PM
LRR-RK subfamily I	AT1G51800.1	1	0	1	6	0	1	PM
CRK11/RLK3 (cysteine-rich RLK11)	AT4G23190.1	1	0	2	2	0	0	PM; ER
<b>Protein folding</b>								
CRT3 (calreticulin 3)	AT1G08450.1	1	0	1	7	0	1	ER
EBS1 (EMS-mutagenized BRI1 suppressor 1); UGGT (UDP-glucose:glycoprotein transferase)	AT1G71220.1	9	6	7	6	5	1	ER
BIP (luminal binding protein)	AT5G42020.1	3	0	3	4	2	1	ER
BIP3	AT1G09080.1	5	2	5	5	1	6	ER
CDC48 (cell division cycle 48) isoform A	AT3G09840.1	2	3	1	3	1	1	ER
DEX1 (defective in exine formation 1)	AT3G09090.1	1	6	2	3	4	1	ER; PM; C
DGL1 (defective glycosylation1)	AT5g66680	2	3	0	0	0	0	ER
<b>ATPases</b>								
AHA3 (Arabidopsis H <sup>+</sup> -ATPase 3)	AT5G57350.1	2	0	1	2	1	0	PM
PDR8/PEN3 (pleiotropic drug resistance 8)	AT1G59870.1	2	2	3	3	1	1	PM
<b>Chloroplastic</b>								
PSAE-2 (photosystem I subunit E-2)	AT2G20260.1	0	1	0	2	1	1	P
TRP1 (tryptophan biosynthesis 1)	AT5G17990.1	3	0	1	3	0	2	P
D1 subunit of photosystem I and II reaction centers	ATCG00340.1	0	0	2	2	0	1	P
PTAC3 (plastid transcriptionally active 3)	AT3G04260.1	1	0	2	1	0	1	P
TOC159 (plasmid protein import 2)	AT4G02510.1	1	1	3	2	0	1	P
Rieske (2Fe-2S) domain-containing protein	AT1G71500.1	0	2	6	0	0	4	P
Acylaminoacyl-peptidase-related	AT4G14570.1	5	0	2	2	0	2	P
NUDT20 (Nudix hydrolase homolog 20)	AT5G19460.1	0	1	1	1	0	2	P
PSAG (photosystem I subunit G)	AT1G55670.1	1	0	2	1	0	0	P
HEME2; uroporphyrinogen decarboxylase	AT2G40490.1	0	0	2	1	2	0	P
AK-HSDH (bifunctional aspartate kinase/homoserine dehydrogenase)	AT4G19710.2	1	0	2	1	0	0	P
CAC2 (acetyl co-enzyme A carboxylase biotin carboxylase (+1))	AT5G35360.1	1	0	0	2	0	1	P
KAS III (3-ketoacyl-acyl carrier protein synthase III)	AT1G62640.1	0	0	0	2	1	0	P
AMI1 (amidase-like protein 1) similar to unknown protein (TAIR:AT3G20510.1); InterPro domain UPF0136, TM (InterPro:IPR005349)	AT1G08980.1	2	1	0	0	1	0	P
	AT3G57280.1	0	0	2	0	0	1	P

**Table 2.1 continued**

Identified Protein *	Accession	no elf18			100 nM elf18			Location <sup>§</sup>
		Rep3	Rep2	Rep1	Rep3	Rep2	Rep1	
<b>Ribosomal proteins</b>								
40S Ribosomal protein S2 (RPS2D)	AT3G57490.1	1	0	2	3	0	0	C
Histidyl-tRNA synthetase, putative	AT3G02760.1	2	1	0	2	0	0	C
40S Ribosomal protein S27+	AT2G45710.1	0	0	1	2	0	1	C
YbaK/prolyl-tRNA synthetase family protein	AT1G44835.1 (+1)	1	0	2	0	0	1	C; N
RPS15 (ribosomal protein S15)	AT1G04270.1 (+1)	0	0	0	2	0	3	PM; V; C
Isoleucyl-tRNA synthetase, putative / isoleucine-tRNA ligase, putative	AT4G10320.1	2	0	0	1	1	0	C
eIF4-gamma/eIF5/eIF2-epsilon domain-containing protein	AT2G34970.1	4	0	1	2	0	1	C; N
tRNA synthetase class I (W and Y) family protein	AT3G04600.1 (+2)	0	0	0	3	0	1	C; N
EMB1473 (embryo defective 1473; 50S ribosomal protein L13)	AT1G78630.1	1	0	2	0	0	2	P
<b>Other</b>								
PLDGAMMA1 (maternal effect embryo arrest 54); phospholipase D	AT4G11850.1	2	0	1	1	0	0	Plastid; M; N
PPC2 (phosphoenolpyruvate carboxylase 2)	AT2G42600.1 (+1)	0	4	0	1	1	1	C
Caffeoyl-CoA 3-O-methyltransferase, putative	AT4G34050.1	1	0	1	2	0	0	C
ATB BETA (Arabidopsis thaliana serine/threonine protein phosphatase 2A 55 kDa regulatory subunit B beta isoform)	AT1G17720.2	0	3	0	1	1	0	C; N
PHB1 (prohibitin 1)	AT4G28510.1	0	0	2	2	0	2	M
CAC3 (acetyl co-enzyme A carboxylase carboxyltransferase alpha subunit)	AT2G38040.1 (+1)	2	1	2	0	0	0	P; M
Pentatricopeptide (PPR) repeat-containing protein	AT1G02150.1	0	0	1	2	0	1	P; M
2-Nitropropane dioxygenase family	AT5G64250.1 (+1)	0	0	1	2	0	1	M/C
Similar to unnamed protein product [Vitis vinifera] (GB:CAO62125.1); contains domain SSF53448	AT1G64980.1	2	1	0	0	0	0	C
<b>Trafficking-related</b>								
Coatomer protein complex, subunit alpha	AT1G62020.1	0	1	2	0	1	1	PM
Coatomer gamma-2 subunit	AT4G34450.1 AT5G22770.1	3	0	1	1	0	2	C
ALPHA-ADR (alpha-adaptin)	(+3)	2	0	1	1	0	0	PM/C

\*All peptides matching protein, not necessarily unique. <sup>§</sup>Localization predicted by SUBA (C=cytosol; M=mitochondrion; N=nucleus; PM=plasma membrane; ER=endoplasmic reticulum; V=vacuole; P=plastid)

Over the three biological replicates that were carried out, a total of 850 proteins were identified by HPLC-MS/MS analysis of EFR immunoprecipitates. Of these, 122 were absent from the *elf-1* control IP, and 50 of these were identified in at least 2/3 biological replicates. The list of putative interacting proteins can be separated into several groups. Firstly, a set of receptor kinases were reproducibly identified in the IPs, referred to as receptor kinases associated with EFR (RAE).

These will be discussed further in Chapter 3 and 4. Secondly, a group of proteins related to receptor folding and quality control ([§ 2.2.2](#)). Trafficking-related candidate interactors include the coatomer subunits alpha and gamma and alpha adaptins. Finally there were numerous mitochondrial, chloroplastic and ribosomal proteins that may play a role in PAMP signaling, or may be non-specifically adhering to the IP beads.

## 2.2.2 EFR *N*-glycosylation and quality control

Interestingly, post-translational modifications of EFR peptides could also be detected by HPLC-MS/MS analysis of EFR IPs. Among these, *N*-glycosylation (N-acetylhexosamine, HexNAc) could reproducibly be detected as a post-translational modification of EFR. EFR protein size based on the primary amino acid sequence is 113 kDa, however the protein migrates at 150 kDa by gel electrophoresis. This discrepancy is likely due to *N*-glycosylation of the LRR domain, which retards the protein migration (Zipfel *et al.*, 2006). EFR has 16 potential *N*-glycosylation sites (Häweker *et al.*, 2010; Albert *et al.*, 2010) ([Appendix Figure A2.1](#)), characterized by the glycosylation sequon NxS/T, where the modified Asn occurs within the tripeptide Asn-X-Ser, the site of glycan addition by oligosaccharyltransferase (OST) to nascent polypeptides in the ER (Helenius and Aebi, 2001).

Two peptides TLANISSLER (N288) and NVDFSNNNLSGR (N571) were modified by *N*-glycosylation in multiple experiments with Mascot ion scores above 20 ([Table 2.2](#)). This suggests that EFR is modified at N288 and N571, which are located in the extracellular LRR domain of EFR. N288 is conserved in Xa21 and N571 is conserved in Xa21 and FLS2 ([Figure 2.2](#)). Xa21 is also a glycosylated protein, and depends on OsBIP3 for correct processing (Park *et al.*, 2010a). The identified glycosylation sites are likely to be true modifications, because in addition to the acceptable Mascot score and spectra ([Appendix Table 2.1](#)), the modified Asn occurs within the glycosylation sequon Asn-X-Ser (Helenius and Aebi, 2001).

**Table 2-2 Glycosylated EFR peptides identified by MS analysis of EFR IPs**

Bio. Rep.	Peptide sequence*	Peptide identification probability <sup>§</sup>	Mascot Ion score <sup>^</sup>	Mascot Identity score <sup>§</sup>	HexNAc (+203.08)
EFR_1	NVDFSNNNNLSGR	95.00%	39.6	30.2	N7
EFR_1	NVDFSNNNNLSGR	95.00%	42.1	30.2	N7
EFR_1	TLANISSLER	89.30%	27.4	31.1	N4
EFR_1	TLANISSLER	95.00%	31.9	30.8	N4
EFR_1	TLANISSLER	95.00%	42.6	29.4	N4
EFR_2	NVDFSNNNNLSGR	95.00%	45.2	26.4	N8
EFR_2	NVDFSNNNNLSGR	95.00%	52.8	26.4	N8
EFR_2	TLANISSLER	95.00%	40.1	27.8	N4
EFR_2	TLANISSLER	95.00%	41.1	27.8	N4
EFR_3	NVDFSNNNNLSGR	95.00%	49.6	30.8	N7
EFR_3	NVDFSNNNNLSGR	95.00%	54.4	30.8	N8
EFR_elf18 1	NVDFSNNNNLSGR	95.00%	35.9	29.9	N6
EFR_elf18 1	NVDFSNNNNLSGR	95.00%	37.7	29.8	N8
EFR_elf18 1	NVDFSNNNNLSGR	95.00%	38.3	27.9	N8
EFR_elf18 1	NVDFSNNNNLSGR	95.00%	49.6	27.9	N8
EFR_elf18 1	TLANISSLER	95.00%	34	30.4	N4
EFR_elf18 2	NVDFSNNNNLSGR	95.00%	70.4	26.6	N6
EFR_elf18 2	TLANISSLER	93.70%	28.4	28	N4

\*: Pink highlighted N indicates N within NxS/T sequon

<sup>§</sup>Peptide ID probability: Scaffold calculated probability that a given protein has been identified correctly

<sup>^</sup>Mascot Ion Score is a measure of how well the observed MS/MS spectrum matches to the stated peptide

<sup>§</sup>Mascot identity score: a minimum ion score threshold. As a rule, the ion score should be above the identity score. identity score=-10\*(log(p/#matches)), where p is your probability threshold (Scaffold uses 1.0), and #matches is the number of precursor matches.

HexNAc: N-acetylhexosamine

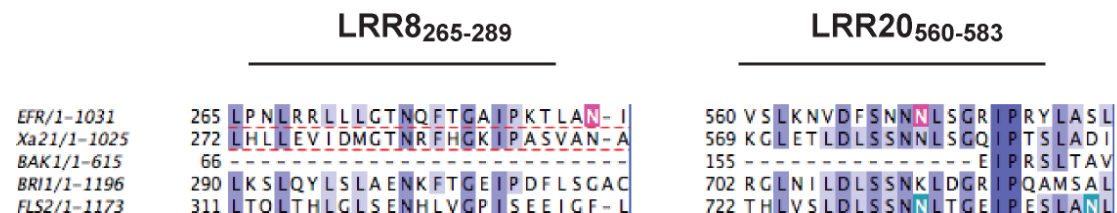


**Figure 2.2 Conservation of N-glycosylation sites in selected LRR-RKs.**

EFR LRR8 and LRR20 aligned with selected LRR-RKs. ClustalW multiple alignment generated using JalView v.12.2, shaded for percentage identity. EFR N-glycosylation sites identified by MS/MS are highlighted pink (N288 in LRR8, N571 in LRR20), predicted N-glycosylation sites are highlighted green.

Recently, genetic screens in *Arabidopsis* have revealed that elements of the endoplasmic reticulum quality control (ER-QC) pathway are specifically required for production of functional EFR. These include UDP-glucose:glycoprotein transferase (UGGT), calreticulin 3 (CRT3), staurosporin and temperature-sensitive 3a (STT3a) and glucosidase II beta (GCSII b) (Saijo *et al.*, 2009; Li *et al.*, 2009a; Häweker *et al.*, 2010; Lu *et al.*, 2009; Li *et al.*, 2009a). Another pathway specifically required for EFR occurs in parallel or in cooperation with the CRT3 pathway and involves the chaperones stromal-derived factor 2

(SDF2), luminal binding protein (BiP) and the Hsp40 ERDj3b (Nekrasov *et al.*, 2009). Importantly, these chaperones act distinctively for EFR folding and none of these pathways are essential to the function of the related FLS2 receptor (Nekrasov *et al.*, 2009; Saijo *et al.*, 2009). This suggests an additional requirement of this more recently evolved receptor for folding assistance. A number of ER-QC-related proteins were also identified as putative EFR-interactors in this work. These include UGGT/EBS1, CRT3, CNX, DGL1 (member of OST complex) and BiP ([Table 2.1](#)). This correlates with the identification of *N. benthamiana* BIP homologs and calnexin-like protein in EFR IPs carried out in *N. benthamiana* ([Chapter 1](#)). Also present in the IP was the AAA-ATPase CDC48, involved in proteasomal retrotranslocation, which was previously identified as an interactor of the LRR-RLK SERK1 (Rienties *et al.*, 2005).

Although no co-IP between EFR and the ER-QC components have been confirmed, it is likely that these are EIPs which interact with EFR during its transit through the ER.

### 2.2.3 EFR Phosphorylation

EFR is a Ser/Thr kinase, and is likely to be phosphorylated, however no phosphorylation sites have previously been reported. However, two potential EFR phosphopeptides were identified during the course of this work. The first peptide KNNASDGNNPSDSTTLGFHEK is located in the internal juxtamembrane region, while TTITESPR, is located in the C-terminal cytoplasmic tail ([Table 2.3](#)). The exact phosphorylation site(s) of the identified peptides is difficult to assign purely from the measurement of neutral loss of phosphate from the peptide (+79.97 Da; [Appendix Figure A2.4](#)). PhosPhat algorithm was used to assess the likelihood of phosphorylation at the various potential sites (Heazlewood *et al.*, 2008; Durek *et al.*, 2009), and in each case the phosphosite was predicted to be possible (score>0). Interestingly the first phosphopeptide overlaps with the potential degradation motif of EFR, which is conserved in Xa21 (see [Figure 1.8](#); [Figure 2.2](#)) and several of the potentially phosphorylated residues in the peptide are also conserved in Xa21 ([Figure 2.3](#)). It is possible that phosphorylation at this site stabilizes the protein, as Xa21 mutants of phosphosites in this area were unstable (Xu *et al.*, 2006a).

**Table 2-3 EFR phosphopeptides\* identified by MS analysis of EFR IPs**

Bio Rep	Peptide sequence	Peptide ID prob. <sup>§</sup>	Mascot Ion score <sup>^</sup>	Mascot Identity score <sup>§</sup>	Other Modifications <sup>*</sup>	PhosPhat score <sup>£</sup>
EFR_3	NNAS <sub>683</sub> DGNPSDSTTLGmFHEK	95%	60.7	22.2	Oxidation	0.176
EFR_3	NNAS <sub>683</sub> DGNPSDSTTLGmFHEK	95%	57.2	22.1	Oxidation	0.176
EFR_3	KNNASDGNPSDSTT <sub>692</sub> LGmFHEK	95%	32.2	23.2	Oxidation	0.18722081
EFRe18-1	TTITES <sub>1010</sub> PR	89.8%	22	23.2		1.549

<sup>§</sup> Peptide ID probability: Scaffold calculated probability that a given protein has been identified correctly.<sup>^</sup> Mascot Ion Score is a measure of how well the observed MS/MS spectrum matches to the stated peptide.<sup>§</sup> Mascot identity score: a minimum ion score threshold. As a rule, the ion score should be above the identity score. identity score=-10\*(log(p/#matches)), where p is your probability threshold (Scaffold uses 1.0), and #matches is the number of precursor matches.

\*Phosphorylation detected as addition of +79.97 Da; variable modifications; oxidation +15.99.

<sup>£</sup> PhosPhat score>0 predicts phosphorylation at site indicated in bold, amino acid number in subscript.

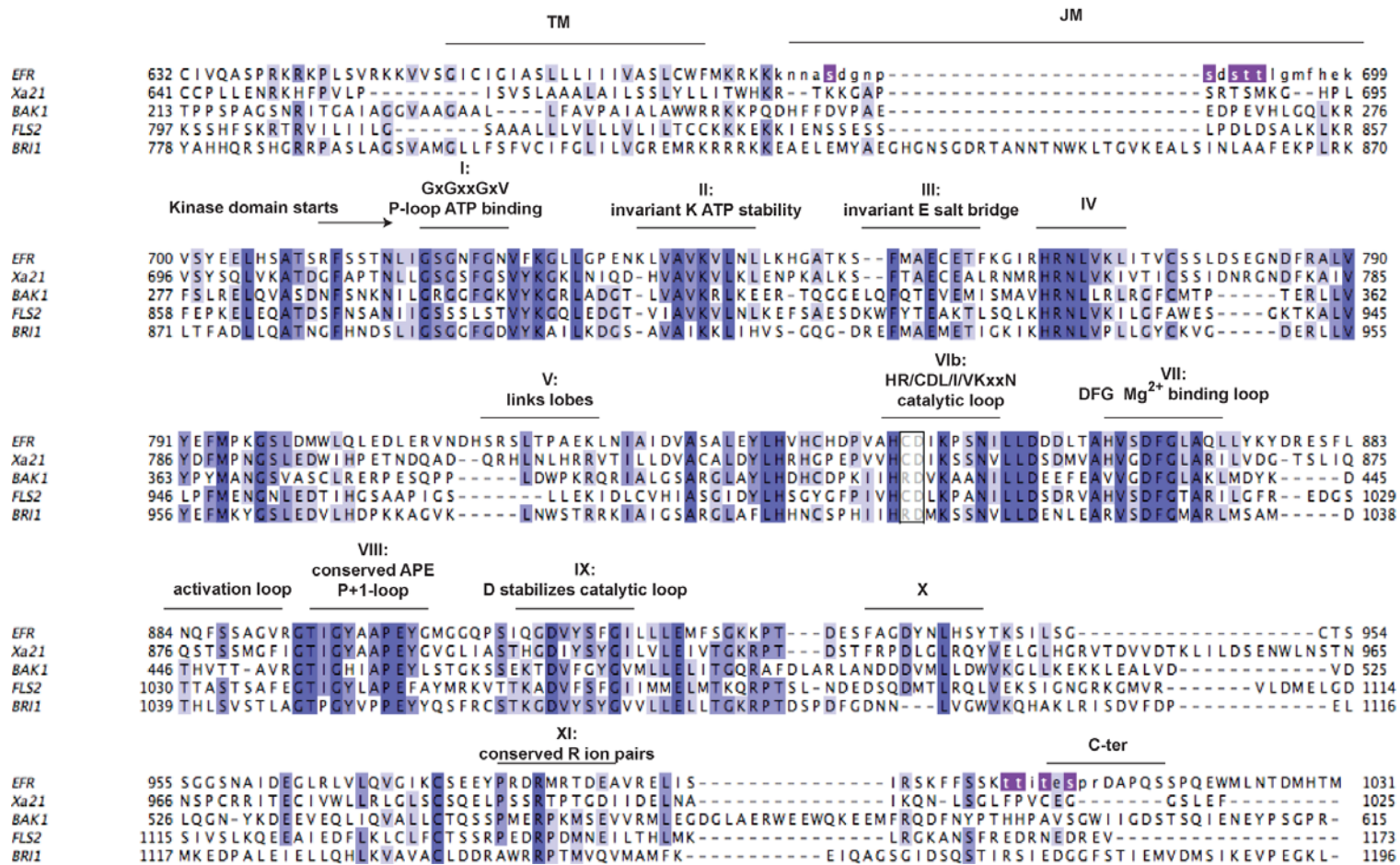


**Figure 2.3 Multiple alignment of EFR, Xa21, FLS2, BRI1, BAK1 cytoplasmic domains**

ClustalW multiple alignment generated using JalView v.12.2, shaded for percentage identity. Phosphopeptides are indicated as lowercase, with potential phosphosites highlighted purple. The kinase subdomains as demarcated by Hanks and Quinn, 1991 are indicated in roman numerals with consensus sequences where applicable. The conserved Asp (D) in the active site, along with the preceding R or C residue are marked by a box. JM: juxtamembrane domain; TM: transmembrane domain.

Domains predicted by UniProt.

Notably, the second peptide has a reduced peptide identification probability, with a low Mascot score, and was only detected in one experiment. This could be an indication that phosphorylation is unlikely, but this has to be experimentally verified.

## 2.2.4 Putative EFR-interacting proteins

*The RKS associated with EFR (RAEs) and SERKs will be discussed separately, in Chapter 3 - Chapter 5.*

### 2.2.4.1 PEN3

Peptides matching PEN3/PDR8 (Penetration resistance 3/pleiotropic drug resistance 8; later referred to as PEN3) were identified in each of the biological replicates of the large-scale IP of EFR in *Arabidopsis* ([Table 2.1](#)). PEN3 is an ATP-binding cassette (ABC) transporter that was identified in a screen for *Arabidopsis* mutants with altered resistance to barley powdery mildew (Stein *et al.*, 2006). PEN3 is required for non-host resistance to fungal pathogens and *pen3* mutants display hyper-induction of SA-induced genes, which correlated with increased resistance to *Pto* DC3000 (Stein *et al.*, 2006; Kobae *et al.*, 2006). *pen3-1* mutants also have reduced flg22-induced callose deposition (Clay *et al.*, 2009) and hyperaccumulation of camalexin and glucosinolates (Bednarek *et al.*, 2009). More recently, PEN3 was also found to play a role in auxin homeostasis (Strader *et al.*, 2010), possibly by enabling efflux of IAA precursor. Certain of the peptides also matched other members of this large family of ABC transporters, including PDR1, 7 and 11, but not PDR12 ([Table 2.4](#); [Appendix Figure 2.2](#)). This was interesting considering the previous detection of *NpPDR1* in EFR IPs in *N. benthamiana* ([Chapter 1](#)), suggesting that the *Arabidopsis* homolog of *NpPDR1* relevant to PAMP signaling may be PEN3.

I sought to confirm whether EFR and PEN3 could interact in *Arabidopsis*. When I immunoprecipitated EFR-eGFP-HA from transgenic EFR-eGFP-HA lines, no PEN3 could be identified by anti-PEN3 (Masayoshi Maeshima, Laboratory of Cell Dynamics, Nagoya University, Japan; Kobae *et al.*, 2006) western blotting

analysis of the EFR immunoprecipitate, before or after elf18 treatment ([Figure 2.4A](#)). To determine whether FLS2 could interact with PEN3, I obtained PEN3-GFP transgenic lines, expressing *PEN3* under the control of its native promoter fused to a C-terminal GFP tag (Shauna Somerville Laboratory, UC Berkeley; (Stein *et al.*, 2006)). I carried out the reciprocal IP of PEN3-GFP from PEN3-GFP lines but also did not detect FLS2 in the PEN3 GFP IP ([Figure 2.4B](#)). I then attempted to confirm interactions by transiently expressing tagged versions of each protein in *N. benthamiana*. Co-IP analysis could not confirm any interaction between PEN3-GFP and EFR-HA<sub>3</sub> (data not shown). In contrast, when pulling down equal amounts of FLS2-Myc, PEN3-GFP could be detected in the IP before and after flg22 treatment ([Figure 2.4C](#)). Yeast two-hybrid analysis of potential interactions done by a collaborator (Bill Underwood; Shauna Somerville Laboratory, UC Berkeley) revealed no interaction between PEN3 and EFR in yeast, but FLS2-PEN3 interaction was detected. It is possible that enrichment of the complex by microsomal fractionation prior to IP, or cross-linking to stabilize the interactions would have facilitated their detection, but this was not attempted.

**Table 2-4 PEN3 peptides identified by MS analysis of EFR IPs**

Biological Rep	Peptide sequence	Mascot Ion score <sup>^</sup>	Mascot ID score <sup>\$</sup>	Matches also
EFR_2	m*TLLLGPSSGK	47.9	29.8	PDR1,6,7,11
EFR_1	GTADFLQEVTSK	69.4	24.4	PDR7
EFR_elf18_3	GTADFLQEVTSK	87.1	23.4	PDR7
EFR_elf18_3	TTLLLALAGKLDK	43.2	10.8	PDR7
EFR_3	DISGVIKPGK	34.6	19	
EFR_1	IQVLGGAPDLTVK	41.7	19.3	
EFR_1	IQVLGGAPDLTVK	52.4	19.4	
EFR_2	NSLVTDYTLK	39.1	18.3	
EFR_2	SLPTLLNVVR	27.6	16.3	
EFR_3	YDLLNELAR	28.1	23.6	
EFR_elf18_3	YDLLNELAR	28	23.4	

\* oxidized +15.99.

All peptides 95 % identification probability (Peptide ID probability: Scaffold calculated probability that a given protein has been identified correctly).

<sup>^</sup> Mascot Ion Score is a measure of how well the observed MS/MS spectrum matches to the stated peptide.

<sup>\$</sup> Mascot identity score: a minimum ion score threshold. As a rule, the ion score should be above the identity score. identity score=-10\*(log(p/#matches)), where p is your probability threshold (Scaffold uses 1.0), and #matches is the number of precursor matches.

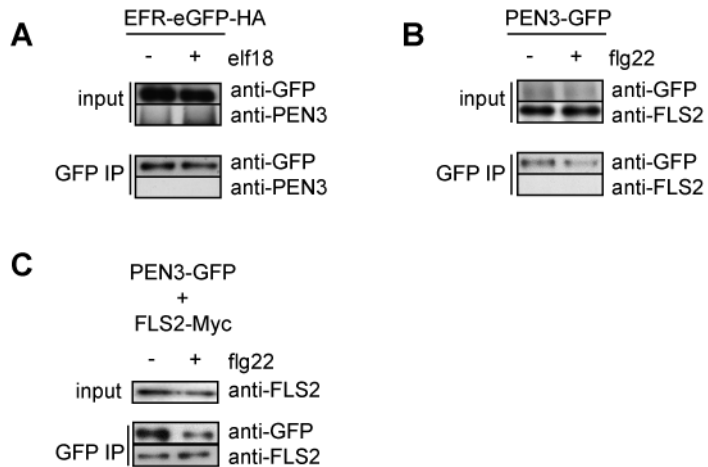


**Figure 2.4 PEN3 interacts with FLS2 but not with EFR under conditions tested.**

A. Co-immunoprecipitation of EFR and PEN3. Transgenic *efr-1* Arabidopsis seedlings expressing EFR-eGFP-HA under the native promoter were treated (+) or not (-) with 100 nM elf18 for 5 minutes. Total proteins (input) were subjected to immunoprecipitation (GFP IP) with GFP Trap beads followed by immunoblot analysis with anti-PEN3 antibodies to detect PEN3 and anti-GFP antibodies to detect EFR-eGFP-HA.

B. Co-immunoprecipitation of FLS2 and PEN3. Transgenic *pen3-1* Arabidopsis seedlings expressing PEN3-GFP under the native promoter were treated (+) or not (-) with 100 nM flg22 for 5 minutes. Total proteins (input) were subjected to immunoprecipitation (GFP IP) with GFP Trap beads followed by immunoblot analysis with anti-FLS2 antibodies to detect FLS2 and anti-GFP antibodies to detect PEN3-GFP.

C. Co-immunoprecipitation of FLS2 and PEN3. *N. benthamiana* leaves expressing FLS2-Myc and PEN3-GFP (2 days post-infiltration) were treated (+) or not (-) with 100 nM flg22 for 5 minutes. Total proteins (input) were subjected to immunoprecipitation with GFP Trap beads followed by immunoblot analysis with anti-FLS2 antibodies to detect FLS2-Myc and anti-GFP antibodies to detect PEN3-GFP.

*pen3* mutants have not been comprehensively characterized for PAMP-induced responses, thus despite no confirmation of an interaction between EFR and PEN3, I proceeded to study these mutants.

Firstly, I assessed the effect of PAMPs on seedling growth in *pen3/pdr8* loss of function lines. The T-DNA insertional mutants *pdr8-1* (Salk\_000578) and *pdr8-2* (Salk\_142256) are null alleles, reportedly accumulating no protein (Kobae *et al.*, 2006) while *pen3-1* is an EMS mutant harbouring a single amino acid substitution in the conserved ABC signature motif, resulting in the formation of a mutant protein (Stein *et al.*, 2006) ([Figure 2.5A](#)). Flg22 severely inhibited growth of Col-0, *pdr8-1* and *pdr8-2* seedlings over 10 days incubation period, with *pdr8-2* mutants being slightly more PAMP sensitive than Col-0 ([Figure 2.5B](#), left panel). At low flg22 concentrations *pen3-1* mutants appeared to be less sensitive to flg22, but this was also true for the complementation line expressing *PEN3-GFP* under the control of the *PEN3* promoter ([Figure 2.5B](#)). At 100 nM flg22, all seedlings

behaved similarly and showed 80 % growth inhibition ([Figure 2.5B](#)). Elf18-induced growth inhibition of all mutants was similar to that of Col-0 over a range of concentrations ([Figure 2.5B](#), right panel). PAMP-induced ROS burst can be detected within 2 minutes of flg22 elicitation in Col-0 leaf tissue, and this was maintained in *pdr8-1* mutants ([Figure 2.5C](#), left panel). *pen3-1* mutants produced less ROS in response to flg22, but this reduction was not reproducible ([Figure 2.5C](#), left panel). Elf18-induced ROS production was similar in Col-0, *pdr8-1* and *pen3-1* ([Figure 2.5C](#), right panel).

Infection by spray inoculation of 4-week-old plants with *Pto* DC3000 results in colonization of Col-0 plants by the bacteria, which is enhanced in *efr-1 fls2* mutants, as reported (Nekrasov *et al.*, 2009). *pdr8-1* plants have wild-type-like susceptibility, while there is slightly increased growth in *pen3-1* ([Figure 2.5D](#)). However, this increased susceptibility of *pen3-1* was not reproducible. Indeed, previous reports indicated increased resistance to syringe-infiltrated *Pseudomonas* infection in *pdr8-1* and *pdr8-2* (Kobae *et al.*, 2006), likely due to accumulation of SA as detected by hyperactivation of SA-induced genes (Stein *et al.*, 2006).

The *Pto* DC3000 strain lacking the type three effectors AvrPto and AvrPtoB ( $\Delta$ AvrPto/ $\Delta$ AvrPtoB) is less virulent and multiplies less in Col-0 than the wild-type *Pto* DC3000 ([Figure 2.5D](#), middle panel). The increased susceptibility of the *efr-1 fls2* double mutant was clear, with growth reaching 1.5 log units cfu/ml more than in Col-0 ([Figure 2.5D](#), middle panel). *pdr8-1* was less susceptible than Col-0, with almost 1 log difference in growth ([Figure 2.5D](#), middle panel), in line with what has been reported (Stein *et al.*, 2006). This was not the case for *pen3-1*, which displayed wild-type-like bacterial growth ([Figure 2.5D](#), middle panel). To further probe for subtle phenotypic differences, I also carried out spray inoculation of the *COR*<sup>-</sup> strain, which lacks the isoleucine-jasmonic acid (Ile-JA) mimic coronatine, preventing it from re-opening stomata and reducing infection of Col-0 plants (Melotto *et al.*, 2006). Again, the *efr-1 fls2* mutant showed increased susceptibility to this strain, while *pdr8-1* was resistant to infection, with 1 log less growth. Conversely, *pen3-1* resembles Col-0 in its susceptibility to this strain ([Figure 2.5D](#), right panel).

Although the phenotypic differences detected in these assays were minor, it is possible that flg22 responses are slightly attenuated in *PEN3* loss-of-function lines, suggesting a potential role for *PEN3* in flg22-induced signaling. If this occurs

through some action of PEN3 on FLS2, this would correlate with the interaction detected by yeast-two-hybrid (data not shown, Bill Underwood, Shauna Somerville Laboratory, UC Berkeley) and the co-IP observed when these proteins were transiently expressed.

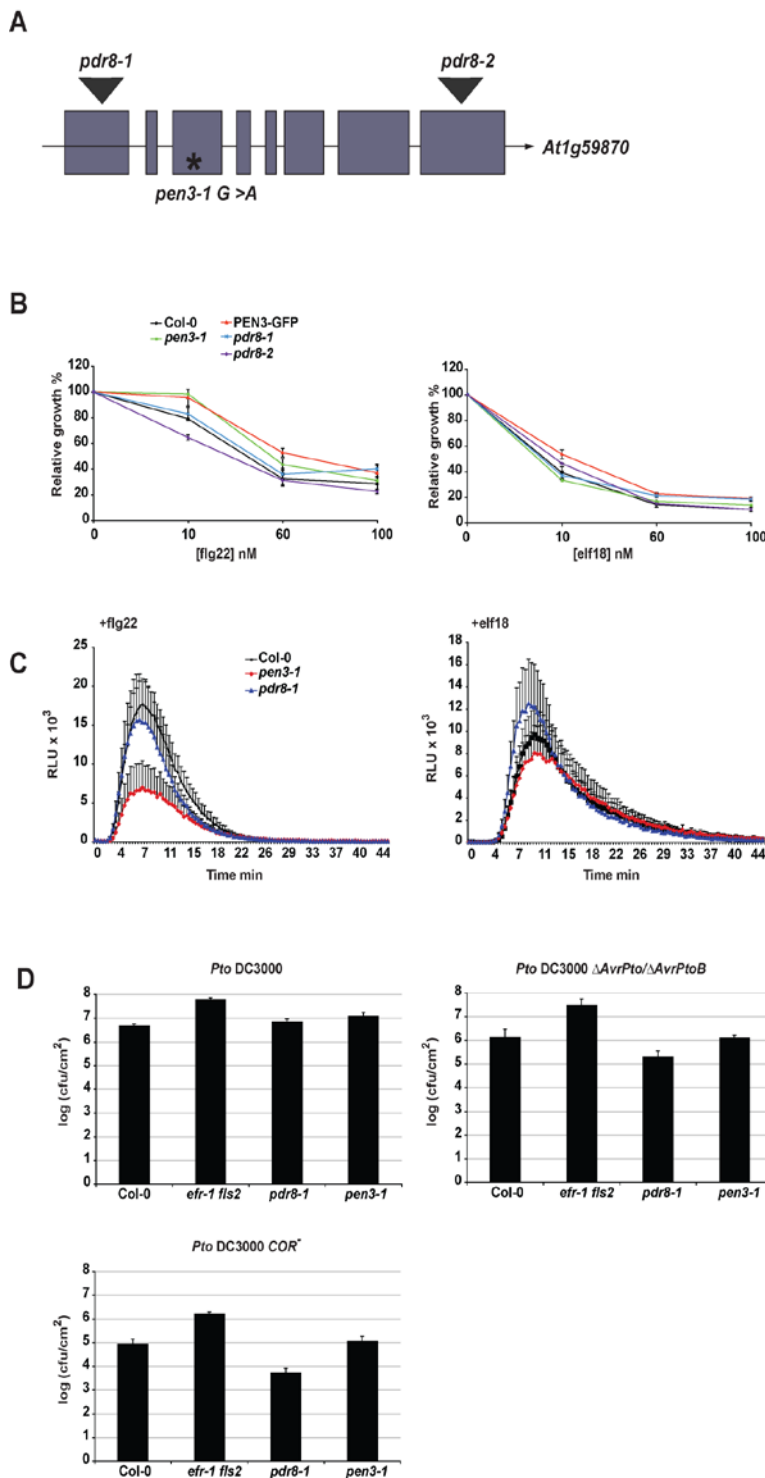


**Figure 2.5** *pen3* mutants do not have severely compromised PTI responses.

A. Schematic diagram illustrating *PEN3* (At1g59870) gene and location of T-DNA insertions *pdr8-1* (Salk\_000578) and *pdr8-2* (Salk\_142256) and *pen3-1* mutation (\*). Exons are represented by filled blue squares, introns by black line.

B. Growth inhibition in response to increasing concentrations of flg22 (left) and elf18 (right) in Col-0, *pdr8-1*, *pdr8-2*, *pen3-1* and *pen3-1/PEN3-GFP* seedlings. Represented as % fresh weight of untreated seedlings. Results are average  $\pm$  standard error ( $n=6$ ). This experiment was repeated once.

C. Production of ROS in Col-0, *pdr8-1*, and *pen3-1* leaf discs in response to 100 nM flg22 (left) or 100 nM elf18 (right) elicitation. RLU = relative light units. Results are average  $\pm$  standard error ( $n=8$ ). This experiment was repeated three times.

D. Bacterial growth (cfu/cm<sup>2</sup>) in Col-0, *efr-1 fls2*, *pdr8-1* and *pen3-1* leaves spray inoculated with  $10^7$  cfu/ml (O.D. 0.02) *P. syringae* pv. *tomato* (Pto) DC3000, Pto DC3000  $\Delta$ AvrPto/ $\Delta$ AvrPtoB or Pto DC3000 COR<sup>+</sup> sampled at 3 dpi. Results are average  $\pm$  standard error ( $n=4$ ). These infections were repeated four times.

## 2.2.4.2 Other putative interacting proteins

### Defective in exine formation (DEX1)

Defective in exine formation (DEX1) is a plant-specific membrane-localized protein involved in pollen exine formation (Paxson-Sowders *et al.*, 2001). This protein possesses FG-GAP repeats in the extracellular domain, as found in the N-terminus of integrin alpha chains, with a possible role in calcium binding (Springer, 1997). *DEX1* is expressed throughout the plant, suggesting that it may have additional functions. Interestingly, *DEX1* is predicted to be co-expressed (ATTED II; BAR) with several genes involved in ER-QC, including RSW3 (GCSII  $\alpha$ ) ALG3, DAD2 and DGL1, strongly suggesting a potential role for DEX1 in EFR quality control. No work was done on this potential candidate and no interaction with EFR was tested. As homozygous T-DNA knockout lines of *dex1* are male sterile (Paxson-Sowders *et al.*, 2001) tissue-specific RNA-silencing of *DEX1* would be a useful tool to develop.

### Arabidopsis H<sup>+</sup>-ATPases (AHA1/2)

Peptides derived from Arabidopsis H<sup>+</sup>-ATPases were present in EFR IPs ([Table 2.1](#)). Due to high sequence conservation, peptides were matched to multiple members of the family of AHAs ([Appendix Table 2.2](#)). However, only AHA1 and AHA2 were represented by unmodified, high quality peptides. AHA1 and AHA2 share 94 % amino acid identity, but one unique peptide could be assigned to AHA1 and four unique peptides matched only AHA2 ([Appendix Table 2.2](#)). This suggests that at least AHA1 and AHA2 are likely to be present in EFR immunoprecipitates, though confirmational co-IPs were not carried out. The majority of peptides were identified from sample post-elf18-elicitation, but this was not exclusively the case, thus the interaction does not appear to be strictly ligand-induced, but may be stabilized by ligand binding.

AHA1 and AHA2 were also identified in RIN4 immunoprecipitates (Liu *et al.*, 2009). RIN4 is known to negatively regulate PTI responses (Mackey *et al.*, 2002; Kim *et al.*, 2005c). Recent work showed that RIN4 acts as a positive regulator of AHA1/2 ATPase activity, ultimately facilitating stomatal aperture in response to *Pto* DC3000, and thereby influencing bacterial susceptibility (Liu *et al.*, 2009). Interestingly, EFR is expressed in guard cells (Liu *et al.*, 2009) where AHA1/2

could be acting, thus could be interacting either directly with AHA1/2 or interacting with AHA1/2 via RIN4 in guard cells (Liu *et al.*, 2009). Consistently, AHA1/2 peptides were also identified in immunoprecipitates of RPS2, the resistance protein that guards and interacts with RIN4 (Qi and Katagiri, 2009). AHA1, AHA2, AHA3 and AHA4 are enriched in detergent-resistant membranes upon flg22 elicitation (Keinath *et al.*, 2010) and AHA1 and AHA2 are phosphorylated in response to flg22 elicitation (Benschop *et al.*, 2007; Nühse *et al.*, 2007), thus AHA activity is regulated in response to PAMP perception. The constitutively active AHA1 mutant *ostD-1* showed reduced flg22-induced ROS burst, likely due to hyperpolarization of the membrane in this mutant, as well as enhanced MAP kinase activation (Keinath *et al.*, 2010). Taken together, these results would suggest the existence of a large immune complex containing components of PTI and ETI, which could act together for a robust immune response. I did not work further on these putative EFR interactors.

## 2.3 Discussion

### 2.3.1 EFR Immunoprecipitation in *Arabidopsis*

The immunoprecipitation of tagged EFR from transgenic *Arabidopsis* has allowed the identification of various interesting candidate EIPs, with potential roles in PAMP signaling.

I detected members of the SERK family as well as ER-QC-related proteins as EFR interactors in both *N. benthamiana* and *Arabidopsis*. BAK1, a SERK family member, and ER-QC components are required for PTI signaling (Heese *et al.*, 2007; Chinchilla *et al.*, 2007; Li *et al.*, 2009a; Lu *et al.*, 2009; Nekrasov *et al.*, 2009; Saijo *et al.*, 2009; Häweker *et al.*, 2010). This illustrates that important partners of EFR, required for EFR biogenesis as well as for signaling, can be identified by using immunoprecipitation and mass spectrometry analysis.

### 2.3.2 ER-QC components as putative EIPs

During the production of plasma membrane-localized transmembrane glycoproteins such as EFR, nascent secretory proteins travel through the ER

where they encounter chaperones, which aid in their folding and ultimately their delivery to the plasma membrane where they function. The correct folding of proteins during this maturation process is monitored by a mechanism called ER quality control (ER-QC) (Ellgaard and Helenius, 2003). If proteins are terminally misfolded or aberrant they are delivered to ER-associated degradation (ERAD) (McCracken and Brodsky, 1996; Vembar and Brodsky, 2008) in the cytosol, or in the vacuole (Pimpl *et al.*, 2006). This ER-QC pathway can follow different routes and is largely conserved from mammals to yeast (Brodsky and McCracken, 1999).

One classical folding pathway relies on retention of misfolded proteins by Hsp70 family member luminal binding protein (BiP). The Hsp40 family member Erdj3b recruits BiP and activates BiP ATPase activity, transferring the client to BiP and releasing Erdj3b (Jin *et al.*, 2008, 2009). In *Arabidopsis*, the unique protein stromal derived factor 2 (SDF2) interacts with Erdj3b and is essential for the correct folding of EFR (Nekrasov *et al.*, 2009).

Another route for ER-QC depends on N-glycosylation of nascent proteins. This co-translational modification of newly synthesized polypeptides is catalyzed by the oligosaccharide transferase (OST) complex (see Part I, Figure 3), comprised of subunits including DAD1/2 (defender against cell death); STT3a and 3b (staurosporine and temperature sensitive) and DGL1 (defective glycosylation1) (Koiwa *et al.*, 2003); (Lerouxel *et al.*, 2005); (Silberstein *et al.*, 1995; Gallois *et al.*, 1997). In this process, a glycosyl moiety  $\text{GlcNaAc}_2\text{Man}_9\text{Glc}_3$  (GlcNAc: N-acetylglucosamine; Man: mannose; Glc: glucose) is conjugated to the Asn (N) of the consensus sequon Asn-X-Ser/Thr (X is any amino acid except Pro). The outermost Glc residues are trimmed by the action of glucosidases I and II (GCSI/II), while the antagonistically acting UDP:glucose:glycoprotein glucosyltransferase (UGGT) specifically recognizes aberrantly folded proteins and adds one glucose. These mono-glucosylated glycan-conjugated proteins are then recognized by the ER lectin-like chaperones calreticulin (CRT) and calnexin (CNX) that act to assist in proper folding. If following glucose removal by glucosidase the protein is properly folded, it will exit the ER; however if it contains hydrophobic patches, it will be recognized by UGGT, which will add another glucose, again targeting the monoglycosylated non-native polypeptide to the CRT/CNX cycle. This continues until the correct conformation is obtained and the protein will be exported to the Golgi to finally arrive at its correct PM destination (Pattison and

Amtmann, 2009). In yeast and mammalian cells, CDC48 (p97) contributes to retrotranslocation of ERAD substrates prior to proteasomal degradation (Braun *et al.*, 2002; Jarosch *et al.*, 2002; Schrader *et al.*, 2009). The Arabidopsis homolog complements yeast *cdc48* (Rancour *et al.*, 2002) and is required for the degradation of aberrant MLO protein (Müller *et al.*, 2005), suggesting that the plant homolog plays a similar role in ERAD, though this protein also functions in cytokinesis and cell expansion (Rancour *et al.*, 2002; Rancour *et al.*, 2004).

The ER-QC components CRT3, UGGT, STT3a, GCSII, SDF2 and Erdj3b have recently been shown to be required for the production of a functional EFR receptor (Häweker *et al.*, 2010; Li *et al.*, 2009a; Lu *et al.*, 2009; Nekrasov *et al.*, 2009; Saijo *et al.*, 2009). Several of these, including CRT3, UGGT, DGL1 and BiP, as well as CDC48, were identified as potential EIPs in the present study. In contrast however, SDF2 and Erdj3b were not identified in EFR IPs, despite their importance for receptor maturation (Nekrasov *et al.*, 2009; Saijo *et al.*, 2009). Although interactions between ER-QC components and EFR were not confirmed by co-IP, it is likely that these proteins interact with EFR during its transit through the ER, hence their presence in the EFR IPs from Arabidopsis and *N. benthamiana*.

The requirement for ER-QC for innate immunity seems to be conserved for the closest rice ortholog of EFR, the PAMP receptor Xa21. The rice homolog of BiP, OsBiP3 was identified as an interactor of Xa21 (Park *et al.*, 2010a), while a rice OsSDF2-silenced line is more susceptible to *Xanthomonas* (Park *et al.*, 2010b). Similarly, the rice chitin receptor OsCERK1 interacts with Hsp90 and its co-chaperone Hop/Sti1 in the ER and these chaperones are required for receptor maturation and innate immunity (Chen *et al.*, 2010a). Furthermore, in *N. benthamiana*, CRT3 and BIP5/GRP78-5 are among the ER-resident chaperones that are up-regulated during N-mediated defense and *CRT3*-silenced plants are compromised in N-mediated TMV resistance (Caplan *et al.*, 2009).

### 2.3.3 N-glycosylation

Two putative glycosylation sites (N288; N571) were repeatedly identified in the EFR LRR domain ([Table 2.2](#)). The biological role of EFR glycosylation was not further investigated, but it would be interesting to determine whether these modifications are required for receptor stability, or perhaps for PAMP binding.

N288 is found within the second LRR of the receptor, and thus falls within the region of the receptor required for elf18 binding (Albert *et al.*, 2010). However, previous work showed that mutagenesis of N288 (N288Q) only marginally compromised ROS production in response to elf18 when the mutant protein was transiently expressed in *N. benthamiana* (Häweker *et al.*, 2010). Furthermore, although there was increased ER-retention of the mutant protein, there was no detectable difference in elf26 binding affinity (Häweker *et al.*, 2010). It is possible that glycosylation at alternative sites could compensate mutational loss of another, however this has not been shown for EFR.

Recently, glycosylation of EFR N143 was shown to be important for elf26 binding, ROS production and receptor stability (Häweker *et al.*, 2010). Although a few peptides covering this region of the protein were obtained in the MS analysis, this modification was not detected. This could be due to the mass spectrometry protocol used, which was not optimized for the detection of N-glycosylation, or due to the low relative abundance of modified peptides (Wuhrer *et al.*, 2007), or this could depend the extraction method or elicitation time used.

### 2.3.4 EFR phosphorylation

Further work is required to fully understand the structure-function relationship of EFR and that is beyond the scope of this thesis. However I did detect some potential phosphorylation sites in the juxtamembrane (JM) (S683; T692) and C-terminal domains of the receptor (S1010). For receptor tyrosine kinases, ligand binding stabilizes receptor dimerization, and this leads to activation of the kinase domain, relieves auto-inhibition and results in auto- and transphosphorylation of receptors, followed by recruitment and phosphorylation of downstream components (Ullrich and Schlessinger, 1990). Most kinases that are regulated by phosphorylation in the activation segment (including the activation loop, P+1 loop and Mg<sup>2+</sup>-binding loop, [Figure 2.3](#)) are RD kinases, featuring an Arg (R) preceding

the conserved Asp (D) in the catalytic loop (Johnson *et al.*, 1996). EGF receptor is an RD kinase but does not require activation loop phosphorylation for activation, rather EGFR is regulated by an allosteric mechanism (Jura *et al.*, 2009; Red Brewer *et al.*, 2009). Phosphorylation of residues within the juxtamembrane and C-terminal domains of the cytoplasmic domain also contribute to RTK regulation (Hubbard, 2004).

EFR is a non-RD kinase, but bears some resemblance to EGFR and may have a similar mode of regulation. During my work I have not detected EFR homooligomerization, but dimerization could be involved in the activation mechanism that leads to receptor transphosphorylation, similarly to EGFR or BRI1 (Heldin, 1995; Wang *et al.*, 2008d).

Auto-phosphorylation of Xa21 occurs at S686, T688 and S689 (Xu *et al.*, 2006a) and these sites are conserved in EFR (S688, S690, T691) ([Figure 2.3](#)). Phosphorylation at these residues appears to be required for Xa21 stability (Xu *et al.*, 2006a), so it is conceivable that EFR may behave similarly. One of the phosphopeptides identified in this study covers this area of the JM domain, and the site of phosphorylation could have been erroneously assigned to S692 (see below).

Furthermore, T705 in the juxtamembrane region of Xa21 is autophosphorylated, and this is required for Xa21 interaction with its signaling partners and function in innate immunity (Chen *et al.*, 2010a). This Thr residue is conserved in many Ser/Thr kinases, including all members of subfamily XII, ERECTA, CERK1, BKK1 and BRI1 (see [Appendix Figure A2.4](#); and (Shan *et al.*, 2008)). This site is also autophosphorylated in the tomato kinase Pto, required for resistance to *Pto* strains carrying AvrPto (Martin *et al.*, 1993; Sessa *et al.*, 2000). Autophosphorylation at this residue (T38) is required for defense signaling, as well as interaction with AvrPto and downstream signaling partners Pti1 and Pti4 (Sessa *et al.*, 2000). The corresponding mutation in FLS2, T867, compromises its function in transgenic plants (Robatzek *et al.*, 2006), but the same residue (T880) is not required for BRI1 function (Wang *et al.*, 2005b). This site is also conserved in EFR (T709), though it has not been identified *in vivo* by mass spectrometry in this work. The similarity in the kinase domains of EFR, FLS2 and Pto was exploited previously to identify these proteins as targets of AvrPto and AvrPtoB (Shan *et al.*, 2008). Given all this evidence, it is likely that phosphorylation at this site is

important for EFR function. Preliminary work indicates that EFR is not functional when the equivalent Thr (T709) is mutated to Ala or Glu (data not shown), but it remains to verify if kinase activity and interaction with downstream targets is maintained in these mutants.

Assessment of the quality of the mass spectra from which the peptide sequences were derived helps to determine whether phosphopeptides have been correctly assigned. During mass spectrometry, a series of b- (where the parent peptide charge is retained on the N-terminal end of the peptide) and y- ions (where the charge is retained on the C-terminal end of the peptide) are generated by successive fragmentation of the peptide backbone within the ionization source (Johnson *et al.*, 1987)([Appendix Figure A2.3](#)). Protein phosphorylation causes a mass shift of 79.99 Da due to the addition of  $\text{HPO}_3$  to the mass of a peptide. Phosphoserine and phosphothreonine lose a phosphoric acid ( $\text{H}_3\text{PO}_4$ ) moiety during high-energy peptide fragmentation, and this can be seen as a neutral loss of 98 Da on spectra (Lehmann *et al.*, 2007). However, when there are several possible phosphorylation sites within a peptide, it is difficult to assign the phosphorylation to a particular amino acid with confidence. This is especially true for low abundance peptides, as the addition of modifications results in more complex MS/MS spectra.

In the MS/MS spectra corresponding to the putative phosphopeptides identified in this work ([Appendix Figure A2.4](#)), the  $b_1$  and  $y_1$  ions are not identified, as expected for data derived from an ion trap mass spectrometer, as these ions are too small to be detected. All the peptides were cleaved at K as is expected for tryptic peptides as trypsin cleaves C-terminal to K or R residues (Olsen *et al.*, 2004). The peptide with the lowest Mascot score (32) is predictably not very convincing: there are several large peaks that remain unassigned, and the signal to noise ratio is not favourable ([Appendix Figure A2.4A](#)). This correlates with the data in the fragmentation table, which shows that only a few of the b and y ions could be assigned to peaks in this case. This phosphopeptide was also identified with higher Mascot scores (57 and 60), with the phosphorylation assigned to S683. In the spectra of the higher scoring peptides, several unassigned peaks remain, however there is a better signal to noise ratio and most of the b and y ions were assigned. Here the addition of 80 Da due to phosphorylation was assigned to S683 ([Appendix Figure A2.4B and C](#)). Finally, the last peptide in [Table 2.3](#)

TTITESPR, has a low Mascot score and accordingly a poor MS/MS spectrum ([Appendix Figure A2.4D](#)). This weak evidence for phosphorylation could be due to low abundance of the phosphopeptides, as the same peptide without any modifications was identified several times ([Appendix Table 2.1](#)).

*In silico* prediction of phosphosites in EFR can be carried out using software such as PhosPhat (<http://phosphat.mpimp-golm.mpg.de>) (Heazlewood *et al.*, 2008; Durek *et al.*, 2009). PhosPhat assigns a score to each putative phosphorylated position, with scores > 0 indicating likelihood of phosphorylation. The phosphosites detected in this study are all predicted to occur by PhosPhat, all with scores > 0 ([Table 2.3](#)).

None of the spectra that were obtained are ideal for the detection of phosphosites, but this is not surprising. Only a subset of EFR protein is likely to be phosphorylated, thus relatively few phosphopeptides are generated for analysis, and peptides with lower intensity are less likely to be identified. Importantly, the aim of this work was not to analyze post-translational modifications, and thus no measures were taken to improve the chances of identification, aside from the addition of phosphatase inhibitors to the extraction buffer. To improve the chances of phosphosite identification, fractionation is usually carried out prior to MS analysis, using immobilized metal affinity or TiO<sub>2</sub> chromatography to enrich for negatively charged phosphopeptides (Schulze, 2010). This could be undertaken in future studies towards *in vivo* EFR phosphosite identification.

To initiate the study of the potential role of these sites in elf18-related signaling, phosphomimetic and phospho-dead mutants need to be created. These could be expressed in *E. coli* (along with their kinase-dead variants as negative controls) in order to determine if these sites affect *in vitro* kinase activity of the receptor. In addition, these mutants could be assessed for their ability to interact with known signaling partners (such as BAK1) to determine whether phosphorylation at either site affects the interaction characteristics of the receptor.

### 2.3.5 PEN3 does not have a clear role in PTI

PEN3 was identified in EFR IPs, both before and after elf18 elicitation. Importantly, although PEN3 is an abundant protein in the plasma membrane, no PEN3 peptides were identified in the *efr-1* control. PEN3/PDR8 belongs to a large

group of ABC transporters, which includes PDR12 ([Figure 1.9](#)). The *Nicotiana* ortholog PDR1 was identified in EFR IPs done in *N. benthamiana* (Part III Chapter 1) although no interaction was confirmed by co-IP. Further work on the Arabidopsis homolog PDR12 did not reveal any role in PTI. Upon identification of this ortholog in EFR IPs, it appeared as though I had previously chosen the wrong homolog to investigate. However, no interaction between EFR and PEN3 could be confirmed, although there was association between PEN3 and FLS2, which was mirrored in yeast two hybrid assays (S. Somerville laboaratory). It is possible that there is an interaction between EFR and PEN3 but the available tools precluded me from detecting if there is any interaction by co-IP. Double-transgenic tagged EFR and PEN3 lines would need to be created in order to investigate the interaction further.

In *pen3* mutant lines, flg22 responses were sometimes reduced, but elf18 responses were similar to Col-0. The fact that there was no striking *pen3* phenotype for PTI responses could be due to redundancy, as another PDR may take over PEN3 function in its absence. However, there is no functional redundancy for PEN3 function in penetration resistance or auxin signaling. Double mutants with the closest homolog PDR7 would need to be assayed for PTI responses to test this possibility. Ultimately, the role of PEN3 may be in an aspect of defense that has not been investigated in this study.

### 3 SERKS: REGULATORY CO-RECEPTORS FOR MULTIPLE RECEPTOR KINASES

*Note: The work in this Chapter was done in equal collaboration with Benjamin Schwessinger (experiments were conducted by both of us together)*

#### 3.1 Preface

BAK1 [brassinosteroid-insensitive 1 (BRI1)-associated receptor kinase] belongs to a sub-class of the subfamily II of LRR-RKs, referred to as the somatic-embryogenesis RK (SERK) family based on sequence homology with the carrot LRR-RK SERK protein (Hecht *et al.*, 2001). The SERK family contains 5 closely related members in *Arabidopsis* with BAK1 corresponding to SERK3. The *Arabidopsis* SERK proteins are involved in diverse signaling pathways and are often functionally redundant (Albrecht *et al.*, 2008).

In addition to BAK1, SERK1 and BAK1-like 1/SERK 4 (BKK1/SERK4) also interact with BRI1 as positive regulators of BR responses (Karlova *et al.*, 2006; He *et al.*, 2007; Albrecht *et al.*, 2008). Furthermore, SERK1 and SERK2 have redundant roles in male sporogenesis (Albrecht *et al.*, 2005; Colcombet *et al.*, 2005; Albrecht *et al.*, 2008), and SERK1 has recently been shown to be involved in organ separation in flowers (Lewis *et al.*, 2010). Importantly, BKK1 and BAK1 are both required to control cell death and senescence (He *et al.*, 2007; Kemmerling *et al.*, 2007; Jeong *et al.*, 2010).

BAK1 was recently found to also form a ligand-dependent complex with FLS2 (Chinchilla *et al.*, 2007; Heese *et al.*, 2007). This association occurs within seconds of flg22 binding, and leads to rapid phosphorylation of FLS2 and BAK1 (Schulze *et al.*, 2010). Loss of BAK1 results in reduced flg22 responses (Chinchilla *et al.*, 2007; Heese *et al.*, 2007). BAK1 is also required for responses triggered by the bacterial PAMPs elf18, lipopolysaccharides (LPS), peptidoglycans (PGN), HrpZ, csp22 (derived from cold-shock protein), the oomycete PAMP INF1, and the DAMP AtPep1 (Chinchilla *et al.*, 2007; Heese *et al.*, 2007; Krol *et al.*, 2010; Shan *et al.*, 2008), suggesting that BAK1 may also form a ligand-dependent complex with their corresponding PRRs. The LRR-RKs PEPR1 and PEPR2, the redundant

receptors for *AtPep1*, have been identified recently as BAK1-interacting proteins in a targeted yeast-two hybrid approach (Postel *et al.*, 2010).

Interestingly, elf26 treatment leads to rapid phosphorylation of BAK1 and of a co-immunoprecipitated protein that migrates at the same size as the glycosylated form of EFR (Schulze *et al.*, 2010). Notably, the effect of *BAK1* loss-of-function on elf18 responses is less marked than for flg22 responses (Chinchilla *et al.*, 2007; Shan *et al.*, 2008), and null *bak1* mutant plants are still sensitive to flg22 and other PAMPs. This indicates that EFR may preferentially interact with other RRs than BAK1, and that additional complex components are required for signaling downstream of FLS2 and EFR.

Following detection of SERK peptides in EFR IPs, I sought to identify which members of the family were present in the complex, and characterize their roles in PTI. Here, I demonstrate that EFR forms a ligand-dependent complex with BAK1 *in vivo*. In addition, I show the ligand-dependent recruitment of additional SERKs in the EFR, FLS2 and BRI1 hetero-oligomeric complexes. Using a novel *bak1* allele that does not exhibit defects in BR and cell death responses, I genetically determined that BAK1 and BKK1 cooperate to regulate multiple PRR-dependent signaling pathways. Furthermore, I demonstrate that BAK1 and BKK1 are major regulators of disease resistance against hemi-biotrophic bacteria and obligate biotrophic oomycetes.

## 3.2 Results

### 3.2.1 Identification of SERKs in the EFR complex

Mass spectrometry analysis of EFR complexes identified the presence of multiple members of the SERK family following elf18 treatment ([Table 2.1](#) and [Table 3.1](#)). Anti-GFP immunoprecipitates were prepared from untreated and elf18-treated transgenic *efr-1/EFR-eGFP-HA* seedlings, as well as from untreated *efr-1* null mutant seedlings to reveal proteins that may bind non-specifically to the GFP beads. Immunoprecipitated proteins were then separated by sodium dodecyl sulphate - polyacrylamide gel electrophoresis (SDS-PAGE), gel slices excised and in-gel trypsin digestion carried out ([Chapter 2](#)). Sequencing of tryptic peptides by liquid chromatography tandem mass spectrometry (LC-MS/MS) identified 28

different peptides matching members of the SERK family. Importantly, these peptides were only present in the elf18-elicited transgenic sample (Table 3.1). Only peptides with sufficiently high Mascot score (>20) were considered as a true indication of the presence of a particular SERK in the immunoprecipitates. Given the high degree of identity among the SERK family (Hecht *et al.*, 2001); (Albrecht *et al.*, 2008), it is difficult to unambiguously assign tryptic peptides to individual specific SERK proteins. After careful analysis of the identified peptides based on multiple alignments of the SERK proteins, three peptides unique to BAK1 were identified in all three biological replicates. For SERK2 and BKK1 only a single specific peptide could be identified for each in all three biological replicates (Table 3.1). No peptides specific to SERK1 or SERK5 were found.

These data revealed the ligand-dependent recruitment of BAK1 and possibly BKK1 and SERK2 into the EFR complex in Arabidopsis.

**Table 3-1 Identification of SERK tryptic peptides by MS analysis of elf18-treated EFR immunoprecipitates**

Peptide sequence	<i>n</i> peptide	Occurrence <sup>a</sup>	Best Mascot score	SERK					Domain <sup>d</sup>
				1	2	3 <sup>b</sup>	4 <sup>c</sup>	5	
NmEGDALHSLR	1	1/3	37.8		+				N-ter
<b>NAEGDALSALK</b>	8	3/3	71.7			+			N-ter
ERPESQPPLDWPKR	2	1/3	51.3			+			N-ter
NAEGDALTQLK	2	1/3	68.5				+		N-ter
KPQDHFFDVPAEEDPEVHLGQLK	1	1/3	35.7		+	+			iJM
<b>ELLVATDNFSNK</b>	4	3/3	57.3				+		iJM
<b>ELQVATDSFSNK</b>	4	3/3	84.8		+				iJM
LmDYKDTHVTTAVR	11	2/3	74.7	+	+	+			Kinase
LRGFcmTPTER	1	1/3	23.6	+	+	+	+	+	Kinase
ERPPSQLPLAWSIR	1	1/3	55.3		+				Kinase
DGTLVAVKR	1	1/3	58.2	+	+	+			Kinase
LANDDDiMLLDWVK	1	1/3	60.9				+	+	Kinase
ERPEGNPALDWPK	1	1/3	70.7				+	+	Kinase
LmNYNDSHVTTAVR	2	1/3	51.5				+	+	Kinase
GRLADGTLVAVKR	2	2/3	54.3	+	+	+			Kinase
LaNDDDVmMLDWVK	2	1/3	71.0	+	+	+	+	+	Kinase
LLVYPYmANGSVAScLR	2	1/3	87.8	+	+	+	+	+	Kinase
MSEVVR	3	1/3	24.7	+	+	+	+	+	Kinase
LADGTLVAVKR	4	2/3	55.8	+	+	+			Kinase
LADGTLVAVK	4	1/3	96.6	+	+	+			Kinase
ERPESQPPLDWPK	7	2/3	61.5			+			Kinase
LADGnLVAVKR	7	2/3	83.9				+	+	Kinase
<b>LADGnLVAVK</b>	10	3/3	72.6				+	+	Kinase
GFcmTPTER	11	2/3	48.0	+	+	+	+	+	Kinase
GTIGHIAPEYLSTGK	13	2/3	84.9	+	+	+	+	+	Kinase
GTIGHIAPEYLSTGK	13	2/3	84.9	+	+	+	+	+	Kinase
<b>ELQVASDNFSNK</b>	28	3/3	78.9			+			Kinase
KLESJVDAELEGK	1	1/3	90.1				+	+	C-ter
mLEGDGLaER	8	2/3	57.2		+	+	+		C-ter

<sup>a</sup>Reproducibility of specific tryptic peptides out of 3 independent biological replicates <sup>b</sup>BAK1 <sup>c</sup> BKK1 <sup>d</sup> N-ter: N-terminal region; iJM: intra-cellular juxta-membrane region; kinase: kinase domain; C-ter: C-terminal extension. Peptides occurring in all 3 replicates are marked in bold. n: number of peptides

### 3.2.2 EFR interacts with BAK1 in Arabidopsis

To confirm the EFR-BAK1 heterodimerization, I used functional transgenic Arabidopsis *efr-1/EFR-eGFP-HA* plants (Nekrasov *et al.*, 2009) in co-immunoprecipitation experiments. BAK1 was detected using recently developed anti-BAK1 peptide antibodies (Schulze *et al.*, 2010). While no BAK1 could be detected in the anti-GFP immunoprecipitate derived from the untreated transgenic EFR-eGFP-HA samples, a strong band was seen following 5 min elicitation with elf18 ([Figure 3.1A](#)). These results suggest a ligand-dependent complex formation between EFR and BAK1 in Arabidopsis.

Although specifically targeted against BAK1, the anti-BAK1 antibodies could potentially cross-react with BKK1 and SERK5 (Schulze *et al.*, 2010). The specificity of the antibodies was further studied by immunoblotting total proteins extracted from wild-type Col-0 or null mutant *bak1-4* seedlings. A specific band around the expected size of 75 kDa was detected in the Col-0 extract that was only faintly detectable in the *bak1-4* total protein extract ([Figure 3.1B](#)). This band was even stronger if anti-BAK1 immunoprecipitation was carried out prior to immunoblotting protein extracts from Col-0 and *bak1-4* ([Figure 3.1B](#)). This suggests that the antibody likely cross-reacts weakly with BKK1 and potentially other SERKs in Arabidopsis seedling total extracts and IPs.

To address the specificity of the EFR-SERK interactions, I took advantage of epitope-tagged constructs of FLS2, EFR or BAK1 for transient expression in *N. benthamiana*. First, I verified that the previously reported flg22-dependent FLS2-BAK1 interaction (Heese *et al.*, 2007; Chinchilla *et al.*, 2009; Schulze *et al.*, 2010) could be recapitulated in *N. benthamiana*. After co-expression of GFP-epitope-tagged FLS2 (FLS2-GFP) and HA<sub>3</sub>-epitope-tagged BAK1 (BAK1-HA<sub>3</sub>), flg22 elicitation could induce an interaction between FLS2 and BAK1 within 5 minutes ([Figure 3.1C](#)). Consistent with the strict ligand-dependency of the FLS2-BAK1 association (Heese *et al.*, 2007; Chinchilla *et al.*, 2009; Schulze *et al.*, 2010) and the inactivity of the flg22 epitope derived from *Agrobacterium tumefaciens* (Felix *et al.*, 1999; Bauer *et al.*, 2001), the FLS2-BAK1 association was not detected in the absence of flg22 treatment ([Figure 3.1C](#)). In addition, the well-characterized interaction between BRI1 and BAK1 (Li *et al.*, 2002; Nam and Li, 2002) was

similarly confirmed using GFP-epitope-tagged BRI1 (BRI1-GFP) and BAK1-HA<sub>3</sub>, and was enhanced by three hours treatment with brassinolide (BL) (Figure 3.1D). Thus, *N. benthamiana* is a useful system to study biologically relevant complex formation between different ligand-binding RKs and BAK1.

When GFP-epitope-tagged EFR (EFR-GFP) and BAK1-HA<sub>3</sub> were co-expressed, BAK1 could be immunoprecipitated with EFR. This interaction was enhanced by the addition of elf18 (Figure 3.1E). The weak constitutive association observed between EFR and BAK1 after mock treatment (Figure 3.1E) may be due to a weak recognition of EF-Tu from *Agrobacterium tumefaciens* by the expressed EFR (Zipfel *et al.*, 2006). However, the EFR-BAK1 interaction could not be further induced by flg22 (Figure 3.1E) confirming that EFR needs to be activated by its ligand to heteromerize with BAK1. Together, these results demonstrate that EFR and BAK1 form a ligand-dependent complex *in planta*.

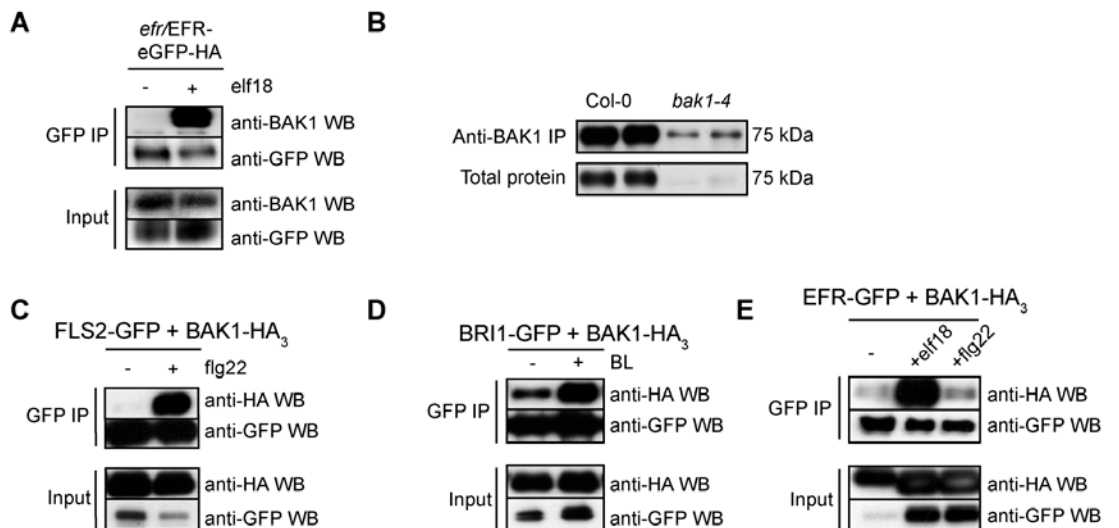


**Figure 3.1 EFR and BAK1 interact in a ligand-specific manner.**

A. Co-immunoprecipitation of EFR and BAK1. Transgenic *efr-1* Arabidopsis seedlings expressing EFR-eGFP-HA under the native promoter were treated (+) or not (-) with 100 nM elf18 for 5 minutes. Total proteins (input) were subjected to immunoprecipitation with GFP Trap beads followed by immunoblot analysis with anti-BAK1 antibodies to detect BAK1 and anti-GFP antibodies to detect EFR-eGFP-HA.

B. Protein extracts derived from 14-day-old Col-0 or *bak1-4* seedlings were separated by SDS-PAGE (10 %) and immunoblotted using anti-BAK1 peptide antibodies (1:500).

C. Co-immunoprecipitation of FLS2 and BAK1. *N. benthamiana* leaves expressing BAK1-HA<sub>3</sub> and FLS2-GFP were treated (+) or not (-) with 100 nM flg22 for 5 minutes. Total proteins (input) were subjected to immunoprecipitation with GFP Trap beads followed by immunoblot analysis with anti-HA antibodies to detect BAK1-HA<sub>3</sub> and anti-GFP antibodies to detect FLS2-GFP.

D. Co-immunoprecipitation of BRI1 and BAK1. *N. benthamiana* leaves expressing BAK1-HA<sub>3</sub> and BRI1-GFP were treated (+) or not (-) with 100 nM BL for 3 hours. Total proteins (input) were subjected to immunoprecipitation with GFP Trap beads followed by immunoblot analysis with anti-HA antibodies to detect BAK1-HA<sub>3</sub> and anti-GFP antibodies to detect BRI1-GFP.

E. Co-immunoprecipitation of EFR and BAK1. *N. benthamiana* leaves expressing BAK1-HA<sub>3</sub> and EFR-GFP were treated (+) or not (-) with 100 nM elf18 or flg22 for 5 minutes. Total proteins (input) were subjected to immunoprecipitation with GFP Trap beads followed by immunoblot analysis with anti-HA antibodies to detect BAK1-HA<sub>3</sub> and anti-GFP antibodies to detect EFR-GFP. These experiments were repeated three times with similar results.

### 3.2.3 Interactions between ligand-binding receptors and regulatory receptor kinases do not require active kinase

EFR, FLS2, BRI1 and BAK1 possess intracellular Ser/Thr kinase domains. Kinase activity of BAK1 is not required for the formation of the FLS2-BAK1 complex, as the general kinase inhibitor K-252a did not prevent complex formation in *Arabidopsis* cells (Schulze *et al.*, 2010).

To characterize the importance of kinase activity for the interaction between EFR, FLS2, BRI1 and their co-receptor BAK1, I used transient co-expression in *N. benthamiana* of wild-type and kinase-dead versions of EFR, FLS2 or BRI1 with kinase-dead or wild-type BAK1. Kinase-dead versions of the receptors were created by mutagenizing the conserved Asp (D) residue in the active site to Asn (N) [EFR D849N; FLS2 D997N; BRI1 D1009N; BAK1 D416N]. EFR-GFP-His was immunoprecipitated from tissue that had been treated with water (-) or 100 nM elf18 (+) for 5 minutes. Both wild-type and kinase-dead BAK1-HA<sub>3</sub> were detected in the IP of wild-type and kinase-dead EFR-GFP-His, with the interaction being induced by elf18 treatment ([Figure 3.2A](#)). Thus, the kinase activity of neither EFR nor BAK1 is required for their interaction. This is despite the requirement of EFR kinase activity for downstream signaling; kinase-inactive EFR does not confer elf18-responsive ROS burst in *N. benthamiana* ([Figure 3.2C](#)).

FLS2-BAK1 interactions followed a similar trend. When FLS2-GFP-His was pulled down in IPs, BAK1 was detected in all IPs following flg22 elicitation, whether or not the kinase of FLS2 or BAK1 was active ([Figure 3.2B](#)). Thus, no kinase-dependent change in interaction intensity was detectable in our system. In contrast, BRI1-BAK1 interactions are affected by their kinase activities (Wang *et al.*, 2008d).

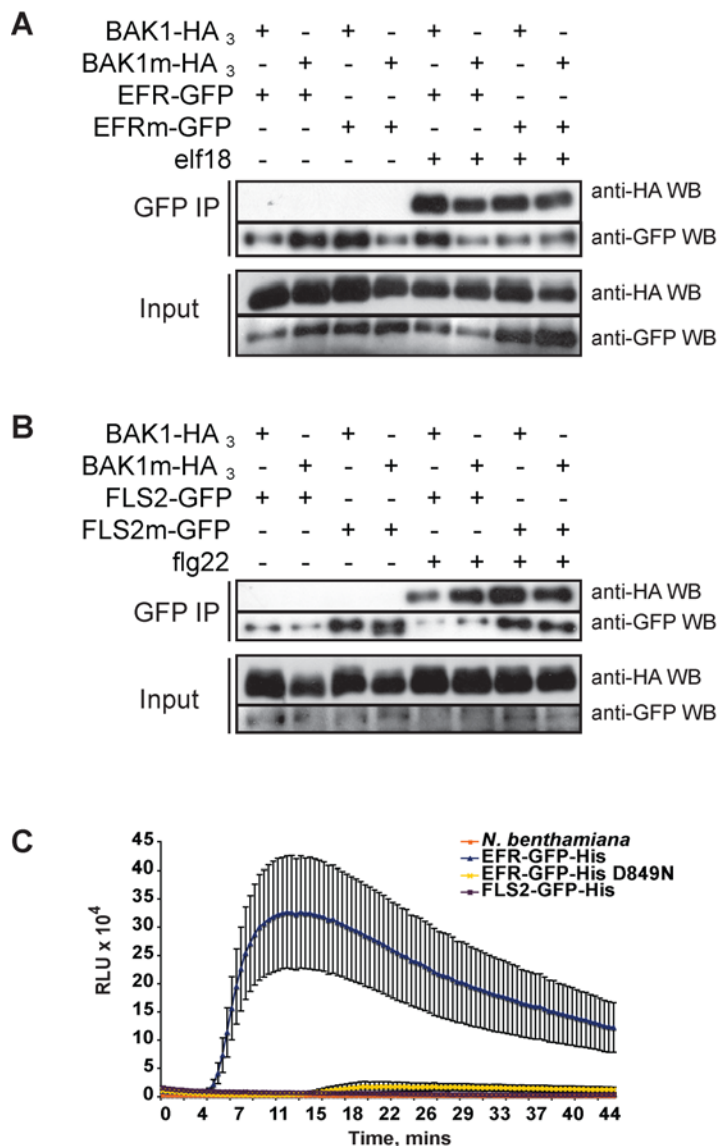


**Figure 3.2 Role of kinase activity for receptor heteromerization and signaling.**

A. Elf18-induced co-immunoprecipitation of EFR and BAK1 before (-) and after (+) 100nM elf18 elicitation in *N. benthamiana* transiently expressing EFR-GFP-His or EFRm-GFP-His (EFRm = D849N) and BAK1-HA<sub>3</sub> or BAK1m-HA<sub>3</sub> (BAK1m = D416N), as indicated. Total proteins were subjected to immunoprecipitation with anti-GFP beads followed by immunoblot analysis with anti-GFP or anti-HA antibodies as indicated.

B. Flg22-induced co-immunoprecipitation of FLS2 and BAK1 before (-) and after (+) 100nM flg22 elicitation in *N. benthamiana* transiently expressing FLS2-GFP-His or FLS2m-GFP-His (FLS2m = D997N) and BAK1-HA<sub>3</sub> or BAK1m-HA<sub>3</sub> (BAK1m = D416N), as indicated. Total proteins were subjected to immunoprecipitation with anti-GFP beads followed by immunoblot analysis with anti-GFP or anti-HA antibodies as indicated.

C. ROS burst in response to 100 nM elf18 elicitation of *N. benthamiana* wild-type (orange line), or transiently expressing EFR-GFP-His (blue line), kinase-dead EFR-GFP-His D849N (yellow line) or FLS2-GFP-His (purple line) 2 days post-agroinfiltration. RLU = relative light units. Results are average  $\pm$  standard error ( $n=8$ ).

These experiments were repeated twice.

### 3.2.4 EFR, FLS2 and BAK1 undergo trans-phosphorylation *in vitro*

EFR, FLS2, BRI1, Xa21 and BAK1 are active Ser/Thr kinases capable of auto-phosphorylation *in vitro* (Oh *et al.*, 2000; Friedrichsen *et al.*, 2000; Gómez-Gómez *et al.*, 2001; Li *et al.*, 2002; Xiang *et al.*, 2008; Lu *et al.*, 2010; Xu *et al.*, 2006a; Liu *et al.*, 2002). BRI1 and BAK1 belong to the class of RD kinases, while FLS2 and EFR are non-RD kinases, which generally exhibit weak auto-phosphorylation activity (Dardick and Ronald, 2006). Indeed, in this work we were unable to detect any kinase activity for FLS2, and this is corroborated by a recent study (Zhang *et al.*, 2010a).

We investigated whether BAK1 and EFR cytoplasmic domains are capable of trans-phosphorylating each other by carrying out *in vitro* kinase assays. We first confirmed the *in vitro* EFR kinase activity under our conditions. The cytoplasmic domain of EFR consisting of the intracellular juxtamembrane and kinase domains (amino acids 682-1031) was expressed in *E. coli* as an MBP fusion protein (MBP-EFR-CD) and purified using amylose resin. When MBP-EFR-CD was incubated with radioactive [<sup>32</sup>P]-γ-ATP *in vitro*, strong phosphorylation of the kinase domain was detected ([Figure 3.3](#)). This activity was abolished in a MBP-epitope-tagged mutant version of the kinase domain where the conserved Asp residue in the active site was mutagenized to Asn (D849N) (MBP-EFRm-CD) ([Figure 3.3](#)), demonstrating that the previously observed phosphorylation is due to auto-phosphorylation of MBP-EFR-CD. The cytoplasmic domain of BAK1 (amino acids 256-615) was expressed as a GST-fusion protein (GST-BAK1-CD) and purified using glutathione beads. In agreement with previously published results (Li *et al.*, 2002; Wang *et al.*, 2008d; Nam and Li, 2002; Wang *et al.*, 2005b), we detected a strong auto-phosphorylation of GST-BAK1-CD when incubated with radioactive [<sup>32</sup>P]-γ-ATP *in vitro* ([Figure 3.3](#)). A kinase-dead mutant of GST-BAK1-CD (GST-BAK1m-CD; D416N) had no auto-phosphorylation activity ([Figure 3.3](#)). No increase of the phosphorylation of EFR-CD or BAK1-CD could be observed when co-incubated, most likely due to their already strong auto-phosphorylation activities ([Figure 3.3](#)).

To test if EFR-CD is capable of trans-phosphorylating BAK1-CD *in vitro*, we co-incubated MBP-EFR-CD with the kinase-inactive GST-BAK1m-CD. Almost no trans-phosphorylation of GST-BAK1m-CD by MBP-EFR-CD could be observed

([Figure 3.3](#)), indicating that EFR is not capable of phosphorylating BAK1 *in vitro*. It is possible that EFR kinase activity needs to be activated by ligand before EFR is capable of transphosphorylating BAK1, and this can only be investigated *in vivo*. Preliminary experiments to pull down ligand-activated EFR from plant tissue followed by *in vitro* incubation with BAK1 kinase domain were unsuccessful. Interestingly, the presence of GST-BAK1m-CD reduced the auto-phosphorylation activity of MBP-EFR-CD ([Figure 3.3](#)), suggesting that a kinase-inactive BAK1 has a dominant-negative effect on the EFR intrinsic kinase activity.

To then test if BAK1-CD is capable of trans-phosphorylating EFR-CD *in vitro*, we co-incubated GST-BAK1-CD with the kinase-inactive MBP-EFRm-CD. A strong trans-phosphorylation of MBP-EFRm-CD could be observed. The presence of MBP-EFRm-CD has no inhibitory effect on the auto-phosphorylation activity of GST-BAK1-CD ([Figure 3.3](#)). Our results demonstrate that EFR and BAK1 are active kinases and that BAK1 trans-phosphorylates EFR *in vitro*.

FLS2 kinase domains were similarly purified and the proteins were stable however no kinase activity could be detected for FLS2 in similar experiments (data not shown). This is in agreement with Zhang *et al.*, who also could not detect significant kinase activity for FLS2 *in vitro* (Zhang *et al.*, 2010a). It is conceivable that FLS2 does possess kinase activity, but it is below the detection limit of these *in vitro* assays.

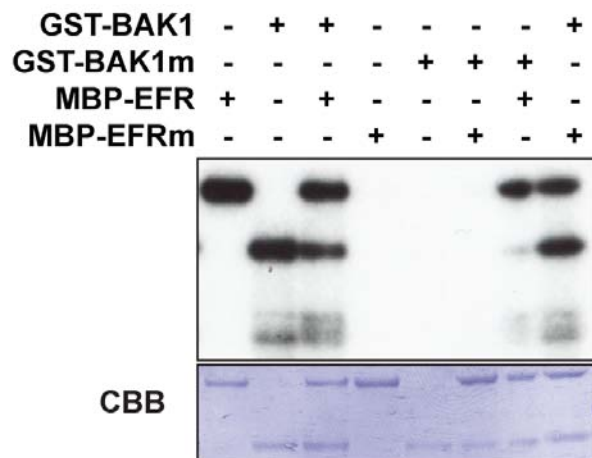


**Figure 3.3: BAK1 transphosphorylates EFR *in vitro*.**

EFR and BAK1 auto- and transphosphorylation *in vitro*. Incubation of equal protein amounts (3 ug) of active and inactive (mBAK1 = D416N and mEFR = D849N) recombinant BAK1 and EFR cytoplasmic domains with [ $\gamma$ -<sup>32</sup>P]ATP shows that GST-BAK1-CD and MBP-EFR-CD can

autophosphorylate and GST-BAK1-CD transphosphorylates MBP-EFR-CD. Coomassie brilliant blue staining (bottom panel) shows protein loading for the autoradiogram (top panel).

### 3.2.5 EFR, FLS2 and BRI1 have differential specificity for SERKs in *N. benthamiana*.

To confirm the interaction between the different SERKs and EFR, I transiently co-expressed individual HA<sub>3</sub>-epitope-tagged SERKs together with EFR-GFP in *N. benthamiana*. Equal amounts of EFR were pulled-down using GFP Trap beads and probed for the presence of SERK-HA<sub>3</sub> using anti-HA immunoblotting. While some SERKs could be sometimes weakly detected in mock-treated samples, elf18 treatment significantly increased the amount of SERK1, SERK2, BAK1 and BKK1 detectable in the EFR immunoprecipitate ([Figure 3.4A](#)). However, no elf18-dependent increase in the amount of SERK5 present in the EFR immunoprecipitate could be observed ([Figure 3.4A](#)). These results suggest that EFR is capable of mounting a ligand-dependent complex with SERK1, SERK2, BAK1 and BKK1 in *N. benthamiana* ([Figure 3.4A](#)).

FLS2 has previously only been reported to heteromerize with BAK1 (Chinchilla *et al.*, 2007; Heese *et al.*, 2007). To test if FLS2 is also capable of interacting with additional SERKs, I transiently co-expressed individual HA<sub>3</sub>-epitope-tagged SERKs together with FLS2-GFP in *N. benthamiana*. Equal amounts of FLS2-GFP-His protein could be immunoprecipitated using GFP Trap beads ([Figure 3.4B](#)). As observed with EFR, all SERKs were weakly detectable in FLS2 immunoprecipitates even in the absence of elicitation ([Figure 3.4B](#)). However, the association between FLS2 and SERK1, SERK2, BAK1 and BKK1 could be enhanced by 5 min of flg22 treatment ([Figure 3.4B](#)). Interestingly, EFR seemed to equally strongly heteromerize with SERK1, SERK2, BAK1 and BKK1 after elf18 treatment. However, FLS2 showed a clear preferential heteromerization with BAK1 ([Figure 3.4B](#)). A less marked flg22-dependent increase in the FLS2 association with SERK1, SERK2 and BKK1 could be detected ([Figure 3.4B](#)). Furthermore, the weak heteromerization with SERK5 could not be enhanced by either ligand treatment ([Figure 3.4A-B](#)).

To compare the affinity of PRRs EFR and FLS2 for the different SERKs with that of BRI1, I transiently co-expressed individual HA<sub>3</sub>-epitope-tagged SERKs together with BRI1-GFP in *N. benthamiana*. Equal amounts of BRI1-GFP-His

protein could be immunoprecipitated using GFP Trap beads (Figure 3.4C). As observed with EFR and FLS2, all SERKs were weakly detectable in BRI1 immunoprecipitates even in the absence of elicitation (Figure 3.4C). However, the association between BRI1 and SERK1, BAK1 and BKK1 could be enhanced by three hours of BL treatment (Figure 3.4C). These data suggest that BRI1 is capable of interacting with SERKs even without addition of exogenous ligand, although there is likely endogenous BL in the leaves. In order to study the ligand-induced interaction properties of BRI1 with the SERKs, pre-treatment with a BR synthesis inhibitor brassinazole (BRZ) is required. Interestingly, these results show that BAK1 is the preferred interactor of FLS2, while EFR shows less selectivity for a particular protein among these SERKs.

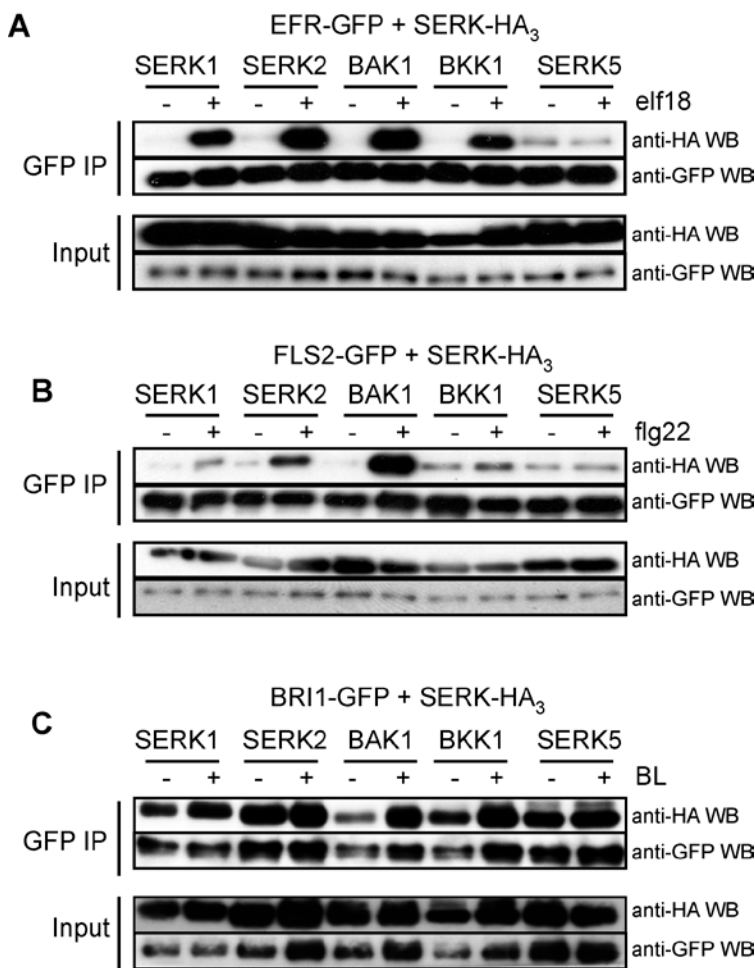


**Figure 3.4 EFR, FLS2 and BRI1 have different specificity for the SERK proteins in *N. benthamiana*.**

A. Co-immunoprecipitation of EFR and SERK proteins. *N. benthamiana* leaves expressing SERK-HA<sub>3</sub> constructs and EFR-GFP were treated (+) or not (-) with 100 nM elf18 for 5 minutes. Total proteins (input) were subjected to immunoprecipitation with GFP Trap beads followed by immunoblot analysis with anti-HA antibodies to detect SERK-HA<sub>3</sub> and anti-GFP antibodies to detect EFR-GFP.

B. Co-immunoprecipitation of FLS2 and SERK proteins. *N. benthamiana* leaves expressing SERK-HA<sub>3</sub> constructs and FLS2-GFP were treated (+) or not (-) with 100 nM flg22 for 5 minutes. Total proteins (input) were subjected to immunoprecipitation with GFP Trap beads followed by immunoblot analysis with anti-HA antibodies to detect SERK-HA<sub>3</sub> and anti-GFP antibodies to detect FLS2-GFP.

C. Co-immunoprecipitation of BRI1 and SERK proteins. *N. benthamiana* leaves expressing SERK-HA<sub>3</sub> constructs and BRI1-GFP were treated (+) or not (-) with 100 nM BL for 3 hours. Total proteins (input) were subjected to immunoprecipitation with GFP Trap beads followed by immunoblot analysis with anti-HA antibodies to detect SERK-HA<sub>3</sub> and anti-GFP antibodies to detect BRI1-GFP.

*N. benthamiana* leaves expressing SERK-HA<sub>3</sub> constructs and BRI1-GFP were treated (+) or not (-) with 100 nM BL for 3 hours. Total proteins (input) were subjected to immunoprecipitation with GFP Trap beads followed by immunoblot analysis with anti-HA antibodies to detect SERK-HA<sub>3</sub> and anti-GFP antibodies to detect BRI1-GFP.

These experiments were repeated twice with similar results.

### 3.2.6 BAK1 and BKK1 are required for EFR-, FLS2- and PEPR1/2-dependent responses

#### 3.2.6.1 *bak1-3 serk4-2* has reduced PTI signaling responses

The biochemical analyses revealed that SERK1, SERK2, BAK1 and BKK1 can form a ligand-dependent complex(es) with EFR and FLS2 *in vivo* (Figures 3.1 and 3.4, Table 2.1; Table 3.1). I then sought to genetically test the biological relevance of these SERKs for EFR- and FLS2-dependent signaling. In agreement with previous reports (Chinchilla *et al.*, 2009; Heese *et al.*, 2007), I found that, with the exception of *bak1* mutants, individual *serk* null mutants were not significantly impaired in flg22 and elf18 responses as measured by the production of a ROS burst and seedling growth inhibition (Figure 3.5). The absence of observable phenotypes in single *serk* mutants could be due to functional redundancy between the related SERK proteins (Albrecht *et al.*, 2008).

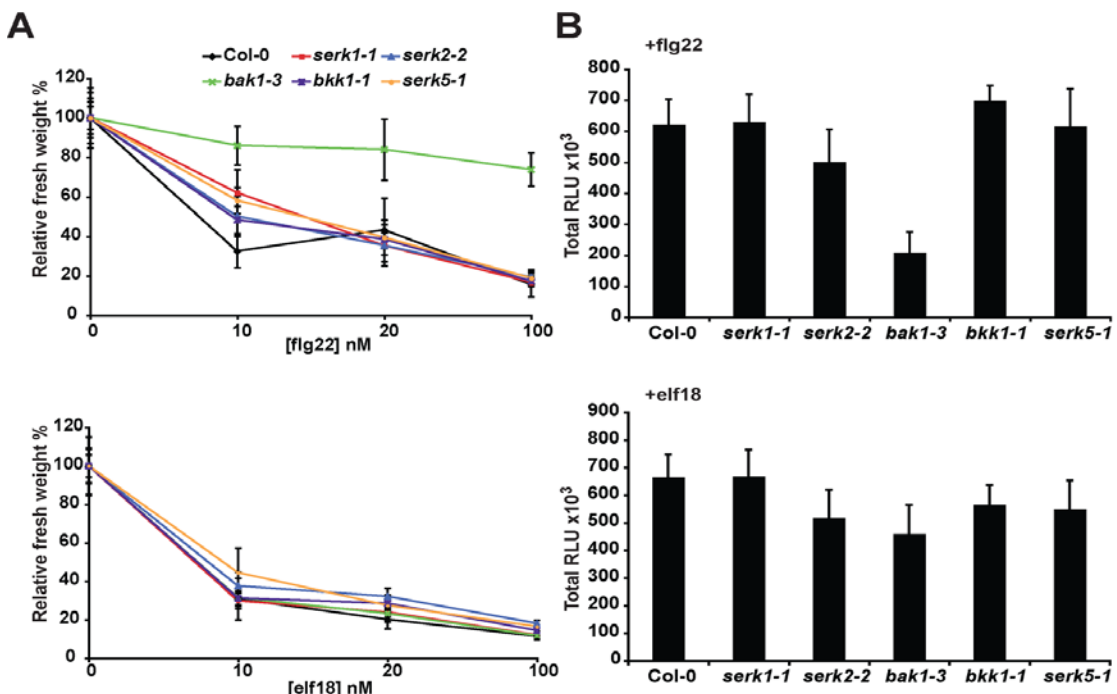


**Figure 3.5 PAMP-induced ROS burst and seedling growth inhibition of single *serk* mutants.**  
A. Seedling growth inhibition in response to increasing concentrations of elf18 or flg22 in Col-0, serk1-1, serk2-2, bak1-3, bkk1-1 and serk5-1 seedlings. Represented as % fresh weight of untreated seedlings. Results are average  $\pm$  standard error ( $n=6$ ).  
B. Total ROS production represented as relative light units (RLU) in Col-0, serk1-1, serk2-2, bak1-3, bkk1-1 and serk5-1 plants after elicitation with 100nM flg22 or elf18. Results are average  $\pm$  standard error ( $n=8$ ).  
All experiments were repeated at least three times with similar results.

To test if SERK1 and SERK2 cooperate with BAK1 to regulate EFR- and FLS2-dependent signaling, I obtained double mutants between the null mutant *bak1-4* (Chinchilla *et al.*, 2007) and the null mutants *serk1-3* (Albrecht *et al.*, 2008) and *serk2-2* (Albrecht *et al.*, 2005) and tested their responsiveness to flg22 and elf18. The double mutants *serk1-3 bak1-4* and *serk2-2 bak1-4* were not further impaired than the *bak1-4* single mutants in the ROS burst produced by flg22 and elf18 (Figure 3.6), suggesting that SERK1 and SERK2 do not play a role in FLS2- and EFR-dependent signaling.

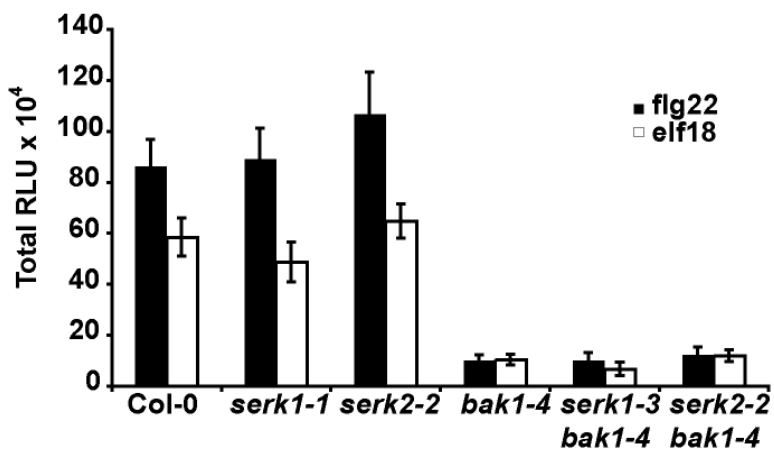


**Figure 3.6 SERK1 and SERK2 are not required for flg22 and elf18 responses in *Arabidopsis*.** Total ROS production of 4-week-old Col-0, *bak1-4*, *serk1-1*, *serk2-2*, *serk1-3* *bak1-4* and *bak1-4* *serk2-2* after elicitation with 100 nM flg22 or elf18. Results are average  $\pm$  standard error ( $n=8$ ). These experiments were repeated four times with similar results.

The seedling lethality of the *bak1-4 bkk1-1* double mutant due to uncontrolled cell death (He *et al.*, 2007) prevented testing whether BKK1 could play a role in elf18 and flg22 responses by acting redundantly to BAK1.

To try to overcome this obstacle, I obtained the double mutant of two weak alleles *bak1-3 serk4-2* (Figure 3.7A), which is not seedling lethal but maintains a developmental phenotype including severely reduced rosette size, early senescence and late flowering (data not shown). *Bak1-3* has reduced flg22 responses, but is more responsive than *bak1-4*, and it thus considered a weak allele although the *BAK1* transcript is not detectable in this mutant by RT-PCR or Northern blot analysis (Chinchilla *et al.*, 2007). The *BKK1* transcript was not detectable in this double mutant when tested by RT-PCR (data not shown). Despite the growth phenotype of this double mutant, it was possible to measure

ROS burst by testing whole seedlings as opposed to leaf discs (Boutrot *et al.*, 2010). Using this method, it was possible to detect a reduced ROS burst in response to elf18 elicitation of the *bak1-3 serk4-2* double mutant when compared to the Col-0 wild-type ([Figure 3.7B](#) and C, left panel). In *bak1-3* there was no detectable reduction in ROS burst, but there was a delay, which was maintained in the double mutant ([Figure 3.7A](#) and B, left panel). The *serk4-2* mutation appears not to affect ROS burst in response to elf18 ([Figure 3.7B](#) and C, left panel). In response to flg22, ROS burst was delayed and reduced to a similar extent in *bak1-3* and *bak1-3 serk4-2* ([Figure 3.7B](#) and C, right panel). The ROS burst in *serk4-2* was higher compared to Col-0 in this experiment, but this was not reproducible, and was often of a similar intensity to Col-0 ([Figure 3.7B](#) and C, right panel). This is in agreement with previous work (Chinchilla *et al.*, 2007), which has indicated that *bak1* null mutants are more compromised in early signaling outputs in response to flg22 than to elf18. Using this weak allele double mutant combination we were able to detect an additive effect of the BAK1 and BKK1 mutations on the elf18-induced ROS phenotype.

In order to further characterize these mutants I studied the temporal changes in the expression of the PAMP-induced gene *At2g17740* (He *et al.*, 2006) in response to elf18 and flg22 elicitation. The expression of *At2g17740* is induced 10-fold after 3 hours of elf18 elicitation in Col-0 seedlings ([Figure 3.7D](#), left panel). In *bak1-3* mutants, this induction is maintained ([Figure 3.7D](#), left panel), as expected from previous work, which has shown reduced early but not late responses of *bak1-3* mutants to elf18 induction (Chinchilla *et al.*, 2007). However, *serk4-2* and *bak1-3 serk4-2* also did not show any reduction in elf18-induced *At2g17740* expression ([Figure 3.7D](#), left panel). In response to three hours of flg22 treatment, *At2g17740* expression is almost 20-fold induced in Col-0 and *serk4-2* ([Figure 3.7D](#), right panel). *Bak1-3* mutants display a 50 % reduction in gene expression, reaching approximately 10-fold over the same period ([Figure 3.7D](#), right panel). Surprisingly, *bak1-3 serk4-2* seedlings achieved a greater induction of *At2g17740* expression, almost reaching Col-0 levels ([Figure 3.7C](#), right panel). This could be due to the likely residual cell death and premature senescence in these double mutants (Jeong *et al.*, 2010), as *At2g17740* expression is upregulated in senescent leaves (eFP browser; [bar.utoronto.ca/](http://bar.utoronto.ca/)).

Col-0 seedling growth is inhibited by 50 – 80 % in response to *elf18* and *flg22* incubation, with *bak1-3* and *serk4-2* being similarly affected ([Figure 3.7E](#)). Counter-intuitively, *bak1-3 serk4-2* mutant seedling growth inhibition is more intense, with high concentrations of *elf18* reducing growth to 10 % of untreated seedlings ([Figure 3.7E](#), left panel). This is in contrast to their reduced *elf18*-responsiveness in the ROS assay (Figure 3.7B and C), and may be a pleiotropic effect of the weak cell death phenotype of these mutants. A similar case is seen in response to *flg22*, with *bak1-3* mutants behaving as Col-0 in response to *flg22*, and the double mutant exhibiting enhanced PAMP sensitivity in this assay ([Figure 3.7E](#)).

Together, these results suggest that both BAK1 and BKK1 are required for early but not late *elf18* responses, while only BAK1 is required for both early and late *flg22*-induced responses.

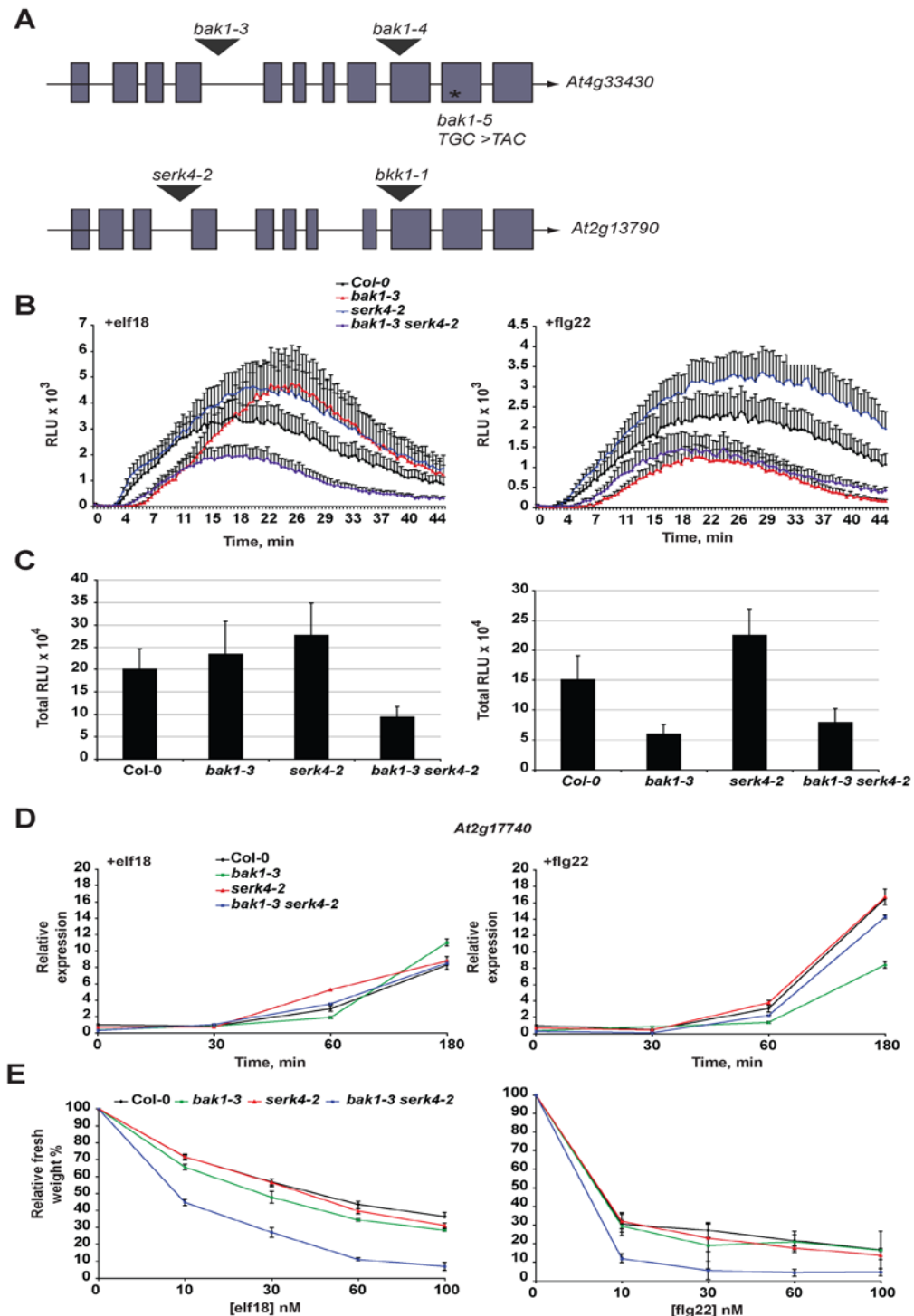


**Figure 3.7 BAK1 and BKK1 are required for flg22 and elf18 responses in Arabidopsis**

A. Schematic representation of *BAK1* and *BKK1* genes and location of T-DNA and *bak1-5*.

B and C. ROS production over time (B) and total ROS production (C) represented as relative light units (RLU) in Col-0, *bak1-3*, *serk4-2* and *bak1-3 serk4-2* seedlings after elicitation with 100 nM elf18 or flg22. Results in B and C are average  $\pm$  standard error ( $n=8$ ).

D. Defense gene induction in response to 100 nM elf18 or flg22 in Col-0, *bak1-3*, *serk4-2* and *bak1-3 serk4-2* seedlings. Gene expression of *At2g17740* was measured by qPCR analysis, normalized to *UBQ10* (housekeeping) expression and plotted relative to Col-0 0 min expression level. Results are average  $\pm$  standard error ( $n=3$ ).

E. Seedling growth inhibition triggered by elf18 or flg22 in Col-0, *bak1-3*, *serk4-2* and *bak1-3 serk4-2* seedlings. Represented as % fresh weight of untreated seedlings. Results are average  $\pm$  standard error ( $n=6$ ).

### 3.2.6.2 *bak1-5 bkk1-1* has reduced PTI signaling responses

In order to study the function of BAK1 and BKK1 in PAMP-induced signaling in the absence of pleiotropic effects such as cell death and early senescence, I took advantage of the newly characterized *bak1-5* allele identified in a forward-genetic screen for *elf18-insensitive* (*elfin*) mutants (Schwessinger *et al.*, *submitted*; Nekrasov *et al.*, 2009). *Bak1-5* harbors a point mutation in the kinase domain of BAK1 ([Figure 3.7](#)), and is more severely impaired in *elf18* and *flg22* responses than the null *bak1-4* mutant (Schwessinger *et al.*, *submitted*; [Figure 3.8](#)). Moreover, *bak1-5* is not impaired in BL responses and does not display uncontrolled cell death when combined with the null *bkk1-1* allele (Schwessinger *et al.*, *submitted*). I thus used the double-mutant *bak1-5 bkk1-1* to study the combined role of BAK1 and BKK1 in EFR- and FLS2-dependent signaling.

The *bak1-5* mutant showed strikingly reduced responses to both *flg22* and *elf18* in all assays conducted. Leaf discs from wild-type Col-0 *Arabidopsis* plants produced a ROS burst upon *flg22* or *elf18* addition, which was significantly reduced in *bak1-5* ([Figure 3.8A](#)). In contrast, *bkk1-1* exhibited a ROS burst comparable to wild-type leaf discs in response to both PAMPs ([Figure 3.8A](#)). Remarkably, leaf discs from *bak1-5 bkk1-1* plants displayed a negligible ROS burst in response to *flg22* or *elf18* ([Figure 3.8A](#)).

I then tested if the combination of the *bak1-5* and *bkk1-1* mutations would similarly impact other responses triggered by *flg22* and *elf18*, which show a different temporal behavior. This was particularly relevant since the null mutant *bak1-4* was reported to be impaired in both early and late responses to *flg22*, but was not impaired in late responses (e.g. seedling growth inhibition) triggered by *elf18* (Chinchilla *et al.*, 2007). The *Arabidopsis* MAP kinases (MPK) MPK3, MPK4 and MPK6 are activated within 5 minutes of *flg22* and *elf18* treatment (Zipfel *et al.*, 2006); [Figure 3.8B](#)). MPK3/6 activation was reduced and delayed in *bak1-5* seedlings in comparison to wild-type and *bkk1-1*, and was almost undetectable in *bak1-5 bkk1-1* seedlings in response to *flg22* and *elf18* over the time course assayed ([Figure 3.8B](#)). Furthermore, MPK4 activation was abolished in *bak1-5* and *bak1-5 bkk1-1* ([Figure 3.8](#)), suggesting that MPK4 activation relies on BAK1.

The expression of over a thousand genes is altered within 30 minutes of *flg22* or *elf18* treatment (Zipfel *et al.*, 2004; Zipfel *et al.*, 2006). The *bak1-4*

mutation had only a minor effect on the expression of PAMP-induced marker genes *At1g51890* and *At2g17740* (He *et al.*, 2006) after flg22 or elf18 treatment, but reduced the expression of *At5g57220* after 3 hours of flg22 treatment ([Figure 3.8C](#)). In agreement with the previously observed weaker effect of the *bak1-4* mutation on elf18 responses (Chinchilla *et al.*, 2007); [Figure 3.8A](#)), the expression of these genes was not significantly altered in this mutant after elf18 treatment ([Figure 3.8C](#)). However, the induction of the three genes was reduced in response to either PAMP in *bak1-5* in comparison to wild-type, *bkk1-1* or *bak1-4* ([Figure 3.8C](#)). Strikingly, the expression of these genes was only minimally induced after flg22 or elf18 treatment in *bak1-5 bkk1-1* ([Figure 3.8C](#)).

An increase in ethylene biosynthesis can be measured within 2 hours of treatment with flg22 or elf18 (Felix *et al.*, 1999; Kunze *et al.*, 2004). A clear flg22- or elf18-induced production of ethylene was measured in Col-0 and *bkk1-1* plants ([Figure 3.8D](#)). In contrast, this was significantly reduced in *bak1-5* leaves and only marginal ethylene production could be measured in *bak1-5 bkk1-1* in response to flg22 or elf18 ([Figure 3.8D](#)). Interestingly, the ROS burst and ethylene production triggered by flg22 and elf18 was sometimes higher in *bkk1-1* leaves than in Col-0 leaves, which may be explained by the weak constitutive cell death and early senescence of this mutant (He *et al.*, 2007; Jeong, *et al.*, 2010).

As shown in Figure 3.8E, seedling growth inhibition in *bkk1-1* was comparable to wild-type, while *bak1-4* seedlings were only impaired in the growth inhibition triggered by flg22, as previously reported (Chinchilla *et al.*, 2007). In comparison to *bak1-4*, *bak1-5* seedlings were further affected in the growth inhibition triggered by flg22, but more interestingly, were now also significantly affected in the growth inhibition triggered by elf18 ([Figure 3.8E](#)). Notably, the seedling growth inhibition triggered by elf18 was even further decreased in *bak1-5 bkk1-1* seedlings ([Figure 3.8E](#)). The combination of the *bak1-5* and *bkk1-1* mutations rendered these plants insensitive to long-term exposure to high concentration (1  $\mu$ M) of either PAMP ([Figure 3.8E](#)), a feature previously only associated to mutations affecting the receptors themselves (Gomez-Gomez and Boller, 2000; Zipfel *et al.*, 2006; Li *et al.*, 2009a; Saijo *et al.*, 2009).

In summary, I could show that loss of *BKK1* further decreased early and late responses of *bak1-5* to elf18 and flg22.

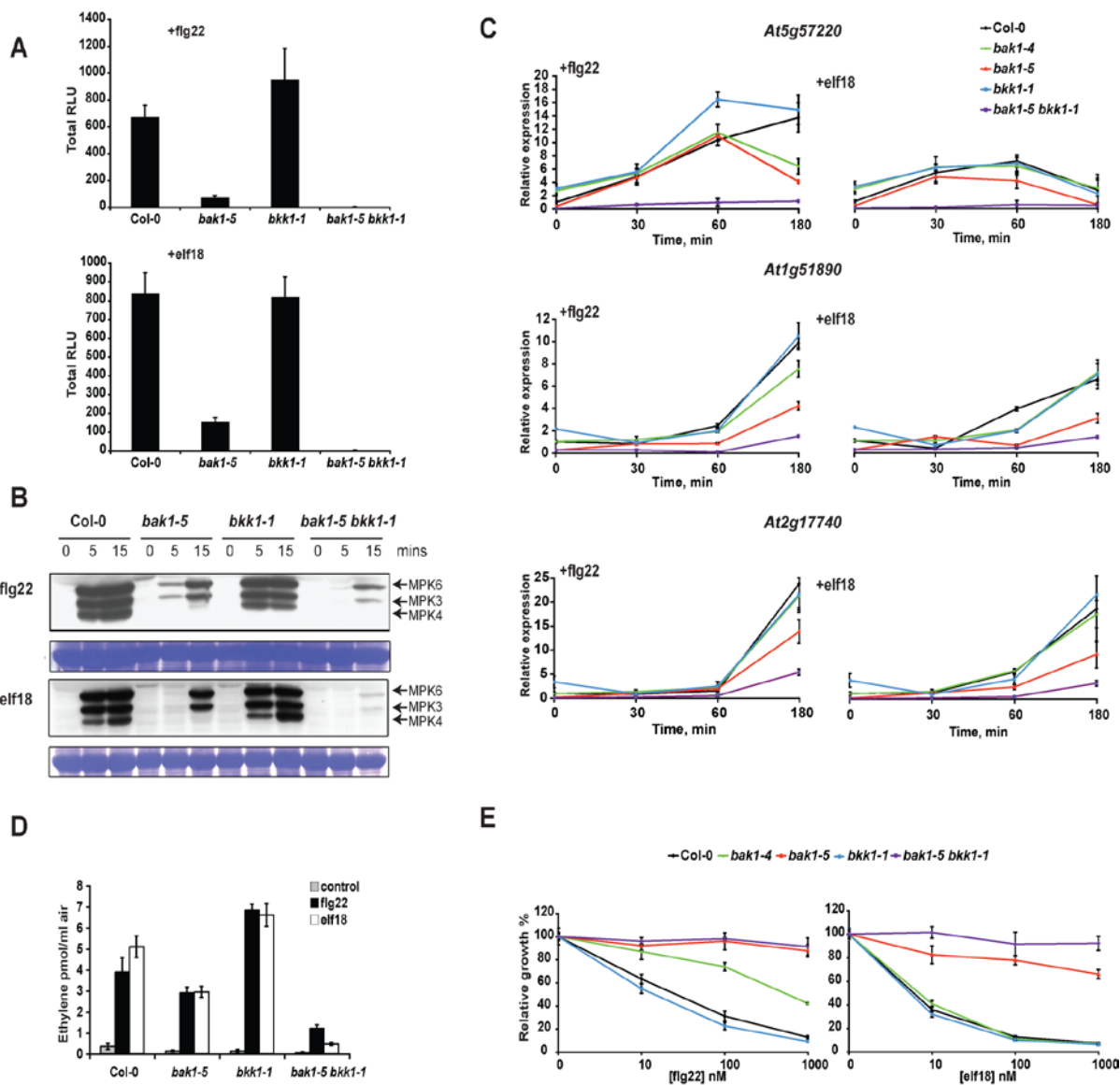


**Figure 3.8 BAK1 and BKK1 are required for flg22 and elf18 responses in *Arabidopsis***

(A) Total ROS production represented as relative light units (RLU) in Col-0, *bak1-5*, *bkk1-1* and *bak1-5 bkk1-1* leaf discs after elicitation with 100 nM flg22 (top) or elf18 (bottom). Results are average  $\pm$  standard error ( $n=8$ ).

(B) Kinetics of MAPK activation after elicitation with 100 nM flg22 or elf18 in Col-0, *bak1-5*, *bkk1-1* and *bak1-5 bkk1-1* seedlings as shown by immunoblot analysis using an anti-p44/42-ERK antibody; immunoblot, upper panel, Coomassie-stained membrane, lower panel. The identity of individual MAPKs as determined by size is indicated by arrows.

(C) Defense gene induction in response to 100 nM flg22 or elf18 of Col-0, *bak1-4*, *bak1-5*, *bkk1-1* and *bak1-5 bkk1-1* seedlings. Gene expression of *At2g17740*, *At5g57220* and *At1g51890* was measured by qPCR analysis, normalized to *UBQ10* (housekeeping) expression and plotted relative to Col-0 0 min expression level. Results are average  $\pm$  standard error ( $n=3$ ).

(D) Ethylene production in Col-0, *bak1-5*, *bkk1-1* and *bak1-5 bkk1-1* leaves after mock (grey bars), 100 nM flg22 (black bars), or elf18 (white bars) treatments. Results are average  $\pm$  standard error ( $n=6$ ).

(E) Seedling growth inhibition triggered by flg22 or elf18 in Col-0, *bak1-4*, *bak1-5*, *bkk1-1* and *bak1-5 bkk1-1* seedlings. Represented as % fresh weight of untreated seedlings. Results are average  $\pm$  standard error ( $n=6$ ).

All experiments were repeated at least twice with similar results.

Recently, BAK1 was identified as an interactor of the *AtPep1* receptors PEPR1 and PEPR2 (Krol *et al.*, 2010; Postel *et al.*, 2010). Thus I tested if BAK1 and BKK1 are also required for PEPR1/2-dependent signaling. I found that the *AtPep1*-induced ROS burst is attenuated in *bak1-4*, further decreased in *bak1-5*, and almost completely abolished in *bak1-5 bkk1-1* (Figure 3.9A). Ethylene production in response to *AtPep1* is also severely compromised in *bak1-5* and is further reduced in *bak1-5 bkk1-1* (Figure 3.9B). *Bkk1-1* plants were not affected in their responsiveness to *AtPep1* (Figure 3.9). This experiment revealed that loss of *BKK1* in a *bak1-5* background also leads to a strong reduction in the responsiveness to the DAMP *AtPep1*.

All together, these results clearly demonstrate that BKK1 cooperates with BAK1 to regulate EFR-, FLS2-, and PEPR1/2-dependent responses.

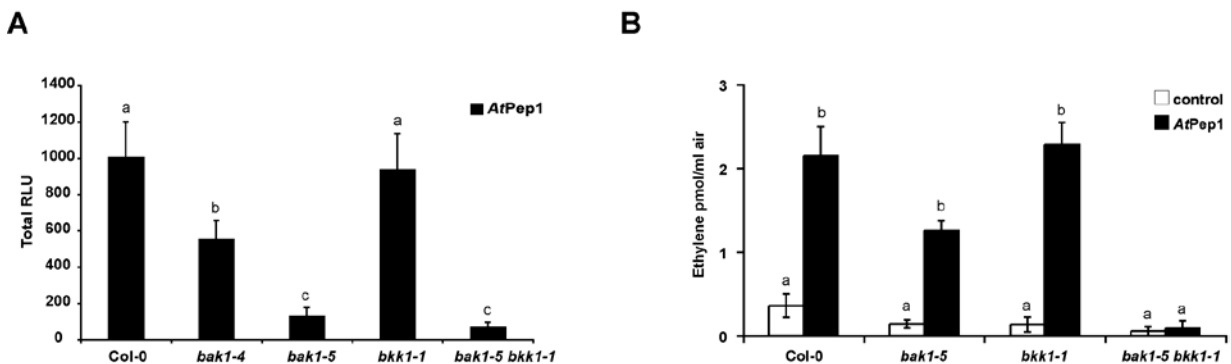


**Figure 3.9 BAK1 and BKK1 are required for *AtPep1* responses.**

A. Total ROS production represented as relative light units (RLU) in *Col-0*, *bak1-4*, *bak1-5*, *bkk1-1* and *bak1-5 bkk1-1* plants after elicitation with 100 nM *AtPep1*. Results are average  $\pm$  standard error ( $n=8$ ). All experiments were repeated at least three times with similar results.

B. Ethylene production in *Col-0*, *bak1-5*, *bkk1-1* and *bak1-5 bkk1-1* leaves after mock (white bars) or 100 nM *AtPep1* (black bars) treatments. Results are average  $\pm$  standard error ( $n=6$ ).

### 3.2.7 BAK1 and BKK1 are required for disease resistance

Next, I assessed whether BAK1 and BKK1 contribute to disease resistance. I first infected plants with the highly virulent hemibiotrophic bacterium *P. syringae* pv. *tomato* (*Pto*) DC3000. As reported previously (Nekrasov *et al.*, 2009), *efr-1 fls2* plants are hyper-susceptible to this strain upon spray-inoculation (Figure 3.10A). The *bak1-4* and *bkk1-1* mutants however exhibited wild-type susceptibility levels

([Figure 3.10A](#)). In contrast, leaves of *bak1-5* and *bak1-5 bkk1-1* allowed more growth of *Pto* DC3000, comparably to *efr-1 fls2* ([Figure 3.10A](#)).

PTI defects can be detected more sensitively with weakly virulent bacterial strains lacking effector molecules, such as AvrPto and AvrPtoB, or the phytotoxin coronatine, that are involved in PTI suppression (Melotto *et al.*, 2006; Xiang *et al.*, 2008; Göhre *et al.*, 2008; Shan *et al.*, 2008; Nekrasov *et al.*, 2009; Xiang *et al.*, 2010). As shown in Figure 3.10B, *efr-1 fls2* mutants were more susceptible to spray-inoculation with *Pto* DC3000  $\Delta$ AvrPto/ $\Delta$ AvrPtoB, while *bak1-4* plants were not. Interestingly, *bak1-5* and *bak1-5 bkk1-1* plants were hyper-susceptible to *Pto* DC3000  $\Delta$ AvrPto/ $\Delta$ AvrPtoB, whereas *bkk1-1* plants exhibited wild-type bacterial susceptibility ([Figure 3.10B](#)). Indeed, *Pto* DC3000  $\Delta$ AvrPto/ $\Delta$ AvrPtoB grew to similar levels in *bak1-5 bkk1-1* as the isogenic wild-type *Pto* DC3000 in Col-0 plants, showing that these mutations almost completely restored the virulence defect associated with the loss of AvrPto and AvrPtoB. A similar pattern was observed when infecting with the *Pto* DC3000 COR<sup>-</sup> strain. This strain already grew to higher numbers in *efr-1 fls2* when compared to Col-0, *bak1-4* or *bkk1-1* ([Figure 3.10C](#)). *Bak1-5* plants were similarly hyper-susceptible as *efr-1 fls2*, while this strain reproducibly colonized *bak1-5 bkk1-1* leaves to a greater extent than *bak1-5* mutant or *efr-1 fls2* ([Figure 3.10C](#)), again reaching levels comparable to those observed with isogenic wild-type *Pto* DC3000 in Col-0 leaves ([Figure 3.10A](#)). Thus, BAK1 and BKK1 both contribute to the basal resistance to *Pto* DC3000 COR<sup>-</sup>.

I then tested if BAK1 and BKK1 play a role in the non-host resistance against the non-adapted bacterium *P. syringae* pv. *tabaci* 6605 (*Pta* 6605), which partially depends on FLS2 (Li *et al.*, 2005) ([Figure 3.10D](#)). Growth in *bak1-4* and *bkk1-1* reached similar low levels as in wild-type Col-0, while the *efr-1 fls2* mutant was significantly more susceptible, supporting up to 2 logs more bacterial growth than Col-0 ([Figure 3.10D](#)). The *bak1-5* and *bak1-5 bkk1-1* mutants were as susceptible to this non-adapted strain as the *efr-1 fls2* double mutant ([Figure 3.10D](#)), suggesting that non-host resistance to *Pta* 6605 is compromised in the absence of functional BAK1 and BKK1.

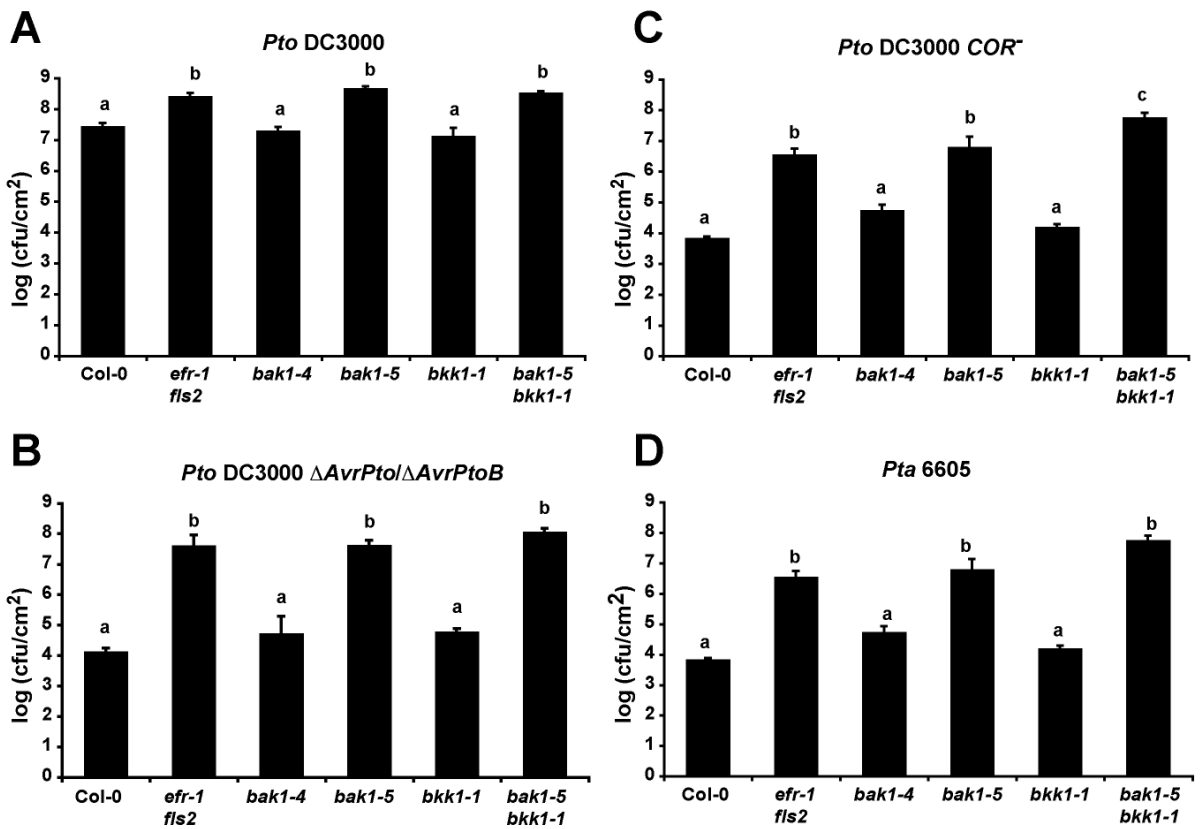


**Figure 3.10 BAK1 and BKK1 are required for resistance to adapted and non-adapted bacteria.**

A. Four-week-old plants (Col-0, *efr-1 fls2*, *bak1-4*, *bak1-5*, *bkk1-1* and *bak1-5 bkk1-1*) were spray-inoculated with *Pseudomonas syringae* pv. *tomato* (*Pto*) DC3000 ( $OD_{600}=0.02$ ).  
 B. Four-week-old plants (Col-0, *efr-1 fls2*, *bak1-4*, *bak1-5*, *bkk1-1* and *bak1-5 bkk1-1*) were spray-inoculated with *Pto DC3000 ΔAvrPto/ΔAvrPtoB* ( $OD_{600}=0.2$ ).  
 C. Four-week-old plants (Col-0, *efr-1 fls2*, *bak1-4*, *bak1-5*, *bkk1-1* and *bak1-5 bkk1-1*) were spray-inoculated with *Pto DC3000 COR<sup>-</sup>* ( $OD_{600}=0.2$ ).  
 D. Four-week-old plants (Col-0, *efr-1 fls2*, *bak1-4*, *bak1-5*, *bkk1-1* and *bak1-5 bkk1-1*) were syringe-inoculated with *P. syringae* pv. *tabaci* 6605 ( $OD_{600}=0.002$ ).  
 Bacterial counts were carried out at 3 days post-inoculation (3 dpi). Results are average  $\pm$  standard error ( $n=4$ ). “a”, “b” or “c” above the graph denotes statistically significant difference  $p<0.0001$  (ANOVA, Bonferroni post-test). All experiments were repeated at least three times with similar results.

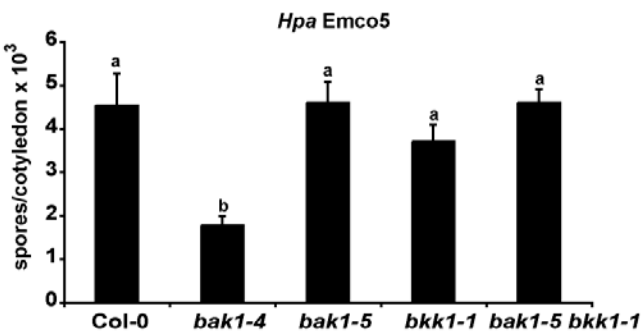
Next I was interested to assess the role of BAK1 and BKK1 in resistance to the obligate biotrophic oomycete pathogen *Hyaloperonospora arabidopsis* (*Hpa*). The *Hpa* infections were done by Nick Holton (Laboratory of M. Tör, HRI, Warwick UK). Infections were performed with the virulent isolate Emco5 that develops abundant sporangiophore and produces spores within 7 days after inoculation (dai) on *Arabidopsis* Col-0 seedlings (McDowell *et al.*, 2005) (Figure 3.11A). In comparison to Col-0, we observed a decreased sporulation on *bak1-4* seedlings (Figure 3.11A), probably due to their increased cell death phenotype upon

infection (Kemmerling *et al.*, 2007). In contrast, no decrease in the number of spores could be observed in *bak1-5*, *bkk1-1* or *bak1-5 bkk1-1* (Figure 3.11A). The absence of noticeable phenotype of *bak1-5 bkk1-1* seedlings could be due to the already high susceptibility of Col-0 to *Hpa* Emco5 that may mask a contribution of PTI.

Next, infections were done with *Hpa* isolates that are only moderately virulent on Col-0 seedlings. Sporulation of the *Hpa* isolate Cala2 on Col-0 seedlings is rare due to the resistance conferred by the R protein RPP2 (Holub *et al.*, 1994). Indeed, we observed only occasional conidiophore formation on Col-0 seedlings inoculated with *Hpa* Cala2 that never resulted in sporulation (Figure 3.11B). In contrast, *bak1-5* and *bkk1-1* seedlings appeared reproducibly more susceptible to this isolate, but only *bak1-5 bkk1-1* seedlings consistently showed statistically significant enhanced susceptibility to *Hpa* Cala2 (Figure 3.11B). Additionally, infection with another weakly virulent isolate, *Hpa* Emoy2, revealed a similar pattern, where resistance in Col-0 is provided by the R protein RPP4 (Holub, 2008). This was in stark contrast to *bak1-5 bkk1-1* seedlings, where statistically significantly increased number of conidiophores could be counted (Figure 3.11C). As observed with the highly virulent isolate Emco5, *bak1-4* seedlings were less susceptible to the *Hpa* isolates Cala2 and Emoy2 (Figure 3.11B-C), as expected due to their deregulated cell death upon infection.

Inoculation of *Arabidopsis* seedlings with crude extracts *Hpa* Emoy2 resulted in induction of the defense-related gene *At1g51890* within 3 hours (Figure 3.11D). This induction was negligible in mock-inoculated plants, suggesting that the gene induction is due to some property of the *Hpa* extracts, possibly PAMPs (Figure 3.11D). To determine whether the enhanced susceptibility of *bak1-5 bkk1-1* is due to compromised PTI signaling, I assessed this *Hpa* extract-induced gene induction in the mutant. The induction of *At1g51890* was reduced by half in *bkk1-1*, further decreased in *bak1-5* and absent in *bak1-5 bkk1-1* seedlings (Figure 3.11D). This hints that BAK1 and BKK1 are likely required for the full function of an as yet uncharacterized PRR(s) that recognize *Hpa* PAMP(s).

All together, these results reveal a role for BAK1 and BKK1 in PTI signaling and resistance to the obligate biotrophic oomycete *Hpa*.

**A**

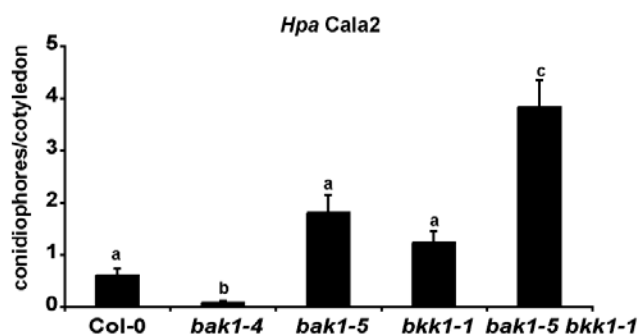
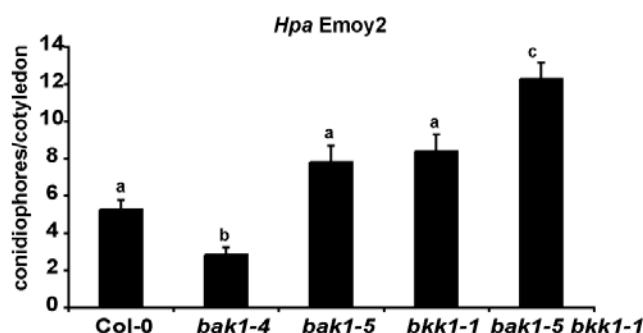
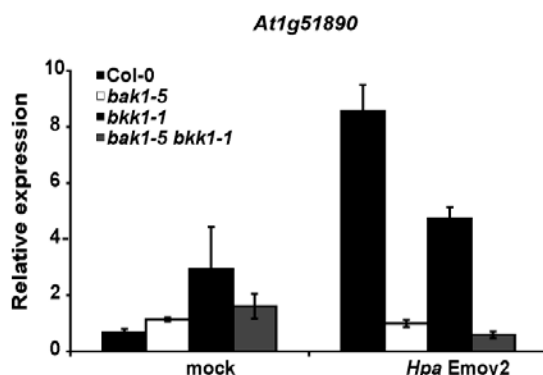
**Figure 3.11 BAK1 and BKK1 are required for resistance to the obligate biotrophic oomycete pathogen *Hyaloperonospora arabidopsisidis*.**

A. Infection of Col-0, *bak1-4*, *bak1-5*, *bkk1-1* and *bak1-5 bkk1-1* seedlings with *H. arabidopsisidis* Emco5. Spores were counted at 7 days post-inoculation (7 dpi). Results are average  $\pm$  standard error ( $n=12$ ).

B. Infection of Col-0, *bak1-4*, *bak1-5*, *bkk1-1* and *bak1-5 bkk1-1* seedlings with *H. arabidopsisidis* Cala2. Conidiophores were counted at 7 dpi. Results are average  $\pm$  standard error ( $n=40$ ).

C. Infection of Col-0, *bak1-4*, *bak1-5*, *bkk1-1* and *bak1-5 bkk1-1* seedlings with *H. arabidopsisidis* Emoy2. Conidiophores were counted at 7 dpi. Results are average  $\pm$  standard error ( $n=40$ ). “a”, “b” or “c” above the graph denotes statistically significant difference  $p < 0.0001$  (ANOVA, Bonferroni post-test). All experiments were repeated at least three times with similar results.

D. Defense gene induction of Col-0, *bak1-5*, *bkk1-1* and *bak1-5 bkk1-1* seedlings in response to 3 hours treatment with crude extracts of uninoculated (mock) or *Hpa Emoy2*-infected leaves. Gene expression of *At1g51890* was measured by qPCR analysis, normalized to *UBQ10* (housekeeping) expression and plotted relative to the expression level in Col-0 at the initial time-point. Results are average  $\pm$  standard error ( $n=3$ ).

**B****C****D**

### 3.3 Discussion

#### 3.3.1 The regulatory LRR-RLK BAK1 interacts *in planta* with several ligand-binding LRR-RKs, including EFR

Over the last few years, it has become evident that BAK1 is an adaptable protein with roles in diverse signaling processes (Chinchilla *et al.*, 2009). BAK1 was initially identified as an interactor of the LRR-RK BRI1 and positive regulator of BR responses (Nam and Li, 2002; Li *et al.*, 2002; Wang *et al.*, 2005b). However, it was recently shown that BAK1 also plays a BR-independent role as a positive regulator of PTI. BAK1 forms a rapid ligand-dependent complex with the PRR FLS2, and is required for full responsiveness to flg22 (Chinchilla *et al.*, 2007; Heese *et al.*, 2007; Schulze *et al.*, 2010). In addition, *bak1* loss-of-function in *Arabidopsis* or *N. benthamiana* results in reduced responsiveness to several other PAMPs and DAMPs, including elf18, csp22, INF1, PGN, LPS and *AtPep1* (Chinchilla *et al.*, 2007; Heese *et al.*, 2007; Shan *et al.*, 2008; Krol *et al.*, 2010).

Furthermore, BAK1 and its closest paralog BKK1 are required for the control of light- and pathogen-induced cell death (Kemmerling *et al.*, 2007; Jeong *et al.*, 2010; He *et al.*, 2007; He *et al.*, 2008). In addition, the LRR-RLK BAK1-interacting RLK 1 (BIR1) interacts with BAK1 *in vivo* and is also necessary to regulate cell death (Gao *et al.*, 2009). It is however unclear if the role of BAK1 and BKK1 in cell death control is linked to their interaction with ligand-binding RKs perceiving an hypothetical endogenous “survival” signal, or if the integrity and/or activity of the BAK1/BIR1/BKK1-containing complex(es) is guarded by hypothetical R protein(s) (Kemmerling *et al.*, 2007; He *et al.*, 2007; Wang *et al.*, 2008; Gao *et al.*, 2009).

Despite these numerous examples of the genetic requirement of BAK1 in different pathways, the *in vivo* heteromerization of BAK1 with ligand-binding RKs has thus far only been demonstrated for BRI1 and FLS2. Several results suggested that BAK1 may also form a ligand-dependent complex with the PRR EFR. First, the null mutant *bak1-4* was affected in elf18-triggered early responses (Chinchilla *et al.*, 2007; Shan *et al.*, 2008). Second, elf18 treatment induced the phosphorylation of a band co-immunoprecipitating with BAK1 that has a similar size as the glycosylated form of EFR (Schulze *et al.*, 2010). In this study, using co-immunoprecipitation experiments in *Arabidopsis* and *N. benthamiana*, we

demonstrated that EFR and BAK1 form a ligand-dependent complex *in vivo*. This interaction occurred rapidly (<5 min) and was specific to elf18 treatment, similarly in nature to the FLS2-BAK1 association triggered by flg22. This provides a third example of ligand-dependent heteromerization between BAK1 and a ligand-binding RK.

### 3.3.2 EFR, FLS2 and BRI1 form complex(es) with multiple SERKs

Null *bak1* mutants are only partially insensitive to flg22 or elf18 (Chinchilla *et al.*, 2007; Heese *et al.*, 2007; Shan *et al.*, 2008), suggesting that BAK1 is not the only rate-limiting component and that additional regulatory proteins are part of the FLS2 and EFR receptor complexes. Since BAK1/SERK3 is part of the multigenic SERK family containing 5 members, it is possible that additional SERKs associate with FLS2 and/or EFR *in vivo*. BRI1 for example, forms a ligand-dependent complex with BAK1, but also with SERK1 and BKK1 (Li *et al.*, 2002; Nam and Li, 2002; Karlova *et al.*, 2006; He *et al.*, 2007). Consistently, LC-MS/MS analysis of *Arabidopsis* anti-GFP immunoprecipitates from elf18-treated transgenic EFR-eGFP-HA seedlings identified specific peptides for SERK2, BAK1 and BKK1, suggesting that these three SERK proteins form ligand-dependent complex(es) with EFR *in vivo*. Notably, nineteen additional peptides matched multiple SERKs and seven peptides matched the highly similar BKK1 and SERK5. The presence of peptides that match several or all SERKs did not allow us to completely exclude the possibility that SERK1 and SERK5 may also be present in the EFR complex. Similarly, specific peptides corresponding to BAK1, SERK1 and SERK2 were also previously identified in HPLC-MS/MS analysis of the FLS2 immuno-complex in *Arabidopsis* (Heese *et al.*, 2007).

Accordingly, independent transient over-expression of epitope-tagged SERK and EFR proteins in *N. benthamiana* suggested that EFR is capable of mounting an elf18-dependent heteromerization with SERK1, SERK2, BAK1 and BKK1. In parallel, the heteromerization between epitope-tagged SERKs and FLS2 was also tested. FLS2 was also capable of forming a ligand-dependent complex with SERK1, SERK2, BAK1 and BKK1. However the amount of SERK1 and BKK1 co-immunoprecipitated with FLS2 was very low. With both FLS2 and EFR, no ligand-dependent association could be detected with SERK5. Our results thus suggest

that FLS2 preferentially interacts with BAK1, and potentially SERK2, while EFR strongly interacts with SERK1, SERK2, BAK1 and BKK1. These results are in agreement with the fact that *bak1* null mutants are more strongly affected in flg22 than elf18 responses (Chinchilla *et al.*, 2007).

### 3.3.3 The regulatory LRR-RKs BAK1 and BKK1 are important regulators of FLS2-, EFR- and PEPR1/2-dependent signaling

Having shown that several SERKs can form a ligand-dependent complex with FLS2 and EFR, it was important to genetically test the importance of these SERKs for flg22 and elf18 responses. Transcripts of *SERK1*, *SERK2*, *SERK3*, *SERK4* are up-regulated in response to PAMP or pathogen treatments (Postel *et al.*, 2010), supporting a potential role for these SERKs in innate immunity.

As previously reported (Chinchilla *et al.*, 2007; Heese *et al.*, 2007), we found that apart from *bak1*, other single null *serk* mutants were not affected in flg22 and elf18, as measured by the production of ROS (early response) and seedling growth inhibition (late response). These results did not disprove that other SERKs could play a role, and could be explained by functional redundancy among different SERKs (Albrecht *et al.*, 2008), in particular BAK1 in this case. Phenotypic analysis of double-mutant between null alleles of *bak1* and *serk1* or *serk2* suggest that SERK1 and SERK2 do not play a role in FLS2- or EFR-triggered signaling, at least in the bioassays used in this study.

Testing the role of BKK1 in the absence of BAK1 is normally hindered by the fact that the double *bak1 bkk1* mutants show constitutive activation of cell death (He *et al.*, 2007). Initial experiments using weak alleles combined as a double mutant *bak1-3 serk4-2* indicated functional BAK1 and BKK1 are required for early elf18-induced responses such as ROS burst. However, the later responses such as SGI and defense gene induction were affected by the weak cell death that could be observed in these mutants.

To circumvent this problem we took advantage of a new *bak1* allele, *bak1-5*, that is not impaired in BR signaling and that does not confer deregulated cell death when combined with *bkk1* mutations (Schwessinger *et al.*, submitted). Importantly, early and late responses to flg22 and elf18 were dramatically reduced in the

double-mutant *bak1-5 bkk1-1*. Interestingly, responses to the DAMP AtPep1 that are also BAK1-dependent (Krol *et al.*, 2010; Postel *et al.*, 2010) were also severely impaired in *bak1-5 bkk1-1*.

One intriguing observation was that MPK4 activation is abrogated in *bak1-5* and *bak1-5 bkk1-1* seedlings, which mirrors the phenotype of *bir1* mutants (Gao *et al.*, 2009). *bir1* mutant plants also have a constitutive cell death phenotype similarly to *bak1-4 bkk1-1* and *mpk4* mutants. The *bir1* cell death phenotype is reverted by increased temperatures, and is dependent on EDS1 and PAD4 (Gao *et al.*, 2009), while that of *bak1-4 bkk1-1* is SA-dependent (He *et al.*, 2007). These are all hallmarks of a R-dependent pathway, suggesting that loss of these components triggers R-mediated HR. It is possible that an unknown R protein guards BIR1, MPK4, BAK1 and BKK1, and this links PTI components with ETI. The lack of MPK4 activation in both *bir1* and *bak1-5 bkk1-1* suggests that this pathway is dependent on BAK1 and BIR1, perhaps through an in/direct interaction with MPK4. It is possible that an interaction is required for MPK4 activation, and this does not occur in *bak1-5* mutants, however further work is required to confirm this hypothesis.

The fact that *bak1-5* was more impaired in flg22 and elf18 responses than *bak1-4* could suggest that this mutation has a dominant-negative effect on SERK1, SERK2 and/or BKK1. However the double-mutants *bak1-4 serk1-3* and *bak1-4 serk2-2* were not less sensitive to flg22 and elf18 than *bak1-4*, indicating that SERK1 and SERK2 do not play a non-redundant role in FLS2 and EFR signaling pathways. In addition, the *bkk1-1* mutation further enhanced the *bak1-5* phenotype, suggesting that the BAK1-5 protein does not impair, at least completely, BKK1 function *per se*.

Our results thus reveal that BKK1 plays a major regulatory role in the FLS2-, EFR- and PEPR1/2-dependent signaling pathways in addition to BAK1.

### **3.3.4 BAK1 and BKK1 are required for immunity to hemi-biotrophic and obligate biotrophic pathogens**

The role of BAK1 and, to a larger extent, BKK1, in plant disease resistance is unclear. An unambiguous analysis of the role of BAK1 and BKK1 in *Arabidopsis* disease resistance is hindered by the constitutive and pathogen-induced cell death

phenotype of *bak1* and *bkk1* single and double null mutants (Kemmerling *et al.*, 2007; He *et al.*, 2007; Jeong *et al.*, 2010).

Accordingly, *bak1-4* plants exhibited pronounced chlorotic lesions upon infection with the hemibiotrophic bacterium *Pto* DC3000, but were not more susceptible to this bacterium (Kemmerling *et al.*, 2007). At the same time, the same mutant plants were more resistant to the obligate biotrophic oomycete *Hpa*, but more susceptible to the necrotrophic fungi *Botrytis cinerea* and *Alternaria brassicicola* (Kemmerling *et al.*, 2007).

Intriguingly, silencing of *NbSERK3/BAK1* in *N. benthamiana* resulted in a clear hyper-susceptibility to the adapted bacterium *Pta* 11528 and the non-adapted bacterium *Pto* DC3000 (Heese *et al.*, 2007). In addition, *SERK3/BAK1* silencing in tomato led to loss of *Verticillium* resistance mediated by the LRR receptor-like protein Ve1 (Fradin *et al.*, 2009).

Several hypotheses could explain the strong impact of *SERK3/BAK1* silencing on disease resistance in *N. benthamiana* and tomato without an apparent impact on cell death control as observed in *Arabidopsis*. First, the silenced gene may not correspond to the true functional ortholog of *AtBAK1*. Second, the silencing fragment may affect the expression of additional *SERK* paralogs whose function and/or identities are currently unknown. Third, hypothetical R protein(s) guarding the *BAK1-BKK1* complex integrity and/or activity may not be present in *N. benthamiana* and tomato. Thus, silencing of *SERK3/BAK1* in these plants does not result in observable cell death phenotypes.

Another issue in interpreting the role of *BAK1* in disease resistance is that the impact of BR signaling in defense is still unclear (Divi and Krishna, 2009). Consequently, conclusions on disease susceptibility of *bak1* mutants always need to be carefully weighed as these lines exhibit defects in hormone signaling, innate immunity and cell death.

We took advantage of the *bak1-5* and *bak1-5 bkk1-1* lines to address the potential role of *BAK1* and *BKK1* in PTI against hemibiotrophic bacteria and the obligate biotrophic oomycete *Hpa*. Our results provide evidence of a role for *BAK1* and *BKK1* in *Arabidopsis* basal and non-host resistances to *Pseudomonas syringae* strains. *Bak1-5* mutants were more susceptible to several strains of *Pto* DC3000 and to the non-adapted strain *Pta* 6605. More importantly, our results also revealed that *BAK1* and *BKK1* are involved in resistance to *Hpa*. Surprisingly,

the isolates Cala2 and Emoy2 that are normally resisted by the R protein RPP2 and RPP4, respectively (Holub, 2008; Holub *et al.*, 1994) grew to a certain extent in *bak1-5 bkk1-1* seedlings. This may suggest that BAK1 and BKK1 are involved in effector-triggered immunity (ETI), although this could also reflect the enhanced growth resulting from the strong loss of PTI in these lines. This latter hypothesis is actually supported by the reduced responsiveness of *bak1-5 bkk1-1* plants to a crude boiled extract from *Hpa*-infected *Arabidopsis* leaves. We speculate that BAK1 and BKK1 might also interact with as yet unidentified PRR(s) for oomycete PAMP(s). Similarly, *bak1-5 bkk1-1* leaves were more susceptible than *efr-1 fls2* to the hypovirulent bacterial strain *Pto* DC3000 *COR*<sup>+</sup>, indicating that at least another PAMP than EF-Tu or flagellin derived from this bacterium is recognized by a BAK1/BKK1-dependent PRR. The identification of these novel PAMPs and corresponding receptors represents an interesting challenge in the future.

### 3.3.5 Possible molecular functions of BAK1 and BKK1

Several questions have been raised by this work, namely: (i) what is the role of BAK1 and BKK1 in the different oligo-heteromeric complexes they are involved in, and (ii) how do they contribute to activation of specific downstream signaling pathways? For both BRI1 and FLS2, BAK1 is not required for ligand binding (Kinoshita *et al.*, 2005; Chinchilla *et al.*, 2007). Therefore, BAK1 is not a co-receptor, but rather a non-ligand-binding regulatory RK.

Binding of BR to BRI1 leads to sequential transphosphorylation events between BRI1 and BAK1 resulting in an increase in BRI1 kinase activity that leads to activation of downstream signaling (Wang *et al.*, 2008d; Li *et al.*, 2002; Nam and Li, 2002; Karlova *et al.*, 2006; He *et al.*, 2007). In this model of receptor activation, BRI1 kinase activity is required for the ligand-induced BRI1-BAK1 association, and BAK1 ultimately enhances the already strong BRI1 kinase activity (Wang *et al.*, 2008d). Although BKK1 and SERK1 can also form a complex with BRI1 (He *et al.*, 2007; Karlova *et al.*, 2006), their role in BRI1 activation is not yet understood.

A model in which they operate as activators of BRI1 kinase activity would correlate with the quantitatively weak and heterogeneous impact of single and double null mutations in *BAK1*, *BKK1* and *SERK1* on different BR-dependent

responses (Li *et al.*, 2002; Nam and Li, 2002; Karlova *et al.*, 2006; He *et al.*, 2007; Albrecht *et al.*, 2008; Jeong *et al.*, 2010).

The regulatory role of BAK1 for FLS2 and EFR however seems distinctive. The null mutant *bak1-4* strongly affects flg22 and elf18 responses (Chinchilla *et al.*, 2007; Heese *et al.*, 2007), while the double-mutant *bak1-5 bkk1-1* is almost insensitive to flg22 and elf18. In addition, BAK1 kinase activity is required for flg22 responses (Schulze *et al.*, 2010) and EFR kinase activity is required for elf18 responses, but the kinase activities of FLS2, EFR, and BAK1 are non-essential for the heteromerization. Indeed, treatment with the general kinase inhibitor K252a does not prevent complex formation between FLS2 and BAK1, and a BAK1 kinase-dead (BAK1-KD) variant still associates with FLS2 in a flg22-dependent manner (Schulze *et al.*, 2010). In addition, kinase-dead variants of FLS2 or EFR still form ligand-dependent complexes with BAK1 (this work and Schwessinger *et al.*, submitted).

A major difference between BRI1 and FLS2 or EFR, is that BRI1 is a RD kinase, while FLS2 and EFR are non-RD kinases. RD kinases carry a conserved arginine (Arg/R) immediately preceding the critical aspartate (Asp/D) in the catalytic loop of the subdomain Vlb, and are regulated by activation loop phosphorylation (Johnson *et al.*, 1996). On the contrary, non-RD kinases present a variable residue in place of the arginine and generally exhibit low autophosphorylation activities. The catalytic loop is the location of the conserved D, which acts as the base or proton-acceptor for the hydroxyl group of the attacking substrate during the phosphotransfer mechanism. The adjacent R is purported to neutralize the negative charge of the  $\gamma$ -phosphate, facilitating phosphotransfer (Johnson *et al.*, 1996). Intriguingly, non-RD kinases are most often associated with immune functions across kingdoms (Dardick and Ronald, 2006).

Given these differences, it is unclear whether the model of activation based on the BRI1-BAK1 system (Wang *et al.*, 2008d) is generally extendable to non-RD kinases. Thus, it is essential in the future to understand the nature and the importance of the phosphorylation events occurring between the non-RD ligand-binding RKs FLS2/EFR and the RD regulatory RLKs BAK1/BKK1.

In the BR pathway, BRI1 activation leads to the phosphorylation of the positive regulatory cytoplasmic kinases BSKs by BRI1 and their release in a BAK1-independent manner from the plasma membrane to activate downstream signaling (Tang *et al.*, 2008; Kim *et al.*, 2009c). Recently, the membrane-associated cytoplasmic kinases BIK1 and related PBS1-LIKE (PBL) proteins were identified as positive regulators of flg22 and elf18 responses (Zhang *et al.*, 2010a); (Lu *et al.*, 2010). BIK1 forms a constitutive complex with FLS2. Flg22 treatment leads to BIK1 and PBL1 phosphorylation within minutes and to the partial dissociation of the FLS2-BIK1 complex. Notably, BIK1 also form a complex with EFR (Zhang *et al.*, 2010a) and elf18 treatment leads to BIK1 phosphorylation (Lu *et al.*, 2010). The FLS2-BIK1 association does not require BAK1 (Lu *et al.*, 2010); (Zhang *et al.*, 2010a), and conversely the FLS2-BAK1 association does not require BIK1 (Lu *et al.*, 2010; Zhang *et al.*, 2010a). However, kinase-active BAK1 and FLS2 are required for flg22-dependent BIK1 phosphorylation, which contribute to its regulatory role (Lu *et al.*, 2010; Zhang *et al.*, 2010a). Whether BAK1 can directly interact with and phosphorylate BIK1 is still controversial (Lu *et al.*, 2010; Zhang *et al.*, 2010a). Interestingly, BIK1 and its paralogs are targeted by the *Pseudomonas syringae* effector AvrPphB (Zhang *et al.*, 2010a) demonstrating the importance of these proteins for PTI. Future work should reveal how the dynamics of the FLS2/EFR-BAK1/BKK1 complexes and the associated phosphorylation events regulate BIK1 and potentially other substrates to trigger downstream signaling.

## 4 RAE5: AN EFR-INTERACTING LRR-RLK FUNCTIONING AS A REGULATOR OF PTI AND ETI

### 4.1 Preface

RAE5 (At4g08850) is a member of the subfamily XII of LRR-RKs, the same subfamily to which EFR and FLS2 belong (Figure 4.1; [Appendix Figure A4.1](#)). This subfamily was already under investigation in the laboratory by Freddy Boutrot in an effort to identify new PAMP receptors. RAE5 is predicted to have 24 LRRs in the extracellular domain, a transmembrane domain and a Ser/Thr kinase domain (Figure 4.2). Interestingly, RAE5 is an RD kinase (Dardick and Ronald, 2006), with an Arg (R) preceding the conserved Asp (D) in the catalytic loop of subdomain VIB.

The only other RD kinase in subfamily XII is the closest relative of RAE5, At1g35710, designated XII1 herein. RAE5 was originally assigned to family XII based on phylogenetic analysis of the kinase domains (Shiu and Bleecker, 2001); subsequent analysis of the full-length sequences placed RAE5 and XII1 in Family XI (Gou *et al.*, 2010). The most recent phylogenetic analysis, which assessed RLK kinase domains in *Arabidopsis*, rice, poplar and grapevine, also placed RAE5 in Family XII (Tang *et al.*, 2010) ([Appendix Figure A4.2](#)), and I have maintained this classification.

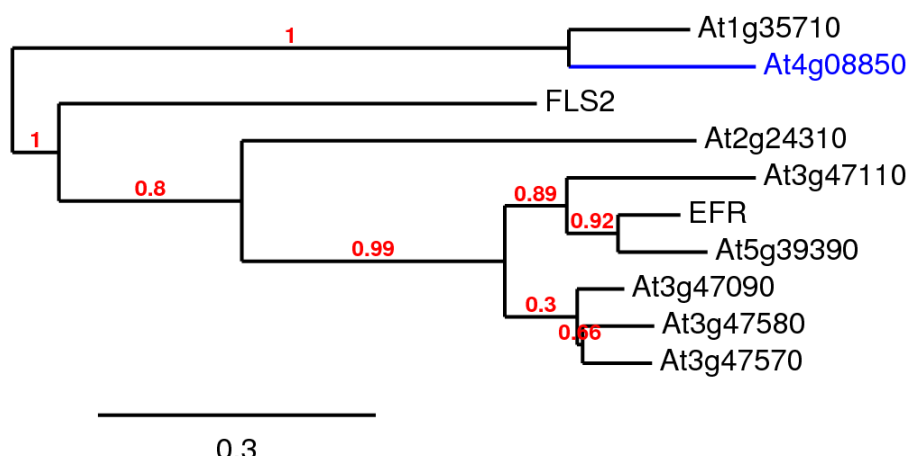


**Figure 4.1. Phylogenetic tree of members of LRR-RK subfamily XII.** Phylogenetic tree was constructed using full-length amino acid sequence, MUSCLE for the alignment, PhyML for the phylogeny and TreeDyn for drawing the tree (at [www.phylogeny.fr](http://www.phylogeny.fr)). The branch support values are shown in red.

A pair of RAE5 orthologs exist in rice (*Oryza sativa* ssp *japonica* cv. *Nipponbare*): Os02g34750 and Os02g34790 (60 % similarity), with highest similarity in the kinase domain. The rice orthologs are closer to each other and RAE5 than to other rice RKs and the each of the pairs fall into a species subclade ([Appendix Figure A4.2](#)). This could hint at a conserved function, but there is no data available for the function of the rice orthologs.

signal peptide 1-43

```

1 MNKTNPERKISLTSFKERMACKEKPRDLQVLLIISIVLSCSFAVSATV 48
49 EEAANALLKWKSTFTNQTSSSKLSSWVNPNTSSFDTSWYGVASLGSI 96
97 RLNLNTNTGIEGTFEDFPFSSLNPNTLTFVDSLNMNRFGTISPLWGRFSKL 144
145 EYFDLSINQLVGIEPPLEGDLISNLDLTLHLVENKLNGSIPSEIGRLTKV 192 LRR
193 TEIAIYDNLLTGPIPSSFGNLTKLVNLYLFINSLSGSIPSEIGNLPNL 240
241 RELCLDRNNTLTKGKIPSSFGNLKNTLNMFENQLSCEIPPEIGNMTAL 288
289 DTLSLHTNKLGPIPSTLGNIKTLAVLHLYLNQLNGSIPPELGEMESM 336
337 IDLEISENKLTGPVPDSFGKLTALEWLFLRDNQLSGPIPPIGIANSTEL 384
385 TVLQLDTNNFTGFLPDTICRGGKLENLTLLDDNHFEGPVPKSLRDCKSL 432
433 IRVRFKGNSFSGDISEAFGVYPTLNFIIDLSNNNFHGQLSANWEQSQKL 480
481 VAFILSNNSITGAIPPEIWNTMQLSQLDLSSNRITGELPESISNINRI 528
529 SKLQLNGNRLSGKIPSGIRLLTNLEYLDLSSNRFSSEIPPTLNNLPRL 576
577 YYMNLSRNLDLDTIPEGLTKLSQLQMLDLSYNQLDGEISSQFRSLQNL 624
625 ERLDLSHNNSLNGQIPPSFKDMALATHVDVSHNNLQGPIDNAAFRNAP 672
673 PDAFEGNKDLGSVNTTQGLKPSITSSKKSHKDRNLIIYILVPIIGA 720 TM
721 IILSVCAGIFICFRKRTKQIEEHTDSESGGETLSIFSFDGKVRYQE 768 JM
769 IKATGEFDPKYLIGTGGHKGVYKAKLPNAIMAVKKLNETTDSSISNPS 816
817 TKQEFLNEIRALTEIRHRNVVKLFGFCSSHRRNTFLVYEYMERGSLRKV 864 Ser/Thr kinase
865 LENDDEAKKLDWGKRINVVKGVAHALSYMHDRSPAIVHRDISSGNIL 912 775-1045
913 LGEDYEAKISDFGTAKLLKPDSSNWSAVAGTYGYVAPELAYAMKVTEK 960
961 CDVYSGVLTLEVIKGEHPGDLVSTLSSPPDATLSLKSISDHRLPEP 1008
1009 TPEIKEEVLEILKVALCLHSDPQARPTMLSISTAFS 1045

```

**Figure 4.2 Primary structure of RAE5 protein.**

Signal peptide (tan; 1-43); Cys pairs indicated in gray text with black box; 24 leucine rich repeats (LRR) in gray, with conserved Leu in purple; potential glycosylation sites in pink (NxS/T); transmembrane domain in light blue; phosphosites in dark green; Ser/Thr kinase domain (775-1045) in light green and pink (indicating location of alternate splicing) with conserved ATP-binding lysine (K802) in purple and conserved D905 of RD motif in brown. Sequence features were obtained from Uniprot (accession Q8VZG8).

In the laboratory of Marc Knight (U. of Durham, UK), RAE5 was found to interact with OXI1 in a yeast two-hybrid screen (M. Knight, personal communication). OXI1 is a protein kinase involved in oxidative stress signaling. OXI1 is required for basal resistance to *Hyaloperonospora arabidopsis* infection and root hair growth. In addition, OXI1 is required for the activation of MPK3 and MPK6 by hydrogen peroxide and cellulase (Rentel *et al.*, 2004). *Oxi1* mutants are more susceptible to virulent and avirulent strains of *P. syringae*, suggesting a role for OXI1 in the regulation of both PTI and ETI (Petersen *et al.*, 2009). Interestingly, RAE5 is predicted to be co-expressed with several defense-related genes, including BIR1 and BIK1, both known BAK1-associated proteins (Gao *et al.*, 2009; Lu *et al.*, 2010), SGT1a and CMPG1 ([Appendix Table A4.1](#)).

Recently, RAE5 was also identified as an interactor of the resistance protein RPS2 in an immunoprecipitation study in *Arabidopsis* (Qi and Katagiri, 2009). Given the interaction between RPS2 and RIN4, and the fact that RIN4 acts as a negative regulator of PTI signaling, this places RAE5 in a position to potentially resolve the links between ETI and PTI signaling. All this evidence points to a potentially important role for RAE5 in PTI, perhaps in a bridge between ETI and PTI.

## 4.2 Results

### 4.2.1 RAE5 was identified in EFR IPs

Mass spectrometry analysis of EFR IPs identified 5 unique peptides matching RAE5, At4g08850.1 ([Table 2.1](#); [Table 4.1](#)). The location of the peptides across the RAE5 sequence is shown in [Appendix Figure A4.1](#). All of these peptides could also correspond to the alternative-splicing product At4g08850.2 ([Appendix Figure A4.3](#)). Interestingly, no modifications were identified in any of the detected peptides.

**Table 4-1: RAE5 peptides identified by MS analysis of EFR IPs**

Bio Rep	Peptide sequence	Mascot Ion score <sup>^</sup>	Mascot ID score <sup>\$</sup>
EFRelf_3	DISSGNILLGEDYEAK	31.6	24.1
EFR_3	ITGELPESISNINR	77.1	22.2
EFRelf_3	ITGELPESISNINR	64.7	22.1
EFR 1	LNETTDSSISNPSTK	49	23.1
EFR 2	LNETTDSSISNPSTK	46.1	18.6
EFR_3	LNETTDSSISNPSTK	95.6	23.7
EFRelf_3	LNETTDSSISNPSTK	68.8	23.7
EFR 1*	LTGPVPDSFGK	25.9	25.5
EFR 2	TVEEANALLK	50.6	30.3
EFR 2	TVEEANALLK	59.4	30.3
EFR_3	TVEEANALLK	35	30.2
EFRelf_3	TVEEANALLK	32.8	30.3

Peptide ID probability (Scaffold calculated probability that a given protein has been identified correctly) 94 % for all

<sup>^</sup>Mascot Ion Score is a measure of how well the observed MS/MS spectrum matches to the stated peptide

<sup>\$</sup>Mascot identity score: a minimum ion score threshold. As a rule, the ion score should be above the identity score. identity score=−10<sup>8</sup>(log(p/#matches)), where p is your probability threshold (Scaffold uses 1.0), and #matches is the number of precursor matches.

### 4.2.2 RAE5 interacts with RLKs in *N. benthamiana*

After identification of RAE5 in EFR IPs, I sought to further characterize the nature of the interactions between these two receptor kinases. First, I had to confirm the interaction by transient expression of C-terminally HA<sub>3</sub>-epitope-tagged RAE5 and receptor-GFP fusion proteins in *N. benthamiana*. Equal amounts of EFR-GFP were pulled-down using GFP Trap beads and probed for the presence of RAE5-HA<sub>3</sub> using anti-HA immunoblotting. While some RAE5 was weakly detected in mock-treated samples, elf18 treatment significantly increased the amount of RAE5 detectable in the EFR immunoprecipitate (GFP IP) ([Figure 4.3A](#)).

Considering that previous work suggests that EFR and FLS2 share several common signaling partners such as the SERKs (Heese *et al.*, 2007; Chinchilla *et al.*, 2007; this work), it is conceivable that both PRRs may interact with RAE5. When equal amounts of FLS2-GFP were pulled-down using GFP Trap beads, RAE5-HA<sub>3</sub> was weakly detected in mock-treated and flg22-treated samples in the GFP immunoprecipitate (GFP IP) ([Figure 4.3B](#)). In an independent experiment (data not shown), there was a slight enhancement of FLS2-RAE5 interaction following flg22 treatment, but never as distinct as that seen for EFR and RAE5.

It is possible that EFR and FLS2 interact with RAE5 directly, or indirectly via another adaptor protein such as BAK1. In order to determine whether RAE5 is capable of interacting with BAK1, I similarly transiently expressed EFR-GFP and BAK1-HA and pulled down equal amounts of BAK1-GFP with GFP Trap beads. Upon anti-HA immunodetection of GFP immunoprecipitates, a faint band was detectable at the correct size corresponding to the tagged RAE5 protein ([Figure 4.3C](#)). This was detected in the presence and absence of flg22 treatment, suggesting a ligand-independent association between these proteins.

Although only a weak interaction with BAK1 was detected, it is possible that RAE5 may have a general function related to receptor kinases. Thus I investigated the specificity of the aforementioned interactions by immunoprecipitating transiently expressed BRI1-GFP, co-expressed with RAE5-HA. Once again, RAE5-HA could be detected in GFP immunoprecipitates, and was slightly enriched following 90-minute treatment with brassinolide ([Figure 4.3D](#)).

This suggests that RAE5 is capable of interacting with diverse receptor kinases. To confirm whether OXI1 is capable of interacting with RAE5 *in planta*, I transiently co-expressed RAE5-GFP and OXI-HA<sub>3</sub> in *N. benthamiana*. When RAE5-GFP was immunoprecipitated using GFP Trap beads, OXI1-HA<sub>3</sub> could be weakly detected at around 65 kDa by anti-HA immunoblotting of mock-treated and flg22-elicited immunoprecipitates ([Figure 4.3E](#)). Thus, RAE5 interacted with all the tested proteins by co-IP in *N. benthamiana*.

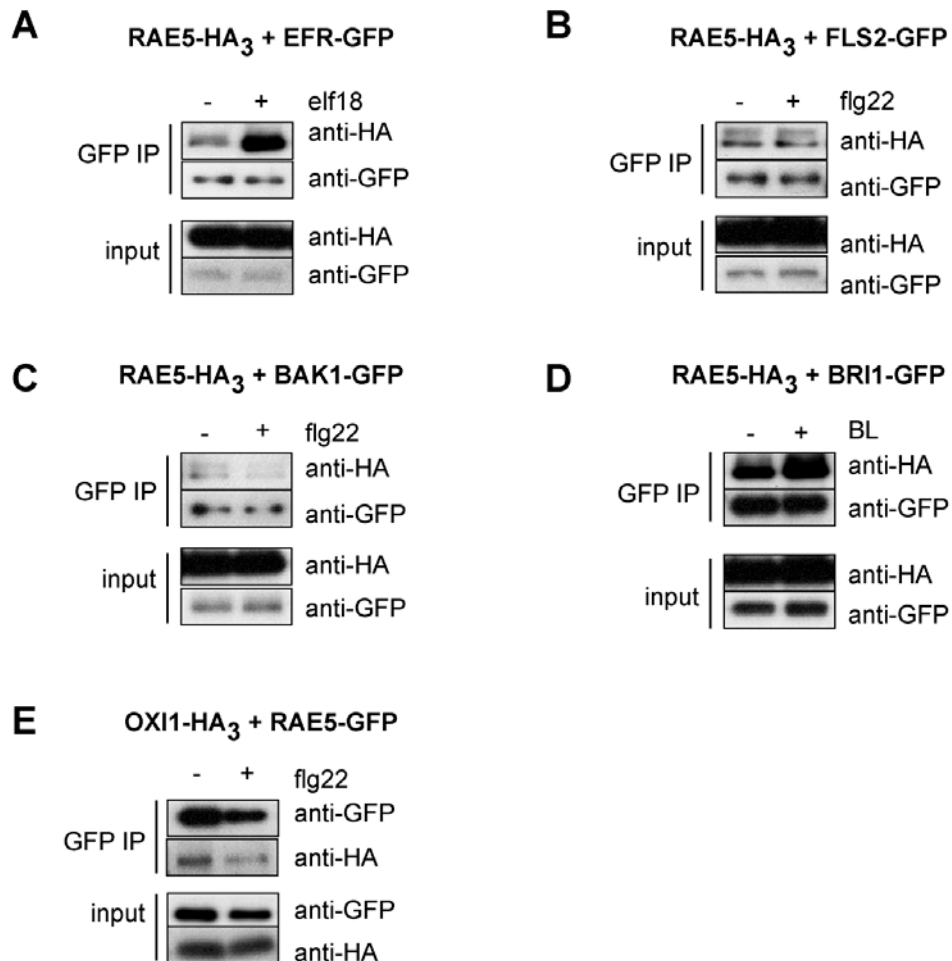


**Figure 4.3. RAE5 is capable of interaction with EFR, FLS2, BRI1, BAK1 and OXI1 in *N. benthamiana*.**

A. Co-immunoprecipitation of EFR and RAE5. *N. benthamiana* leaves expressing RAE5-HA<sub>3</sub> constructs and EFR-GFP were treated (+) or not (-) with 100 nM elf18 for 5 minutes. Total proteins (input) were subjected to immunoprecipitation with GFP Trap beads followed by immunoblot analysis with anti-HA antibodies to detect RAE5-HA<sub>3</sub> and anti-GFP antibodies to detect EFR-GFP. This experiment was repeated three times.

B. Co-immunoprecipitation of FLS2 and RAE5. *N. benthamiana* leaves expressing RAE5-HA<sub>3</sub> constructs and FLS2-GFP were treated (+) or not (-) with 100 nM flg22 for 5 minutes. Total proteins (input) were subjected to immunoprecipitation with GFP Trap beads followed by immunoblot analysis with anti-HA antibodies to detect RAE5-HA<sub>3</sub> and anti-GFP antibodies to detect FLS2-GFP. This experiment was repeated three times.

C. Co-immunoprecipitation of BAK1 and RAE5. *N. benthamiana* leaves expressing RAE5-HA<sub>3</sub> constructs and BAK1-GFP were treated (+) or not (-) with 100 nM flg22 for 5 minutes. Total proteins (input) were subjected to immunoprecipitation with GFP Trap beads followed by immunoblot analysis with anti-HA antibodies to detect RAE5-HA<sub>3</sub> and anti-GFP antibodies to detect BAK1-GFP. This experiment was repeated twice.

D. Co-immunoprecipitation of BRI1 and RAE5. *N. benthamiana* leaves expressing RAE5-HA<sub>3</sub> constructs and BRI1-GFP were treated (+) or not (-) with 100 nM BL for 90 minutes. Total proteins (input) were subjected to immunoprecipitation with GFP Trap beads followed by immunoblot analysis with anti-HA antibodies to detect RAE5-HA<sub>3</sub> and anti-GFP antibodies to detect BRI1-GFP. This experiment was repeated three times.

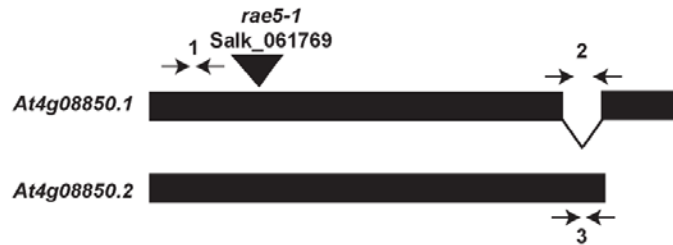
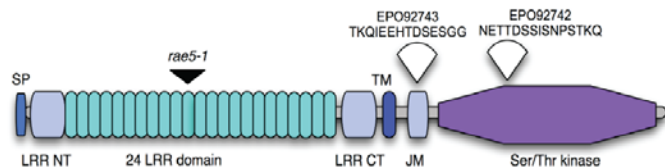
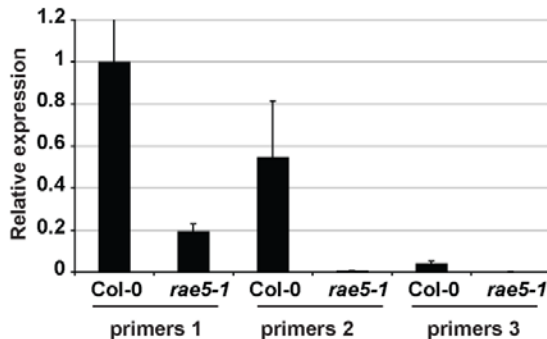
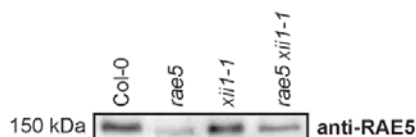
E. Co-immunoprecipitation of RAE5 and OXI1. *N. benthamiana* leaves expressing OXI1-HA<sub>3</sub> constructs and RAE5-GFP were treated (+) or not (-) with 100 nM flg22 for 5 minutes. Total proteins (input) were subjected to immunoprecipitation with GFP Trap beads followed by immunoblot analysis with anti-HA antibodies to detect OXI1-HA<sub>3</sub> and anti-GFP antibodies to detect RAE5-GFP. This experiment was repeated twice.

#### 4.2.3 Anti-RAE5 antibody development

In order to study the complex formation involving RAE5 *in planta*, the ideal would be to use native anti-RAE5 antibodies to detect protein behaviour under native conditions. To this end, I sought to obtain specific, sensitive anti-RAE antibodies for immunoprecipitation in *Arabidopsis*. Two peptides, one from the juxtamembrane region (EPO92743: TKQIEEHTDSESGG), another from the kinase domain (EPO92742: NETTDSSISNPSTKQ) were selected for their unique sequence ([Figure 4.4B](#); [Appendix Figure A4.1](#)). Two independent rabbits were immunized with each peptide and the specificity and affinity of the antisera were assessed by the manufacturer (Eurogentec; data not shown).

Large bleeds derived from both rabbits were purified against each peptide, and tested for affinity and specificity. Firstly, testing by dot-blotting indicated that the antiserum derived from purification against EPO92743 peptides did not cross-react with any proteins in crude *Arabidopsis* protein extracts, while EPO92742-purified antibodies detected an antigen in plant extracts (data not shown). In order to confirm the specificity of the antibodies for RAE5, null mutant *rae5* lines were required as a negative control. Thus, Freddy Boutrot obtained and genotyped homozygous *rae5-1* T-DNA insertion line (Salk\_061769), as well as an insertion line for XII1 (At1g35710), the gene most closely related to RAE5 ([Figure 4.1](#)), *xii1-1* (Gabi-Kat\_031G02). The T-DNA insertion in *rae5-1* is predicted to be within the 12<sup>th</sup> LRR repeat of *RAE5* ([Figure 4.4A-B](#)). RAE5 is subject to alternative splicing, and produces two possible transcripts, designated herein as *RAE5.1* for the canonical transcript in which the intron is spliced out, and *RAE5.2* for the alternative transcript, in which the intron is partially transcribed. The impact of this on the protein sequence can be seen in the pairwise alignment in [Appendix Figure A4.3](#). In order to determine whether *rae5-1* is a null mutant, I used qPCR analysis to monitor transcript levels of either *RAE5.1* or *RAE5.2* in Col-0 and *rae5-1* ([Figure 4.4C](#)). Primer set 1 is designed to amplify both transcripts, primer set 2 should amplify only *RAE5.1* and primer set 3 should amplify *RAE5.2*. I found evidence for the expression of both alternative transcripts in Col-0 seedlings, although less *RAE5.2* transcript was detected ([Figure 4.4C](#)). Although a small amount of each transcript remains in *rae5-1*, this is significantly reduced compared to Col-0 irrespective of the primer set used ([Figure 4.4C](#)).

Total proteins extracted from Col-0 were compared to those derived from *rae5-1* and *xii1-1*, as well as the double mutant *rae5-1 xii1-1*. Anti-RAE5 antibodies (purified against EPO92742) at a 1:500 dilution cross-reacted with protein present in Col-0 and *xii1-1* protein extracts, where an intense band could be detected in crude total protein extracts ([Figure 4.4D](#)). A faint band remained in the *rae5-1* and *rae5-1 xii1-1* protein extracts, suggesting that the antibody may also cross-react with other proteins present. Interestingly, the size of the band corresponding to RAE5 is around 150 kDa, which is higher than the predicted molecular weight of 115 kDa. This suggests that RAE5, similarly to EFR and FLS2 is subject to *N*-glycosylation. This will be tested later by PNGase treatment to de-glycosylate proteins. Antibodies purified against EPO92743 did not cross-react with any proteins (data not shown).

**A****B****C****D****Figure 4.4. Anti-RAE5 antibodies can detect RAE5 in total protein extracts**

A. Representation of *RAE5* (At4g08850.1) gene arrangement and splice variant At4g08850.2. T-DNA insertion *rae5-1* (Salk\_061769) indicated. Exons are represented by black rectangles; the intron is represented by the line linking exons. The paired arrows indicate binding of qPCR primers used in (C).

B. Schematic representation of RAE5 protein structure. Peptide sequences chosen for antibodies indicated above (EPO94742/3). SP: signal peptide; LRR:leucine rich repeat; NT: N-ter; CT: C-ter; TM: transmembrane domain; JM: juxtamembrane domain.

C. *Rae5-1* has reduced levels of *RAE5* transcript. Gene expression of *RAE5* was measured by qPCR analysis, normalized to *UBQ10* (housekeeping) expression and plotted relative to Col-0 expression level. Primers used as indicated; binding positions shown in A. Results are average  $\pm$  standard error ( $n=3$ ).

D. Immunoblot analysis of anti-RAE5 antibodies. Total protein extracts derived from Col-0, *rae5-1*, *xii1-1* (GK\_031G02) and *rae5-1 xii1-1* were separated by SDS-PAGE and immunoblotted with anti-RAE5 antibodies (1:500).

#### 4.2.4 RAE5 interactions in Arabidopsis

In the first instance, I observed the behaviour of RAE5 during its immunoprecipitation from *Arabidopsis* Col-0 seedlings. Total protein was extracted from Col-0 seedlings using a non-denaturing detergent and subjected to immunoprecipitation using Trueblot beads and anti-RAE5 antibodies. An intense band could be detected in total protein extracts derived from Col-0 and *bak1-4*, while there was only a faint smear in *rae5-1* extracts ([Figure 4.5A](#), top panel). Unfortunately, no distinct RAE5-specific band could be detected in anti-RAE5 immunoprecipitates from any *Arabidopsis* genotype ([Figure 4.5A](#), bottom panel). This suggests that while the anti-RAE5 antibody can be used to detect RAE5 in total protein extracts, it cannot be used to immunoprecipitate the native, folded RAE5 protein.

In an effort to circumvent this problem, I attempted to detect immunoprecipitated RAE5 pulled down with EFR, FLS2 or BAK1 in *Arabidopsis*. For EFR immunoprecipitation, I made use of transgenic *Arabidopsis* seedlings expressing EFR-eGFP under the control of its own promoter. EFR-eGFP was pulled down using GFP Trap beads, with *efr-1* null mutants as a negative control for the immunoprecipitation. An intense band was detected by anti-GFP immunoblotting of GFP immunoprecipitates, in the mock-treated and *elf18*-treated EFR-eGFP IPs, which was absent from the *efr-1* control lane ([Figure 4.5B](#), top panel). When probing the same immunoprecipitates with anti-RAE5 antibodies, no RAE5-specific band could be detected ([Figure 4.5B](#), bottom panel). Thus, in *Arabidopsis*, no RAE5 could be detected in EFR immunoprecipitates.

To determine whether RAE5 could be detected in immunoprecipitates of other proteins associated with RAE5 when transiently expressed in *N. benthamiana*, I carried out immunoprecipitation of FLS2 or BAK1 in *Arabidopsis*, followed by anti-RAE5 immunoblotting. For FLS2, anti-FLS2 combined with Trueblot beads could immunoprecipitate FLS2 from Col-0 but not *fls2* seedlings. Anti-FLS2 immunoblotting detected an intense band for FLS2 pulled down in Col-0, *bak1-4* and *rae5-1* seedlings ([Figure 4.5C](#)). Furthermore, the flg22 treatment was able to induce an interaction between FLS2 and BAK1, as anti-BAK1 immunoblotting of FLS2 IPs identified a band, which was absent prior to PAMP treatment and absent from *bak1-4* immunoprecipitates. However, when probing

the same immunoprecipitates with anti-RAE5 antibodies, no RAE5-specific band could be detected (Figure 4.5C, bottom panel). There did appear to be a mild reduction in the amount of BAK1 detected in FLS2 IPs derived from *rae5-1* tissue, however there was no detectable reduction in the amount of total FLS2 or BAK1 protein detectable in *rae5-1*. Thus, in Arabidopsis, no RAE5 could be detected in FLS2 immunoprecipitates.

In the reciprocal IP, BAK1 was pulled down using anti-BAK1 antibodies with Trueblot beads. Following anti-BAK1 immunoblotting of the IPs, an intense band corresponding to immunoprecipitated BAK1 could be detected in Col-0 and *rae5-1* seedlings (Figure 4.5D). A faint band was detected in *bak1-4* seedlings owing to weak recognition of a related SERK by the antibodies, as discussed in Chapter 3. In addition, FLS2 could be detected in BAK1 IPs derived from flg22-treated Col-0 and *rae5-1* seedlings, but was absent from *bak1-4* IPs (Figure 4.5D). However, once again RAE5 could not be detected in the IPs, providing no evidence of RAE5 interactions with receptors in Arabidopsis.

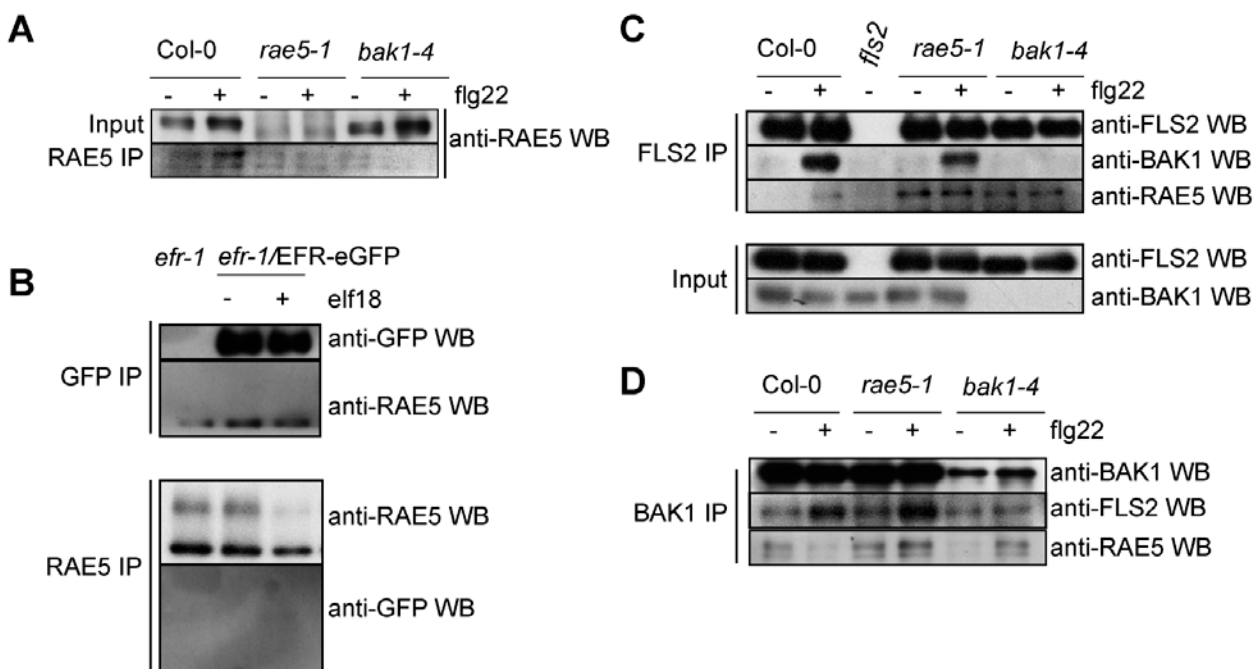


**Figure 4.5. RAE5 complex formation in Arabidopsis.**

A. Immunoprecipitation of RAE5 from Arabidopsis Col-0, *rae5-1* or *bak1-4* seedlings. Tissue was treated (+) or not (-) with 100 nM flg22 for 5 minutes. Total proteins (input) were subjected to immunoprecipitation with Trueblot beads and anti-RAE5 antibodies, followed by immunoblot analysis with anti-RAE5 antibodies.

B. Immunoprecipitation of RAE5 or EFR-GFP from *Arabidopsis efr-1* or *efr-1/EFR-eGFP* seedlings. Tissue was treated (+) or not (-) with 100 nM elf18 for 5 minutes. Total proteins (input) were subjected to immunoprecipitation with GFP Trap beads (GFP IP, top) or Trueblot beads and anti-RAE5 antibodies (RAE5 IP, bottom), followed by immunoblot analysis with anti-RAE5 or anti-GFP antibodies.

C. Immunoprecipitation of FLS2 from *Arabidopsis Col-0, fls2, rae5-1* or *bak1-4* seedlings. Tissue was treated (+) or not (-) with 100 nM flg22 for 5 minutes. Total proteins (input) were subjected to immunoprecipitation with Trueblot beads and anti-FLS2 antibodies, followed by immunoblot analysis with anti-FLS2, anti-BAK1 or anti-RAE5 antibodies.

D. Immunoprecipitation of BAK1 from *Arabidopsis Col-0, rae5-1* or *bak1-4* seedlings. Tissue was treated (+) or not (-) with 100 nM flg22 for 5 minutes. Total proteins (input in (C)) were subjected to immunoprecipitation with Trueblot beads and anti-BAK1 antibodies, followed by immunoblot analysis with anti-FLS2, anti-BAK1 or anti-RAE5 antibodies.

These experiments were repeated twice.

#### 4.2.5 RAE5 is present at the plasma membrane

RAE5 has a predicted transmembrane domain, and its identification as a potential EIP suggests membrane localization. Upon transient overexpression in *N. benthamiana*, RAE5-GFP can be detected at the cell periphery within two days of agro-infiltration ([Figure 4.6A](#)). This localization is likely to be at the plasma membrane because upon plasmolysis by the incubation of leaf tissue with NaCl, the fluorescent signal can be seen retracting from the cell wall ([Figure 4.6B](#)). This is also true for a mutant variant of RAE5 harbouring a D to N mutation in the conserved aspartic acid (D905N) within the activation loop of the kinase domain ([Figure 4.6C and D](#)).

Thus, RAE5 is localized to the plasma membrane, and this does not appear to depend on its kinase activity.

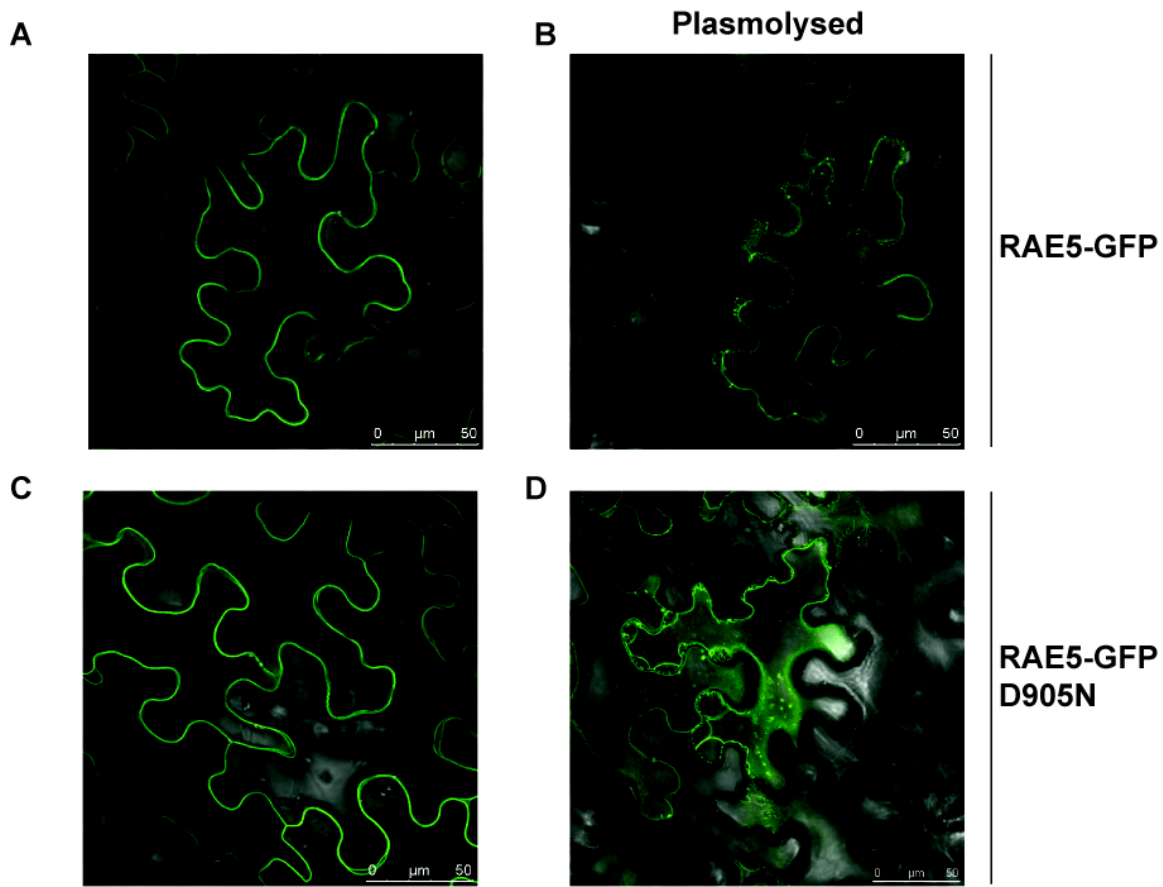


**Figure 4.6. Transiently over-expressed RAE5 is localized in the plasma membrane.**

A and C. Confocal microscopy analysis of the leaf epidermis of *N. benthamiana* transiently expressing 35S::RAE5-GFP-His (A) and 35S::RAE5-GFP-His mutant D905N (C).  
 B and D. Plasmolysed tissue - 35S::RAE5-GFP-His (B) and 35S::RAE5-GFP-His mutant D905N (D) 20 minutes after addition of 1 M NaCl.

#### 4.2.6 RAE5 is required for optimal PAMP-triggered ROS responses

In order to understand the role played by RAE5 in PTI signaling, Freddy Boutrot has studied several PTI signaling responses in *rae5-1* mutants (Figure 4.6) and has obtained similar results using alternative *RAE5* loss-of-function lines (data not shown). Initial experiments indicate that RAE5 is required for ROS burst in response to *elf18* and *flg22*, as *rae5-1* mutants are significantly compromised in PAMP responsiveness in this assay (Figure 4.7A and B). Further phenotypic characterization is ongoing (Freddy Boutrot) and will be briefly referred to in the Discussion (§ 4.3).

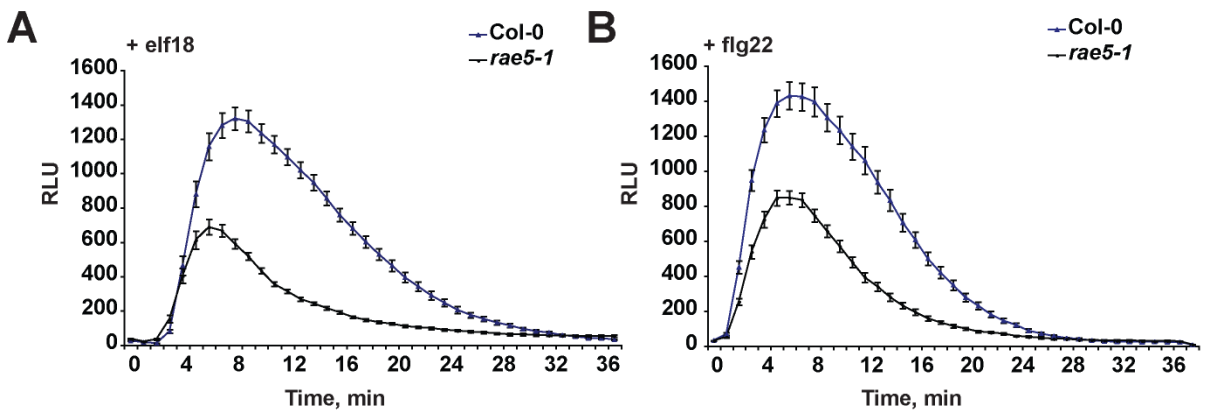


**Figure 4.7. RAE5 is a positive regulator of ROS burst.**

ROS production over time represented as relative light units (RLU) in Col-0 and *rae5-1* seedlings after elicitation with 100 nM elf18 (A) or flg22 (B). Results are average  $\pm$  standard error ( $n=8$ ).

### 4.3 Discussion

#### 4.3.1 RAE5: PRR regulator?

RAE5 was identified as a putative EFR-interacting protein based on its presence in EFR IPs (Table 2.1 and 4.1). RAE5 peptides were detected before and after elf18 elicitation, suggesting that the interaction is already in place prior to PAMP perception. The MS data is not quantitative, thus it is not possible to assess the differential abundance of RAE5. Immunoprecipitation analysis of co-expressed proteins in *N. benthamiana* however does suggest that interactions are enhanced by PAMPs. This could indicate a ligand-enhanced complex formation, at least under the conditions used here. Further control experiments should be done to confirm whether RAE5 is sticking to anti-GFP IP beads, for example co-expression with an unrelated kinase, for example CLAVATA1-GFP (CLV1) followed by GFP IP. In parallel, interactions could be assessed using a different experimental method such as split-YFP analysis.

It was not possible to study the interaction properties of RAE5 in *Arabidopsis*, likely due to low endogenous levels of RAE5 protein, a fraction of which may be engaged in complex formation. Unfortunately, the anti-RAE5 antibodies were unable to detect RAE5 during immunoprecipitation experiments, suggesting that the recognition epitope is hidden within the folded protein. There are several possible reasons for the inability to detect RAE5 in *Arabidopsis* IPs of EFR, FLS2 or BAK1, in contrast to evidence obtained in *N. benthamiana*. One possibility is that there is no interaction and the peptides detected in the MS

analysis of EFR IPs were false positives, purely sticking non-specifically to the GFP beads.

A more probable explanation is that an interaction occurs but cannot be detected by co-IP analysis of proteins at native expression levels in Arabidopsis. RAE5 peptides were identified in EFR IPs by mass spectrometry, which has a femtogram detection limit, while the immunoblotting experiments conducted here were at the picogram detection limit. To overcome this limitation, these experiments could be repeated using an ultra-sensitive chemiluminescent substrate and bulking up the amount of immunoprecipitate used for Western blotting. In addition, microsomal preparation prior to immunoprecipitation could enrich for RAE5 and its membrane-associated interactions. With these experimental improvements, we will attempt to characterize the RAE5 complexes. In addition, we have prepared transgenic Arabidopsis lines expressing C-terminally-tagged RAE5 under the control of the 35S promoter in a *rae5-1* background. We have also combined these with tagged EFR transgenic lines to obtain double transgenic lines for co-immunoprecipitation experiments. Further analysis of complex kinetics and specificity will be assessed when transgenic tagged lines become available.

Data obtained so far point to a role for RAE5 as a positive regulator of PTI. ROS burst in response to *elf18* and *flg22* was compromised in *rae5-1*, however MAP kinase activation and seedling growth inhibition are maintained (Freddy Boutrot, data not shown). However, we have yet to place RAE5 in the signaling network and have not determined its mode of action.

According to Dardick and Ronald, RD kinases are associated with roles in plant defense, and tend to require activation loop phosphorylation for their function (Dardick and Ronald, 2006). RAE5, in contrast to EFR and FLS2, is an RD kinase (see alignment [Appendix Figure A4.1](#)). In future work, we need to address the potential role of RAE5 as an activator of PRRs via a mechanism of transphosphorylation. Interestingly, differential RAE5 phosphorylation has previously been detected in response to *flg22* and xylanase elicitation in large-scale proteomic studies (Nühse *et al.*, 2004; Benschop *et al.*, 2007). Unusually, the phosphosites detected (T745, S747; S749) were in the juxtamembrane and C-terminal regions of the kinase domain, and not in the activation loop where several

RD kinases are commonly activated (Johnson *et al.*, 1996), suggesting another method of regulation may be required for RAE5. EGF receptor is not activated by transphosphorylation of the activation loop, rather an allosteric mechanism promotes dimerization and activates the receptor (Jura *et al.*, 2009; Red Brewer *et al.*, 2009). It is possible that such a regulatory mechanism exists for RAE5, but much work remains to be done before gaining a deeper understanding of its mechanism of action.

Of further interest, one of the detected RAE5 phosphosites, T745, corresponds to a putative EFR phosphosite (S683) detected by MS/MS analysis in this work ([Table 2.3](#)). The fact that phosphorylation has been detected at the same location on these related receptor kinases may point to a shared regulatory mechanism. However, the phosphorylation of RAE5 T745 detected by Benschop *et al.*, 2007 was differentially modified in response to flg22 elicitation, while the EFR S683 phosphorylation was detected in untreated EFR IPs. Of course these results were obtained in separate laboratories and thus cannot be directly compared.

RAE5 may act as a general co-activator of PTI components through transphosphorylation of the kinase domain of PRRs or associated RKs (SERKs or other RAEs), thus the kinase activity of RAE5 will need to be tested. I have cloned constructs for *in vitro* expression of RAE5 kinase domains in order to test for autophosphorylation and transphosphorylation of artificial substrates as well as EFR, FLS2, BRI1, OXI1 and BAK1 kinase domains. Preliminary expression trials indicate that the RAE5 kinase domain (wild-type and kinase-dead versions) can be expressed in *E. coli* as soluble protein, thus the purification and *in vitro* assays remain to be done. In addition, it would be useful to create phosphodead and phosphomimetic mutant constructs to test the importance of the previously detected RAE5 phosphorylation sites. I have already initiated transgenic lines expressing kinase-dead (D905N mutant) RAE5 to determine the phenotypic consequences of loss-of-function of RAE5 kinase activity in defense signaling.

#### 4.3.2 RAE5 and its potential link with OXI1, lipid signaling and cell death control

RAE5 was identified as a yeast-two hybrid interactor of OXI1, and this interaction was confirmed by co-IP of these proteins in *N. benthamiana*. OXI1 is a Ser/Thr kinase of the AGC VIIb subfamily, originally identified due to its induction in response to ROS (Rentel *et al.*, 2004). OXI1 was subsequently shown to be required for resistance to infection by hemi-biotrophic bacterial and biotrophic oomycete pathogens (Rentel *et al.*, 2004; Petersen *et al.*, 2009). The role of OXI1 in *Arabidopsis* defense remains elusive, as the preceding work has only partially addressed this question. So far, it is known that phosphorylation of OXI1 is induced by peroxide and cellulase, which also induce MPK3 and MPK6 activation. *Oxi1* mutants are compromised in MPK3/6 activation, placing OXI1 upstream of MPK activation and downstream of ROS (Rentel *et al.*, 2004).

In addition, glycerophospholipid metabolism is also linked to OXI1-mediated signaling. Phospholipase D (PLD) hydrolyzes lipid head groups to produce phosphatidic acid (PA), which acts as a second messenger in plants. Phosphatidic acid (PA) is also produced by the sequential reactions catalyzed by phospholipase C (PLC) and diacylglycerol (DAG) kinase (DGK) (Testerink and Munnik, 2005). PLC hydrolyzes phosphatidylinositol-4,5-biphosphate (PtdIns(4,5)P<sub>2</sub>) into inositol-1,4,5,-triphosphate (Ins(4,5)P<sub>3</sub>) and DAG. DAG is phosphorylated by DGK to form PA (Testerink and Munnik, 2005) ([Appendix Figure A4.4](#)). The role of PA in signaling can be either in the modification of enzyme activity or by acting as docking sites for recruitment of proteins. PA plays important roles in diverse signaling pathways, including responses to ABA, H<sub>2</sub>O<sub>2</sub>, cold and osmotic stress (Wang *et al.*, 2006b). PA production is induced by the application of flg22 and xylanase to tomato cells (van der Luit *et al.*, 2000) and by Avr4 elicitation of Cf4 tobacco (de Jong *et al.*, 2004). PA binds to several targets in plants in order to mediate signaling.

Another plant PA target is PDK1 (phosphatidyl-inositol-dependent protein kinase 1), whose activity is enhanced by binding PA and PtdIns(4,5)P<sub>2</sub> (Anthony *et al.*, 2004). PDK1 has been shown to activate OXI1 via PA, as well as to phosphorylate OXI1 at a conserved site *in vitro* (Anthony *et al.*, 2004).

PA also binds to MPK6 in response to salt stress (Yu *et al.*, 2010), while in *Vicia faba* guard cells, ABA-induced PA inhibits protein phosphatase 1C and H<sup>+</sup>-ATPases to inhibit blue-light induced stomatal opening (Takemiya and Shimazaki, 2010).

Importantly however, another prominent PA target is NADPH oxidases (Zhang *et al.*, 2009b). PA binds to and activates AtRbohD, linking PA to ROS production, which may be responsible for OXI1 activation (Zhang *et al.*, 2009b). This is corroborated by earlier studies with evidence for PA-induced ROS production. When *PLD $\alpha$*  is silenced in Arabidopsis, PA and AtRboh-derived superoxide levels are decreased and this can be reversed by the application of exogenous PA (Sang *et al.*, 2001). Chitooligosaccharides induce a biphasic ROS burst in rice cells, which correlates with phospholipase activities (Yamaguchi *et al.*, 2005). The first ROS peak is PLC and PLD-dependent while the second peak is dependent on PLD activity (Yamaguchi *et al.*, 2005). Application of PA or DG also induces expression of defense genes and phytoalexin production (Yamaguchi *et al.*, 2005).

OXI1-interacting proteins include the Arabidopsis relatives of tomato S/Pti1, PTI1-1, PTI1-2 and PTI1-3 (see [Appendix Figure A4.5](#)) (Anthony *et al.*, 2006), identified in Y2H assays. The kinase activity of PTI1-2, a phosphorylation target of OXI1, was enhanced by treatment with flg22, xylanase and PA (Anthony *et al.*, 2006), but it is not yet known what role this plays in disease resistance or cell death control, if any.

Rice OsOXI1 is transcriptionally regulated by ROS, and phosphorylated in response to H<sub>2</sub>O<sub>2</sub> and chitin (Matsui *et al.*, 2010). Furthermore, OsOXI overexpression lines are more resistant to *X. oryzae* pv. *oryzae*, suggesting a role for OsOXI1 in basal resistance. Furthermore, OsOXI also interacts with and phosphorylates OsPti1a, the modification of which is required for disease resistance (Matsui *et al.*, 2010).

Interestingly, the Arabidopsis OXI1 interactor PTI1-1 is predicted to be co-expressed (ATTED II) with the LCB2 (long chain base 2) subunit of serine palmitoyltransferase (SPT), an enzyme upstream of ceramide synthase in the ceramide (N-acetylsphingosine) biosynthetic pathway (see [Appendix Figure A4.6](#);

(Shi *et al.*, 2007). Mutations in this pathway, such as *acd11*, which is mutated in sphingosine transfer protein, lead to constitutive cell death (Brodersen *et al.*, 2002). Furthermore, the penultimate products of this pathway, sphingosine and dihydrosphingosine, have antagonistic roles in the induction of cell death (Shi *et al.*, 2007). Tomato and rice *Pti1* homologs are involved in cell death suppression, but *Pti1* loss-of-function lines have yet to be tested (Zhou *et al.*, 1995; Matsui *et al.*). Similar experiments have also not yet been done for *Arabidopsis Pti* homologs, and their biological role remains unknown. *oxi1* mutants do not have a lesion mimic phenotype, but this could be due to redundancy at this level in the pathway. Overall, the connection between *OXI1*, *Pti1* and PA-related signaling supports the role of *OXI1* in oxidative stress-induced signaling, but the link to plant defense or possibly cell death control remains to be explored.

Using confocal analysis, Freddy Boutrot has detected *OXI1-GFP* at the cell periphery, but the subcellular localization of its substrates has not been tested in rice or *Arabidopsis*. Loss-of-function lines for rice and *Arabidopsis Pti1* orthologs have to be assessed for the influence of *Pti* on disease resistance, as well as PTI signaling. Thus far *oxi1* mutants have not been found to be compromised in PTI signaling (Freddy Boutrot), although *oxi1* mutants display reduced activation of MPK3 and MPK6 (Rentel *et al.*, 2004). It is possible that the role of *OXI1* is somehow linked with that of *RAE5*, perhaps as a rapid means of activating cell death in the presence of avirulent pathogens. In our hands, *rae5-1* mutants do not display a lesion mimic phenotype or enhanced cell death in response to inoculation with *Pto DC3000* (Freddy Boutrot), however a collaborator has observed spontaneous cell death and premature senescence in *rae5* mutants (Birgit Kemmerling, U. of Tübingen, personal communication).

To assess the potential role of *RAE5* in oxidative stress, Freddy Boutrot will test ion leakage of *rae5* mutants in response to peroxide, ozone, paraquat and light. In parallel, we will make use of wild-type and *rae5* plants expressing the  $H_2O_2$  sensor HyperC (Belousov *et al.*, 2006) to monitor the production of ROS *in planta*. To probe the role of *RAE5* in defense responses, we are testing *rae5* disease resistance to virulent and avirulent strains of *Pseudomonas* and *Hpa*, as well as PAMP-induced MAP kinase activation and defense gene induction. Freddy

will determine role of RAE5 in ETI responses by measuring ion leakage in response to infiltration with *Pto* DC3000 expressing AvrRpm1 or AvrRpt2.

#### 4.3.3 RAE5 complex dynamics and potential ETI-PTI bridge

RAE5 was recently identified by MS analysis as part of RPS2 immunocomplexes (Qi and Katagiri, 2009), invoking a novel role for RAE5 in a putative PTI-ETI bridging complex, which may serve to rapidly activate the more intense ETI signaling responses when PTI is unable to overcome initial pathogen ingress. To test this hypothesis, it would be necessary to identify the components of the complex. It is known that RPS2 interacts with RIN4 at the plasma membrane (Belkhadir *et al.*, 2004), and RIN4 is a puzzling protein with no domains of known function and an unknown mechanism of action. Modification of RIN4 by AvrRpt2, AvrRpm1 or AvrB results in the activation of RPS2 or RPM1, and HR (Mackey *et al.*, 2002, 2003). However, AvrRpt2, AvrRpm1 and AvrB retain virulence functions in the absence of their cognate resistance proteins and RIN4 (Belkhadir *et al.*, 2004), suggesting there are alternative effector targets, protected by RIN4 acting as a decoy. Alternatively, some as yet uncharacterized manipulation of RIN4 by these effectors may promote pathogen virulence.

It is conceivable that a large complex occurs at the membrane, comprising PTI components such as FLS2, EFR, RAE5, BAK1, BKK1, and this is in turn loosely associated with ETI components such as RPS2, perhaps via RIN4. *Bak1-4 bkk1-1*, *bir1* and *mpk4* mutants suffer from constitutive cell death (He *et al.*, 2007; Gao *et al.*, 2009) (Petersen *et al.*, 2000), which could be a hypersensitive cell death reaction induced by resistance proteins when they detect the loss of a guardee. A similar situation has been proposed for the lesion mimic mutant *acd11*, as a resistance protein was identified in an *acd11*-suppressor screen (Palma *et al.*, 2010). We have preliminary data suggesting an interaction between FLS2 and MPK4, which is abolished in the presence of flg22 (data not shown). MPK4 is also targeted by AvrB, which indirectly leads to MPK4 phosphorylation (Cui *et al.*, 2010). Normally, MPK4 sequesters WRKY33 in a ternary complex with MKS1 (Qiu *et al.*, 2008). Following treatment with flg22 or infection with *Pto* AvrRpm1, WRKY33 is released from MPK4 and upregulates *PAD3* expression (Qiu *et al.*, 2008). MPK4 likely negatively regulates SA-mediated defenses, which are active

against biotrophic pathogens such as *Pto* DC3000, thus MPK4 targeting is part of the virulence strategy. Similarly, RIN4 is required for JA responses, which are induced in plants ectopically expressing AvrB (Cui *et al.*, 2010).

NB-LRRs have limited variability in their substrate binding specificity, thus it is possible that RPM1 and RPS2 are expanding their repertoire of guardees by indirectly guarding PTI components such as RAE5. Recently, the RLCKs BIK1 and PBS1 were found to interact with FLS2 *in planta* and dissociate in response to PAMP treatment (Lu *et al.*, 2010; Zhang *et al.*, 2010a). Importantly, PBS1 is cleaved by the *P. syringae* effector AvrPphB, and this activity is guarded by RPS5 (Ade *et al.*, 2007). This provides yet another link between PTI and ETI.

One hypothesis is that prior to PAMP activation a complex/es exist(s) comprising FLS2, EFR, BAK1, RAE5, RIN4, MPK4, BIK1, PBS1 and PBLs, which in effect sequester defense in a negatively regulated state. This complex uses RIN4 as a scaffold to mediate interactions with the associated R proteins RPM1, RPS2 and RPS5, possibly via NDR1. Upon PAMP treatment, BAK1 and BKK1 associate more closely with the PRRs, possibly to cause transphosphorylation of the receptors. This may explain the subsequent release of BIK1 and MPK4, which are freed to carry out downstream signaling functions such as target phosphorylation and defense gene activation. In the presence of an effector (and in the absence/presence of the cognate R gene), these defenses would be overcome by effector-mediated PTI suppression, through degradation of PBS1 by AvrPphB, or BAK1 inhibition by AvrPto, or FLS2 degradation by AvrPtoB for example. In the presence of the cognate R gene, PTI responses would need to be modulated by ETI machinery to create a more fatal reaction to suppress further infection by virulent pathogens. Now effector activity on host virulence targets would alert the R proteins to their presence. As PTI and ETI signaling components are hooked together by RIN4, defense responses initiated by PTI could be appropriated by ETI to deliver a lethal defense response to the offending pathogens.

In order to biochemically test parts of these hypotheses, we will test for the following interactions: FLS2-RAE5, BAK1-RAE5, RPS2-RAE5, RAE5-RIN4; FLS2-BIK1. In order to determine whether interactions are direct or via other proteins, the same IPs will be done in *bak1-4*, *fls2*, *oxi1* and *rae5-1* mutants. RAE5 over-expression lines, which are currently at the T2 stage, will be used to facilitate detection of RAE5-PRR interactions. I have done experiments to detect whether

FLS2 and EFR can interact with RIN4, and I have not been able to detect interactions by co-IP in Arabidopsis (data not shown). However, the interaction may be weak and detectable using cross-linking or Dex-inducible RIN4 lines for enhanced RIN4 detectability.

The next set of experiments will assess the effect of effectors, such as AvrRpt2, on putative complex formation of FLS2-RAE5 and RPS2-RAE5. Assuming these interactions occur via RIN4, they should be abolished in the presence of AvrRpt2. This model also needs to be tested genetically. Experiments done by F. Boutrot indicate that RAE5 is required for AvrRpt2-induced HR, as *rae5-1* mutants display reduced ion leakage in response to this effector. These data correlate with the identification of RAE5 in immunoprecipitates of RPS2, and suggests an exciting link between PTI and ETI signaling components.

Finally, the function, if any, of the alternate *RAE5.2* transcript should also be tested. *RAE5.2* has been cloned and will be transiently expressed in *N. benthamiana* to determine whether the protein can be detected by confocal microscopy as well as Western blotting. If the *RAE5.2* protein is detected, the next step will be to determine whether it is also associated with RKs by transient co-expression and immunoprecipitation. Depending on the result, further experiments would need to be done, for example determining whether *RAE5.2* is a negative or positive regulator of EFR or RAE5 itself.

Finally, it is important to consider a possible role for RAE5 in brassinosteroid (BR) signaling, as RAE5 was associated with BRI1 when transiently co-expressed. *rae5-1* and *rae5-1 xii1-1* plants do not display the cabbage-like phenotype characteristic of brassinosteroid mutants, suggesting that their role in BR signaling would likely be indirect. Initially, it is necessary to confirm whether RAE5 interacts with BRI1 in Arabidopsis, using anti-BRI1 to probe RAE5 pulled down in tagged RAE5 transgenic lines (in progress). To study BR signaling, several assays need to be carried out in *rae5-1* plants. For example, testing BR-responsiveness of etiolated seedlings by assessing growth in the presence of different concentrations of BL and the BR synthesis inhibitor BRZ. Furthermore, the expression of BL-responsive marker genes could be tested in *rae5-1* and *rae5-1 xii1-1*. To reveal any genetic requirement of *RAE5* for brassinosteroid signaling, double mutants will be created with the weak *bri1* allele *bri1-103* as well as *bak1-4*.

## 5 Parting shots - RAEs of insight

### 5.1 Preface

During my dissertation I was able only to do a few initial experiments towards the characterization of the other RAEs identified in the EFR IPs in *Arabidopsis*. Nonetheless, I think this section merits mentioning, as candidate EFR interactors could hold the keys to unlocking downstream PAMP-induced signaling.

RAE6 (At3g14840) is a member of the subfamily VIII-2 of LRR-RKs I (Shiu and Bleecker, 2001), consisting of 14 members ([Appendix Figure A5.1](#)), 3 of which also encode alternative transcripts (alignment of alternative transcript [Appendix Figure A5.2](#)). Interestingly, RAE6, and most of the other family members, possesses an N-terminal malectin-like domain, in addition to LRR and kinase domains found in other LRR-RKs. Malectin is an ER-membrane-anchored protein initially identified in *Xenopus laevis*, and domains resembling this protein have subsequently been found in many other species (Schallus *et al.*, 2008). Malectin recognizes and binds Glc<sub>2</sub>-N-glycan, suggesting a possible role as chaperone or recruiter of chaperones in the early N-glycosylation of proteins (Schallus *et al.*, 2008). The malectin domain has low homology to the mammalian sequence, and the residues mediating the carbohydrate interaction are not conserved. However, the possibility exists that the protein still mediates a related function in *Arabidopsis*. Interestingly, the N-glycosylation machinery is vitally important for EFR function, as demonstrated in several recent publications (Li *et al.*, 2009a; Lu *et al.*, 2009; Nekrasov *et al.*, 2009; Saijo *et al.*, 2009; Häweker *et al.*, 2010). Furthermore, RAE6 is predicted to be co-expressed with several genes related to plant defense, including FLS2, PEN3 and MKK1 ([Appendix Table A5.1](#)).

RAE7 (At1g51800) is LRR-RK of subfamily I ([Appendix Figure A5.3](#)) (Shiu and Bleecker, 2001), members of which have 3 LRRs in the extracellular domain. Importantly, expression of RAE7 is enhanced by PAMP treatment (BAR <http://www.bar.utoronto.ca/>). Another member of this family is flagellin-induced receptor kinase 1 (FRK1), which is rapidly induced by flg22 treatment of

Arabidopsis protoplasts, leaves, and seedlings (Asai *et al.*, 2002; He *et al.*, 2006). Accordingly, several PAMP-induced marker genes are co-expressed with *RAE7* ([Appendix Table A5.2](#)) including LRR-RK subfamily I members *FRK1* and *At1g51890*, as well as unrelated DC1-domain-containing protein *At2g17740* (He *et al.*, 2006).

*RAE8* (*CRK11*, *At4g23190*) is a member of the cysteine-rich RKs, which feature two copies of the DUF26 C-X8-C-X2-C motif in their extracellular domains. This is a large family, with over 40 members in Arabidopsis ([Appendix Figure A5.4](#)) often arranged in tandem arrays in the genome (Chen, 2001). *CRK11* is most closely related to *CRK22* and *CRK13*. The cysteine-rich motif shared by this group of RKs could be subject to redox regulation, and alterations in the disulphide-bonding pattern in the extracellular region could act as a stress signaling mechanism. In addition to six other CRKs, *CRK11* gene expression is induced by salicylic acid (SA), bacterial pathogen infection and oxidative stress (Czernic *et al.*, 1999; Du and Chen, 2000). Interestingly, the *CRK11* gene contains W boxes in the promoter, which may allow its regulation by the binding of WRKY transcription factors (Du and Chen, 2000). Recent work has shown that *CRK11* gene expression is 10-fold up-regulated in response to *flg22*, and altered in *sid2* and *npr1* backgrounds, depending on growth conditions (Wrzaczek *et al.*, 2010). Previous work has shown enhanced resistance to *Pto* DC3000 in plants over-expressing *CRK5* but not *CRK11* (Chen *et al.*, 2003). Inducible expression of *CRK4*, *5*, *19* and *20* led to cell death, which at least for *CRK5* was independent of SA (Chen *et al.*, 2003). In contrast, over-expression of *CRK13* led to enhanced resistance to *Pto* DC3000 linked to increased SA levels (Acharya *et al.*, 2007).

Analysis of RK subfamilies induced by particular biotic stressors has revealed that certain subfamilies are over-represented among responsive genes ([Figure 5.1](#) from Lehti-Shiu *et al.*, 2009). Interestingly, the RAEs all belong to subfamilies whose expression is generally upregulated in response to biotic stresses including DUF26 (*CRK11* member), LRR-I (*RAE7* member), LRR-VIII-2 (*RAE6* member), LRR-Xb, RLCK-VIIa, SD1, SD-2b, L-LEC, WAK and WAK-LRK10L-1.

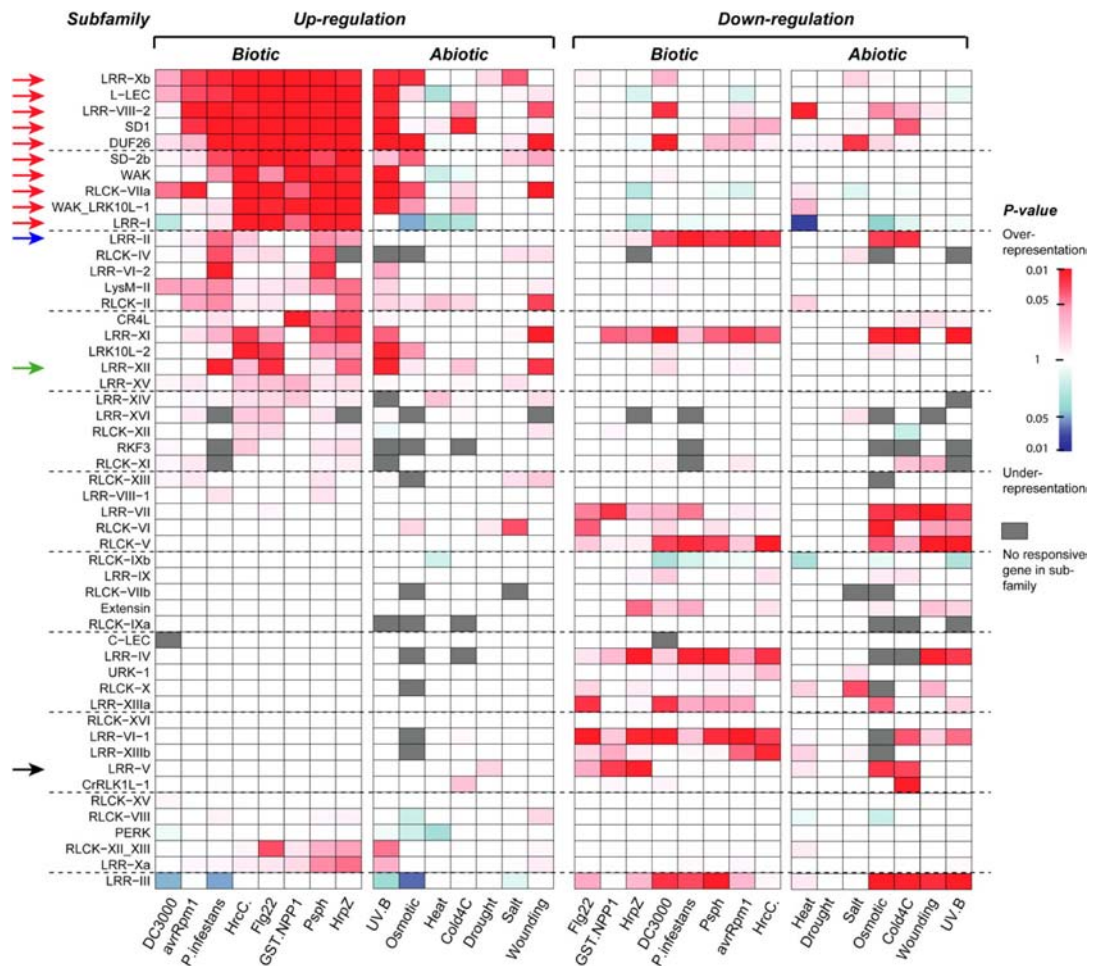


**Figure 5.1 RLK/Pelle subfamilies enriched in up- and down-regulated genes under abiotic and biotic stress conditions from Lehti-Shiu et al., 2009.**

Enrichment of stress-responsive members in each subfamily was determined by Fisher's exact test, with red shading indicating overrepresentation and blue shading indicating underrepresentation. A gray box indicates that no gene in that subfamily was up or down-regulated. Red arrows indicate subfamilies with responsiveness to a broad range of biotic signals. The black arrow indicates the LRR-V subfamily whose members have functions in development, and the blue arrow indicates the LRR-II subfamily whose members function in both development and disease resistance, and include the SERKs. The green arrow indicates the LRR-XII subfamily.

## 5.2 Preliminary results

By mass spectrometric analysis of EFR IPs, 8 RAE6-specific peptides were identified with Mascot scores above 20 and peptide identification probability of 95 % (Table 5.1). Only one of these peptides also matches other members of the subfamily VIII-2; the others are unique to RAE6. The peptide matches are distributed across the length of the protein, as indicated in [Appendix Figure A5.2](#) where peptides are lowercase.

RAE7 was identified by MS analysis of EFR IPs, with 6 matching peptides, 5 of which are unique to RAE7 and one of which matches several of the subfamily LRR-I members ([Table 5.1](#)).

RAE8/CRK11 is represented by 3 peptides, although only one of these, located at the C-terminus of the protein, is specific to CRK11 ([Table 5.1](#)).

I did not yet confirm the interaction between RAE6, 7 or 8 and EFR, and no antibodies are available for these proteins. Constructs for transient expression as well as transgenic lines expressing tagged RAE need to be generated towards this end.

**Table 5-1 RAE peptides identified by MS analysis of EFR immunoprecipitates**

Bio. Rep.	Peptide sequence	Mascot Ion score <sup>^</sup>	Mascot ID score <sup>\$</sup>	Other matches
<b>RAE6 At3g14840.2</b>				
EFRefl_3	ATNVLLDKELNPK	46.5	19.1	
EFRefl_3	EQNTLLEVVDPR	50.2	21.5	
EFRefl_3	EVKDFNIVDEAK	37	23.9	
EFR 2	GlmTDGTVIAVK	58.2	29.7	
EFR 1	ISDFGLAK	38	25.9	At1g5342/3/40; At1g56130; At1g07650
EFRefl_3	LLEASVNNEKDEESVR	44.5	23.8	
EFRefl_3	LLEASVNNEKDEESVR	91.7	23.7	
EFRefl_3	RYFDIYVQGK	38.8	23	
EFR_elf18 1	VATDNFDPANK	29.8	22.9	
EFR 2	VATDNFDPANK	48.5	18.9	
EFR 1	VATDNFDPANK	50.2	22.5	
EFRefl_3	VATDNFDPANK	69	22.4	
<b>RAE7 At1g51800</b>				
EFR 2	ADVGATVNQGYR	57.7	19.1	
EFRefl_3	ADVGATVNQGYR	63.8	23.3	
EFRefl_2	ADVGATVNQGYR	67.9	20.1	
EFR 2	AEVELLLR	23.8	21.4	Several in family
EFRefl_3	AEVELLLR	37.9	20.1	Several in family
EFRefl_3	KLTYIDVVK	30	15.9	
EFRefl_3	RGPSILTWEGR	36.2	21.5	
EFRefl_3	TQFQQQTWNLR	59.3	23.4	
EFRefl_3	YGIDVFDR	41.3	23	
<b>RAE8 At4g23190 (CRK11)</b>				
EFR 2	ASNILLDADmNPK	44.5	29	12 members
EFR 2	ASNILLDADmNPK	69.9	29	12 members
EFRefl_3	GILYLHQDSR	37.8	22.6	18 members
EFR 2	LVSEGSESDQYTSK	45.3	15.4	
EFRefl_3	LVSEGSESDQYTSK	97.5	23.3	

lowercase m indicates modification by oxidation (+15.99);

all peptides have peptide ID probability (Scaffold calculated probability that a given protein has been identified correctly) of 95%.

<sup>^</sup> Mascot Ion Score is a measure of how well the observed MS/MS spectrum matches to the stated peptide

<sup>\$</sup> Mascot identity score: a minimum ion score threshold. As a rule, the ion score should be above the identity score. identity score=-10\*(log(p/#matches)), where p is your probability threshold (Scaffold uses 1.0), and #matches is the number of precursor matches.

In order to evaluate the potential role of RAE6 in PTI signaling, I obtained several homozygous *rae6* loss-of-function lines. ROS burst in response to flg22 and elf18 in *rae6-1* (Salk\_040386) is similar to that of Col-0, albeit slightly delayed in response to elf18 ([Figure 5.2A](#)). Compared to Col-0, *rae6-1* appeared to be slightly less sensitive to elf18 and flg22 in the seedling growth inhibition assay ([Figure 5.2B](#)). The T-DNA insertion in *rae6-1* is predicted to be within the 16<sup>th</sup> exon, encoding the malectin domain. Semi-quantitative RT-PCR analysis of *rae6-1* indicates the presence of a truncated transcript, not a true knockout in this line, as primers annealing at 670 bp, but not primers that anneal closer to the C-terminus at position 1450 bp of the transcript could amplify a product (data not shown). Additional insertion lines *rae6-2* (Salk\_030855) and *rae6-3* (Salk\_094512) were obtained in an attempt to isolate a *RAE6* null mutant line. *rae6-2* insertion is predicted within the 2<sup>nd</sup> intron while *rae6-3* insertion is predicted within the 5' UTR. ROS burst occurred in both *rae6-2* and *rae6-3* with a similar amplitude and timing to Col-0 responding to elf18 and flg22 ([Figure 5.2C](#)). Elf18 and flg22-induced seedling growth inhibition of these mutants also did not appear to be compromised ([Figure 5.2D](#)).

It is possible that the *rae6* alleles tested displayed wild-type PAMP response due to redundancy, and the relative transcript abundance of *RAE6* in *rae6-2* and *rae6-3* remains to be tested. A closely related LRR-RK (At1g53420) with 60% homology on the protein level may be able to assume RAE6 function in its absence ([Appendix Figure A5.2](#)). I have obtained homozygous insertion lines for this gene in order to produce double mutants.

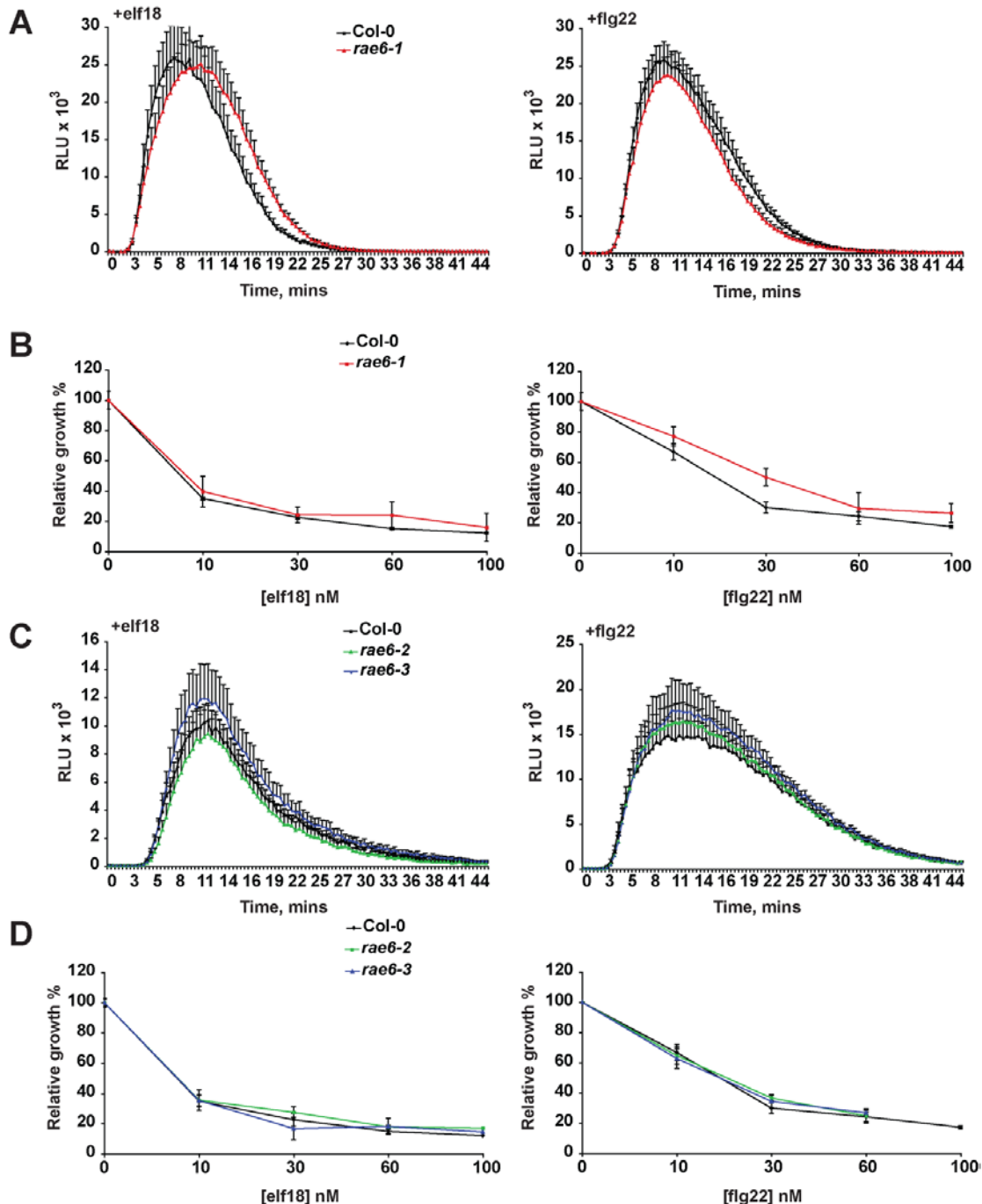


**Figure 5.2 rae6 single mutants respond with wild-type-like ROS burst and seedling growth inhibition.**

A. Production of ROS in Col-0 and *rae6-1* leaf discs in response to 100 nM elf18 (left) or 100 nM flg22 (right) elicitation. RLU = relative light units. Results are average  $\pm$  standard error ( $n=8$ ). This experiment was repeated twice.

B. Growth inhibition in response to increasing concentrations of elf18 (left) or flg22 (right) in Col-0 and *rae6-1* seedlings. Represented as % fresh weight of untreated seedlings. Results are average  $\pm$  standard error ( $n=6$ ). This experiment was repeated twice.

C. Production of ROS in Col-0, *rae6-2* and *rae6-3* leaf discs in response to 100 nM elf18 (left) or 100 nM flg22 (right) elicitation. RLU = relative light units. Results are average  $\pm$  standard error ( $n=8$ ). This experiment was repeated once.

D. Growth inhibition in response to increasing concentrations of elf18 (left) or flg22 (right) in Col-0 *rae6-2* and *rae6-3* seedlings. Represented as % fresh weight of untreated seedlings. Results are average  $\pm$  standard error ( $n=6$ ). This experiment was repeated once.

### 5.3 Discussion

No co-IP experiments have been carried out to confirm any of the RAEs as true EFR interactors, and this will be the primary goal of future work. Nonetheless, the mass spectrometry data provides compelling evidence of the presence of multiple RRs associated with EFR ([Table 2.1](#) and [Table 5.1](#)).

The localization of these interactions will also need to be characterized. This could be addressed in a cell biological approach employing fluorescently tagged RAEs and EFR, transiently expressed and/or in transgenic lines. To this end, I have initiated production of transgenic lines expressing RAE6-eYFP for crossing with EFR-eGFP transgenic lines. Co-localization by confocal microscopy in parallel with known subcellular marker lines could be combined with split-YFP to confirm interactions.

Next, it will be important to determine what the function of confirmed interacting RAEs might be for EFR function or associated signaling pathways. To this end, several independent loss-of-function lines will need to be obtained for each RAE and closely related members. For RAE7 and RAE8, several closely related RRs are present ([Appendix Figure A5.3](#) and [A5.4](#)). Thus a microRNA silencing approach will likely be necessary to overcome redundancy. In parallel, a gain-of-function approach, by over-expression of RAEs, could be informative.

It is conceivable that RAE6 for example could constitute an ER-localized EFR-RAE complex, as the presence of a malectin-like domain in this protein hints at a function in ER-QC. If *elf18* signaling is compromised in *rae6* double mutant knockout lines, EFR *N*-glycosylation could be studied using EndoH assays to characterize the nature of *N*-glycans present in EFR when expressed from a *rae6* mutant background. Alternatively, RAE6 may be required for correct targeting of EFR to the PM. For example, the RLP CLV2 (CLAVATA2), involved in the regulation of stem cells in the meristem, interacts with the kinase CRN (CORYNE) (Bleckmann *et al.*, 2010; Zhu *et al.*, 2010b), and these proteins rely on each other to achieve membrane localization. In the absence of either one, they are retained in the ER (Bleckmann *et al.*, 2010).

Putative RAE6-co-expressed genes ([Appendix Table A5.1](#); Expression Angler; Pearson correlation co-efficient > 0.5) include a cellulose synthase-like gene (CSLC4), a putative  $\beta$ -D-glucan exohydrolase, galactosyltransferase, supporting a

possible role for RAE6 in glycosylation or ER-QC. Interestingly, RAE6 is predicted to be co-expressed with PEN3, MKK1, PCS1 and FLS2, linking RAE6 with defense responses. In fact, co-expression analysis of all RAEs reveals several genes commonly co-expressed, hinting that these genes function in the same pathway (Appendix Tables [A5.1-A5.3](#)).

All of the RAEs are RD kinases, in contrast to EFR, which is a non-RD kinase. As mentioned in the [discussion](#) in Chapter 4, receptor transphosphorylation is a common mechanism of activation, and RAEs could play a role in this mechanism.

The link between ROS and the RAEs could be mediated through OXI1 and CRK11. Publicly available gene expression data shows the *CRK11* is induced by abiotic stress such as UV and osmotic stress, and in response to flg22, NPP1 and HrpZ (<http://www.bar.utoronto.ca/>). A recent study employed *in silico* analysis of CRK family gene expression responding to ozone and biotic stress (from the same source) to try to discern any connections between these receptors and responses to oxidative stress (Wrzaczek *et al.*, 2010). Hypothetically, the cysteine-rich DUF26 motif could act as a redox sensor and its modification could signal changes such as oxidative stress or ROS burst in response to pathogens, which could then be transmitted downstream to intracellular changes to enhance cellular defenses.

So far, no data supports this notion, however it is tempting to imagine such redox-related CRK11 modification as a rapid switch to engage defenses, possibly to create a positive feedback loop for signal amplification in response to PAMP detection. So far, over-expression or RNAi of *CRK11* has had no impact on disease resistance responses (Chen *et al.*, 2003), however in this study the authors did not provide evidence for CRK11 protein accumulation in their knock-down or over-expression lines. To further study CRK function in PAMP signaling, double *crk11 crk22* mutants may be necessary. RNAi could be used to silence *CRK11* and its closest homolog *CRK22*, as it is likely to be difficult to obtain double mutants of such chromosomally proximal genes.

*This project is being continued by a postdoc in the laboratory, Vladimir Nekrasov.*

## 6 General Conclusions and Outlooks

Signal transduction is expedited by the formation of signaling complexes, usually comprised of enzymes (kinases/phosphatases), their substrates and adaptor or scaffolding proteins. These complexes may be associated with the plasma membrane through protein-protein interactions, for example with transmembrane receptor proteins, as in the case of EFR. Complex assembly enhances signaling efficiency and specificity, and thus complex composition is of great interest. Several questions arise when considering signaling complexes: what is complex composition and stoichiometry? When and where are complex(es) formed? How do complex(es) affect downstream signaling? Answering all these questions requires a combination of techniques including proteomics, microscopy and genetic approaches. The affinity purification approach used in this thesis has been extensively employed in other complex purification studies (Gingras *et al.*, 2007). We have not answered all the questions regarding the EFR signaling complex, but we have taken the first steps.

It is possible that the EIPs identified in this study actually comprise a population of distinct multiprotein complexes, perhaps with varying tissue or subcellular localization, which could not be resolved using co-immunoprecipitation. Future work might use blue-native PAGE or gel filtration chromatography to isolate the EFR complex(es) from different tissues or under different conditions (un/elicited/with effectors/infected tissues). This would be complemented by studies of subcellular co-localization of EFR and EIPs, under several conditions and in different tissues, or with truncations to determine the molecular site of interactions. Furthermore, a cell biological approach employing microscopic detection of fluorescently tagged EFR and RAEs will provide valuable insight into the subcellular localization of RAE complexes. These could also be used to assess the effect of RAEs on potential EFR endocytosis, or differential localization induced by interaction with different RAEs.

A good example is found in the LRR-RK CLAVATA 1 (CLV1), expressed in specific regions of the shoot apical meristem (SAM), that binds the ligand CLE

peptide CLV3 to regulate stem cell specification and inhibits cell division in the SAM (Ogawa *et al.*, 2008). This requires the LRR-RLP CLV2, which is expressed more widely and required for several organ development pathways (Jeong *et al.*, 1999) (Fiers *et al.*, 2005; Wang *et al.*, 2010a). Genetic analysis revealed another regulator, CORYNE (CRN) required for this pathway (Muller *et al.*, 2008). Confocal microscopy, luciferase complementation imaging as well as fluorescence resonance energy transfer (FRET) analysis of heterologously expressed proteins were used to study the signaling complex comprising CLV1, CLV2 and CRN. This work has resulted in the identification of 3 possible receptor assemblies for signal transmission. First, CLV1 monomers or homodimers at the PM can bind CLV3 (Ogawa *et al.*, 2008); second, CLV2-CRN heterodimers combine to form tetramers (Muller *et al.*, 2008; Meng and Feldman, 2010; Zhu *et al.*, 2010b); third, CLV1 homodimerizes independently of CLV2-CRN heterodimers (Bleckmann *et al.*, 2010; Zhu *et al.*, 2010b). Importantly, CRN and CLV2 interact in the ER and require each other to reach the PM (Bleckmann *et al.*, 2010). Furthermore, CLV1 and CRN homodimers may already be assembled in the ER (Bleckmann *et al.*, 2010).

This illustrates the importance of complex localization to understand the function of the interaction. Thus a combination of confocal microscopy (co-localization) and biochemical techniques are useful to study independent complexes, although it was more difficult to assess the effect of the ligand, as it is active in the SAM and did not have an effect on heterologously expressed proteins. EFR may oligomerize and/or combine with different RAEs depending on subcellular location, to form a large super-complex, or perhaps to achieve novel recognition specificity. Alternatively, RAEs may act as a bridge to attach EFR to a different complex, with which it interacts indirectly. RAEs may also be required to target EFR to the PM, by already forming a complex in the ER and guiding EFR to its proper localization for function.

Phosphorylation is an important aspect of complex composition as this modification could cause conformational changes, regulate the interactions in which EFR is engaged, or altering binding sites on EFR and its partners. To assess post-translational modification of EFR complex components, a two-dimensional electrophoresis approach could be taken. This technique is a high-

resolution means of separating different protein isoforms when combined with MS (Wittmann-Liebold *et al.*, 2007). Alternatively, chromatographic enrichment of phosphoproteins might be used to improve chances of MS identification (Collins *et al.*, 2007). Collision-induced dissociation (CID) is often used to fragment peptides for MS, and this method was employed for the current study. The phosphoester bond is more labile than the peptide backbone, leading to release of a distinctive product ion that gives rise to a specific spectral peak, which can be monitored to trigger MS/MS sequencing of the candidate phosphopeptide (Collins *et al.*, 2007). Analysis of such spectra becomes complicated for multiply phosphorylated peptides, which may lead to limited or weak fragment ion spectra.

Electron capture dissociation (ECD) (Zubarev *et al.*, 1998) and electron transfer dissociation (ETD) (Syka *et al.*, 2004) are recently developed alternative gentler fragmentation techniques, where cleavage occurs along the peptide backbone to preserve the phosphate moiety. This technique could be employed, usually with FT-ICR (Fourier transform ion cyclotron resonance) MS to improve EFR phosphopeptide identification. To obtain further insight into the possible structure of the EFR complex, the functional groups on the surface of EFR and an interaction partner could be chemically cross-linked using a protein interaction reporter (PIR), followed by trypsin digestion (Zhang *et al.*, 2009a). The cross-linked peptides could then be analyzed by MS to identify the site of interaction (Sinz, 2006).

Overall the strategy used in this thesis was successful, and several EIPs were identified, in *N. benthamiana* and Arabidopsis. Transiently expressed EFR is functional in *N. benthamiana*, suggesting that the signaling components used by different plant species are conserved. Encouragingly, several EIPs were identified in both species, further supporting the existence of a common signaling mechanism. These common EIPs include the chaperones BiP, calnexin and calreticulin, as well as members of the SERK family of LRR-RKs. Several other ribosomal, chloroplastic and mitochondrial proteins were repeatedly identified in immunoprecipitates but were not further investigated.

Several peptides corresponding to *N. benthamiana* SERKs were identified in EFR IPs, but it is not possible to be sure how many SERKs are present in *N. benthamiana*, thus we also cannot conclude which may be EIPs. However, the

majority of peptides resembled the *Arabidopsis* ortholog BAK1, suggesting that NbBAK1 is the EIP detected. Only 5 SERK peptides were identified in *N. benthamiana* EFR IPs, compared to 28 SERK peptides detected in *Arabidopsis* EFR IPs. Furthermore, 16 *N. benthamiana* EIPs were present in 2/3 biological replicates, compared to 50 EIPs in *Arabidopsis*. Taken together, these data suggest that *Arabidopsis* is a more amenable system to work with for large-scale immunoprecipitation studies, due to the boundaries imposed by limited sequence availability for *N. benthamiana*.

Several modifications of EFR were discovered in this work, such as *N*-glycosylation and phosphorylation. Characterization of EFR post-translational modifications will require extensive future work. It is known that correct *N*-glycosylation of EFR is required for its function, and that EFR is more sensitive than FLS2 to perturbations in its glycosylation patterns (Häweker *et al.*, 2010) (Nekrasov *et al.*, 2009). OST complex mutant *sst3a* does not bind elf18 and is more susceptible to bacterial pathogens (Häweker *et al.*, 2010). DGL1 is an OST complex component identified as a putative EIP in this work. Previous screens for elf18-insensitive mutants have not isolated *dg1* alleles, possibly due to the seedling lethality of this mutant. FLS2 protein was not detectable in *dg1* seedlings, but similar experiments have not been done for EFR (Häweker *et al.*, 2010). CRT3 and UGGT, which are also required for correct EFR folding (Li *et al.*, 2009a; Saijo *et al.*, 2009), were identified as potential EIPs in this work. EFR protein can be detected in the ER (Häweker *et al.*, 2010), and this is likely the location of these interactions.

*N*-glycosylation specifically at N143 is required for elf18 binding (Häweker *et al.*, 2010), though this site was not identified in the present study. Glycosylation at the conserved N288 site, detected in this work, was previously found to be required for correct folding or targeting of EFR to the PM, as N288Q mutants display increased ER-retention (Häweker *et al.*, 2010).

Phosphorylation is another important means of receptor regulation. In general, ligand binding causes conformational changes that promote receptor dimerization and auto- and transphosphorylation. Phosphorylation creates binding sites to engage with downstream signaling components, which may also phosphorylate

the receptor to transduce the signals. Plants encode hundreds of Ser/Thr RKs, but not RTKs, although extensive tyrosine phosphorylation has been detected in *Arabidopsis* (Sugiyama *et al.*, 2008). Despite their classification as Ser/Thr kinases, the LRR-RKs SERK1, BAK1 and BRI1 all appear to be dual-specificity kinases (Karlova *et al.*, 2009; Oh *et al.*, 2009). Little is known about the phosphorylation of PRRs in plants, and this is complicated by the fact that EFR and FLS2 have less active kinases than the better characterized BRI1 and BAK1 (this work; (Zhang *et al.*, 2010a). This lower activity could be because EFR and FLS2 are non-RD kinases, known to be less active. Nonetheless, it will be important to characterize EFR phosphorylation, to study phosphorylation dynamics in relation to PAMP elicitation and to identify the kinases and phosphatases responsible for the regulation of EFR phosphorylation as well as EFR substrates. It will be interesting to identify which, if any, of the EIPs are substrates of the FR kinase activity, using an *in vitro* radioactive kinase assay. If phosphorylation creates docking sites for the recruitment of signaling partners as it does for EGFR, it would be interesting to manipulate these to understand interaction mechanisms.

Post-translational modification could also play a role in receptor localization. Endocytosis of receptors plays an important role in signal regulation. Endocytosed receptors can be degraded to down-regulate signaling or signaling can occur from endocytic compartments (von Zastrow and Sorkin, 2007). FLS2 undergoes endocytosis following flg22 binding, although the importance of endocytosis for signaling has not been proven. Endocytosis is however dependent on the FLS2 kinase activity and BAK1 (Chinchilla *et al.*, 2007), and is abolished in the presence of kinase inhibitors or upon mutation of the potential phosphosite T867 in the juxtamembrane region. The tomato PAMP receptor LeEIX2 undergoes endocytosis and this relies on the endocytic signal Yxx $\phi$  (where  $\phi$  is hydrophobic) and is required for HR. Interestingly, LeEIX1, which can also bind EIX but is not required for signaling, can oligomerize with LeEIX2 and inhibit its endocytosis (Bar *et al.*, 2010). This endocytosis inhibition is dependent on BAK1 (Bar *et al.*, 2010). The EFR juxtamembrane domain harbours such a sorting signal, which in mammals serves to recruit proteins to clathrin-mediated endocytic pathways (Marti *et al.*, 2010). It is not known whether EFR is subject to ligand-induced endocytosis,

or what role this may play in elf18-induced signaling. The identification of coatomers and adaptin as potential EIPs suggests a clathrin-mediated endocytic mechanism could be in place, but this requires extensive further study.

Partial degradation of EFR was previously observed in *Arabidopsis* extracts, where a 150 kDa-band corresponding to the full-length protein as well as a 100kDa-band were observed upon cross-linking elf26 (Häweker *et al.*, 2010). I also noted this degradation, which was particularly obvious in immunoprecipitates, and occurred in the presence of a cocktail of protease inhibitors. It is possible that EFR degradation occurs at a conserved degradation motif, in a similar manner as was observed for the closely related rice Xa21 PRR (Xu *et al.*, 2006a), as well as EGF receptor (Yuan *et al.*, 2003). Following ligand binding, RTKs are commonly subject to downregulation by several mechanisms, such as dephosphorylation or internalization followed by degradation, to control signaling (Stuible and Tremblay, 2010). The heregulin receptor kinase ErbB-4 is not subject to endocytosis as a means of downregulation, but rather undergoes cleavage to produce an 80 kDa TM and cytoplasmic domain that is ubiquitinated and subsequently degraded by the proteasome (Vecchi and Carpenter, 1997). This occurs independently of ligand binding, and interestingly the cleavage product retains kinase activity. Thus degradation, mediated by metalloproteases, is a means of controlling receptor output (Vecchi and Carpenter, 1997). In contrast to ErbB-4, TrkA binding of nerve growth factor induces ectodomain shedding (Cabrera *et al.*, 1996). Cell surface metalloproteases responsible for cleavage of receptors (ectodomain shedding) are called sheddases, and cleave receptors adjacent to the membrane (Seals and Courtneidge, 2003). Sheddases have a wide substrate range including ligands such as TGF- $\alpha$ , TNF- $\alpha$  and cytokines (Seals and Courtneidge, 2003), as well as receptors including EGF receptor, discoidin domain receptor 1 (Vogel, 2002) and vascular endothelial growth factor receptor (Rahimi *et al.*, 2009). Although the ADAM family of sheddases responsible for ectodomain shedding of EGFR and other RTKs are absent from plants (Seals and Courtneidge, 2003), an alternative mechanism may exist. Considering that diverse receptor kinases are subject to ectodomain shedding and are cleaved adjacent to the membrane where

sequences may be divergent, it is likely that the proteases responsible recognize a secondary structure as opposed to a particular amino acid sequence.

In this work, several RKs (RAEs) were identified as EIPs. These may phosphorylate EFR, to positively or negatively regulate the receptor depending on the phosphorylation site. BAK1 plays an important role in the transphosphorylation and activation of BRI1 (Wang *et al.*, 2008d), and a similar mechanism could exist for EFR activation. We have observed that BAK1 can transphosphorylate EFR *in vitro*, and that BAK1 as well as EFR kinase activity is required for elf18 signaling. Now it is necessary to determine the effect of BAK1 phosphorylation on elf18 signaling. Our studies of *in vitro* incubation of EFR and BAK1 kinase domains followed by MS analysis has not revealed any EFR phosphorylation sites, however this could be due to technical limitations, and we will next investigate using alternative ionization to optimize phosphopeptide detection. To determine the role of ligand activation for trans-phosphorylation events *in vitro*, we could carry out kinase assays of elf18-treated EFR-expressing plant extracts incubated with purified BAK1 kinase domains and a radioactive phosphate source. Ultimately, *In vivo* studies would be most revealing, as ligand-induced differential phosphorylation would provide insight into receptor activation.

Recently it was shown that BAK1 autophosphorylation at a C-terminal Tyr (Y610) is necessary for brassinosteroid signaling and defense gene expression in uninfected *Arabidopsis*, but not for flg22-induced seedling growth inhibition or cell death control (Oh *et al.*, 2010b). Interestingly, the basal expression of several defense-related genes was down-regulated in BAK1 Y610F mutants, which also showed enhanced susceptibility to bacterial infection (Oh *et al.*, 2010b). Among the down-regulated genes were *RAE5* (-3 fold) and the close relative *At1g35710/XII1* (-64 fold); *RAE6* (-2 fold); *RAE7* and *At1g51790* (-4.8 fold), CRK11-related genes, *CRK6* (-27 fold) and *CRK7* (-11 fold). This supports a potentially important role for the RAEs in anti-bacterial immunity.

Another important point to note about the data yielded from this project is that the majority of EIPs are membrane-associated proteins. While this is logical considering the localization of EFR, surely some cytoplasmic proteins would interact with the EFR intracellular domain in the cytoplasm. For example, the

receptor cytoplasmic kinase BIK1 interacts with FLS2 and is phosphorylated in response to elf18, suggesting a possible association *in planta*. In order to reveal potential cytoplasmic EIPs, or weak/transient interactions, EFR immunoprecipitation could be repeated using lower amounts of detergent and minimal washing. This approach is being undertaken by Yasuhiro Kadota in this laboratory. He will combine this with  $^{15}\text{N}$ -labelling to obtain quantitative data about the ligand-induced differential interactions.

In conclusion, this study has improved our knowledge about receptor complexes involved in PAMP-regulated signaling and has also opened up a new set of questions and challenges for the next years.

## APPENDIX

Appendix Table A1.1 EFR peptides identified in comparison extraction methods

Peptide score*	Pep_expect <sup>§</sup>	TOTAL PROTEIN EXTRACTION		Variable Mods
		Peptide sequence		
38.82	0.00057	VLNLLK		
22.5	0.024	VLNLLK		
48.82	2.50E-05	VLNLLK		
45.62	5.20E-05	VLNLLK		
23.45	0.0084	VLNLLK		
24.36	0.007	VLNLLK		
45.77	5.00E-05	VLNLLK		
22.01	0.12	ELISIR		
35.89	0.0047	ELISIR		
26.06	0.045	ELISIR		
20.11	0.17	IPQSLGR		
32.04	0.011	IPQSLGR		
38.59	0.0024	IPQSLGR		
22.2	0.1	IPQSLGR		
31.74	0.012	IPQSLGR		
31.35	0.013	IPQSLGR		
49.67	0.00019	IPQSLGR		
22.17	0.1	GLLGPENK		
27.39	0.03	GLLGPENK		
41.29	0.0012	GLLGPENK		
24.32	0.013	LAILDLSK		
24.53	0.079	VPTTGVFR		
34.38	0.0075	VPTTGVFR		
28.81	0.027	VPTTGVFR		
26.36	0.047	VPTTGVFR		
24.94	0.066	VPTTGVFR		
31.89	0.013	VPTTGVFR		
23.65	0.088	VPTTGVFR		
26.85	0.042	VPTTGVFR		
32.71	0.011	VPTTGVFR		
21.93	0.13	VPTTGVFR		
22.17	0.12	VPTTGVFR		
44.63	0.00062	GEIPDEVAR		
20.03	0.18	GEIPDEVAR		
53.43	4.10E-05	YLASLPSLR		
21.22	0.068	YLASLPSLR		
54.66	2.20E-05	VISLNLLGGFK		
23.11	0.089	TLANISSLER		
44.24	0.00083	ALVYEFMPK	Oxidation (M)	
33.84	0.0091	ALVYEFMPK	Oxidation (M)	
25.12	0.064	ALVYEFMPK	Oxidation (M)	
22.29	0.14	ALVYEFMPK	Oxidation (M)	
41.48	0.0019	LDFAYNQMR		
40.3	0.0025	LDFAYNQMR		
54.44	8.40E-05	LDFAYNQMR		
35.55	0.0086	LDFAYNQMR	Oxidation (M)	
39.93	0.0023	LDFAYNQMR	Oxidation (M)	
21.36	0.17	LDFAYNQMR	Oxidation (M)	
22.27	0.14	LDFAYNQMR	Oxidation (M)	
68.9	3.10E-06	LDFAYNQMR	Oxidation (M)	
45.5	0.00077	LDFAYNQMR	Oxidation (M)	
51.95	0.00014	SFMAECETFK		
50.08	0.00019	SFMAECETFK	Oxidation (M)	
68.31	3.40E-06	ADFGYLLPNLR		
30.02	0.023	ADFGYLLPNLR		
20.48	0.19	ADFGYLLPNLR		
41.61	0.0014	ADFGYLLPNLR		

38.78	0.004	LHLNSNSFHGR
86.6	7.50E-08	LHLNSNSFHGR
35.35	0.0091	LHLNSNSFHGR
45.01	0.00099	LHLNSNSFHGR

**Appendix Table A1.1 EFR peptides identified in comparison extraction methods (continued)**

Peptide score	Pep_expect	TOTAL PROTEIN EXTRACTION	
		Peptide sequence	Variable Mods
62.92	1.60E-05	LHLNSNSFHGR	
22.52	0.18	LHLNSNSFHGR	
23.71	0.13	LHLNSNSFHGR	
48.16	0.00045	LHLNSNSFHGR	
37.82	0.0054	NVDFSNNNLSGR	
47.51	0.00067	VSYEELHSATSR	
60.78	3.20E-05	VSYEELHSATSR	
38.57	0.0052	VSYEELHSATSR	
36.71	0.0081	VSYEELHSATSR	
21.53	0.27	VSYEELHSATSR	
26.32	0.081	VSYEELHSATSR	
60.01	3.40E-05	VSYEELHSATSR	
39.67	0.0037	VSYEELHSATSR	
23.05	0.17	VSYEELHSATSR	
23.9	0.17	ESFLNQFSSAGVR	
33.73	0.016	ESFLNQFSSAGVR	
34.8	0.013	ESFLNQFSSAGVR	
47.94	0.00063	ESFLNQFSSAGVR	
<b>33.47</b>	0.018	ESFLNQFSSAGVR	
28.58	0.053	ESFLNQFSSAGVR	
36.04	0.0096	ESFLNQFSSAGVR	
36.45	0.01	ESFLNQFSSAGVR	
41.55	0.0032	ESFLNQFSSAGVR	
23.46	0.2	ESFLNQFSSAGVR	
60.06	4.30E-05	YLLDLWMDTNR	Oxidation (M)
25.68	0.12	YLLDLWMDTNR	Oxidation (M)
39.83	0.0045	YLLDLWMDTNR	Oxidation (M)
21.37	0.061	LLLGTNQFTGAIPK	
37.32	0.0016	LLLGTNQFTGAIPK	
42.93	0.00044	LLLGTNQFTGAIPK	
64.71	2.90E-06	LLLGTNQFTGAIPK	
43.73	0.00036	LLLGTNQFTGAIPK	
34.12	0.003	LLLGTNQFTGAIPK	
27.77	0.013	LLLGTNQFTGAIPK	
32.39	0.0044	LLLGTNQFTGAIPK	
29.79	0.0081	LLLGTNQFTGAIPK	
51.11	6.10E-05	LLLGTNQFTGAIPK	
54.38	2.60E-05	LLLGTNQFTGAIPK	
68.53	1.20E-06	LLLGTNQFTGAIPK	
59.76	9.80E-06	LLLGTNQFTGAIPK	
60.69	7.80E-06	LLLGTNQFTGAIPK	
45.45	0.00026	LLLGTNQFTGAIPK	
27.6	0.017	RLLLGTNQFTGAIPK	
47.84	0.00062	EMQLKPCIVQASPR	
25.35	0.13	EMQLKPCIVQASPR	Oxidation (M)
23.1	0.21	EMQLKPCIVQASPR	Oxidation (M)
32.27	0.026	EMQLKPCIVQASPR	Oxidation (M)
44.08	0.0012	LLNLADNSFGSTIPQK	
28.84	0.039	LLNLADNSFGSTIPQK	
32.69	0.016	LLNLADNSFGSTIPQK	
21.51	0.21	LLNLADNSFGSTIPQK	
21.29	0.22	LLNLADNSFGSTIPQK	
31.88	0.019	LLNLADNSFGSTIPQK	
22.97	0.15	LLNLADNSFGSTIPQK	
31.14	0.022	LLNLADNSFGSTIPQK	
32.32	0.017	LLNLADNSFGSTIPQK	
27.24	0.054	LLNLADNSFGSTIPQK	
32.67	0.015	LLNLADNSFGSTIPQK	
46.67	0.00067	LLNLADNSFGSTIPQK	
28.83	0.041	LLNLADNSFGSTIPQK	
52.5	0.00018	LLNLADNSFGSTIPQK	
<b>73.42</b>	1.40E-06	LLNLADNSFGSTIPQK	
61.47	2.20E-05	LLNLADNSFGSTIPQK	

34.6	0.019	GSLSMWLQLEDLER	Oxidation (M)
88.05	1.00E-07	LITVCSSLSEGNDFR	
68.74	8.20E-06	YDRESFLNQFSSAGVR	
57.8	0.00011	SILSGCTSSGGSNAIDEGLR	

**Appendix Table A1.1 EFR peptides identified in comparison extraction methods (continued)**

TOTAL PROTEIN EXTRACTION			
Peptide score	Pep_expect	Peptide sequence	Variable Mods
70.69	5.50E-06	SILSGCTSSGGSNAIDEGLR	
88.17	9.60E-08	SILSGCTSSGGSNAIDEGLR	
<b>23.41</b>	0.27	NNASDGPNPSDSTTLGMFHEK	
25.42	0.17	NNASDGPNPSDSTTLGMFHEK	
21.7	0.42	NNASDGPNPSDSTTLGMFHEK	
96.48	1.40E-08	NNASDGPNPSDSTTLGMFHEK	
31.31	0.046	NNASDGPNPSDSTTLGMFHEK	Oxidation (M)
41.23	0.0048	NNASDGPNPSDSTTLGMFHEK	Oxidation (M)
26.63	0.17	LDFAYNQMRGEIPDEVAR	Oxidation (M)
20.45	0.4	NNASDGPNPSDSTTLGMFHEK	Oxidation (M); Phos (ST)
25.67	0.22	KNNASDGPNPSDSTTLGMFHEK	
61.9	5.50E-05	KNNASDGPNPSDSTTLGMFHEK	Oxidation (M)
42.15	0.0033	LSTVDLSSNHLGHGVPELGSLSK	
MICROSOMAL PROTEIN EXTRACTION			
28	0.028	VPTTGVFR	
17	0.37	GEIPDEVAR	
12	0.68	YLASLPSLR	
14	0.83	ALVYEFMPK	
14	1	ADFGYLLPNLR	
27	0.064	LHLNSNSFHGR	
34	0.014	ESFLNQFSSAGVR	
55	2.80E-05	LLLGTNQFTGAIPK	
3	25	FSNETDMQALLEFK	

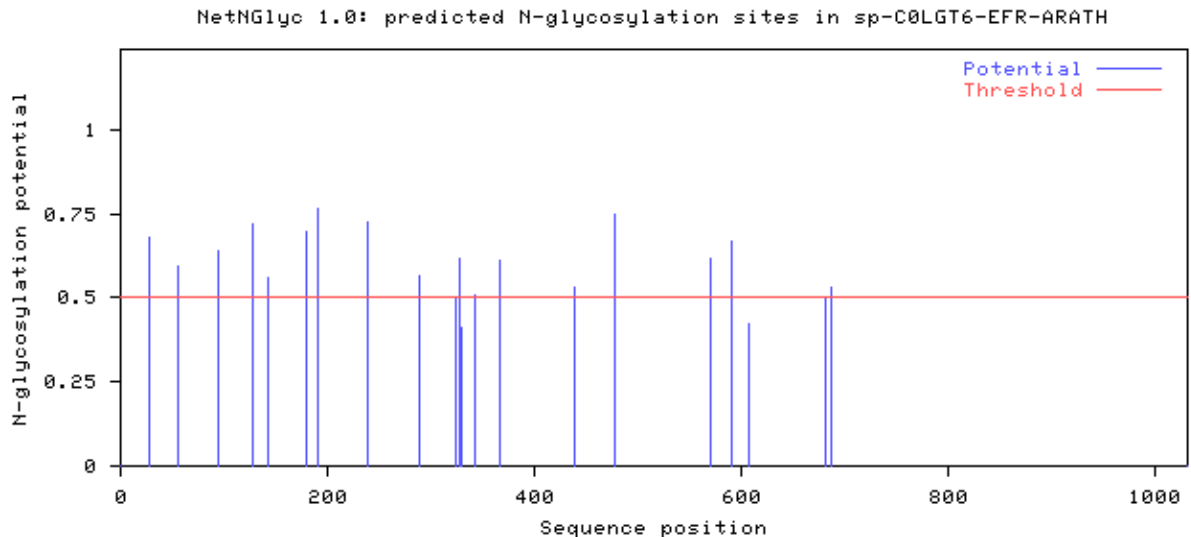
<sup>\*</sup> In Mascot, the ions score for an MS/MS match is based on the calculated probability, P, that the observed match between the experimental data and the database sequence is a random event. The reported score is -10Log(P). So, during a search, if 1500 peptides fell within the mass tolerance window about the precursor mass, and the significance threshold was chosen to be 0.05, (a 1/20 chance of being a false positive), this would translate into a score threshold of 45.

<sup>§</sup> Pep\_expect score is Expectation value for the peptide match. (The number of times we would expect to obtain an equal or higher score, purely by chance. The lower this value, the more significant the result).



**Appendix Table A1.3 NbSERK MS/MS data**

Bio rep	Peptide sequence	Prev aa	Next aa	Pept ID Prob (%)	Mascot Ion score	Mascot ID score	Variable Mods	Observed m/z	Actual peptide mass (AMU)	Calculated +1H Peptide Mass (AMU)
EFR elf 2	TQGGELQFQTEVEMISMAVHR	R	N	95	48	22.6		797.7204	2,390.14	2,391.14
EFR elf 2	LANDDDVMILLDWVK	R	G	95	79.7	24		823.91	1,645.80	1,646.81
EFR elf 3	mLEGDGLAER	R	W	95	38.9	21.1	m1: Oxidation (+15.99)	553.7615	1,105.51	1,106.52
EFR elf 3	ELQVASDNFSNK	R	N	95	47.8	22.9		676.3284	1,350.64	1,351.65
EFR elf 3	GTIGHIAPEYLSTGK	R	S	95	45.8	23.7		772.4104	1,542.81	1,543.81



### Appendix Figure A2.1. Putative N-glycosylation sites in EFR.

Predicted by NetNGlyc 1.0 server (<http://www.cbs.dtu.dk/services/NetNGlyc/>) (Blom *et al.*, 2004). Asn-Xaa-Ser/Thr sequons in the sequence output are highlighted in **blue**. Asparagines predicted to be N-glycosylated are highlighted in **red**. The graph illustrates predicted N-glycosylation sites across the protein chain (x-axis represents protein length from N- to C-terminal). A position with a potential (vertical lines) crossing the threshold (horizontal line at 0.5) is predicted glycosylated.

## Appendix Figure A2.2 Multiple sequence alignment of PDR family members. Part 1/3.

Clustal W multiple alignment generated using Jalview v.12.2, shaded for percentage identity. PEN3 peptides identified by MS/MS analysis highlighted in green, NpPDR1 peptides in purple. The conserved ATP binding sites are highlighted red.

**Appendix Figure A2.2 (continued) Multiple sequence alignment of PDR family members.**

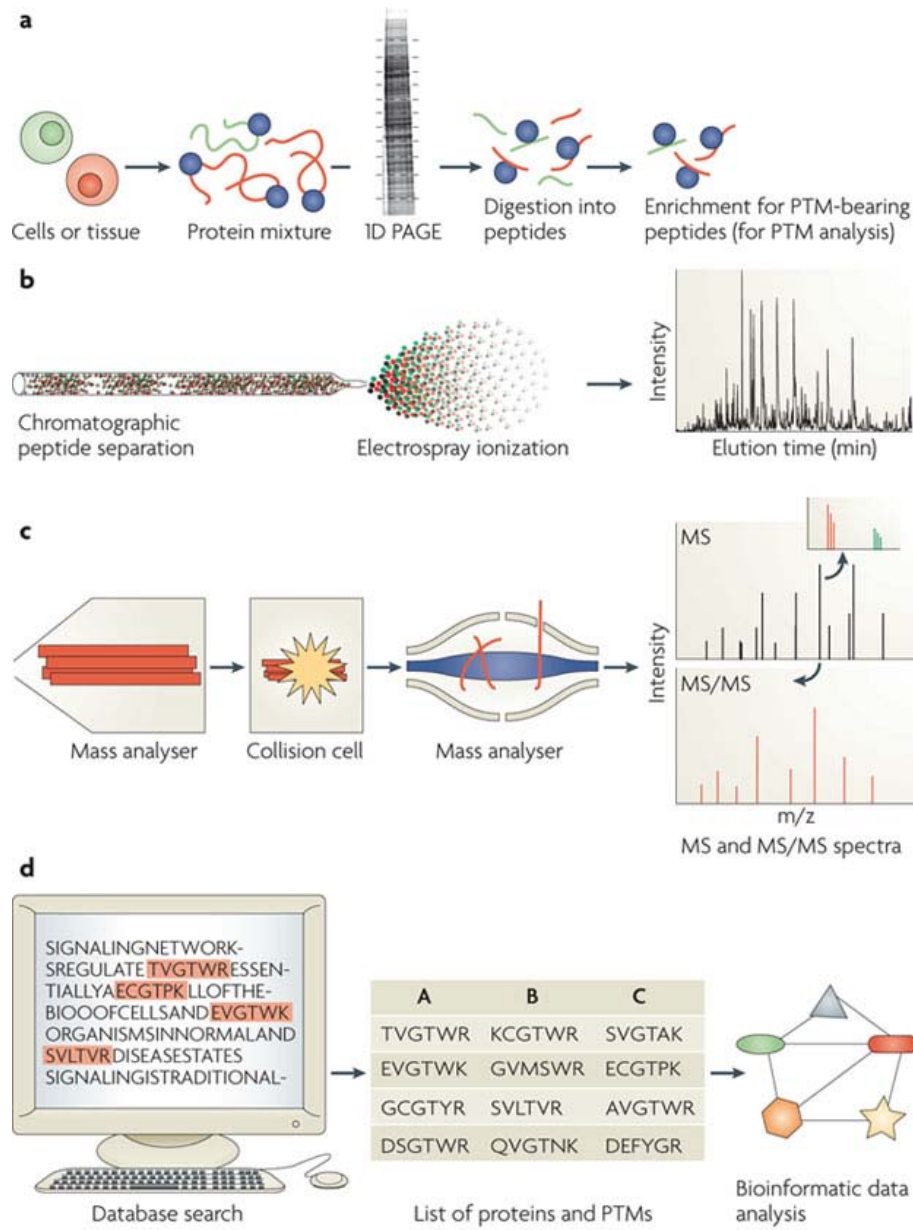
## Part 2/3.

Clustal W multiple alignment generated using Jalview v.12.2, shaded for percentage identity. PEN3 peptides identified by MS/MS analysis highlighted in green, NpPDR1 peptides in purple. The conserved ATP binding sites are highlighted red.

**Appendix Figure A2.2 (continued) Multiple sequence alignment of PDR family members.**

### Part 3/3.

Clustal W multiple alignment generated using Jalview v.12.2, shaded for percentage identity. PEN3 peptides identified by MS/MS analysis highlighted in green, NpPDR1 peptides in purple. The conserved ATP binding sites are highlighted red.

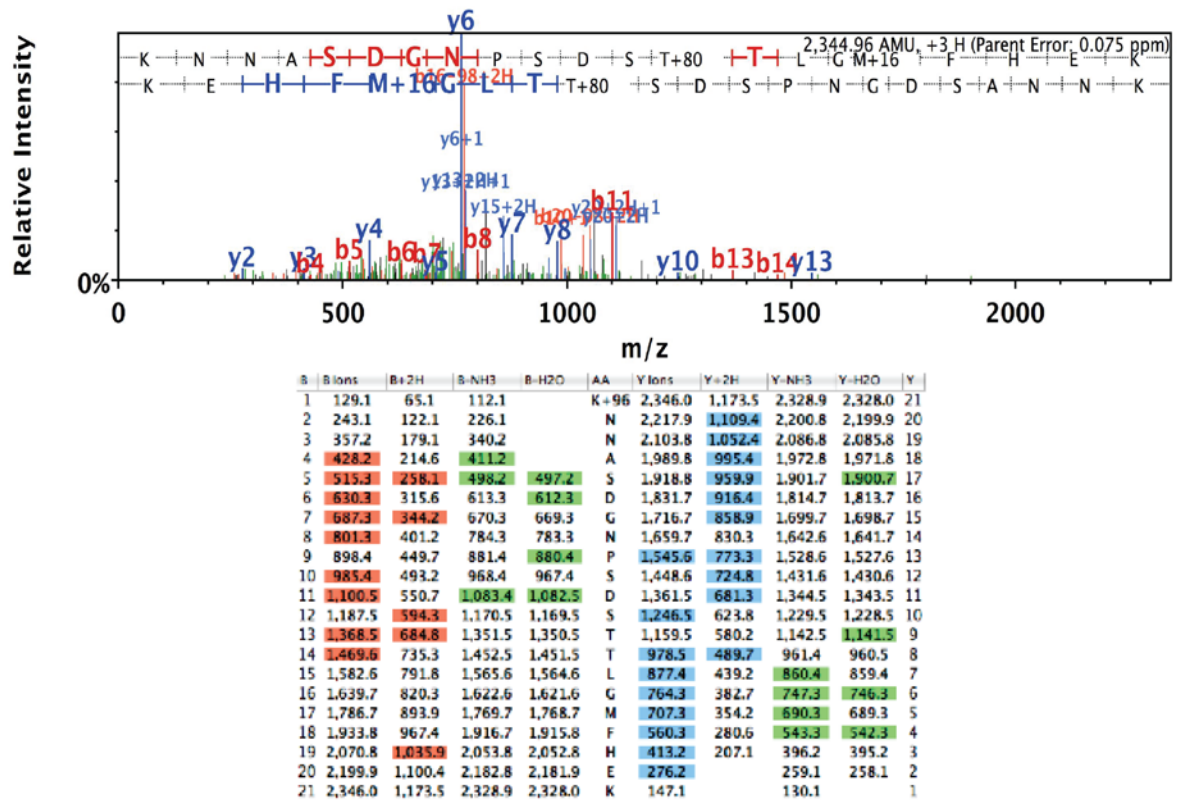


Nature Reviews | Molecular Cell Biology

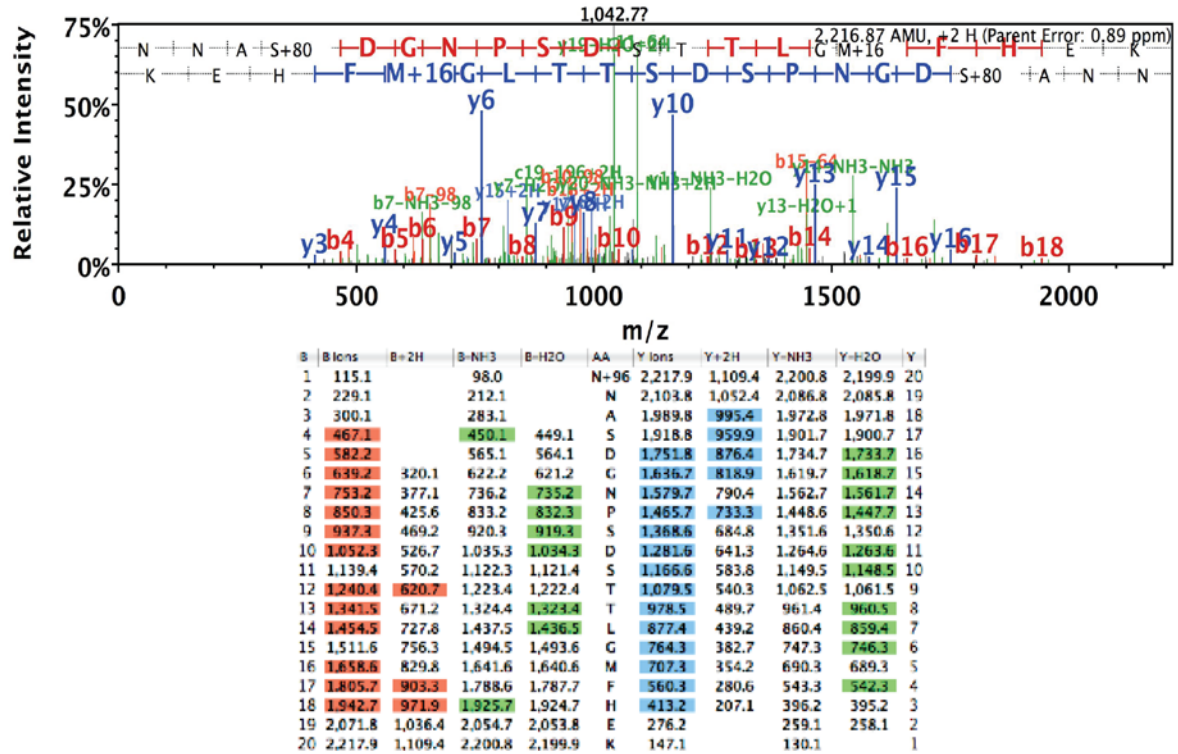
#### Appendix Figure A2.3 Workflow for identification of PTMs. (Choudhary and Mann, 2010)

Proteins extracted from organs, tissues or cells are separated by one-dimensional polyacrylamide gel electrophoresis (1D PAGE) and 'in-gel digested' into peptides using proteases such as trypsin. The peptides containing specific post-translational modifications (PTMs) can be enriched using different approaches. Non-modified peptides are used to identify and quantify total cellular proteins. **b** | Purified peptides are separated on a miniaturized reverse phase chromatography column with an organic solvent gradient. Peptides eluting from the column are ionized by electrospray at the tip of the column, directly in front of the mass spectrometer (known as on-line coupling). **c** | The electrosprayed ions are transferred into the vacuum of the mass spectrometer. In the mass spectrometry (MS) mode, all ions are moved to the orbitrap mass analyser, where they are measured at high resolution (top mass spectrum). The first mass analyser then selects a particular peptide ion and fragments it in a collision cell. The inset in the MS panel indicates the stable isotope labelling by amino acids in cell culture (SILAC) ratio of one of the peptides. The MS/MS spectrum can be obtained in the ion trap mass analyser at low resolution or in the orbitrap at high resolution. For modified peptides, the peptide mass will be shifted by the mass of the modification, as will all fragments containing the modification, allowing the unambiguous placement of the PTM on the sequence. **d** | The mass and list of fragment masses for each peptide are scanned against protein sequence databases, resulting in a list of identified peptides and proteins. *With the omission of the SILAC, this is the workflow that was used for MS/MS analysis in this project.*

**A KNNASDGNPSDSTTL score 32**

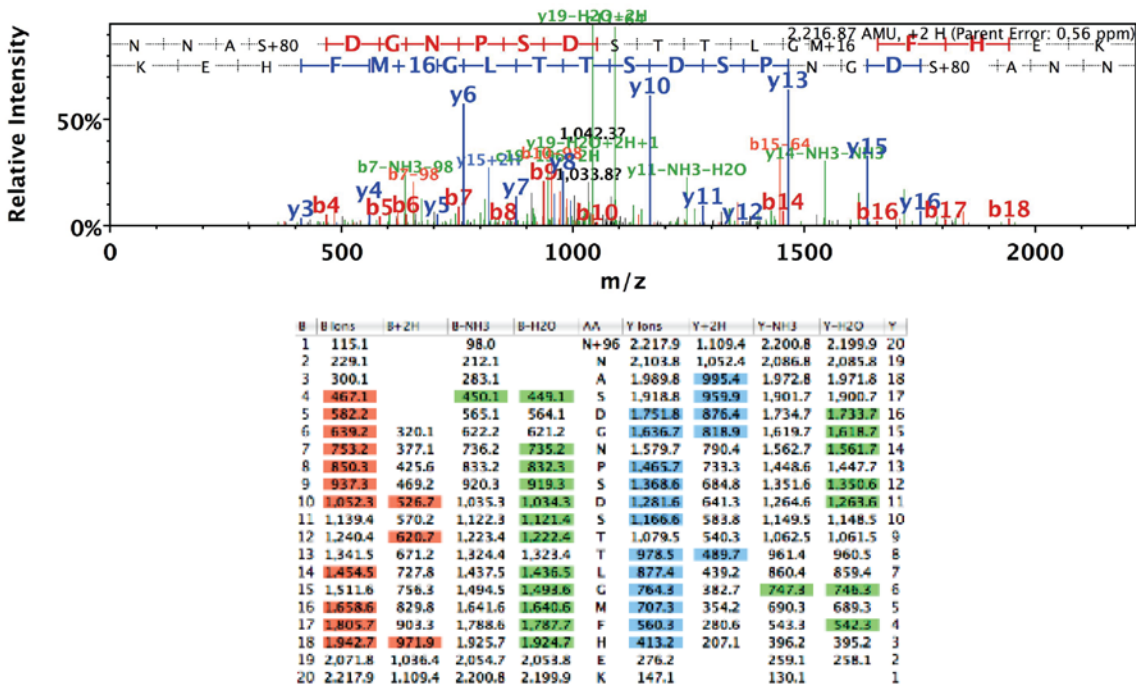


**B KNNASDGNPSDSTTL score 57**

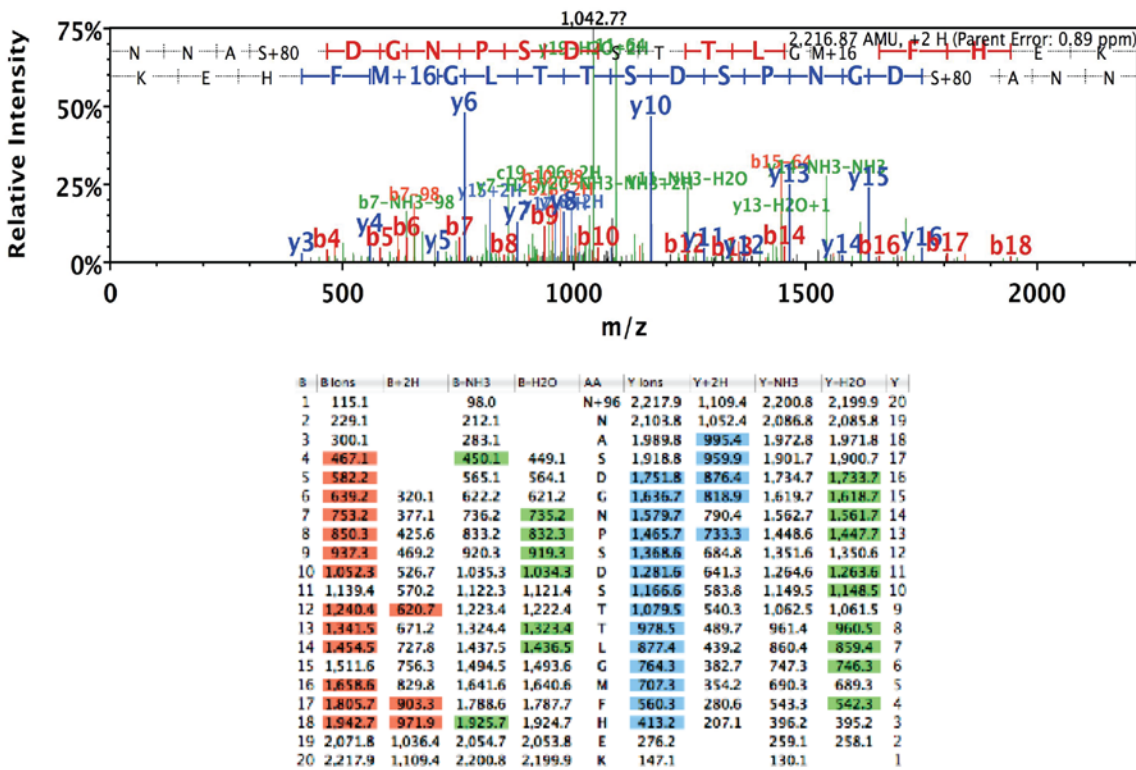


Appendix Figure A2.4 EFR phosphopeptides spectra and fragmentation tables. (continues)

**C KNNASDGNPSDSTTL score 60**



**D TTITESPR score 22**



**Appendix Figure A2.4 EFR phosphopeptides spectra and fragmentation tables (continued).**

MS/MS spectra (top panel) and fragmentation table showing ions detected in MS analyzer (bottom). y ions are blue and b ions red, parent ions green in spectra and unassigned peaks black. The masses of the corresponding ions are shown highlighted if assigned in the table below each spectrum.

Appendix Table A2.1. Detailed MS/MS data of *Arabidopsis* IPs (attached .xls file)

Appendix Table 2.2: AHA peptides identified by MS/MS analysis of EFR IPs

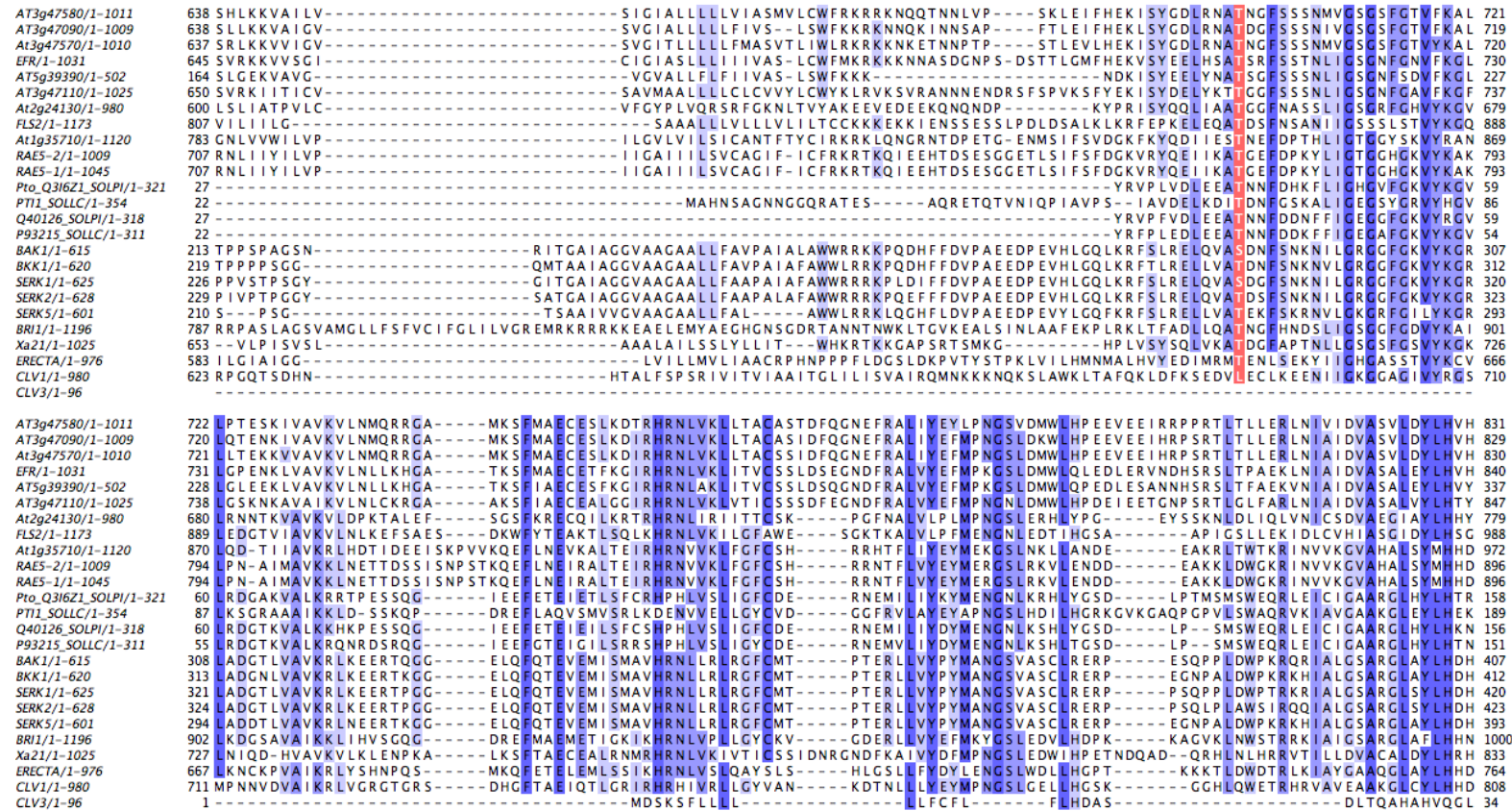
Bio Rep	Peptide sequence	Peptide ID Prob	Mascot Ion score	Mascot ID score	Variable Mods	Matches
EFRelf_3	<b>IVIFGPNKLEEK</b>	95.00%	30	20.6		AHA1
EFRelf_3	<b>sGLEDIKNETVDLEK</b>	95.00%	69	34.8	s1: Acetyl (+42.01)	AHA1
EFRelf_3	<b>sGLEDIKNETVDLEK</b>	95.00%	75.1	34.7	s1: Acetyl (+42.01)	AHA1
EFR_3	<b>DANLASIPVEELIEK</b>	95.00%	37.8	22.3		AHA2
EFRelf_3	<b>DANLASIPVEELIEK</b>	94.50%	26.5	21.8		AHA2
EFR 2	<b>GAPEQILELAK</b>	95.00%	25.4	18.5		AHA2
EFR 2	<b>GAPEQILELAK</b>	95.00%	34.8	18.5		AHA2
EFR+elf18 2	<b>GAPEQILELAK</b>	93.70%	25.4	18.5		AHA2
EFR+elf18 2	<b>GAPEQILELAK</b>	95.00%	38.3	18.5		AHA2
EFR+elf18 2	<b>GAPEQILELAK</b>	95.00%	50	18.5		AHA2
efr-KO 2	<b>GAPEQILELAK</b>	95.00%	28.7	18.5		AHA2
EFRelf_3	<b>KVLSIIDKYAER</b>	95.00%	49.3	16.9		AHA2
EFR 2	<b>SLEDIKNETVDLEK</b>	95.00%	29.5	29.5		AHA2
EFR 2	<b>EAQWAhAQR</b>	90.90%	26.5	28	h6: His->Leu (H) (-23.97) a13: Ala->Val (A) (+28.03)	AHA3
EFRelf_3	<b>VDQSALTGESLPaTK</b>	95.00%	51.1	33.7		AHA3
EFR_3	<b>AAHLVDSTNnVGHFQK</b>	94.40%	38.6	35.3	n10: Methyl (+14.02)	AHA6
EFRelf_3	<b>AAHLVDSTNnVGHFQK</b>	95.00%	54.5	35.4	n10: Methyl (+14.02) r14: Arg->Lys (R) (-28.01)	AHA6
EFRelf_3	<b>TAITYIDTNGEWr</b>	79.50%	30.1	34.5		AHA6
EFR_3	<b>EGLTTEAADER</b>	95.00%	44.2	24.2		AHA11
EFR_3	<b>GDkEEVLEAVLK</b>	95.00%	61.7	32	k3: Acetyl (+42.01) n-term: Acetyl (+42.01)	AHA11
EFR_3	<b>gDKEEVLEAVLK</b>	95.00%	44.5	32.6		AHA11
EFR 2	<b>ADIGIAVADATDAAR</b>	95.00%	62.5	20.7		AHA1, 2, 3, 11
EFR 2	<b>ADIGIAVADATDAAR</b>	95.00%	84.3	20.8		AHA1, 2, 3, 11
EFR 2	<b>ADIGIAVADATDAAR</b>	95.00%	62.5	20.7		AHA1, 2, 3, 11
EFR+elf18 2	<b>ADIGIAVADATDAAR</b>	95.00%	57.3	20.7		AHA1, 2, 3, 11
EFR+elf18 2	<b>ADIGIAVADATDAAR</b>	95.00%	68.9	20.7		AHA1, 2, 3, 11
EFRelf_3	<b>ADIGIAVADATDAAR</b>	95.00%	55.6	23.3		AHA1, 2, 3, 11
EFRelf_3	<b>ADIGIAVADATDAAR</b>	95.00%	56	23.3		AHA1, 2, 3, 11
EFRelf_3	<b>ADIGIAVADATDAAR</b>	95.00%	55.6	23.3		AHA1, 2, 3, 11
EFRelf_3	<b>ADIGIAVADATDAAR</b>	95.00%	56	23.3		AHA1, 2, 3, 11
EFRelf_3	<b>ADIGIAVADATDAAR</b>	95.00%	55.6	23.3		AHA1, 2, 3, 11
EFRelf_3	<b>ADIGIAVADATDAAR</b>	95.00%	56	23.3		AHA1, 2, 3, 11
EFR 2	<b>ADIGIAVADATDAAR</b>	95.00%	84.3	20.8		AHA1, 2, 3, 11
EFR_3	<b>KADIGIAVADATDAAR</b>	95.00%	100	22.3		AHA1, 2, 3, 11
EFR_3	<b>KADIGIAVADATDAAR</b>	95.00%	117	22.3		AHA1, 2, 3, 11
EFR_3	<b>KADIGIAVADATDAAR</b>	95.00%	100	22.3		AHA1, 2, 3, 11
EFR_3	<b>KADIGIAVADATDAAR</b>	95.00%	117	22.3		AHA1, 2, 3, 11
EFRelf_3	<b>KADIGIAVADATDAAR</b>	95.00%	109	22		AHA1, 2, 3, 11
EFRelf_3	<b>KADIGIAVADATDAAR</b>	95.00%	107	22.5		AHA1, 2, 3, 11
EFRelf_3	<b>KADIGIAVADATDAAR</b>	95.00%	107	22.5		AHA1, 2, 3, 11
EFR 2	<b>ELSEIAEQAK</b>	95.00%	25.1	21.9		AHA1,2
EFR+elf18 2	<b>ELSEIAEQAK</b>	95.00%	37.9	21.9		AHA1,2
EFR 2	<b>ELSEIAEQAKR</b>	95.00%	32.6	22.4		AHA1,2
EFR_3	<b>NLVEVFcK</b>	88.70%	24	22.1	c7: Carbamidomethyl (+57.02)	AHA1,2
EFR_3	<b>IPIEEVFQQLK</b>	95.00%	60.4	21		AHA1,2,3
EFR_3	<b>IPIEEVFQQLK</b>	95.00%	63.9	20.7		AHA1,2,3
EFR_3	<b>IPIEEVFQQLK</b>	95.00%	63.9	20.7		AHA1,2,3
EFRelf_3	<b>IPIEEVFQQLK</b>	95.00%	45.3	22.1		AHA1,2,3

**Appendix Table 2.2 (continued): AHA peptides identified by MS/MS analysis of EFR IPs**

Bio Rep	Peptide sequence	Peptide ID Prob	Mascot Ion score	Mascot ID score	Variable Mods	Matches
EFRelf_3	IPIEEVFQQLK	95.00%	45.3	22.1		AHA1,2,3
EFR_3	KADIGIAVADATDAAR	95.00%	100	22.3		AHA1,2,3
EFR_3	KADIGIAVADATDAAR	95.00%	117	22.3		AHA1,2,3
EFRelf_3	KADIGIAVADATDAAR	95.00%	107	22.5		AHA1,2,3
EFR 2	LGDIIPADAR	95.00%	48.7	20.5		AHA1,2,3
EFR 2	LGDIIPADAR	95.00%	43.4	20.5		AHA1,2,3
EFR 2	LGDIIPADAR	95.00%	46.5	20.5		AHA1,2,3
EFR 2	LGDIIPADAR	95.00%	43.4	20.5		AHA1,2,3
EFR 2	LGDIIPADAR	95.00%	46.5	20.5		AHA1,2,3
EFR+elf18 2	LGDIIPADAR	95.00%	26.8	20.5		AHA1,2,3
EFR+elf18 2	LGDIIPADAR	95.00%	45.5	20.5		AHA1,2,3
EFR+elf18 2	LGDIIPADAR	86.70%	21.9	20.5		AHA1,2,3
EFRelf_3	LGDIIPADAR	95.00%	31.4	20.8		AHA1,2,3
efr-KO 2	LGDIIPADAR	95.00%	29.7	20.5		AHA1,2,3
EFR_3	HIVGmTGDGVNDAPALKK	94.70%	28.8	23.8	m5: Oxidation (+15.99)	AHA1,2,6
EFR_3	HIVGmTGDGVNDAPALKK	94.70%	28.8	23.8	m5: Oxidation (+15.99)	AHA1,2,6
EFRelf_3	HIVGmTGDGVNDAPALKK	95.00%	34.5	23.8	m5: Oxidation (+15.99)	AHA1,2,6
EFRelf_3	HIVGmTGDGVNDAPALKK	95.00%	34.5	23.8	m5: Oxidation (+15.99)	AHA1,2,6
EFR_3	KHIVGmTGDGVNDAPALKK	95.00%	51.9	22	m6: Oxidation (+15.99)	AHA1,2,6
EFR_3	KHIVGmTGDGVNDAPALKK	95.00%	51.9	22	m6: Oxidation (+15.99)	AHA1,2,6
EFRelf_3	KHIVGmTGDGVNDAPALKK	87.70%	25.5	21.4	m6: Oxidation (+15.99)	AHA1,2,6
EFRelf_3	KHIVGmTGDGVNDAPALKK	87.70%	25.5	21.4	m6: Oxidation (+15.99)	AHA1,2,6
EFRelf_3	KHIVGmTGDGVNDAPALKK	87.70%	25.5	21.4	m6: Oxidation (+15.99)	AHA1,2,6
					m1: Oxidation (+15.99), a10: Ala->Gly (A) (- 14.02)	
EFR_3	mITGDQLAlaK	95.00%	47.3	30.8	m1: Carbamyl (M) (+43.01)	AHA1,2,6,11
EFR+elf18 2	<b>mITGDQLAIGK</b>	95.00%	40.2	30.4		AHA1,2,6,11
EFR 2	<b>mITGDQLAIGK</b>	95.00%	31.1	27.7	m1: Oxidation (+15.99)	AHA1,2,6,11
EFR 2	<b>mITGDQLAIGK</b>	95.00%	41.8	30.2	m1: Oxidation (+15.99)	AHA1,2,6,11
EFR 2	<b>mITGDQLAIGK</b>	95.00%	61.5	29.6	m1: Oxidation (+15.99)	AHA1,2,6,11
EFR+elf18 2	<b>mITGDQLAIGK</b>	95.00%	76.8	29.3	m1: Oxidation (+15.99)	AHA1,2,6,11
EFR+elf18 2	<b>mITGDQLAIGK</b>	95.00%	30.7	29.3	m1: Oxidation (+15.99)	AHA1,2,6,11
EFR+elf18 2	<b>mITGDQLAIGK</b>	88.20%	26.9	29.5	m1: Oxidation (+15.99)	AHA1,2,6,11
efr-KO 2	<b>mITGDQLAIGK</b>	91.60%	28.2	28.6	m1: Oxidation (+15.99) n-term: Carbamyl (+43.01)	AHA1,2,6,11
EFR 2	<b>mITGDQLAIGK</b>	95.00%	42.5	31		AHA1,2,6,11
EFRelf_3	IPIEEVFQQLK	95.00%	45.3	22.1		AHA2,3
EFRelf_3	HIVGmTGDGVNDAPALKK	95.00%	34.5	23.8	m5: Oxidation (+15.99)	AHA2,6
EFR 2	RALdLGVNVK	95.00%	61.9	26.7	d4: Asp->Asn (D) (- 0.98)	AHA3, 6
EFR_3	RALdLGVNVK	95.00%	44.4	27.1	d4: Asp->Asn (D) (- 0.98)	AHA3, 6
EFR_3	RALdLGVNVK	95.00%	44.4	27.1	d4: Asp->Asn (D) (- 0.98)	AHA3, 6
EFRelf_3	RALdLGVNVK	95.00%	44.8	27.2	d4: Asp->Asn (D) (- 0.98)	AHA3, 6
EFRelf_3	RALdLGVNVK	95.00%	44.8	27.2	d4: Asp->Asn (D) (- 0.98)	AHA3, 6

Peptides with modifications unlikely to represent biologically relevant are indicated in gray.

Mascot identity score: an estimate of the minimum ion score necessary to achieve a 95% confidence.  $10^*(\log(p/\#matches))$  where p is 0.95 and #matches is the number of peptides in the database that have the same parent ion mass. This takes the database size into consideration, but it doesn't take the complexity of the sample, or instrument type, or any number of other factors into consideration.



**Appendix Figure A2.5 Multiple sequence alignment of various receptor-like kinases.** ClustalW multiple alignment, generated in Jalview, colored by percentage sequence identity. Green highlighted residue indicates conserved catalytic Asp in kinase active site. Pink indicates conservation of important Thr (T38 in Pto, essential for autophosphorylation and interaction with Pt1).

AT3g47580/1-1011	938 LALPEK-VFEIADKAI LH-----IGLRVGFRTAECLTLVLEVGLRCC E EYPTNR LATSEAKELISIRERFFKTRRTPRR-----	1011
AT3g47090/1-1009	936 AALPER-VLDIADKSILH-----SGLR VGF P VLECLKG I LDVGLRCC E E S P L N R LATSEA A KELISIRERFFKTRRTARR-----	1009
At3g47570/1-1010	937 SALPER-ILDIVDESILH-----IGLRVGF P VVECLTMVFEVGLRCC E E S P M N R LATSI V KELISIRERFFKASRTTWR-----	1010
EFR/1-1031	947 S I L S G C - T S S G G S N -----A I D E G L R L V L Q V G I K C S E E Y P R D R M R T D E A V R E L I S I R S K F F S K T T I T E S P R D A P Q S S P Q E W M L N T D M H T M -----	1031
AT5g39390/1-502	444 S V L S C S - T S R G G R T -----M V D E W L R L V L E V G I K C S E E Y P R D R M G M A E A V R E L V S I K S K F T T S S R -----	502
AT3g47110/1-1025	954 S A L Q K R Q A L D I T D E T I L R -----G A Y A Q H F N M V E C L T L V F R V G V S C S E E S P V N R I S M A E A I S K L V S I R E S F F R D E E T -----	1025
At2g24130/1-980	891 S H Y P D S - L E G I I E Q A L S R W K P Q -----G K P E K C E K L W R E V I L E M I E L G L V C T Q Y N P S T R P D M L D V A H E M G R L K E Y L F A C P S L L H F S S Q E T Q G E A S S -----	980
FLS2/1-1173	1095 K S I G N G R K G M V R V L D M E L G -----D S I V S L K Q E E A I E D F L K L C L F C T S S R P E D R P D M N E I L T H L M K L R G K A N S F R E D R N E D R E V -----	1173
At1g35710/1-1120	1066 P - G E A L S L R S I S D E R V L E -----P R G Q N R E K L L K M V E M A L L C L Q A N P E S R P T M L S I S T T F S -----	1120
RAE5/2/1-1009	970 R V E I M V R F G L F G L N -----F N Q I K T K M F C F G --L K F F L T M G W I W F S F -----	1009
RAE5/1/1-1045	990 P P D A T L S L K S I S D H R L P E -----P T P E I K E V E L I L K V A L L C L H S D P Q A R P T M L S I S T A F S -----	1045
Pto_Q3I6Z1_SOLPI/1-321	258 E S H N N G Q L E Q I V D P N L A D -----K I R P E S L R K F G - D T A V K C L A L S S E D R P S M G D V L -----W K L E Y A L R L Q E S V I -	321
PTI1_SOLLC/1-354	292 P R L S E D K V K Q C V D A R L N T -----D Y P P K A I A K M A - A V A A L C V Q Y E A D F R P N M S I V V K A L Q P L L P -----R P V P S -----	354
Q40126_SOLPI/1-318	250 E T Q K M G Q L E Q I V D P T I A A -----K I R P E S L R K F G - E T A I K C L A P S S K N R P S M G D V L -----W K L E Y A L C L Q E P T I Q	318
P93215_SOLLC/1-311	248 E S H N N G Q L E Q I V D P N L A D -----K I R P E S L R K F G - E T A V K C L A L S S E D R P S M G D V L -----W K L E Y A L R L Q E S V I -	311
BAK1/1-615	511 G L L K E K K L E A L V D V D L Q C -----N Y K D E E V E Q L I - Q V A L L C T Q S S P M E R P K M S E V V R M L E G D G L A E R W E E W Q K E E M F R Q D F N Y P T H H P A V S G W I I G D S T S Q I E N E Y P	611
BKK1/1-620	516 E V L K E K K L E S L V D A E L E G -----K Y V E T E V E Q L I - Q M A L L C T Q S S A M E R P K M S E V V R M L E G D G L A E R W E E W Q K E E M P I H D F N Y Q A Y P H A G T D W L I P Y S N S L I E N D Y P	616
SERK1/1-625	524 G L L K E K K L E M L V D P D L Q T -----N Y E E R E L E Q V I - Q V A L L C T Q G S P M E R P K M S E V V R M L E G D G L A E K W D E W Q K V E I L R E E I D L S P N P N S - D W I L D S T Y N L H A V E L	621
SERK2/1-628	527 G L L K E K K L E M L V D P D L Q S -----N Y T E A E V E Q L I - Q V A L L C T Q S S P M E R P K M S E V V R M L E G D G L A E K W D E W Q K V E V L R Q E V E L S S H P T S - D W I L D S T D N L H A M E L	624
SERK5/1-601	497 E V L K E K K L E S L V D A E L E G -----K Y V E T E V E Q L I - Q M A L L C T Q S S A M E R P K M S E V V R M L E G D G L A E R W E E W Q K E E M P I H D F N Y Q A Y P H A G T D W L I P Y S N S L I E N D Y P	597
BRI1/1-1196	1102 - Q H A K L R I S D V F D P E L M K -----E D P A L E I E L L Q H L K V A V A C L D D R A W R R P T M V Q V M A M F K E I Q A G S G I D S Q S T I R S I E D G G F S T I E M V D M S I K E V P E G K L -----	1196
Xa21/1-1025	939 L G L H G R - V T D V V D T K L I L D S E N W L N S T N N S P C R R I T E C I V W L L R L G L S C S Q E L P S S R T P T G D I I D E L N A I K Q N L S G L F P V C E G G S L E F -----	1025
ERECTA/1-976	861 S K T G N N E V M E M A D P D I T S -----T C K D L G V V K K V F - Q L A L L C T K R Q P N D R P T M H Q V T R V L G S F M L S E Q P P A T D T S A T L A G S C Y V D E Y A N L K T P H S V N C S S M S A S D A Q	962
CLV1/1-980	913 E I T Q P S D A A I V V A I V D P R -----L T G Y P L T S V I H V F K I A M M C V E E E A A R P T M R E V V H M E T N -----P P K S V A N L I A F -----	980
CLV3/1-96	- -----	
AT3g47580/1-1011	- -----	
AT3g47090/1-1009	- -----	
At3g47570/1-1010	- -----	
EFR/1-1031	- -----	
AT5g39390/1-502	- -----	
AT3g47110/1-1025	- -----	
At2g24130/1-980	- -----	
FLS2/1-1173	- -----	
At1g35710/1-1120	- -----	
RAE5/2/1-1009	- -----	
RAE5/1/1-1045	- -----	
Pto_Q3I6Z1_SOLPI/1-321	- -----	
PTI1_SOLLC/1-354	- -----	
Q40126_SOLPI/1-318	315 D D P E -----	318
P93215_SOLLC/1-311	- -----	
BAK1/1-615	612 S G P R -----	615
BKK1/1-620	617 S G P R -----	620
SERK1/1-625	622 S G P R -----	625
SERK2/1-628	625 S G P R -----	628
SERK5/1-601	598 S G P R -----	601
BRI1/1-1196	- -----	
Xa21/1-1025	- -----	
ERECTA/1-976	963 L F L R F G Q V I S Q N S E -----	976
CLV1/1-980	- -----	
CLV3/1-96	- -----	

**Appendix Figure A2.5 Multiple sequence alignment of various receptor-like kinases.** ClustalW multiple alignment, generated using JalView v.12.2, colored by percentage sequence identity. Green highlighted residue indicates conserved catalytic Asp in kinase active site. Pink indicates conservation of important Thr (T38 in Pto, essential for autophosphorylation and interaction with Pt1).

**Table A4.1 RAE5-co-expressed genes predicted by Expression Angler<sup>1</sup>**

TAIR accession	r <sup>2</sup>	Annotation
<b>At5g48380</b>	<b>0.834</b>	<b>BIR1 LRR-RK</b>
At1g66910	0.821	protein kinase, putative
At2g39210	0.804	nodulin family protein
At5g01540	0.797	LECRKA4.1 (lectin receptor kinase A4.1)
<b>At5g44070</b>	<b>0.793</b>	<b>ARA8/PCS1/CAD1(phytochelain synthase1)</b>
At1g70520	0.786	CRK2_protein kinase family protein
At5g23490	0.783	unknown protein
<b>At3g54420</b>	<b>0.778</b>	<b>AtCHITIV; chitinase</b>
At5g25440	0.771	protein kinase family protein
At5g40780	0.762	LTH1 amino acid transmembrane transporter
At1g10340	0.761	ankyrin repeat family protein
At4g13510	0.759	AtAMT1 (1 ammonium transporter 1;1)
At5g39020	0.746	protein kinase family protein
<b>At1g02920</b>	<b>0.74</b>	<b>ATGST11_ATGSTF7_ATGST8</b>
<b>At5g61210</b>	<b>0.736</b>	<b>ATSNAP33 (soluble n-ethylmaleimide-sensitive factor adaptor protein 33)</b>
At2g02220	0.735	ATPSKR1 (phytosulfokin receptor 1)
<b>At1g66160</b>	<b>0.733</b>	<b>ATCMPG1 (U-box domain-containing protein</b>
At2g42360	0.733	zinc finger (C3HC4-type RING finger) family protein
<b>At2g39660</b>	<b>0.733</b>	<b>BIK1 (botrytis-induced kinase1); kinase</b>
<b>At4g23570</b>	<b>0.731</b>	<b>SGT1A; protein binding</b>
At5g20050	0.728	protein kinase family protein
At3g09830	0.725	protein kinase, putative
At4g23200	0.722	CRK12_protein kinase family protein
At2g37710	0.721	RLK (receptor lectin kinase); kinase
At4g38550	0.721	LOCATED IN: chloroplast;

<sup>1</sup>Genes co-expressed with RAE5 according to NASCArrays392 data set obtained at Expression Angler ([http://www.bar.utoronto.ca/ntools/cgi-bin/ntools\\_expression\\_angler.cgi](http://www.bar.utoronto.ca/ntools/cgi-bin/ntools_expression_angler.cgi))

<sup>2</sup> r: Pearson correlation coefficient

signal peptide

AT3g47580/1-1011	1	-----M <b>KLF</b> LLL <b>SFS</b> AH-LLL <b>GADG</b> -----	<b>FTD</b> EDTRQ <del>ALL</del> E <b>FK</b> SQVSEG-KRDV <del>L</del> <b>SSWNS</b> -----	50
AT3g47090/1-1009	1	-----M <b>RLL</b> FLLA <b>FA</b> NAL-M <b>QLE</b> AY <b>G</b> -----	<b>FTD</b> EDTRQ <del>ALL</del> E <b>I</b> K <b>SQVSE</b> S-KRD <b>AL</b> S <b>ANHNS</b> -----	50
AT3g47570/1-1010	1	-----M <b>RLL</b> FLLA <b>FA</b> NAL-M <b>LE</b> TH <b>G</b> -----	<b>FTD</b> EDTRQ <del>ALL</del> E <b>I</b> K <b>SQVSE</b> D-KRV <b>L</b> S <b>WNS</b> -----	50
EFR/1-1031	1	-----M <b>KLS</b> FLV <b>N</b> ALTL <b>L</b> QVC <b>I</b> -----	<b>FA</b> Q <b>AR</b> F <b>S</b> NET <b>DMQ</b> ALL <b>E</b> F <b>K</b> S <b>QVSE</b> N <b>KREV</b> L <b>ASWNS</b> -----	57
AT5g39390/1-502	1	-----M <b>KIS</b> FLFA <b>N</b> AL-M <b>L</b> QVC <b>I</b> LV <b>F</b> Q <b>AR</b> F <b>S</b> NET <b>DMQ</b> ALL <b>E</b> F <b>K</b> S <b>QVTE</b> N <b>KREV</b> L <b>ASWNS</b> -----	57	
AT3g47110/1-1025	1	-----M <b>G</b> V <b>P</b> C <b>I</b> V <b>R</b> L <b>I</b> V <b>S</b> AL <b>V</b> S <b>L</b> -----	<b>E</b> HS <b>D</b> M <b>V</b> CA <b>Q</b> T <b>I</b> R <b>L</b> T <b>E</b> DK <b>Q</b> -----	65
AT2g24130/1-980	1	-----M <b>DY</b> C <b>S</b> LL <b>V</b> S <b>F</b> LT <b>V</b> TM <b>V</b> TL <b>A</b> S-----	-----K <b>EN</b> D <b>HE</b> I <b>K</b> NP <b>Q</b> NS <b>L</b> SS <b>W</b> SS <b>S</b> SS <b>S</b> SS <b>S</b> -----	50
FLS2/1-1173	1	-----M <b>M</b> K <b>L</b> S <b>T</b> K <b>F</b> -----	-----L <b>LT</b> T <b>F</b> F <b>G</b> IA <b>L</b> AK <b>Q</b> FS <b>E</b> -----	57
At1g35710/1-1120	1	-----M <b>G</b> FA <b>E</b> KN <b>LY</b> D <b>F</b> R <b>F</b> LL <b>F</b> -----	I <b>S</b> I <b>I</b> L <b>S</b> C <b>S</b> I <b>S</b> A <b>S</b> A <b>T</b> I <b>E</b> A <b>N</b> ALL <b>K</b> W <b>K</b> S <b>T</b> F <b>T</b> N-----	62
RAES-2/1-1009	1	-----M <b>M</b> N <b>K</b> T <b>N</b> P <b>E</b> K <b>I</b> S <b>L</b> T <b>S</b> F <b>K</b> E <b>M</b> ACK <b>E</b> -----	P <b>R</b> D <b>L</b> Q <b>V</b> LL <b>I</b> I <b>S</b> V <b>L</b> S <b>C</b> F <b>A</b> V <b>S</b> A <b>T</b> E <b>V</b> E <b>E</b> AN <b>A</b> ALL <b>K</b> W <b>K</b> S <b>T</b> F <b>T</b> N <b>T</b> Q <b>S</b> S <b>S</b> SS <b>L</b> S <b>W</b> V <b>N</b> -----	79
RAES-5/1-1045	1	-----M <b>M</b> N <b>K</b> T <b>N</b> P <b>E</b> K <b>I</b> S <b>L</b> T <b>S</b> F <b>K</b> E <b>M</b> ACK <b>E</b> -----	P <b>R</b> D <b>L</b> Q <b>V</b> LL <b>I</b> I <b>S</b> V <b>L</b> S <b>C</b> F <b>A</b> V <b>S</b> A <b>T</b> E <b>V</b> E <b>E</b> -----	79
AT3g47580/1-1011	51	<b>F</b> PL <b>C</b> N <b>K</b> W <b>V</b> T-----	-----G <b>R</b> K <b>H</b> K <b>R</b> V <b>H</b> L <b>N</b> LG <b>G</b> Q <b>U</b> G <b>I</b> V <b>S</b> P <b>S</b> I <b>G</b> N <b>V</b> S <b>F</b> I-----	109
AT3g47090/1-1009	51	<b>F</b> PL <b>C</b> SH <b>K</b> W <b>V</b> R-----	-----G <b>R</b> K <b>H</b> K <b>R</b> V <b>T</b> R <b>L</b> D <b>G</b> Q <b>L</b> Q <b>G</b> V <b>I</b> S <b>P</b> S <b>S</b> I <b>G</b> N <b>S</b> F-----	109
AT3g47570/1-1010	51	<b>F</b> PL <b>C</b> N <b>K</b> W <b>V</b> C <b>T</b> -----	-----G <b>R</b> K <b>N</b> K <b>R</b> V <b>H</b> L <b>E</b> -----	109
EFR/1-1031	58	S <b>P</b> FC <b>C</b> N <b>W</b> I <b>G</b> T-----	-----G <b>R</b> R <b>E</b> R <b>M</b> I <b>S</b> LN <b>R</b> -----	116
AT5g39390/1-502	58	<b>F</b> PL <b>C</b> W <b>H</b> I <b>G</b> T-----	-----G <b>R</b> Q <b>E</b> R <b>T</b> S <b>L</b> D <b>G</b> F <b>L</b> S <b>C</b> I <b>S</b> P <b>S</b> I <b>G</b> N <b>S</b> F-----	115
AT3g47110/1-1025	66	L <b>P</b> LC <b>S</b> T <b>C</b> V <b>I</b> T-----	-----G <b>L</b> K <b>H</b> R <b>V</b> T <b>G</b> D <b>L</b> G <b>G</b> L <b>K</b> T <b>C</b> V <b>F</b> G <b>V</b> G <b>N</b> L <b>S</b> F-----	124
AT2g24130/1-980	51	V <b>D</b> V <b>C</b> N <b>W</b> S <b>C</b> K-----	-----N <b>K</b> E <b>S</b> T <b>Q</b> M <b>I</b> E <b>D</b> I <b>S</b> G <b>R</b> D <b>G</b> E-----	124
FLS2/1-1173	58	L <b>R</b> H <b>E</b> N <b>Y</b> T <b>G</b> T-----	-----D <b>S</b> T <b>G</b> -H <b>M</b> V <b>S</b> S <b>W</b> L <b>E</b> K <b>Q</b> G <b>V</b> E-----	115
At1g35710/1-1120	63	F <b>S</b> C <b>T</b> W <b>Y</b> G <b>V</b> S-----	-----S <b>N</b> R <b>G</b> S <b>I</b> E <b>E</b> N <b>L</b> N <b>L</b> T <b>N</b> T <b>G</b> I <b>E</b> G <b>T</b> F <b>Q</b> D <b>F</b> P-----	145
RAES-2/1-1009	80	S <b>F</b> C <b>T</b> W <b>Y</b> G <b>V</b> A-----	-----S <b>L</b> G <b>S</b> I <b>I</b> R <b>L</b> N <b>L</b> T <b>N</b> T <b>G</b> I <b>E</b> G <b>T</b> F <b>ED</b> F <b>P</b> F <b>S</b> S <b>L</b> P-----	161
RAES-5/1-1045	80	S <b>F</b> C <b>T</b> W <b>Y</b> G <b>V</b> A-----	-----S <b>L</b> G <b>S</b> I <b>I</b> R <b>L</b> N <b>L</b> T <b>N</b> T <b>G</b> I <b>E</b> G <b>T</b> F <b>ED</b> F <b>P</b> F <b>S</b> S <b>L</b> P-----	161
AT3g47580/1-1011	110	V <b>C</b> N <b>I</b> F-----	-----L <b>E</b> H <b>Y</b> MA <b>F</b> N <b>S</b> L <b>E</b> E <b>C</b> I <b>P</b> A-----	168
AT3g47090/1-1009	110	M <b>C</b> N <b>I</b> F-----	-----L <b>K</b> Y <b>L</b> A <b>V</b> C <b>F</b> N <b>I</b> Y <b>L</b> E-----	168
AT3g47570/1-1010	110	V <b>C</b> Q <b>L</b> S-----	-----L <b>E</b> Y <b>L</b> D <b>M</b> C <b>I</b> N <b>Y</b> L <b>R</b> P <b>I</b> P <b>L</b> G <b>L</b> Y <b>N</b> C <b>S</b> R <b>L</b> L <b>N</b> L <b>R</b> -----	168
EFR/1-1031	117	V <b>R</b> F-----	-----L <b>Q</b> Y <b>L</b> N <b>M</b> S <b>Y</b> N <b>L</b> E-----	175
AT5g39390/1-502	125	V <b>C</b> N <b>I</b> F-----	-----Q <b>Y</b> L <b>N</b> M <b>S</b> N <b>L</b> F-----	183
AT3g47110/1-1025	125	V <b>C</b> N <b>I</b> F-----	-----Q <b>Y</b> L <b>N</b> M <b>S</b> N <b>L</b> F-----	183
AT2g24130/1-980	110	I <b>C</b> S <b>L</b> H <b>E</b> T-----	-----L <b>K</b> Q <b>L</b> S <b>L</b> E <b>N</b> -----	162
FLS2/1-1173	116	I <b>C</b> K-----	-----L <b>E</b> N <b>Q</b> P <b>Q</b> E <b>G</b> L <b>Q</b> -----	198
At1g35710/1-1120	146	L <b>C</b> N-----	-----L <b>T</b> V <b>L</b> L <b>H</b> Q <b>N</b> Y <b>L</b> T-----	204
RAES-2/1-1009	162	L <b>C</b> D <b>L</b> S-----	-----L <b>D</b> T <b>L</b> H <b>V</b> E <b>N</b> K <b>L</b> N-----	220
RAES-5/1-1045	162	L <b>C</b> D <b>L</b> S-----	-----L <b>D</b> T <b>L</b> H <b>V</b> E <b>N</b> K <b>L</b> N-----	220
AT3g47580/1-1011	169	L <b>G</b> R <b>N</b> L <b>K</b> G <b>K</b> L-----	-----P <b>R</b> S <b>L</b> G <b>N</b> L <b>T</b> K <b>S</b> -----	250
AT3g47090/1-1009	169	L <b>G</b> L <b>D</b> L <b>K</b> F-----	-----P <b>R</b> F <b>V</b> I <b>R</b> N <b>L</b> T-----	250
AT3g47570/1-1010	169	L <b>G</b> Y <b>N</b> N <b>M</b> R <b>G</b> K-----	-----P <b>R</b> S <b>L</b> G <b>N</b> L <b>T</b> K <b>S</b> -----	250
EFR/1-1031	176	L <b>S</b> K <b>N</b> N <b>T</b> C <b>N</b> F-----	-----P <b>R</b> S <b>L</b> G <b>N</b> L <b>T</b> K <b>S</b> -----	250
AT5g39390/1-502	184	L <b>G</b> R <b>N</b> T <b>K</b> F-----	-----P <b>R</b> S <b>L</b> G <b>N</b> L <b>T</b> K <b>S</b> -----	250
AT3g47110/1-1025	184	L <b>G</b> R <b>N</b> T <b>K</b> F-----	-----P <b>R</b> S <b>L</b> G <b>N</b> L <b>T</b> K <b>S</b> -----	265
AT2g24130/1-980	163	-----G <b>S</b> S <b>S</b> S-----	-----P <b>R</b> S <b>L</b> G <b>N</b> L <b>T</b> K <b>S</b> -----	231
FLS2/1-1173	199	A <b>G</b> A <b>N</b> H <b>L</b> T <b>C</b> S-----	-----P <b>R</b> S <b>L</b> G <b>N</b> L <b>T</b> K <b>S</b> -----	280
At1g35710/1-1120	205	L <b>E</b> Y <b>N</b> E <b>L</b> T <b>C</b> V-----	-----P <b>R</b> S <b>L</b> G <b>N</b> L <b>T</b> K <b>S</b> -----	286
RAES-2/1-1009	221	L <b>E</b> F <b>I</b> N <b>S</b> L <b>C</b> S-----	-----P <b>R</b> S <b>L</b> G <b>N</b> L <b>T</b> K <b>S</b> -----	302
RAES-5/1-1045	221	L <b>E</b> F <b>I</b> N <b>S</b> L <b>C</b> S-----	-----P <b>R</b> S <b>L</b> G <b>N</b> L <b>T</b> K <b>S</b> -----	302
AT3g47580/1-1011	251	K <b>P</b> D <b>F</b> -----	-----P <b>R</b> S <b>L</b> G <b>N</b> L <b>T</b> K <b>S</b> -----	255
AT3g47090/1-1009	251	K <b>P</b> D <b>F</b> -----	-----P <b>R</b> S <b>L</b> G <b>N</b> L <b>T</b> K <b>S</b> -----	255
AT3g47570/1-1010	251	R <b>P</b> D <b>L</b> G-----	-----P <b>R</b> S <b>L</b> G <b>N</b> L <b>T</b> K <b>S</b> -----	255
EFR/1-1031	258	R <b>A</b> D <b>F</b> C-----	-----P <b>R</b> S <b>L</b> G <b>N</b> L <b>T</b> K <b>S</b> -----	262
AT5g39390/1-502	266	R <b>P</b> D <b>F</b> C-----	-----P <b>R</b> S <b>L</b> G <b>N</b> L <b>T</b> K <b>S</b> -----	270
AT3g47110/1-1025	232	P <b>S</b> Q <b>V</b> I-----	-----P <b>R</b> S <b>L</b> G <b>N</b> L <b>T</b> K <b>S</b> -----	298
AT2g24130/1-980	281	P <b>A</b> E <b>L</b> N <b>V</b> Q <b>L</b> Q <b>A</b> R <b>I</b> Y <b>K</b> N-----	-----P <b>R</b> S <b>L</b> G <b>N</b> L <b>T</b> K <b>S</b> -----	369
FLS2/1-1173	287	P <b>S</b> S <b>L</b> C <b>N</b> K <b>N</b> L <b>T</b> L <b>S</b> L <b>F</b> Q <b>N</b> Y <b>L</b> T <b>G</b> I <b>P</b> P <b>K</b> L <b>G</b> N <i>IES</i> <b>M</b> I <b>D</b> <b>L</b> E <b>L</b> S <b>N</b> K <b>N</b> L <b>T</b> G <b>S</b> I <b>P</b> S <b>S</b> L <b>G</b> N <i>LN</i> <b>K</b> N <b>L</b> T <b>I</b> I <b>L</b> Y <b>E</b> N <i>Y</i> <b>L</b> T <b>G</b> V <i>P</i> <b>E</b> L <b>G</b> N <i>M</i> <b>E</b> <b>S</b> -----	307	
At1g35710/1-1120	303	P <b>S</b> T <b>L</b> G-----	-----P <b>R</b> S <b>L</b> G <b>N</b> L <b>T</b> K <b>S</b> -----	307
RAES-2/1-1009	303	P <b>S</b> T <b>L</b> G-----	-----P <b>R</b> S <b>L</b> G <b>N</b> L <b>T</b> K <b>S</b> -----	307
RAES-5/1-1045	303	P <b>S</b> T <b>L</b> G-----	-----P <b>R</b> S <b>L</b> G <b>N</b> L <b>T</b> K <b>S</b> -----	307

## Appendix Figure A4.1-1. Multiple alignment of members of Family XII of LRR-RKs - Part 1: Signal peptide and LRR domain.

ClustalW multiple alignment generated using JalView v.12.2, shaded for percentage identity.

RAE5 peptides identified by MS analysis of EFR IPs highlighted in green. The region corresponding to the signal peptide is indicated.

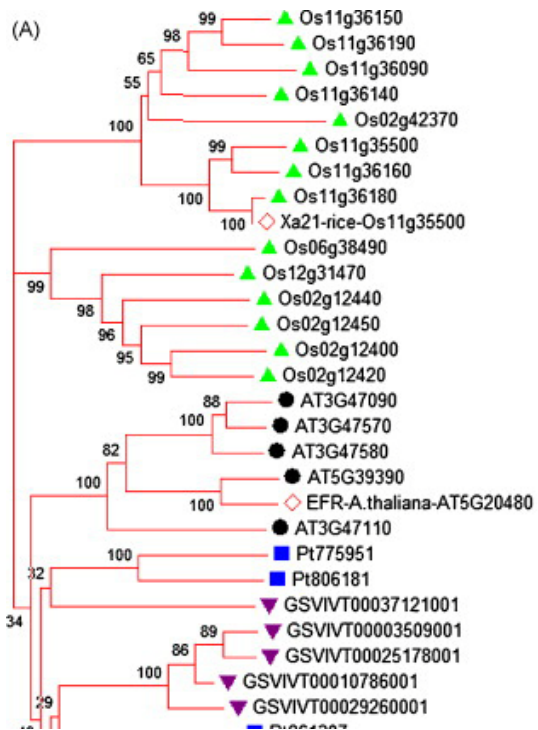
**Appendix Figure A4.1-2. Multiple alignment of members of Family XII of LRR-RKs (continued) - Part 2: LRR domain.**

ClustalW multiple alignment generated using JalView v.12.2, shaded for percentage identity. RAE5 peptides identified by MS analysis of EFR IPs highlighted in green.

AT3g47580/1-1011 621 K L K P C L A Q E P P V E T K H S S H L K K V A I L V S I C I A L L L L V I A S M V L C W F R K R R K N Q Q T N N L V P - - - S K L E I F H E K I S Y G D L R N A 699  
 AT3g47090/1-1009 621 K L K P C I A Q A P P V E T R H P S L L K K V A I G V S V C I A L L L L F I V S - - - L S W F K K R R K N Q Q I N N S A P - - - F T L E I F H E K I S Y G D L R N A 697  
 At3g47570/1-1010 620 Q L K P C L S Q A P S V V K K H S S R L K K V V I G V S V C I T L L L L F M A S V T L I W L R K R K K N K E T N N P T P - - - S T L E V L H E I S Y G D L R N A 698  
 EFR/1-1031 628 Q L K P C I V Q A S P R K R K P L S V R K V V V S G C I C I A S L L L I I V A S - - - L C W F M K R K K K N A S D G N P S - D S T I L G M F H E K V S E E L H S A 708  
 AT5g39390/1-502 149 Q L K P C I E - - S P R K R K P F S L G E K V A V G - - - V C V A L L F L I I V A S - - - L S W F K K K - - - - - N D K I S Y E E L Y N A 205  
 AT3g47110/1-1025 636 Q L Q P C S V E L P R R H S - - - S V R K I I T I C V S A V M A A L L L C L C V V Y L C W Y K L R V K S V R A N N N E N D R S F S P V K S F Y E I S Y D E L Y K T 715  
 At2g24130/1-980 583 Q A C K K K H K Y P S V L L P V L L S I A T P V L C V F C Y P L V Q R S R F G K N L T V V A K E E V E D E E K Q N Q N D P - - - - - K Y P R I S Y Q Q L I A 657  
 FLS2/1-1173 790 K P C T I K Q K S S H F S K R T R V I L I I L G S A A A L L L V L L V L I L T C C K K K E K K I E N S S E S S L P D L D S - - - - - A L K L K R F E P K E L E Q A 866  
 At1g35710/1-1120 768 Q R L K P C - - R E L K K P K K G N G N L V V W I L V P I L C V L V I L I V P I I C A I I I L S V C A G I F - I C F R K R T K Q I E E H T D S E S G G E T L S I F S F D C V R Y Q E I I K A 847  
 RAE5-2/1-1009 690 Q G L K P C S I T S S K K S H K D R N L I I Y I L V P I I C A I I I L S V C A G I F - I C F R K R T K Q I E E H T D S E S G G E T L S I F S F D C V R Y Q E I I K A 771  
 RAE5-1/1-1045 690 Q G L K P C S I T S S K K S H K D R N L I I Y I L V P I I C A I I I L S V C A G I F - I C F R K R T K Q I E E H T D S E S G G E T L S I F S F D C V R Y Q E I I K A 771  
 AT3g47580/1-1011 700 T N G F S S S N M V G S C S F G T V F A A L P T E S K I I A V K V L N M Q R R G A M K S - - - F M A E C E S L K D T R H R N L V K L L T A C A S T D F Q G N E F R 778  
 AT3g47090/1-1009 698 T D G F S S S N M V G S C S F G T V Y V A R L Q T E N K I I A V K V L N M Q R R G A M K S - - - F M A E C E S L K D I I R H R N L V K L L T A C S S I D F Q G N E F R 776  
 At3g47570/1-1010 699 T N G F S S S N M V G S C S F G T V Y V A R L Q T E N K I I A V K V L N M Q R R G A M K S - - - F M A E C E S L K D I I R H R N L V K L L T A C S S I D F Q G N E F R 777  
 EFR/1-1031 709 T S R F S S T N L I C S G N F G N V F N G L G P E N K L V A V K V L N L L K H G A T K S - - - F M A E C E T F K G I R H R N L V K L L T V C S S L D E S G N D F R 787  
 AT5g39390/1-502 206 T S G F S S S N L I G S C S F D S V F N G L G L E E K L V A V K V L N L L K H G A T K S - - - F M A E C E S F K G I R H R N L V K L L T V C S S L D E S G N D F R 284  
 AT3g47110/1-1025 716 T G G S S S N L I G S C S F N G A V F R G F L G S K N K A V A I K V L N L L K C R G A A K S - - - F M A E C E A L G G I R H R N L V K L V T I I S S S D F E G N D F R 794  
 At2g24130/1-980 658 T G G F N A S S L I C S R F G H V V Y V G L R N N T S V A V K V L D P K T A E F S G S - - - F K R E Q C I L K R V N L T R I I T E S P K G - - - - - F N 731  
 FLS2/1-1173 867 T D S F N S A N I I C S S S L S T V Y V Q L E D G - T V I A V K V L N L K E F S A E S D K - - W F Y T E A K T L S O L K H R N L V K I I L G F A W E S G - - - K T K 942  
 At1g35710/1-1120 848 T N E F D P T H L I G T C G Y S K V Y R A N Q D T I I A V K R L H D T I D E E I S K P V V K Q E F L N E V K A L T E I R H R N V V K L I F G F C H R R - - - H T 925  
 RAE5-2/1-1009 772 T G E F D P K Y L I G T C G H G K V Y M A K L P N A I M A K K L N E T T D S S I S N P S T K Q E F L N E I R A L T E I R H R N V V K L I F G F C H R R - - - N T 849  
 RAE5-1/1-1045 772 T G E F D P K Y L I G T C G H G K V Y M A K L P N A I M A K K L N E T T D S S I S N P S T K Q E F L N E I R A L T E I R H R N V V K L I F G F C H R R - - - N T 849  
 AT3g47580/1-1011 779 A L I Y E Y L P N G S V D M W L H P E E V E E I R R P R T L T L L E R L N I V D V A S V I D Y L I V H C H E P I A I C D L K P S N V L L E D D L T A H V S D F G L 861  
 AT3g47090/1-1009 777 A L I Y E F P M P N G S L D K W L H P E E V E E I H R P S R T L T L L E R L N I A I D V A S V I D Y L I V H C H E P I A I C D L K P S N I L L D D D L T A H V S D F G L 859  
 At3g47570/1-1010 778 A L I Y E F P M P N G S L D M W L H P E E V E E I H R P S R T L T L L E R L N I A I D V A S V I D Y L I V H C H E P I A I C D L K P S N V L L D D D L T A H V S D F G L 860  
 EFR/1-1031 788 A L V Y E F P M P K G S L D M W L Q P E D L E S A N N H S R S L T F A E K V N I A I D V A S A L E Y L I V H C H D P V A C D I K P S N V L L D D D L T A H V S D F G L 870  
 AT5g39390/1-502 285 A L V Y E F P M P K G S L D M W L Q P E D L E S A N N H S R S L T F A E K V N I A I D V A S A L E Y L I V H C H D P V A C D I K P S N V L L D D D L T A H V S D F G L 367  
 AT3g47110/1-1025 795 A L V Y E F P M P G N D L M W L H P D E I E E T G N P S R T L G L F A R L N I A I D V A S A L V Y L I V H C H D P V A C D I K P S N V L L D D D L T A H V S D F G L 877  
 At2g24130/1-980 732 A L V L P L M P N G S L E R H Y P G - - - E Y S S K N D L I Q L V N I C S D V A E G T A L Y L H H Y S P V K V V D C L K P S N I L L D D E M A T A L V T D F G I 809  
 FLS2/1-1173 943 A L V L P L M P N G S L E R H Y P G - - - E Y S S K N D L I Q L V N I C S D V A E G T A L Y L H H Y S P V K V V D C L K P S N I L L D D E M A T A L V T D F G I 1018  
 At1g35710/1-1120 926 F L I Y E Y M E R G S L R K V I E N D D - - - E A K K L D W G K R I N V V K G V A H A L S Y M H H D R S P A I V R D I S S C N I L L D N E Y T A K I E D F C T 1002  
 RAE5-2/1-1009 850 F L I Y E Y M E R G S L R K V I E N D D - - - E A K K L D W G K R I N V V K G V A H A L S Y M H H D R S P A I V R D I S S C N I L L D N E Y T A K I E D F C T 926  
 RAE5-1/1-1045 850 F L I Y E Y M E R G S L R K V I E N D D - - - E A K K L D W G K R I N V V K G V A H A L S Y M H H D R S P A I V R D I S S C N I L L D N E Y T A K I E D F C T 926  
 AT3g47580/1-1011 862 A R L L L K F D K E S F L N Q L S S A G - - - V R G T I C Y A A P E Y G M G Q Q P S I H G D V Y S F G V V L L E M F T G K R P T - - D E L F G G N L T L H S Y T K 937  
 AT3g47090/1-1009 860 A R L L L K F D Q E S F F N Q L S S A G - - - V R G T I C Y A A P E Y G M G Q Q P S I H G D V Y S F G V V L L E M F T G K R P T - - N E L F G G N F T L L H S Y T K 935  
 At3g47570/1-1010 861 A R L L L K F D E E S F F N Q L S S A G - - - V R G T I C Y A A P E Y G M G Q Q P S I N C D V Y S F G I I L L E M F T G K R P T - - N E L F G G N F T L L H S Y T K 936  
 EFR/1-1031 871 A Q L L K Y K D R E S F L N Q F S S A G - - - V R G T I C Y A A P E Y G M G Q Q P S I Q C D V Y S F G I I L L E M E S G K G P T - - D E S F A G D Y N L H S Y T K 946  
 AT5g39390/1-502 368 A R L L L K F D E K T F L N Q F S S A G - - - V R G T I C Y A A P E Y G M G S K P S I Q C D V Y S F G V V L L E M F T G K R P T - - D N S F G G G Y N L H G Y T K 443  
 AT3g47110/1-1025 878 A Q L L K F D R D T F H I Q F S S A G - - - V R G T I C Y A A P E Y G M G Q H P S I M C D V Y S F G I V V L L E M F T G K R P T - - N K L F V D G L T L H S F T K 953  
 At2g24130/1-980 810 S R L V Q Q V E E T V S T D D S V F S E T D G L L C G S V C Y I A P E Y G M G K R A S T H D V Y S F G V V L L E I V S G R P T - - D V L V N E G S S L H E F M K 890  
 FLS2/1-1173 1019 A R L L K F D R E G D T S T A S F A E G - - - T I C Y L A P E F A Y M R K V T K A D V F S G I I I M M E L M T K Q R P T S L N D E D S Q D M T L R Q L V E 1094  
 At1g35710/1-1120 1003 A K L L K T - - - D S S N W S A V A G - - - T I C Y V A P G T L F D P - - - - - L D K L V V D L T R - - - - - L W S G R V E I M V R F 977  
 RAE5-2/1-1009 927 A K L L K P - - - D S S N W S A V A G - - - T I C Y V A P G T L F D P - - - - - L D K L V V D L T R - - - - - L W S G R V E I M V R F 977  
 RAE5-1/1-1045 927 A K L L K P - - - D S S N W S A V A G - - - T I C Y V A P E L A Y A M V T E K C D V Y S F G V V L L E I I C K H P G D L V S S L S S P - - G E A L S 1072  
 AT3g47580/1-1011 938 L A L P E K - V F E I A D K A I L H I G L - - - R V G F R T A E C U T L V L E V G L R C C E E Y P T N I L A T S E V A K E L I S I R E R F F K T R T P R R - - - 1011  
 AT3g47090/1-1009 936 A A L P E R - V L D A K D S I L H S G L - - - R V G F P V L E C L K G I I D V G L R C C E E S P L N I L A T S E A A K E L I S I R E R F F K T R T R A R R - - - 1009  
 At3g47570/1-1010 937 S A L P E R - I L D I V D E S I L H I G L - - - R V G F P V E C L T M V F E V G L R C E E S P M N I L A T S I V V K E L I S I R E R F F K A S R T T W R - - - 1010  
 EFR/1-1031 947 S I L S G C - T S S G G S N - - - A I D E C U R L V L O V G I K C S E E Y P D R M R T D E A V R E L I S I R E R F F K F S S K T T I T E S P R D 1013  
 AT5g39390/1-502 444 S V L S C S - T S R G G R T - - - M V D E W L R L V L E V G I K C S E E Y P D R M R T D E A V R E L I S I R E R F F K F S S K T T I T E S P R D 502  
 AT3g47110/1-1025 954 S A L Q K R Q A L D I T D E T I L R G A Y - - - A Q H F N M V E C L T L V F R V G V S C S E E S P V N N I S M A E A I S K L V S I R E S F F R D E E T - - - 1025  
 At2g24130/1-980 891 S H Y P D S L E G I I E Q A L S R W K P Q G K P E K C E K L W R E V I L E M I E L G L V C T Q Y N P S T R P D M L D V A H E M G R L K E Y L F A C P S L L H F S S Q E 973  
 FLS2/1-1173 1095 K S I G N G R K G M V R V L D M E L G D S - - - I V S L K Q E E A I E D F L K L C L F C T S R P E D P M D N E I L T H L M K L R C K A N S F R E D R N E D R E V 1173  
 At1g35710/1-1120 1073 R S I S D E R V L E P R C Q - - - N R E K L L K M Y E M A L L C L Q A N P E S B P T M L S I S T T F S - - - 1120  
 RAE5-2/1-1009 978 G L F G L N - - - F N Q I K T K M F C F G - - - L K F F L T M G W I F S F - - - 1009  
 RAE5-1/1-1045 998 K S I S D H R L P E P T P E - - - I K T E V L E I L K V A L L C L H S D P Q A P T M L S I S T A F S - - - 1045  
 AT3g47580/1-1011 - - - - -  
 AT3g47090/1-1009 - - - - -  
 At3g47570/1-1010 - - - - -  
 EFR/1-1031 1014 A P Q S S P Q E W M L N T D M H T M - - - 1031  
 AT5g39390/1-502 - - - - -  
 AT3g47110/1-1025 - - - - -  
 At2g24130/1-980 974 T Q G E A S S - - - - - 980  
 FLS2/1-1173 - - - - -  
 At1g35710/1-1120 - - - - -  
 RAE5-2/1-1009 - - - - -  
 RAE5-1/1-1045 - - - - -

**Appendix Figure A4.1-3. Multiple alignment of members of Family XII of LRR-RKs (continued)- Part 3: Transmembrane (TM), juxtamembrane (JM) and kinase domain.**

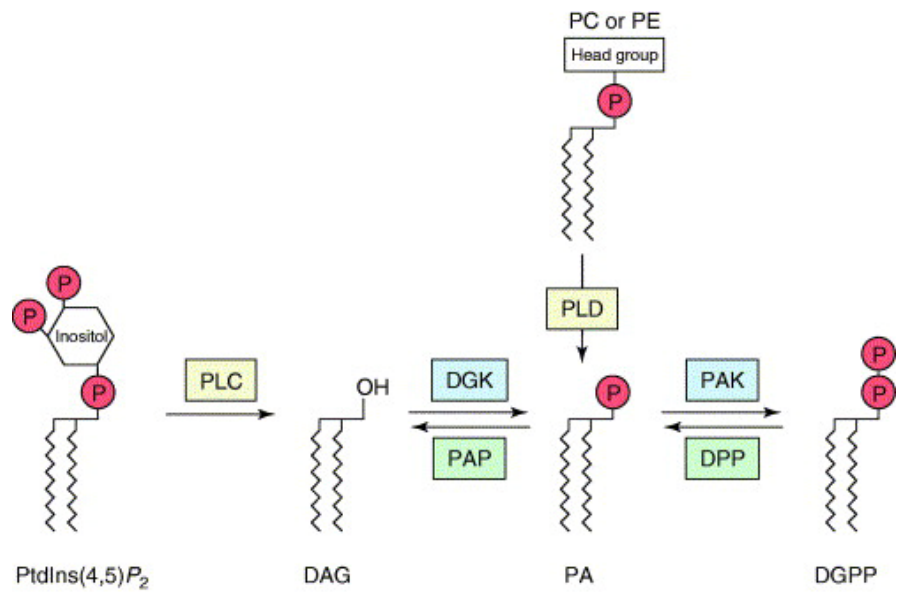
ClustalW multiple alignment generated using JalView v.12.2, shaded for percentage identity. RAE5 peptides identified by MS analysis of EFR IPs highlighted in green. The peptides for EFR antibodies are highlighted in gray text with a pink box; peptides for RAE5 antibodies are black text boxed in pink. The RD or CD in the kinase activation loop is boxed in orange. Putative or MS-detected phosphorylation sites are highlighted mustard yellow [RAE5: T745, S747, S749, S988, S989; EFR: S683; T692; FLS2: T867].



**Appendix Figure A4.2 Kinase domain phylogeny of selected LRR-RLK genes in four plant species;** selected members from Tang *et al.*, 2010. ●, ▲, ■, ▼ represents genes identified from *A. thaliana*, rice, poplar and grapevine, respectively.

RAE5-1/1-1045	1	MNKTPNPERKISLTSFKERMACKEKPRDLQVLLIISIVLSCSFAVSATVEEANALL	55
RAE5-2/1-1009	1	MNKTPNPERKISLTSFKERMACKEKPRDLQVLLIISIVLSCSFAVSATVEEANALL	55
RAE5-1/1-1045	56	KWKSTFTNQTSSSKLSSWVNPNTSSFCSTSWSVGVACSLGSIIRLNLTNTGIEGTFE	110
RAE5-2/1-1009	56	KWKSTFTNQTSSSKLSSWVNPNTSSFCSTSWSVGVACSLGSIIRLNLTNTGIEGTFE	110
RAE5-1/1-1045	111	DFFFSSLPNLTVDLSMNRSGTISPLWGRFSKLEYFDLSINQLVGEIPPELGDL	165
RAE5-2/1-1009	111	DFFFSSLPNLTVDLSMNRSGTISPLWGRFSKLEYFDLSINQLVGEIPPELGDL	165
RAE5-1/1-1045	166	SNLDLTLHLENKLNGLSIPSEIGRLTKVTEIAIYDNLNTGPIPSSFGNLTKLVNL	220
RAE5-2/1-1009	166	SNLDLTLHLENKLNGLSIPSEIGRLTKVTEIAIYDNLNTGPIPSSFGNLTKLVNL	220
RAE5-1/1-1045	221	LFINSLSGSIPSEIGNLPNLRELCRDRNNLTGKIPSSFGNLKNVTLLNMFENQLS	275
RAE5-2/1-1009	221	LFINSLSGSIPSEIGNLPNLRELCRDRNNLTGKIPSSFGNLKNVTLLNMFENQLS	275
RAE5-1/1-1045	276	GEIPPEIGNMTALDTLSLHTNKLGTGIPSTLGNIKTLAVLHLYLNQLNGLSIPPEL	330
RAE5-2/1-1009	276	GEIPPEIGNMTALDTLSLHTNKLGTGIPSTLGNIKTLAVLHLYLNQLNGLSIPPEL	330
RAE5-1/1-1045	331	GEMESMIDLEISENKLTGPVPDSFGKLTALEEWLFLRDNQLSGPIPPIGANSTELT	385
RAE5-2/1-1009	331	GEMESMIDLEISENKLTGPVPDSFGKLTALEEWLFLRDNQLSGPIPPIGANSTELT	385
RAE5-1/1-1045	386	VLQLQDTNNFTGFLPDTICRGGKLENLTDDNHFEGPVPKSLRDCKSLIRVRFKGN	440
RAE5-2/1-1009	386	VLQLQDTNNFTGFLPDTICRGGKLENLTDDNHFEGPVPKSLRDCKSLIRVRFKGN	440
RAE5-1/1-1045	441	SFSGDISEAFGVYPTLNFIDLSNNNFGQLSANWEQSQKLVAFILSNNNSITGAIP	495
RAE5-2/1-1009	441	SFSGDISEAFGVYPTLNFIDLSNNNFGQLSANWEQSQKLVAFILSNNNSITGAIP	495
RAE5-1/1-1045	496	PEIWNMTQLSQLDLSSNRITGELPESISNINRISKLQLNGNRLSGKIPSGIRLLT	550
RAE5-2/1-1009	496	PEIWNMTQLSQLDLSSNRITGELPESISNINRISKLQLNGNRLSGKIPSGIRLLT	550
RAE5-1/1-1045	551	NLEYLDLSSNRFSSEIPPTLNNLPRLYYMMNLSRNDLDQTIP EGLTKLSQLQMLDL	605
RAE5-2/1-1009	551	NLEYLDLSSNRFSSEIPPTLNNLPRLYYMMNLSRNDLDQTIP EGLTKLSQLQMLDL	605
RAE5-1/1-1045	606	SYNQLDGIESSQFRSLQNLERLDLSHNNLSGQIPPSFKDMALATHVDVSHNNLQG	660
RAE5-2/1-1009	606	SYNQLDGIESSQFRSLQNLERLDLSHNNLSGQIPPSFKDMALATHVDVSHNNLQG	660
RAE5-1/1-1045	661	PIDPNAAFRNAPPDAFEGNKGDLGCSVNTTQGLKPCSITSSKKSHKDRNLIYILV	715
RAE5-2/1-1009	661	PIDPNAAFRNAPPDAFEGNKGDLGCSVNTTQGLKPCSITSSKKSHKDRNLIYILV	715
RAE5-1/1-1045	716	PIIGAIILSVCAGIFICFRKRTKQIEEHTDSESGGETLSIFSFDGKVRYQEIIK	770
RAE5-2/1-1009	716	PIIGAIILSVCAGIFICFRKRTKQIEEHTDSESGGETLSIFSFDGKVRYQEIIK	770
RAE5-1/1-1045	771	ATGEFDPKYLIGTGGHGKVYKAKLPNAIMAVKKLNETTDSSISNPSTKQEFNLNEI	825
RAE5-2/1-1009	771	ATGEFDPKYLIGTGGHGKVYKAKLPNAIMAVKKLNETTDSSISNPSTKQEFNLNEI	825
RAE5-1/1-1045	826	RALTEIRHRNVVKLFGFCSSHRRNTFLVYEYMERGSLRKVLENDDEAKKLDWGKRI	880
RAE5-2/1-1009	826	RALTEIRHRNVVKLFGFCSSHRRNTFLVYEYMERGSLRKVLENDDEAKKLDWGKRI	880
RAE5-1/1-1045	881	NVVKGVAHALSYMHHDRSPAIVHRDISSGNILLGEDYEAKISDFGTAKKLLKPDSS	935
RAE5-2/1-1009	881	NVVKGVAHALSYMHHDRSPAIVHRDISSGNILLGEDYEAKISDFGTAKKLLKPDSS	935
RAE5-1/1-1045	936	NWSAVAGTYGYVAPELAY--AMKVTKEKCDVYSFGVLTLEVIK--GEHPGDLVST	985
RAE5-2/1-1009	936	NWSAVAGTYGYVAPGTLFDPLDKLWVDLTRLWSGRVEIMVRFGFLGPNFNQIKTK	990
RAE5-1/1-1045	986	LSSSPPDATLSLKSISDHR	1004
RAE5-2/1-1009	991	MFCFGLKFFLTMGWIWFSF	1009

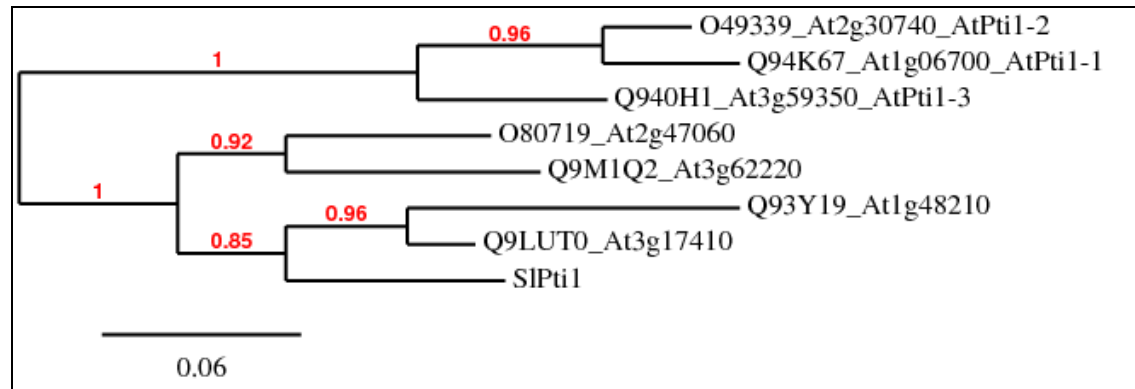
**Appendix Figure A4.3. Pairwise alignment for comparison of proteins encoded by alternative RAE5 transcripts**



TRENDS in Plant Science

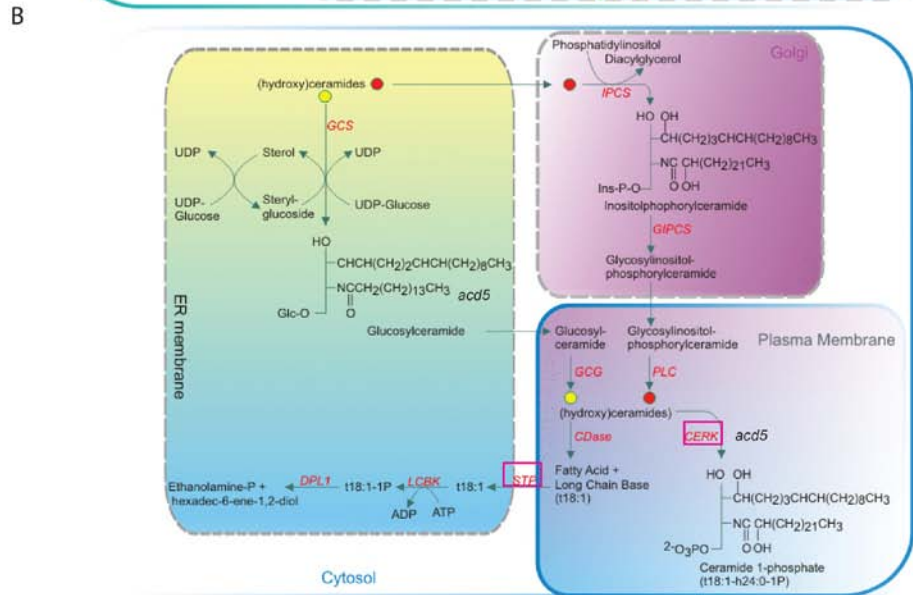
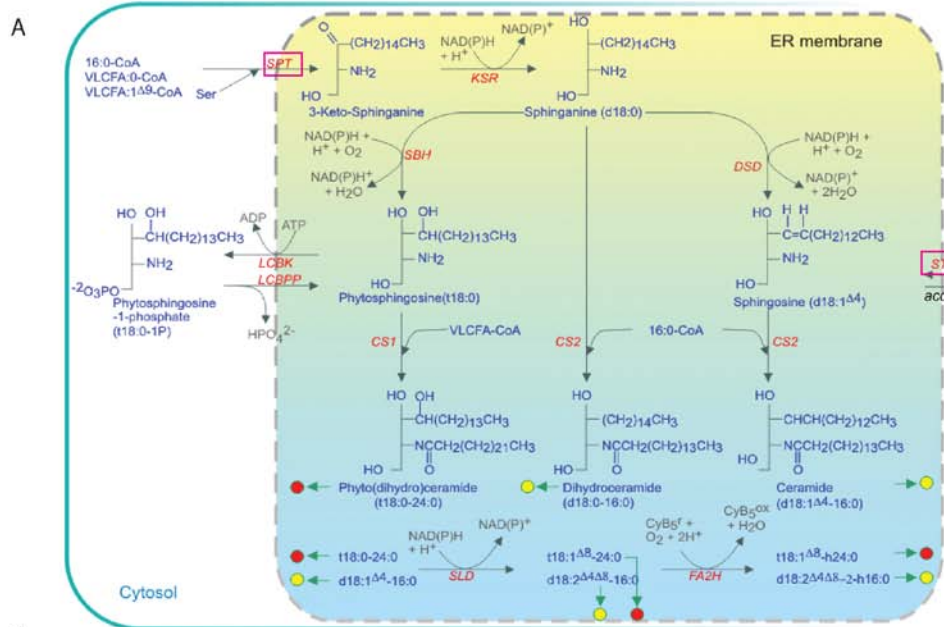
#### Appendix Figure A4.4 Formation and attenuation of phosphatidic acid (PA).

Phospholipases are highlighted in yellow, lipid kinases in blue and lipid phosphatases in green. DAG, diacylglycerol; DGPP, DAG pyrophosphate; DPP, DGPP phosphatase; P, phosphate; PAK, PA kinase; PAP, PA phosphatase; PC, phosphatidylcholine; PE, phosphatidylethanolamine; PtdIns(4,5)P<sub>2</sub>, phosphatidylinositol-(4,5)-bisphosphate (Testerink and Munnik, 2005).



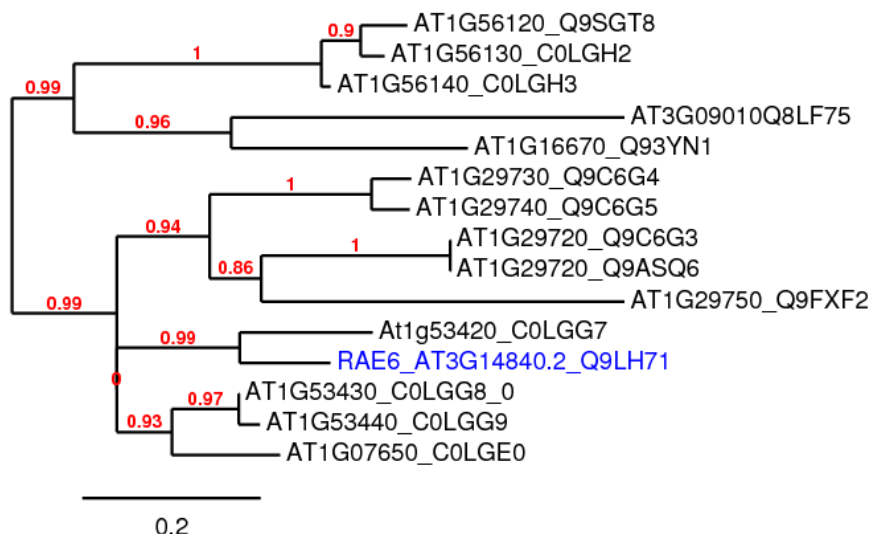
#### Appendix Figure A4.5: Phylogenetic tree of Pti1-related *Arabidopsis* protein kinases.

Protein accessions indicated from Uniprot and TAIR. SIPti1: Q41328.



**Appendix Figure A4.6 Pathway for sphingolipid metabolism (Li-Beisson et al., 2010)**

[http://aralip.plantbiology.msu.edu/pathways/sphingolipid\\_biosynthesis](http://aralip.plantbiology.msu.edu/pathways/sphingolipid_biosynthesis)



**Appendix Figure A5.1 Phylogenetic tree of RAE6 family VIII-2 members.**

AT3G14840.1/1-112	1	-----	MSLNRLQLLFTYYFIVSLILFSDFVSSATLPKEEVDALQSVATALKSNWN 50
AT3G14840.2/1-1042	1	-----	MSLNRLQLLFTYYFIVSLILFSDFVSSATLPKEEVDALQSVATALKSNWN 50
At1g53420/1-953	1	-----	MSLNRLQLLFTSFSSFLFFIVH--FASSATLPTQECEAFKVVLTTLKKTNID 48
AT3G14840.1/1-112	51	F SV DPCDET LSEG GWRNP-----	NAAKG FED AVTC NCSSV ICHVT NM CV----- 94
AT3G14840.2/1-1042	51	F SV DPCDET LSEG GWRNP-----	NAAKG FED AVTC NCSSV ICHVT NIVLKAQD LQGS LPTDL 107
At1g53420/1-953	49	LNVDPCCEV S STG NEWSTI-----	SRNLKRENLQGSLPKELVGLPLLQE----- 92
AT3G14840.1/1-112	95	-----LLSF STS YL-----	FFVK III INI----- 112
AT3G14840.2/1-1042	108	SCLPFLQELDLTRNYLN G SIPP EWGASSLLNISLLGN- RISGSIPKELGNLTLSGLVLEYNQ 169	
At1g53420/1-953	93	-----DL SRNYLN G SIPP EWQVLPLVNIWLLGN- RLTGP IPK EFGN ITTLTSLVLEANQ 145	
AT3G14840.1/1-112	170	-----LSGKIPPE LGNL PNLK RLLL SNNL SGEIPSTFAKL-----	TTLTDLRISDNQFTGAIPDFIQNWKG L 232
AT3G14840.2/1-1042	146	LSGELP LE LGNL PNIQ QMIL LSSNNFNGEIPSTFAKL-----	TTLRLDFR VSDNQLSGTIPDFIQKWTKL 208
At1g53420/1-953	-----	-----	
AT3G14840.1/1-112	233	EKLV IQAS G L VGP I P S A I G L L G T L T D L R I T D L S G P E S P - FPPL R N M T S M K Y L I L R N C N L T G D L 294	
AT3G14840.2/1-1042	209	ERLF IQAS G L VGP I P I A I A S L V E L K D L R I S D L N G P E S P - FPQL R N I K K M E T L I L R N C N L T G D L 270	
At1g53420/1-953	-----	-----	
AT3G14840.1/1-112	295	PAYLG-QNRK LKNLDLSFNKLSGP I P A T Y S G L S D V D F I Y F T S N M L N G Q V P S W M V D Q G D T I D I T 356	
AT3G14840.2/1-1042	271	PDYLG-KITSFKFLDLSFNKLSGA I P N T Y I N L R D G G Y I Y F T G N M L N G S V P D W M V N K G Y K I D L S 332	
At1g53420/1-953	-----	-----	
AT3G14840.1/1-112	357	YNNFSKDKTEECQQKS V N T F S S T S P L V A N N S S N V S C L S K Y T C P K K P Y R L I P T C V S D L S S V T N H 419	
AT3G14840.2/1-1042	333	YNNF S V D P T N A V C K Y N N -----VLSCMRNYQCPKTFN----- 364	
At1g53420/1-953	-----	-----	
AT3G14840.1/1-112	420	L F S A F Y G L H I N C G G N E I T S N E T K Y D A D T W D T P G - YYDSKNGWV S S N T G N F L D D D R T N N G K S K W 481	
AT3G14840.2/1-1042	365	-----ALH I N C G G D E M S I N G T I Y E S D K Y D R L E S W Y E S R N G W F S S N N V G F V D D K H V P E R V T I E 421	
At1g53420/1-953	-----	-----	
AT3G14840.1/1-112	482	SNSSEL KIT N S S I D F R L Y T Q A R L S A I S L T Y Q A L C L G K G N Y T V N L H F A E I M F N E K N M - Y S N L G 542	
AT3G14840.2/1-1042	422	SNSSELN-----VVDFGLYTQ A R I S A I S L T Y Y A C L E N G N Y N V N L H F A E I M F N G N N N - Y Q S L G 478	
At1g53420/1-953	-----	-----	
AT3G14840.1/1-112	543	Rryfd i yvqgk r E V K D F N I V D E A K G V G K A V V K K F P V M V T N G - K L E I R L Q W A G K G T Q A I P V R G V 604	
AT3G14840.2/1-1042	479	R R F F D I Y I Q R K L E V K D F N I A K E A K D V G N V V I K T F P V E I K D G - K L E I R L Y W A G R G T T V I P K E R V 540	
At1g53420/1-953	-----	-----	
AT3G14840.1/1-112	605	Y C P L I S A V S V D P D F I P P K E P G T G T G G G S S V G T V V G S V I A S T V F L V L L I G G I L W W R G C L R P K S Q 667	
AT3G14840.2/1-1042	541	Y C P L I S A I S V D S S V N P S P R N G -----M S T G T L H T L V V I L S I F I V F L V F G T L W K K G Y L R S K S Q 597	
At1g53420/1-953	-----	-----	
AT3G14840.1/1-112	668	MEKDFKNLDFQ I S S F S L R Q I K V a t d n f d p a n k I G E G G F G P V H K g i m t d g t v i a v k Q L S A K S K Q 730	
AT3G14840.2/1-1042	598	MEKDFKS L E L M I A S F S L R Q I K I A T N N F D S A N R I G E G G F G P V Y K G K L F D G T I I A V K Q L S T G S K Q 660	
At1g53420/1-953	-----	-----	
AT3G14840.1/1-112	731	G N R E F L N E I A M I S A L Q H P H L V K L Y G C C V E G D Q L L L V Y E Y L E N N S L A R A L F G P -- Q E T Q I P L N W 791	
AT3G14840.2/1-1042	661	G N R E F L N E I G M I S A L H P N L V K L Y G C C V E G G Q L L L V Y E F V E N N S L A R A L F G P -- Q E T Q L R L D W 721	
At1g53420/1-953	-----	-----	
AT3G14840.1/1-112	792	P M R Q K I C V G I A R G L A Y L H E E S R L K I V H R D I K a t n v l l d k e l n p k i s d f g i a k l D E E E N T H I S T 854	
AT3G14840.2/1-1042	722	P T R R K I C I G V A R G L A Y L H E E S R L K I V H R D I K A T N V L L D K Q L N P K I S D F G L A K L D E E D S T H I S T 784	
At1g53420/1-953	-----	-----	
AT3G14840.1/1-112	855	R V A G T Y G Y M A P E Y A M R G H L T D K A D V Y S F G V V A L E I V H G K S N T S S R S K A D T F Y - L L D W V H V L R e 916	
AT3G14840.2/1-1042	785	R I A G T F G Y M A P E Y A M R G H L T D K A D V Y S F G I V A L E I V H G R S N K I E R S K N N T F Y - L I D W V E V L R e 846	
At1g53420/1-953	-----	-----	
AT3G14840.1/1-112	917	q n t l l e v v d p r L G T D Y N K Q E A L M M I Q I G M L C T S P A P G D R P S M S T V V S M L E G - H S T V N V E K I I e 978	
AT3G14840.2/1-1042	847	K N N L L E L V D P R L G S E Y N R E E A M T M I Q I A I M C T S S E P C E R P S M S E V V K M L E G - K K M V E V E K L E E 908	
At1g53420/1-953	-----	-----	
AT3G14840.1/1-112	979	a s v n n e k d e e s v r A M K R H Y A T I G E E E I T N T T T D G P F T S S S T S T A N A N D L Y P V K L D S A Y W N T R 1041	
AT3G14840.2/1-1042	909	A S V H R E T K R L E N M M T M K Y Y E M I G Q E I S T S M S M I M S D R S E S S A D H ----- 953	
At1g53420/1-953	-----	-----	

### Appendix Figure A5.2 Multiple alignment of RAE6 family VII-2 members RAE6/At3g14840.2 and splice variant At3g14840.1 and closest relative At1g53420.

Colour coded predicted sequence features: features assigned by Pfam and Uniprot, Lilac indicates low complexity region; green indicates Ser/Thr kinase domain; orange is transmembrane; burgundy is malectin-like domain; pink is LRR; mustard indicates signal peptide. Peptides identified by MS indicated as lowercase in sequence.

**Table A5.1 RAE6-co-expressed genes predicted by Expression Angler<sup>1</sup>**

Locus	r <sup>2</sup>	Description
At3g14310*	0.554	AtPME3; pectinesterase
At3g28180	0.545	AtCSLC4 (cellulose-synthase like C4); cellulose synthase/transferase
At5g66420	0.54	Unknown protein
At2g40940*	0.529	ERS1 (ethylene response sensor 1); ethylene binding / protein histidine kinase/ receptor
At4g33300	0.529	ADR1-L1 (ADR1-like 1); ATP binding
At5g20950	0.525	glycosyl hydrolase family 3 protein
<b>At1g59870<sup>**</sup></b>	<b>0.525</b>	<b>PDR8/PEN3</b>
At4g26940	0.51	galactosyltransferase family protein
<b>At5g46330</b>	<b>0.51</b>	<b>FLS2</b>
<b>At2g02930</b>	<b>0.509</b>	<b>GST16/ATGSTF3 (glutathione s-transferase F3)</b>
<b>At4g26070*</b>	<b>0.509</b>	<b>AtMKK1</b>
<b>At4g23470</b>	<b>0.504</b>	<b>hydroxyproline-rich glycoprotein family protein</b>
At1g53440*	0.502	LRR-RK (family VIII-2)
At1g20980	0.498	AtSPL14 (squamos transcription factor
At1g08930	0.498	ERD6 (early response to dehydration 6) sugar:hydrogen symporter
At3g47670	0.496	pectinesterase inhibitor
At1g30900	0.494	vacuolar sorting receptor, putative
At4g00330 <sup>§</sup>	0.493	CRCK2; Ser.Thr protein kinase
At3g28940	0.492	avirulence-responsive protein, putative / avirulence induced gene (AIG) protein, putative
At2g30870*	0.49	AtGSTF10/ERD13 (glutathione s-transferase phi 10)
At5g18470	0.488	curculin-like (mannose-binding) lectin
At4g38550 <sup>§</sup>	0.486	LOCATED IN: chloroplast;
At2g28940	0.483	protein kinase family protein
At5g65670	0.481	IAA9; transcription factor
<b>At5g44070*</b>	<b>0.479</b>	<b>PCS1/CAD1 (Cadmium sensitive1)</b>

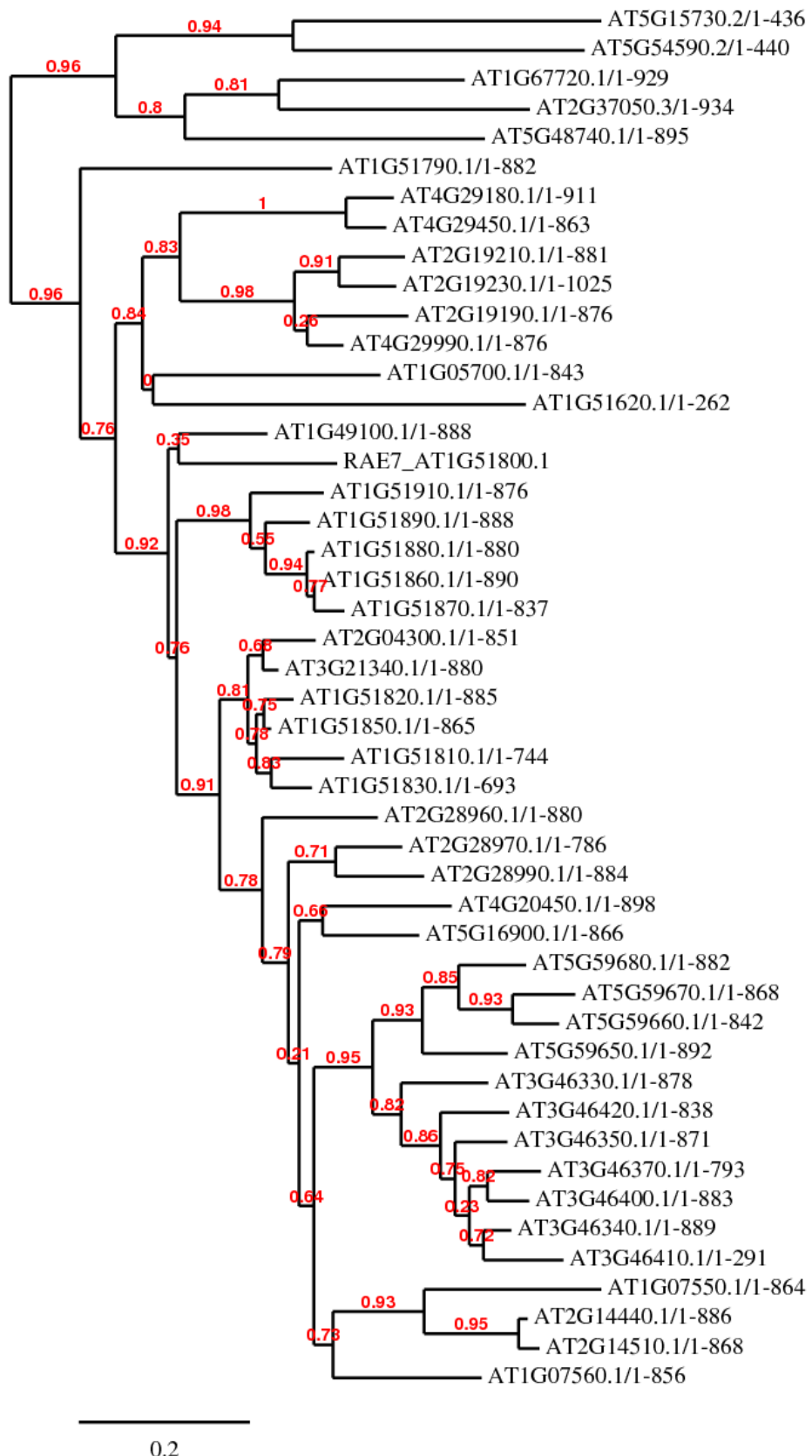
<sup>1</sup>Genes co-expressed with RAE6 according to NASCArrays392 data set obtained at Expression Angler ([http://www.bar.utoronto.ca/ntools/cgi-bin/ntools\\_expression\\_angler.cgi](http://www.bar.utoronto.ca/ntools/cgi-bin/ntools_expression_angler.cgi)). Bold indicates proteins with a known role in defense.

<sup>2</sup> r: Pearson correlation coefficient

\*: also co-expressed on ATTEDII

§: also co-expressed with RAE5

<sup>\*\*</sup>: putative EFR-interacting protein



**Appendix Figure A5.3 Phylogenetic tree of RAE7 family members.** Based on full-length amino acid sequence.

**Table A5.2 RAE7 co-expressed gene predicted by Expression Angler<sup>1</sup>**

Locus	r <sup>2</sup>	Description
<b>At2g19190</b>	<b>0.979</b>	<b>FRK1 (Flg22-induced receptor-like kinase 1) LRR-RK family I</b>
At1g51790 <sup>*</sup>	0.975	LRR-RK family LRR I
<b>At2g39200<sup>*</sup></b>	<b>0.97</b>	<b>ATMLO12 (mildew resistance locus o 12); calmodulin binding</b>
At3g46280	0.963	protein kinase-related
At3g22060	0.955	receptor protein kinase-related
At3g45060	0.954	NRT2.6_ATNRT2.6; nitrate transmembrane transporter
<b>At2g17740</b>	<b>0.944</b>	<b>DC1 domain-containing protein</b>
<b>At1g51890</b>	<b>0.941</b>	<b>leucine-rich repeat protein kinase, putative</b>
At1g26420	0.94	FAD-binding domain-containing protein
<b>At3g52450</b>	<b>0.937</b>	<b>PUB22 (plant U-box 22); ubiquitin-protein ligase</b>
At1g51850	0.931	leucine-rich repeat protein kinase, putative
At1g61380 <sup>§</sup>	0.929	SD1-29 (S-domain-1 29); carbohydrate binding protein kinase
At1g61360 <sup>§</sup>	0.928	S-locus lectin protein kinase family protein
At2g27660 <sup>§</sup>	0.921	DC1 domain-containing protein
At5g61560	0.914	protein kinase family protein
<b>At4g23210</b>	<b>0.913</b>	<b>CRK13_protein kinase family protein (same family as RAE8)</b>
<b>At2g35930</b>	<b>0.913</b>	<b>PUB23 (PLANT U-BOX 23); ubiquitin-protein ligase</b>
		protease inhibitor/seed storage/lipid transfer protein (LTP) family protein
At4g22470	0.912	
At5g48540	0.91	33 kDa secretory protein-related
At2g25735	0.909	unknown protein
At3g47380	0.908	invertase/pectin methylesterase inhibitor family protein
		AtNRT3.1/WR3 (wound-responsive 3); nitrate transmembrane transporter
At5g50200	0.904	
At2g38290	0.903	AtAMT2;1 (ammonium transporter 2)
At1g52200	0.903	unknown protein
<b>At4g01700</b>	<b>0.902</b>	<b>chitinase, putative</b>

<sup>1</sup>Genes co-expressed with RAE7 according to NASCArrays392 data set obtained at Expression Angler ([http://www.bar.utoronto.ca/ntools/cgi-bin/ntools\\_expression\\_angler.cgi](http://www.bar.utoronto.ca/ntools/cgi-bin/ntools_expression_angler.cgi)). Bold indicates proteins with a known role in defense.

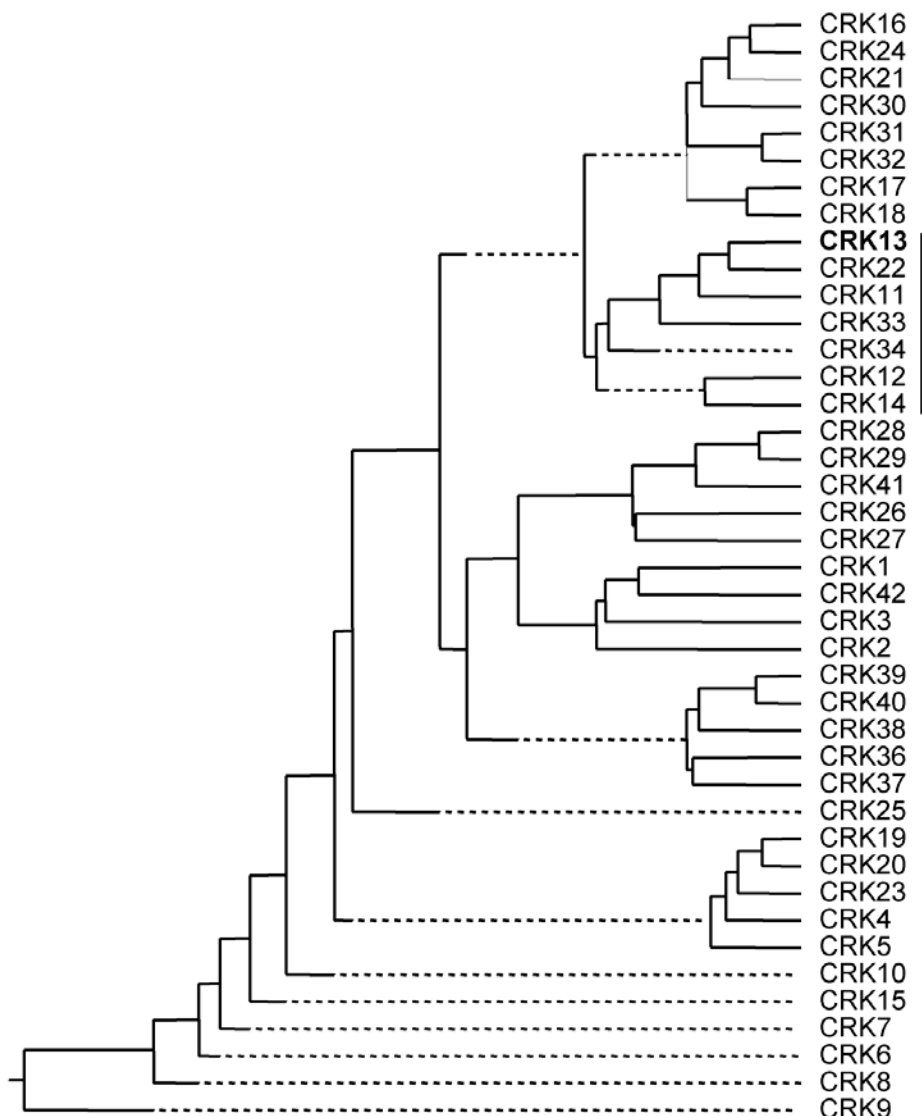
<sup>2</sup> r: Pearson correlation co-efficient

<sup>\*</sup>: also co-expressed on ATTEDII

<sup>§</sup>: also predicted by ATTEDII

<sup>§</sup>: also co-expressed with RAE5

<sup>§</sup>: also co-expressed with RAE8



**Appendix Figure A5.4 Phylogenetic analysis of the CRK family.** Phylogenetic analysis was performed by CLUSTALW method. The vertical line shows the subgroup of 7 members to which CRK11 belongs (from Acharya *et al.*, 2007).

**Table A5.3: RAE8 co-expressed genes predicted by Expression Angler**

Locus	$r^2$	Description
At1g61360	0.849	S-locus lectin protein kinase family protein
At4g04510	0.844	CRK38 (Same as RAE8 family)
<b>At2g35930<sup>\$</sup></b>	<b>0.835</b>	<b>PUB23 (PLANT U-BOX 23); ubiquitin-protein ligase</b>
At3g53810	0.822	lectin protein kinase, putative
At2g27660 <sup>\$</sup>	0.822	DC1 domain-containing protein
At1g51820	0.81	LRR-RK family I
At4g25350	0.801	SHB1 (SHORT HYPOCOTYL UNDER BLUE1) protein kinase family protein / peptidoglycan-binding LysM domain-containing
At2g23770	0.798	protein kinase family protein
At5g61560	0.797	SD1-29 (S-DOMAIN-1 29); carbohydrate binding / kinase/protein
At1g61380 <sup>*\$</sup>	0.796	LRR-RK family I
At4g39830	0.782	L-ascorbate oxidase, putative
At5g44370	0.78	PHT4;6 (PHOSPHATE TRANSPORTER 4;6)
At5g23490	0.777	unknown protein
At4g31980	0.777	unknown protein
At1g18390	0.774	serine/threonine kinase/ protein tyrosine kinase
At1g51800 <sup>^</sup>	0.768	LRR-RK I (RAE7)
At5g45000	0.768	transmembrane receptor
At5g01540	0.766	LECRKA4.1 (LECTIN RECEPTOR KINASE A4.1); kinase
At4g01750	0.764	RGXT2 (rhamnogalacturonan xylosyltransferase 2); UDP-xylosyltransferase
At4g18250	0.764	receptor serine/threonine kinase, putative
At5g54720	0.764	ankyrin repeat family protein

<sup>1</sup>Genes co-expressed with RAE8 according to NASCArrays392 data set obtained at Expression Angler ([http://www.bar.utoronto.ca/ntools/cgi-bin/ntools\\_expression\\_angler.cgi](http://www.bar.utoronto.ca/ntools/cgi-bin/ntools_expression_angler.cgi)). Bold indicates proteins with a known role in defense.

<sup>2</sup>  $r$ : Pearson correlation coefficient

<sup>\*</sup>: also co-expressed on ATTEDII

<sup>\$</sup>: also co-expressed with RAE5

<sup>^</sup>: putative EFR-interacting protein

## Acknowledgements

Funding for this work was from Marie Curie Early Stage Training fellowship 019727, ERA-PG PRR-CROP (BBSRC grant BB/G024936/1), and The Gatsby Charitable Foundation.

I dedicate this thesis to my long-suffering mother, who taught me to have the guts to do what I want to and to believe in myself.

It's been a journey of discovery and I was lucky to meet a lot of great people along the way. Thanks to JIC/TSL for setting up the rotation program that made it possible for a South African girl like me to come to the UK and study in one of the best institutes in the world. To my supervisor Cyril, we had an anxious start but we have done so well together and I appreciate your patience with me, and I value your enthusiasm for science, it has been motivational (and for tolerating my long sentences....). Thanks for your kindness and gentle handling of my fledgling ego. Thanks to John Rathjen for battering the aforementioned ego and teaching me to think and be critical. Thanks to my advisor Alex Jones for all your support and good advice. Thanks to Silke Robatzek for being a part of my committee in the last years and giving good guidance. Thanks to the CZ lab, the founding members Valerie, Vlad, Martine, and Ben, we have all grown up together; then later Roda, Frederikke, Cecile, Freddy, Yasu and Jackie - it was fun working with you guys. To my lab partner Ben, we were in it together from the start and working together was sometimes hard but also really good; You are a true friend and I will miss you very much when we part. Thanks to the great friends I made in Norwich, especially Sophie, Hale and Anne-Claire, you made the experience. Thanks to my lab mother Karen, you have been nurturing and helpful and I will miss our morning coffees. Thanks to SL for the delicious free coffee. Thanks to Tim Wells who has green fingers and a good heart. Thanks to Jan Sklenar for putting so much effort into the mass spectrometry, I appreciate it. Thanks to Matthew and Jodi for transformations and good advice. Thanks to Neil Hastings for always hooking me up with IT.

And most of all thanks to my husband Chris for supporting me all the way and enduring the long hours, stress and lab-related mood swings, jy is my wêreld engel.

## References

Aarts, N., Metz, M., Holub, E., Staskawicz, B.J., Daniels, M.J., and Parker, J.E. (1998). Different requirements for EDS1 and NDR1 by disease resistance genes define at least two R gene-mediated signaling pathways in *Arabidopsis*. *PNAS USA* 95, 10306.

Abramovitch, R.B., Anderson, J.C., and Martin, G.B. (2006). Bacterial elicitation and evasion of plant innate immunity. *Nat Rev Mol Cell Biol* 7, 601-611.

AbuQamar, S., Chen, X., Dhawan, R., Bluhm, B., Salmeron, J., Lam, S., Dietrich, R.A., and Mengiste, T. (2006). Expression profiling and mutant analysis reveals complex regulatory networks involved in *Arabidopsis* response to *Botrytis* infection. *Plant J* 48, 28 - 44.

Acharya, B.R., Raina, S., Maqbool, S.B., Jagadeeswaran, G., Mosher, S.L., Appel, H.M., Schultz, J.C., Klessig, D.F., and Raina, R. (2007). Overexpression of CRK13, an *Arabidopsis* cysteine-rich receptor-like kinase, results in enhanced resistance to *Pseudomonas syringae*. *Plant J* 50, 488-499.

Ade, J., DeYoung, B.J., Golstein, C., and Innes, R.W. (2007). Indirect activation of a plant nucleotide binding site-ileucine-rich repeat protein by a bacterial protease. *PNAS* 104, 2531-2536.

Agorio, A., and Vera, P. (2007). ARGONAUTE4 Is Required for Resistance to *Pseudomonas syringae* in *Arabidopsis*. *Plant Cell* 19, 3778-3790.

Agostini, L., Martinon, F., Burns, K., McDermott, M.F., Hawkins, P.N., and Tschopp, J.r. (2004). NALP3 forms an IL-1-processing inflammasome with increased activity in Muckle-Wells autoinflammatory disorder. *Immunity* 20, 319-325.

Ajuh, P., Sleeman, J., Chusainow, J., and Lamond, A.I. (2001). A Direct Interaction between the carboxyl-terminal region of CDC5L and the WD40 domain of PLRG1 Is essential for pre-mRNA splicing. *Journal of Biological Chemistry* 276, 42370-42381.

Al-Daoude, A., de Torres Zabala, M., Ko, J.-H., and Grant, M. (2005). RIN13 Is a positive regulator of the plant disease resistance protein RPM1. *Plant Cell* 17, 1016-1028.

Albert, M., Jehle, A.K., Mueller, K., Eisele, C., Lipschis, M., and Felix, G. (2010). *Arabidopsis thaliana* pattern recognition receptors for bacterial elongation factor tu and flagellin can be combined to form functional chimeric receptors. *Journal of Biological Chemistry* 285, 19035-19042.

Albrecht, C., Russinova, E., Hecht, V., Baaijens, E., and de Vries, S. (2005). The *Arabidopsis thaliana* SOMATIC EMBRYOGENESIS RECEPTOR-LIKE KINASES1 and 2 control male sporogenesis. *Plant Cell* 17, 3337-3349.

Albrecht, C., Russinova, E., Kemmerling, B., Kwaaitaal, M., and de Vries, S.C. (2008). *Arabidopsis* SOMATIC EMBRYOGENESIS RECEPTOR KINASE proteins serve brassinosteroid-dependent and -independent signaling pathways. *Plant Physiol.* 148, 611-619.

Ali, G.S., Prasad, K.V.S.K., Day, I., and Reddy, A.S.N. (2007a). Ligand-dependent reduction in the membrane mobility of FLAGELLIN SENSITIVE2, an *Arabidopsis* receptor-like kinase. *Plant and Cell Physiology* 48, 1601-1611.

Ali, R., Ma, W., Lemtiri-Chlieh, F., Tsaltas, D., Leng, Q., von Bodman, S., and Berkowitz, G.A. (2007b). Death don't have no mercy and neither does calcium: *Arabidopsis* CYCLIC NUCLEOTIDE GATED CHANNEL2 and innate immunity. *Plant Cell* 19, 1081-1095.

Almagro, L., Gómez Ros, L.V., Belchi-Navarro, S., Bru, R., Ros Barceló, A., and Pedreño, M.A. (2009). Class III peroxidases in plant defense reactions. *Journal of Experimental Botany* 60, 377-390.

Alonso, J.M., Hirayama, T., Roman, G., Nourizadeh, S., and Ecker, J.R. (1999). EIN2, a bifunctional transducer of ethylene and stress responses in *Arabidopsis*. *Science* 284, 2148-2152.

Alvarez-Venegas, R., Abdallat, A., Guo, M., Alfano, J.R., and Avramova, Z. (2007). Epigenetic control of a transcription factor at the cross section of two antagonistic pathways. *Epigenetics* 2, 106-113.

Alvarez-Venegas, R., Sadder, M., Hlavacka, A., Baluska, F.e., Xia, Y., Lu, G., Firsov, A., Sarath, G., Moriyama, H., Dubrovsky, J.G., and Avramova, Z. (2006). The *Arabidopsis* homolog of trithorax, ATX1, binds phosphatidylinositol 5-phosphate, and the two regulate a common set of target genes. *PNAS* 103, 6049-6054.

An, F., Zhao, Q., Ji, Y., Li, W., Jiang, Z., Yu, X., Zhang, C., Han, Y., He, W., Liu, Y., Zhang, S., Ecker, J.R., and Guo, H. (2010). Ethylene-induced stabilization of ETHYLENE INSENSITIVE3 and EIN3-LIKE1 is mediated by proteasomal degradation of EIN3 binding F-Box 1 and 2 that requires EIN2 in *Arabidopsis*. *Plant Cell* 22, 2384-2401.

Andreasson, E., Jenkins, T., Brodersen, P., Thorgrimsen, S., Petersen, N.H., Zhu, S., Qiu, J.L., Micheelsen, P., Rocher, A., Petersen, M., Newman, M.A., Bjorn Nielsen, H., Hirt, H., Somssich, I., Mattsson, O., and Mundy, J. (2005). The MAP kinase substrate MKS1 is a regulator of plant defense responses. *Embo J* 24, 2579-2589.

Anthony, R.G., Khan, S., Costa, J., Pais, M.S., and Bögre, L. (2006). The Arabidopsis protein kinase PTI1-2 is activated by convergent phosphatidic acid and oxidative stress signaling pathways downstream of PDK1 and OXI1. *Journal of Biological Chemistry* 281, 37536-37546.

Anthony, R.G., Henriques, R., Helfer, A., Meszaros, T., Rios, G., Testerink, C., Munnik, T., Deak, M., Koncz, C., and Bogre, L. (2004). A protein kinase target of a PDK1 signaling pathway is involved in root hair growth in Arabidopsis. *Embo J* 23, 572-581.

Arbibe, L., Kim, D.W., Batsche, E., Pedron, T., Mateescu, B., Muchardt, C., Parsot, C., and Sansonetti, P.J. (2007). An injected bacterial effector targets chromatin access for transcription factor NF- $\kappa$ B to alter transcription of host genes involved in immune responses. *Nat Immunol* 8, 47-56.

Asai, T., Tena, G., Plotnikova, J., Willmann, M.R., Chiu, W.L., Gomez-Gomez, L., Boller, T., Ausubel, F.M., and Sheen, J. (2002). MAP kinase signaling cascade in Arabidopsis innate immunity. *Nature* 415, 977-983.

Aslam, S.N., Newman, M.-A., Erbs, G., Morrissey, K.L., Chinchilla, D., Boller, T., Jensen, T.T., De Castro, C., Ierano, T., Molinaro, A., Jackson, R.W., Knight, M.R., and Cooper, R.M. (2008). Bacterial polysaccharides suppress induced innate immunity by calcium chelation. *Current biology* 18, 1078-1083.

Ausubel, F.M. (2005). Are innate immune signaling pathways in plants and animals conserved? *Nat Immunol* 6, 973-979.

Axtell, M.J., Chisholm, S.T., Dahlbeck, D., and Staskawicz, B.J. (2003). Genetic and molecular evidence that the *Pseudomonas syringae* type III effector protein AvrRpt2 is a cysteine protease. *Molecular Microbiology* 49, 1537-1546.

Ayers, A.R., Ebel, J., Finelli, F., Berger, N., and Albersheim, P. (1976). Host-pathogen interactions: IX. Quantitative assays of elicitor activity and characterization of the elicitor present in the extracellular medium of cultures of *Phytophthora megasperma* var. *sojae*. *Plant Physiol.* 57, 751-759.

Azevedo, C., Sadanandom, A., Kitagawa, K., Freialdenhoven, A., Shirasu, K., and Schulze-Lefert, P. (2002). The RAR1 interactor SGT1, an essential component of *R* gene-triggered disease resistance. *Science* 295, 2073-2076.

Bailey, B. A. (1995). Purification of a protein from culture filtrates of *Fusarium oxysporum* that induces ethylene and necrosis in leaves of *Erythroxylum coca*. *Phytopathology* 85, 1250-1255.

Bailey, B.A., Dean, J.F.D., and Anderson, J.D. (1990). An ethylene biosynthesis-inducing endoxylanase elicits electrolyte leakage and necrosis in *Nicotiana tabacum* cv *Xanthi* leaves. *Plant Physiol.* 94, 1849-1854.

Bailey, B.A., Korcak, R.F., and Anderson, J.D. (1992). Alterations in *Nicotiana tabacum* L. cv *Xanthi* cell membrane function following treatment with an ethylene biosynthesis-inducing endoxylanase. *Plant Physiol.* 100, 749-755.

Balague, C., Lin, B., Alcon, C., Flottes, G., Malmstrom, S., Kohler, C., Neuhaus, G., Pelletier, G., Gaymard, F., and Roby, D. (2003). HLM1, an essential signaling component in the hypersensitive response, is a member of the cyclic nucleotide-gated channel ion channel family. *Plant Cell* 15, 365-379.

Bar, M., and Avni, A. (2009). EHD2 inhibits ligand-induced endocytosis and signaling of the leucine-rich repeat receptor-like protein LeEix2. *Plant J* 59, 600-611.

Bar, M., Sharfman, M., Ron, M., and Avni, A. (2010). BAK1 is required for the attenuation of ethylene-inducing xylanase (Eix)-induced defense responses by the decoy receptor LeEix1. *Plant J*, no-no.

Bargmann, B.O., Laxalt, A.M., Riet, B.t., Schouten, E., Van Leeuwen, W., Dekker, H.L., De Koster, C.G., Haring, M.A., and Munnik, T. (2006). LePLD $\beta$ 1 activation and relocalization in suspension-cultured tomato cells treated with xylanase. *Plant J* 45, 358-368.

Bauer, Z., Gomez-Gomez, L., Boller, T., and Felix, G. (2001). Sensitivity of different ecotypes and mutants of *Arabidopsis thaliana* toward the bacterial elicitor flagellin correlates with the presence of receptor-binding sites. *J Biol Chem* 276, 45669-45676.

Bedini, E., De Castro, C., Erbs, G., Mangoni, L., Dow, J.M., Newman, M.A., Parrilli, M., and Unverzagt, C. (2005). Structure-dependent modulation of a pathogen response in plants by synthetic O-antigen polysaccharides. *J Am Chem Soc* 127, 2414-2416.

Bednarek, P., Pislewska-Bednarek, M., Svatos, A., Schneider, B., Doubsky, J., Mansurova, M., Humphry, M., Consonni, C., Panstruga, R., Sanchez-Vallet, A., Molina, A., and Schulze-Lefert, P. (2009). A glucosinolate metabolism pathway in living plant cells mediates broad-spectrum antifungal defense. *Science* 323, 101-106.

Belkhadir, Y., Nimchuk, Z., Hubert, D.A., Mackey, D., and Dangl, J.L. (2004). *Arabidopsis* RIN4 negatively regulates disease resistance mediated by RPS2 and RPM1 downstream or independent of the NDR1 signal modulator and is not required for the virulence functions of bacterial type iii effectors AvrRpt2 or AvrRpm1. *Plant Cell* 16, 2822-2835.

Belousov, V.V., Fradkov, A.F., Lukyanov, K.A., Staroverov, D.B., Shakhbazov, K.S., Terskikh, A.V., and Lukyanov, S. (2006). Genetically encoded fluorescent indicator for intracellular hydrogen peroxide. *Nat Meth* 3, 281-286.

Benschop, J.J., Mohammed, S., O'Flaherty, M., Heck, A.J.R., Slijper, M., and Menke, F.L.H. (2007). Quantitative phosphoproteomics of early elicitor signaling in *Arabidopsis*. *Molecular & Cellular Proteomics* 6, 1198-1214.

Bent, A.F., and Mackey, D. (2007). Elicitors, effectors, and R genes: The new paradigm and a lifetime supply of questions. *Annu Rev Phytopathol* 45, 399-436.

Bergey, D.R., Howe, G.A., and Ryan, C.A. (1996). Polypeptide signaling for plant defensive genes exhibits analogies to defense signaling in animals. *PNAS* 93, 12053-12058.

Berin, M.C., Darfeuille-Michaud, A., Egan, L.J., Miyamoto, Y., and Kagnoff, M.F. (2002). Role of EHEC O157:H7 virulence factors in the activation of intestinal epithelial cell NF- $\kappa$ B and MAP kinase pathways and the upregulated expression of interleukin 8. *Cell Microbiol* 4, 635-648.

Berr, A., McCallum, E., Alioua, A., Heintz, D., Heitz, T., and Shen, W.-H. (2010). *Arabidopsis* histone methyltransferase SDG8 mediates induction of the jasmonate/ethylene-pathway genes in plant defense response to necrotrophic fungi. *Plant Physiol.*, pp.110.161497.

Bestwick, C.S., Brown, I.R., Bennett, M.H.R., and Mansfield, J.W. (1997). localization of hydrogen peroxide accumulation during the hypersensitive reaction of lettuce cells to *Pseudomonas syringae* pv *phaseolicola*. *Plant Cell* 9, 209-221.

Bethke, G., Unthan, T., Uhrig, J.F., Pröschl, Y., Gust, A.A., Scheel, D., and Lee, J. (2009). Flg22 regulates the release of an ethylene response factor substrate from MAP kinase 6 in *Arabidopsis thaliana* via ethylene signaling. *PNAS* 106, 8067-8072.

Bhoj, V.G., and Chen, Z.J. (2009). Ubiquitylation in innate and adaptive immunity. *Nature* 458, 430-437.

Bi, D., Cheng, Y.T., Li, X., and Zhang, Y. (2010). Activation of plant immune responses by a gain-of-function mutation in an atypical receptor-like kinase. *Plant Physiol.*, pp.110.158501.

Bieri, S., Mauch, S., Shen, Q.H., Peart, J., Devoto, A., Casais, C., Ceron, F., Schulze, S., Steinbiss, H.H., Shirasu, K., and Schulze-Lefert, P. (2004). RAR1 positively controls steady state levels of barley MLA resistance proteins and enables sufficient MLA6 accumulation for effective resistance. *Plant Cell* 16, 3480-3495.

Bindschedler, L.V., Dewdney, J., Blee, K.A., Stone, J.M., Asai, T., Plotnikov, J., Denoux, C., Hayes, T., Gerrish, C., Davies, D.R., Ausubel, F.M., and Paul Bolwell, G. (2006). Peroxidase-dependent apoplastic oxidative burst in *Arabidopsis* required for pathogen resistance. *Plant J* 47, 851-863.

Birch, P.R.J., Armstrong, M., Bos, J., Boevink, P., and Gilroy, E.M. (2009). Towards understanding the virulence functions of RXLR effectors of the oomycete plant pathogen *Phytophthora infestans*. *J. Exp. Bot.* 60, 1133.

Birker, D., Heidrich, K., Takahara, H., Narusaka, M., Deslandes, L., Narusaka, Y., Reymond, M., Parker, J.E., and O'Connell, R. (2009). A locus conferring resistance to *Colletotrichum higginsianum* is shared by four geographically distinct *Arabidopsis* accessions. *Plant J.* 60, 602-613.

Bisgrove, S.R., Simonich, M.T., Smith, N.M., Sattler, A., and Innes, R.W. (1994). A disease resistance gene in *arabidopsis* with specificity for two different pathogen avirulence genes. *Plant Cell* 6, 927-933.

Bishop, P.D., Makus, D.J., Pearce, G., and Ryan, C.A. (1981). Proteinase inhibitor-inducing factor activity in tomato leaves resides in oligosaccharides enzymically released from cell walls. *PNAS* 78, 3536-3540.

Bisson, M.M.A., Bleckmann, A., Allekotte, S., and Groth, G. (2009). EIN2, the central regulator of ethylene signaling, is localized at the ER membrane where it interacts with the ethylene receptor ETR1. *Biochemical Journal* 424, 1-6.

Bleckmann, A., Weidtkamp-Peters, S., Seidel, C.A.M., and Simon, R. (2010). Stem cell signaling in *Arabidopsis* requires CRN to localize CLV2 to the plasma membrane. *Plant Physiol.* 152, 166-176.

Block, A., Schmelz, E., Jones, J.B., and Klee, H.J. (2005). Coronatine and salicylic acid: the battle between *Arabidopsis* and *Pseudomonas* for phytohormone control. *Molecular Plant Pathology* 6, 79-83.

Block, A., Li, G., Fu, Z.Q., and Alfano, J.R. (2008). Phytopathogen type III effector weaponry and their plant targets. *Current Opinion in Plant Biology* 11, 396-403.

Blom, N., Sicheritz-Pontén, T., Gupta, R., Gammeltoft, S., and Brunak, S. (2004). Prediction of post-translational glycosylation and phosphorylation of proteins from the amino acid sequence. *Proteomics* 4, 1633-1649.

Boch, J., and Bonas, U. (2010). *Xanthomonas AvrBs3* family-type III effectors: discovery and function. *Annu Rev Phytopathol* 48, 419-436.

Bogdanove, A.J., Schornack, S., and Lahaye, T. (2010). TAL effectors: finding plant genes for disease and defense. *Current Opinion in Plant Biology* 13, 394-401.

Bögre, L., Ökrész, L., Henriques, R., and Anthony, R.G. (2003). Growth signaling pathways in *Arabidopsis* and the AGC protein kinases. *Trends in Plant Science* 8, 424-431.

Boller, T., and Felix, G. (2009). A Renaissance of Elicitors: perception of microbe-associated molecular patterns and danger signals by pattern-recognition receptors. *Annual Review of Plant Biology* 60, 379-406.

Borner, G.H.H., Sherrier, D.J., Weimar, T., Michaelson, L.V., Hawkins, N.D., MacAskill, A., Napier, J.A., Beale, M.H., Lilley, K.S., and Dupree, P. (2005). Analysis of detergent-resistant membranes in *Arabidopsis*. evidence for plasma membrane lipid rafts. *Plant Physiol.* 137, 104-116.

Bos, J.I.B., Armstrong, M.R., Gilroy, E.M., Boevink, P.C., Hein, I., Taylor, R.M., Zhendong, T., Engelhardt, S., Vetukuri, R.R., Harrower, B., Dixelius, C., Bryan, G., Sadanandom, A., Whisson, S.C., Kamoun, S., and Birch, P.R.J. (2010). *Phytophthora infestans* effector AVR3a is essential for virulence and manipulates plant immunity by stabilizing host E3 ligase CMPG1. *PNAS* 107, 9909-9914.

Botér, M., Amigues, B., Peart, J., Breuer, C., Kadota, Y., Casais, C., Moore, G., Kleanthous, C., Ochsenbein, F., Shirasu, K., and Guerois, R. (2007). Structural and functional analysis of SGT1 reveals that its interaction with HSP90 is required for the accumulation of Rx, an R protein involved in plant immunity. *Plant Cell* 19, 3791-3804.

Boudsocq, M., Willmann, M.R., McCormack, M., Lee, H., Shan, L., He, P., Bush, J., Cheng, S.-H., and Sheen, J. (2010). Differential innate immune signaling via  $\text{Ca}^{2+}$  sensor protein kinases. *Nature* 464, 418-422.

Boursiac, Y., Lee, S.M., Romanowsky, S.M., Blank, R.R., Sladek, C., Chung, W.S., and Harper, J.F. (2010). Disruption of the vacuolar calcium-ATPases in *Arabidopsis* results in the activation of a salicylic acid-dependent programmed cell death pathway. *Plant Physiol.*

Boutrot, F., Segonzac, C.c., Chang, K.N., Qiao, H., Ecker, J.R., Zipfel, C., and Rathjen, J.P. (2010). Direct transcriptional control of the *Arabidopsis* immune receptor FLS2 by the ethylene-dependent transcription factors EIN3 and EIL1. *PNAS* 107, 14502-14507.

Bowling, S.A., Clarke, J.D., Liu, Y.D., Klessig, D.F., and Dong, X.N. (1997). The *cpr5* mutant of *Arabidopsis* expresses both NPR1-dependent and NPR1-independent resistance. *Plant Cell* 9, 1573-1584.

Bowling, S.A., Guo, A., Cao, H., Gordon, A.S., Klessig, D.F., and Dong, X. (1994). A mutation in *Arabidopsis* that leads to constitutive expression of systemic acquired resistance. *Plant Cell* 6, 1845 - 1857.

Brancaccio, M., Fratta, L., Notte, A., Hirsch, E., Poulet, R., Guazzone, S., De Acetis, M., Vecchione, C., Marino, G., Altruda, F., Silengo, L., Tarone, G., and Lembo, G. (2003). Melusin, a muscle-specific integrin  $\beta(1)$ -interacting protein, is required to prevent cardiac failure in response to chronic pressure overload. *Nat Med* 9, 68-75.

Braun, S., Matuschewski, K., Rape, M., Thoms, S., and Jentsch, S. (2002). Role of the ubiquitin-selective CDC48 UFD1/NPL4 chaperone (segregase) in ERAD of OLE1 and other substrates. *Embo J* 21, 615-621.

Brodersen, P., Petersen, M., and Pike, H.M. (2002). Knockout of *Arabidopsis ACCELERATED-CELL-DEATH11* encoding a sphingosine transfer protein causes activation of programmed cell death and defense. *Genes Dev* 16, 490-502.

Brodsky, J.L., and McCracken, A.A. (1999). ER protein quality control and proteasome-mediated protein degradation. *Seminars in Cell and Developmental Biology* 10, 507-513.

Brooks, D.M., Hernandez-Guzman, G., Kloek, A.P., Alarcon-Chaidez, F., Sreedharan, A., Rangaswamy, V., Penalosa-Vazquez, A., Bender, C.L., and Kunkel, B.N. (2004). Identification and characterization of a well-defined series of coronatine biosynthetic mutants of *Pseudomonas syringae* pv. *tomato* DC3000. *MPMI* 17, 162-174.

Brunner, F., Rosahl, S., Lee, J., Rudd, J.J., Geiler, C., Kauppinen, S., Rasmussen, G., Scheel, D., and Nurnberger, T. (2002). Pep-13, a plant defense-inducing pathogen-associated pattern from *Phytophthora* transglutaminases. *Embo J* 21, 6681-6688.

Bultreys, A., Trombik, T., Drozak, A., and Boutry, M. (2009). *Nicotiana plumbaginifolia* plants silenced for the ATP-binding cassette transporter gene *NpPDR1* show increased susceptibility to a group of fungal and oomycete pathogens. *Molecular Plant Pathology* 10, 651-663.

Burch-Smith, T.M., Schiff, M., Caplan, J.L., Tsao, J., Czymbek, K., and Dinesh-Kumar, S.P. (2007). A novel role for the TIR domain in association with pathogen-derived elicitors. *PLoS Biol* 5, e68.

Burmeister, W.P., Cottaz, S., Driguez, H., Iori, R., Palmieri, S., and Henrissat, B. (1997). The crystal structures of *Sinapis alba* myrosinase and a covalent glycosyl-enzyme intermediate provide insights into the substrate recognition and active-site machinery of an S-glycosidase. *Structure* 5, 663-675.

Cabrera, N., Díaz-Rodríguez, E., Becker, E., Martín-Zanca, D., and Pandiella, A. (1996). TrkA receptor ectodomain cleavage generates a tyrosine-phosphorylated cell-associated fragment. *The Journal of Cell Biology* 132, 427-436.

Campbell, E.J., Schenk, P.M., Kazan, K., Penninckx, I.A.M.A., Anderson, J.P., Maclean, D.J., Cammue, B.P.A., Ebert, P.R., and Manners, J.M. (2003). Pathogen-responsive expression of a putative ATP-binding cassette transporter gene conferring resistance to the diterpenoid sclareol is regulated by multiple defense signaling pathways in *Arabidopsis*. *Plant Physiol.* 133, 1272-1284.

Cao, H., Bowling, S.A., Gordon, A.S., and Dong, X. (1994). Characterization of an *Arabidopsis* mutant that is nonresponsive to inducers of systemic acquired resistance. *Plant Cell* 6, 1583-1592.

Caplan, J.L., Mamillapalli, P., Burch-Smith, T.M., Czermek, K., and Dinesh-Kumar, S.P. (2008). Chloroplastic protein NRIP1 mediates innate immune receptor recognition of a viral effector. *Cell* 132, 449-462.

Caplan, J.L., Zhu, X., Mamillapalli, P., Marathe, R., Anandalakshmi, R., and Dinesh-Kumar, S.P. (2009). Induced ER chaperones regulate a receptor-like kinase to mediate antiviral innate immune response in plants 6, 457-469.

Catlett, M.G., and Kaplan, K.B. (2006). Sgt1p is a unique co-chaperone that acts as a client adaptor to link Hsp90 to Skp1p. *Journal of Biological Chemistry* 281, 33739-33748.

Cesbron, S., Paulin, J.P., Tharaud, M., Barny, M.A., and Brisset, M.N. (2006). The alternative  $\sigma$  factor HrpL negatively modulates the flagellar system in the phytopathogenic bacterium *Erwinia amylovora* under *hrp*-inducing conditions. *FEMS Microbiology Letters* 257, 221-227.

Chandran, D., Tai, Y.C., Hather, G., Dewdney, J., Denoux, C., Burgess, D.G., Ausubel, F.M., Speed, T.P., and Wildermuth, M.C. (2009). Temporal global expression data reveal known and novel salicylate-impacted processes and regulators mediating powdery mildew growth and reproduction on *Arabidopsis*. *Plant Physiol.* 149, 1435-1451.

Chang, H.Y., and Yang, X. (2000). Proteases for cell suicide: Functions and regulation of caspases. *Microbiol. Mol. Biol. Rev.* 64, 821-846.

Chao, Q., Rothenberg, M., Solano, R., Roman, G., Terzaghi, W., and Ecker, J.R. (1997). Activation of the ethylene gas response pathway in *Arabidopsis* by the nuclear protein ETHYLENE-INSENSITIVE3 and related proteins. *Cell* 89, 1133-1144.

Charroux, B., Rival, T., Narbonne-Reveau, K., and Royet, J. (2010). Bacterial detection by *Drosophila* peptidoglycan recognition proteins. *Microbes and Infection* 11, 631-636.

Che, F.-S., Nakajima, Y., Tanaka, N., Iwano, M., Yoshida, T., Takayama, S., Kadota, I., and Isogai, A. (2000). Flagellin from an incompatible strain of *Pseudomonas avenae* induces a resistance response in cultured rice cells. *Journal of Biological Chemistry* 275, 32347-32356.

Chen, F., Gao, M.-J., Miao, Y.-S., Yuan, Y.-X., Wang, M.-Y., Li, Q., Mao, B.-Z., Jiang, L.-W., and He, Z.-H. (2010a). Plasma membrane localization and potential endocytosis of constitutively expressed Xa21 proteins in transgenic rice. *Mol Plant*, ssq038.

Chen, L., Hamada, S., Fujiwara, M., Zhu, T., Thao, N.P., Wong, H.L., Krishna, P., Ueda, T., Kaku, H., Shibuya, N., Kawasaki, T., and Shimamoto, K. (2010b). The Hop/Sti1-Hsp90 chaperone complex facilitates the maturation and transport of a PAMP receptor in rice innate immunity 7, 185-196.

Chen, X., Chern, M., Canlas, P.E., Ruan, D., Jiang, C., and Ronald, P.C. (2010c). An ATPase promotes autophosphorylation of the pattern recognition receptor XA21 and inhibits XA21-mediated immunity. PNAS 107, 8029-8034.

Chen, Z., Agnew, J.L., Cohen, J.D., He, P., Shan, L., Sheen, J., and Kunkel, B.N. (2007). *Pseudomonas syringae* type III effector AvrRpt2 alters *Arabidopsis thaliana* auxin physiology. PNAS 104, 20131-20136.

Chen, K., Du, L., and Chen, Z. (2003). Sensitization of defense responses and activation of programmed cell death by a pathogen-induced receptor-like protein kinase in *Arabidopsis*. Plant Mol Biol 53, 61 - 74.

Cheng, H., Sugiura, R., Wu, W., Fujita, M., Lu, Y., Sio, S.O., Kawai, R., Takegawa, K., Shunthoh, H., and Kuno, T. (2002). Role of the Rab GTP-binding protein Ypt3 in the Fission yeast exocytic pathway and its connection to calcineurin function. Mol. Biol. Cell 13, 2963-2976.

Chen, Z. (2001). A superfamily of proteins with novel cysteine-rich repeats. Plant Physiol. 126, 473-476.

Cheng, Y.T., Germain, H., Wiermer, M., Bi, D., Xu, F., Garcia, A.V., Wirthmueller, L., Despres, C., Parker, J.E., Zhang, Y., and Li, X. (2009). Nuclear pore complex component MOS7/Nup88 is required for innate immunity and nuclear accumulation of defense regulators in *Arabidopsis*. Plant Cell 21, 2503-2516.

Chico, J.M., Chini, A., Fonseca, S., and Solano, R. (2008). JAZ repressors set the rhythm in jasmonate signaling. Current Opinion in Plant Biology 11, 486-494.

Chinchilla, D., Shan, L., He, P., de Vries, S., and Kemmerling, B. (2009). One for all: the receptor-associated kinase BAK1. Trends in Plant Science 14, 535-541.

Chinchilla, D., Zipfel, C., Robatzek, S., Kemmerling, B., Nürnberg, T., Jones, J.D., Felix, G., and Boller, T. (2007). A flagellin-induced complex of the receptor FLS2 and BAK1 initiates plant defense. Nature 448, 497-500.

Chinchilla, D., Bauer, Z., Regenass, M., Boller, T., and Felix, G. (2006). The *Arabidopsis* receptor kinase FLS2 binds flg22 and determines the specificity of flagellin perception. Plant Cell 18, 465-476.

Chini, A., Boter, M., and Solano, R. (2009a). Plant oxylipins: COI1/JAZs/MYC2 as the core jasmonic acid-signaling module. FEBS Journal 276, 4682-4692.

Chini, A., Fonseca, S., Chico, J.M., Fernández-Calvo, P., and Solano, R. (2009b). The ZIM domain mediates homo- and heteromeric interactions between Arabidopsis JAZ proteins. *Plant J* 59, 77-87.

Chini, A., Fonseca, S., Fernandez, G., Adie, B., Chico, J.M., Lorenzo, O., Garcia-Casado, G., Lopez-Vidriero, I., Lozano, F.M., Ponce, M.R., Micol, J.L., and Solano, R. (2007). The JAZ family of repressors is the missing link in jasmonate signaling. *Nature* 448, 666-671.

Chisholm, S.T., Coaker, G., Day, B., and Staskawicz, B.J. (2006). Host-microbe interactions: shaping the evolution of the plant immune response. *Cell* 124, 803-814.

Choi, J., Huh, S.U., Kojima, M., Sakakibara, H., Paek, K.-H., and Hwang, I. (2010). The cytokinin-activated transcription factor ARR2 promotes plant immunity via TGA3/NPR1-dependent salicylic acid signaling in Arabidopsis. *Developmental Cell* 19, 284-295.

Choudhary, C., and Mann, M. (2010). Decoding signaling networks by mass spectrometry-based proteomics. *Nat Rev Mol Cell Biol* 11, 427-439.

Chow, C.-M., Neto, H., Foucart, C., and Moore, I. (2008). Rab-A2 and Rab-A3 GTPases define a trans-golgi endosomal membrane domain in arabidopsis that contributes substantially to the cell plate. *Plant Cell* 20, 101-123.

Christensen, A., Svensson, K., Thelin, L., Zhang, W., Tintor, N., Prins, D., Funke, N., Michalak, M., Schulze-Lefert, P., Saijo, Y., Sommarin, M., Widell, S., and Persson, S. (2010). Higher plant calreticulins have acquired specialized functions in Arabidopsis. *PLoS ONE* 5, e11342.

Chung, H.S., and Howe, G.A. (2009). A critical role for the TIFY motif in repression of jasmonate signaling by a stabilized splice variant of the JASMONATE ZIM-domain protein JAZ10 in Arabidopsis. *Plant Cell* 21, 131-145.

Clark, K.L., Larsen, P.B., Wang, X., and Chang, C. (1998). Association of the Arabidopsis CTR1 Raf-like kinase with the ETR1 and ERS ethylene receptors. *PNAS* 95, 5401-5406.

Clay, N.K., Adio, A.M., Denoux, C., Jander, G., and Ausubel, F.M. (2009). Glucosinolate metabolites required for an Arabidopsis innate immune response. *Science* 323, 95-101.

Clough, S.J., Fengler, K.A., Yu, I.C., Lippok, B., Smith, R.K., and Bent, A.F. (2000). The Arabidopsis *dnd1* "defense, no death" gene encodes a mutated cyclic nucleotide-gated ion channel. *PNAS* 97, 9323 - 9328.

Cobb, M.H., Sang, B.C., Gonzalez, R., Goldsmith, E., and Ellis, L. (1989). Autophosphorylation activates the soluble cytoplasmic domain of the insulin

receptor in an intermolecular reaction. *Journal of Biological Chemistry* 264, 18701-18706.

Colcombet, J., Boisson-Dernier, A., Ros-Palau, R., Vera, C.E., and Schroeder, J.I. (2005). *Arabidopsis SOMATIC EMBRYOGENESIS RECEPTOR KINASES1 and 2* are essential for tapetum development and microspore maturation. *Plant Cell* 17, 3350-3361.

Collier, S.M., and Moffett, P. (2009). NB-LRRs work a "bait and switch" on pathogens. *Trends in Plant Science* 14, 521-529.

Collins, M.O., Yu, L., and Choudhary, J.S. (2007). Analysis of protein phosphorylation on a proteome-scale. *Proteomics* 7, 2751-2768.

Collmer, A., Schneider, D.J., and Lindeberg, M. (2009). Lifestyles of the effector rich: genome-enabled characterization of bacterial plant pathogens. *Plant Physiol.* 150, 1623-1630.

Collmer, A., Badel, J.L., Charkowski, A.O., Deng, W.-L., Fouts, D.E., Ramos, A.R., Rehm, A.H., Anderson, D.M., Schneewind, O., van Dijk, K., and Alfano, J.R. (2000). *Pseudomonas syringae* Hrp type III secretion system and effector proteins. *PNAS* 97, 8770-8777.

Craig, A., Ewan, R., Mesmar, J., Gudipati, V., and Sadanandom, A. (2009). E3 ubiquitin ligases and plant innate immunity. *Journal of Experimental Botany* 60, 1123-1132.

Creelman, R.A., and Mullet, J.E. (1997). Biosynthesis and action of jasmonates in plants. *Annual Review of Plant Physiology and Plant Molecular Biology* 48, 355-381.

Crouzet, J., Trombik, T., Fraysse, A.S., and Boutry, M. (2006). Organization and function of the plant pleiotropic drug resistance ABC transporter family. *FEBS Letters* 580, 1123-1130.

Cui, H., Wang, Y., Xue, L., Chu, J., Yan, C., Fu, J., Chen, M., Innes, R.W., and Zhou, J.-M. (2010). *Pseudomonas syringae* effector protein AvrB perturbs *Arabidopsis* hormone signaling by activating MAP kinase 4. *Cell Host & Microbe* 7, 164-175.

Czernic, P., Chen Huang, H., and Marco, Y. (1996). Characterization of *hsr201* and *hsr515*, two tobacco genes preferentially expressed during the hypersensitive reaction provoked by phytopathogenic bacteria. *Plant Molecular Biology* 31, 255-265.

Czernic, P., Visser, B., Sun, W., Savouré, A., Deslandes, L., Marco, Y., Van Montagu, M., and Verbruggen, N. (1999). Characterization of an *Arabidopsis thaliana* receptor-like protein kinase gene activated by oxidative stress and pathogen attack. *Plant J* 18, 321-327.

da Silva Correia, J., Miranda, Y., Leonard, N., and Ulevitch, R. (2007). SGT1 is essential for Nod1 activation. *PNAS* 104, 6764-6769.

da Silva, F.G., Shen, Y., Dardick, C., Burdman, S., Yadav, R.C., de Leon, A.L., and Ronald, P.C. (2004). Bacterial genes involved in Type I secretion and sulfation are required to elicit the rice Xa21-mediated innate immune response. *MPMI* 17, 593-601.

Dangl, J.L., and Jones, J.D.G. (2001). Plant pathogens and integrated defense responses to infection. *Nature* 411, 826.

Daniel, X., Lacomme, C., Morel, J.B., and Roby, D. (1999). A novel *myb* oncogene homologue in *Arabidopsis thaliana* related to hypersensitive cell death. *Plant J* 20, 57-66.

Dardick, C., and Ronald, P. (2006). Plant and animal pathogen recognition receptors signal through non-RD kinases. *PLoS Pathog* 2, e2.

Day, B., Dahlbeck, D., and Staskawicz, B.J. (2006). NDR1 interaction with RIN4 mediates the differential activation of multiple disease resistance pathways in *Arabidopsis*. *Plant Cell* 18, 2782-2791.

Day, B., Dahlbeck, D., Huang, J., Chisholm, S.T., Li, D., and Staskawicz, B.J. (2005). Molecular basis for the RIN4 negative regulation of RPS2 disease resistance. *Plant Cell* 17, 1292-1305.

de Jong, C.F., Laxalt, A.M., Bargmann, B.O., P.J., d.W., Joosten, M.H., and Munnik, T. (2004). Phosphatidic acid accumulation is an early response in the Cf-4/Avr4 interaction. *Plant J* 39, 1-12.

De Smet, I., Vassileva, V., De Rybel, B., Levesque, M.P., Grunewald, W., Van Damme, D., Van Noorden, G., Naudts, M., Van Isterdael, G., De Clercq, R., Wang, J.Y., Meuli, N., Vanneste, S., Friml, J., Hilson, P., Jurgens, G., Ingram, G.C., Inze, D., Benfey, P.N., and Beeckman, T. (2008). Receptor-like kinase ACR4 restricts formative cell divisions in the *Arabidopsis* root. *Science* 322, 594-597.

de Torres, M., Sanchez, P., Fernandez-Delmond, I., and Grant, M. (2003). Expression profiling of the host response to bacterial infection: the transition from basal to induced defense responses in RPM1-mediated resistance. *Plant J* 33, 665-676.

de Torres, M., Mansfield, J.W., Grabov, N., Brown, I.R., Ammounah, H., Tsiamis, G., Forsyth, A., Robatzek, S., Grant, M., and Boch, J. (2006). *Pseudomonas syringae* effector AvrPtoB suppresses basal defense in *Arabidopsis*. *Plant J* 47, 368-382.

de Torres Zabala, M., Bennett, M.H., Truman, W.H., and Grant, M.R. (2009). Antagonism between salicylic and abscisic acid reflects early host-pathogen conflict and moulds plant defense responses. *Plant J* 59, 375-386.

de Torres-Zabala, M., Truman, W., Bennett, M.H., Lafforgue, G., Mansfield, J.W., Rodriguez Egea, P., Bogre, L., and Grant, M. (2007). *Pseudomonas syringae* pv.

*tomato* hijacks the *Arabidopsis* abscisic acid signaling pathway to cause disease. *Embo J* 26, 1434-1443.

Delaney, T.P., Friedrich, L., and Ryals, J.A. (1995). *Arabidopsis* signal transduction mutant defective in chemically and biologically induced disease resistance. *PNAS* 92, 6602-6606.

Denoux, C., Galletti, R., Mammarella, N., Gopalan, S., Werck, D.I., De Lorenzo, G., Ferrari, S., Ausubel, F.M., and Dewdney, J. (2008). Activation of defense response pathways by OGS and flg22 elicitors in *Arabidopsis* seedlings. *Molecular Plant* 1, 423-445.

Desaki, Y., Miya, A., Venkatesh, B., Tsuyumu, S., Yamane, H., Kaku, H., Minami, E., and Shibuya, N. (2006). Bacterial lipopolysaccharides induce defense responses associated with programmed cell death in rice cells. *Plant and Cell Physiology* 47, 1530-1540.

Deslandes, L., Olivier, J., Peeters, N., Feng, D.X., and Khounlotham, M. (2003). Physical interaction between RRS1-R, a protein conferring resistance to bacterial wilt, and PopP2, a type III effector targeted to the plant nucleus. *PNAS* 100, 8024.

Despres, C., Chubak, C., Rochon, A., Clark, R., Bethune, T., Desveaux, D., and Fobert, P.R. (2003). The *Arabidopsis* NPR1 disease resistance protein is a novel cofactor that confers redox regulation of DNA binding activity to the basic domain/leucine zipper transcription factor TGA1. *Plant Cell* 15, 2181-2191.

Devarenne, T.P., Ekengren, S.K., Pedley, K.F., and Martin, G.B. (2006). Adi3 is a Pdk1-interacting AGC kinase that negatively regulates plant cell death. *Embo J* 25, 255-265.

Devoto, A., Nieto-Rostro, M., Xie, D., Ellis, C., Harmston, R., Patrick, E., Davis, J., Sherratt, L., Coleman, M., and Turner, J.G. (2002). COI1 links jasmonate signaling and fertility to the SCF ubiquitin-ligase complex in *Arabidopsis*. *Plant J* 32, 457-466.

Dhawan, R., Luo, H., Foerster, A.M., AbuQamar, S., Du, H.-N., Briggs, S.D., Scheid, O.M., and Mengiste, T. (2009). Histone monoubiquitination1 interacts with a subunit of the mediator complex and regulates defense against necrotrophic fungal pathogens in *Arabidopsis*. *Plant Cell* 21, 1000-1019.

Dickman, M.B., and Mitra, A. (1992). *Arabidopsis thaliana* as a model for studying *Sclerotinia sclerotiorum* pathogenesis. *Physiological and Molecular Plant Pathology* 41, 255-263.

Dietrich, R.A., Richberg, M.H., Schmidt, R., Dean, C., and Dangl, J.L. (1997). A novel zinc finger protein is encoded by the *Arabidopsis* *LSD1* gene and functions as a negative regulator of plant cell death. *Cell* 88, 685-694.

Divi, U.K., and Krishna, P. (2009). Brassinosteroid: a biotechnological target for enhancing crop yield and stress tolerance. *New Biotechnology* 26, 131-136.

Dobler, S. (2001). Evolutionary aspects of defense by recycled plant compounds in herbivorous insects. *Basic and Applied Ecology* 2, 15-26.

Dodd, A.N., Kudla, J.r., and Sanders, D. (2010). The language of calcium signaling. *Annual Review of Plant Biology* 61, 593-620.

Dong, C.-H., Jang, M., Scharein, B., Malach, A., Rivarola, M., Liesch, J., Groth, G., Hwang, I., and Chang, C. (2010). Molecular association of the *Arabidopsis* ETR1 ethylene receptor and a regulator of ethylene signaling, RTE1. *Journal of Biological Chemistry*.

Dong, C.H., Rivarola, M., Resnick, J.S., Maggin, B.D., and Chang, C. (2008). Subcellular co-localization of *Arabidopsis* RTE1 and ETR1 supports a regulatory role for RTE1 in ETR1 ethylene signaling. *Plant J* 53, 275-286.

Dou, D.L., Kale, S.D., Wang, X., Jiang, R.H.Y., and Bruce, N.A. (2008). RXLR-mediated entry of *Phytophthora sojae* effector Avr1b into soybean cells does not require pathogen-encoded machinery. *Plant Cell* 20, 1930.

Du, L., and Chen, Z. (2000). Identification of genes encoding receptor-like protein kinases as possible targets of pathogen- and salicylic acid-induced WRKY DNA-binding proteins in *Arabidopsis*. *Plant J* 24, 837-847.

Dunn, T.M., Lynch, D.V., Michaelson, L.V., and Napier, J.A. (2004). A post-genomic approach to understanding sphingolipid metabolism in *Arabidopsis thaliana*. *Annals of Botany* 93, 483-497.

Dunning, F.M., Sun, W., Jansen, K.L., Helft, L., and Bent, A.F. (2007). Identification and mutational analysis of *arabidopsis* FLS2 leucine-rich repeat domain residues that contribute to flagellin perception. *Plant Cell* 19, 3297-3313.

Durek, P., Schmidt, R., Heazlewood, J.L., Jones, A., MacLean, D., Nagel, A., Kersten, B., and Schulze, W.X. (2009). PhosPhAt: the *Arabidopsis thaliana* phosphorylation site database. An update. *Nucleic acids research* 38, D828-D834.

Durrant, W.E., and Dong, X. (2004). Systemic acquired resistance. *Annu Rev Phytopathol* 42, 185-209.

Earley, K.W., Haag, J.R., Pontes, O., Opper, K., Juehne, T., Song, K., and Pikaard, C.S. (2006). Gateway-compatible vectors for plant functional genomics and proteomics. *Plant J* 45, 616-629.

Eitas, T.K., and Dangl, J.L. (2010) NB-LRR proteins: pairs, pieces, perception, partners, and pathways. *Current Opinion in Plant Biology* 13, 472-477.

Eitas, T.K., Nimchuk, Z.L., and Dangl, J.L. (2008). *Arabidopsis TAO1* is a TIR-NB-LRR protein that contributes to disease resistance induced by the *Pseudomonas syringae* effector AvrB. *PNAS* 105, 6475-6480.

Ek-Ramos, M.a.J., Avila, J., Cheng, C., Martin, G.B., and Devarenne, T.P. (2010). The T-loop extension of the tomato protein kinase AvrPto-dependent pto-interacting protein 3 (Adi3) directs nuclear localization for suppression of plant cell death. *Journal of Biological Chemistry* 285, 17584-17594.

Elbaz, M., Avni, A., and Weil, M. (2002). Constitutive caspase-like machinery executes programmed cell death in plant cells. *Cell Death Differ* 9, 726-733.

Ellgaard, L., and Helenius, A. (2003). Quality control in the endoplasmic reticulum. *Nat Rev Mol Cell Biol* 4, 181-191.

Ellis, J.G., Dodds, P.N., and Lawrence, G.J. (2007). Flax rust resistance gene specificity is based on direct resistance-avirulence protein interactions. *Annu. Rev. Phytopathol.* 45, 289.

Engelhardt, S., Lee, J., Gäßler, Y., Kemmerling, B., Haapalainen, M.L., Li, C.M., Wei, Z., Keller, H., Joosten, M., Taira, S., and Nürnberg, T. (2009). Separable roles of the *Pseudomonas syringae* pv. *phaseolicola* accessory protein HrpZ1 in ion-conducting pore formation and activation of plant immunity. *Plant J* 57, 706-717.

Epple, P., Apel, K., and Bohlmann, H. (1995). An *Arabidopsis thaliana* thionin gene is inducible via a signal transduction pathway different from that for pathogenesis-related proteins. *Plant Physiol.* 109, 813-820.

Erbs, G., Silipo, A., Aslam, S., De Castro, C., Liparoti, V., Flagiello, A., Pucci, P., Lanzetta, R., Parrilli, M., Molinaro, A., Newman, M.-A., and Cooper, R.M. (2008). Peptidoglycan and muropeptides from pathogens *Agrobacterium* and *Xanthomonas* elicit plant innate immunity: structure and activity. *Chemistry & biology* 15, 438-448.

Escobar-Restrepo, J.M., Huck, N., Kessler, S., Gagliardini, V., Gheyselinck, J., Yang, W.C., and Grossniklaus, U. (2007). The FERONIA receptor-like kinase mediates male-female interactions during pollen tube reception. *Science* 317, 656 - 660.

Eulgem, T., and Somssich, I.E. (2007). Networks of WRKY transcription factors in defense signaling. *Curr Opin Plant Biol* 10, 366 - 371.

Fahlgren, N., Howell, M.D., Kasschau, K.D., Chapman, E.J., Sullivan, C.M., Cumbie, J.S., Givan, S.A., Law, T.F., Grant, S.R., Dangl, J.L., and Carrington, J.C. (2007). High-throughput sequencing of *Arabidopsis* microRNAs: Evidence for frequent birth and death of *miRNA* genes. *PLoS ONE* 2, e219.

Fan, W., and Dong, X. (2002). *In vivo* interaction between NPR1 and transcription factor TGA2 leads to salicylic acid-mediated gene activation in *Arabidopsis*. *Plant Cell* 14, 1377-1389.

Felix, G., and Boller, T. (2003). Molecular sensing of bacteria in plants. The highly conserved RNA-binding motif RNP-1 of bacterial cold shock proteins is recognized as an elicitor signal in tobacco. *J Biol Chem* 278, 6201-6208.

Felix, G., Duran, J.D., Volko, S., and Boller, T. (1999). Plants have a sensitive perception system for the most conserved domain of bacterial flagellin. *Plant J* 18, 265-276.

Fellbrich, G., Romanski, A., Varet, A., Blume, B., Brunner, F., Engelhardt, S., Felix, G., Kemmerling, B., Krzymowska, M., and Nürnberg, T. (2002). NPP1, a *Phytophthora*-associated trigger of plant defense in parsley and *Arabidopsis*. *Plant J* 32, 375-390.

Felton, G.W., and Korth, K.L. (2000). Trade-offs between pathogen and herbivore resistance. *Current Opinion in Plant Biology* 3, 309-314.

Ferrari, S., Galletti, R., Denoux, C., De Lorenzo, G., Ausubel, F.M., and Dewdney, J. (2007). Resistance to *Botrytis cinerea* induced in *Arabidopsis* by elicitors is independent of salicylic acid, ethylene, or jasmonate signaling but requires PHYTOALEXIN DEFICIENT3. *Plant Physiol.* 144, 367-379.

Feys, B.J., Moisan, L.J., Newman, M.-A., and Parker, J.E. (2001). Direct interaction between the *Arabidopsis* disease resistance signaling proteins, EDS1 and PAD4. *Embo J* 20, 5400-5411.

Feys, B.J.F., Benedetti, C.E., Penfold, C.N., and Turner, J.G. (1994). *Arabidopsis* mutants selected for resistance to the phytotoxin coronatine are male sterile, insensitive to methyl jasmonate, and resistant to a bacterial pathogen. *Plant Cell* 6, 751-759.

Fiers, M., Golemiec, E., Xu, J., van der Geest, L., Heidstra, R., Stiekema, W., and Liu, C.-M. (2005). The 14-amino acid CLV3, CLE19, and CLE40 peptides trigger consumption of the root meristem in *Arabidopsis* through a CLAVATA2-dependent pathway. *Plant Cell* 17, 2542-2553.

Flor, H.H. (1971). Current status of the gene-for-gene concept. *Annu Rev Phytopathol* 9, 275-296.

Fonseca, S., Chini, A., Hamberg, M., Adie, B., Porzel, A., Kramell, R., Miersch, O., Wasternack, C., and Solano, R. (2009). (+)-7-iso-Jasmonoyl-L-isoleucine is the endogenous bioactive jasmonate. *Nat Chem Biol* 5, 344-350.

Fradin, E.F., Zhang, Z., Juarez Ayala, J.C., Castroverde, C.D.M., Nazar, R.N., Robb, J., Liu, C.-M., and Thomma, B.P.H.J. (2009). Genetic dissection of *Verticillium* wilt resistance mediated by tomato Ve1. *Plant Physiol.* 150, 320-332.

Franchi, L., Stoolman, J., Kanneganti, T.D., Verma, A., Ramphal, R., and Núñez, G. (2007). Critical role for Ipaf in *Pseudomonas aeruginosa*-induced caspase-1 activation. European Journal of Immunology 37, 3030-3039.

Franchi, L., Amer, A., Body-Malapel, M., Kanneganti, T., Özören, N., Jagirdar, R., Inohara, N., Vandenabeele, P., Bertin, J., Coyle, A., Grant, E.P., and Núñez, G. (2006). Cytosolic flagellin requires Ipaf for activation of caspase-1 and interleukin 1 in salmonella-infected macrophage. Nat Immunol 7, 576 - 582.

Freialdenhoven, A., Scherag, B., Hollricher, K., Collinge, D.B., Thordal-Christensen, H., and Schulze-Lefert, P. (1994). *Nar-1* and *Nar-2*, Two Loci Required for Mla12-specified race-specific resistance to powdery mildew in barley. Plant Cell 6, 983-994.

Friedrichsen, D.M., Joazeiro, C.A.P., Li, J., Hunter, T., and Chory, J. (2000). Brassinosteroid-Insensitive-1 Is a ubiquitously expressed leucine-rich repeat receptor serine/threonine kinase. Plant Physiol. 123, 1247-1256.

Fritz-Laylin, L.K., Krishnamurthy, N., Tor, M., Sjolander, K.V., and Jones, J.D.G. (2005). Phylogenomic analysis of the receptor-like proteins of rice and Arabidopsis. Plant Physiol. 138, 611-623.

Froidure, S., Canonne, J., Daniel, X., Jauneau, A., Brière, C., Roby, D., and Rivas, S. (2010). AtsPLA2 $\alpha$  nuclear relocalization by the Arabidopsis transcription factor AtMYB30 leads to repression of the plant defense response. PNAS 107, 15281-15286.

Fu, D.-Q., Ghabrial, S., and Kachroo, A. (2008). GmRAR1 and GmSGT1 are required for basal, *R* Gene-mediated and systemic acquired resistance in soybean. MPMI 22, 86-95.

Fu, Z.Q., Guo, M., Jeong, B.R., Tian, F., Elthon, T.E., Cerny, R.L., Staiger, D., and Alfano, J.R. (2007). A type III effector ADP-ribosylates RNA-binding proteins and quells plant immunity. Nature 447, 284-288.

Fuchs, Y., Saxena, A., Gamble, H.R., and Anderson, J.D. (1989). Ethylene biosynthesis-inducing protein from cellulysin is an endoxylanase. Plant Physiol. 89, 138-143.

Fujiwara, M., Hamada, S., Hiratsuka, M., Fukao, Y., Kawasaki, T., and Shimamoto, K. (2009). Proteome analysis of detergent-resistant membranes (DRMs) associated with OsRac1-mediated innate immunity in rice. Plant and Cell Physiology 50, 1191-1200.

Furman-Matarasso, N., Cohen, E., Du, Q., Chejanovsky, N., Hanania, U., and Avni, A. (1999). A point mutation in the ethylene-inducing xylanase elicitor inhibits the beta-1,4-endoxylanase activity but not the elicitation activity. Plant Physiol. 121, 345-352.

Gagne, J.M., Smalle, J., Gingerich, D.J., Walker, J.M., Yoo, S.-D., Yanagisawa, S., and Vierstra, R.D. (2004). Arabidopsis EIN3-binding F-box 1 and 2 form ubiquitin-protein ligases that repress ethylene action and promote growth by directing EIN3 degradation. *PNAS* 101, 6803-6808.

Galletti, R., Denoux, C., Gambetta, S., Dewdney, J., Ausubel, F.M., De Lorenzo, G., and Ferrari, S. (2008). The AtrbohD-mediated oxidative burst elicited by oligogalacturonides in Arabidopsis is dispensable for the activation of defense responses effective against *Botrytis cinerea*. *Plant Physiol.* 148, 1695-1706.

Gallois, P., Makishima, T., Hecht, V., Despres, B., Laudié, M., Nishimoto, T., and Cooke, R. (1997). An *Arabidopsis thaliana* cDNA complementing a hamster apoptosis suppressor mutant. *Plant J* 11, 1325-1331.

Gao, M., Liu, J., Bi, D., Zhang, Z., Cheng, F., Chen, S., and Zhang, Y. (2008). MEKK1, MKK1/MKK2 and MPK4 function together in a mitogen-activated protein kinase cascade to regulate innate immunity in plants. *Cell Res* 18, 1190-1198.

Gao, M., Wang, X., Wang, D., Xu, F., Ding, X., Zhang, Z., Bi, D., Cheng, Y.T., Chen, S., Li, X., and Zhang, Y. (2009). Regulation of cell death and innate immunity by two receptor-like kinases in Arabidopsis. *Cell Host & Microbe* 6, 34-44.

Garcia-Brunner, A., Lamotte, O., Vandelle, E., Bourque, S.p., Lecourieux, D., Poinssot, B., Wendehenne, D., and Pugin, A. (2006). Early signaling events induced by elicitors of plant defenses. *MPMI* 19, 711-724.

Garcia-Ranea, J.A., Mirey, G., Camonis, J., and Valencia, A. (2002). p23 and HSP20/[alpha]-crystallin proteins define a conserved sequence domain present in other eukaryotic protein families. *FEBS Letters* 529, 162-167.

Gassmann, W., Hinsch, M.E., and Staskawicz, B.J. (1999). The Arabidopsis *RPS4* bacterial-resistance gene is a member of the TIR-NBS-LRR family of disease-resistance genes. *Plant J* 20, 265-277.

Geldner, N., and Robatzek, S. (2008). Plant receptors go endosomal: a moving view on signal transduction. *Plant Physiol.* 147, 1565-1574.

Geldner, N., Hyman, D.L., Wang, X., Schumacher, K., and Chory, J. (2007). Endosomal signaling of plant steroid receptor kinase BRI1. *Genes Dev* 21, 1598-1602.

Gewirtz, A.T., Simon, P.O., Schmitt, C.K., Taylor, L.J., Hagedorn, C.H., O'Brien, A.D., Neish, A.S., and Madara, J.L. (2001). *Salmonella typhimurium* translocates flagellin across intestinal epithelia, inducing a proinflammatory response. *The Journal of Clinical Investigation* 107, 99-109.

Gifford, M.L., Dean, S., and Ingram, G.C. (2003). The Arabidopsis *ACR4* gene plays a role in cell layer organisation during ovule integument and sepal margin development. *Development* 130, 4249-4258.

Gifford, M.L., Robertson, F.C., Soares, D.C., and Ingram, G.C. (2005). ARABIDOPSIS CRINKLY4 function, internalization, and turnover are dependent on the extracellular crinkly repeat domain. *Plant Cell* 17, 1154-1166.

Gijzen, M., and Nrnberger, T. (2006). Nep1-like proteins from plant pathogens: Recruitment and diversification of the NPP1 domain across taxa. *Phytochemistry* 67, 1800-1807.

Gilchrist, D. (1997). Mycotoxins reveal connections between plants and animals in apoptosis and ceramide signaling. *Cell Death Differ* 4, 689-698.

Gimenez-Ibanez, S., Ntoukakis, V., and Rathjen, J.P. (2009a). The LysM receptor kinase CERK1 mediates bacterial perception in *Arabidopsis*. *Plant Signal Behav* 4, 539-541.

Gimenez-Ibanez, S., Hann, D.R., Ntoukakis, V., Petutschnig, E., Lipka, V., and Rathjen, J.P. (2009b). AvrPtoB targets the lsm receptor kinase CERK1 to promote bacterial virulence on plants. *Current biology* 19, 423-429.

Gingras, A.-C., Gstaiger, M., Raught, B., and Aebersold, R. (2007). Analysis of protein complexes using mass spectrometry. *Nat Rev Mol Cell Biol* 8, 645-654.

Glazebrook, J. (2005). Contrasting mechanisms of defense against biotrophic and necrotrophic pathogens. *Annu Rev Phytopathol* 43, 205-227.

Glazebrook, J., Zook, M., Mert, F., Kagan, I., Rogers, E.E., Crute, I.R., Holub, E.B., Hammerschmidt, R., and Ausubel, F.M. (1997). Phytoalexin- deficient mutants of *Arabidopsis* reveal that *PAD4* encodes a regulatory factor and that four *PAD* genes contribute to downy mildew resistance. *Genetics* 146, 381-392.

Glazebrook, J., Rogers, E.E., and Ausubel, F.M. (1996). Isolation of *Arabidopsis* mutants with enhanced disease susceptibility by direct screening. *Genetics* 143, 973-982.

Glazebrook, J., and Ausubel, F.M. (1994). Isolation of phytoalexin-deficient mutants of *Arabidopsis thaliana* and characterization of their interactions with bacterial pathogens. *Proc Natl Acad Sci USA* 91, 8955-8959.

Göhre, V., Spallek, T., Häweker, H., Mersmann, S., Mentzel, T., Boller, T., de Torres, M., Mansfield, J.W., and Robatzek, S. (2008). Plant pattern-recognition receptor FLS2 is directed for degradation by the bacterial ubiquitin ligase AvrPtoB. *Current Biology* 18, 1824-1832.

Gómez-Gómez, L., Bauer, Z., and Boller, T. (2001). Both the extracellular leucine-rich repeat domain and the kinase activity of FSL2 are required for flagellin binding and signaling in *Arabidopsis*. *Plant Cell* 13, 1155-1163.

Gómez-Gómez, L., and Boller, T. (2000). FLS2: an LRR receptor-like kinase involved in the perception of the bacterial elicitor flagellin in *Arabidopsis*. *Mol Cell* 5, 1003 - 1011.

Gómez-Gómez, L., Felix, G., and Boller, T. (1999). A single locus determines sensitivity to bacterial flagellin in *Arabidopsis thaliana*. *Plant J* 18, 277-284.

Gonzalez-Lamothe, R., Tsitsigiannis, D.I., Ludwig, A.A., Panicot, M., Shirasu, K., and Jones, J.D.G. (2006). The U-Box Protein *cmpg1* is required for efficient activation of defense mechanisms triggered by multiple resistance genes in tobacco and tomato. *Plant Cell* 18, 1067-1083.

Goodin, M.M., Zaitlin, D., Naidu, R.A., and Lommel, S.A. (2008). *Nicotiana benthamiana*: its history and future as a model for plant-pathogen Interactions. *MPMI* 21, 1015-1026.

Goritschnig, S., Zhang, Y., and Li, X. (2007). The ubiquitin pathway is required for innate immunity in *Arabidopsis*. *Plant J* 49, 540 - 551.

Gou, M., Su, N., Zheng, J., Huai, J., Wu, G., Zhao, J., He, J., Tang, D., Yang, S., and Wang, G. (2009). An F-box gene, *CPR30*, functions as a negative regulator of the defense response in *Arabidopsis*. *Plant J* 60, 757-770.

Gou, X., He, K., Yang, H., Yuan, T., Lin, H., Clouse, S., and Li, J. (2010). Genome-wide cloning and sequence analysis of leucine-rich repeat receptor-like protein kinase genes in *Arabidopsis thaliana*. *BMC Genomics* 11, 19.

Granato, D., Bergonzelli, G.E., Pridmore, R.D., Marvin, L., Rouvet, M., and Corthesy-Theulaz, I.E. (2004). Cell surface-associated elongation factor tu mediates the attachment of *Lactobacillus johnsonii* NCC533 (*La1*) to human intestinal cells and mucins. *Infect. Immun.* 72, 2160-2169.

Grant, M., Brown, I., Adams, S., Knight, M., Ainslie, A., and Mansfield, J. (2000). The *RPM1* plant disease resistance gene facilitates a rapid and sustained increase in cytosolic calcium that is necessary for the oxidative burst and hypersensitive cell death. *Plant J* 23, 441-450.

Grant, M.R., Godiard, L., Straube, E., Ashfield, T., Lewald, J., Sattler, A., Innes, R.W., and Dangl, J.L. (1995). Structure of the *Arabidopsis RPM1* gene enabling dual specificity disease resistance. *Science* 269, 843-846.

Grant, S.R., Fisher, E.J., Chang, J.H., Mole, B.M., and Dangl, J.L. (2006). Subterfuge and manipulation: type III effector proteins of phytopathogenic bacteria. *Annu. Rev. Microbiol.* 60, 425.

Green, T.R., and Ryan, C.A. (1972). Wound-induced proteinase inhibitor in plant leaves: a possible defense mechanism against insects. *Science* 175, 776-777.

Guan, R., and Mariuzza, R.A. (2007). Peptidoglycan recognition proteins of the innate immune system. *Trends in Microbiology* 15, 127-134.

Guo, H., and Ecker, J.R. (2003). Plant responses to ethylene gas are mediated by *scfEBF1/EBF2*-dependent proteolysis of EIN3 transcription factor. *Cell* 115, 667-677.

Guo, H., Li, L., Ye, H., Yu, X., Algreen, A., and Yin, Y. (2009). Three related receptor-like kinases are required for optimal cell elongation in *Arabidopsis thaliana*. PNAS 106, 7648-7653.

Gust, A.A., Biswas, R., Lenz, H.D., Rauhut, T., Ranf, S., Kemmerling, B., Gotz, F., Glawischnig, E., Lee, J., Felix, G., and Nürnberger, T. (2007). Bacteria-derived peptidoglycans constitute pathogen-associated molecular patterns triggering innate immunity in *Arabidopsis*. J Biol Chem 208, 32338-32348.

Guttman, D.S., Gropp, S.J., Morgan, R.L., and Wang, P.W. (2006). Diversifying selection drives the evolution of the type iii secretion system pilus of *Pseudomonas syringae*. Molecular Biology and Evolution 23, 2342-2354.

Haapalainen, M., Engelhardt, S., Kühner, I., Li, C.M., Nürnberger, T., Lee, J., Romantschuk, M., and Taira, S. (2010). Functional mapping of harpin HrpZ of *Pseudomonas syringae* reveals the sites responsible for protein oligomerization, lipid interactions and plant defense induction. Molecular Plant Pathology, no-no.

Hahlbrock, K., Scheel, D., Logemann, E., Nürnberger, T., Parniske, M., Reinold, S., Sacks, W.R., and Schmelzer, E. (1995). Oligopeptide elicitor-mediated defense gene activation in cultured parsley cells. PNAS 92, 4150-4157.

Hahn, J.-S. (2005). Regulation of Nod1 by Hsp90 chaperone complex. FEBS Letters 579, 4513-4519.

Halim, V.A., Hunger, A., Macioszek, V., Landgraf, P., Nurnberger, T., Scheel, D., and Rosahl, S. (2004). The oligopeptide elicitor Pep-13 induces salicylic acid-dependent and -independent defense reactions in potato. Physiological and Molecular Plant Pathology 64, 311-318.

Ham, J.H., Kim, M.G., Lee, S.Y., and Mackey, D. (2007). Layered basal defenses underlie non-host resistance of *Arabidopsis* to *Pseudomonas syringae* pv. *phaseolicola*. Plant J 51, 604-616.

Hammond-Kosack, K.E., and Jones, J.D.G. (1997). Plant disease resistance genes. Annual Review of Plant Physiology and Plant Molecular Biology 48, 575-607.

Hammond-Kosack, K.E., and Parker, J. (2003). Deciphering plant-pathogen communication: fresh perspectives for molecular resistance breeding. Curr Opin Biotechnol 14, 177-193.

Hanks, S.K., and Quinn, A.M. (1991). Protein kinase catalytic domain sequence database: identification of conserved features of primary structure and classification of family members.

Hann, D.R., and Rathjen, J.P. (2007). Early events in the pathogenicity of *Pseudomonas syringae* on *Nicotiana benthamiana*. Plant J 49, 607-618.

Hann, D.R., Gimenez-Ibanez, S., and Rathjen, J.P. (2010). Bacterial virulence effectors and their activities. *Current Opinion in Plant Biology* 13, 388-393.

Häweker, H., Rips, S., Koiwa, H., Salomon, S., Saijo, Y., Chinchilla, D., Robatzek, S., and von Schaewen, A. (2010). Pattern recognition receptors require N-glycosylation to mediate plant immunity. *Journal of Biological Chemistry* 285, 4629-4636.

Hayashi, F., Smith, K.D., Ozinsky, A., Hawn, T.R., Yi, E.C., Goodlett, D.R., Eng, J.K., Akira, S., Underhill, D.M., and Aderem, A. (2001). The innate immune response to bacterial flagellin is mediated by Toll-like receptor 5. *Nature* 410, 1099-1103.

He, K., Gou, X., Powell, R.A., Yang, H., Yuan, T., Guo, Z., and Li, J. (2008). Receptor-like protein kinases, BAK1 and BKK1, regulate a light-dependent cell-death control pathway. *Plant Signaling and Behaviour* 3, 813-815.

He, K., Gou, X., Yuan, T., Lin, H., Asami, T., Yoshida, S., Russell, S.D., and Li, J. (2007). BAK1 and BKK1 regulate brassinosteroid-dependent growth and brassinosteroid-independent cell-death pathways. *Curr Biol* 17, 1109-1115.

He, P., Shan, L., Lin, N.C., Martin, G.B., Kemmerling, B., Nurnberger, T., and Sheen, J. (2006). Specific bacterial suppressors of MAMP signaling upstream of MAPKKK in *Arabidopsis* innate immunity. *Cell* 125, 563-575.

Heazlewood, J.L., Durek, P., Hummel, J., Selbig, J., Weckwerth, W., Walther, D., and Schulze, W.X. (2008). PhosPhAt: a database of phosphorylation sites in *Arabidopsis thaliana* and a plant-specific phosphorylation site predictor. *Nucleic acids research* 36, D1015-D1021.

Hecht, V., Vielle-Calzada, J.-P., Hartog, M.V., Schmidt, E.D.L., Boutilier, K., Grossniklaus, U., and de Vries, S.C. (2001). The *Arabidopsis* somatic embryogenesis receptor kinase 1 gene is expressed in developing ovules and embryos and enhances embryogenic competence in culture. *Plant Physiol.* 127, 803-816.

Heese, A., Hann, D.R., Gimenez-Ibanez, S., Jones, A.M., He, K., Li, J., Schroeder, J.I., Peck, S.C., and Rathjen, J.P. (2007). The receptor-like kinase SERK3/BAK1 is a central regulator of innate immunity in plants. *Proc Natl Acad Sci U S A* 104, 12217-12222.

Heldin, C.-H. (1995). Dimerization of cell surface receptors in signal transduction. *Cell* 80, 213-223.

Helenius, A., and Aebi, M. (2001). Intracellular functions of N-linked glycans. *Science* 291, 2364-2369.

Herbers, K., Conrads-Strauch, J., and Bonas, U. (1992). Race-specificity of plant resistance to bacterial spot disease determined by repetitive motifs in a bacterial avirulence protein. *Nature* 356, 172-174.

Higgins, C.F. (2007). Multiple molecular mechanisms for multidrug resistance transporters. *Nature* 446, 749-757.

Hitmi, A., Coudret, A., and Barthomeuf, C. (2000). The production of pyrethrins by plant cell and tissue cultures of *Chrysanthemum cinerariaefolium* and *Tagetes* species. *Crit Rev Biochem Mol Biol.* 35, 317-337.

Hofius, D., Schultz-Larsen, T., Joensen, J., Tsitsigiannis, D.I., Petersen, N.H.T., Mattsson, O., Jørgensen, L.B., Jones, J.D.G., Mundy, J., and Petersen, M. (2009). Autophagic components contribute to hypersensitive cell death in *Arabidopsis* 137, 773-783.

Holt, B.F., Boyes, D.C., Ellerström, M., Siefers, N., Wiig, A., Kauffman, S., Grant, M.R., and Dangl, J.L. (2002). An evolutionarily conserved mediator of plant disease resistance gene function is required for normal *arabidopsis* development. *Developmental Cell* 2, 807-817.

Holton, N., Cano-Delgado, A., Harrison, K., Montoya, T., Chory, J., and Bishop, G.J. (2007). Tomato BRASSINOSTEROID INSENSITIVE1 is required for systemin-induced root elongation in *Solanum pimpinellifolium* but is not essential for wound signaling. *Plant Cell* 19, 1709-1717.

Holub, E. (2008). Natural history of *Arabidopsis thaliana* and oomycete symbioses. *European Journal of Plant Pathology* 122, 91-109.

Holub, E.B., Beynon, L.J., and Crute, I.R. (1994). Phenotypic and genotypic characterization of interactions between isolates of *Peronospora parasitica* and accessions of *Arabidopsis thaliana*. *Mol. Plant-Microbe Interact.* 7, 223.

Hong, Z., Jin, H., Tzfira, T., and Li, J. (2008). Multiple mechanism-mediated retention of a defective brassinosteroid receptor in the endoplasmic reticulum of *Arabidopsis*. *Plant Cell* 20, 3418-3429.

Hu, J., Barlet, X., Deslandes, L., Hirsch, J., Feng, D.X., Somssich, I., and Marco, Y. (2008). Transcriptional Responses of *Arabidopsis thaliana* during wilt disease caused by the soil-borne phytopathogenic bacterium, *Ralstonia solanacearum*. *PLoS ONE* 3, e2589.

Hua, J., and Meyerowitz, E.M. (1998). Ethylene responses are negatively regulated by a receptor gene family in *Arabidopsis thaliana*. *Cell* 94, 261-271.

Hua, J., Grisafi, P., Cheng, S.-H., and Fink, G.R. (2001). Plant growth homeostasis is controlled by the *Arabidopsis BON1* and *BAP1* genes. *Genes Dev* 15, 2263-2272.

Huang, Y., Li, H., Hutchison, C.E., Laskey, J., and Kieber, J.J. (2003). Biochemical and functional analysis of CTR1, a protein kinase that negatively regulates ethylene signaling in *Arabidopsis*. *Plant J* 33, 221-233.

Hubbard, S.R. (2004). Juxtamembrane autoinhibition in receptor tyrosine kinases. *Nat Rev Mol Cell Biol* 5, 464-471.

Huckelhoven, R. (2007). Cell wall-associated mechanisms of disease resistance and susceptibility. *Annu. Rev. Phytopathol.* 45, 2.1–2.27.

Huffaker, A., and Ryan, C.A. (2007). Endogenous peptide defense signals in *Arabidopsis* differentially amplify signaling for the innate immune response. *PNAS* 104, 10732-10736.

Huffaker, A., Pearce, G., and Ryan, C.A. (2006). An endogenous peptide signal in *Arabidopsis* activates components of the innate immune response. *PNAS* 103, 10098-10103.

Ichimura, K., Casais, C., Peck, S.C., Shinozaki, K., and Shirasu, K. (2006). MEKK1 is required for MPK4 activation and regulates tissue-specific and temperature-dependent cell death in *Arabidopsis*. *J Biol Chem* 281, 36969-36976.

Iizasa, E.i., Mitsutomi, M., and Nagano, Y. (2010). Direct binding of a plant LysM receptor-like kinase, LysM RLK1/CERK1, to chitin *in vitro*. *Journal of Biological Chemistry* 285, 2996-3004.

Inaba, T., Nagano, Y., Nagasaki, T., and Sasaki, Y. (2002). Distinct localization of two closely related Ypt3/Rab11 proteins on the trafficking pathway in higher plants. *Journal of Biological Chemistry* 277, 9183-9188.

Jabs, T., Dietrich, R.A., and Dangl, J.L. (1996). Initiation of runaway cell death in an *Arabidopsis* mutant by extracellular superoxide. *Science* 273, 1853-1856.

Jacob, Y., Feng, S., LeBlanc, C.A., Bernatavichute, Y.V., Stroud, H., Cokus, S., Johnson, L.M., Pellegrini, M., Jacobsen, S.E., and Michaels, S.D. (2009). ATXR5 and ATXR6 are H3K27 monomethyltransferases required for chromatin structure and gene silencing. *Nat Struct Mol Biol* 16, 763-768.

Jacobs, A.K., Lipka, V., Burton, R.A., Panstruga, R., Strizhov, N., Schulze-Lefert, P., and Fincher, G.B. (2003). An *Arabidopsis* callose synthase, GSL5, is required for wound and papillary callose formation. *Plant Cell* 15, 2503-2513.

Janeway, C.A. (1989). Approaching the asymptote? Evolution and revolution in immunology. *Cold Spring Harb. Symp. Quant. Biol.* 54, 1-13.

Janeway, C.A., and Medzhitov, R. (2002). Innate immune recognition. *Annual Review of Immunology* 20, 197-216.

Janjusevic, R., Abramovitch, R.B., Martin, G.B., and Stebbins, C.E. (2006). A bacterial inhibitor of host programmed cell death defenses is an E3 ubiquitin ligase. *Science* 311, 222-226.

Jarosch, E., Taxis, C., Volkwein, C., Bordallo, J., Finley, D., Wolf, D.H., and Sommer, T. (2002). Protein dislocation from the ER requires polyubiquitination and the AAA-ATPase Cdc48. *Nat Cell Biol* 4, 134-139.

Jasinski, M., Stukkens, Y., Degand, H., Purnelle, B., Marchand-Brynaert, J., and Boutry, M. (2001). A plant plasma membrane ATP binding cassette-type transporter is involved in antifungal terpenoid secretion. *Plant Cell* 13, 1095-1107.

Jeong, S., Trotochaud, A.E., and Clark, S.E. (1999). The *Arabidopsis* CLAVATA2 gene encodes a receptor-like protein required for the stability of the CLAVATA1 receptor-like kinase. *Plant Cell* 11, 1925-1934.

Jeong, Y.J., Yun, S.; Kim, B.H.; Kim, S.Y.; Song, J.H.; Lee, J.S.; Lee, M.M.; Li, J. and Nam, K-H. (2010). BAK7 displays unequal genetic redundancy with BAK1 in brassinosteroid signaling and early senescence in *Arabidopsis*. *Molecules and Cells* 29, 259-266.

Jeworutzki, E., Roelfsema, M.R.G., Anschütz, U., Krol, E., Elzenga, J.T.M., Felix, G., Boller, T., Hedrich, R., and Becker, D. (2010). Early signaling through the *Arabidopsis* pattern recognition receptors FLS2 and EFR involves  $\text{Ca}^{2+}$ -associated opening of plasma membrane anion channels. *Plant J* 62, 367-378.

Jia, Y., McAdams, S.A., Bryan, G.T., Hershey, H.P., and Valent, B. (2000). Direct interaction of resistance gene and avirulence gene products confers rice blast resistance. *EMBO J* 19, 4004.

Jin, H., Yan, Z., Nam, K.H., and Li, J. (2007). Allele-specific suppression of a defective brassinosteroid receptor reveals a physiological role of UGGT in ER quality control. *Molecular Cell* 26, 821-830.

Jin, H., Hong, Z., Su, W., and Li, J. (2009a). A plant-specific calreticulin is a key retention factor for a defective brassinosteroid receptor in the endoplasmic reticulum. *PNAS* 106, 13612-13617.

Jin, Y., Zhuang, M., and Hendershot, L.M. (2009b). ERdj3, a luminal ER DnaJ homologue, binds directly to unfolded proteins in the mammalian ER: identification of critical residues. *Biochemistry* 48, 41-49.

Jin, Y., Awad, W., Petrova, K., and Hendershot, L.M. (2008). Regulated release of ERdj3 from unfolded proteins by BiP. *Embo J* 27, 2873-2882.

Jirage, D., Zhou, N., Cooper, B., Clarke, J.D., Dong, X., and Glazebrook, J. (2001). Constitutive salicylic acid-dependent signaling in *cpr1* and *cpr6* mutants requires PAD4. *Plant J* 26, 395-407.

Johnson, C., Boden, E., and Arias, J. (2003). Salicylic acid and NPR1 induce the recruitment of trans-activating TGA factors to a defense gene promoter in *Arabidopsis*. *Plant Cell* 15, 1846-1858.

Johnson, L.N., Noble, M.E.M., and Owen, D.J. (1996). Active and inactive protein kinases: structural basis for regulation. *Cell* 85, 149-158.

Johnson, R.S., Martin, S.A., Biemann, K., Stults, J.T., and Watson, J.T. (1987). Novel fragmentation process of peptides by collision-induced decomposition in a tandem mass spectrometer: differentiation of leucine and isoleucine. *Analytical Chemistry* 59, 2621-2625.

Jones, D.A., Thomas, C.M., Hammond-Kosack, K.E., Balint-Kurti, P.J., and Jones, J.D. (1994). Isolation of the tomato *Cf-9* gene for resistance to *Cladosporium fulvum* by transposon tagging. *Science* 266, 789-793.

Jones, J.D., and Dangl, J.L. (2006). The plant immune system. *Nature* 444, 323-329.

Jourdan, E., Henry, G., Duby, F., Dommes, J., Barthélemy, J.P., Thonart, P., and Ongena, M. (2009). Insights into the defense-related events occurring in plant cells following perception of surfactin-type lipopeptide from *Bacillus subtilis*. *MPMI* 22, 456-468.

Journot-Catalino, N., Somssich, I.E., Roby, D., and Kroj, T. (2006). The transcription factors WRKY11 and WRKY17 act as negative regulators of basal resistance in *Arabidopsis thaliana*. *Plant Cell* 18, 3289-3302.

Jura, N., Endres, N.F., Engel, K., Deindl, S., Das, R., Lamers, M.H., Wemmer, D.E., Zhang, X., and Kuriyan, J. (2009). Mechanism for activation of the EGF receptor catalytic domain by the juxtamembrane segment. *Cell* 137, 1293-1307.

Kadota, Y., Amigues, B., Ducassou, L., Madaoui, H., Ochsenbein, F., Guerois, R., and Shirasu, K. (2008). Structural and functional analysis of SGT1-HSP90 core complex required for innate immunity in plants. *EMBO Rep* 9, 1209-1215.

Kaku, H., Nishizawa, Y., Ishii-Minami, N., Akimoto-Tomiyama, C., Dohmae, N., Takio, K., Minami, E., and Shibuya, N. (2006). Plant cells recognize chitin fragments for defense signaling through a plasma membrane receptor. *PNAS* 103, 11086-11091.

Kanemaki, M., Kurokawa, Y., Matsu-ura, T., Makino, Y., Masani, A., Okazaki, K.-i., Morishita, T., and Tamura, T.-a. (1999). TIP49b, a new RuvB-like DNA helicase, is included in a complex together with another RuvB-like DNA helicase, TIP49a. *Journal of Biological Chemistry* 274, 22437-22444.

Kanemaki, M., Makino, Y., Yoshida, T., Kishimoto, T., Koga, A., Yamamoto, K., Yamamoto, M., Moncollin, V., Egly, J.-M., Muramatsu, M., and Tamura, T.-a. (1997). Molecular cloning of a rat 49-kDa TBP-interacting protein (TIP49) that is highly homologous to the bacterial RuvB. *Biochemical and Biophysical Research Communications* 235, 64-68.

Kang, H.-G., Kuhl, J.C., Kachroo, P., and Klessig, D.F. (2008). CRT1, an Arabidopsis ATPase that interacts with diverse resistance proteins and modulates disease resistance to turnip crinkle virus. *Cell Host & Microbe* 3, 48-57.

Kang, H.-G., Oh, C.-S., Sato, M., Katagiri, F., Glazebrook, J., Takahashi, H., Kachroo, P., Martin, G.B., and Klessig, D.F. (2010). Endosome-associated crt1 functions early in resistance gene-mediated defense signaling in Arabidopsis and tobacco. *Plant Cell* 22, 918-936.

Kang, J.-G., Yun, J., Kim, D.-H., Chung, K.-S., Fujioka, S., Kim, J.-I., Dae, H.-W., Yoshida, S., Takatsuto, S., Song, P.-S., and Park, C.-M. (2001). Light and brassinosteroid signals are integrated via a dark-induced small g protein in etiolated seedling growth. *Cell* 105, 625-636.

Karlova, R., Boeren, S., Russinova, E., Aker, J., Vervoort, J., and de Vries, S. (2006). The Arabidopsis SOMATIC EMBRYOGENESIS RECEPTOR-LIKE KINASE1 protein complex includes BRASSINOSTEROID-INSENSITIVE1. *Plant Cell* 18, 626-638.

Karlova, R., Boeren, S., van Dongen, W., Kwaaitaal, M., Aker, J., Vervoort, J., and de Vries, S.C. (2009). Identification of *in vitro* phosphorylation sites in the *Arabidopsis thaliana* somatic embryogenesis receptor-like kinases. *Proteomics* 9, 368-379.

Kaschani, F., Shabab, M., Bozkurt, T., Shindo, T., Schornack, S., Gu, C., Ilyas, M., Win, J., Kamoun, S., and van der Hoorn, R.A.L. (2010). An effector-targeted protease contributes to defense against *Phytophthora infestans* and is under diversifying selection in natural hosts. *Plant Physiol.*, pp.110.158030.

Katagiri, F., and Tsuda, K. (2010). Understanding the plant immune system. *MPMI* xx.

Katiyar-Agarwal, S., Gao, S., Vivian-Smith, A., and Jin, H. (2007). A novel class of bacteria-induced small RNAs in Arabidopsis. *Genes Dev* 21, 3123-3134.

Katiyar-Agarwal, S., Morgan, R., Dahlbeck, D., Borsani, O., Villegas, A., Jr., Zhu, J.K., Staskawicz, B.J., and Jin, H. (2006). A pathogen-inducible endogenous siRNA in plant immunity. *PNAS* 103, 18002-18007.

Katsir, L., Schilmiller, A.L., Staswick, P.E., He, S.Y., and Howe, G.A. (2008). COI1 is a critical component of a receptor for jasmonate and the bacterial virulence factor coronatine. *PNAS* 105, 7100-7105.

Kawasaki, T., Nam, J., Boyes, D.C., Holt, B.F., Hubert, D.A., Wiig, A., and Dangl, J.L. (2005). A duplicated pair of Arabidopsis RING-finger E3 ligases contribute to the RPM1- and RPS2-mediated hypersensitive response. *Plant J* 44, 258-270.

Kawchuk, L.M., Hachey, J., Lynch, D.R., Kulcsar, F., van Rooijen, G., Waterer, D.R., Robertson, A., Kokko, E., Byers, R., Howard, R.J., Fischer, R., and Prüfer, D. (2001). Tomato Ve disease resistance genes encode cell surface-like receptors. *PNAS* 98, 6511-6515.

Kay, S., Hahn, S., Marois, E., Hause, G., and Bonas, U. (2007). A bacterial effector acts as a plant transcription factor and induces a cell size regulator. *Science* 318, 648-651.

Keen, N.T., Partridge, J.E., and Zaki, A. (1972). Pathogen-produced elicitor of a chemical defense mechanism in soybean monogenically resistant to *Phytophthora megasperma* var. *sojae*. *Phytopathology* 62, 768.

Keinath, N.F., Kierszniowska, S., Lorek, J., Bourdais, G., Kessler, S.A., Asano, H., Grossniklaus, U., Schulze, W., Robatzek, S., and Panstruga, R. (2010). PAMP-induced changes in plasma membrane compartmentalization reveal novel components of plant immunity. *Journal of Biological Chemistry*.

Keller, T., Damude, H.G., Werner, D., Doerner, P., Dixon, R.A., and Lamb, C. (1998). A plant homolog of the neutrophil NADPH oxidase gp91phox subunit gene encodes a plasma membrane protein with  $\text{Ca}^{2+}$  binding motifs. *Plant Cell* 10, 255-266.

Kemmerling, B., Schwedt, A., Rodriguez, P., Mazzotta, S., Frank, M., Qamar, S.A., Mengiste, T., Betsuyaku, S., Parker, J.E., Mussig, C., Thomma, B.P., Albrecht, C., de Vries, S.C., Hirt, H., and Nürnberg, T. (2007). The BRI1-associated kinase 1, BAK1, has a brassinolide-independent role in plant cell-death control. *Curr Biol* 17, 1116-1122.

Khan, M.A.S., Kang, J., and Steiner, T.S. (2004). Enteroaggregative *Escherichia coli* flagellin-induced interleukin-8 secretion requires Toll-like receptor 5-dependent p38 MAP kinase activation. *Immunology* 112, 651-660.

Khush, G.S., Bacalangco, E., and Ogawa, T. (1990). A new gene for resistance to bacterial blight from *O. longistaminata*. *Rice Genetics Newsletter* 7, 121-122.

Kieber, J.J., Rothenberg, M., Roman, G., Feldmann, K.A., and Ecker, J.R. (1993). CTR1, a negative regulator of the ethylene response pathway in *Arabidopsis*, encodes a member of the Raf family of protein kinases. *Cell* 72, 427-441.

Kierszniowska, S., Seiwert, B., and Schulze, W.X. (2009). Definition of *Arabidopsis* sterol-rich membrane microdomains by differential treatment with methyl-cyclodextrin and quantitative proteomics. *Molecular & Cellular Proteomics* 8, 612-623.

Kim, H.S., Jung, M.S., Lee, S.M., Kim, K.E., Byun, H., Choi, M.S., Park, H.C., Cho, M.J., and Chung, W.S. (2009a). An S-locus receptor-like kinase plays a role as a negative regulator in plant defense responses. *Biochemical and Biophysical Research Communications* 381, 424-428.

Kim, M.G., Geng, X., Lee, S.Y., and Mackey, D. (2009b). The *Pseudomonas syringae* type III effector AvrRpm1 induces significant defenses by activating the *Arabidopsis* nucleotide-binding leucine-rich repeat protein RPS2. *Plant J* 57, 645-653.

Kim, T.-W., Guan, S., Sun, Y., Deng, Z., Tang, W., Shang, J.-X., Sun, Y., Burlingame, A.L., and Wang, Z.-Y. (2009c). Brassinosteroid signal transduction from cell-surface receptor kinases to nuclear transcription factors. *Nat Cell Biol* 11, 1254-1260.

Kim, J.S., Jung, H.J., Lee, H.J., Kim, K.A., Goh, C.H., Woo, Y., Oh, S.H., Han, Y.S., and Kang, H. (2008a). Glycine-rich RNA-binding protein7 affects abiotic stress responses by regulating stomata opening and closing in *Arabidopsis thaliana*. *Plant J* 55, 455-466.

Kim, K.-C., Lai, Z., Fan, B., and Chen, Z. (2008b). Arabidopsis WRKY38 and WRKY62 transcription factors interact with histone Deacetylase 19 in basal defense. *Plant Cell* 20, 2357-2371.

Kim, H.-S., Desveaux, D., Singer, A.U., Patel, P., Sondek, J., and Dangl, J.L. (2005a). The *Pseudomonas syringae* effector AvrRpt2 cleaves its C-terminally acylated target, RIN4, from Arabidopsis membranes to block RPM1 activation. *Proc Natl Acad Sci U S A* 102, 6496-6501.

Kim, M.G., da Cunha, L., McFall, A.J., Belkhadir, Y., and DebRoy, S. (2005b). Two *Pseudomonas syringae* type III effectors inhibit RIN4-regulated basal defense in Arabidopsis. *Cell* 121, 749.

Kim, M.G., da Cunha, L., McFall, A.J., Belkhadir, Y., DebRoy, S., Dangl, J.L., and Mackey, D. (2005c). Two *Pseudomonas syringae* type III effectors inhibit RIN4-regulated basal defense in Arabidopsis. *Cell* 121, 749-759.

Kinkema, M., Fan, W., and Dong, X. (2000). Nuclear localization of NPR1 is required for activation of *PR* gene expression. *Plant Cell* 12, 2339-2350.

Kinoshita, T., Cano-Delgado, A., Seto, H., Hiranuma, S., Fujioka, S., Yoshida, S., and Chory, J. (2005). Binding of brassinosteroids to the extracellular domain of plant receptor kinase BRI1. *Nature* 433, 167-171.

Kishimoto, K., Kouzai, Y., Kaku, H., Shibuya, N., Minami, E., and Nishizawa, Y. (2010). Perception of the chitin oligosaccharides contributes to disease resistance to blast fungus *Magnaporthe oryzae* in rice. *Plant J*, no-no.

Kitagawa, K., Skowyra, D., Elledge, S.J., Harper, J.W., and Hieter, P. (1999). SGT1 encodes an essential component of the yeast kinetochore assembly pathway and a novel subunit of the SCF ubiquitin ligase complex. *Mol Cell* 4, 21-33.

Kobae, Y., Sekino, T., Yoshioka, H., Nakagawa, T., Martinoia, E., and Maeshima, M. (2006). Loss of AtPDR8, a plasma membrane ABC transporter of *Arabidopsis thaliana*, causes hypersensitive cell death upon pathogen infection. *Plant Cell Physiol* 47, 309-318.

Kobayashi, M., Ohura, I., Kawakita, K., Yokota, N., Fujiwara, M., Shimamoto, K., Doke, N., and Yoshioka, H. (2007). Calcium-dependent protein kinases regulate the production of reactive oxygen species by potato NADPH oxidase. *Plant Cell* 19, 1065-1080.

Koiba, H., Li, F., McCully, M.G., Mendoza, I., Koizumi, N., Manabe, Y., Nakagawa, Y., Zhu, J., Rus, A., Pardo, J.M., Bressan, R.A., and Hasegawa, P.M. (2003). The STT3a subunit isoform of the *Arabidopsis* oligosaccharyltransferase controls adaptive responses to salt/osmotic stress. *Plant Cell* 15, 2273-2284.

Koornneef, A., and Pieterse, C.M.J. (2008). Cross talk in defense signaling. *Plant Physiol.* 146, 839-844.

Korasick, D.A., McMichael, C., Walker, K.A., Anderson, J.C., Bednarek, S.Y., and Heese, A. (2010). Novel functions of stomatal cytokinesis-defective 1 (SCD1) in innate immune responses against bacteria. *Journal of Biological Chemistry* 285, 23342-23350.

Krasileva, K.V., Dahlbeck, D., and Staskawicz, B.J. (2010). Activation of an *Arabidopsis* resistance protein is specified by the in planta association of its leucine-rich repeat domain with the cognate oomycete effector. *Plant Cell* 22, 2444-2458.

Krol, E., Mentzel, T., Chinchilla, D., Boller, T., Felix, G., Kemmerling, B., Postel, S., Arents, M., Jeworutzki, E., Al-Rasheid, K.A.S., Becker, D., and Hedrich, R. (2010). Perception of the *Arabidopsis* danger signal peptide 1 involves the pattern recognition receptor AtPEPR1 and its close homologue AtPEPR2. *Journal of Biological Chemistry* 285, 13471-13479.

Kudla, J., Batistic, O., and Hashimoto, K. (2010). Calcium signals: the lead currency of plant information processing. *Plant Cell* 22, 541-563.

Kunkel, B.N., Bent, A.F., Dahlbeck, D., Innes, R.W., and Staskawicz, B.J. (1993). RPS2, an *Arabidopsis* disease resistance locus specifying recognition of *Pseudomonas syringae* strains expressing the avirulence gene *avrRpt2*. *Plant Cell* 5, 865-875.

Kunze, G., Zipfel, C., Robatzek, S., Niehaus, K., Boller, T., and Felix, G. (2004). The N terminus of bacterial elongation factor Tu elicits innate immunity in *Arabidopsis* plants. *Plant Cell* 16, 3496-3507.

Kvitko, B.H., Ramos, A.R., Morello, J.E., Oh, H.-S., and Collmer, A. (2007). Identification of harpins in *Pseudomonas syringae* pv. *tomato* DC3000, which are functionally similar to HrpK1 in promoting translocation of type III secretion system effectors. *J. Bacteriol.* 189, 8059-8072.

Lacombe, S., Rougon-Cardoso, A., Sherwood, E., Peeters, N., Dahlbeck, D., van Esse, H.P., Smoker, M., Rallapalli, G., Thomma, B.P.H.J., Staskawicz, B., Jones, J.D.G.,

and Zipfel, C. (2010). Interfamily transfer of a plant pattern-recognition receptor confers broad-spectrum bacterial resistance. *Nat Biotech* 28, 365-369.

Lan, L., Deng, X., Zhou, J., and Tang, X. (2006). Genome-Wide Gene Expression Analysis of *Pseudomonas syringae* pv. *tomato* DC3000 reveals overlapping and distinct pathways regulated by *hrpL* and *hrpRS*. *MPMI* 19, 976-987.

Lecourieux, D., Lamotte, O., Bourque, S., Wendehenne, D., and Mazars, C. (2005). Proteinaceous and oligosaccharidic elicitors induce different calcium signatures in the nucleus of tobacco cells. *Cell Calcium* 38, 527.

Lee, M., Lee, K., Lee, J., Noh, E.W., and Lee, Y. (2005). AtPDR12 contributes to lead resistance in *Arabidopsis*. *Plant Physiol* 138, 827-836.

Lee, M.W., Jelenska, J., and Greenberg, J.T. (2008). *Arabidopsis* proteins important for modulating defense responses to *Pseudomonas syringae* that secrete HopW1-1. *Plant J* 54, 452-465.

Lee, S.W., Han, S.W., Sririanum, M., Park, C.J., Seo, Y.S., and Ronald, P.C. (2009). A type I-secreted, sulfated peptide triggers XA21-mediated innate immunity. *Science* 326, 850 - 824.

Lee, T.-F., and McNellis, T. (2009). Evidence that the BONZAI1/COPINE1 protein is a calcium- and pathogen-responsive defense suppressor. *Plant Molecular Biology* 69, 155-166.

Lee, Y.T., Jacob, J., Michowski, W., Nowotny, M., Kuznicki, J., and Chazin, W.J. (2004). Human Sgt1 binds HSP90 through the CHORD-Sgt1 domain and not the tetratricopeptide repeat domain. *J Biol Chem* 279, 16511-16517.

Lehmann, W.D., Knöger, R., Salek, M., Hung, C.-W., Wolschin, F., and Weckwerth, W. (2007). Neutral loss-based phosphopeptide recognition: a collection of caveats. *Journal of Proteome Research* 6, 2866-2873.

Lehti-Shiu, M.D., Zou, C., Hanada, K., and Shiu, S.H. (2009). Evolutionary history and stress regulation of plant receptor-like kinase/pelle genes. *Plant Physiol* 150, 12 - 26.

Leister, R.T., Dahlbeck, D., Day, B., Li, Y., Chesnokova, O., and Staskawicz, B.J. (2005). Molecular genetic evidence for the role of SGT1 in the intramolecular complementation of Bs2 protein activity in *Nicotiana benthamiana*. *Plant Cell* 17, 1268-1278.

Lemmon, M.A., and Schlessinger, J. (2010). Cell signaling by receptor tyrosine kinases. *Cell* 141, 1117-1134.

Leon-Reyes, A., Van der Does, D., De Lange, E., Delker, C., Wasternack, C., Van Wees, S., Ritsema, T., and Pieterse, C. (2010). Salicylate-mediated suppression of

jasmonate-responsive gene expression in *Arabidopsis* is targeted downstream of the jasmonate biosynthesis pathway. *Planta* 32, 1423-1432.

Lerouxel, O., Mouille, G., Andème-Onzighi, C., Bruyant, M.P., Séveno, M., Loutelier-Bourhis, C., Driouich, A., Höfte, H., and Lerouge, P. (2005). Mutants in DEFECTIVE GLYCOSYLATION, an *Arabidopsis* homolog of an oligosaccharyltransferase complex subunit, show protein underglycosylation and defects in cell differentiation and growth. *Plant J* 42, 455-468.

Lewis, M.W., Leslie, M.E., Fulcher, E.H., Darnielle, L., Healy, P.N., Youn, J.Y., and Liljegren, S.J. (2010). The SERK1 receptor-like kinase regulates organ separation in *Arabidopsis* flowers. *Plant J* 62 817-828

Li, J. (2010). Multi-tasking of somatic embryogenesis receptor-like protein kinases. *Current Opinion in Plant Biology* In Press, Corrected Proof.

Li, Y., Tessaro, M.J., Li, X., and Zhang, Y. (2010a). Regulation of the expression of plant resistance gene *SNC1* by a protein with a conserved BAT2 domain. *Plant Physiol.* 153, 1425-1434.

Li, Y., Zhang, Q., Zhang, J., Wu, L., Qi, Y., and Zhou, J.-M. (2010b). Identification of microRNAs involved in pathogen-associated molecular pattern-triggered plant innate immunity. *Plant Physiol.* 152, 2222-2231.

Li, J., Zhao-Hui, C., Batoux, M., Nekrasov, V., Roux, M., Chinchilla, D., Zipfel, C., and Jones, J.D.G. (2009a). Specific ER quality control components required for biogenesis of the plant innate immune receptor EFR. *PNAS* 106, 15973-15978.

Li, Y., Pennington, B.O., and Hua, J. (2009b). Multiple *R*-Like Genes Are Negatively Regulated by BON1 and BON3 in *Arabidopsis*. *MPMI* 22, 840-848.

Li, H., Xu, H., Zhou, Y., Zhang, J., Long, C., Li, S., Chen, S., Zhou, J.M., and Shao, F. (2007). The phosphothreonine lyase activity of a bacterial type III effector family. *Science* 315, 1000-1003.

Li, J., Brader, G., Kariola, T., and Tatio Palva, E. (2006). WRKY70 modulates the selection of signaling pathways in plant defense. *Plant J* 46, 477-491.

Li, X., Lin, H., Zhang, W., Zou, Y., Zhang, J., Tang, X., and Zhou, J.M. (2005). Flagellin induces innate immunity in nonhost interactions that is suppressed by *Pseudomonas syringae* effectors. *Proc Natl Acad Sci U S A* 102, 12990-12995.

Li, J., Brader, G., and Palva, E.T. (2004). The WRKY70 transcription factor: a node of convergence for jasmonate-mediated and salicylate-mediated signals in plant defense. *Plant Cell* 16, 319-331.

Li, J., Wen, J., Lease, K.A., Doke, J.T., Tax, F.E., and Walker, J.C. (2002). BAK1, an *Arabidopsis* LRR receptor-like protein kinase, interacts with BRI1 and modulates brassinosteroid signaling. *Cell* 110, 213-222.

Li, X., Clarke, J.D., Zhang, Y., and Dong, X. (2001). Activation of an EDS1-mediated *R*-gene pathway in the *snc1* mutant leads to constitutive, NPR1-independent pathogen resistance. *Mol Plant Microbe Interact* 14, 1131 - 1139.

Li-Beisson, Y., Shorrosh, B., Beisson, F., Andersson, M., Aronidel, V., Bates, P., Baud, S., Bird, D., DeBono, A., Durrett, T., Franke, R., Graham, I., Katayama, K., Kelly, A., Larson, T., Markham, J., Miquel, M., Molina, I., Nishida, I., Rowland, O., Samuels, L., Schmid, K., Wada, H., Welti, R., Xu, C., Zallot, R., and J., O. (2010). Acyl-Lipid Metabolism In The *Arabidopsis* Book. Rockville, MD: American Society of Plant Biologists.

Liang, H., Yao, N., and Song, J.T. (2003). Ceramides modulate programmed cell death in plants. *Genes Dev* 17, 2636-2641.

Lieberherr, D., Thao, N.P., Nakashima, A., Umemura, K., Kawasaki, T., and Shimamoto, K. (2005). A sphingolipid elicitor-inducible mitogen-activated protein kinase is regulated by the small gtpase osract1 and heterotrimeric G-protein in rice. *Plant Physiol.* 138, 1644-1652.

Lightfield, K.L., Persson, J., Brubaker, S.W., Witte, C.E., von Moltke, J., Dunipace, E.A., Henry, T., Sun, Y.-H., Cado, D., Dietrich, W.F., Monack, D.M., Tsolis, R.M., and Vance, R.E. (2008). Critical function for Naip5 in inflammasome activation by a conserved carboxy-terminal domain of flagellin. *Nat Immunol* 9, 1171-1178.

Lin, N.-C., and Martin, G.B. (2005). An *avrPto/avrPtoB* mutant of *Pseudomonas syringae* pv. *tomato* DC3000 does not elicit pto-mediated resistance and is less virulent on tomato. *MPMI* 18, 43-51.

Lin, Z., Zhong, S., and Grierson, D. (2009). Recent advances in ethylene research. *Journal of Experimental Botany* 60, 3311-3336.

Liu, G.-Z., Pi, L.-Y., Walker, J.C., Ronald, P.C., and Song, W.-Y. (2002). Biochemical characterization of the kinase domain of the rice disease resistance receptor-like kinase Xa21. *Journal of Biological Chemistry* 277, 20264-20269.

Liu, J., Elmore, J.M., Fuglsang, A.T., Palmgren, M.G., Staskawicz, B.J., and Coaker, G. (2009). RIN4 functions with plasma membrane H<sup>+</sup>-ATPases to regulate stomatal apertures during pathogen attack. *PLoS Biol* 7, e1000139.

Liu, Y., and Zhang, S. (2004). Phosphorylation of 1-aminocyclopropane-1-carboxylic acid synthase by MPK6, a stress-responsive mitogen-activated protein kinase, induces ethylene biosynthesis in *Arabidopsis*. *The Plant cell* 16, 3386-3399.

Liu, Y., Burch-Smith, T., Schiff, M., Feng, S., and Dinesh-Kumar, S.P. (2004). Molecular chaperone Hsp90 associates with resistance protein N and Its signaling proteins SGT1 and Rar1 to modulate an innate immune response in plants. *Journal of Biological Chemistry* 279, 2101-2108.

Lu, D., Wu, S., Gao, X., Zhang, Y., Shan, L., and He, P. (2010). A receptor-like cytoplasmic kinase, BIK1, associates with a flagellin receptor complex to initiate plant innate immunity. *PNAS* 107, 496-501.

Lu, X., Tintor, N., Mentzel, T., Kombrink, E., Boller, T., Robatzek, S., Schulze-Lefert, P., and Saijo, Y. (2009). Uncoupling of sustained MAMP receptor signaling from early outputs in an *Arabidopsis* endoplasmic reticulum glucosidase II allele. *PNAS* 106, 22522-22527.

Luan, S., Lan, W., and Chul Lee, S. (2009). Potassium nutrition, sodium toxicity, and calcium signaling: connections through the CBL-CIPK network. *Current Opinion in Plant Biology* 12, 339-346.

Lukasik, E., and Takken, F.L.W. (2009). STANDING strong, resistance proteins instigators of plant defense. *Current Opinion in Plant Biology* 12, 427-436.

Lumbreras, V., Vilela, B., Irar, S., Solé, M., Capellades, M., Valls, M., Coca, M., and Pagès, M. (2010). MAPK phosphatase MKP2 mediates disease responses in *Arabidopsis* and functionally interacts with MPK3 and MPK6. *Plant J.* no-no.

Luo, Y., Caldwell, K.S., Wroblewski, T., Wright, M.E., and Michelmore, R.W. (2009). Proteolysis of a negative regulator of innate immunity is dependent on resistance genes in tomato and *Nicotiana benthamiana* and induced by multiple bacterial effectors. *Plant Cell* 21, 2458-2472.

Ma, W., and Berkowitz, G.A. (2007). The grateful dead: calcium and cell death in plant innate immunity. *Cell Microbiol* 9, 2571-2585.

Ma, W., Smiegel, A., Verma, R., and Berkowitz, G.A. (2009). Cyclic nucleotidegated channels and related signaling components in plant innate immunity. *Plant Signal Behav* 4, 272 - 282.

Ma, W., Smigel, A., Tsai, Y.-C., Braam, J., and Berkowitz, G.A. (2008). Innate immunity signaling: cytosolic  $Ca^{2+}$  elevation is linked to downstream nitric oxide generation through the action of calmodulin or a calmodulin-like protein. *Plant Physiol.* 148, 818-828.

Mackey, D., Holt, B.F., 3rd, Wiig, A., and Dangl, J.L. (2002). RIN4 interacts with *Pseudomonas syringae* type III effector molecules and is required for RPM1-mediated resistance in *Arabidopsis*. *Cell* 108, 743-754.

Mackey, D., Belkhadir, Y., Alonso, J.M., Ecker, J.R., and Dangl, J.L. (2003). *Arabidopsis* RIN4 Is a target of the type III virulence effector AvrRpt2 and modulates RPS2-mediated resistance. *Cell* 112, 379-389.

Maga, G., and Hubscher, U. (2003). Proliferating cell nuclear antigen (PCNA): a dancer with many partners. *J Cell Sci* 116, 3051-3060.

Malinovsky, F.G., Brodersen, P., Fiil, B.K., McKinney, L.V., Thorgrimsen, S., Beck, M., Nielsen, H.B.r., Pietra, S., Zipfel, C., Robatzek, S., Petersen, M., Hofius, D., and Mundy, J. (2010). Lazarus1, a DUF300 protein, contributes to programmed cell death associated with *Arabidopsis acd11* and the hypersensitive response. *PLoS ONE* 5, e12586.

Malinowski, R., Higgins, R., Luo, Y., Piper, L., Nazir, A., Bajwa, V., Clouse, S., Thompson, P., and Stratmann, J. (2009). The tomato brassinosteroid receptor BRI1 increases binding of systemin to tobacco plasma membranes, but is not involved in systemin signaling. *Plant Molecular Biology* 70, 603-616.

Marmor, M.D., and Yarden, Y. (2010). Role of protein ubiquitylation in regulating endocytosis of receptor tyrosine kinases. *Oncogene* 23, 2057-2070.

Marti, L., Fornaciari, S., Renna, L., Stefano, G., and Brandizzi, F. (2010). COPII-mediated traffic in plants. *Trends in Plant Science* 15, 522-528.

Martin, G.B., Brommonschenkel, S.H., Chunwongse, J., Frary, A., Ganal, M.W., Spivey, R., Wu, T., Earle, E.D., and Tanksley, S.D. (1993). Map-based cloning of a protein kinase gene conferring disease resistance in tomato. *Science* 262, 1432-1436.

Martinon, F., Burns, K., and Tschoopp, J.r. (2002). The inflammasome: a molecular platform triggering activation of inflammatory caspases and processing of proIL- $\beta$ . *Mol Cell* 10, 417-426.

Matsui, H., Yamazaki, M., Kishi-Kaboshi, M., Takahashi, A., and Hirochika, H. (2010). AGC kinase OsOxi1 positively regulates basal resistance through suppression of OsPti1a-mediated negative regulation. *Plant and Cell Physiology*.

Matsuzawa, A., Saegusa, K., Noguchi, T., Sadamitsu, C., Nishitoh, H., Nagai, S., Koyasu, S., Matsumoto, K., Takeda, K., and Ichijo, H. (2005). ROS-dependent activation of the TRAF6-ASK1-p38 pathway is selectively required for TLR4-mediated innate immunity. *Nat Immunol* 6, 587-592.

Matzinger, P. (2002). The danger model: a renewed sense of self. *Science* 296, 301-305.

Mayor, A., Martinon, F., De Smedt, T., Petrilli, V., and Tschoopp, J. (2007). A crucial function of SGT1 and HSP90 in inflammasome activity links mammalian and plant innate immune responses. *Nat Immunol* 8, 497-503.

McCracken, A.A., and Brodsky, J.L. (1996). Assembly of ER-associated protein degradation *in vitro*: dependence on cytosol, calnexin, and ATP. *The Journal of Cell Biology* 132, 291-298.

McDowell, J.M., and Simon, S.A. (2006). Recent insights into *R* gene evolution. *Molecular Plant Pathology* 7, 437-448.

McDowell, J.M., Williams, S.G., Funderburg, N.T., Eulgem, T., and Dangl, J.L. (2005). Genetic analysis of developmentally regulated resistance to downy mildew (*Hyaloperonospora parasitica*) in *Arabidopsis thaliana*. *MPMI* 18, 1226-1234.

McDowell, J.M., Cuzick, A., Can, C., Beynon, J., Dangl, J.L., and Holub, E.B. (2000). Downy mildew (*Peronospora parasitica*) resistance genes in *Arabidopsis* vary in functional requirements for NDR1, EDS1, NPR1 and salicylic acid accumulation. *Plant J* 22, 523-529.

McSorley, S.J., Ehst, B.D., Yu, Y., and Gewirtz, A.T. (2002). Bacterial flagellin is an effective adjuvant for CD4+ T cells *in vivo*. *J Immunol* 169, 3914-3919.

Medzhitov, R. (2007). Recognition of microorganisms and activation of the immune response. *Nature* 449, 819-826.

Medzhitov, R., Preston-Hurlburt, P., Kopp, E., Stadlen, A., Chen, C., Ghosh, S., and Janeway, C.A. (1998). MyD88 Is an adaptor protein in the hToll/IL-1 receptor family signaling pathways. *Mol Cell* 2, 253-258.

Melotto, M., Underwood, W., Koczan, J., Nomura, K., and He, S.Y. (2006). Plant stomata function in innate immunity against bacterial invasion. *Cell* 126, 969-980.

Melotto, M., Mecey, C., Niu, Y., Chung, H.S., Katsir, L., Yao, J., Zeng, W., Thines, B., Staswick, P., Browse, J., Howe, G., A., and He, S.Y. (2008). A critical role of two positively charged amino acids in the Jas motif of *Arabidopsis* JAZ proteins in mediating coronatine- and jasmonoyl isoleucine-dependent interactions with the COI1 F-box protein. *Plant J* 55, 979-988.

Meng, L., and Feldman, L. (2010). CLE14/CLE20 peptides may interact with CLAVATA2/CORYNE receptor-like kinases to irreversibly inhibit cell division in the root meristem of *Arabidopsis*. *Planta* 232, 1061-1074.

Meng, P.H., Raynaud, C.c., Tcherkez, G., Blanchet, S., Massoud, K., Domenichini, S.v., Henry, Y., Soubigou-Taconnat, L., Lelarge-Trouverie, C., Saindrenan, P., Renou, J.P., and Bergounioux, C. (2009). Crosstalks between myo-inositol metabolism, programmed cell death and basal immunity in *Arabidopsis*. *PLoS ONE* 4, e7364.

Meszaros, T., Helfer, A., Hatzimasoura, E., Magyar, Z., Serazetdinova, L., Rios, G., Bardoczy, V., Teige, M., Koncz, C., Peck, S., and Bögre, L. (2006). The *Arabidopsis* MAP kinase kinase MKK1 participates in defense responses to the bacterial elicitor flagellin. *Plant J* 48, 485-498.

Metraux, J.P., Signer, H., Ryals, J., Ward, E., Wyss-Benz, M., Gaudin, J., Raschdorf, K., Schmid, E., Blum, W., and Inverardi, B. (1990). Increase in salicylic acid at the onset of systemic acquired resistance in cucumber. *Science* 250, 1004-1006.

Meyers, B.C., Kozik, A., Griego, A., Kuang, H., and Michelmore, R.W. (2003). Genome-wide analysis of NBS-LRR-encoding genes in *Arabidopsis*. *Plant Cell* 15, 809 - 834.

Miao, E.A., Alpuche-Aranda, C., Dors, M., Clark, A.E., Bader, M.W., Miller, S.I., and Aderem, A. (2006). Cytoplasmic flagellin activates caspase-1 and secretion of interleukin 1 via Ipaf. *Nat Immunol* 7, 569 - 575

Miller, G., Schlauch, K., Tam, R., Cortes, D., Torres, M.A., Shulaev, V., Dangl, J.L., and Mittler, R. (2009). The plant NADPH oxidase RBOHD mediates rapid systemic signaling in response to diverse stimuli. *Sci Signal* 2, ra45.

Mishina, T.E., and Zeier, J. (2007a). Bacterial non-host resistance: interactions of *Arabidopsis* with non-adapted *Pseudomonas syringae* strains. *Physiologia Plantarum* 131, 448-461.

Mishina, T.E., and Zeier, J. (2007b). Pathogen-associated molecular pattern recognition rather than development of tissue necrosis contributes to bacterial induction of systemic acquired resistance in *Arabidopsis*. *Plant J* 50, 500-513.

Miya, A., Albert, P., Shinya, T., Desaki, Y., Ichimura, K., Shirasu, K., Narusaka, Y., Kawakami, N., Kaku, H., and Shibuya, N. (2007). CERK1, a LysM receptor kinase, is essential for chitin elicitor signaling in *Arabidopsis*. *PNAS* 104, 19613-19618.

Molina-Torres, J., García-Chávez, A., and Ramírez-Chávez, E. (1999). Antimicrobial properties of alkamides present in flavouring plants traditionally used in Mesoamerica: affinin and capsaicin. *Journal of Ethnopharmacology* 64, 241-248.

Monaghan, J., Xu, F., Gao, M., Zhao, Q., Palma, K., Long, C., Chen, S., Zhang, Y., and Li, X. (2009). Two Prp19-like U-box proteins in the MOS4-associated complex play redundant roles in plant innate immunity. *PLoS Pathog* 5, e1000526.

Mongrand, S.b., Morel, J., Laroche, J., Claverol, S.p., Carde, J.-P., Hartmann, M.-A.e., Bonneau, M., Simon-Plas, F.o., Lessire, R., and Bessoule, J.-J. (2004). Lipid rafts in higher plant cells. *Journal of Biological Chemistry* 279, 36277-36286.

Moors, M.A., Li, L., and Mizel, S.B. (2001). Activation of interleukin-1 receptor-associated kinase by gram-negative flagellin. *Infect Immun* 69, 4424 - 4429.

Morel, J., Claverol, S.P., Mongrand, S.B., Furt, F., Fromentin, J., Bessoule, J.-J., Blein, J.-P., and Simon-Plas, F. (2006). Proteomics of plant detergent-resistant membranes. *Molecular & Cellular Proteomics* 5, 1396-1411.

Morel, J.B., and Dangl, J.L. (1997). The hypersensitive response and the induction of cell death in plants. *Cell Death Differ* 4, 671-683.

Moscou, M.J., and Bogdanove, A.J. (2009). A simple cipher governs DNA recognition by TAL effectors. *Science* 326, 1501-.

Mou, Z., Fan, W., and Dong, X. (2003). Inducers of plant systemic acquired resistance regulate NPR1 function through redox changes. *Cell* 113, 935-944.

Moynagh, P.N. (2009). The Pellino family: IRAK E3 ligases with emerging roles in innate immune signaling. *Trends in immunology* 30, 33-42.

Mucyn, T.S., Clemente, A., Andriotis, V.M., Balmuth, A.L., Oldroyd, G.E., Staskawicz, B.J., and Rathjen, J.P. (2006). The tomato NBARC-LRR protein Prf interacts with Pto kinase *in vivo* to regulate specific plant immunity. *Plant Cell* 18, 2792-2806.

Müller, J., Piffanelli, P., Devoto, A., Miklis, M., Elliott, C., Ortmann, B., Schulze-Lefert, P., and Panstruga, R. (2005). Conserved ERAD-like quality control of a plant polytopic membrane protein. *Plant Cell* 17, 149-163.

Muller, R., Bleckmann, A., and Simon, R. (2008). The receptor kinase CORYNE of *Arabidopsis* transmits the stem cell-limiting signal CLAVATA3 independently of CLAVATA1. *Plant Cell* 20, 934-946.

Münch, S., Lingner, U., Floss, D.S., Ludwig, N., Sauer, N., and Deising, H.B. (2008). The hemibiotrophic lifestyle of *Colletotrichum* species. *Journal of Plant Physiology* 165, 41-51.

Mur, L.A.J., Kenton, P., Lloyd, A.J., Ougham, H., and Prats, E. (2008). The hypersensitive response; the centenary is upon us but how much do we know? *J. Exp. Bot.* 59, 501-520.

Muskett, P.R., Kahn, K., Austin, M.J., Moisan, L.J., Sadanandom, A., Shirasu, K., Jones, J.D.G., and Parker, J.E. (2002). *Arabidopsis* RAR1 exerts rate-limiting control of *R* gene-mediated defenses against multiple pathogens. *Plant Cell* 14, 979-992.

Naito, K., Ishiga, Y., Toyoda, K., Shiraishi, T., and Ichinose, Y. (2007). N-terminal domain including conserved flg22 is required for flagellin-induced hypersensitive cell death in *Arabidopsis thaliana*. *Journal of General Plant Pathology* 73, 281-285.

Nakagami, H., Soukupova, H., Schikora, A., Zarsky, V., and Hirt, H. (2006). A Mitogen-activated protein kinase kinase kinase mediates reactive oxygen species homeostasis in *Arabidopsis*. *J Biol Chem* 281, 38697-38704.

Nakashima, A., Chen, L., Thao, N.P., Fujiwara, M., Wong, H.L., Kuwano, M., Umemura, K., Shirasu, K., Kawasaki, T., and Shimamoto, K. (2008). RACK1 functions in rice innate immunity by interacting with the Rac1 immune complex. *Plant Cell* 20, 2265-2279.

Nam, K.H., and Li, J. (2002). BRI1/BAK1, a receptor kinase pair mediating brassinosteroid signaling. *Cell* 110, 203-212.

Narusaka, M., Shirasu, K., Noutoshi, Y., Kubo, Y., Shiraishi, T., Iwabuchi, M., and Narusaka, Y. (2009). *RRS1* and *RPS4* provide a dual resistance-gene system against fungal and bacterial pathogens. *Plant J* 60, 218-226.

Narváez-Vásquez, J., and Ryan, C. (2004). The cellular localization of prosystemin: a functional role for phloem parenchyma in systemic wound signaling. *Planta* 218, 360-369.

Narváez-Vásquez, J., Pearce, G., and Ryan, C.A. (2005). The plant cell wall matrix harbors a precursor of defense signaling peptides. *PNAS* 102, 12974-12977.

Navarro, L., Zipfel, C., Rowland, O., Keller, I., and Robatzek, S. (2004). The transcriptional innate immune response to flg22. Interplay and overlap with *Avr* gene-dependent defense responses and bacterial pathogenesis. *Plant Physiol.* 135, 1113.

Navarro, L., Jay, F., Nomura, K., He, S.Y., and Voinnet, O. (2008). Suppression of the microRNA pathway by bacterial effector proteins. *Science* 321, 964-967.

Navarro, L., Dunoyer, P., Jay, F., Arnold, B., Dharmasiri, N., Estelle, M., Voinnet, O., and Jones, J.D. (2006). A plant miRNA contributes to antibacterial resistance by repressing auxin signaling. *Science* 312, 436-439.

Nawrath, C., and Metraux, J.-P. (1999). Salicylic acid induction-deficient mutants of *Arabidopsis* express *PR-2* and *PR-5* and accumulate high levels of camalexin after pathogen inoculation. *Plant Cell* 11, 1393-1404.

Neale, A.D., Wahleithner, J.A., Lund, M., Bonnett, H.T., Kelly, A., Meeks-Wagner, D.R., Peacock, W.J., and Dennis, E.S. (1990). Chitinase,  $\beta$ -1,3-glucanase osmotin, and extensin are expressed in tobacco explants during flower formation. *Plant Cell* 2, 673-684.

Neff, M.M., Turk, E., and Kalishman, M. (2002). Web-based primer design for single nucleotide polymorphism analysis. *Trends in Genetics* 18, 613-615.

Neish, A.S. (2007). TLRS in the Gut. II. Flagellin-induced inflammation and antiapoptosis. *Am J Physiol Gastrointest Liver Physiol* 292, G462-466.

Nekrasov, V., Li, J., Batoux, M., Roux, M., Chu, Z.-H., Lacombe, S., Rougon, A., Bittel, P., Kiss-Papp, M., Chinchilla, D., van Esse, H.P., Jorda, L., Schwessinger, B., Nicaise, V., Thomma, B.P.H.J., Molina, A., Jones, J.D.G., and Zipfel, C. (2009). Control of the pattern-recognition receptor EFR by an ER protein complex in plant immunity. *Embo J* 28, 3428-3438.

Nelson, A.J. (1998). Sequence announcements. *Plant Molecular Biology* 38, 911-912.

Nennstiel, D., Scheel, D., and Nrnberger, T. (1998). Characterization and partial purification of an oligopeptide elicitor receptor from parsley (*Petroselinum crispum*). *FEBS Letters* 431, 405-410.

Newman, M.A., Dow, J.M., Molinaro, A., and Parrilli, M. (2007). Priming, induction and modulation of plant defense responses by bacterial lipopolysaccharides. *Journal of endotoxin research* 13, 69-84.

Nicaise, V., Roux, M., and Zipfel, C. (2009). Recent advances in PAMP-triggered immunity against bacteria: pattern recognition receptors watch over and raise the alarm. *Plant Physiol.* 150, 1638-1647.

Nickstadt, A., Thomma, B.P.H.J., Feussner, I., KangasjÄRvi, J., Zeier, J., Loeffler, C., Scheel, D., and Berger, S. (2004). The jasmonate-insensitive mutant *jin1* shows increased resistance to biotrophic as well as necrotrophic pathogens. *Molecular Plant Pathology* 5, 425-434.

Nishimura, M.T., Stein, M., Hou, B.-H., Vogel, J.P., Edwards, H., and Somerville, S.C. (2003). Loss of a callose synthase results in salicylic acid-dependent disease resistance. *Science* 301, 969-972.

Noma, K.-i., Allis, C.D., and Grewal, S.I.S. (2001). Transitions in distinct histone h3 methylation patterns at the heterochromatin domain boundaries. *Science* 293, 1150-1155.

Nomura, K., Debroy, S., Lee, Y.H., Pumplin, N., Jones, J., and He, S.Y. (2006). A bacterial virulence protein suppresses host innate immunity to cause plant disease. *Science* 313, 220-223.

Noutoshi, Y., Ito, T., Seki, M., Nakashita, H., Yoshida, S., Marco, Y., Shirasu, K., and Shinozaki, K. (2005). A single amino acid insertion in the WRKY domain of the *Arabidopsis* TIR–NBS–LRR–WRKY-type disease resistance protein SLH1 (sensitive to low humidity 1) causes activation of defense responses and hypersensitive cell death. *Plant J* 43, 873-888.

Ntoukakis, V., Mucyn, T.S., Gimenez-Ibanez, S., Chapman, H.C., Gutierrez, J.R., Balmuth, A.L., Jones, A.M.E., and Rathjen, J.P. (2009). Host inhibition of a bacterial virulence effector triggers immunity to infection. *Science* 324, 784-787.

Nühse, T.S., Stensballe, A., Jensen, O.N., and Peck, S.C. (2004). phosphoproteomics of the *Arabidopsis* plasma membrane and a new phosphorylation site database. *Plant Cell* 16, 2394-2405.

Nühse, T.S., Bottrill, A.R., Jones, A.M., and Peck, S.C. (2007). Quantitative phosphoproteomic analysis of plasma membrane proteins reveals regulatory mechanisms of plant innate immune responses. *Plant J* 51, 931-940.

Nürnberg, T., and Lipka, V. (2005). Non-host resistance in plants: new insights into an old phenomenon. *Molecular Plant Pathology* 6, 335-345.

Nürnberg, T., Nennstiel, D., Hahlbrock, K., and Scheel, D. (1995). Covalent cross-linking of the *Phytophthora megasperma* oligopeptide elicitor to its receptor in parsley membranes. *PNAS* 92, 2338-2342.

Nürnberg, T., Colling, C., Hahlbrock, K., Jabs, T., Renelt, A., Sacks, W.R., and Scheel, D. (1994). Perception and transduction of an elicitor signal in cultured parsley cells. *Biochem Soc Symp.* 60, 173-182.

O'Donnell, P.J., Schmelz, E.A., Moussatche, P., Lund, S.T., Jones, J.B., and Klee, H.J. (2003). Susceptible to intolerance--a range of hormonal actions in a susceptible *Arabidopsis* pathogen response. *Plant J* 33, 245-257.

Ogawa, M., Shinohara, H., Sakagami, Y., and Matsubayashi, Y. (2008). *Arabidopsis* CLV3 peptide directly binds CLV1 ectodomain. *Science* 319, 294.

Oh, H.-S., Park, D.H., and Collmer, A. (2010a). Components of the *Pseudomonas syringae* type III secretion system can suppress and may elicit plant innate immunity. *MPMI* 23, 727-739.

Oh, M.-H., Wang, X., Wu, X., Zhao, Y., Clouse, S.D., and Huber, S.C. (2010b). Autophosphorylation of Tyr-610 in the receptor kinase BAK1 plays a role in brassinosteroid signaling and basal defense gene expression. *PNAS*.

Oh, M.-H., Ray, W.K., Huber, S.C., Asara, J.M., Gage, D.A., and Clouse, S.D. (2000). Recombinant brassinosteroid insensitive 1 receptor-like kinase autophosphorylates on serine and threonine residues and phosphorylates a conserved peptide motif *in vitro*. *Plant Physiol.* 124, 751-766.

Oh, M.-H., Wang, X., Kota, U., Goshe, M.B., Clouse, S.D., and Huber, S.C. (2009). Tyrosine phosphorylation of the BRI1 receptor kinase emerges as a component of brassinosteroid signaling in *Arabidopsis*. *PNAS* 106, 658-663.

Olsen, J.V., Ong, S.-E., and Mann, M. (2004). Trypsin cleaves exclusively c-terminal to arginine and lysine residues. *Molecular & Cellular Proteomics* 3, 608-614.

Olson, D., Davis, R., Wäckers, F., Rains, G., and Potter, T. (2008). Plant–herbivore–carnivore interactions in cotton - *Gossypium hirsutum* linking belowground and aboveground. *Journal of Chemical Ecology* 34, 1341-1348.

Ortiz-Martín, I., Thwaites, R., Macho, A.P., Mansfield, J.W., and Beuzón, C.R. (2010). Positive regulation of the Hrp type III secretion system in *Pseudomonas syringae* pv. *phaseolicola*. *MPMI* 23, 665-681.

Ottmann, C., Luberacki, B., Küfner, I., Koch, W., Brunner, F.d.r., Weyand, M., Mattinen, L., Pirhonen, M., Anderluh, G., Seitz, H.U., Nürnberg, T., and Oecking, C. (2009). A common toxin fold mediates microbial attack and plant defense. *PNAS* 106, 10359-10364.

Palma, K., Zhao, Q., Cheng, Y.T., Bi, D., Monaghan, J., Cheng, W., Zhang, Y., and Li, X. (2007). Regulation of plant innate immunity by three proteins in a complex conserved across the plant and animal kingdoms. *Genes Dev* 21, 1484-1493.

Palma, K., Thorgrimsen, S., Malinovsky, F.G., Fiil, B.K., Nielsen, H.B.r., Brodersen, P., Hofius, D., Petersen, M., and Mundy, J. (2010). Autoimmunity in *Arabidopsis acd11* is mediated by epigenetic regulation of an immune receptor. *PLoS Pathog* 6, e1001137.

Pandey, S., Roccaro, M., Schön, M., Logemann, E., and Somssich, I. (2010). Transcriptional reprogramming regulated by WRKY18 and WRKY40 facilitates powdery mildew infection of *Arabidopsis*. *Plant J* accepted article.

Pandey, S.P., and Somssich, I.E. (2009). The role of WRKY transcription factors in plant immunity. *Plant Physiol.* 150, 1648-1655.

Park, C.-J., Bart, R., Chern, M., Canlas, P.E., Bai, W., and Ronald, P.C. (2010a). Overexpression of the Endoplasmic Reticulum Chaperone BiP3 regulates xa21-mediated innate immunity in rice. *PLoS ONE* 5, e9262.

Park, C.-J., Peng, Y., Chen, X., Dardick, C., Ruan, D., Bart, R., Canlas, P.E., and Ronald, P.C. (2008). Rice XB15, a protein phosphatase 2C, negatively regulates cell death and Xa21-mediated innate immunity. *PLoS Biol* 6, e231.

Park, C.J., Han, S.W., Chen, X., and Ronald, P.C. (2010b). Elucidation of Xa21-mediated innate immunity. *Cell Microbiol* 12, 1017-1025.

Passardi, F., Penel, C., and Dunand, C. (2004). Performing the paradoxical: how plant peroxidases modify the cell wall. *Trends in Plant Science* 9, 534-540.

Pattison, R.J., and Amtmann, A. (2009). N-glycan production in the endoplasmic reticulum of plants. *Trends in Plant Science* 14, 92-99.

Pauwels, L., Morreel, K., De Witte, E., Lammertyn, F., Van Montagu, M., Boerjan, W., Inzé, D., and Goossens, A. (2008). Mapping methyl jasmonate-mediated transcriptional reprogramming of metabolism and cell cycle progression in cultured *Arabidopsis* cells. *PNAS* 105, 1380-1385.

Pauwels, L., Barbero, G.F., Geerinck, J., Tillemen, S., Grunewald, W., Perez, A.C., Chico, J.M., Bossche, R.V., Sewell, J., Gil, E., Garcia-Casado, G., Witters, E., Inze, D., Long, J.A., De Jaeger, G., Solano, R., and Goossens, A. (2010). NINJA connects the co-repressor TOPLESS to jasmonate signaling. *Nature* 464, 788-791.

Paxson-Sowders, D.M., Dodrill, C.H., Owen, H.A., and Makaroff, C.A. (2001). DEX1, a novel plant protein, is required for exine pattern formation during pollen development in *Arabidopsis*. *Plant Physiol.* 127, 1739-1749.

Pearce, G., and Ryan, C.A. (2003). Systemic signaling in tomato plants for defense against herbivores. *Journal of Biological Chemistry* 278, 30044-30050.

Pearce, G., Johnson, S., and Ryan, C.A. (1993). Purification and characterization from tobacco (*Nicotiana tabacum*) leaves of six small, wound-inducible, proteinase iso-inhibitors of the potato inhibitor II family. *Plant Physiol.* 102, 639-644.

Pearce, G., Siems, W.F., Bhattacharya, R., Chen, Y.-C., and Ryan, C.A. (2007). Three hydroxyproline-rich glycopeptides derived from a single petunia polyprotein precursor activate defensin I, a pathogen defense response gene. *Journal of Biological Chemistry* 282, 17777-17784.

Pearce, L.R., Komander, D., and Alessi, D.R. (2010). The nuts and bolts of AGC protein kinases. *Nat Rev Mol Cell Biol* 11, 9-22.

Peer, M., Stegmann, M., Mueller, M.J., and Waller, F. (2010). *Pseudomonas syringae* infection triggers de novo synthesis of phytosphingosine from sphinganine in *Arabidopsis thaliana*. *FEBS Letters* 584, 4053-4056.

Pemberton, C.L., and Salmond, G.P.C. (2004). The Nep1-like proteins—a growing family of microbial elicitors of plant necrosis. *Molecular Plant Pathology* 5, 353-359.

Peng, Y., Bartley, L.E., Chen, X., Dardick, C., Chern, M., Ruan, R., Canlas, P.E., and Ronald, P.C. (2008). OsWRKY62 is a Negative Regulator of Basal and Xa21-Mediated Defense against *Xanthomonas oryzae* pv. *oryzae* in Rice. *Molecular Plant* 1, 446-458.

Penninckx, I., Thomma, B., Buchala, A., Metraux, J.P., and Broekaert, W.F. (1998). Concomitant activation of jasmonate and ethylene response pathways is required for induction of a plant defensin gene in *Arabidopsis*. *Plant Cell* 10, 2103 - 2113.

Petersen, L.N., Ingle, R.A., Knight, M.R., and Denby, K.J. (2009). OXI1 protein kinase is required for plant immunity against *Pseudomonas syringae* in *Arabidopsis*. *Journal of Experimental Botany* 60, 3727-3735.

Petersen, M., Brodersen, P., Naested, H., Andreasson, E., Lindhart, U., Johansen, B., Nielsen, H.B., Lacy, M., Austin, M.J., Parker, J.E., Sharma, S.B., Klessig, D.F., Martienssen, R., Mattsson, O., Jensen, A.B., and Mundy, J. (2000). *Arabidopsis* MAP kinase 4 negatively regulates systemic acquired resistance. *Cell* 103, 1111-1120.

Petnicki-Ocwieja, T., van Dijk, K., and Alfano, J.R. (2005). The *hrpK* Operon of *Pseudomonas syringae* pv. *tomato* DC3000 encodes two proteins secreted by the Type III (Hrp) protein secretion system: HopB1 and HrpK, a putative type III translocator. *J. Bacteriol.* 187, 649-663.

Petutschnig, E.K., Jones, A.M.E., Serazetdinova, L., Lipka, U., and Lipka, V. (2010). The lysin motif receptor-like kinase (LysM-RLK) CERK1 is a major chitin-binding protein in *Arabidopsis thaliana* and subject to chitin-induced phosphorylation. *Journal of Biological Chemistry* 285, 28902-28911.

Pfund, C., Tans-Kersten, J., Dunning, F.M., Alonso, J.M., Ecker, J.R., Allen, C., and Bent, A.F. (2004). Flagellin is not a major defense elicitor in *Ralstonia solanacearum* cells or extracts applied to *Arabidopsis thaliana*. *MPMI* 17, 696-706.

Pieterse, C.M.J., and Van Loon, L.C. (2004). NPR1: the spider in the web of induced resistance signaling pathways. *Current Opinion in Plant Biology* 7, 456-464.

Pimpl, P., Taylor, J.P., Snowden, C., Hillmer, S., Robinson, D.G., and Denecke, J. (2006). Golgi-mediated vacuolar sorting of the endoplasmic reticulum chaperone BiP may play an active role in quality control within the secretory pathway. *Plant Cell* 18, 198-211.

Postel, S., Kühner, I., Beuter, C., Mazzotta, S., Schwedt, A., Borlotti, A., Halter, T., Kemmerling, B., and Nürnberg, T. (2010). The multifunctional leucine-rich repeat receptor kinase BAK1 is implicated in *Arabidopsis* development and immunity. *European Journal of Cell Biology* 89, 169-174.

Potuschak, T., Lechner, E., Parmentier, Y., Yanagisawa, S., Grava, S., Koncz, C., and Genschik, P. (2003). EIN3-dependent regulation of plant ethylene hormone signaling by two *Arabidopsis* F box proteins: EBF1 and EBF2. *Cell* 115, 679-689.

Qi, Y., and Katagiri, F. (2009). Purification of low-abundance *Arabidopsis* plasma-membrane protein complexes and identification of candidate components. *Plant J* 57, 932-944.

Qi, Y., Tsuda, K., Joe, A., Sato, M., Nguyen, L.V., Glazebrook, J., Alfano, J.R., Cohen, J.D., and Katagiri, F. (2010). A putative RNA-binding protein positively regulates salicylic acid-mediated immunity in *Arabidopsis*. *MPMI*: epub ahead of print.

Qiao, H., Chang, K.N., Yazaki, J., and Ecker, J.R. (2009). Interplay between ethylene, ETP1/ETP2 F-box proteins, and degradation of EIN2 triggers ethylene responses in *Arabidopsis*. *Genes Dev* 23, 512-521.

Qiu, J.-L., Füll, B.K., Petersen, K., Nielsen, H.B., Botanga, C.J., Thorgrimsen, S., Palma, K., Suarez-Rodriguez, M.C., Sandbech-Clausen, S., Lichota, J., Brodersen, P., Grasser, K.D., Mattsson, O., Glazebrook, J., Mundy, J., and Petersen, M. (2008). *Arabidopsis* MAP kinase 4 regulates gene expression through transcription factor release in the nucleus. *Embo J* 27, 2214-2221.

Qutob, D., Kemmerling, B., Brunner, F., Kühner, I., Engelhardt, S., Gust, A.A., Luberacki, B., Seitz, H.U., Stahl, D., Rauhut, T., Glawischnig, E., Schween, G., Lacombe, B., Watanabe, N., Lam, E., Schlichting, R., Scheel, D., Nau, K., Dodt, G., Hubert, D., Gijzen, M., and Nürnberg, T. (2006). Phytotoxicity and innate immune responses induced by Nep1-like proteins. *Plant Cell* 18, 3721-3744.

Radutoiu, S., Madsen, L.H., Madsen, E.B., Felle, H.H., Umehara, Y., Gronlund, M., Sato, S., Nakamura, Y., Tabata, S., Sandal, N., and Stougaard, J. (2003). Plant recognition of symbiotic bacteria requires two LysM receptor-like kinases. *Nature* 425, 585-592.

Raffaele, S., Vailleau, F., Leger, A., Joubes, J., Miersch, O., Huard, C., Blee, E., Mongrand, S., Domergue, F., and Roby, D. (2008). A MYB transcription factor regulates very-long-chain fatty acid biosynthesis for activation of the hypersensitive cell death response in *Arabidopsis*. *Plant Cell* 20, 752-767.

Rahimi, N., Golde, T.E., and Meyer, R.D. (2009). Identification of ligand-induced proteolytic cleavage and ectodomain shedding of VEGFR-1/FLT1 in leukemic cancer cells. *Cancer research* 69, 2607-2614.

Rairdan, G.J., and Delaney, T.P. (2002). Role of salicylic acid and NIM1/NPR1 in race-specific resistance in *Arabidopsis*. *Genetics* 161, 803-811.

Rairdan, G.J., Collier, S.M., Sacco, M.A., Baldwin, T.T., Boetttrich, T., and Moffett, P. (2008). The coiled-coil and nucleotide binding domains of the potato Rx disease resistance protein function in pathogen recognition and signaling. *Plant Cell* 20, 739-751.

Ralston, L., Kwon, S.T., Schoenbeck, M., Ralston, J., Schenk, D.J., Coates, R.M., and Chappell, J. (2001). Cloning, heterologous expression, and functional characterization of 5-epi-aristolochene-1,3-dihydroxylase from tobacco (*Nicotiana tabacum*). *Archives of Biochemistry and Biophysics* 393, 222-235.

Rancour, D.M., Dickey, C.E., Park, S., and Bednarek, S.Y. (2002). Characterization of AtCDC48. Evidence for multiple membrane fusion mechanisms at the plane of cell division in plants. *Plant Physiol.* 130, 1241-1253.

Rancour, D.M., Park, S., Knight, S.D., and Bednarek, S.Y. (2004). Plant UBX domain-containing protein 1, PUX1, regulates the oligomeric structure and activity of *Arabidopsis* CDC48. *Journal of Biological Chemistry* 279, 54264-54274.

Raynaud, C., Sozzani, R., Glab, N., Domenichini, S., Perennes, C., Cella, R., Kondorosi, E., and Bergounioux, C. (2006). Two cell-cycle regulated SET-domain proteins interact with proliferating cell nuclear antigen (PCNA) in *Arabidopsis*. *Plant J* 47, 395-407.

Red Brewer, M., Choi, S.H., Alvarado, D., Moravcevic, K., Pozzi, A., Lemmon, M.A., and Carpenter, G. (2009). The juxtamembrane region of the egf receptor functions as an activation domain. *Mol Cell* 34, 641-651.

Rehmany, A.P., Gordon, A., Rose, L.E., Allen, R.L., and Armstrong, M.R. (2005). Differential recognition of highly divergent downy mildew avirulence gene alleles by *RPP1* resistance genes from two *Arabidopsis* lines. *Plant Cell* 17, 1839.

Reina-Pinto, J.J., and Yephremov, A. (2009). Surface lipids and plant defenses. *Plant Physiology and Biochemistry* 47, 540-549.

Reinbothe, C., Springer, A., Samol, I., and Reinbothe, S. (2009). Plant oxylipins: role of jasmonic acid during programmed cell death, defense and leaf senescence. *FEBS Journal* 276, 4666-4681.

Rentel, M.C., Lecourieux, D., Ouaked, F., Usher, S.L., Petersen, L., Okamoto, H., Knight, H., Peck, S.C., Grierson, C.S., Hirt, H., and Knight, M.R. (2004). OXI1 kinase is necessary for oxidative burst-mediated signaling in *Arabidopsis*. *Nature* 427, 858-861.

Rienties, I.M., Vink, J., Borst, J.W., Russinova, E., and Vries, S.C.d. (2005). The *Arabidopsis* SERK1 protein interacts with the AAA-ATPase CDC48, the 14-3-3 protein GF14 $\lambda$  and the PP2C phosphatase KAPP. *Planta* 221, 394-405.

Ritter, C., and Dangl, J.L. (1995). The *avrRpm1* gene of *Pseudomonas syringae* pv. *maculicola* is required for virulence on *Arabidopsis*. *MPMI* 8, 444-453.

Ritter, C., and Dangl, J.L. (1996). Interference between two specific pathogen recognition events mediated by distinct plant disease resistance genes. *Plant Cell* 8, 251-257.

Robatzek, S., Chinchilla, D., and Boller, T. (2006). Ligand-induced endocytosis of the pattern recognition receptor FLS2 in *Arabidopsis*. *Genes Dev* 20, 537-542.

Robatzek, S., Bittel, P., Chinchilla, D., Koechner, P., Felix, G., Shiu, S., and Boller, T. (2007). Molecular identification and characterization of the tomato flagellin receptor LeFLS2, an orthologue of *Arabidopsis* FLS2 exhibiting characteristically different perception specificities. *Plant Molecular Biology*.

Roine, E., Wei, W., Yuan, J., Nurmiaho-Lassila, E.-L., Kalkkinen, N., Romantschuk, M., and He, S.Y. (1997). Hrp pilus: An *hrp*-dependent bacterial surface appendage produced by *Pseudomonas syringae* pv. *tomato* DC3000. *PNAS* 94, 3459-3464.

Romeis, T., Piedras, P., and Jones, J.D.G. (2000). Resistance gene-dependent activation of a calcium-dependent protein kinase in the plant defense response. *Plant Cell* 12, 803-816.

Romeis, T., Ludwig, A.A., Martin, R., and Jones, J.D.G. (2001). Calcium-dependent protein kinases play an essential role in a plant defense response. *Embo J* 20, 5556-5567.

Romeis, T., Piedras, P., Zhang, S., Klessig, D.F., Hirt, H., and Jones, J.D.G. (1999). Rapid Avr 9- and Cf-9 -dependent activation of map kinases in tobacco cell cultures and leaves: convergence of resistance gene, elicitor, wound, and salicylate responses. *Plant Cell* 11, 273-288.

Romer, P., Strauss, T., Hahn, S., Scholze, H., Morbitzer, R., Grau, J., Bonas, U., and Lahaye, T. (2009). Recognition of AvrBs3-like proteins is mediated by specific binding to promoters of matching pepper Bs3 alleles. *Plant Physiol.* 150, 1697-1712.

Ron, M., and Avni, A. (2004). The receptor for the fungal elicitor ethylene-inducing xylanase is a member of a resistance-like gene family in tomato. *Plant Cell* 16, 1604-1615.

Ron, M., Kantety, R., Martin, G.B., Avidan, N., Eshed, Y., Zamir, D., and Avni, A. (2000). High-resolution linkage analysis and physical characterization of the EIX-responding locus in tomato. *TAG Theoretical and Applied Genetics* 100, 184-189.

Rothbauer, U., Zolghadr, K., Muyldermans, S., Schepers, A., Cardoso, M.C., and Leonhardt, H. (2008). A versatile nanotrap for biochemical and functional studies with fluorescent fusion proteins. *Molecular & Cellular Proteomics* 7, 282-289.

Rothbauer, U., Zolghadr, K., Tillib, S., Nowak, D., Schermelleh, L., Gahl, A., Backmann, N., Conrath, K., Muyldermans, S., Cardoso, M.C., and Leonhardt, H. (2006). Targeting and tracing antigens in live cells with fluorescent nanobodies. *Nat Meth* 3, 887-889.

Russinova, E., Borst, J.-W., Kwaaitaal, M., Cano-Delgado, A., Yin, Y., Chory, J., and de Vries, S.C. (2004). Heterodimerization and endocytosis of arabidopsis brassinosteroid receptors BRI1 and AtSERK3 (BAK1). *Plant Cell* 16, 3216-3229.

Ryals, J., Weymann, K., Lawton, K., Friedrich, L., Ellis, D., Steiner, H.Y., Johnson, J., Delaney, T.P., Jesse, T., Vos, P., and Uknas, S. (1997). The Arabidopsis NIM1 protein shows homology to the mammalian transcription factor inhibitor  $\text{Ik}\beta$ . *Plant Cell* 9, 425-439.

Ryals, J.A., Neuenschwander, U.H., Willits, M.G., Molina, A., Steiner, H.Y., and Hunt, M.D. (1996). Systemic acquired resistance. *Plant Cell* 8, 1809-1819.

Ryan, C.A., and Pearce, G. (2003). Systemins: A functionally defined family of peptide signals that regulate defensive genes in Solanaceae species. *Proc Natl Acad Sci U S A* 100, 14577-14580.

Sagi, M., and Fluhr, R. (2001). Superoxide production by plant homologues of the gp91phox NADPH oxidase. modulation of activity by calcium and by tobacco mosaic virus infection. *Plant Physiol.* 126, 1281-1290.

Saijo, Y., Tintor, N., Lu, X., Rauf, P., Pajerowska-Mukhtar, K., Haweker, H., Dong, X., Robatzek, S., and Schulze-Lefert, P. (2009). Receptor quality control in the endoplasmic reticulum for plant innate immunity. *Embo J* 28, 3439-3449.

Saleh, A., Alvarez-Venegas, R., Yilmaz, M., Le, O., Hou, G., Sadder, M., Al-Abdallat, A., Xia, Y., Lu, G., Ladunga, I., and Avramova, Z. (2008). The highly similar Arabidopsis homologs of trithorax ATX1 and ATX2 encode proteins with divergent biochemical functions. *Plant Cell* 20, 568-579.

Samuels, L., Kunst, L., and Jetter, R. (2008). Sealing plant surfaces: cuticular wax formation by epidermal cells. *Annual Review of Plant Biology* 59, 683-707.

Sánchez-Fernández, R., Davies, T.G.E., Coleman, J.O.D., and Rea, P.A. (2001). The *Arabidopsis thaliana* abc protein superfamily, a complete inventory. *Journal of Biological Chemistry* 276, 30231-30244.

Sanders, D., Pelloux, J., Brownlee, C., and Harper, J.F. (2002). Calcium at the crossroads of signaling. *Plant Cell* 14, S401.

Sang, Y., Cui, D., and Wang, X. (2001). Phospholipase D and phosphatidic acid-mediated generation of superoxide in *Arabidopsis*. *Plant Physiol.* 126, 1449-1458.

Sasabe, M., Toyoda, K., Shiraishi, T., Inagaki, Y., and Ichinose, Y. (2002). cDNA cloning and characterization of tobacco ABC transporter: *NtPDR1* is a novel elicitor-responsive gene. *FEBS Letters* 518, 164-168.

Schallus, T., Jaeckh, C., Feher, K., Palma, A.S., Liu, Y., Simpson, J.C., Mackeen, M., Stier, G., Gibson, T.J., Feizi, T., Pieler, T., and Muhle-Goll, C. (2008). Malectin: a novel carbohydrate-binding protein of the endoplasmic reticulum and a candidate player in the early steps of protein n-glycosylation. *Mol. Biol. Cell* 19, 3404-3414.

Schenk, P.M., Kazan, K., Manners, J.M., Anderson, J.P., Simpson, R.S., Wilson, I.W., Somerville, S.C., and Maclean, D.J. (2003). Systemic gene expression in *arabidopsis* during an incompatible interaction with *Alternaria brassicicola*. *Plant Physiol.* 132, 999-1010.

Schilmiller, A.L., and Howe, G.A. (2005). Systemic signaling in the wound response. *Current Opinion in Plant Biology* 8, 369-377.

Schlessinger, J. (1988). Signal transduction by allosteric receptor oligomerization. *Trends Biochem Sci.* 13, 443-447.

Schlessinger, J. (2002). Ligand-induced, receptor-mediated dimerization and activation of EGF receptor. *Cell* 110, 669-672.

Schmelz, E.A., Engelberth, J., Alborn, H.T., O'Donnell, P., Sammons, M., Toshima, H., and Tumlinson, J.H. (2003). Simultaneous analysis of phytohormones, phytotoxins, and volatile organic compounds in plants. *PNAS* 100, 10552-10557.

Schrader, E.K., Harstad, K.G., and Matouschek, A. (2009). Targeting proteins for degradation. *Nat Chem Biol* 5, 815-822.

Schreiber, L. (2010). Transport barriers made of cutin, suberin and associated waxes. *Trends in Plant Science* 15, 546-553.

Schulze, B., Mentzel, T., Jehle, A.K., Mueller, K., Beeler, S., Boller, T., Felix, G., and Chinchilla, D. (2010). Rapid heteromerization and phosphorylation of ligand-activated plant transmembrane receptors and their associated kinase BAK1. *Journal of Biological Chemistry* 285, 9444-9451.

Schulze, W.X. (2010). Proteomics approaches to understand protein phosphorylation in pathway modulation. *Current Opinion in Plant Biology* 13, 279-286.

Schwessinger, B., Roux, M., Sklenar, J., Kadota, Y., Jones, A., Zipfel, C. (2010). Phosphorylation-dependent differential regulation of plant growth, cell death and innate immunity by the regulatory receptor-like kinase BAK1. *PLOS Biology*, *submitted*.

Scofield, S.R., Tobias, C.M., Rathjen, J.P., Chang, J.H., and Lavelle, D.T. (1996). Molecular basis of gene-for-gene specificity in bacterial speck disease of tomato. *Science* 274, 2063.

Seals, D.F., and Courtneidge, S.A. (2003). The ADAMs family of metalloproteases: multidomain proteins with multiple functions. *Genes Dev* 17, 7-30.

Segonzac, C. and Zipfel, C. (2010). Activation of plant pattern recognition receptors by bacteria. *Curr. Opin. Microbiol.* *submitted*.

Sels, J., Mathys, J., De Coninck, B.M.A., Cammue, B.P.A., and De Bolle, M.F.C. (2008). Plant pathogenesis-related (PR) proteins: A focus on PR peptides. *Plant Physiology and Biochemistry* 46, 941-950.

Seong, H.-A., Jung, H., Ichijo, H., and Ha, H. (2010). Reciprocal NEGATIVE REGULATION of PDK1 and ASK1 SIGNALING BY DIRECT INTERACTION AND PHOSPHORYLATION. *Journal of Biological Chemistry* 285, 2397-2414.

Sessa, G., D'Ascenzo, M., and Martin, G.B. (2000). Thr38 and Ser198 are Pto autophosphorylation sites required for the AvrPto-Pto-mediated hypersensitive response. *Embo J* 19, 2257-2269.

Shah, J., Tsui, F., and Klessig, D.F. (1997). Characterization of a salicylic acid-insensitive mutant (*sai1*) of *Arabidopsis thaliana*, identified in a selective screen utilizing the SA-inducible expression of the *tms2* gene. *MPMI* 10, 69-78.

Shan, L., He, P., Li, J., Heese, A., Peck, S.C., Nrnberger, T., Martin, G.B., and Sheen, J. (2008). Bacterial effectors target the common signaling partner BAK1 to disrupt multiple MAMP receptor-signaling complexes and impede plant immunity. *Cell Host & Microbe* 4, 17-27.

Shao, F., Golstein, C., Ade, J., Stoutemyer, M., Dixon, J.E., and Innes, R.W. (2003). Cleavage of *Arabidopsis* PBS1 by a bacterial type III effector. *Science* 301, 1230-1233.

Shapiro, A.D., and Zhang, C. (2001). The role of NDR1 in avirulence gene-directed signaling and control of programmed cell death in *Arabidopsis*. *Plant Physiol.* 127, 1089-1101.

Shen, Q.H., Saijo, Y., Mauch, S., Biskup, C., Bieri, S., Keller, B., Seki, H., Ulker, B., Somssich, I.E., and Schulze-Lefert, P. (2007). Nuclear activity of MLA immune receptors links isolate-specific and basal disease-resistance responses. *Science* 315, 1098 - 1103.

Shi, L., Bielawski, J., Mu, J., Dong, H., Teng, C., Zhang, J., Yang, X., Tomishige, N., Hanada, K., Hannun, Y.A., and Zuo, J. (2007). Involvement of sphingoid bases in mediating reactive oxygen intermediate production and programmed cell death in *Arabidopsis*. *Cell Res* 17, 1030-1040.

Shibata, Y., Kawakita, K., and Takemoto, D. (2010). Age-related resistance of *Nicotiana benthamiana* against hemibiotrophic pathogen *Phytophthora infestans* requires both ethylene- and salicylic acid-mediated signaling pathways. *MPMI* 23, 1130-1142.

Shimizu, R., Taguchi, F., Marutani, M., Mukaihara, T., Inagaki, Y., Toyoda, K., Shiraishi, T., and Ichinose, Y. (2003). The *fliD* mutant of *Pseudomonas syringae* pv. *tabaci*, which secretes flagellin monomers, induces a strong hypersensitive reaction (HR) in non-host tomato cells. *Molecular Genetics and Genomics* 269, 21-30.

Shimizu, T., Nakano, T., Takamizawa, D., Desaki, Y., Ishii-Minami, N., Nishizawa, Y., Minami, E., Okada, K., Yamane, H., Kaku, H., and Shibuya, N. (2010). Two LysM receptor molecules, CEBiP and OsCERK1, cooperatively regulate chitin elicitor signaling in rice. *Plant J*, no-no.

Shirano, Y., Kachroo, P., Shah, J., and Klessig, D.F. (2002). A gain-of-function mutation in an *Arabidopsis* toll interleukin1 receptor-nucleotide binding site-leucine-rich repeat type *R* Gene triggers defense responses and results in enhanced disease resistance. *Plant Cell* 14, 3149-3162.

Shirasu, K. (2009). The HSP90-SGT1 chaperone complex for NLR immune sensors. *Annual Review of Plant Biology* 60, 139-164.

Shirasu, K., and Schulze-Lefert, P. (2003). Complex formation, promiscuity, and multi-functionality: protein interactions in disease resistance pathways. *Trends Plant Sci* 8, 252-258.

Shiu, S.H., and Bleecker, A.B. (2001). Receptor-like kinases from *Arabidopsis* form a monophyletic gene family related to animal receptor kinases. *PNAS* 98, 10763 - 10768.

Shiu, S.H., Karlowski, W.M., Pan, R., Tzeng, Y.H., Mayer, K.F.X., and Li, W.H. (2004). Comparative analysis of the receptor-like kinase family in *Arabidopsis* and rice. *Plant Cell* 16, 1220 - 1234.

Silberstein, S., Collins, P.G., Kelleher, D.J., and Gilmore, R. (1995). The essential OST2 gene encodes the 16-kD subunit of the yeast oligosaccharyltransferase, a highly conserved protein expressed in diverse eukaryotic organisms. *The Journal of Cell Biology* 131, 371-383.

Silipo, A., Erbs, G., Shinya, T., Dow, J.M., Parrilli, M., Lanzetta, R., Shibuya, N., Newman, M.-A., and Molinaro, A. (2010). Glyco-conjugates as elicitors or suppressors of plant innate immunity. *Glycobiology* 20, 406-419.

Sims, J.K., Houston, S.I., Magazinnik, T., and Rice, J.C. (2006). A trans-tail histone code defined by monomethylated H4 Lys-20 and H3 Lys-9 demarcates distinct regions of silent chromatin. *Journal of Biological Chemistry* 281, 12760-12766.

Sinz, A. (2006). Chemical cross-linking and mass spectrometry to map three-dimensional protein structures and protein-protein interactions. *Mass Spectrom. Rev.* 25, 663-682.

Smith, K.D., Andersen-Nissen, E., Hayashi, F., Strobe, K., Bergman, M.A., Barrett, S.L.R., Cookson, B.T., and Aderem, A. (2003). Toll-like receptor 5 recognizes a conserved site on flagellin required for protofilament formation and bacterial motility. *Nat Immunol* 4, 1247-1253.

Solano, R., Stepanova, A., Chao, Q., and Ecker, J.R. (1998). Nuclear events in ethylene signaling: a transcriptional cascade mediated by ETHYLENE-INSENSITIVE3 and ETHYLENE-RESPONSE-FACTOR1. *Genes Dev* 12, 3703-3714.

Song, W.-Y., Wang, G.-L., Chen, L.-L., Kim, H.-S., Pi, L.-Y., Holsten, T., Gardner, J., Wang, B., Zhai, W.-X., Zhu, L.-H., Fauquet, C., and Ronald, P. (1995). A receptor kinase-like protein encoded by the rice disease resistance gene, Xa21. *Science* 270, 1804-1806.

Spoel, S.H., Johnson, J.S., and Dong, X. (2007). Regulation of tradeoffs between plant defenses against pathogens with different lifestyles. *PNAS* 104, 18842-18847.

Spoel, S.H., Mou, Z., Tada, Y., Spivey, N.W., Genschik, P., and Dong, X. (2009). Proteasome-mediated turnover of the transcription coactivator NPR1 plays dual roles in regulating plant immunity. *Cell* 137, 860-872.

Springer, T.Ä. (1997). Folding of the N-terminal, ligand-binding region of integrin  $\alpha$ -subunits into  $\beta$ -propeller domain. *PNAS* 94, 65-72.

Stahl, Y., Wink, R.H., Ingram, G.C., and Simon, R.d. (2009). A signaling module controlling the stem cell niche in *Arabidopsis* root meristems. *Current biology : CB* 19, 909-914.

Stanislas, T., Bouyssie, D., Rossignol, M., Vesa, S., Fromentin, J.r.m., Morel, J., Pichereaux, C., Monsarrat, B., and Simon-Plas, F.o. (2009). Quantitative proteomics reveals a dynamic association of proteins to detergent-resistant membranes upon elicitor signaling in tobacco. *Molecular & Cellular Proteomics* 8, 2186-2198.

Staswick, P.E. (2008). JAzing up jasmonate signaling. *Trends in Plant Science* 13, 66-71.

Staswick, P.E., and Tiryaki, I. (2004). The oxylipin signal jasmonic acid is activated by an enzyme that conjugates it to isoleucine in *Arabidopsis*. *Plant Cell* 16, 2117-2127.

Stein, M., Dittgen, J., Sanchez-Rodriguez, C., Hou, B.H., Molina, A., Schulze-Lefert, P., Lipka, V., and Somerville, S. (2006). *Arabidopsis* PEN3/PDR8, an ATP binding cassette transporter, contributes to nonhost resistance to inappropriate pathogens that enter by direct penetration. *Plant Cell* 18, 731-746.

Stotz, H.U., Thomson, J.G., and Wang, Y. (2009). Plant defensins. Defense, development and application. *Plant Signal Behav* 4, 1010-1012.

Strader, L.C., Culler, A.H., Cohen, J.D., and Bartel, B. (2010). Conversion of endogenous indole-3-butyric acid to indole-3-acetic acid drives cell expansion in *Arabidopsis* seedlings. *Plant Physiol.* 153, 1577-1586.

Stuible, M., and Tremblay, M.L. (2010). In control at the ER: PTP1B and the down-regulation of RTKs by dephosphorylation and endocytosis. *Trends in Cell Biology* In Press, Corrected Proof.

Stukkens, Y., Bultreys, A., Grec, S., Trombik, T., Vanham, D., and Boutry, M. (2005). NpPDR1, a pleiotropic drug resistance-type ATP-binding cassette transporter from *Nicotiana plumbaginifolia*, plays a major role in plant pathogen defense. *Plant Physiol.* 139, 341-352.

Suarez-Rodriguez, M.C., Adams-Phillips, L., Liu, Y., Wang, H., Su, S.H., Jester, P.J., Zhang, S., Bent, A.F., and Krysan, P.J. (2007). MEKK1 is required for flg22-induced MPK4 activation in *Arabidopsis* plants. *Plant Physiol.* 143, 661-669.

Sugiyama, N., Nakagami, H., Mochida, K., Daudi, A., Tomita, M., Shirasu, K., and Ishihama, Y. (2008). Large-scale phosphorylation mapping reveals the extent of tyrosine phosphorylation in *Arabidopsis*. *Mol Syst Biol* 4.

Sun, W., Dunning, F.M., Pfund, C., Weingarten, R., and Bent, A.F. (2006). Within-species flagellin polymorphism in *Xanthomonas campestris* pv *campestris* and its impact on elicitation of *Arabidopsis* FLAGELLIN SENSING2-dependent defenses. *Plant Cell* 18, 764-779.

Swiderski, M.R., and Innes, R.W. (2001). The *Arabidopsis* PBS1 resistance gene encodes a member of a novel protein kinase subfamily. *Plant J* 26, 101-112.

Swiderski, M.R., Birker, D., and Jones, J.D.G. (2009). The TIR domain of TIR-NB-LRR resistance proteins is a signaling domain involved in cell death induction. *MPMI* 22, 157-165.

Syka, J.E.P., Coon, J.J., Schroeder, M.J., Shabanowitz, J., and Hunt, D.F. (2004). Peptide and protein sequence analysis by electron transfer dissociation mass spectrometry. *PNAS* 101, 9528-9533.

Tada, Y., Spoel, S.H., Pajerowska-Mukhtar, K., Mou, Z., Song, J., Wang, C., Zuo, J., and Dong, X. (2008). plant immunity requires conformational charges of NPR1 via S-nitrosylation and thioredoxins. *Science* 321, 952-956.

Taguchi, F., Shimizu, R., Inagaki, Y., Toyoda, K., Shiraishi, T., and Ichinose, Y. (2003). Post-translational modification of flagellin determines the specificity of HR induction. *Plant and Cell Physiology* 44, 342-349.

Taguchi, F., Suzuki, T., Takeuchi, K., Inagaki, Y., Toyoda, K., Shiraishi, T., and Ichinose, Y. (2009). Glycosylation of flagellin from *Pseudomonas syringae* pv. *tabaci* 6605 contributes to evasion of host tobacco plant surveillance system. *Physiological and Molecular Plant Pathology* 74, 11-17.

Taguchi, F., Takeuchi, K., Katoh, E., Murata, K., Suzuki, T., Marutani, M., Kawasaki, T., Eguchi, M., Katoh, S., Kaku, H., Yasuda, C., Inagaki, Y., Toyoda, K., Shiraishi, T., and Ichinose, Y. (2006). Identification of glycosylation genes and glycosylated amino acids of flagellin in *Pseudomonas syringae* pv. *tabaci*. *Cell Microbiol* 8, 923-938.

Takabatake, R., Karita, E., Seo, S., Mitsuhashi, I., Kuchitsu, K., and Ohashi, Y. (2007). Pathogen-induced calmodulin isoforms in basal resistance against bacterial and fungal pathogens in tobacco. *Plant Cell Physiol* 48, 414-423.

Takahashi, H., Miller, J., Nozaki, Y., Sukamto, and Takeda, M. (2002). *RCY1*, an *Arabidopsis thaliana* RPP8/HRT family resistance gene, conferring resistance to cucumber mosaic virus requires salicylic acid, ethylene and a novel signal transduction mechanism. *Plant J*. 32, 655.

Takahashi, Y., Berberich, T., Kanzaki, H., Matsumura, H., Saitoh, H., Kusano, T., and Terauchi, R. (2009). Serine palmitoyltransferase, the first step enzyme in sphingolipid biosynthesis, is involved in nonhost resistance. *MPMI* 22, 31-38.

Takai, R., Isogai, A., Takayama, S., and Che, F.-S. (2008). Analysis of flagellin perception mediated by flg22 receptor OsFLS2 in rice. *MPMI* 21, 1635-1642.

Takemiya, A., and Shimazaki, K.-i. (2010). Phosphatidic acid inhibits blue light-induced stomatal opening via inhibition of protein phosphatase 1. *Plant Physiol*. 153, 1555-1562.

Takeuchi, K., Taguchi, F., Inagaki, Y., Toyoda, K., Shiraishi, T., and Ichinose, Y. (2003). Flagellin glycosylation island in *Pseudomonas syringae* pv. *glycinea* and its role in host specificity. *J. Bacteriol*. 185, 6658-6665.

Takeuchi, K., Ono, H., Yoshida, M., Ishii, T., Katoh, E., Taguchi, F., Miki, R., Murata, K., Kaku, H., and Ichinose, Y. (2007). Flagellin glycans from two pathovars of *Pseudomonas syringae* contain rhamnose in D and L configurations in different ratios and modified 4-amino-4,6-dideoxyglucose. *J. Bacteriol*. 189, 6945-6956.

Tallant, T., Deb, A., Kar, N., Lupica, J., de Veer, M., and DiDonato, J. (2004). Flagellin acting via TLR5 is the major activator of key signaling pathways leading to NF- $\kappa$ B and proinflammatory gene program activation in intestinal epithelial cells. *BMC Microbiology* 4, 33.

Tameling, W.I.L., Elzinga, S.D.J., Darmin, P.S., Vossen, J.H., Takken, F.L.W., Haring, M.A., and Cornelissen, B.J.C. (2002). The tomato *R* gene products I-2 and Mi-1 are functional ATP binding proteins with ATPase activity. *Plant Cell* 14, 2929-2939.

Tang, P., Zhang, Y., Sun, X., Tian, D., Yang, S., and Ding, J. (2010). Disease resistance signature of the leucine-rich repeat receptor-like kinase genes in four plant species. *Plant Science* 179, 399-406.

Tang, W., Kim, T.-W., Oses-Prieto, J.A., Sun, Y., Deng, Z., Zhu, S., Wang, R., Burlingame, A.L., and Wang, Z.-Y. (2008). BSKs mediate signal transduction from the receptor kinase BRI1 in *Arabidopsis*. *Science* 321, 557-560.

Tang, X.Y., Frederick, R.D., Zhou, J.M., Halterman, D.A., Jia, Y.L., and Martin, G.B. (1996). Initiation of plant disease resistance by physical interaction of AvrPto and Pto kinase. *Science* 274, 2060.

Tao, Y., Xie, Z.Y., Chen, W.Q., Glazebrook, J., Chang, H.S., Han, B., Zhu, T., Zou, G.Z., and Katagiri, F. (2003). Quantitative nature of *Arabidopsis* responses during compatible and incompatible interactions with the bacterial pathogen *Pseudomonas syringae*. *Plant Cell* 15, 317-330.

Teis, D., Wunderlich, W., and Huber, L.A. (2002). Localization of the MP1-MAPK scaffold complex to endosomes is mediated by p14 and required for signal transduction. *Developmental Cell* 3, 803-814.

Tellstrom, V., Usadel, B., Thimm, O., Stitt, M., Kuster, H., and Niehaus, K. (2007). The lipopolysaccharide of *Sinorhizobium meliloti* suppresses defense-associated gene expression in cell cultures of the host plant *Medicago truncatula*. *Plant Physiol* 143, 825-837.

Testerink, C., and Munnik, T. (2005). Phosphatidic acid: a multifunctional stress signaling lipid in plants. *Trends in Plant Science* 10, 368-375.

Thao, N.P., Chen, L., Nakashima, A., Hara, S.-i., Umemura, K., Takahashi, A., Shirasu, K., Kawasaki, T., and Shimamoto, K. (2007). RAR1 and HSP90 form a complex with Rac/Rop GTPase and function in innate-immune responses in rice. *Plant Cell* 19, 4035-4045.

Thilmony, R., Underwood, W., and He, S.Y. (2006). Genome-wide transcriptional analysis of the *Arabidopsis thaliana* interaction with the plant pathogen *Pseudomonas syringae* pv. *tomato* DC3000 and the human pathogen *Escherichia coli* O157:H7. *Plant J* 46, 34-53.

Thines, B., Katsir, L., Melotto, M., Niu, Y., Mandaokar, A., Liu, G., Nomura, K., He, S.Y., Howe, G.A., and Browse, J. (2007). JAZ repressor proteins are targets of the SCFCOI1 complex during jasmonate signaling. *Nature* 448, 661-665.

Thoma, I., Krischke, M., Loeffler, C., and Mueller, M.J. (2004). The isoprostanoid pathway in plants. *Chemistry and Physics of Lipids* 128, 135-148.

Thomma, B.P.H.J., Eggermont, K., Penninckx, I.A.M.A., Mauch-Mani, B., Vogelsang, R., Cammue, B.P.A., and Broekaert, W.F. (1998). Separate jasmonate-dependent and salicylate-dependent defense-response pathways in *Arabidopsis* are essential for resistance to distinct microbial pathogens. *PNAS* 95, 15107-15111.

Tian, D., Traw, M.B., Chen, J.Q., Kreitman, M., and Bergelson, J. (2003). Fitness costs of *R*-gene-mediated resistance in *Arabidopsis thaliana*. *Nature* 423, 74-77.

Tischner, R., Koltermann, M., Hesse, H., and Plath, M. (2010). Early responses of *Arabidopsis thaliana* to infection by *Verticillium longisporum*. *Physiological and Molecular Plant Pathology* 74, 419-427.

Tör, M., Gordon, P., Cuzick, A., Eulgem, T., Sinapidou, E., Mert-Turk, F., Can, C., Dangl, J.L., and Holub, E.B. (2002). *Arabidopsis* SGT1b is required for defense signaling conferred by several downy mildew resistance genes. *Plant Cell* 14, 993-1003.

Tornero, P., Merritt, P., Sadanandom, A., Shirasu, K., Innes, R.W., and Dangl, J.L. (2002). RAR1 and NDR1 contribute quantitatively to disease resistance in *Arabidopsis*, and their relative contributions are dependent on the *R* gene assayed. *Plant Cell* 14, 1005-1015.

Torres, M.A., Dangl, J.L., and Jones, J.D.G. (2002). *Arabidopsis* gp91phox homologues AtrbohD and AtrbohF are required for accumulation of reactive oxygen intermediates in the plant defense response. *PNAS* 99, 517-522.

Torres, M.A., Jones, J.D.G., and Dangl, J.L. (2006). Reactive oxygen species signaling in response to pathogens. *Plant Physiol.* 141, 373-378.

Townley, H.E., McDonald, K., Jenkins, G.I., Knight, M.R., and Leaver, C.J. (2005). Ceramides induce programmed cell death in *Arabidopsis* cells in a calcium-dependent manner. *Biological Chemistry* 386, 161-166.

Trujillo, M., and Shirasu, K. (2010). Ubiquitination in plant immunity. *Current Opinion in Plant Biology* 13, 402-408.

Trujillo, M., Ichimura, K., Casais, C., and Shirasu, K. (2008). Negative regulation of PAMP-triggered immunity by an E3 ubiquitin ligase triplet in *Arabidopsis*. *Current biology : CB* 18, 1396-1401.

Truman, W., Bennett, M.H., Kubigsteltig, I., Turnbull, C., and Grant, M. (2007). *Arabidopsis* systemic immunity uses conserved defense signaling pathways and is mediated by jasmonates. *PNAS* 104, 1075-1080.

Tsuda, K., and Katagiri, F. (2010). Comparing signaling mechanisms engaged in pattern-triggered and effector-triggered immunity. *Current Opinion in Plant Biology* 13, 459-465.

Tsuda, K., Sato, M., Glazebrook, J., Cohen, J.D., and Katagiri, F. (2008). Interplay between MAMP-triggered and SA-mediated defense responses. *Plant J* 53, 763-775.

Tsuda, K., Sato, M., Stoddard, T., Glazebrook, J., and Katagiri, F. (2009). Network properties of robust immunity in plants. *PLoS Genet* 5, e1000772.

Ullrich, A., and Schlessinger, J. (1990). Signal transduction by receptors with tyrosine kinase activity. *Cell* 61, 203-212.

Underwood, W., Zhang, S., and He, S.Y. (2007). The *Pseudomonas syringae* type III effector tyrosine phosphatase HopAO1 suppresses innate immunity in *Arabidopsis thaliana*. *Plant J* 52, 658-672.

Upchurch, R. (2008). Fatty acid unsaturation, mobilization, and regulation in the response of plants to stress. *Biotechnology Letters* 30, 967-977.

Urquhart, W., Gunawardena, A., Moeder, W., Ali, R., Berkowitz, G., and Yoshioka, K. (2007). The chimeric cyclic nucleotide-gated ion channel ATCNGC11/12 constitutively induces programmed cell death in a  $\text{Ca}^{2+}$ -dependent manner. *Plant Molecular Biology* 65, 747-761.

Vailleau, F., Daniel, X., Tronchet, M., Montillet, J.-L., Triantaphylidès, C., and Roby, D. (2002). A R2R3-MYB gene, *AtMYB30*, acts as a positive regulator of the hypersensitive cell death program in plants in response to pathogen attack. *PNAS* 99, 10179-10184.

van der Biezen, E.A., Freddie, C.T., Kahn, K., Parker, J.E., and Jones, J.D.G. (2002). *Arabidopsis RPP4* is a member of the RPP5 multigene family of TIR-NB-LRR genes and confers downy mildew resistance through multiple signaling components. *Plant J*. 29, 439.

van der Hoorn, R.A.L., and Kamoun, S. (2008). From guard to decoy: a new model for perception of plant pathogen effectors. *Plant Cell* 20, 2009.

van der Luit, A.H., Piatti, T., van Doorn, A., Musgrave, A., Felix, G., Boller, T., and Munnik, T. (2000). Elicitation of suspension-cultured tomato cells triggers the formation of phosphatidic acid and diacylglycerol pyrophosphate. *Plant Physiol*. 123, 1507-1516.

van Kan, J.A.L. (2006). Licensed to kill: the lifestyle of a necrotrophic plant pathogen. *Trends in Plant Science* 11, 247-253.

van Loon, L.C., Rep, M., and Pieterse, C.M.J. (2006). Significance of inducible defense-related proteins in infected plants. *Annu Rev Phytopathol* 44, 135-162.

van Wees, S.C.M., Chang, H.-S., Zhu, T., and Glazebrook, J. (2003). Characterization of the Early Response of Arabidopsis to *Alternaria brassicicola* Infection Using Expression Profiling. *Plant Physiol.* 132, 606-617.

Vecchi, M., and Carpenter, G. (1997). Constitutive proteolysis of the ErbB-4 receptor tyrosine kinase by a unique, sequential mechanism. *The Journal of Cell Biology* 139, 995-1003.

Vembar, S.S., and Brodsky, J.L. (2008). One step at a time: endoplasmic reticulum-associated degradation. *Nat Rev Mol Cell Biol* 9, 944-957.

Veronese, P., Nakagami, H., Bluhm, B., AbuQamar, S., Chen, X., Salmeron, J., Dietrich, R.A., Hirt, H., and Mengiste, T. (2006). The membrane-anchored BOTRYTIS-INDUCED KINASE1 plays distinct roles in Arabidopsis resistance to necrotrophic and biotrophic pathogens. *Plant Cell* 18, 257-273.

Vijay-Kumar, M., Aitken, J., and Gewirtz, A. (2008). Toll like receptor-5: protecting the gut from enteric microbes. *Seminars in Immunopathology* 30, 11-21.

Vinatzer, B.A., Patocchi, A., Gianfranceschi, L., Tartarini, S., Zhang, H.-B., Gessler, C., and Sansavini, S. (2001). Apple contains receptor-like genes homologous to the *Cladosporium fulvum* resistance gene family of tomato with a cluster of genes cosegregating with *Vf* apple scab resistance. *MPMI* 14, 508-515.

Vogel, W.F. (2002). Ligand-induced shedding of discoidin domain receptor 1. *FEBS Letters* 514, 175-180.

von Zastrow, M., and Sorkin, A. (2007). Signaling on the endocytic pathway. *Current Opinion in Cell Biology* 19, 436-445.

Walley, J.W., Rowe, H.C., Xiao, Y., Chehab, E.W., Kliebenstein, D.J., Wagner, D., and Dehesh, K. (2008). The chromatin remodeler SPLAYED regulates specific stress signaling pathways. *PLoS Pathog* 4, e1000237.

Wan, J., Zhang, X.-C., Neece, D., Ramonell, K.M., Clough, S., Kim, S.-y., Stacey, M.G., and Stacey, G. (2008). A LysM receptor-like kinase plays a critical role in chitin signaling and fungal resistance in Arabidopsis. *Plant Cell* 20, 471-481.

Wang, G., Zhang, Z., Angenent, G.C., and Fiers, M. (2010a). New aspects of CLAVATA2, a versatile gene in the regulation of Arabidopsis development. *Journal of Plant Physiology In Press, Corrected Proof*.

Wang, Y., Li, J., Hou, S., Wang, X., Li, Y., Ren, D., Chen, S., Tang, X., and Zhou, J.-M. (2010b). A *Pseudomonas syringae* ADP-ribosyltransferase inhibits arabidopsis mitogen-activated protein kinase kinases. *Plant Cell*, tpc.110.075697.

Wang, L., Tsuda, K., Sato, M., Cohen, J.D., Katagiri, F., and Glazebrook, J. (2009). Arabidopsis CaM binding protein CBP60g contributes to MAMP-induced SA

Accumulation and is involved in disease resistance against *Pseudomonas syringae*. PLoS Pathog 5, e1000301.

Wang, G., Ellendorff, U., Kemp, B., Mansfield, J.W., Forsyth, A., Mitchell, K., Bastas, K., Liu, C.M., Woods-Tor, A., Zipfel, C., de Wit, P.J., Jones, J.D., Tor, M., and Thomma, B.P. (2008a). A genome-wide functional investigation into the roles of receptor-like proteins in Arabidopsis. Plant Physiol 147, 503-517.

Wang, L., Mitra, R.M., Hasselmann, K.D., Sato, M., Lenarz-Wyatt, L., Cohen, J.D., Katagiri, F., and Glazebrook, J. (2008b). The genetic network controlling the Arabidopsis transcriptional response to *Pseudomonas syringae* pv. *maculicola*: roles of major regulators and the phytotoxin coronatine. MPMI 21, 1408-1420.

Wang, W., Yang, X., Tangchaiburana, S., Ndeh, R., Markham, J.E., Tsegaye, Y., Dunn, T.M., Wang, G.-L., Bellizzi, M., Parsons, J.F., Morrissey, D., Bravo, J.E., Lynch, D.V., and Xiao, S. (2008c). An inositolphosphorylceramide synthase is involved in regulation of plant programmed cell death associated with defense in Arabidopsis. Plant Cell 20, 3163-3179.

Wang, X., Kota, U., He, K., Blackburn, K., Li, J., Goshe, M.B., Huber, S.C., and Clouse, S.D. (2008d). Sequential transphosphorylation of the BRI1/BAK1 receptor kinase complex impacts early events in brassinosteroid signaling. Developmental Cell 15, 220-235.

Wang, D., Pajerowska-Mukhtar, K., Culler, A.H., and Dong, X. (2007). Salicylic acid inhibits pathogen growth in plants through repression of the auxin signaling pathway. Current biology 17, 1784-1790.

Wang, W., Esch, J.J., Shiu, S.-H., Agula, H., Binder, B.M., Chang, C., Patterson, S.E., and Bleecker, A.B. (2006a). Identification of important regions for ethylene binding and signaling in the transmembrane domain of the ETR1 ethylene receptor of Arabidopsis. Plant Cell 18, 3429-3442.

Wang, X., Devaiah, S.P., Zhang, W., and Welti, R. (2006b). Signaling functions of phosphatidic acid. Progress in Lipid Research 45, 250-278.

Wang, Y.-S., Pi, L.-Y., Chen, X., Chakrabarty, P.K., Jiang, J., De Leon, A.L., Liu, G.-Z., Li, L., Benny, U., Oard, J., Ronald, P.C., and Song, W.-Y. (2006c). Rice XA21 binding protein 3 is a ubiquitin ligase required for full Xa21-mediated disease resistance. Plant Cell 18, 3635-3646.

Wang, X., Li, X., Meisenhelder, J., Hunter, T., Yoshida, S., Asami, T., and Chory, J. (2005a). Autoregulation and homodimerization are involved in the activation of the plant steroid receptor BRI1. Developmental Cell 8, 855-865.

Wang, X., Goshe, M.B., Soderblom, E.J., Phinney, B.S., Kuchar, J.A., Li, J., Asami, T., Yoshida, S., Huber, S.C., and Clouse, S.D. (2005b). identification and functional

analysis of *in vivo* phosphorylation sites of the *Arabidopsis* BRASSINOSTEROID-INSENSITIVE1 receptor kinase. *Plant Cell* 17, 1685-1703.

Ward, E.R., Uknes, S.J., Williams, S.C., Dincher, S.S., Wiederhold, D.L., Alexander, D.C., Ahl-Goy, P., Metraux, J.P., and Ryals, J.A. (1991). Coordinate gene activity in response to agents that induce systemic acquired resistance. *Plant Cell* 3, 1085-1094.

Warren, S.E., Mao, D.P., Rodriguez, A.E., Miao, E.A., and Aderem, A. (2008). Multiple Nod-like receptors activate caspase 1 during *Listeria monocytogenes* infection. *J Immunol* 180, 7558-7564.

Wasternack, C. (2007). Jasmonates: an update on biosynthesis, signal transduction and action in plant stress response, growth and development. *Ann Bot* 100, 681-697.

Wasternack, C., and Kombrink, E. (2009). Jasmonates: structural requirements for lipid-derived signals active in plant stress responses and development. *ACS Chemical Biology* 5, 63-77.

Watanabe, M., Tanaka, H., Watanabe, D., Machida, C., and Machida, Y. (2004). The ACR4 receptor-like kinase is required for surface formation of epidermis-related tissues in *Arabidopsis thaliana*. *Plant J* 39, 298-308.

Watt, S.A., Tellström, V., Patschkowski, T., and Niehaus, K. (2006). Identification of the bacterial superoxide dismutase (SodM) as plant-inducible elicitor of an oxidative burst reaction in tobacco cell suspension cultures. *Journal of Biotechnology* 126, 78-86.

Whalen, M.C., Innes, R.W., Bent, A.F., and Staskawicz, B.J. (1991). Identification of *Pseudomonas syringae* pathogens of *Arabidopsis* and a bacterial locus determining avirulence on both *Arabidopsis* and soybean. *Plant Cell* 3, 49-59.

White, R.F. (1979). Acetylsalicylic acid (aspirin) induces resistance to tobacco mosaic virus in tobacco. *Virology* 99, 410-412.

Widjaja, I., Naumann, K., Roth, U., Wolf, N., Mackey, D., Dangl, J.L., Scheel, D., and Lee, J. (2009). Combining subproteome enrichment and Rubisco depletion enables identification of low abundance proteins differentially regulated during plant defense. *Proteomics* 9, 138-147.

Widjaja, I., Lassowskat, I., Bethke, G., Eschen-Lippold, L., Long, H.H., Naumann, K., Dangl, J.L., Scheel, D., and Lee, J. (2010). A protein phosphatase 2C, responsive to the bacterial effector AvrRpm1 but not to the AvrB effector, regulates defense responses in *Arabidopsis*. *Plant J* 61, 249-258.

Wildermuth, M.C., Dewdney, J., Wu, G., and Ausubel, F.M. (2001). Isochorismate synthase is required to synthesize salicylic acid for plant defense. *Nature* 414, 562-565.

Williams, L.T. (1989). Signal transduction by the platelet-derived growth factor receptor involves association of the receptor with cytoplasmic molecules. *Clin Research* 37, 564-568.

Wilton, M., Subramaniam, R., Elmore, J., Felsensteiner, C., Coaker, G., and Desveaux, D. (2010). The type III effector HopF2 Pto targets *Arabidopsis* RIN4 protein to promote *Pseudomonas syringae* virulence. *PNAS* 107, 2349-2354.

Wirthmueller, L., Zhang, Y., Jones, J.D.G., and Parker, J.E. (2007). Nuclear accumulation of the *arabidopsis* immune receptor RPS4 is necessary for triggering EDS1-dependent defense. *Current biology* 17, 2023-2029.

Wittmann-Liebold, B., Graack, H.R., and Pohl, T. (2007). Two-dimensional gel electrophoresis as tool for proteomics studies in combination with protein identification by mass spectrometry. *Proteomics* 7, 824-824.

Wong, H.L., Sakamoto, T., Kawasaki, T., Umemura, K., and Shimamoto, K. (2004). Down-regulation of metallothionein, a reactive oxygen scavenger, by the small GTPase OsRac1 in rice. *Plant Physiol.* 135, 1447-1456.

Wrzaczek, M., Brosche, M., Salojarvi, J., Kangasjarvi, S., Idanheimo, N., Mersmann, S., Robatzek, S., Karpinski, S., Karpinska, B., and Kangasjarvi, J. (2010). Transcriptional regulation of the CRK/DUF26 group of Receptor-like protein kinases by ozone and plant hormones in *Arabidopsis*. *BMC Plant Biology* 10, 95.

Wuhrer, M., Catalina, M.I., Deelder, A.M., and Hokke, C.H. (2007). Glycoproteomics based on tandem mass spectrometry of glycopeptides. *Journal of Chromatography B* 849, 115-128.

Xiang, T., Zong, N., Zhang, J., Chen, J., Chen, M., and Zhou, J. (2010). FLS2, but not BAK1, is a target of the *Pseudomonas syringae* effector AvrPto. *MPMI* online.

Xiang, T., Zong, N., Zou, Y., Wu, Y., Zhang, J., Xing, W., Li, Y., Tang, X., Zhu, L., Chai, J., and Zhou, J.-M. (2008). *Pseudomonas syringae* effector AvrPto blocks innate immunity by targeting receptor kinases. *Current Biology* 18, 74-80.

Xing, D.-H., Lai, Z.-B., Zheng, Z.-Y., Vinod, K.M., Fan, B.-F., and Chen, Z.-X. (2008). Stress- and pathogen-induced *Arabidopsis* WRKY48 is a transcriptional activator that represses plant basal defense. *Molecular Plant* 1, 459-470.

Xing, W., Zou, Y., Liu, Q., Liu, J., Luo, X., Huang, Q., Chen, S., Zhu, L., Bi, R., Hao, Q., Wu, J.-W., Zhou, J.-M., and Chai, J. (2007). The structural basis for activation of plant immunity by bacterial effector protein AvrPto. *Nature* 449, 243-247.

Xu, L., Liu, F., Lechner, E., Genschik, P., Crosby, W.L., Ma, H., Peng, W., Huang, D., and Xie, D. (2002). The SCFCOI1 ubiquitin-ligase complexes are required for jasmonate response in *Arabidopsis*. *Plant Cell* 14, 1919-1935.

Xu, W.H., Wang, Y.S., Liu, G.Z., Chen, X., Tinjuangjun, P., Pi, L.Y., and Song, W.Y. (2006a). The autophosphorylated Ser686, Thr688, and Ser689 residues in the intracellular juxtamembrane domain of XA21 are implicated in stability control of rice receptor-like kinase. *Plant J* 45, 740-751.

Xu, X., Chen, C., Fan, B., and Chen, Z. (2006b). Physical and functional interactions between pathogen-induced *Arabidopsis* WRKY18, WRKY40, and WRKY60 transcription factors. *Plant Cell* 18, 1310-1326.

Yakushiji, S., Ishiga, Y., Inagaki, Y., Toyoda, K., Shiraishi, T., and Ichinose, Y. (2009). Bacterial DNA activates immunity in *Arabidopsis thaliana*. *Journal of general plant pathology* 75, 227-234.

Yamaguchi, T., Minami, E., Ueki, J., and Shibuya, N. (2005). Elicitor-induced activation of phospholipases plays an important role for the induction of defense responses in suspension-cultured rice cells. *Plant and Cell Physiology* 46, 579-587.

Yamaguchi, Y., Pearce, G., and Ryan, C.A. (2006). The cell surface leucine-rich repeat receptor for AtPep1, an endogenous peptide elicitor in *Arabidopsis*, is functional in transgenic tobacco cells. *PNAS* 103, 10104-10109.

Yamaguchi, Y., Huffaker, A., Bryan, A.C., Tax, F.E., and Ryan, C.A. (2010). PEPR2 is a second receptor for the Pep1 and Pep2 peptides and contributes to defense responses in *Arabidopsis*. *Plant Cell* 22, 508-522.

Yan, J., Zhang, C., Gu, M., Bai, Z., Zhang, W., Qi, T., Cheng, Z., Peng, W., Luo, H., Nan, F., Wang, Z., and Xie, D. (2009). The *Arabidopsis* CORONATINE INSENSITIVE1 protein is a jasmonate receptor. *Plant Cell* 21, 2220-2236.

Yang, B., Sugio, A., and White, F.F. (2005). Avoidance of host recognition by alterations in the repetitive and C-terminal regions of AvrXa7, a type III effector of *Xanthomonas oryzae* pv. *oryzae*. *MPMI* 18, 142-149.

Yang, C.W., Gonzalez-Lamothe, R., Ewan, R.A., Rowland, O., Yoshioka, H., Shenton, M., Ye, H., O'Donnell, E., Jones, J.D., and Sadanandom, A. (2006a). The E3 ubiquitin ligase activity of *arabidopsis* PLANT U-BOX17 and its functional tobacco homolog ACRE276 are required for cell death and defense. *Plant Cell* 18, 1084-1098.

Yang, S., Yang, H., Grisafi, P., Sanchatjate, S., Fink, G.R., Sun, Q., and Hua, J. (2006b). The BON/CPN gene family represses cell death and promotes cell growth in *Arabidopsis*. *Plant J* 45, 166-179.

Yang, S., and Hua, J. (2004). A haplotype-specific resistance gene regulated by BONZAI1 mediates temperature-dependent growth control in *Arabidopsis*. *Plant Cell* 16, 1060-1071.

Yasuda, M., Ishikawa, A., Jikumaru, Y., Seki, M., Umezawa, T., Asami, T., Maruyama-Nakashita, A., Kudo, T., Shinozaki, K., Yoshida, S., and Nakashita, H. (2008).

Antagonistic interaction between systemic acquired resistance and the abscisic acid-mediated abiotic stress response in *Arabidopsis*. *The Plant cell* 20, 1678-1692.

Yi, H., and Richards, E.J. (2007). A cluster of disease resistance genes in *Arabidopsis* is coordinately regulated by transcriptional activation and rna silencing. *Plant Cell* 19, 2929-2939.

Yi, H., and Richards, E. (2008). Phenotypic instability of *Arabidopsis* alleles affecting a disease Resistance gene cluster. *BMC Plant Biology* 8, 36.

Yoo, S.D., Cho, Y.H., Tena, G., Xiong, Y., and Sheen, J. (2008). Dual control of nuclear EIN3 by bifurcate MAPK cascades in C2H4 signaling. *Nature* 451, 789-795.

Yoshikawa, M., Matama, M., and Masago, H. (1981). Release of a soluble phytoalexin elicitor from mycelial walls of *Phytophthora megasperma* var. *sojae* by soybean tissues. *Plant Physiol.* 67, 1032-1035.

Yu, L., Nie, J., Cao, C., Jin, Y., Yan, M., Wang, F., Liu, J., Xiao, Y., Liang, Y., and Zhang, W. (2010). Phosphatidic acid mediates salt stress response by regulation of MPK6 in *Arabidopsis thaliana*. *New Phytologist*, earlyview.

Yu, Y., Zeng, H., Lyons, S., Carlson, A., Merlin, D., Neish, A.S., and Gewirtz, A.T. (2003). TLR5-mediated activation of p38 MAPK regulates epithelial IL-8 expression via posttranscriptional mechanism. *Am J Physiol Gastrointest Liver Physiol* 285, G282-290.

Yuan, C.-X., Lasut, A.L., Wynn, R., Neff, N.T., Hollis, G.F., Ramaker, M.L., Rupar, M.J., Liu, P., and Meade, R. (2003). Purification of Her-2 extracellular domain and identification of its cleavage site. *Protein Expression and Purification* 29, 217-222.

Zagrobelny, M., Bak, S., Rasmussen, A.V., Jorgensen, B., Naumann, C.M., and Lindberg Moller, B. (2004). Cyanogenic glucosides and plant-insect interactions. *Phytochemistry* 65, 293-306.

Zeidler, D., Zahringer, U., Gerber, I., Dubery, I., Hartung, T., Bors, W., Hutzler, P., and Durner, J. (2004). Innate immunity in *Arabidopsis thaliana*: lipopolysaccharides activate nitric oxide synthase (NOS) and induce defense genes. *PNAS* 101, 15811-15816.

Zeng, H., Carlson, A.Q., Guo, Y., Yu, Y., Collier-Hyams, L.S., Madara, J.L., Gewirtz, A.T., and Neish, A.S. (2003). Flagellin is the major proinflammatory determinant of enteropathogenic *Salmonella*. *J Immunol* 171, 3668-3674.

Zhang, J., Li, W., Xiang, T., Liu, Z., Laluk, K., Ding, X., Zou, Y., Gao, M., Zhang, X., Chen, S., Mengiste, T., Zhang, Y., and Zhou, J.-M. (2010a). Receptor-like cytoplasmic kinases integrate signaling from multiple plant immune receptors and are targeted by a *Pseudomonas syringae* effector. *Cell Host & Microbe* 7, 290-301.

Zhang, M., Kadota, Y., Prodromou, C., Shirasu, K., and Pearl, L.H. (2010b). Structural basis for assembly of Hsp90-Sgt1-CHORD protein complexes: implications for chaperoning of NLR innate immunity receptors. *Mol Cell* 39, 269-281.

Zhang, Y., Yang, Y., Fang, B., Gannon, P., Ding, P., Li, X., and Zhang, Y. (2010c). *Arabidopsis snc2-1D* activates receptor-like protein-mediated immunity transduced through WRKY70. *Plant Cell*, tpc.110.074120.

Zhang, H., Tang, X., Munske, G.R., Tolic, N., Anderson, G.A., and Bruce, J.E. (2009a). Identification of protein-protein interactions and topologies in living cells with chemical cross-linking and mass spectrometry. *Molecular & Cellular Proteomics* 8, 409-420.

Zhang, Y., Zhu, H., Zhang, Q., Li, M., Yan, M., Wang, R., Wang, L., Welti, R., Zhang, W., and Wang, X. (2009b). Phospholipase D $\alpha$ 1 and phosphatidic acid regulate NADPH oxidase activity and production of reactive oxygen species in ABA-mediated stomatal closure in *Arabidopsis*. *Plant Cell* 21, 2357-2377.

Zhang, M., Boter, M., Li, K., Kadota, Y., Panaretou, B., Prodromou, C., Shirasu, K., and Pearl, L.H. (2008). Structural and functional coupling of Hsp90- and Sgt1-centred multi-protein complexes. *Embo J* 27, 2789-2798.

Zhang, Y., and Turner, J.G. (2008). Wound-induced endogenous jasmonates stunt plant growth by inhibiting mitosis. *PLoS ONE* 3, e3699.

Zhang, J., Shao, F., Li, Y., Cui, H., Chen, L., Li, H., Zou, Y., Long, C., Lan, L., Chai, J., Chen, S., Tang, X., and Zhou, J.-M. (2007). A *Pseudomonas syringae* effector inactivates MAPKs to suppress PAMP-induced immunity in plants. *Cell Host & Microbe* 1, 175-185.

Zhang, Y., and Li, X. (2005). A putative nucleoporin 96 Is required for both basal defense and constitutive resistance responses mediated by suppressor of *npr1-1*, *constitutive 1*. *Plant Cell* 17, 1306 - 1316.

Zhang, Y., Cheng, Y.T., Bi, D., Palma, K., and Li, X. (2005). MOS2, a protein containing G-patch and KOW motifs, is essential for innate immunity in *Arabidopsis thaliana*. *Curr Biol* 15, 1936 - 1942.

Zhang, Y., Tessaro, M.J., Lassner, M., and Li, X. (2003a). Knockout analysis of *Arabidopsis* transcription factors *TGA2*, *TGA5*, and *TGA6* reveals their redundant and essential roles in systemic acquired resistance. *Plant Cell* 15, 2647-2653.

Zhang, Y., Goritschnig, S., Dong, X., and Li, X. (2003b). A gain-of-function mutation in a plant disease resistance gene leads to constitutive activation of downstream signal transduction pathways in *suppressor of npr1-1, constitutive 1*. *Plant Cell* 15, 2636 - 2646.

Zheng, Z., Qamar, S.A., Chen, Z., and Mengiste, T. (2006). Arabidopsis WRKY33 transcription factor is required for resistance to necrotrophic fungal pathogens. *Plant J* 48, 592-605.

Zheng, Z., Mosher, S.L., Fan, B., Klessig, D.F., and Chen, Z. (2007). Functional analysis of Arabidopsis WRKY25 transcription factors in plant defense against *Pseudomonas syringae*. *BMC Plant Biol* 7, 2.

Zheng, W. and He, S.Y. (2010). A prominent role of the flagellin receptor FLAGELLIN SENSING2 in mediating stomatal response to *Pseudomonas syringae* p. *tomato* DC3000 in Arabidopsis. *Plant Physiol.* 153, 1188-1198.

Zhou, J., Loh, Y.-T., Bressan, R.A., and Martin, G.B. (1995). The tomato gene *Pti1* encodes a serine/threonine kinase that is phosphorylated by Pto and is involved in the hypersensitive response. *Cell* 83, 925-935.

Zhou, J.-M., and Chai, J. (2008). Plant pathogenic bacterial type III effectors subdue host responses. *Current Opinion in Microbiology* 11, 179-185.

Zhou, N., Tootle, T.L., and Glazebrook, J. (1999). Arabidopsis *PAD3*, a gene required for camalexin biosynthesis, encodes a putative cytochrome P450 monooxygenase. *Plant Cell* 11, 2419-2428.

Zhu, X., Caplan, J., Mamillapalli, P., Czymbek, K., and Dinesh-Kumar, S.P. (2010a). Function of endoplasmic reticulum calcium ATPase in innate immunity-mediated programmed cell death. *Embo J* 29, 1007-1018.

Zhu, Y., Wang, Y., Li, R., Song, X., Wang, Q., Huang, S., Jin, J.B., Liu, C.M., and Lin, J. (2010b). Analysis of interactions among the CLAVATA3 receptors reveals a direct interaction between CLAVATA2 and CORYNE in Arabidopsis. *Plant J* 61, 223-233.

Zhu, Z., Xu, F., Zhang, Y., Cheng, Y.T., Wiermer, M., Li, X., and Zhang, Y. (2010c). Arabidopsis resistance protein SNC1 activates immune responses through association with a transcriptional corepressor. *PNAS* 107, 13960-13965.

Zipfel, C. (2009). Early molecular events in PAMP-triggered immunity. *Current Opinion in Plant Biology* 12, 414-420.

Zipfel, C., Kunze, G., Chinchilla, D., Caniard, A., Jones, J.D., Boller, T., and Felix, G. (2006). Perception of the bacterial PAMP EF-Tu by the receptor EFR restricts Agrobacterium-mediated transformation. *Cell* 125, 749-760.

Zipfel, C., and Felix, G. (2005). Plants and animals: a different taste for microbes? *Current Opinion in Plant Biology* 8, 353-360.

Zipfel, C., Robatzek, S., Navarro, L., Oakeley, E.J., Jones, J.D., Felix, G., and Boller, T. (2004). Bacterial disease resistance in Arabidopsis through flagellin perception. *Nature* 428, 764-767.

Zubarev, R.A., Kelleher, N.L., and McLafferty, F.W. (1998). Electron capture dissociation of multiply charged protein cations. a nonergodic process. Journal of the American Chemical Society 120, 3265-3266.